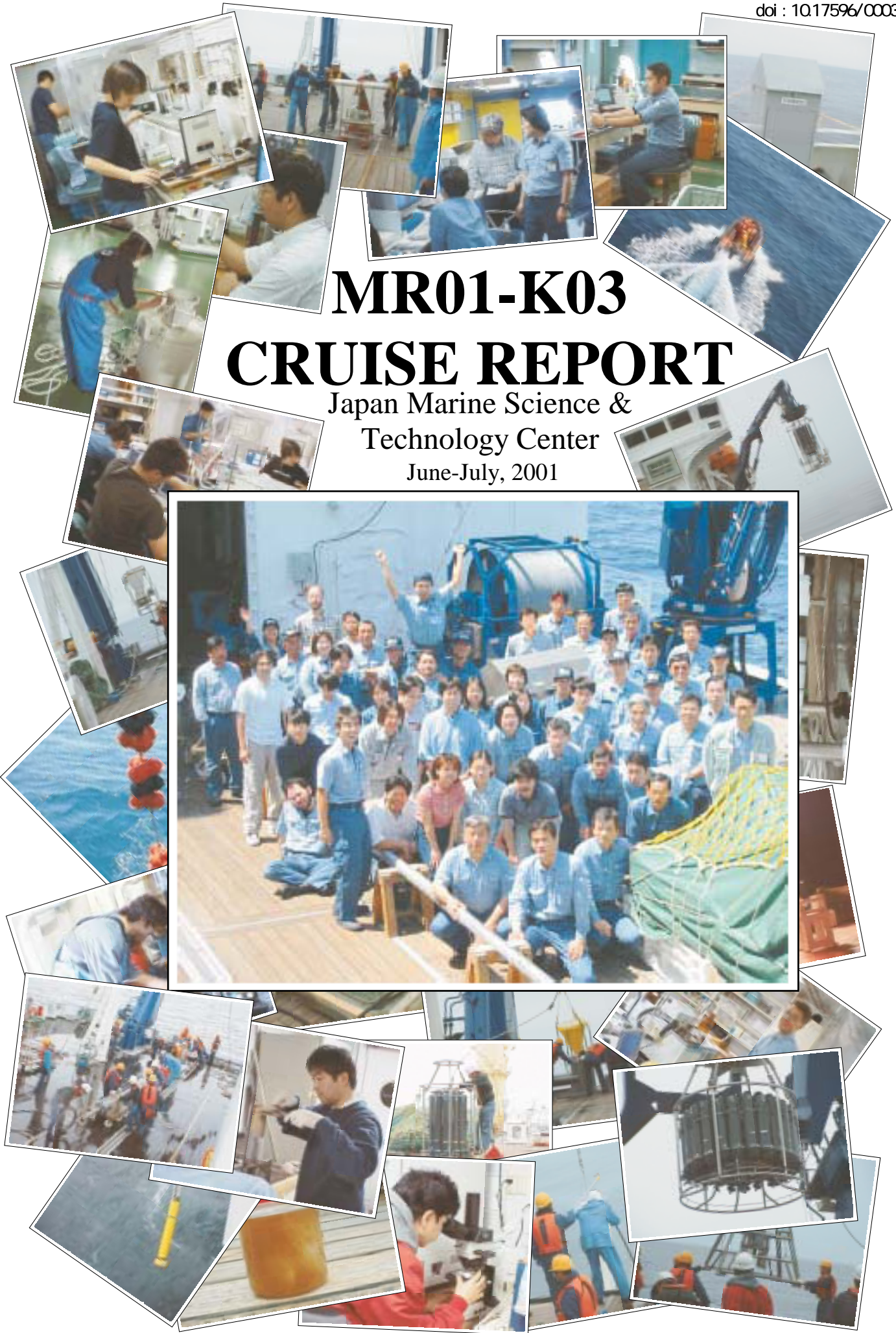


MR01-K03

CRUISE REPORT

Japan Marine Science &
Technology Center
June-July, 2001



Contents

1. Preface
2. Outline of MR01-K03
 - 2.1 Cruise Summary
 - 2.2 Cruise Log and cruise track
 - 2.3 List of participants
3. Observation
 - 3.1 Meteorological observation
 - 3.1.1 Surface meteorological observation
 - 3.1.2 Ceilometer Observation
 - 3.2 CTD/CWS, Lowering ADCP
 - 3.3 Hydrocast
 - 3.3.1 Salinity
 - 3.3.2 Dissolved oxygen
 - 3.3.3 Nutrients
 - 3.3.4 pH
 - 3.3.5 Total dissolved inorganic carbon
 - 3.3.6 Total alkalinity
 - 3.3.7 Carbon-13
 - 3.3.8 Carbon-14
 - 3.3.9 Iodine-129
 - 3.3.10 Freon
 - 3.3.11 Ar/N₂/O₂
 - 3.3.12 DMS/DMSP
 - 3.3.13 Chlorophyll-a and pigment
 - 3.3.14 CREST samples
 - 3.4 Hydrocast for trace metals
 - 3.5 Optical observation and primary production
 - 3.6 Plankton net
 - 3.7 Time-series sediment trap experiment
 - 3.7.1 JAMSTEC sediment trap
 - 3.7.2 Hokkaido Univ. sediment trap

- 3.8 Sediment
- 3.9 Atmospheric observation
 - 3.9.1 Aerosol
 - 3.9.2 Radiometer / particle counter
- 3.10 Surface water underway observations
 - 3.10.1 pCO₂ (JAMSTEC)
 - 3.10.2 pCO₂ (CREST)
 - 3.10.3 Salinity, temperature, dissolved oxygen, and fluorescence
 - 3.10.4 Nutrients
 - 3.10.5 Total dissolved inorganic carbon
- 3.11 Eddy observations
- 3.12 ARGO buoy
- 3.13 Shipboard ADCP
- 3.14 Geological and geophysical observation
 - 3.14.1 Sea beam
 - 3.14.2 Sea surface gravity
 - 3.14.3 Surface three component magnetometer

Appendix

- A1. Hydrocast List
- A2. Nutrient Data for Toyama Univ.
- A3. Nutrient Data for Hokkaido Univ.
- A4. Site Survey Maps for the Sediment Sampling
- A5. WHPO Publication 90-1 Revision 2 / Chapter-4: Hydrographic Data Formats

1. Preface

MR01-K03 cruise observation was carried out in the western North Pacific. Previous cruises of R/V Mirai organized by JAMSTEC biogeochemistry group were carried out to obtain a lot of information for biogeochemical cycle of carbon and its related materials, and to join the JGOFS time series observation in the western North Pacific. Results obtained at the JGOFS time series observation station (KNOT) suggested that it is important of observations in the section along longitude in the western North Pacific. We started the observation along 155° E from MR01-K03 R/V Mirai cruise to detect the long time environmental change in this area.

Tow Russian scientists joined to study the eddy in the western North Pacific relating the water and some material transport. This study is related with the purpose of this cruise deeply.

This cruise was carried out over 40 days. On behalf of cruise participants, I acknowledge captain Hashimoto and the crew for their hard works and effort on board during the long cruise. I also thank marine technicians from Marine Work Japan and Global Ocean Development for their kindly support.

MR01-K03 Cruise Chief Scientist
Shuichi Watanabe
Japan Marine Science and Technology Center

2. Outline of MR01-K03

2.1 Cruise summary

This cruise was conducted chiefly to study the global biogeochemical cycle and to make a database for detecting an environmental change in the western North Pacific. We collected water samples at 25 stations, sediments at 5 stations and recovered sediments traps at 3 stations for this cruise's purpose. XBT/XCTD observations were also carried out in several eddies. R/V Mirai left Sekinehama on June 4, 2001 and returned on July 19. Seven institutions (JAMSTEC, Kanazawa Univ., Hokkaido Univ., Tsukuba Univ., Toyama Univ., NIES in Japan and POI in Russia) participated in this cruise.

We conducted several observations and analysis in this cruise as follows.

1) Hydrocasting

Water samples at 13 stations from 26° N to 44° N along 155° E were collected with CWS (Carousel Water Sampler) attached CTD (SBE 9 plus) for the detection of the seasonal variation of materials related the climate change in the western North Pacific. We also collected water samples at 12 stations near the area deployed the sediment trap array and others. Salinity, dissolved oxygen gas, nutrients, carbonate species, some trace metal, DMS, CFCs, and others were determined.

2) Underway measurements

Temperature, salinity, nutrients, pCO₂ and TCO₂ in surface seawater were measured continuously along this cruise track. Surface current of seawater was also measured using ADCP attached with R/V Mirai.

3) XBT/XCTD observations

XBT/XCTD observations were carried out for the eddy study with the CTD-CWS observation. We obtained temperature and salinity profiles inside several eddies which located off Sanriku coast and along/near 160° E.

4) Sediments coring

Sediments for analyzing the history of the environments around and near the last glacial period were collected at 5 stations.

5) Time-series sediments trap experiments

Sediments traps were deployed in three stations to determine the seasonal particle flux in the high latitude area of the western North Pacific. In this cruise, we recovered two sediment trap arrays.

6) Others

The observations related with atmospheric science, geology and others were conducted in this cruise.

2.2 Cruise Log and Cruise track

Date	Start Time (U.T.C.)	Date	Start Time (S.M.T.)	Station	Position (start)		Events
					Lat.	Lon.	
6.4	04:54	6.4	13:54	-	41-21.9N	141-14.3E	Departure from Sekinehama
	22:31	6.5	07:31	-	41-22.0N	141-14.3E	Arrival at Hachinome
6.5	04:53		13:53	-	-	-	Departure from Hachinohe
6.6	04:48	6.6	13:48	TEST	40-10.0N	146-57.3E	Arrival at Station TEST
	05:11		14:11	TEST	40-09.8N	146-57.7E	Small CTD/Carousel Water Sampler (CWS) cast (500m)
	05:23		14:23	TEST	40-09.9N	146-58.0E	Profiling Reflectance Radiometer (PRR) measurement
	06:07		15:07	TEST	40-09.9N	146-58.1E	Large CTD/CWS cast (1,000m)
	07:21		16:21	TEST	40-09.7N	146-58.5E	Small CTD/CWS cast (300m)
	08:00		17:00	TEST	-	-	Departure from Stn. TEST
6.7	11:48	6.7	20:48	KNOT	44-00.0N	155-00.0E	Arrival at Station KNOT
	12:01		21:01	KNOT	44-00.0N	155-00.0E	Large CTD/CWS cast (5,298m)
	15:25	6.8	00:25	KNOT	44-00.1N	155-00.0E	Small CTD/CWS cast (5,000m)
	18:42		03:42	KNOT	43-59.9N	154-59.7E	Large CTD/CWS cast (900m)
	19:10		04:10	KNOT	44-00.0N	154-59.8E	Surface water sampling
	20:10		05:10	KNOT	44-00.0N	155-00.1E	Small CTD/CWS cast (300m)
6.8	03:26		12:26	KNOT	44-00.1N	155-00.2E	PRR measurement
	03:34		12:34	KNOT	44-00.1N	155-00.0E	Plankton net (500m)
	03:59		12:59	KNOT	44-00.1N	155-00.0E	Plankton net (150m)
	14:29		23:29	KNOT	43-59.9N	155-00.1E	Plankton net (500m)
	14:37		23:37	KNOT	44-00.0N	155-00.1E	Surface water sampling
	14:52		23:52	KNOT	44-00.0N	155-00.1E	Plankton net (150m)
	15:07	6.9	00:07	KNOT	43-59.9N	155-00.1E	Small CTD/CWS cast (200m)
	15:36		00:36	KNOT	-	-	Departure from Stn. KNOT
	19:00		04:00	-	44-42.6N	155-37.9E	Arrival at sediment trap recovery point
	22:58		07:58	-	44-42.6N	155-37.4E	Sediment trap (Hokkaido Univ.) recovery
6.9	01:18		10:18	-	-	-	Departure from sediment trap recovery point
	07:30		16:30	2	45-30.0N	157-30.0E	Arrival at Stn. 2
	07:30		16:30	2	45-29.9N	157-29.9E	PRR measurement
	07:38		16:38	2	45-29.8N	157-29.9E	Small CTD/CWS cast (300m)
	08:16		17:16	2	45-29.7N	157-29.8E	Large CTD/CWS cast (4,900m)
	10:44		19:44	2	45-30.3N	157-30.1E	Surface water sampling
	11:32		20:32	2	45-30.1N	157-30.2E	Plankton net (518m)
	11:57		20:57	2	45-30.1N	157-30.1E	Plankton net (150m)
	12:11		21:11	2	45-30.1N	157-30.0E	Small CTD/CWS cast (200m)
	12:36		21:36	-	-	-	Departure from Stn. 2
	22:00	6.10	07:00	3	47-00.0N	160-00.0E	Arrival at Stn. 3
	22:57		07:57	3	47-00.0N	159-59.9E	PRR measurement
	23:03		08:03	3	46-59.9N	159-59.9E	Plankton net (500m)
	23:27		08:27	3	46-59.8N	159-59.8E	Plankton net (150m)
	23:44		08:44	3	46-59.7N	159-59.8E	Small CTD/CWS cast (300m)
6.10	00:20		09:20	3	46-59.4N	159-59.8E	Large CTD/CWS cast (5,188m)
	02:46		11:46	3	47-00.1N	160-00.0E	Surface water sampling

Date	Start Time (U.T.C.)	Date	Start Time (S.M.T.)	Station	Positon (start)		Events
					Lat.	Lon.	
6.10	03:23	6.10	12:23	3	47-00.1N	159-59.8E	Surface water sampling
	03:51		12:51	3	47-00.1N	159-59.8E	Small CTD/CWS cast (200m)
	04:18		13:18	3	-	-	Departure from Stn. 3
	13:06		22:06	4	48-25.0N	162-30.0E	Arrival at Stn. 4
	13:22		22:22	4	48-25.1N	162-30.2E	Small CTD/CWS cast (300m)
	14:02		23:02	4	48-25.1N	162-30.2E	Large CTD/CWS cast (5,178m)
	16:39	6.11	01:39	4	48-25.0N	162-29.8E	Surface water sampling
	17:44		02:44	4	48-24.9N	162-29.9E	Plankton net (533m)
	18:07		03:07	4	48-24.8N	162-29.9E	Plankton net (150m)
	18:18		03:18	4	-	-	Departure from Stn. 4
6.11	03:24		12:24	5	50-00.0N	165-00.0E	Arrival at Stn. 5
	03:32		12:32	5	50-01.3N	165-00.7E	PRR measurement
	03:46		12:46	5	50-01.2N	165-00.3E	Sediment trap recovery
	07:20		16:20	5	49-59.8N	165-00.1E	Small CTD/CWS cast (5,000m)
	10:22		19:22	5	50-00.4N	165-00.4E	Large CTD/CWS cast (5,468m)
	13:38		22:38	5	49-59.4N	165-00.1E	Plankton net (500m)
	14:00		23:00	5	49-59.4N	165-00.2E	Plankton net (150m)
	14:16		23:16	5	49-59.4N	165-00.3E	Small CTD/CWS cast (200m)
	14:51		23:51	5	49-59.5N	165-00.4E	Large CTD/CWS cast (900m)
	15:00	6.12	00:00	5	49-59.8N	165-00.2E	Surface water sampling
	16:00		01:00	5	49-59.9N	165-00.1E	Small CTD/CWS cast (300m)
	16:48		01:48	5	-	-	Departure from Stn. 5
	20:46		05:46	XC01	49-00.0N	165-00.0E	XCTD observation
	22:45		07:45	XC02	48-30.0N	165-00.1E	XCTD observation
6.12	00:46		09:46	XC03	48-00.0N	165-00.1E	XCTD observation
	02:49		11:49	XC04	47-30.0N	165-00.0E	XCTD observation
	05:00		14:00	7	47-00.0N	165-00.0E	Arrival at Stn. 7
	22:57	6.13	07:57	7	46-59.9N	165-00.3E	PRR measurement
	23:10		08:10	7	46-59.9N	165-00.6E	Small CTD/CWS cast (300m)
	238:54		08:54	7	47-00.0N	165-00.9E	Large CTD/CWS cast (5874m)
6.13	02:39		11:39	7	46-59.4N	165-00.7E	Surface water sampling
	03:50		12:50	7	46-59.7N	165-01.0E	Plankton net (500m)
	04:11		13:11	7	46-59.8N	165-01.3E	Plankton net (150m)
	04:23		13:23	7	46-59.8N	165-01.5E	Small CTD/CWS cast (200m)
	04:57		13:57	7	46-59.8N	165-01.9E	ARGO float deployment
	04:57		13:57	XC05	46-59.8N	165-01.8E	XCTD observation
	05:00		14:00	7	-	-	Departure from Stn. 7
	07:09		16:09	XC06	46-30.0N	165-00.0E	XCTD observation
	09:17		18:17	XC07	46-00.0N	165-00.1E	XCTD observation
	11:25		20:25	XC08	45-30.0N	164-59.9E	XCTD observation
	13:03		22:03	8	-	-	Site survey at Stn. 8

Date	Start Time (U.T.C.)	Date	Start Time (S.M.T.)	Station	Positon (start)		Events
					Lat.	Lon.	
6.13	13:42	6.13	22:42	8	45-00.0N	165-00.0E	Arrival at Stn. 8
	23:00	6.14	08:00	8	44-59.9N	165-00.2E	PRR measurement
	23:12		08:12	8	45-00.0N	165-00.1E	Small CTD/CWS cast (300m)
	23:50		08:50	8	45-00.1N	165-00.1E	Large CTD/CWS cast (5,916m)
6.14	02:31		11:31	8	45-00.0N	165-00.0E	Surface water sampling
	03:49		12:49	8	44-59.9N	165-00.0E	Plankton net (500m)
	04:10		13:10	8	44-59.9N	165-00.1E	Plankton net (150m)
	04:28		13:28	8	44-59.8N	165-00.1E	Small CTD/CWS cast (200m)
	04:57		13:57	8	44-59.6N	165-00.5E	ARGO float deployment
	05:00		14:00	8	-	-	Departure from Stn. 8
	05:12		14:12	XC09	44-59.6N	165-04.4E	XCTD observation
	07:42		16:42	XC10	45-00.0N	166-00.3E	XCTD observation
	10:24		19:24	XC11	45-00.1N	167-00.0E	XCTD observation
	13:06		22:06	XC12	44-59.9N	168-00.0E	XCTD observation
	15:49	6.15	00:49	XC13	45-00.0N	169-00.0E	XCTD observation
	18:18		03:18	XC14	45-00.0N	169-55.3E	XCTD observation
	18:18		03:18	9	-	-	Site survey at Stn. 9
	18:18		03:18	9	45-00.0N	170-00.0E	Arrival at Stn. 9
6.15	00:47		09:47	9	45-02.7N	170-14.8E	Multiple core sampling (2,651m)
	04:09		13:09	9	45-02.5N	170-14.4E	Piston core sampling (2,649m)
	07:12		16:12	9	-	-	Site survey at Stn. 9
	23:07	6.16	08:07	9	44-57.5N	170-21.6E	Multiple core sampling (3,141m)
6.16	01:16		10:16	9	44-57.5N	170-21.6E	Piston core sampling (3,142m)
	04:30		13:30	9	-	-	Departure from Stn. 9
	21:00	6.17	06:00	8	45-00.0N	165-00.0E	Arrival at Stn. 8
	23:05		08:05	8	45-00.5N	164-57.1E	Multiple core sampling (6,028m)
6.17	02:18		11:18	8	-	-	Departure from Stn. 8
	04:16		13:16	XC15	44-30.0N	164-58.8E	XCTD observation
	06:15		15:15	XC16	44-00.1N	164-59.7E	XCTD observation
	08:14		17:14	XC17	43-30.1N	164-58.9E	XCTD observation
	10:12		19:12	XC18	43-00.0N	164-59.5E	XCTD observation
	12:14		21:14	-	42-30.0N	165-00.0E	ARGO float deployment
	12:15		21:15	XC19	42-29.8N	165-00.0E	XCTD observation
	14:17		23:17	XC20	42-00.0N	165-00.0E	XCTD observation
	16:19	6.18	01:19	XC21	41-30.0N	165-00.5E	XCTD observation
	18:22		03:22	XC22	41-00.0N	165-00.8E	XCTD observation
	20:23		05:23	XC23	40-30.0N	165-01.0E	XCTD observation
	22:30		07:30	11	40-00.0N	165-00.0E	Arrival at Stn. 11
	22:33		07:33	XC24	40-00.0N	165-00.8E	XCTD observation
6.18	00:28		09:28	11	40-00.0N	165-00.0E	PRR measurement
	00:36		09:36	11	39-59.9N	165-00.0E	Large CTD/CWS cast (900m)

Date	Start Time (U.T.C.)	Date	Start Time (S.M.T.)	Station	Positon (start)		Events
					Lat.	Lon.	
6.18	01:11	6.18	10:11	11	40-00.0N	165-00.0E	Surface water sampling
	01:29		10:29	11	40-00.1N	165-00.0E	Surface water sampling
	02:03		11:03	11	40-00.1N	165-00.0E	Plankton net (500m)
	02:25		11:25	11	40-00.0N	165-00.3E	Plankton net (150m)
	02:41		11:41	11	39-59.8N	165-00.6E	Small CTD/CWS cast (300m)
	03:57		12:57	11	40-00.0N	165-00.0E	Large CTD/CWS cast (5,411m)
	13:57		22:57	11	40-00.0N	165-00.0E	Small CTD/CWS cast (200m)
	23:04		08:04	11	40-00.2N	165-01.0E	Sediment trap recovery
6.19	02:22	6.19	11:22	11	-	-	Departure from Stn. 11
	03:27		12:27	XC25	39-48.2N	164-47.7E	XCTD observation
	04:36		13:36	XC26	39-57.7N	164-30.0E	XCTD observation
	05:42		14:42	XC27	40-06.7N	164-12.5E	XCTD observation
	06:48		15:48	XC28	40-15.8N	163-55.4E	XCTD observation
	07:54		16:54	XC29	40-24.7N	163-38.0E	XCTD observation
	09:02		18:02	XC30	40-33.6N	163-20.4E	XCTD observation
	10:35		19:35	XC31	40-45.7E	163-57.0E	XCTD observation
	12:24		21:24	12	41-00.0N	162-30.0E	Arrival at Stn. 12
	12:26		21:26	12	40-59.9N	162-30.1E	Plankton net (500m)
	12:49		21:49	12	40-59.8N	162-30.3E	Plankton net (150m)
	13:07		22:07	12	41-00.1N	162-30.5E	Small CTD/CWS cast (300m)
	13:49		22:49	12	41-00.2N	162-30.5E	Large CTD/CWS cast (5,508m)
17:18	02:18	12	-	-	D 12		
6.20	01:42	6.20	10:42	13	42-00.0N	160-00.0E	Arrival at Stn. 13
	01:45		10:45	13	41-59.9N	160-00.2E	PRR measurement
	01:51		10:51	13	42-00.0N	160-00.3E	Small CTD/CWS cast (300m)
	02:33		11:33	13	42-00.2N	160-00.1E	Large CTD/CWS cast (5,588m)
	05:15		14:15	13	41-59.9N	160-00.1E	Surface water sampling
	05:55		14:55	13	42-00.0N	160-00.1E	Plankton net (500m)
	06:18		15:18	13	42-00.0N	160-00.3E	Plankton net (150m)
	06:30		15:30	13	42-00.0N	160-00.4E	Small CTD/CWS cast (200m)
	07:00		16:00	13	-	-	Departure from Stn. 13
22:00	07:00	10	42-30.0N	165-00.0E	Arrival at Stn. 10		
23:01	08:01	10	42-30.0N	164-59.9E	PRR measurement		
23:13	08:13	10	42-29.9N	164-59.7E	Small CTD/CWS cast (1300m)		
6.21	00:23	6.21	09:23	10	42-29.3N	164-57.8E	Plankton net (500m)
	00:44		09:44	10	42-29.1N	164-58.6E	Plankton net (150m)
	00:57		09:57	10	42-28.9N	164-58.4E	Small CTD/CWS cast (200m)
	04:05		13:05	10	42-29.9N	165-00.1E	Large CTD/CWS cast (5,018m)
	06:42		15:42	10	42-30.6N	164-59.2E	Surface water sampling
	07:54		16:54	10	-	-	Departure from Stn. 10
	18:00		06:00	8	45-00.0N	165-00.0E	Arrival at Stn. 8
23:11	08:11	8	45-00.5N	164-57.3E	PC (6,026m)		
6.22	04:00		13:00	8	-	-	Departure from Stn. 8

Date	Start Time (U.T.C.)	Date	Start Time (S.M.T.)	Station	Positon (start)		Events
					Lat.	Lon.	
6.23	03:30	6.23	12:30	14	43-00.0N	157-30.0E	Arrival at Stn. 14
	03:53		12:53	14	43-00.0N	157-30.0E	PRR measurement
	04:00		13:00	14	43-00.0N	157-30.0E	Small CTD/CWS cast (300m)
	04:35		13:35	14	43-00.0N	157-30.0E	Large CTD/CWS cast (5,510m)
	07:13		16:13	14	43-00.0N	157-29.8E	Surface water sampling
	07:58		16:58	14	43-00.0N	157-29.7E	Plankton net (500m)
	08:20		17:20	14	42-59.9N	157-29.8E	Plankton net (150m)
	08:32		17:32	14	42-59.9N	157-29.9E	Small CTD/CWS cast (200m)
	09:00		18:00	14	-	-	Departure from Stn. 14
	17:00	6.24	02:00	KNOT	44-00.0N	155-00.0E	Arrival at Station KNOT
	22:58		07:58	KNOT	43-57.9N	155-02.9E	PRR measurement
6.24	03:55		12:55	KNOT	44-00.1N	155-00.2E	Large CTD/CWS cast (5,260m)
	07:06		16:06	KNOT	44-00.0N	154-59.9E	Plankton net (500m)
	07:29		16:29	KNOT	44-00.0N	155-00.0E	Plankton net (150m)
	07:42		16:42	KNOT	44-00.0N	155-00.1E	Small CTD/CWS cast (300m)
	08:27		17:27	KNOT	44-00.0N	155-00.1E	Large CTD/CWS cast (900m)
	08:40		17:40	KNOT	44-00.0N	155-00.1E	Surface water sampling
	09:30		18:30	KNOT	44-00.0N	155-00.1E	Surface water sampling
	13:56		22:56	KNOT	44-00.0N	155-00.0E	Small CTD/CWS cast (200m)
	14:24		23:24	KNOT	-	-	Departure from Stn. KNOT
	22:00	6.25	07:00	15	42-30.0N	155-00.0E	Arrival at Stn. 15
	22:58		07:58	15	42-30.0N	155-00.0E	Large CTD/CWS cast (5,132m)
6.25	01:25		10:25	15	42-30.0N	155-00.0E	Surface water sampling
	02:06		11:06	15	-	-	Departure from Stn. 15
	08:00		17:00	16	41-00.0N	155-00.0E	Arrival at Stn. 16
	08:58		17:58	16	41-00.3N	155-00.2E	Large CTD/CWS cast (5,475m)
	12:17		21:17	16	40-59.9N	154-59.6E	Small CTD/CWS cast (300m)
	13:15		22:15	16	41-00.2N	155-00.1E	Large CTD/CWS cast (900m)
	13:45		22:45	16	41-00.0N	154-59.9E	Surface water sampling
	14:24		23:24	16	-	-	Departure from Stn. 16
	15:34	6.26	00:34	XC33	41-10.0N	154-39.9E	XCTD observation
	16:49		01:49	XC34	41-20.1N	154-19.9E	XCTD observation
	17:54		02:54	E001	41-20.0N	154-00.0E	Arrival at Stn. E001
	22:59		07:59	E001	41-20.1N	154-00.1E	Small CTD/CWS cast (1,500m)
6.26	00:06		09:06	E001	-	-	Departure from Stn. E001
	01:09		10:09	XC35	41-20.0N	153-39.8E	XCTD observation
	01:53		10:53	XB01	41-20.1N	153-24.9E	XBT observation
	02:37		11:37	XB02	41-20.0N	153-09.7E	XBT observation
	03:06		12:06	XB03	41-20.0N	152-59.9E	XBT observation
	03:54		12:54	E002	41-20.0N	152-45.0E	Arrival at Stn. E002
	03:57		12:57	E002	41-20.0N	152-44.9E	Small CTD/CWS cast (1,500m)
	05:06		14:06	E002	-	-	Departure from Stn. E002

Date	Start Time (U.T.C.)	Date	Start Time (S.M.T.)	Station	Positon (start)		Events
					Lat.	Lon.	
6.26	05:59	6.26	14:59	XB04	41-20.2N	152-29.8E	XBT observation
	06:44		15:44	XB05	41-20.0N	152-14.7E	XBT observation
	07:48		16:48	E003	41-20.0N	151-55.0E	Arrival at Stn. E003
	08:57		17:57	E003	41-19.9N	151-55.0E	Small CTD/CWS cast (5,188m)
	12:06		21:06	E003	-	-	Departure from Stn. E003
	13:18		22:18	XC36	41-20.1N	151-29.8E	XCTD observation
	16:56	6.27	01:56	XC37	42-00.2N	152-20.2E	XCTD observation
	20:06		05:06	E004	42-40.0N	153-00.0E	Arrival at Stn. E004
	22:58		07:58	E004	42-40.0N	153-00.0E	Small CTD/CWS cast (5,169m)
6.27	02:18		11:18	E004	-	-	Departure from Stn. E004
	03:48		12:48	E005	42-20.0N	153-00.0E	Arrival at Stn. E005
	04:01		13:01	E005	42-00.0N	153-00.3E	Small CTD/CWS cast (1,500m)
	05:24		14:24	E005	-	-	Departure from Stn. E005
	06:54		15:54	E006	42-00.0N	153-00.0E	Arrival at Stn. E006
	06:55		15:55	E006	42-00.1N	152-59.9E	Small CTD/CWS cast (4,916m)
	10:12		19:12	E006	-	-	Departure from Stn. E006
	11:36		20:36	E007	41-40.0N	153-00.0E	Arrival at Stn. E007
	11:41		20:41	E007	41-40.0N	153-00.0E	Small CTD/CWS cast (1,500m)
	12:54		21:54	E007	-	-	Departure from Stn. E007
	13:35		22:35	XB06	41-30.0N	153-00.0E	XBT observation
	14:34		23:34	XB07	41-15.0N	153-00.0E	XBT observation
	15:18	6.28	00:18	XB08	41-04.9N	152-59.9E	XBT observation
	16:08		01:08	XB09	41-05.0N	152-45.0E	XBT observation
	17:00		02:00	E008	41-12.0N	152-52.0E	Arrival at Stn. E008
	22:59		07:59	E008	41-12.0N	152-51.9E	Small CTD/CWS cast (5,000m)
6.28	02:00		11:00	E008	-	-	Departure from Stn. E008
	03:00		12:00	E009	41-00.0N	153-00.0E	Arrival at Stn. E009
	03:25		12:25	E009	41-00.2N	152-59.8E	Small CTD/CWS cast (1,500m)
	04:36		13:36	E009	-	-	Departure from Stn. E009
	05:28		14:28	XC38	40-48.4N	153-00.0E	XCTD observation
	06:06		15:06	E010	40-40.0N	153-00.0E	Arrival at Stn. E010
	06:07		15:07	E010	40-40.1N	153-00.0E	Small CTD/CWS cast (1,500m)
	07:18		16:18	E010	-	-	Departure from Stn. E010
	08:05		17:05	XB10	40-29.7N	153-00.1E	XBT observation
	08:48		17:48	E011	40-20.0N	153-00.0E	Arrival at Stn. E011

Date	Start Time (U.T.C.)	Date	Start Time (S.M.T.)	Station	Positon (start)		Events
					Lat.	Lon.	
6.28	08:48	6.28	17:48	E011	40-20.1N	152-59.8E	Small CTD/CWS cast (5,000m)
	11:48		20:48	E011	-	-	Departure from Stn. E011
	13:08		22:08	XC39	39-59.8N	153-00.0E	XCTD observation
	14:08		23:08	XC40	39-50.0N	153-00.0E	XCTD observation
	15:12		00:12	E012	39-30.0N	153-30.0E	Arrival at Stn. E012
6.29	22:56	6.29	07:56	E012	39-29.9N	152-29.9E	Small CTD/CWS cast (5,000m)
	02:00		11:00	E012	-	-	Departure from Stn. E012
	03:26		12:26	XC41	39-29.9N	153-30.0E	XCTD observation
	04:54		13:54	XC42	39-30.1N	153-56.9E	XCTD observation
	06:41		15:41	XC43	39-30.1N	154-30.1E	XCTD observation
	08:51		17:51	17	39-30.0N	155-00.0E	Arrival at Stn. 17
	08:51		17:51	17	39-30.1N	155-00.0E	Large CTD/CWS cast (5,598m)
	11:38		20:38	17	39-29.9N	155-00.0E	Surface water sampling
	12:18		21:18	17	-	-	Departure from Stn. 17
	16:14		01:14	XC44	38-30.0N	155-00.0E	XCTD observation
	6.30		18:18	6.30	03:18	18	38-00.0N
21:02		06:02	18		38-00.0N	155-00.1E	Large CTD/CWS cast (5,960m)
00:50		09:50	18		37-59.9N	155-00.0E	Small CTD/CWS cast (300m)
01:49		10:49	18		38-00.0N	155-00.1E	Large CTD/CWS cast (900m)
02:25		11:25	18		37-59.9N	155-00.1E	Surface water sampling
02:54		11:54	18		-	-	Departure from Stn. 18
04:12		13:12	XC45		37-42.9N	154-50.0E	XCTD observation
05:34		14:34	XC46		37-24.9N	154-39.5E	XCTD observation
06:48		15:48	XC47		37-09.0N	154-30.0E	XCTD observation
08:20		17:20	XC48		36-49.1N	154-45.1E	XCTD observation
7.1	09:48	7.1	18:48	19	36-30.0N	155-00.0E	Arrival at Stn. 19
	09:50		18:50	19	36-29.9N	154-59.7E	Large CTD/CWS cast (5,683m)
	12:36		21:36	19	36-29.9N	154-59.6E	Surface water sampling
	13:18		22:18	19	-	-	Departure from Stn. 19
	14:38		23:38	XC49	36-09.9N	155-00.0E	XCTD observation
	16:38		01:38	XC50	35-40.8N	155-00.0E	XCTD observation
	19:42		04:42	20	35-00.0N	155-00.0E	Arrival at Stn. 20
	20:56		05:56	20	35-00.0N	155-00.0E	Large CTD/CWS cast (5,603m)
7.1	00:28	7.1	09:28	20	35-00.0N	155-00.0E	Small CTD/CWS cast (300m)
	01:34		10:34	20	35-00.0N	154-59.9E	Large CTD/CWS cast (900m)
	02:01		11:01	20	35-00.0N	155-00.0E	Surface water sampling
	02:42		11:42	20	-	-	Departure from Stn. 20
	06:54		15:54	25	27-30.0N	155-00.0E	Arrival at Stn. 25

Date	Start Time (U.T.C.)	Date	Start Time (S.M.T.)	Station	Positon (start)		Events
					Lat.	Lon.	
7.2	08:16	7.2	17:16	25	27-30.0N	155-00.1E	Large CTD/CWS cast (5,994m)
	11:08		20:08	25	27-29.7N	154-59.9E	Surface water sampling
	11:48		20:48	25	-	-	Departure from Stn. 25
	17:18	7.3	02:18	26	26-00.0N	155-00.0E	Arrival at Stn. 26
	21:56		06:56	26	26-00.0N	155-00.0E	Large CTD/CWS cast (5,587m)
7.3	00:21		09:21	26	26-00.0N	155-00.0E	Surface water sampling
	01:16		10:16	26	26-00.0N	155-00.0E	PRR measurement
	01:22		10:22	26	26-00.0N	155-00.0E	Small CTD/CWS cast (300m)
	02:31		11:31	26	26-00.0N	155-00.0E	Large CTD/CWS cast (900m)
	03:13		12:13	26	26-00.0N	155-00.0E	Surface water sampling
	03:45		12:45	26	25-59.9N	155-00.0E	Small CTD/CWS cast (200m)
	04:12		13:12	26	-	-	Departure from Stn. 26
	16:18	7.4	01:18	24	29-00.0N	155-00.0E	Arrival at Stn. 24
	19:54		04:54	24	28-59.9N	154-59.9E	Large CTD/CWS cast (5,881m)
	23:27		08:27	24	29-00.1N	155-00.0E	Small CTD/CWS cast (300m)
7.4	00:28		09:28	24	29-00.0N	155-00.0E	Large CTD/CWS cast (900m)
	00:57		09:57	24	29-00.0N	154-59.9E	Surface water sampling
	01:36		10:36	24	-	-	Departure from Stn. 24
	07:12		16:12	23	30-30.0N	155-00.0E	Arrival at Stn. 23
	07:17		16:17	23	30-30.0N	154-59.9E	Large CTD/CWS cast (5,710m)
	10:00		19:00	23	30-30.0N	155-00.1E	Surface water sampling
	10:42		19:42	23	-	-	Departure from Stn. 23
	16:30	7.5	01:30	22	32-00.0N	155-00.0E	Arrival at Stn. 22
	19:56		04:56	22	32-00.0N	155-00.1E	Large CTD/CWS cast (4,420m)
	22:42		07:42	22	32-00.1N	155-00.0E	Small CTD/CWS cast (300m)
	23:32		08:32	22	32-00.0N	155-00.1E	Large CTD/CWS cast (900m)
7.5	00:04		09:04	22	32-00.0N	155-00.1E	Surface water sampling
	00:36		09:36	22	-	-	Departure from Stn. 22
	06:30		15:30	21	33-30.0N	155-00.0E	Arrival at Stn. 21
	06:31		15:31	21	33-30.1N	155-00.2E	Large CTD/CWS cast (5,761m)
	09:18		18:18	21	33-30.0N	154-59.8E	Surface water sampling
	09:54		18:54	21	-	-	Departure from Stn. 21
7.6	03:54	7.6	12:54	27	35-00.0N	150-00.0E	Arrival at Stn. 27
	03:58		12:58	27	35-00.0N	150-00.0E	Large CTD/CWS cast (6,050m)
	06:45		15:45	27	35-00.0N	150-00.1E	Surface water sampling
	07:42		16:42	27	-	-	Departure from Stn. 27
7.7	00:42	7.7	09:42	28	35-00.0N	145-00.0E	Arrival at Stn. 28
	00:42		09:42	28	35-00.1N	144-59.9E	Large CTD/CWS cast (5,745m)
	03:40		12:40	28	35-00.2N	144-59.9E	Surface water sampling
	04:24		13:24	28	-	-	Departure from Stn. 28
	14:28		23:28	XC51	37-30.1N	145-13.3E	XCTD observation

Date	Start Time (U.T.C.)	Date	Start Time (S.M.T.)	Station	Positon (start)		Events
					Lat.	Lon.	
7.7	16:12	7.8	01:12	XC52	37-54.6N	145-15.0E	XCTD observation
	17:14		02:14	XC53	38-08.6N	145-16.2E	XCTD observation
7.8	00:33		09:33	29	-	-	Site survey at Stn. 29
	10:30		19:30	30	41-07.0N	142-33.0E	Arrival at Stn. 30
	10:30		19:30	30	-	-	Site survey at Stn. 30
	23:52	7.9	08:52	30	41-07.1N	142-24.1E	Multiple core sampling (1,360m)
7.9	04:09		13:09	30	41-07.1N	142-24.1E	Piston core sampling (1,360m)
	22:09	7.10	07:09	30	41-07.1N	142-24.2E	Piston core sampling (1,360m)
7.10	00:12		09:12	30	-	-	Departure from Stn. 30
	03:44		12:44	XC54	41-24.0N	143-25.5E	XCTD observation
	07:42		16:42	31	42-16.0N	144-07.0E	Arrival at Stn. 31
	07:45		16:45	31	-	-	Site survey at Stn. 31
7.11	02:40	7.11	11:40	31	42-21.5N	144-13.4E	Piston core sampling (1,069m)
	04:24		13:24	31	-	-	Departure from Stn. 31
	08:47		17:47	XC55	41-25.0N	144-37.5E	XCTD observation
	14:36		23:36	29	39-58.0N	145-26.0E	Arrival at Stn. 29
	14:36		23:36	29	-	-	Site survey at Stn. 29
	22:59	7.12	07:59	29	39-57.6N	145-29.7E	Multiple core sampling (5,265m)
7.12	02:30		11:30	29	39-57.6N	145-29.8E	Piston core sampling (5,266m)
	06:06		15:06	29	-	-	Departure from Stn. 29
	06:50		15:50	XC56	39-50.0N	145-35.0E	XCTD observation
	07:48		16:48	XB11	39-57.1N	145-23.8E	XBT observation
	08:30		17:30	XB12	40-04.1N	145-12.9E	XBT observation
	09:11		18:11	XB13	40-11.1N	145-02.2E	XBT observation
	09:53		18:53	XB14	40-18.1N	144-51.2E	XBT observation
	10:36		19:36	XB15	40-25.1N	144-40.2E	XBT observation
	11:18		20:18	XB16	40-32.1N	144-29.2E	XBT observation
	12:01		21:01	XB17	40-39.0N	144-18.1E	XBT observation
	12:45		21:45	XB18	40-46.0N	144-07.2E	XBT observation
	13:34		22:34	XC56	40-53.5N	143-55.2E	XCTD observation
	15:58	7.13	00:58	XB19	40-20.3N	143-57.0E	XBT observation
	18:01		03:01	XB20	39-50.3N	143-58.3E	XBT observation
	22:00		07:00	R01	39-00.0N	144-00.0E	Arrival at Stn. R01
	23:34		08:34	R01	39-00.1N	143-59.9E	Small CTD/CWS cast (1,500m)
7.13	01:00		10:00	R01	-	-	Departure from Stn. R01
	01:46		10:46	XC57	38-49.0N	143-55.1E	XCTD observation

Date	Start Time (U.T.C.)	Date	Start Time (S.M.T.)	Station	Positon (start)		Events
					Lat.	Lon.	
7.13	02:42	7.13	11:42	R02	38-38.0N	143-49.0E	Arrival at Stn. R02
	03:43		12:43	R02	38-38.1N	143-48.7E	Small CTD/CWS cast (5,447m)
	07:00		16:00	R02	-	-	Departure from Stn. R02
	07:47		16:47	XC59	38-27.1N	143-43.0E	XCTD observation
	08:36		17:36	R03	38-16.0N	143-37.0E	Arrival at Stn. R03
	08:40		17:40	R03	38-16.1N	143-37.0E	Small CTD/CWS cast (3,580m)
	11:00		20:00	R03	-	-	Departure from Stn. R03
	11:59		20:59	XC60	38-03.0N	143-29.9E	XCTD observation
	13:31		22:31	XB21	38-10.0N	143-53.2E	XBT observation
	14:44		23:44	XB22	38-16.0N	144-15.2E	XBT observation
	16:13	7.14	01:13	XB23	38-23.1N	144-37.5E	XBT observation
	16:58		01:58	XB24	38-25.9N	144-25.4E	XBT observation
	17:40		02:40	XC61	38-30.1N	144-13.2E	XCTD observation
	18:25		03:25	XB25	38-34.1N	144-01.1E	XBT observation
	19:51		04:51	XB26	38-42.1N	143-37.0E	XBT observation
	20:32		05:32	XB27	38-46.0N	143-25.0E	XBT observation
	21:14		06:14	XB28	38-49.9N	143-12.8E	XBT observation
	21:57		06:57	XC62	38-54.3N	143-00.3E	XCTD observation
	23:23		08:23	XB29	39-00.1N	143-22.4E	XBT observation
7.14	00:28		09:28	XB30	39-06.1N	143-43.4E	XBT observation
	01:46		10:46	XC63	39-13.0N	144-08.2E	XCTD observation
	03:00		12:00	R04	39-29.0N	144-17.0E	Arrival at Stn. R04
	03:00		12:00	R04	39-29.0N	144-17.2E	Small CTD/CWS cast (6,000m)
	04:45		13:45	R04	39-29.5N	144-17.2E	Surface water sampling
	06:18		15:18	R04	-	-	Departure from Stn. R04
	07:28		16:28	XC64	39-46.0N	144-25.1E	XCTD observation
	08:30		17:30	R05	40-00.0N	144-32.0E	Arrival at Stn. R05
	08:32		17:32	R05	40-00.0N	144-32.1E	Small CTD/CWS cast (1,500m)
	09:42		18:42	R05	-	-	Departure from Stn. R05
	10:07		19:07	XB31	40-05.5N	144-35.1E	XBT observation
	10:32		19:32	XC65	40-11.0N	144-38.1E	XCTD observation
	10:58		19:58	XB32	40-16.6N	144-40.9E	XBT observation
	11:24		20:24	R06	40-22.0N	144-44.0E	Arrival at Stn. R06
	11:27		20:27	R06	40-22.0N	144-44.0E	Small CTD/CWS cast (6,000m)
	14:48		23:48	R06	-	-	Departure from Stn. R06
	15:20	7.15	00:20	XB33	40-27.5N	144-46.8E	XBT observation
	15:44		00:44	XC66	40-33.25N	144-49.6E	XCTD observation
	16:08		01:08	XB34	40-38.3N	144-52.2E	XBT observation
	16:36		01:36	R07	40-44.0N	144-55.0E	Arrival at Stn. R07

Date	Start Time (U.T.C.)	Date	Start Time (S.M.T.)	Station	Positon (start)		Events
					Lat.	Lon.	
7.14	21:56	7.15	06:56	R07	40-44.0N	144-55.1E	Small CTD/CWS cast (6,000m)
7.15	01:12		10:12	R07	-	-	Departure from Stn. R07
	02:01		11:01	XC67	40-54.6N	145-01.2E	XCTD observation
	02:48		11:48	R08	41-05.0N	145-07.0E	Arrival at Stn. R08
	02:48		11:48	R08	41-05.0N	145-07.1E	Small CTD/CWS cast (1,500m)
	04:06		13:06	R08	-	-	Departure from Stn. R08
	05:02		14:02	XC68	41-18.1N	145-14.3E	XCTD observation
	06:00		15:00	R09	41-32.0N	145-22.0E	Arrival at Stn. R09
	06:05		15:05	R09	41-31.9N	145-22.0E	Small CTD/CWS cast (5,950m)
	09:36		18:36	R09	-	-	Departure from Stn. R09
	14:39		23:39	XB35	40-22.4N	146-03.7E	XBT observation
	15:27	7.16	00:27	XB36	40-22.1N	145-51.9E	XBT observation
	16:18		01:18	R10	40-22.0N	145-44.0E	Arrival at Stn. R10
	21:59		06:59	R10	40-22.0N	145-44.0E	Small CTD/CWS cast (1,500m)
	23:06		08:06	R10	-	-	Departure from Stn. R10
	23:56		08:56	XC69	40-22.0N	145-25.1E	XCTD observation
7.16	00:43		09:43	XC70	40-22.0N	145-10.0E	XCTD observation
	02:54		11:54	R11	40-22.0N	144-28.0E	Arrival at Stn. R11
	02:55		11:55	R11	40-22.1N	144-28.0E	Small CTD/CWS cast (6,000m)
	06:24		15:24	R11	-	-	Departure from Stn. R11
	07:13		16:13	XB37	40-22.0N	144-14.1E	XBT observation
	08:57		17:57	XB38	40-22.2N	143-41.8E	XBT observation
	09:52		18:52	XC71	40-22.0N	143-24.9E	XCTD observation
	12:51		21:51	XB39	41-03.3N	143-46.2E	XBT observation
	13:44		22:44	XB40	41-13.9N	143-36.1E	XBT observation
7.18	22:44	7.19	07:44	-	41-21.9N	141-14.3E	Arrival at Sekinehama

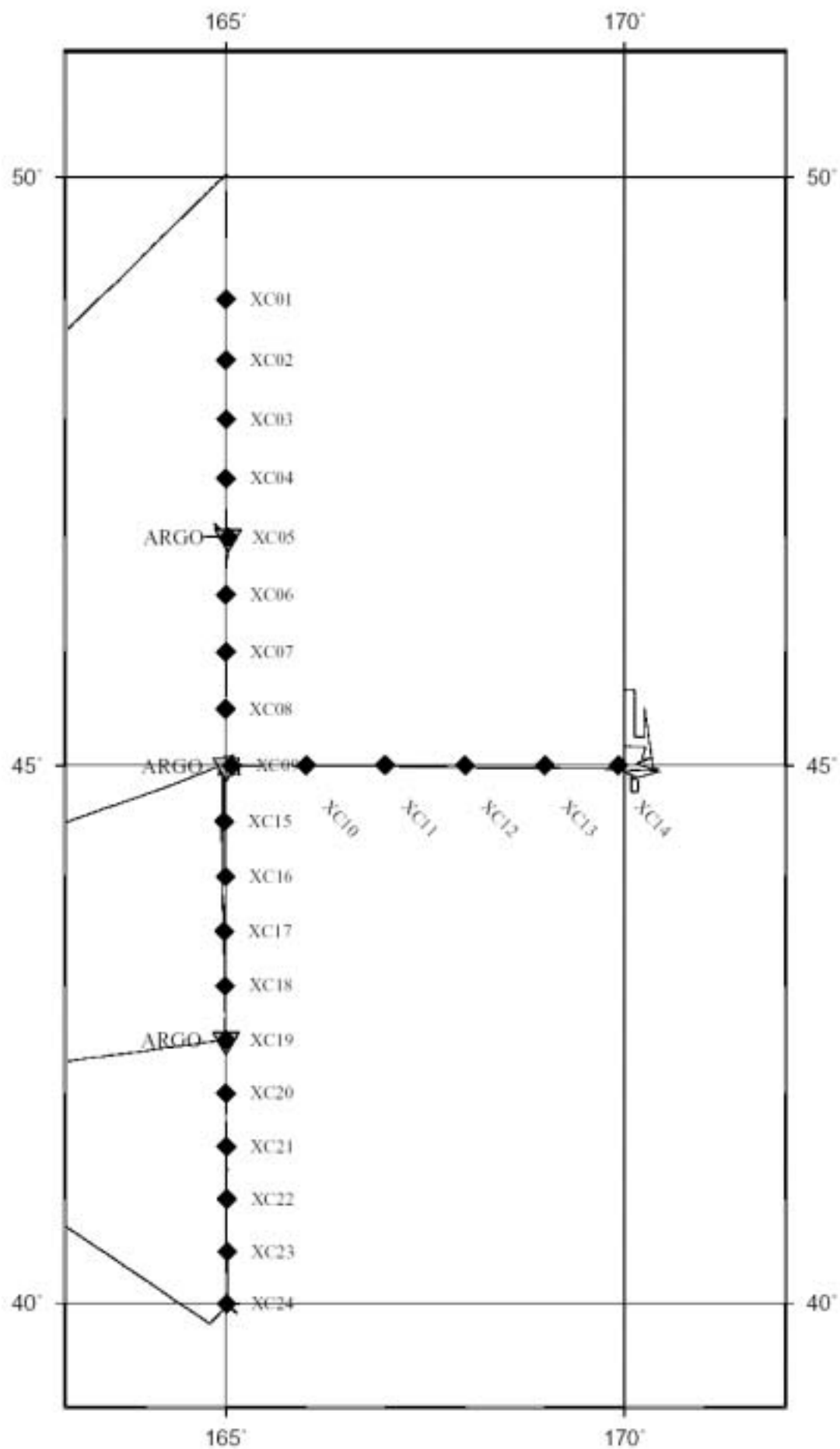


fig 2.2-1 ARGO float & XCTD

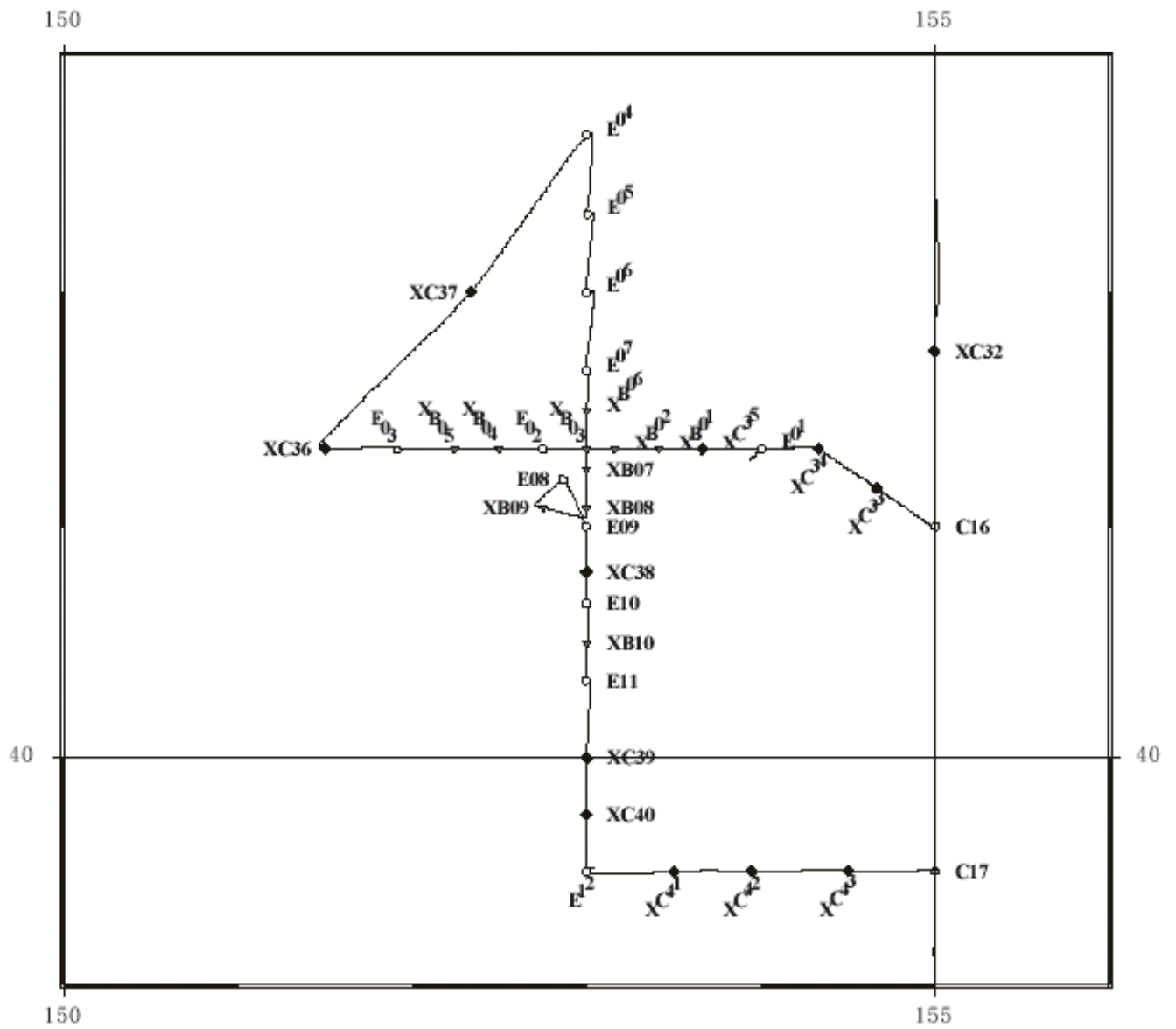


fig2.2-2 Eddy Study Area No.1

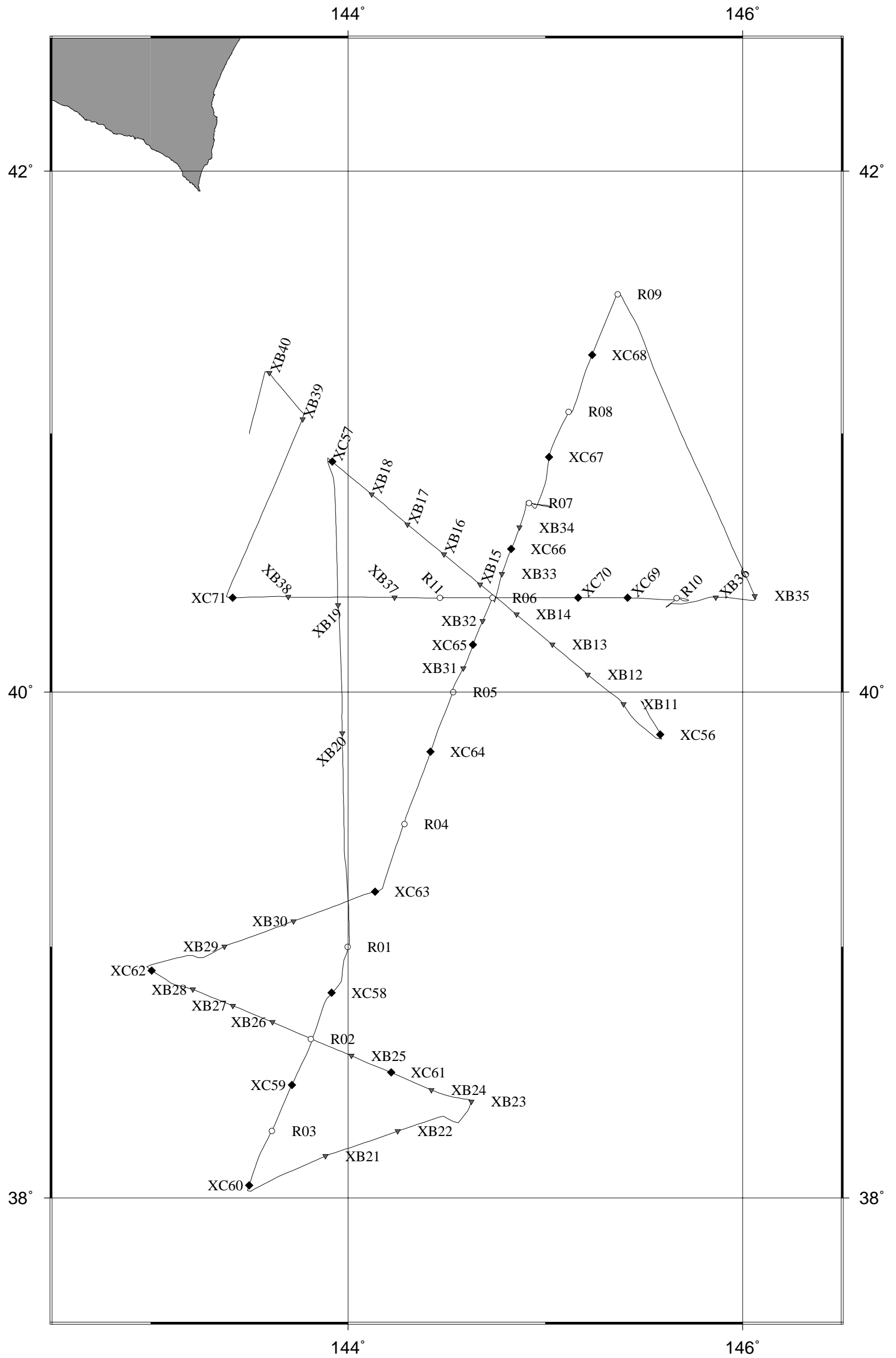


fig2.2-3 Eddy Study Area No.2

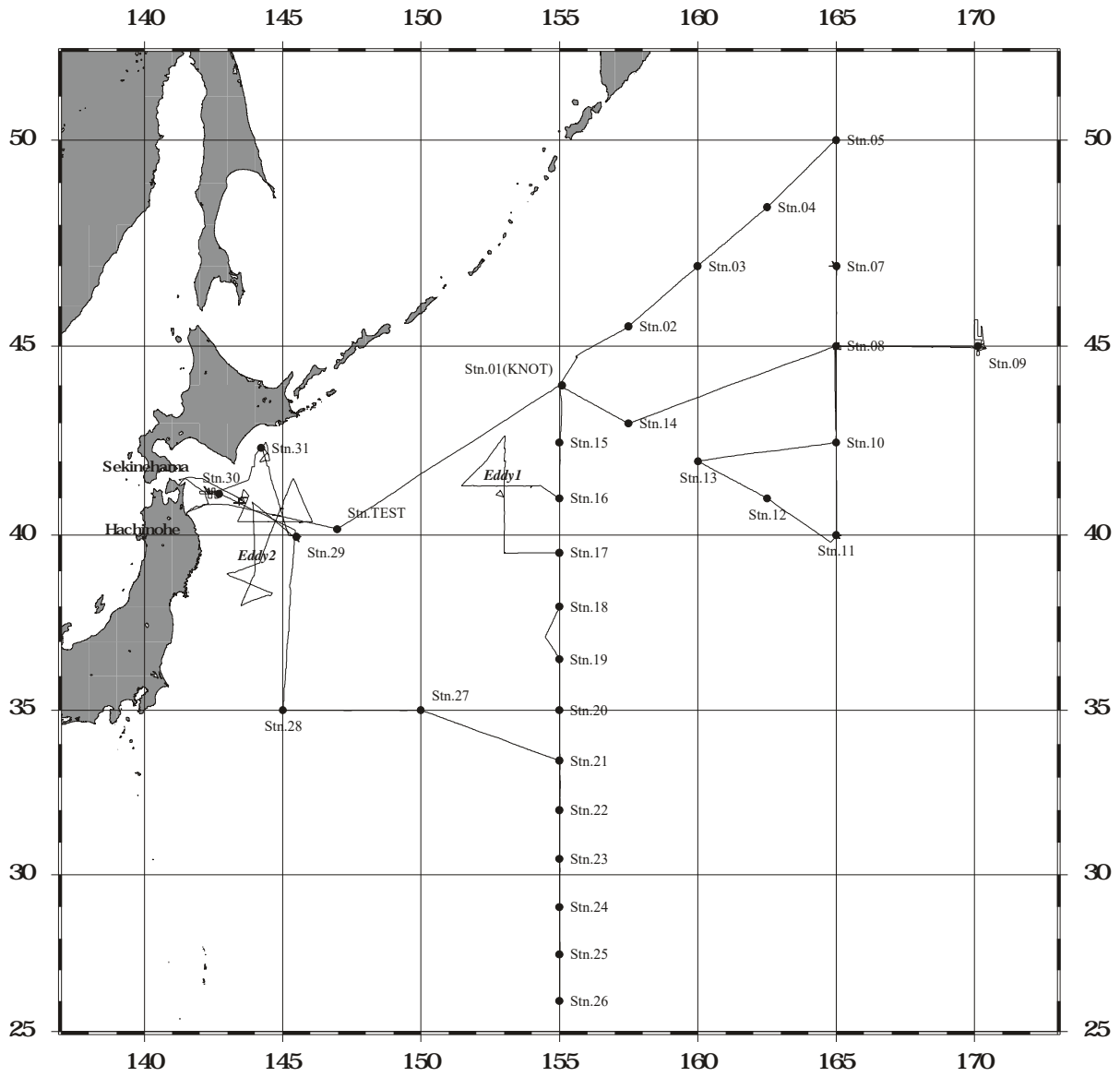


fig2.2-4 Curise Track MR01-K03

2.3 List of participants

Name	Affiliation	Address	Tel Fax E-mail
Shuichi WATANABE	Japan Marine Science & Technology Center (JAMSTEC)	2-15 Natsushima-cho Yokosuka 237-0061, Japan	
Yuichiro KUMAMOTO	JAMSTEC	2-15 Natsushima-cho Yokosuka 237-0061, Japan	
Naokazu AHAGON	JAMSTEC	690 Kitasekine, Sekine Mutsu 035-0022, Japan	
Andrey ANDREEV	JAMSTEC	2-15 Natsushima-cho Yokosuka 237-0061, Japan	
Masao UCHIDA	JAMSTEC	2-15 Natsushima-cho Yokosuka 237-0061, Japan	
Toshiaki MISHIMA	JAMSTEC	2-15 Natsushima-cho Yokosuka 237-0061, Japan	
Vyacheslav LOBANOV	Pacific Oceanological Insitute (POI)	Baltiysuaya 43 Vladivostok 690041, Russia	+7-4232-31-1400 +7-4232-31-2573
Igor JABINE	POI	Baltiysuaya 43 Vladivostek 690041, Russia	+7-4232-31-1400 +7-4232-31-2573
Kenichi OKUSHI	Tsukuba University	1-1-1 Tennodai Tsukuba 305-0006, Japan	
Hisashi NARITA	Hokkaido University	N10, W5 Kita-ku Sapporo 060-0810, Japan	
Nobue KASAMATSU	Hokkaido University	N10, W5 Kita-ku Sapporo 060-0810, Japan	
Shinichi TANAKA	Hokkaido University	N10, W5 Kita-ku Sapporo 060-0810, Japan	
Naoyuki SATO	Kanazawa University	2-40-20 Kodatsuno Kanazawa 920-8667, Japan	
Jiahong WU	Toyama University	3190 Gofuku Toyama 930-8555, Japan	
Fujio SHIMANO	Japan Science and Technology Copration (JST)	16-2 Onogawa Tsukuba 305-0053, Japan	
Takeshi EGASHIRA	JST	16-2 Onogawa Tsukuba 305-0053, Japan	

Name	Affiliation	Address	Tel Fax E-mail
Hirokatsu UNO	Marine Works Japan Ltd. (MWJ)	Live Pier Kanazawahakkei 2F 1-1-7 Mitsuura Kanagawa-ku Yokohama 236-0031, Japan	
Fujio KOBAYASHI	MWJ	Live Pier Kanazawahakkei 2F 1-1-7 Mitsuura Kanagawa-ku Yokohama 236-0031, Japan	
Miki YOSHIKE	MWJ	Live Pier Kanazawahakkei 2F 1-1-7 Mitsuura Kanagawa-ku Yokohama 236-0031, Japan	
Kenichi KATAYAMA	MWJ	Live Pier Kanazawahakkei 2F 1-1-7 Mitsuura Kanagawa-ku Yokohama 236-0031, Japan	
Kei SUMINAGA	MWJ	Live Pier Kanazawahakkei 2F 1-1-7 Mitsuura Kanagawa-ku Yokohama 236-0031, Japan	
Fuyuki SHIBATA	MWJ	Live Pier Kanazawahakkei 2F 1-1-7 Mitsuura Kanagawa-ku Yokohama 236-0031, Japan	
Mikio KITADA	MWJ	Live Pier Kanazawahakkei 2F 1-1-7 Mitsuura Kanagawa-ku Yokohama 236-0031, Japan	
Kenichiro SATO	MWJ	Live Pier Kanazawahakkei 2F 1-1-7 Mitsuura Kanagawa-ku Yokohama 236-0031, Japan	
Keisuke WATAKI	MWJ	Live Pier Kanazawahakkei 2F 1-1-7 Mitsuura Kanagawa-ku Yokohama 236-0031, Japan	
Kaori AKIZAWA	MWJ	Live Pier Kanazawahakkei 2F 1-1-7 Mitsuura Kanagawa-ku Yokohama 236-0031, Japan	
Minoru KAMATA	MWJ	Live Pier Kanazawahakkei 2F 1-1-7 Mitsuura Kanagawa-ku Yokohama 236-0031, Japan	
Takayoshi SEIKE	MWJ	Live Pier Kanazawahakkei 2F 1-1-7 Mitsuura Kanagawa-ku Yokohama 236-0031, Japan	
Junko HAMANAKA	MWJ	Live Pier Kanazawahakkei 2F 1-1-7 Mitsuura Kanagawa-ku Yokohama 236-0031, Japan	
Tomoko MIYASHITA	MWJ	Live Pier Kanazawahakkei 2F 1-1-7 Mitsuura Kanagawa-ku Yokohama 236-0031, Japan	
Soichi MORIYA	MWJ	Live Pier Kanazawahakkei 2F 1-1-7 Mitsuura Kanagawa-ku Yokohama 236-0031, Japan	
Hiroaki MURAKI	MWJ	Live Pier Kanazawahakkei 2F 1-1-7 Mitsuura Kanagawa-ku Yokohama 236-0031, Japan	

Name	Affiliation	Address	Tel Fax E-mail
Aya KATO	MWJ	Live Pier Kanazawahakkei 2F 1-1-7 Mitsuura Kanagawa-ku Yokohama 236-0031, Japan	
Kazuhiro SUGIYAMA	MWJ	Live Pier Kanazawahakkei 2F 1-1-7 Mitsuura Kanagawa-ku Yokohama 236-0031, Japan	
Masumi ISHIMORI	MWJ	Live Pier Kanazawahakkei 3F 1-1-7 Mitsuura Kanagawa-ku Yokohama 236-0031, Japan	
Satoshi OKUMURA	Global Ocean Development, Inc. (GODI)	3-65 Oppamahigashi-cho Yokosuka 237-0063, Japan	
Wataru TOKUNAGA	GODI	3-65 Oppamahigashi-cho Yokosuka 237-0063, Japan	

3. Observation

3.1 Meteorological observation

3.1.1 Surface meteorological observation

Satoshi Okumura (GODI)

Wataru Tokunaga (GODI)

(1) Objectives

The surface meteorological parameters are observed as a basic dataset of the meteorology. These parameters bring us the information about temporal variation of the meteorological condition surrounding the ship.

(2) Methods

The surface meteorological parameters were observed throughout MR01-K03 cruise from the departure of Sekinehama, Japan on 4 June 2001 to the arrival of Sekinehama, Japan on 18 July 2001.

This cruise, we used 2 systems for the surface meteorological observation.

1. Mirai meteorological observation system
2. Shipboard Oceanographic and Atmospheric Radiation (SOAR) system

The measured parameters of each system are listed in Table 3.1.1-1, 3.1.1-2, 3.1.1-3 and 3.1.1-4.

(3-1) Mirai meteorological observation system

Instruments and archived parameters of Mirai meteorological observation system are listed in the table below. Data was collected and processed by KOAC-7800 weather data processor made by Koshin Denki, Japan. The data set has 6-second averaged every 6-second record and 10-minute averaged every 10-minute record.

Table 3.1.1-1 Instrument and their installation locations
of Mirai meteorological observation system

Sensors	Type	Manufacturer	Location (altitude from base line)
Anemometer	KE-500	Koshin Denki, Japan	Foremast (30m)
Thermometer	FT	Koshin Denki, Japan	Compass deck (27m)
Dewpoint meter	DW-1	Koshin Denki, Japan	Compass deck (27m)
Barometer	F451	Yokogawa, Japan	Captain deck (20m)
			Weather station room (tubing outside)
Rain gauge	50202	R. M. Young, USA	Compass deck (25m)
Optical Rain gauge	ORG-115DR	ScTi, USA	Compass deck (25m)

Table 3.1.1-1 (continued)

Radiometer (short wave)	MS-801	Eiko Seiki, Japan	Radar mast (28m)
Radiometer (long wave)	MS-200	Eiko Seiki, Japan	Radar mast (28m)
Wave height meter	MW-2	Tsurumi-seiki, Japan	Bow (16m)

Table 3.1.1-2 Parameter of Mirai meteorological observation systems

Parameter	Units	Remarks
1 Latitude	Degree	
2 Longitude	Degree	
3 Ship's speed	Knot	Mirai log
4 Ship's heading	Degree	Mirai gyro
5 Relative wind speed	m/s	6 sec. / 10 min. average
6 Relative wind direction	Degree	6 sec. / 10 min. average
7 True wind speed	m/s	6 sec. / 10 min. average
8 True wind direction	Degree	6 sec. / 10 min. average
9 Barometric pressure	hPa	6 sec. / 10 min. average Adjusted to the sea surface level
10 Air temperature (starboard side)	deg-C	6 sec. / 10 min. average
11 Air temperature (port side)	deg-C	6 sec. / 10 min. average
12 Dewpoint temperature (starboard side)	deg-C	6 sec. / 10 min. average
13 Dewpoint temperature (port side)	deg-C	6 sec. / 10 min. average
14 Relative humidity (starboard side)	%	6 sec. / 10 min. average
15 Relative humidity (port side)	%	6 sec. / 10 min. average
16 Rain rate (optical rain gauge)	mm/hr	1 hr / 12 hr accumulated
17 Rain rate (capacitive rain gauge)	mm/hr	1 hr / 12 hr accumulated
18 Down welling shotwave radiometer		Momentary / 12 hr accumulated
19 Down welling infra-red radiometer		Momentary / 12 hr accumulated
20 Sea surface temperature	deg-C	Under the water line –5 m
21 Significant wave height (fore)	M	3 hourly
22 Significant wave height (aft)	M	3 hourly
23 Significant wave period (fore)	Second	3 hourly
24 Significant wave period (aft)	Second	3 hourly

(3-2) Shipboard Oceanographic and Atmospheric Radiation (SOAR) system

SOAR system, designed by BNL (Brookhaven National Laboratory, USA), is consisted of 3 parts.

1. Portable Radiation Package (PRP) designed by BNL – short and long wave down welling radiation.
2. Zeno meteorological system designed by BNL – wind, Tair/RH, pressure and rainfall measurement.

3. Scientific Computer System (SCS) designed by NOAA (National Oceanographic and Atmospheric Administration, USA) – centralized data acquisition and logging of all data sets.

SCS recorded PRP data every 6.5 seconds and Zeno meteorological data every 10 seconds. Instruments and their location are listed in Table 3.1.1-3. The archived parameters are in Table 3.1.1-4.

Table 3.1.1-3 Instruments installation locations of SOAR system

Sensor	Type	Manufacturer	Location (altitude from base line)
Anemometer	05106	R. M. Young, USA	Foremast (31m)
Tair/RH	HMP45A	R. M. Young, USA	Foremast (29m)
	With 43408 Gill aspirated radiation shield (R. M. Young)		
Barometer	61201	R. M. Young, USA	Foremast (30m)
	With 61002 Gill pressure port (R. M. Young)		
Tipping bucket rain gauge	50202	R. M. Young, USA	Foremast (30m)
Optical rain gauge	ORG-115DA	ScTi, USA	Foremast (30m)
Radiometer (short wave)	PSP	Eppley labs, USA	Foremast (31m)
Radiometer (long wave)	PIR	Eppley labs, USA	Foremast (31m)
Fast rotating Shadowband radiometer		Yankee, USA	Foremast (31m)

Table 3.1.1-4 Parameters of SOAR system

Parameters	Units	Remarks
1 Latitude	Degree	
2 Longitude	Degree	
3 Sog	Knot	
4 Cog	Degree	
5 Relative wind speed	m/s	
6 Relative wind direction	Degree	
7 Barometric pressure	HPa	
8 Air temperature	deg-C	
9 Relative humidity	%	
10 Rain rate (optical rain gauge)	mm/hr	
11 Precipitation (capacitive rain gauge)	Mm	Reset at 50 mm
12 Down welling shortwave radiation	W/m ²	
13 Down welling infra-red radiation	W/m ²	
14 Defuse irradiation	W/m ²	

(4) Preliminary results

Wind (converted to U, V component), Air temperature, Relative Humidity, Rainfall and surface pressure observed during the cruise from Mirai meteorological observation system via navigation system are shown in Fig.3.1.1-1.

(5) Data archives

These raw data obtained in this cruise will be submitted to the Data Management Office (DMO) in JAMSTEC just after the cruise.

Remarks concerning about data quality are as follows;

1. Radiometers for upwelling radiation measurement of Mirai meteorological observation system were not installed during this cruise.
2. Restarted the PRP PC. (0250 to 0310 UTC, 18 July)

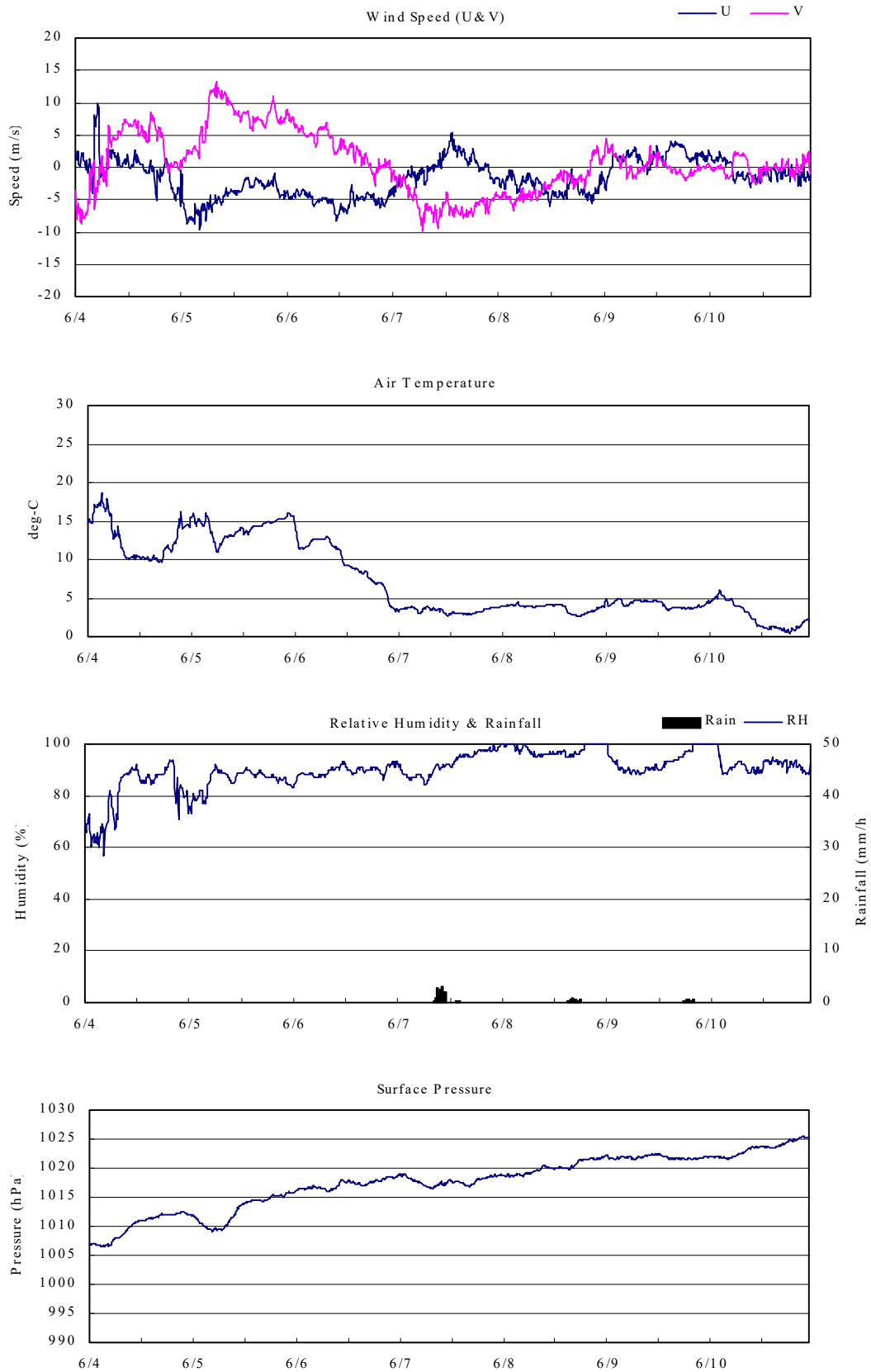


Fig. 3.1.1-1 Time series of measured parameter by Mirai meteorological observation system

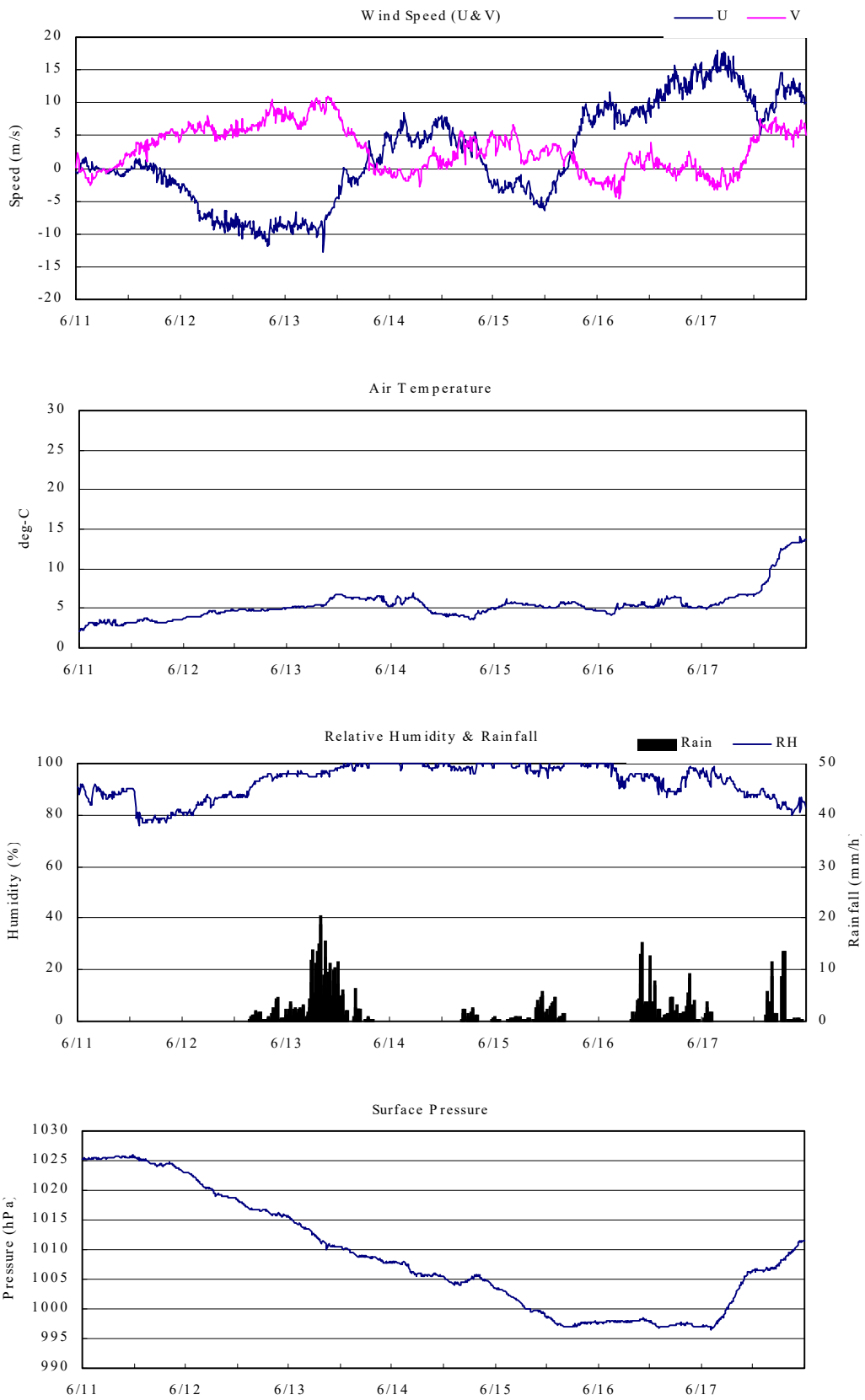


Fig. 3.1.1-1 (continued)

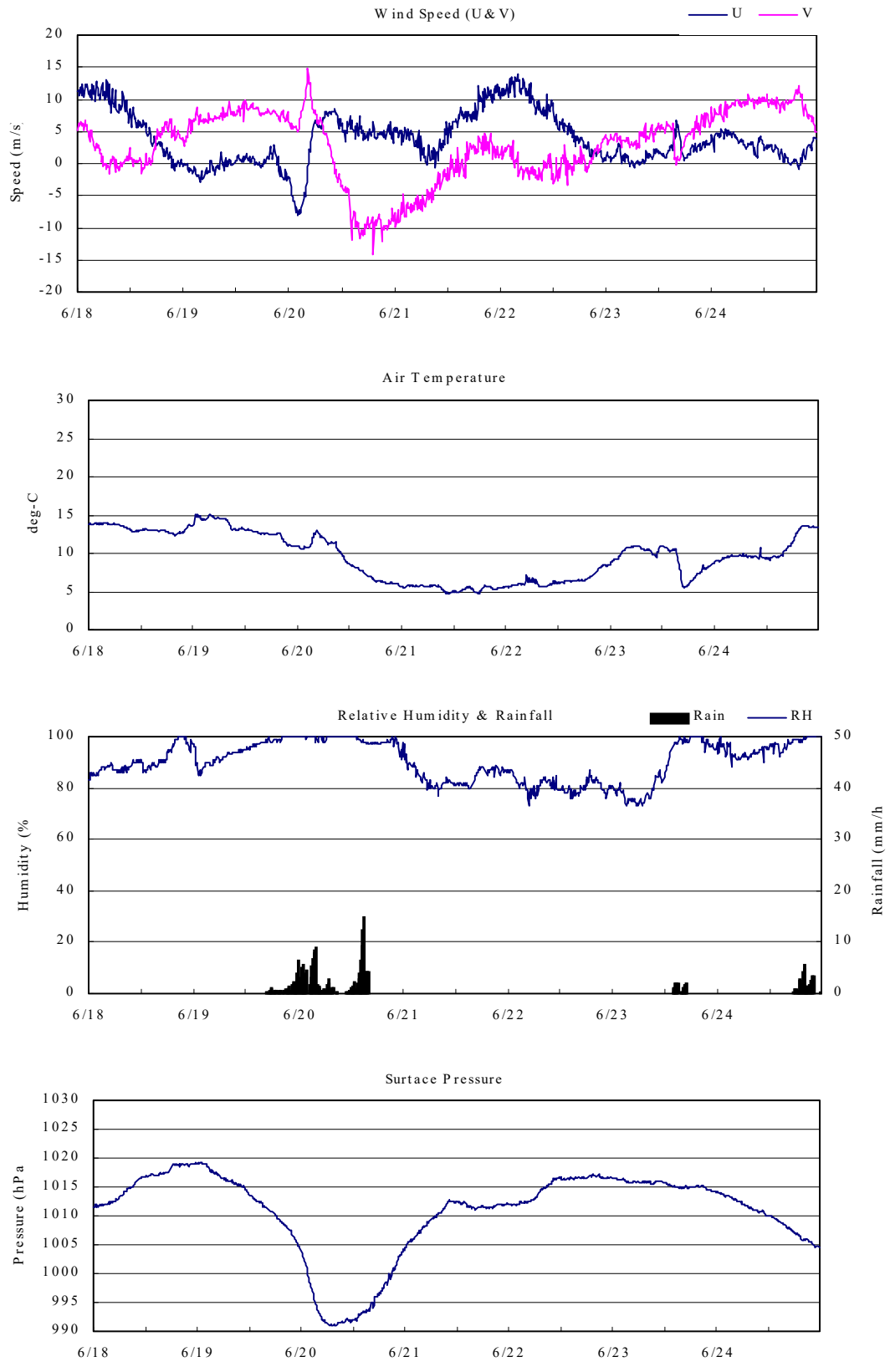


Fig. 3.1.1-1 (continued)

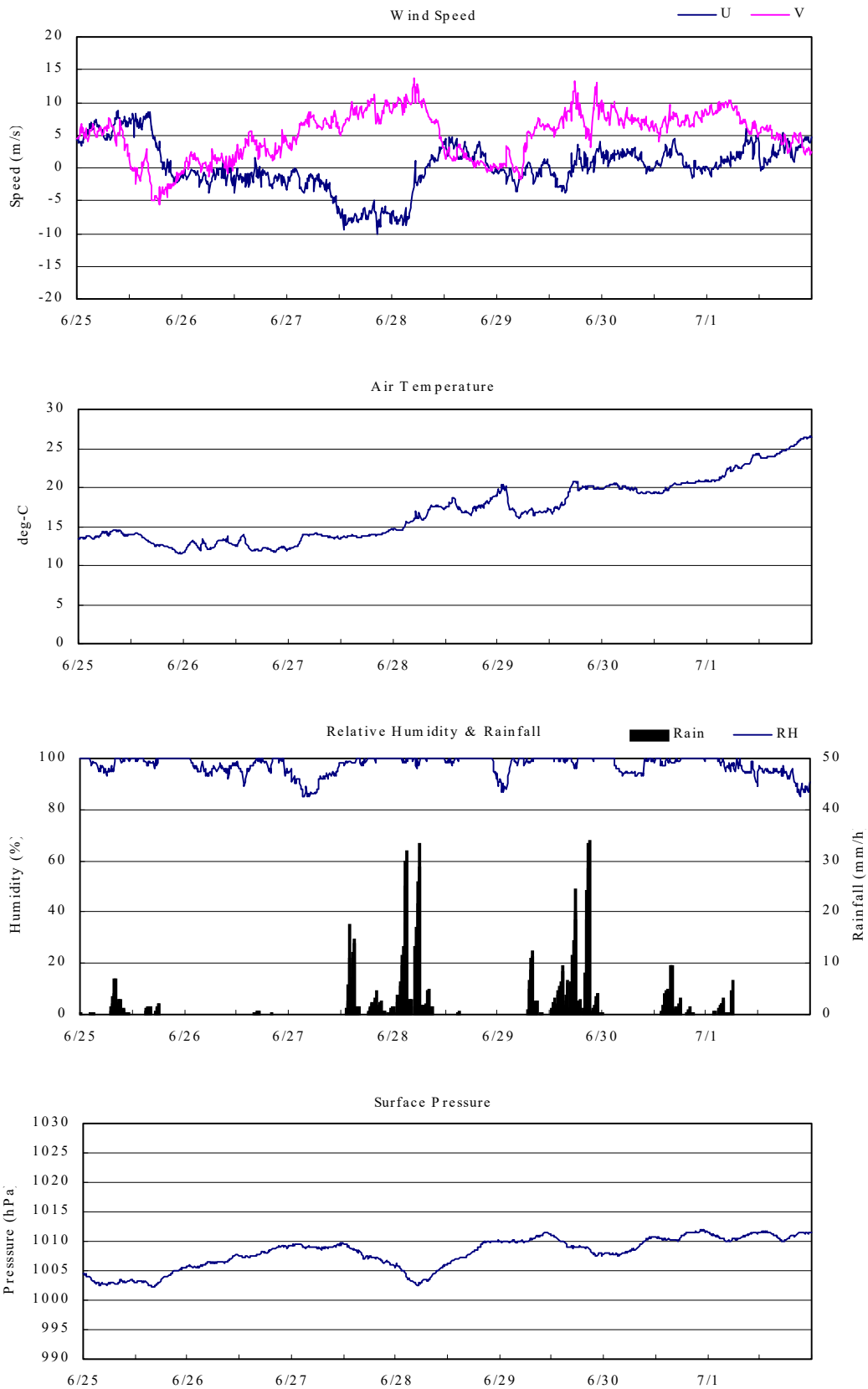


Fig. 3.1.1-1 (continued)

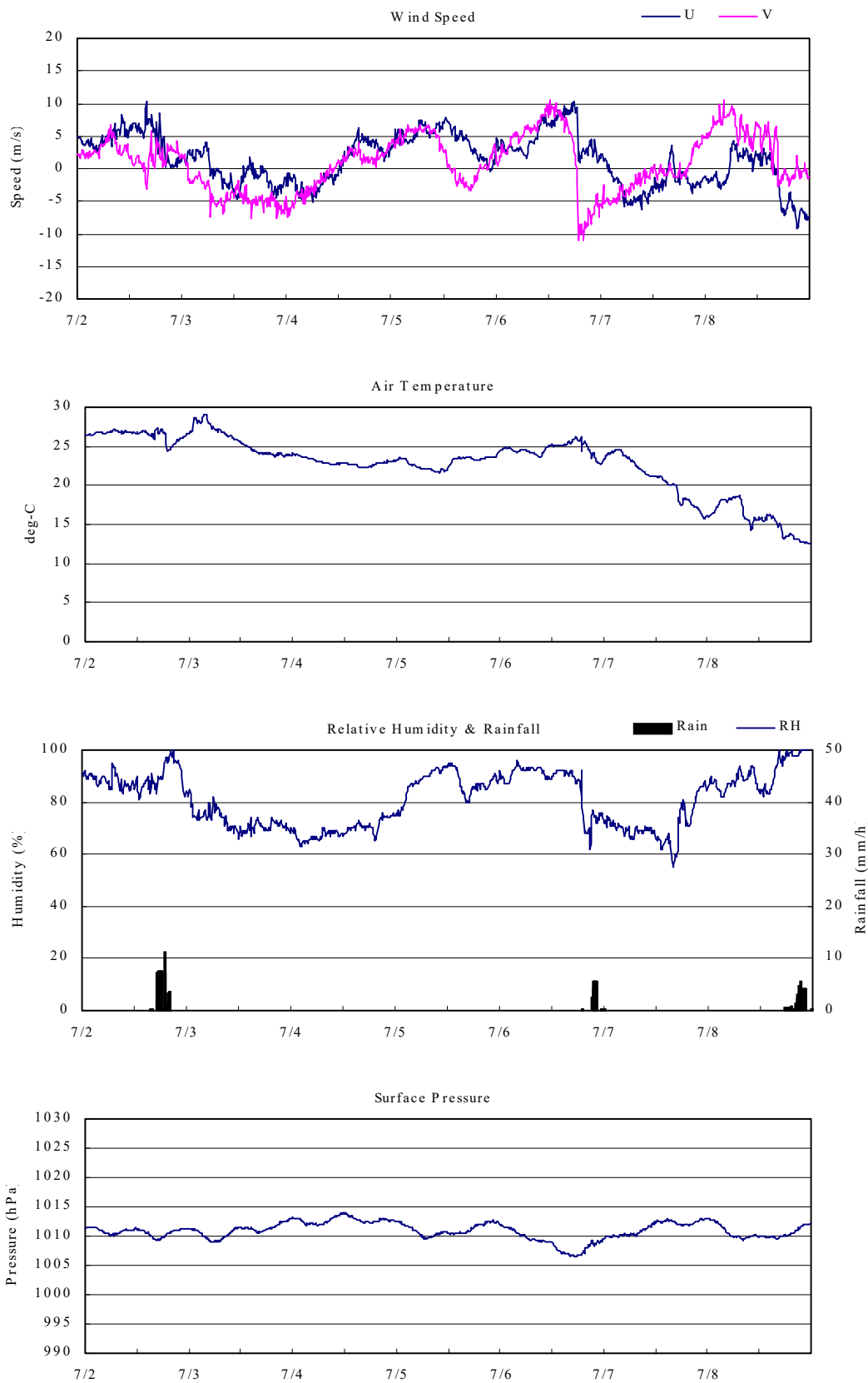


Fig. 3.1.1-1 (continued)

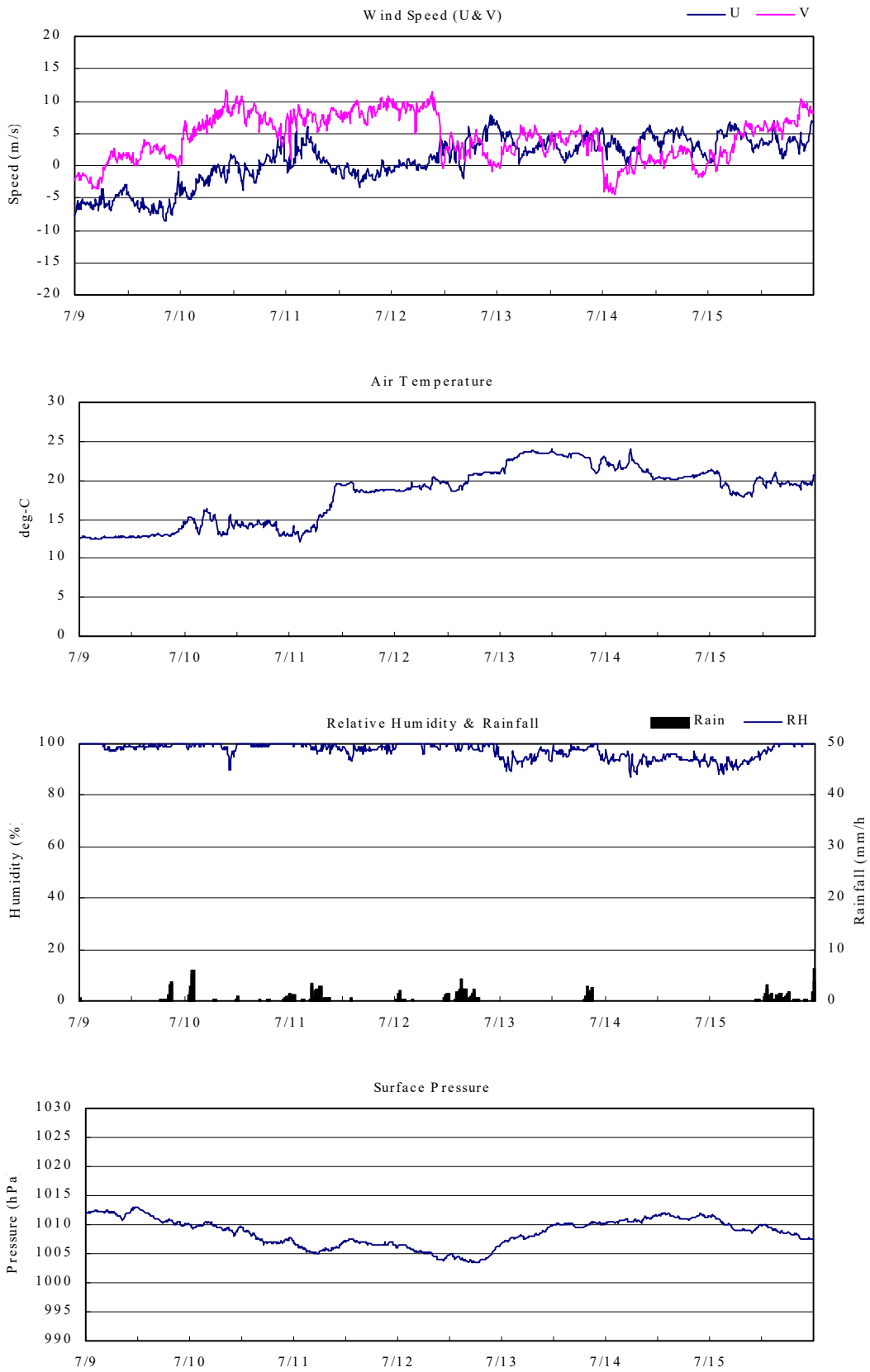


Fig. 3.1.1-1 (continued)

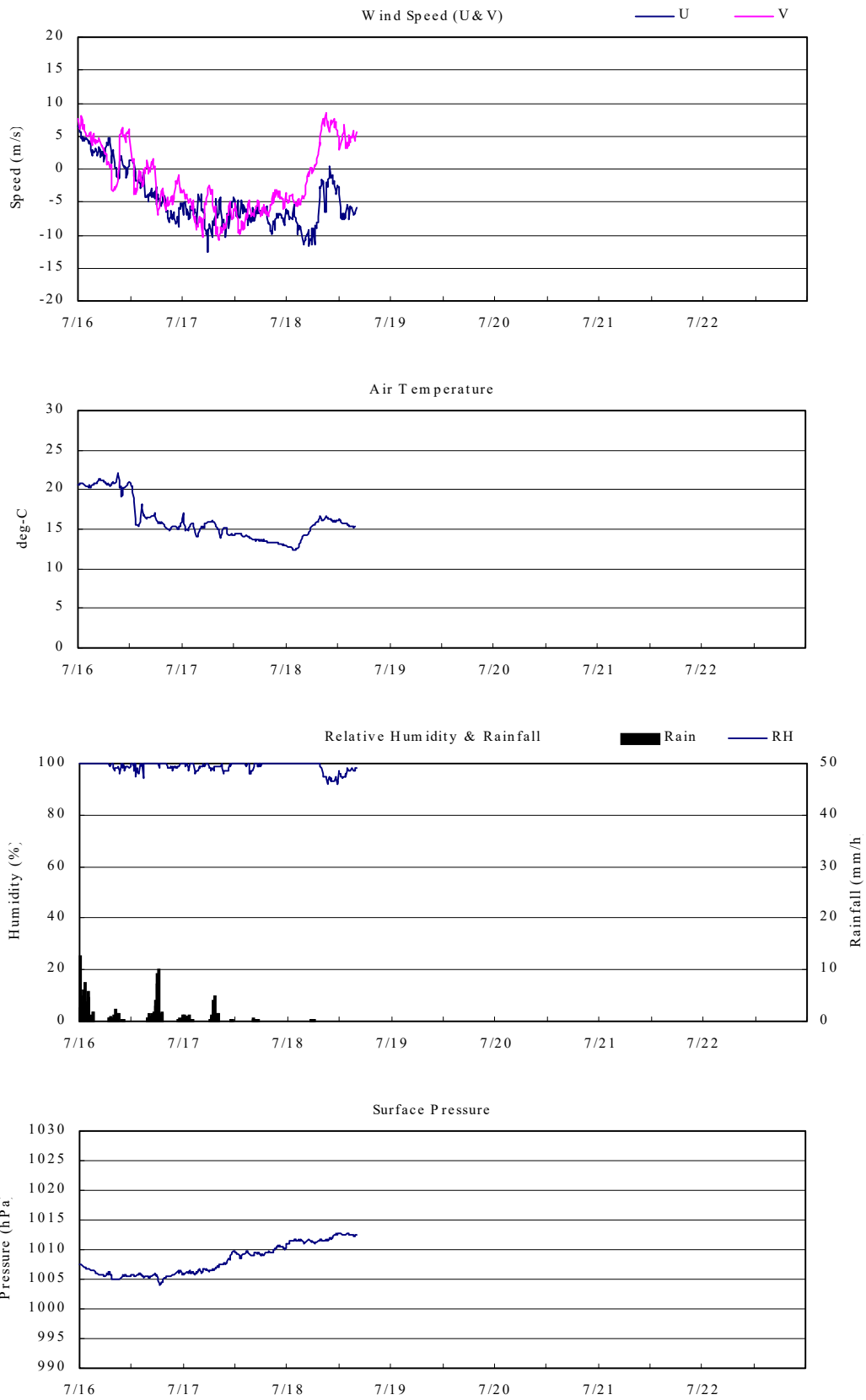


Fig. 3.1.1-1 (continued)

3.1.2 Ceilometer Observation

Satoshi Okumura (GODI)

Wataru Tokunaga (GODI)

(1) Objectives

The information of the cloud base height and the liquid water amount around cloud base is important to understand the processes on formation the cloud. As one of the methods to measure them, the ceilometer observation was carried out.

(2) Parameters

(3-1) Cloud base height [m]

(3-2) Backscatter profile, sensitivity and range normalized at 30m resolution

(3) Methods

We measured cloud base height and backscatter profiles using CT-25K ceilometer (Vaisara, Finland) throughout MR01-K03 cruise from the departure of Sekinehama, Japan on 4 June 2001 to the arrival of Sekinehama, Japan on 18 July 2001.

Major parameters for the measurement configuration are as follows;

Laser source:	Indium Gallium Arsenide (InGaAs) Diode Laser
Transmitting wavelength:	905 +/- 5 nm at 25 deg-C
Transmitting average power:	8.9 mW
Repetition rate:	5.57 kHz
Detector:	Silicon Avalanche Photodiode (APD)
Responsively at 905 nm:	65 A/W
Measurement range:	0 ~ 7.5 km
Resolution:	50 ft. in full range
Sampling rate:	60 sec.

(4) Preliminary results

The time series of the detected cloud base height is shown in Fig. 3.1.2-1. "C1" is the lowest cloud base height, "C2" is the second lowest cloud base height, and "C3" is the highest cloud base height. The results will be public after the analyses in the future.

(5) Data archives

Ceilometer data obtained in this cruise will be submitted to the DMO (Data Management Office), in JAMSTEC and will be available via "R/V Mirai Data Web Page" in JAMSTEC home page.

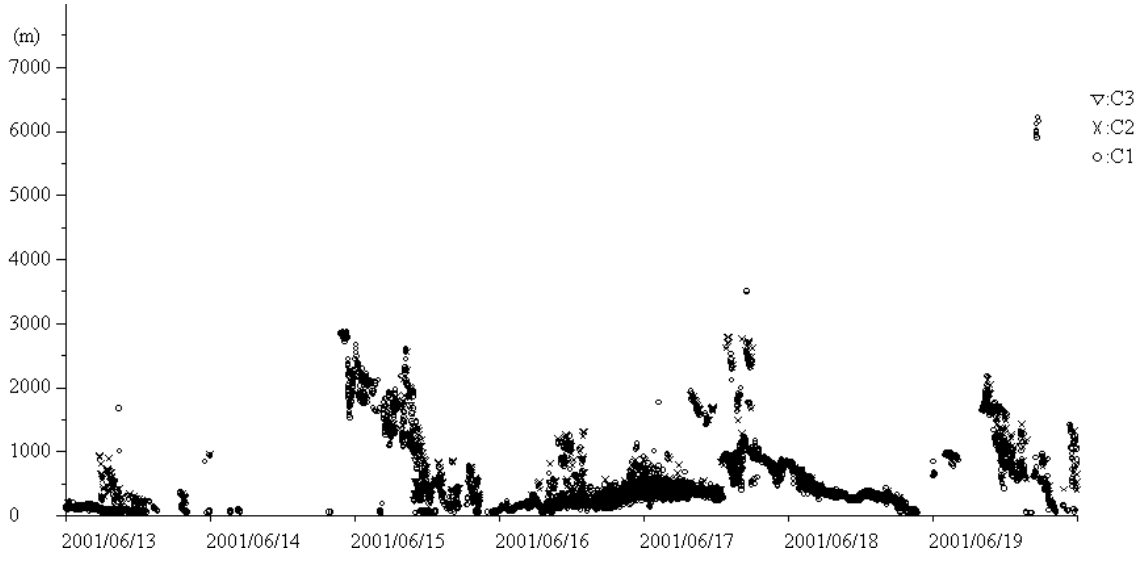
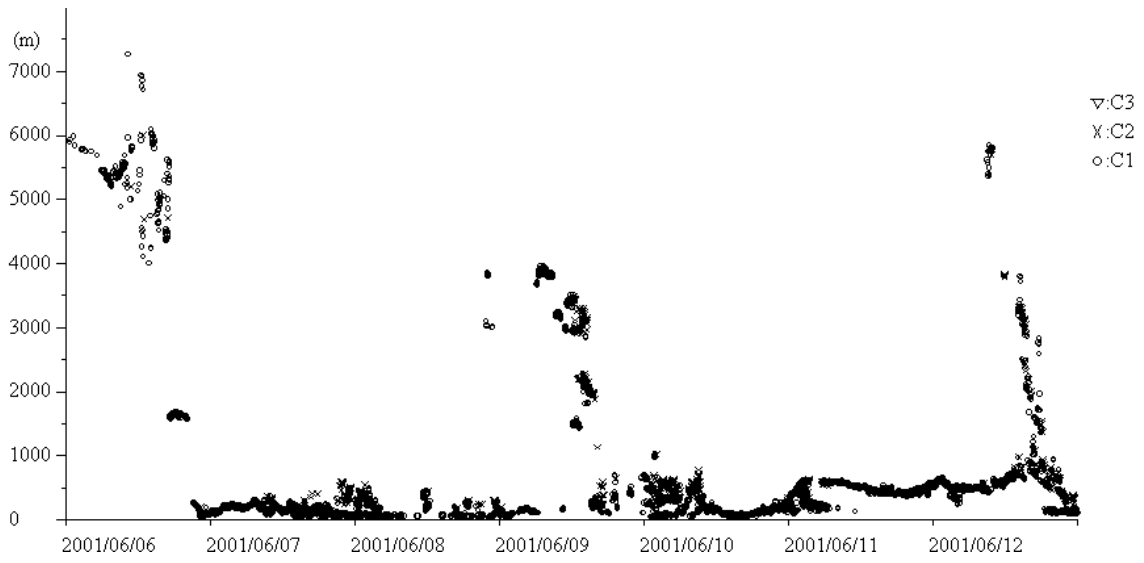


Fig. 3.1.2-1 Cloud base height

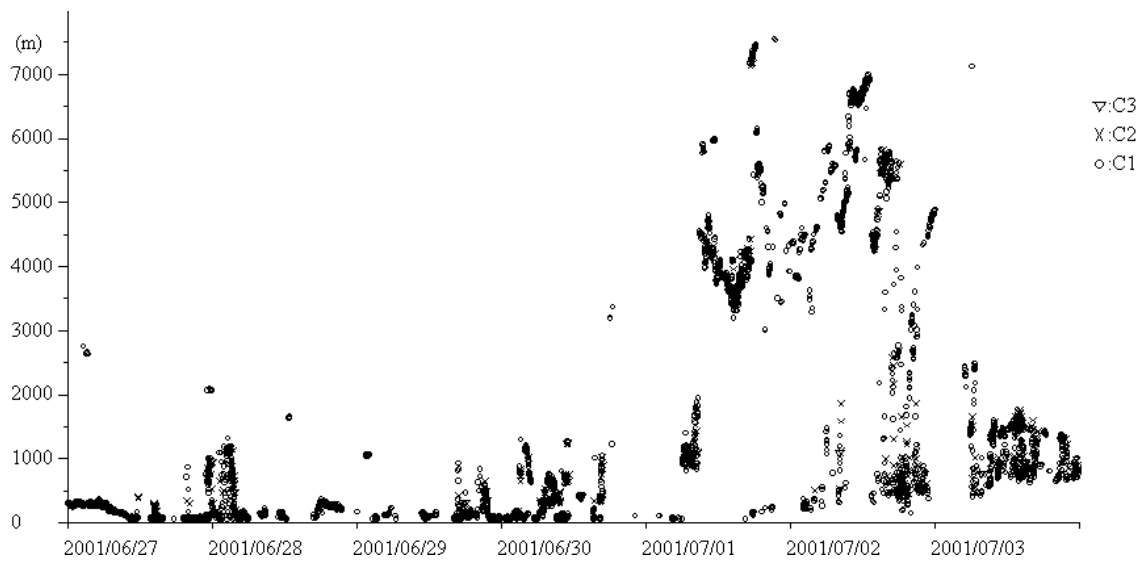
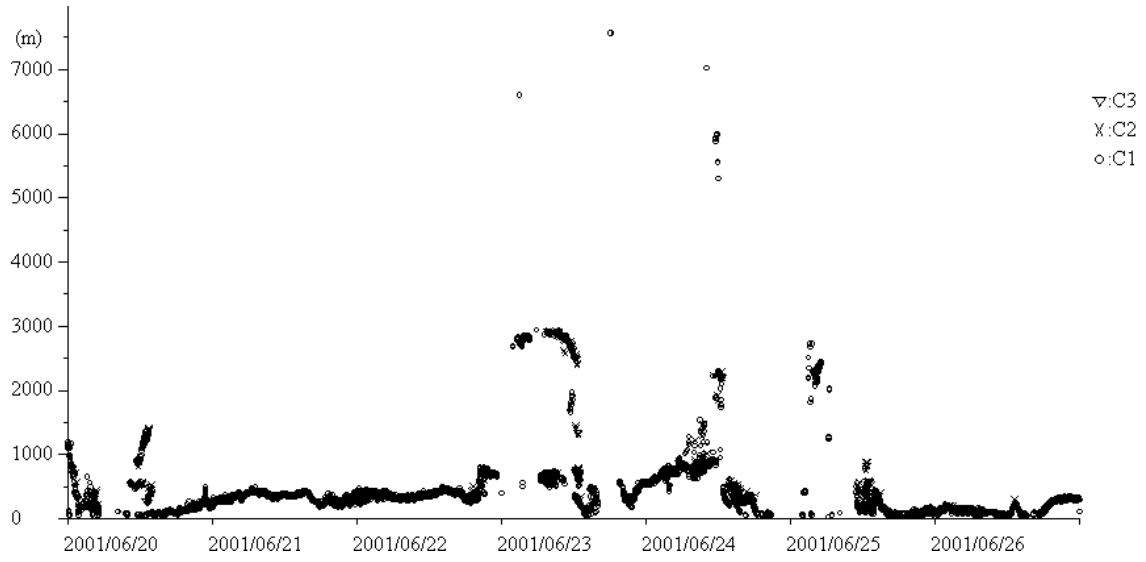


Fig. 3.1.2-1(continued)

3.2 CTD/CWS, Lowered ADCP

Hirokatsu UNO, Fujio KOBAYASHI, Miki YOSHIKE, Kenichi KATAYAMA,
and Kei SUMINAGA

(Marine Works Japan Ltd.)

(1) Introduction

Temperature and salinity were measured with CTD (SBE911*plus*; Sea-Bird Electronics, Inc.) and seawater sampling for chemical analysis was conducted with Carousel Water Sampler (CWS: SBE32; Sea-Bird Electronics, Inc.). In addition, a dissolved oxygen sensor and Lowered Acoustic Doppler Current Profiler (LADCP: RD Instruments) were attached with the CTD system for dissolved oxygen and current velocity. In this section, we describe the outlines of the CTD/CWS and LADCP observations in MR01-K03 cruise on R/V MIRAI from 6 June to 16 July 2001.

(2) Methods

(a) CTD/CWS systems

We used two sets of CTD/CWS system, the Large-CTD System and the Small-CTD System. The former and latter are equipped with the 30-liters 24-positions and the 12-liters 12-positions Carousel Water Sampler, respectively. For the Small-CTD System, Niskin-X External Spring Water Samplers were usually used and Niskin Water Sampler were used only for Eddy Study casts.

Conductivity, temperature, depth, and dissolved oxygen were measured from sea surface to 6,051 m (Large-CTD System) or 6,002 m (Small-CTD System). Seawater was collected at 51 stations. The 96 water-sampling casts were carried for the chemical analysis of nutrient, dissolved gas, pH, alkalinity, pigment, and so on.

The sensors and their configurations are listed in Table 3.2.1.

(b) Operation during Observation

The Large-CTD System was deployed and recovered with the A-frame in the stern and the Small-CTD System was with another frame (Dynacon, Inc.) on starboard side. The CTD raw data was acquired on real time by

using a SEASAVE utility in SEASOFT (version 4.232) provided by Sea-Bird Electronics, Inc. and stored on the hard disk of the personal computer set in the After Wheel-house. Water sampling was made during up cast by sending a fire command from the computer. Detail information such as station name, file name, date, time, location at the start/bottom/end of observations, water sampling layers, and events were recorded in CTD cast log sheets.

(c) CTD data processing

The CTD raw data were processed by SEASOFT (version 4.232) on another computer. Procedure of the data processing and used utilities in SEASOFT were as following:

- DATCNV: Convert raw data (binary format) to engineering units (ASCII format). Output items are scan number, pressure, depth, temperature, conductivity, oxygen current, oxygen temperature, descent rate, altimeter, oxygen, salinity, density (sigma-theta), potential temperature, and density (sigma-t). This utility makes a file that includes the data when the bottles were closed.
- SECTION: Exclude the data in air. Write out selected rows of converted data to a new file.
- ALIGNCTD: Align oxygen measurements in time relative to pressure. This ensures that calculation of dissolved oxygen concentration is made using measurements from the same parcel of water.
- WILDEDIT: Mark wild points by setting their values to the bad value specified in the input file header.
- CELLTM: Use a recursive filter to remove conductivity cell thermal mass effects from the measured conductivity.
- FILTER: Low pass filter pressure with a time constant to increase pressure resolution for LOOPEDIT.
- LOOPEDIT: Mark scans "bad" by setting the flag value associated with the scan to bad flag in input files that have pressure reversals.
- DERIVE: Compute oxygen.

BINAVG: Average data into depth bins.
DERIVE: Compute salinity, density, and potential temperature.
SPLIT: Split the data into up cast and down cast files. The filename of down cast is d*.CNV and that of up cast is u*.CNV.
ROSSUM: Write out a summary of the bottle data to a file with a .BTL extension.

(3) Preliminary results

The information of water sampling by the CWS of each CTD cast was summarized in Appendix. Profiles for routine sampling casts in every station and all casts during Eddy Study are shown from Fig. 3.2.1 to Fig. 3.2.51.

As CTD Cast Table in Appendix, we could not help stopping the CTD observation five times through this cruise because of setting the false bottle position (File Name: 004L01.DAT), quitting the SEASAVE software (016L02.DAT), the dissolved oxygen sensor trouble (025L01.DAT), and the pump trouble second times (R01S01.DAT and R02S01.DAT). The restart of these casts caused the data files, 004L02.DAT, 016L03.DAT, 025L02.DAT, R01S02.DAT, and R02S02.DAT, respectively. In addition, LADCP observation was incomplete because of low battery at Station 23 (023L01.DAT).

The information for casts with noises and sensor maintenance are shown in Table 3.2.2.

Note: Management of the CTD data

A file name of each cast consists of station name, CTD system type and cast number, e.g., 001L01. After SPLIT utility was used, up/down identification was added. As a result of data processing, 9 files were made every cast, such as .BL, .CON, .DAT, .HDR, .ROS, .BTL, d*.CNV, u*.CNV, and *.CNV files.

Raw and processed CTD data files were copied into 3.5 inches magnetic optical disks (MO disks).

Table 3.2-1. CTD System Configuration

		Date (UTC) Stations	6/6 - 6/25 Test - 16	6/25 - 6/29 E01 - E12	6/29 - 7/1 17 - 20	7/2 - 7/7 25 - 28	7/13 - 7/16 R01-R11
CTD/CWS Type	Sensors		Serial Number	Serial Number	Serial Number	Serial Number	Serial Number
Large-CTD System	Underwater Unit	SBE <i>9plus</i>	0575	-	0575	0575	-
	Pressure	415K-187	79492	-	79492	79492	-
	Temperature	SBE 3	031525	-	031525	031525	-
	Conductivity	SBE 4	041202	-	041202	041202	-
	Dissolved Oxygen*	SBE 13	130339	-	130339	130575	-
	Altimeter	Benthos 2110-2	228	-	228	228	-
	Carousel	SBE 32	0240	-	0240	0240	-
	LADCP	RDI WH-M-300kHz	0545	-	0545	0545	-
Small-CTD System	Underwater Unit	SBE <i>9plus</i>	0280	0280	0280	0280	0280
	Pressure	410K-105	51190	51190	51190	51190	51190
	Temperature	SBE 3	032453	032453	032453	032453	032453
	Conductivity	SBE 4	041088	041088	041088	041088	041088
	Dissolved Oxygen*(Primary)	SBE 13	130575	130339	130575	-	130575
	Dissolved Oxygen*(Secondary)	SBE 13	-	130575	-	-	-
	Altimeter	Benthos 2110-2	206	206	206	206	206
	Carousel	SBE 32	0171	0171	0171	0171	0171
LADCP	RDI WH-M-300-I-SP2	-	TSN-1512	-	-	TSN-1512	
Deck Unit	Deck Unit	SBE <i>11plus</i>	0308	0308	0308	0308	0308
		Remarks		for Eddy Study		D.O. sensor trouble	for Eddy Study

*There is a systematic difference between two oxygen sensors, serial number 130339 (DO sensor A) and 130575 (DO sensor B). These data should be corrected by the bottle DO data (see the Appendix).

Table 3.2-2. Information for Casts with Noises and Sensor Maintenance

Station	File Name	Event
TEST	UTSTL01	Noises for D.O. (Oxygen current and Oxygen temperature)
	DTSTS02	Noises for D.O. (Oxygen current)
01	U001S01	Noises for D.O. (Oxygen current)
	U001L02	Noises for D.O. (Oxygen current and Oxygen temperature)
	D001S02	Noises for D.O. (Oxygen current)
	U001S02	Noises for D.O. (Oxygen current)
	D001S03	Noises for D.O. (Oxygen current)
	U001S03	Noises for D.O. (Oxygen current)
05	U005S01	Noises for D.O. (Oxygen current)
	D005S02	Noises for D.O. (Oxygen current)
	U005S02	Noises for D.O. (Oxygen current)
	D005S03	Noises for D.O. (Oxygen current)
	U005S03	Noises for D.O. (Oxygen current)
05 - 06	-	D.O. sensor maintenance (S/N 130575)
11	D011S01	Noises for D.O. (Oxygen current)
	U011S01	Noises for D.O. (Oxygen current and Oxygen temperature)
	D011S02	Noises for D.O. (Oxygen current)
	U011S02	Noises for D.O. (Oxygen current)
12	D012S01	Noises for D.O. (Oxygen current)
12 - 13	-	D.O. sensor maintenance (S/N 130575)
14	D014S01	Noises for D.O. (Oxygen current)
	U014S01	Noises for D.O. (Oxygen current and Oxygen temperature)
16	U016L01	Noises for D.O. (Oxygen current and Oxygen temperature)
	D016S01	Noises for D.O. (Oxygen current)
16 - E01	-	D.O. sensor was changed. (Small-CTD System: from S/N 130575 to S/N 130339)
E12 - 17	-	D.O. sensor was changed. (Small-CTD System: from S/N 130339 to S/N 130575)
18	D018L01	Noises for Temperature, Salinity, and D.O. (Oxygen current and Oxygen temperature)
	D018S01	Noises for D.O. (Oxygen current)
	U018S01	Noises for D.O. (Oxygen current and Oxygen temperature)
19	D019L01	Noises for D.O. (Oxygen temperature)
	U019L01	Noises for D.O. (Oxygen current and Oxygen temperature)
20	U020S01	Noises for D.O. (Oxygen current)
	D020L02	Noises for D.O. (Oxygen temperature)
	U020L02	Noises for D.O. (Oxygen temperature)
20 - 25	-	D.O. sensor maintenance (S/N 130575)
25	025L01 - 025L02	D.O. sensor was changed. (Large-CTD System: from S/N 130339 to S/N 130575)
26	D026L01	Noises for D.O. (Oxygen current)
	U026L02	Noises for D.O. (Oxygen current and Oxygen temperature)
24	D024L01	Noises for D.O. (Oxygen current)
	U024L01	Noises for D.O. (Oxygen current and Oxygen temperature)
	D024L02	Noises for D.O. (Oxygen current)
	U024L02	Noises for D.O. (Oxygen current)
24 - 23	-	D.O. sensor maintenance (S/N 130575)
28 - R01	-	D.O. sensor was attached. (Small-CTD System: S/N 130575)

3.2-6

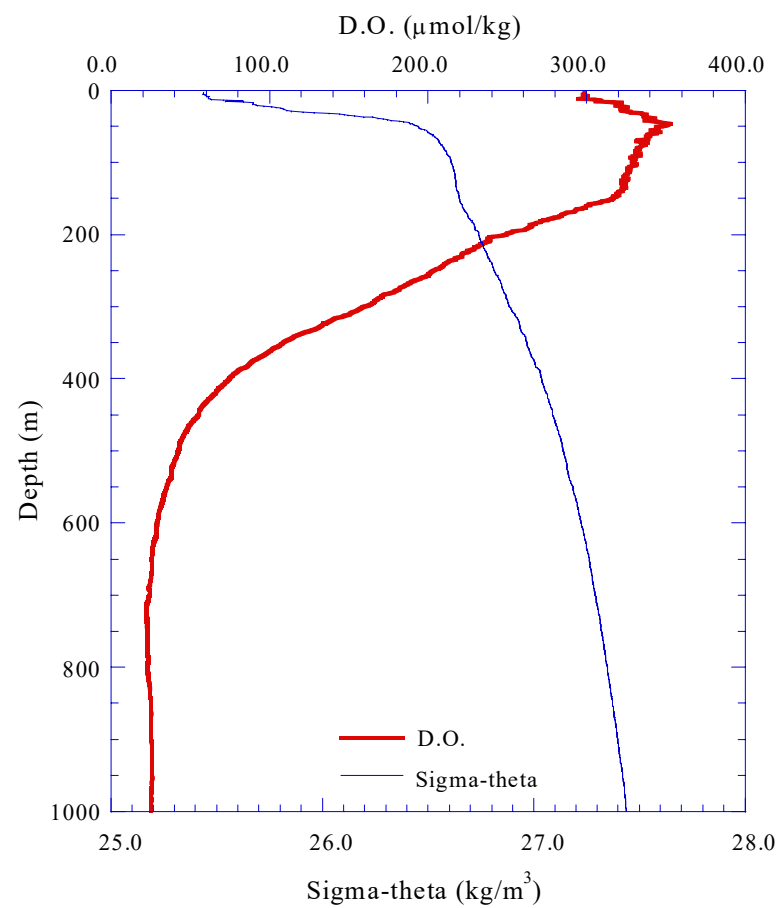
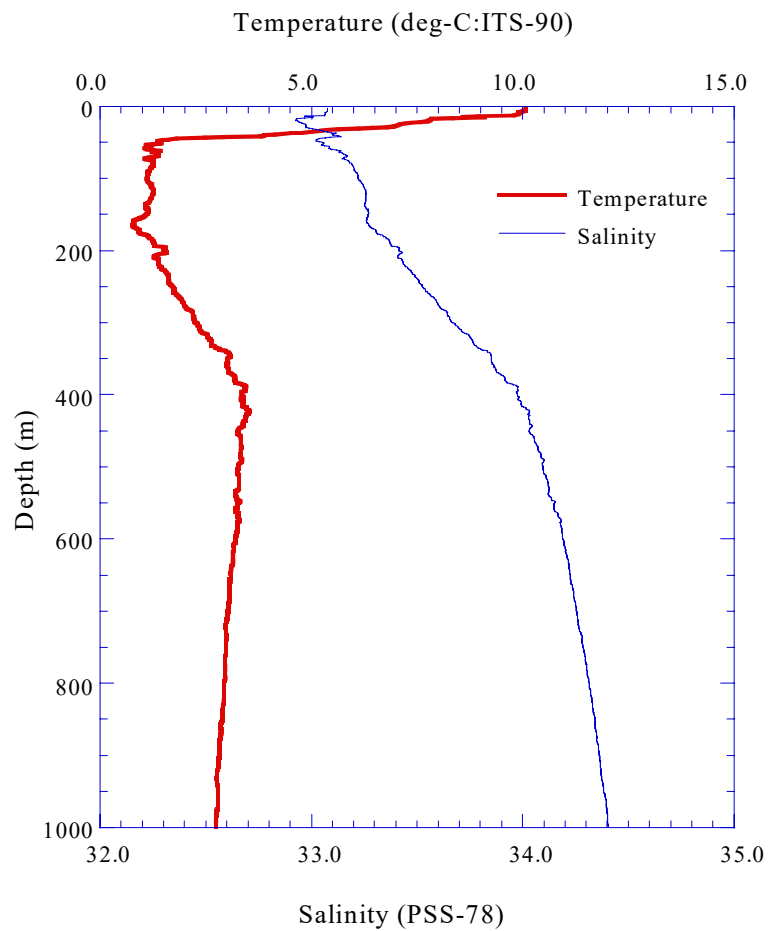


Fig.3.2.1 CTD profile (Stn.TEST;TSTL01)

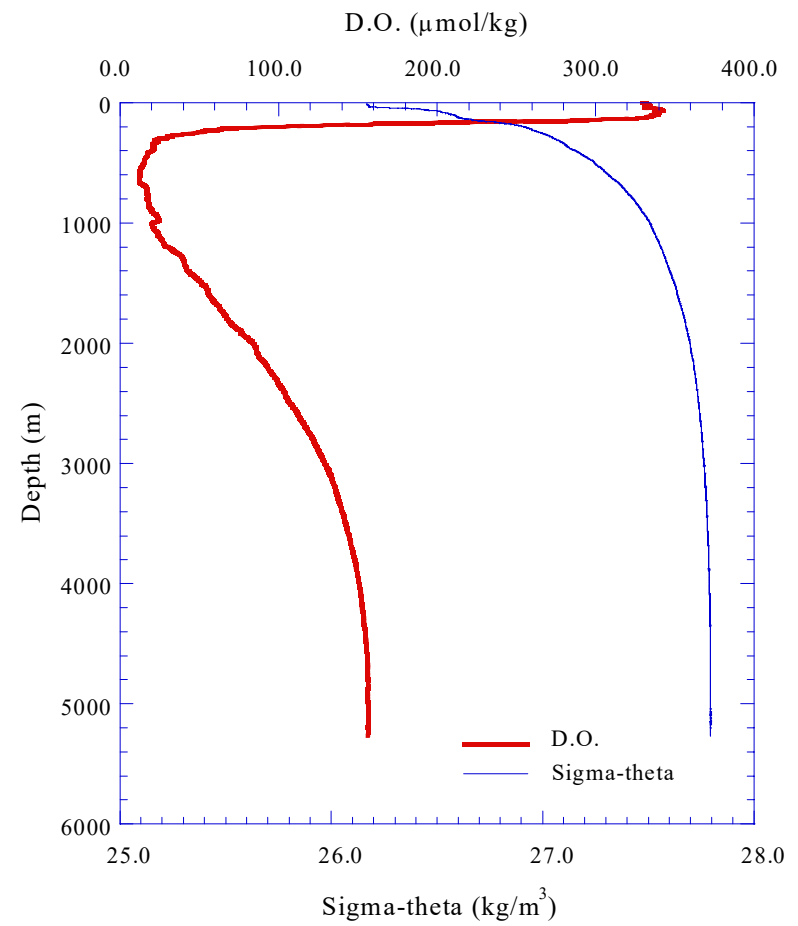
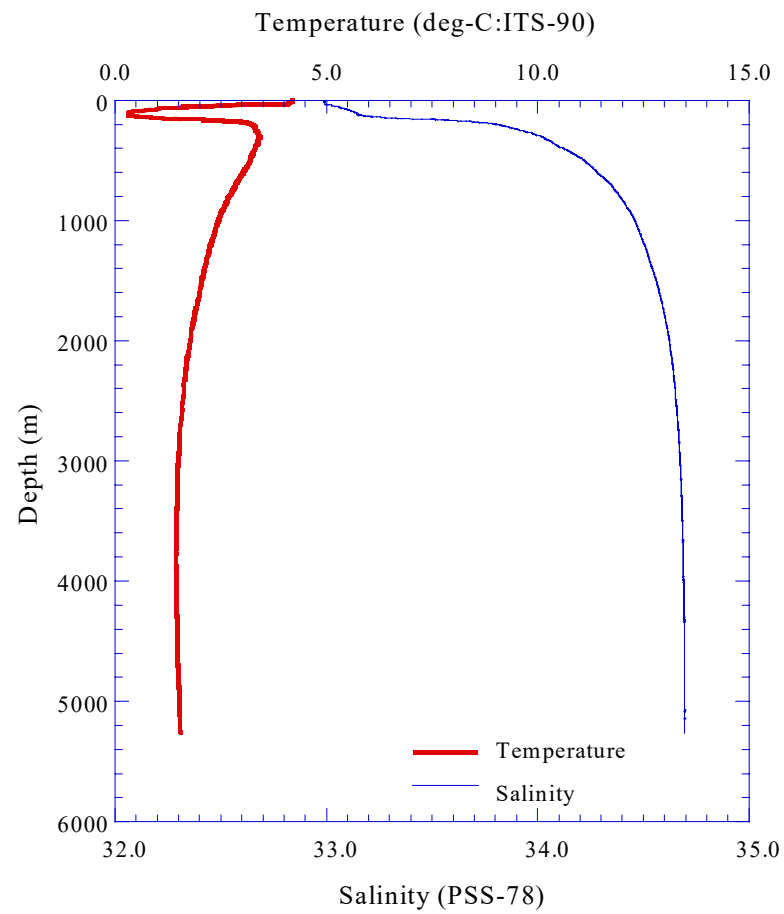


Fig.3.2.2.(a) CTD profile (Stn.01;001L01)

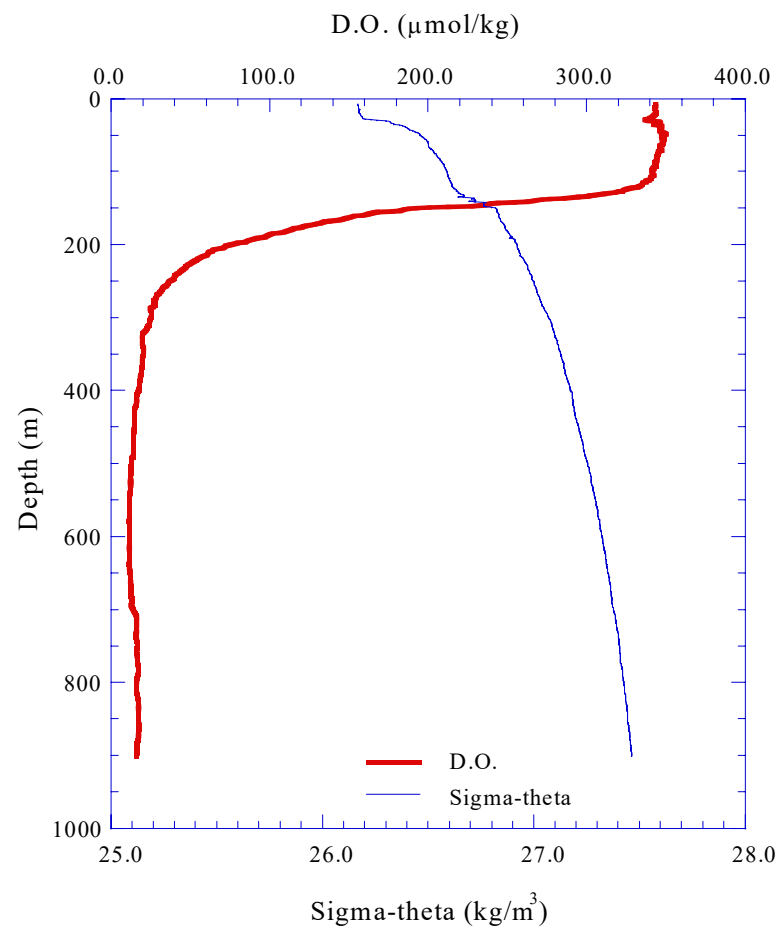
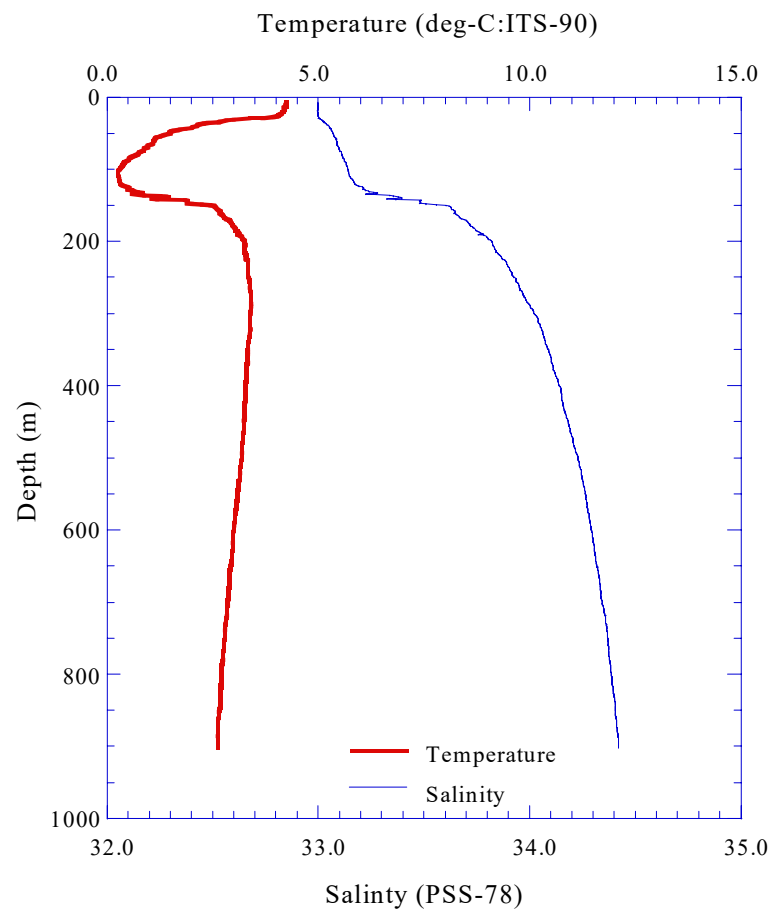


Fig.3.2.2.(b) CTD profile to 1,000m (Stn.01;001L02)

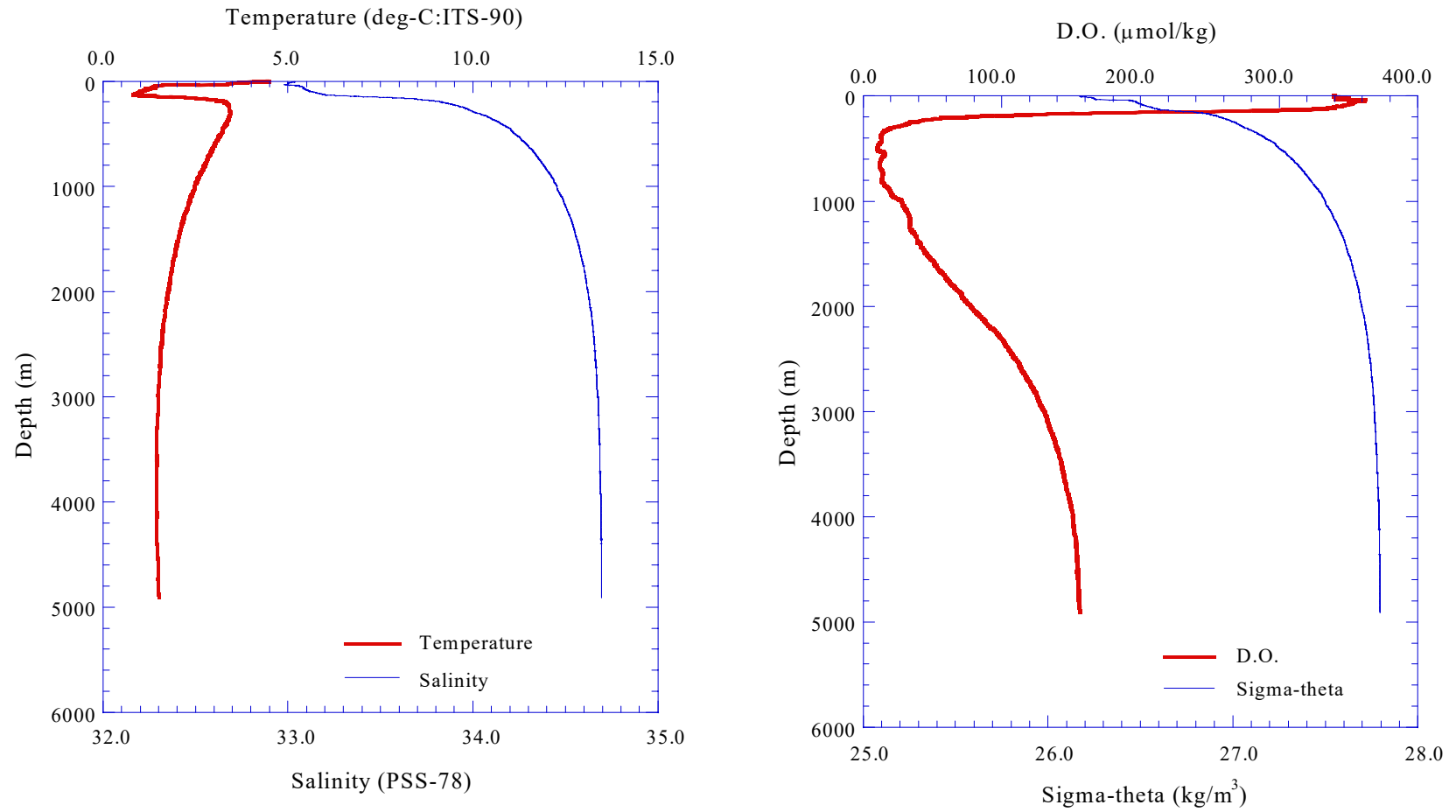


Fig.3.2.3.(a) CTD profile (Stn.02;002L01)

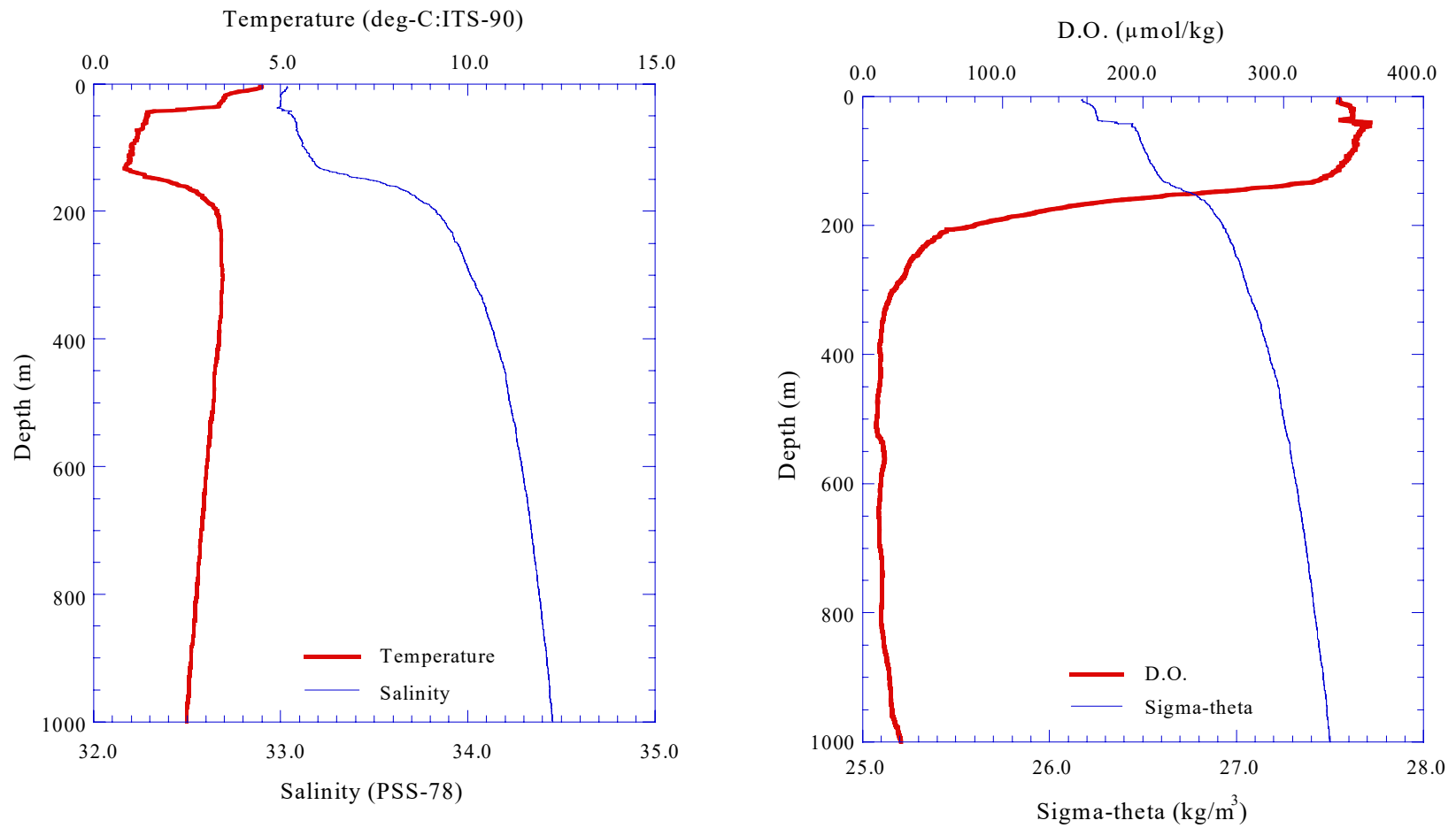


Fig.3.2.3.(b) CTD profile to 1,000m (Stn.02;002L01)

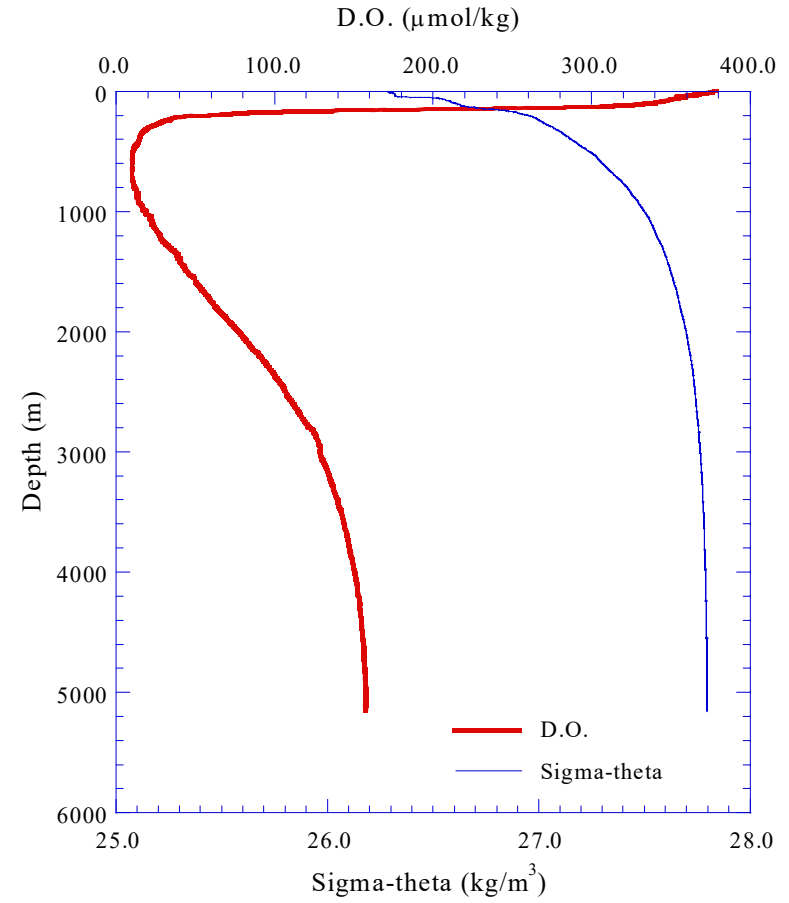
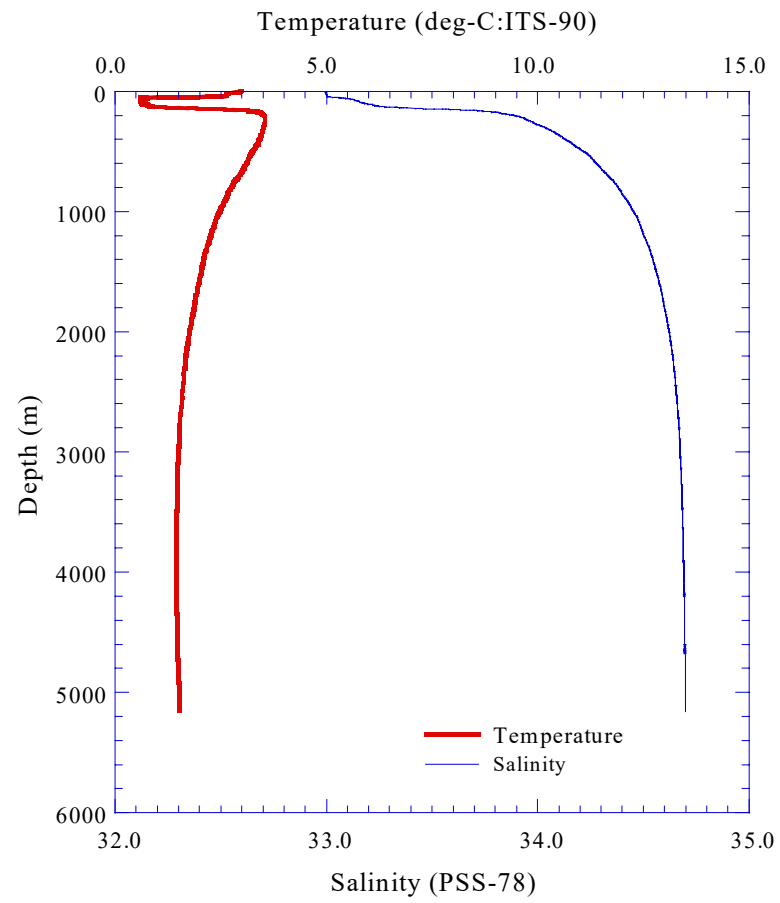


Fig.3.2.4.(a) CTD profile (Stn.03;003L01)

3.2-12

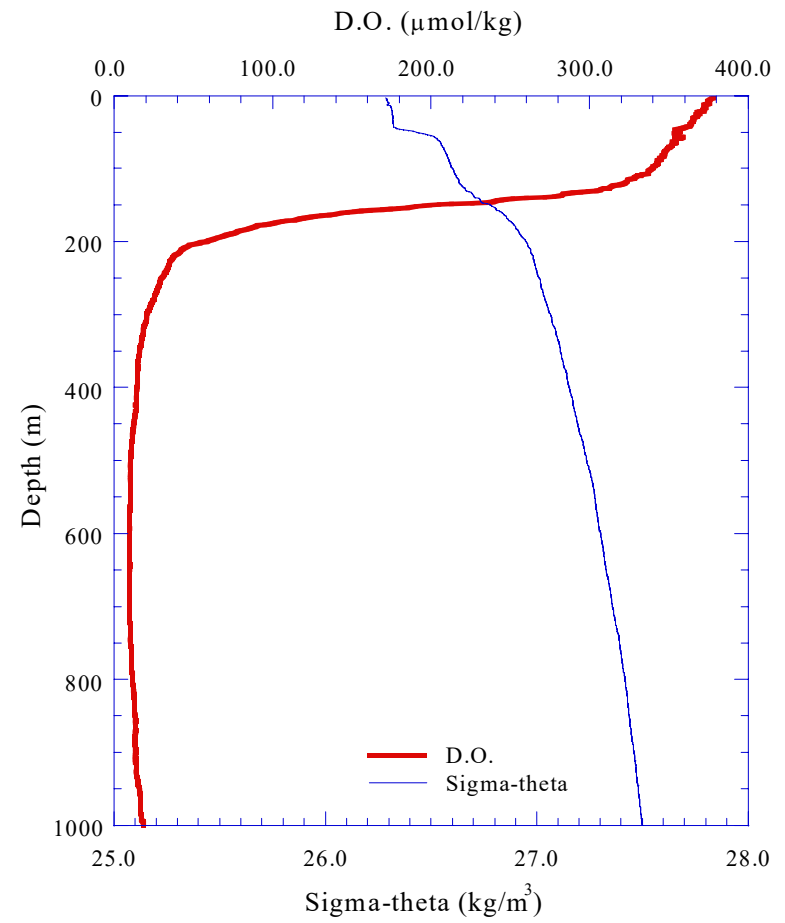
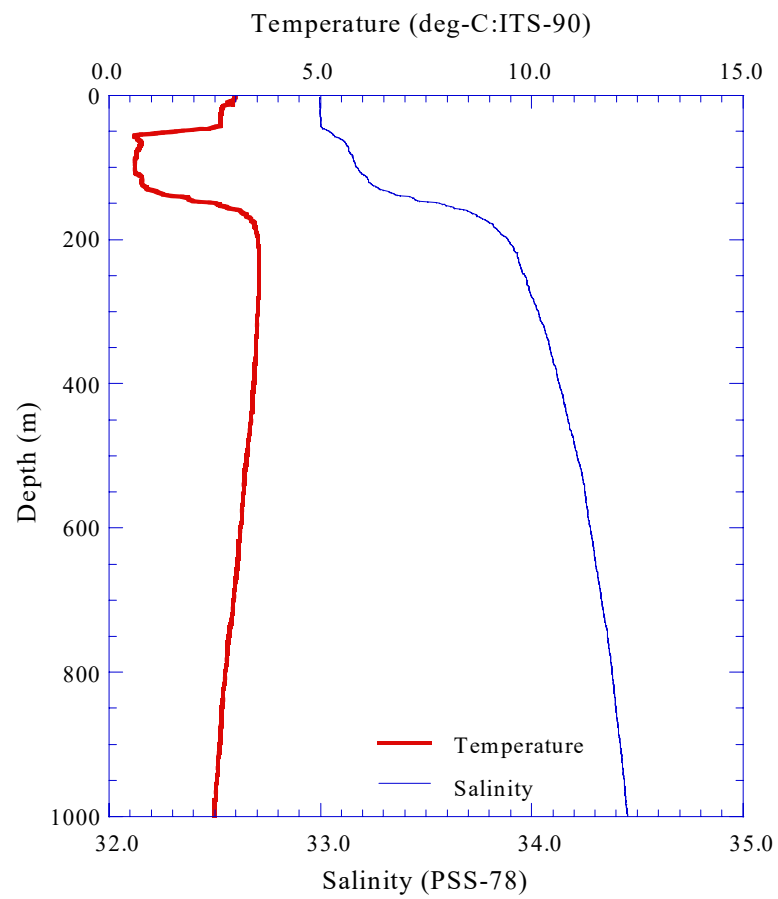


Fig.3.2.4.(b) CTD profile to 1,000m (Stn.03;003L01)

3.2-13

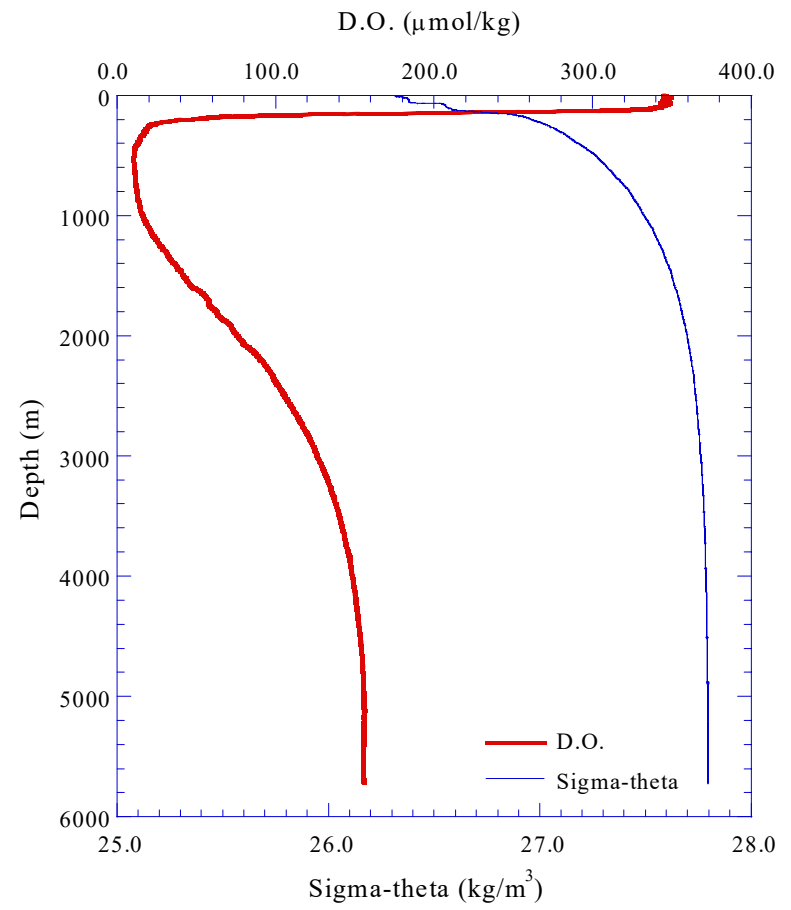
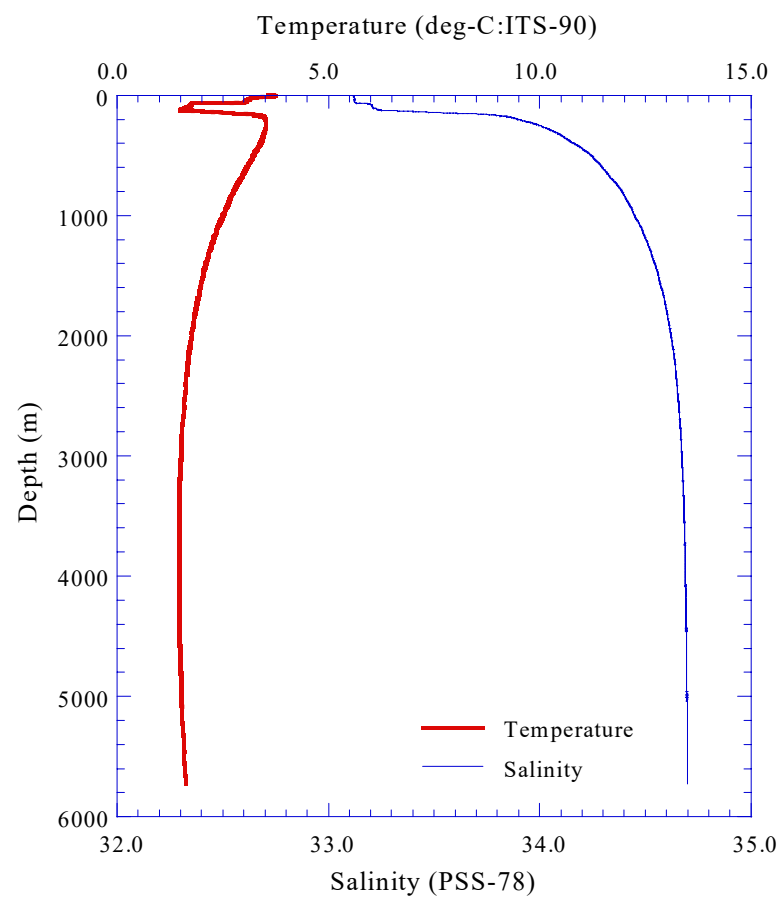


Fig.3.2.5.(a) CTD profile (Stn.04;004L01)

3.2-14

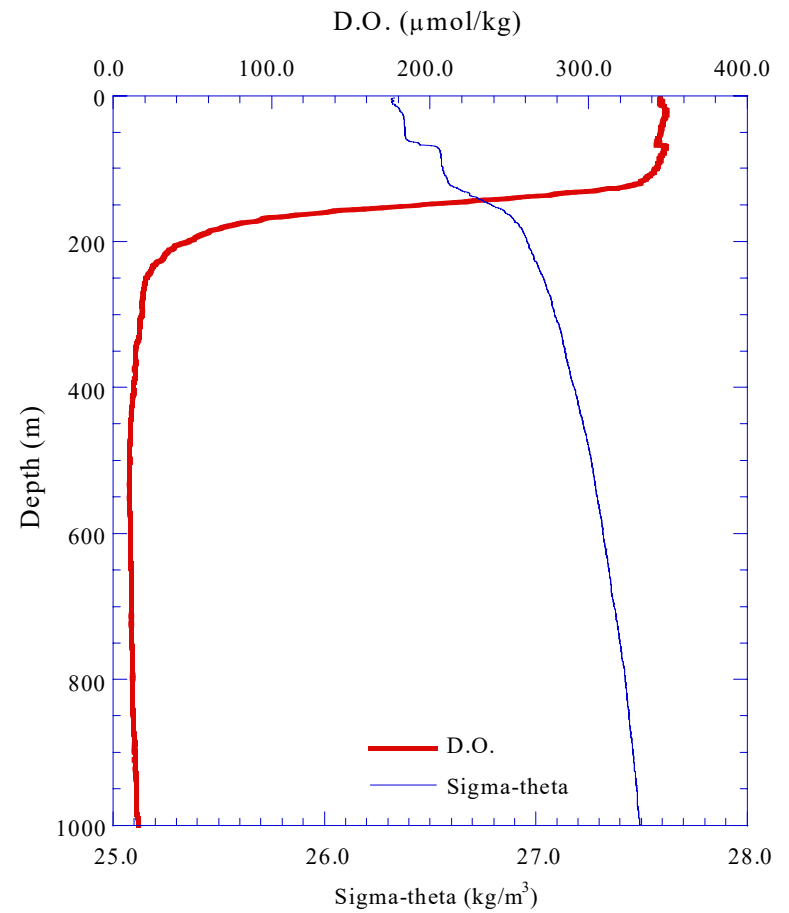
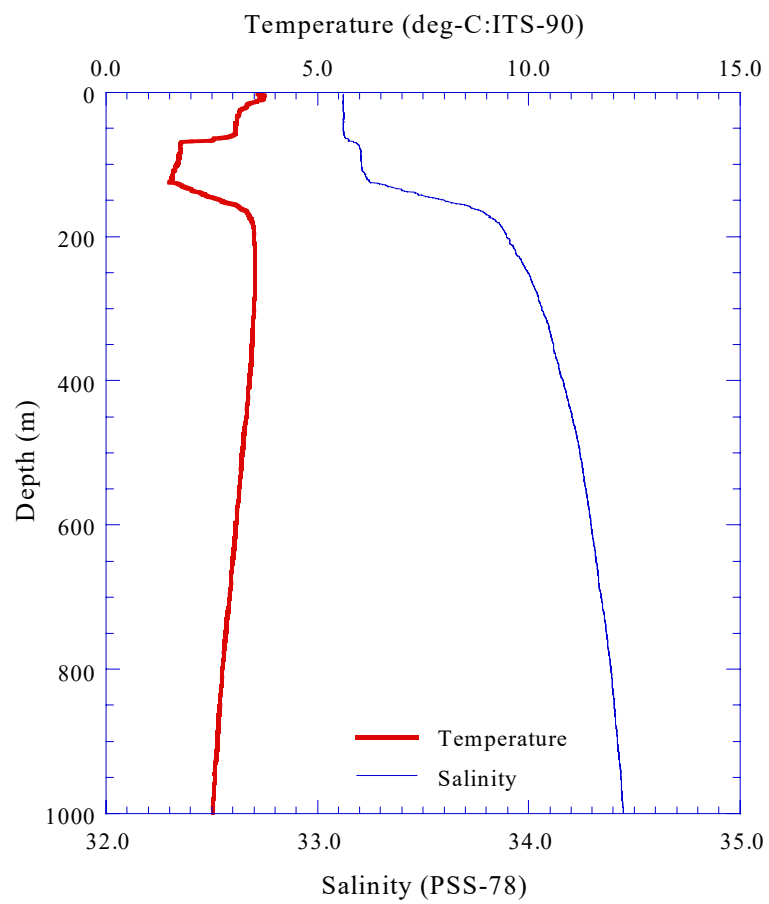


Fig.3.2.5.(b) CTD profile to 1,000m (Stn.04;004L01)

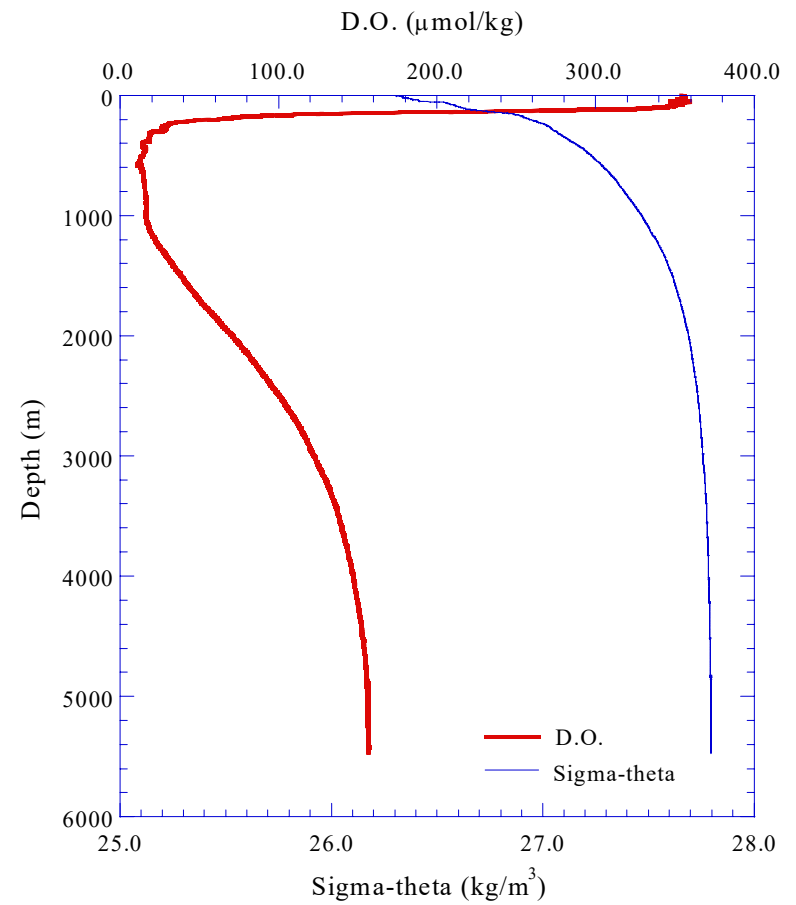
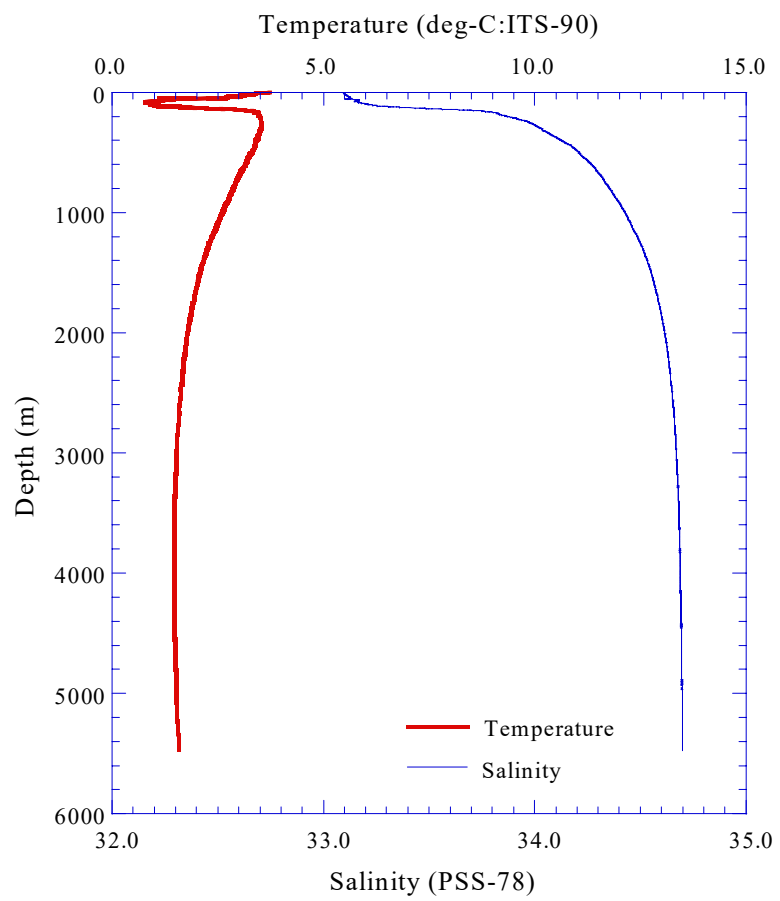


Fig.3.2.6.(a) CTD profile (Stn.05;005L01)

3.2-16

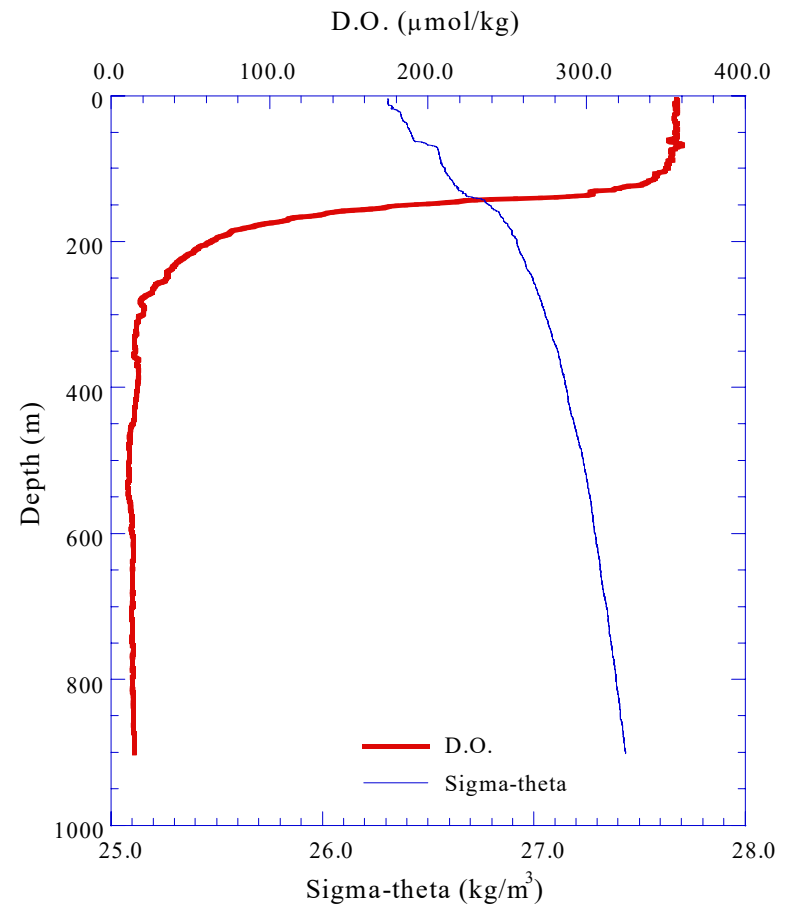
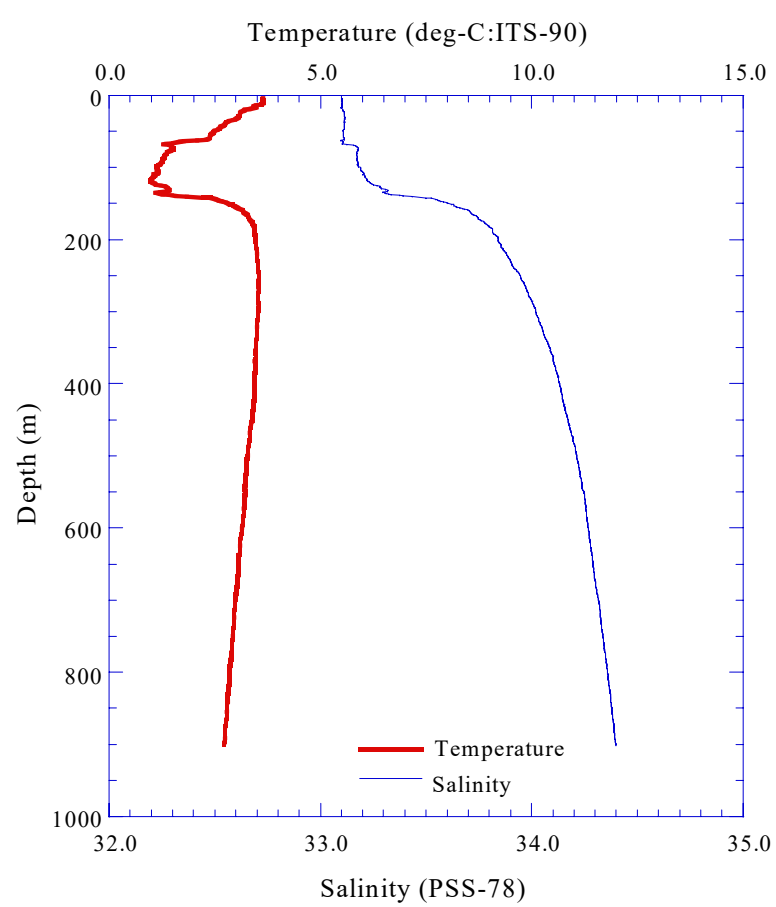


Fig.3.2.6.(b) CTD profile to 1,000m (Stn.05;005L02)

3.2-17

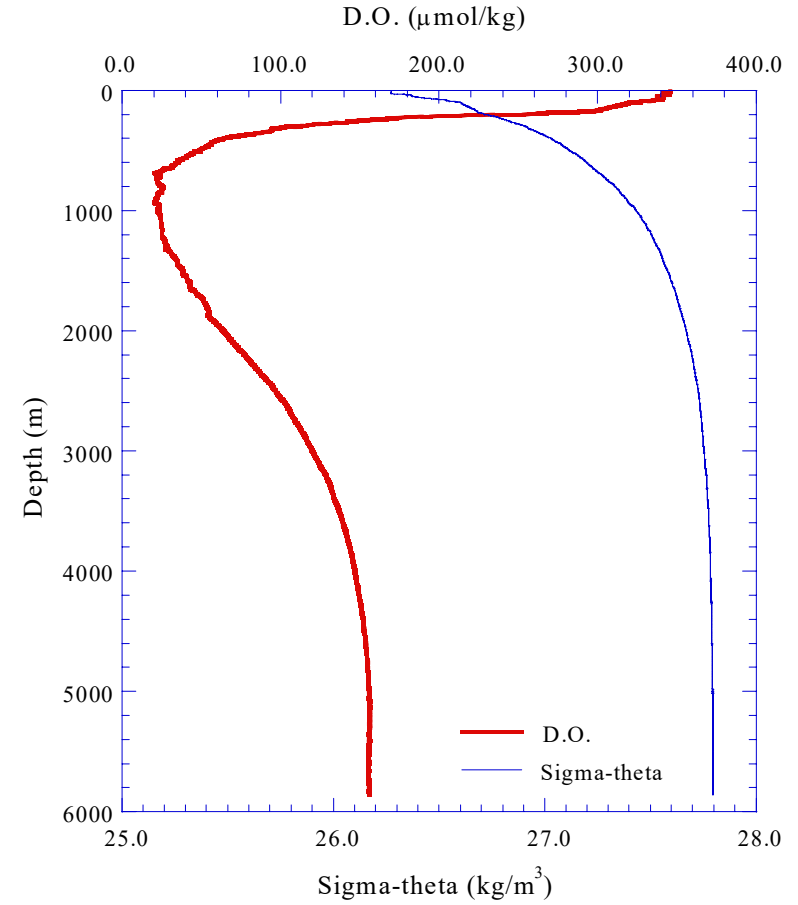
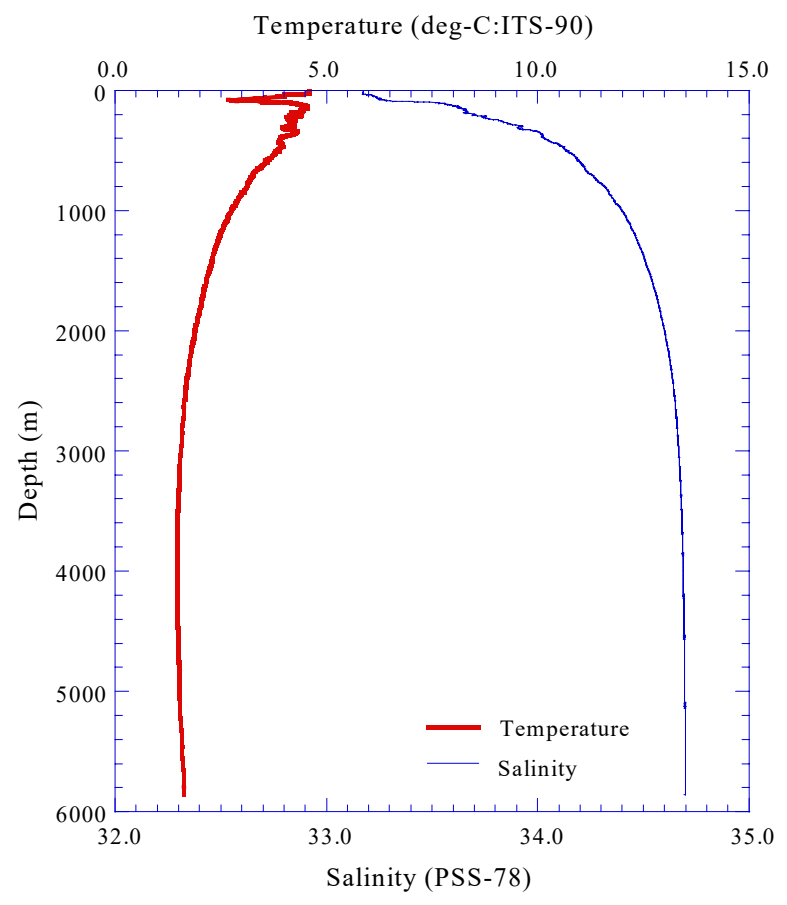


Fig.3.2.7.(a) CTD profile (Stn.07;007L01)

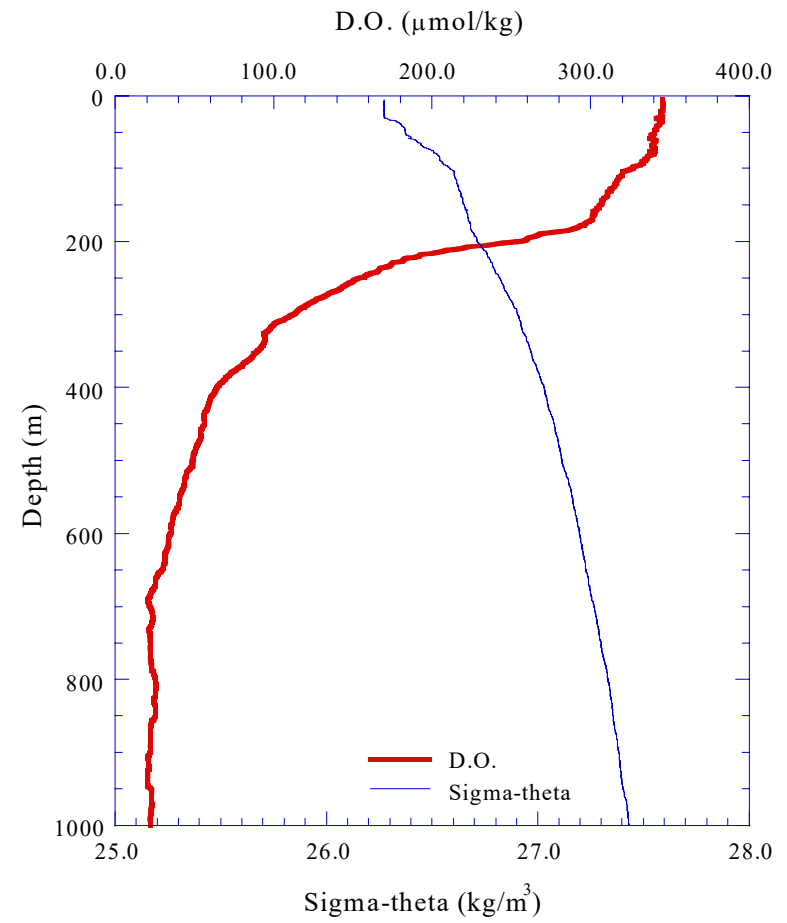
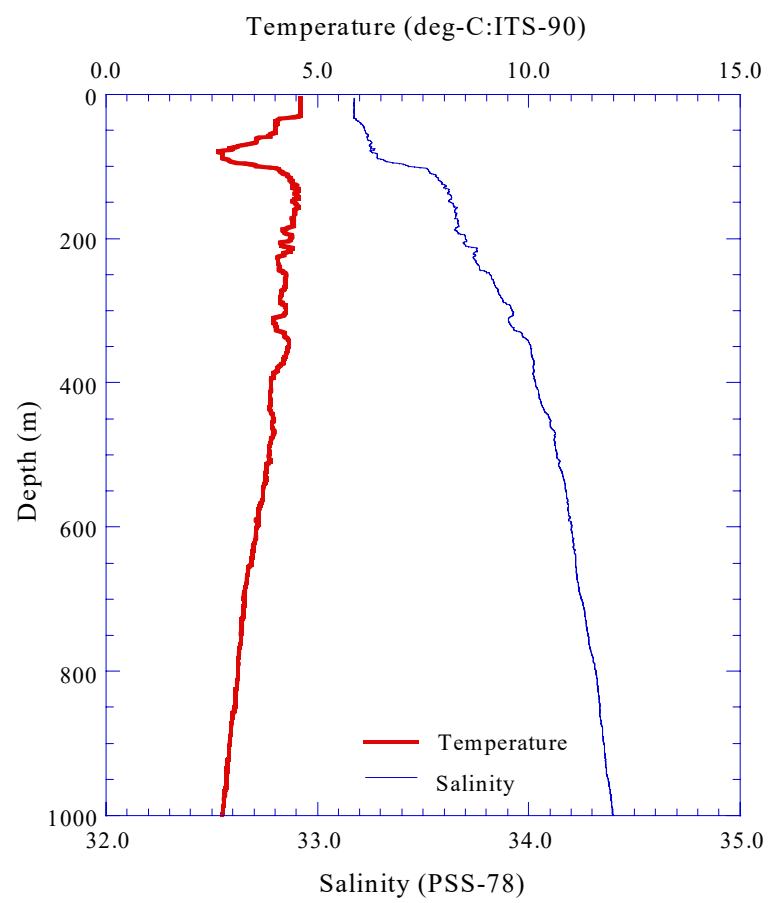


Fig.3.2.7.(b) CTD profile to 1,000m (Stn.07;007L01)

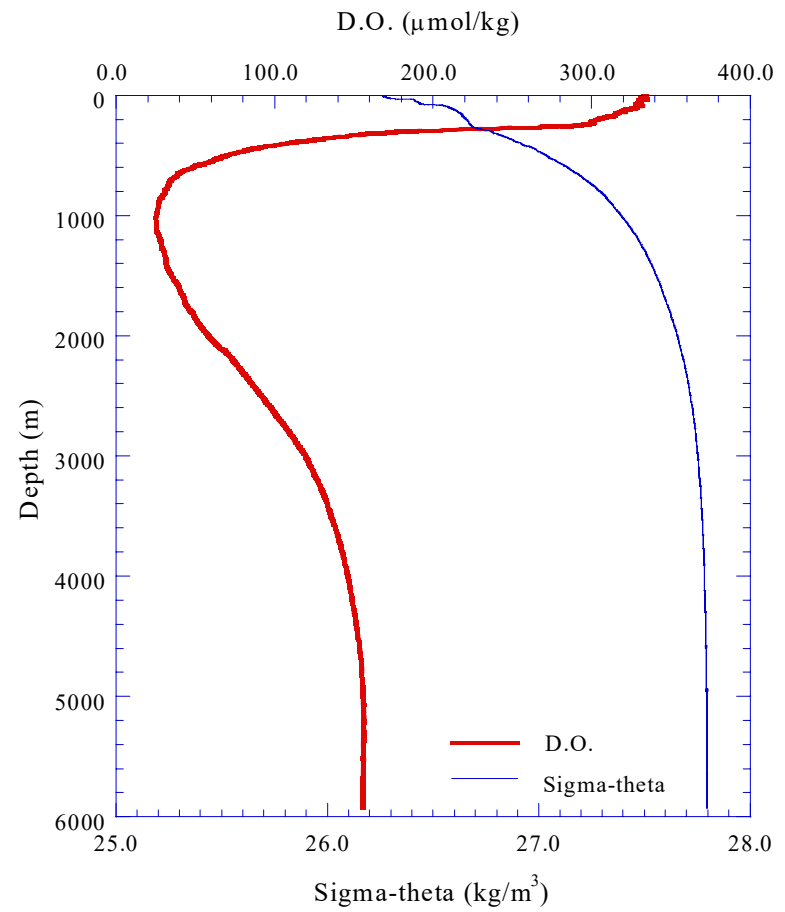
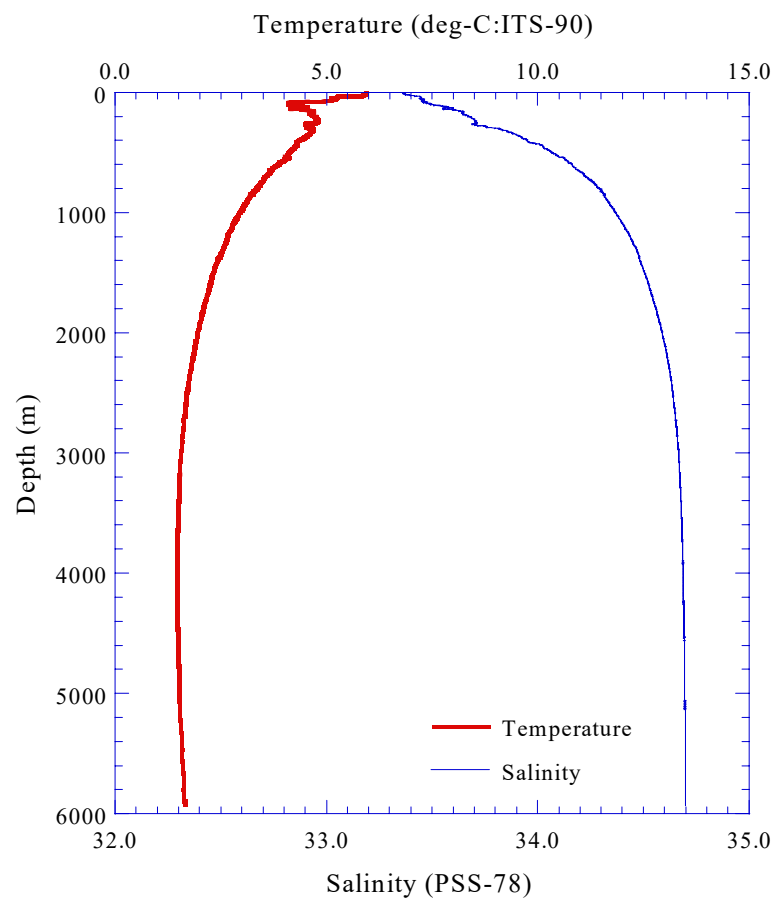


Fig.3.2.8.(a) CTD profile (Stn.08;008L01)

3.2-20

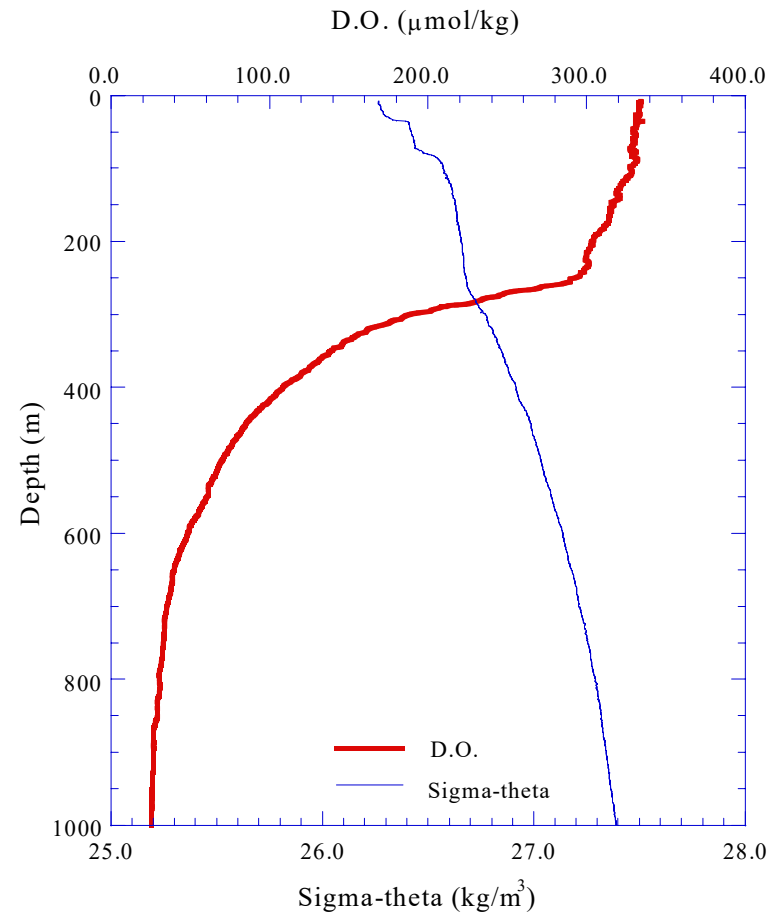
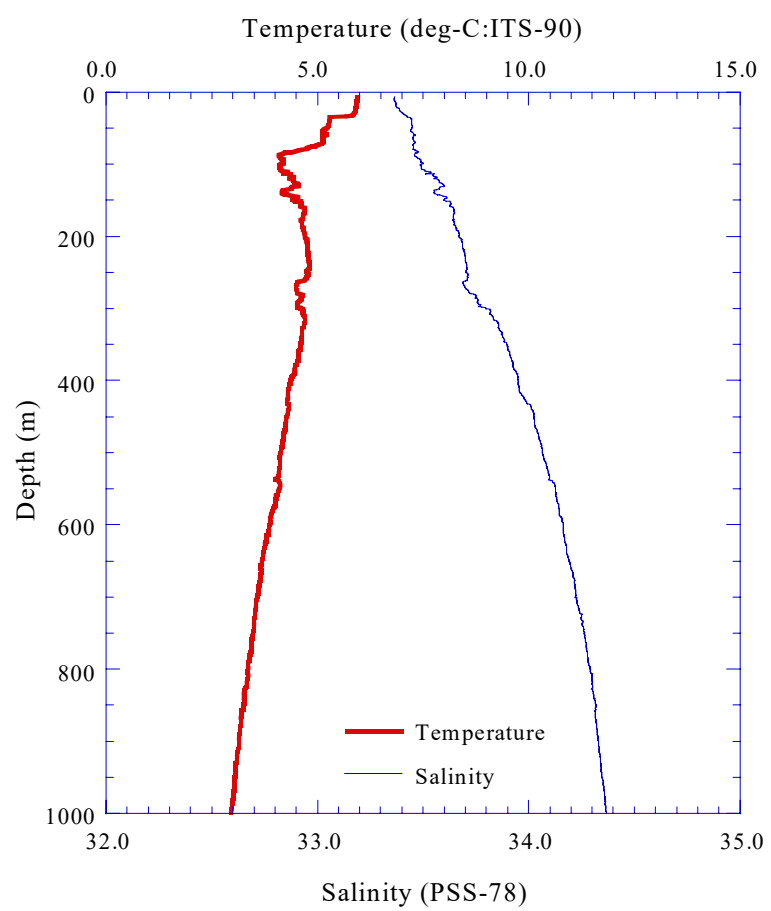


Fig.3.2.8.(b) CTD profile to 1,000m (Stn.08;008L01)

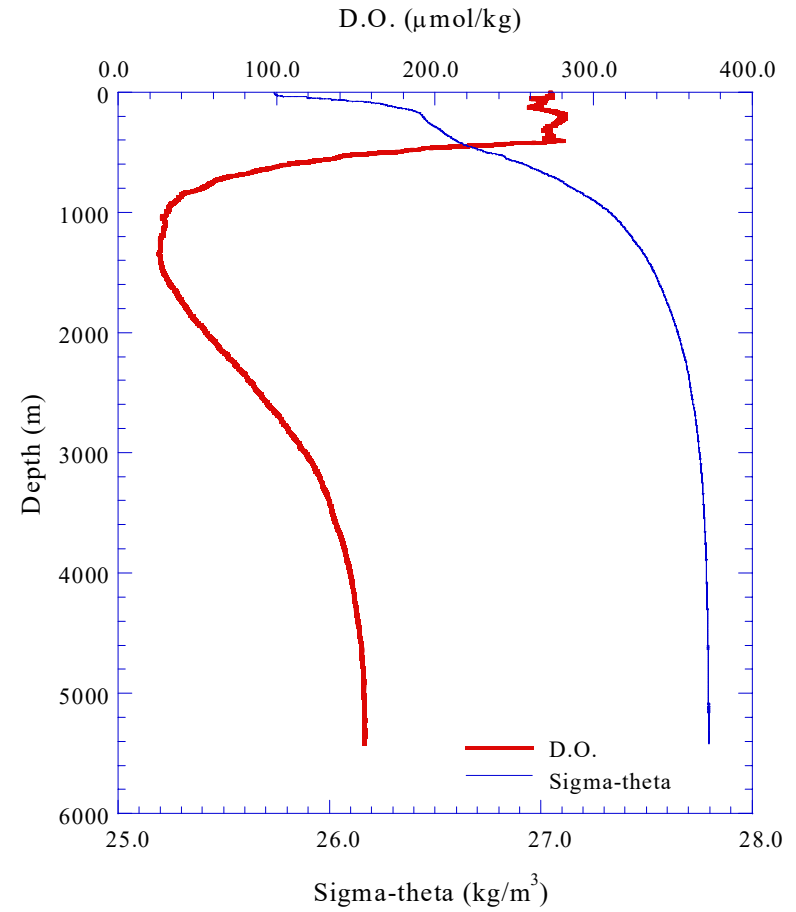
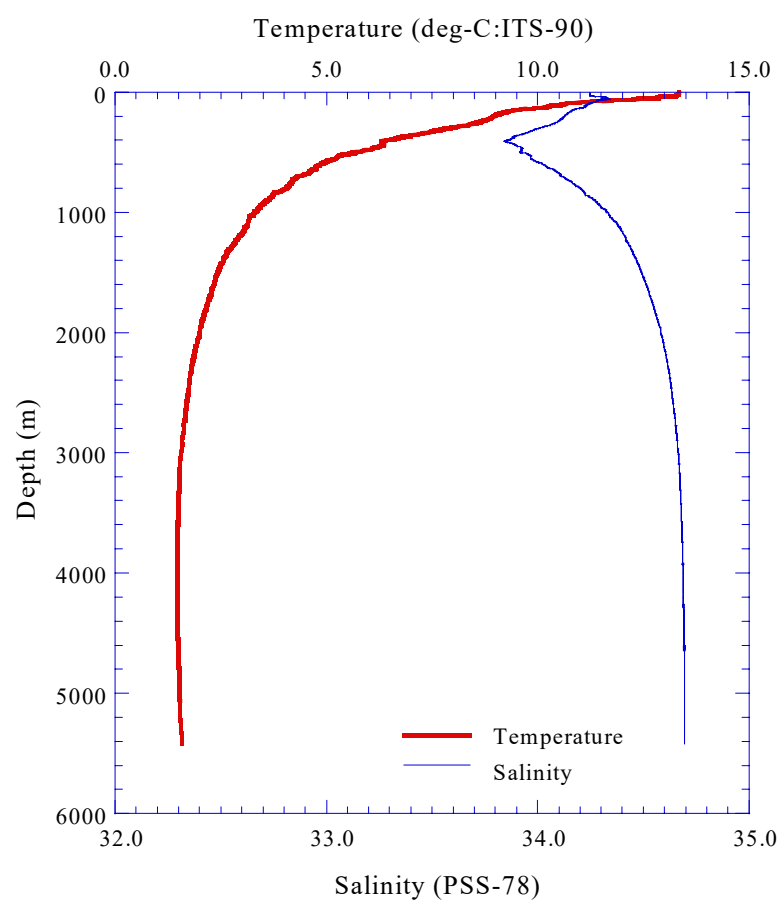


Fig.3.2.9.(a) CTD profile (Stn.11;011L02)

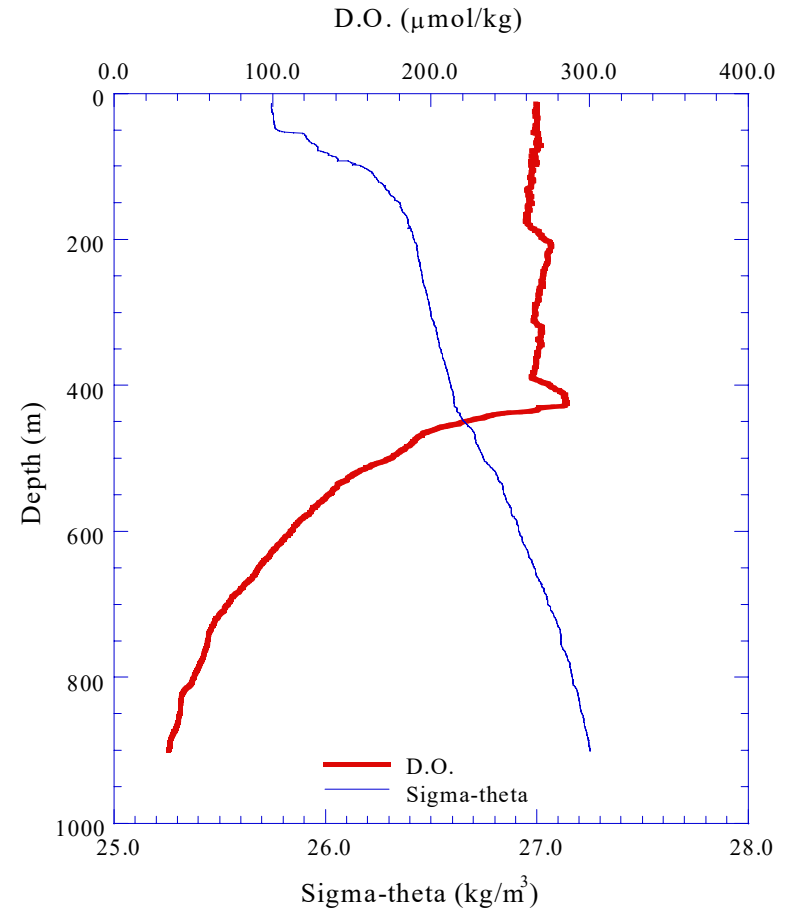
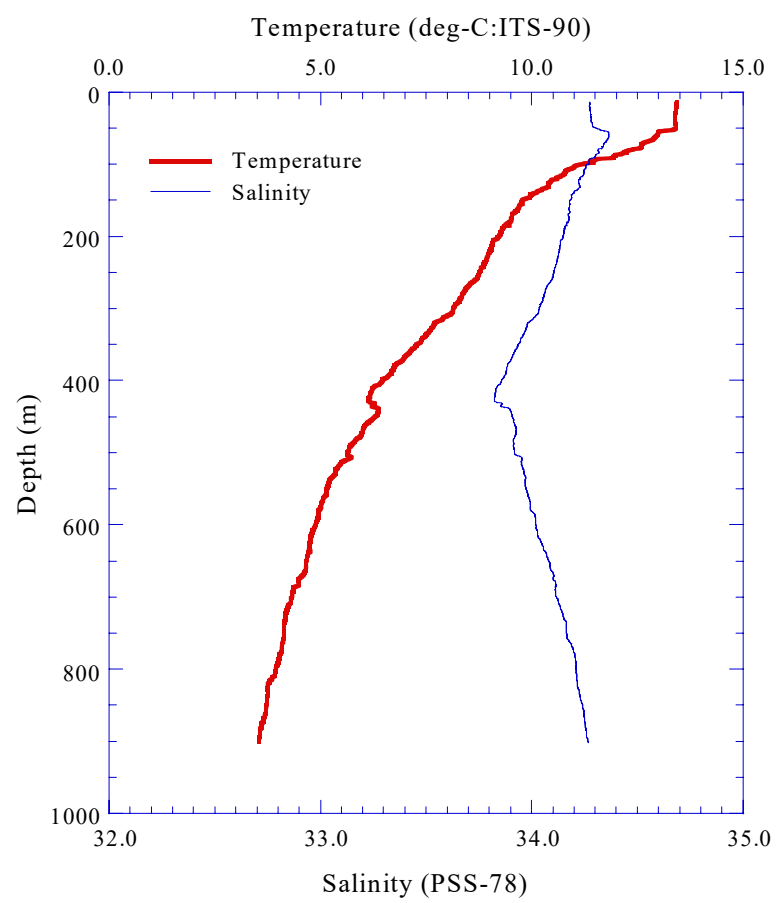


Fig.3.2.9.(b) CTD profile to 1,000m (Stn.11;011L01)

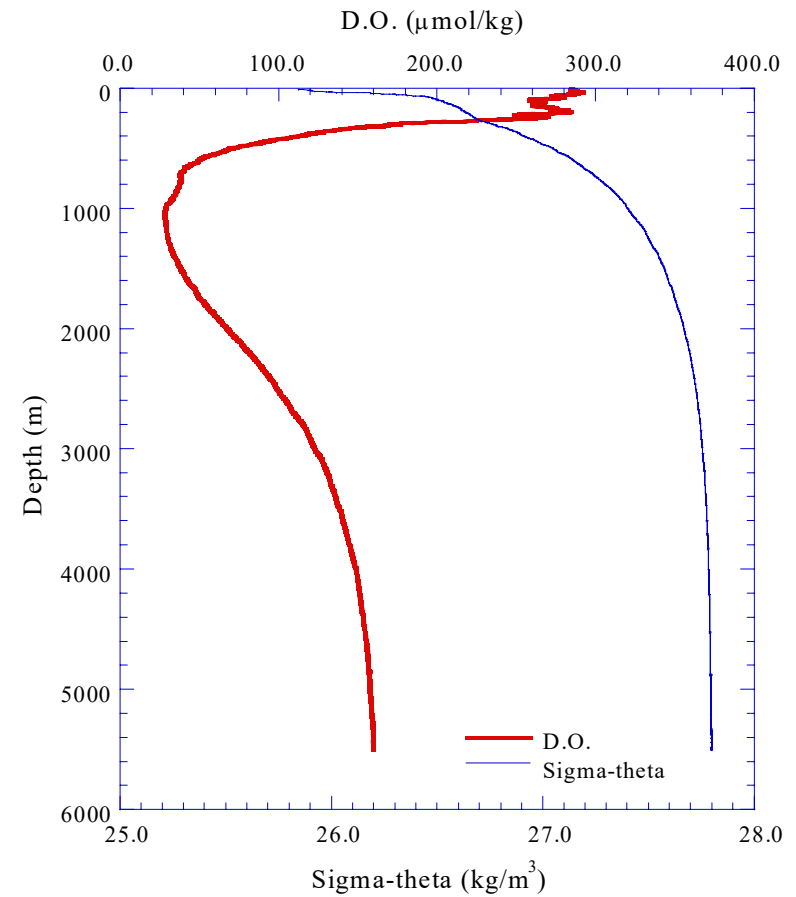
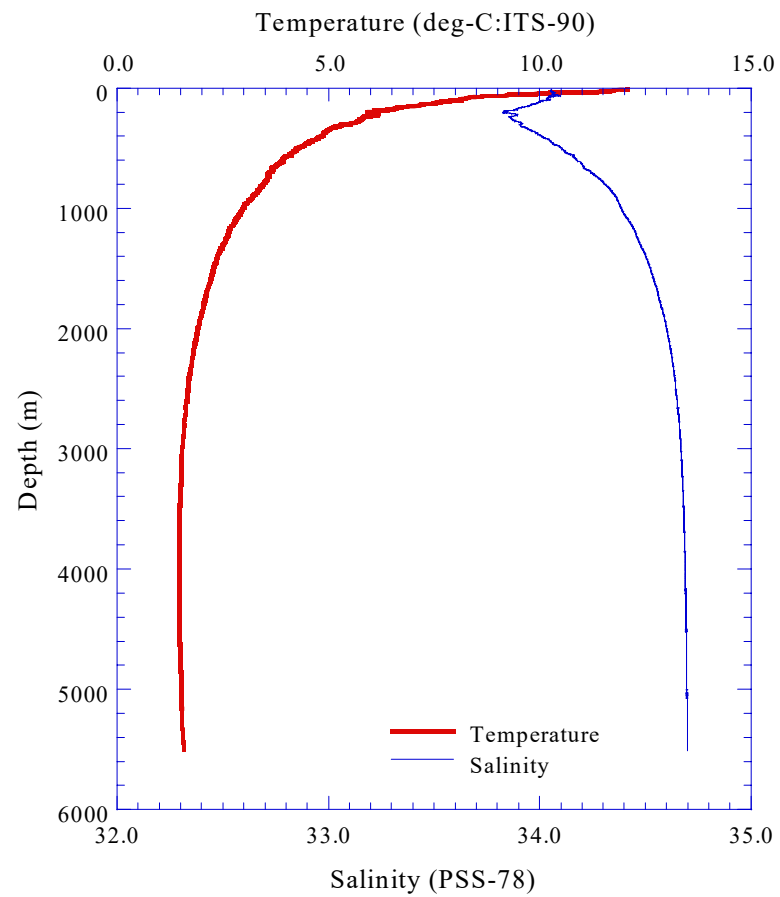


Fig.3.2.10.(a) CTD profile (Stn.12;012L01)

3.2-24

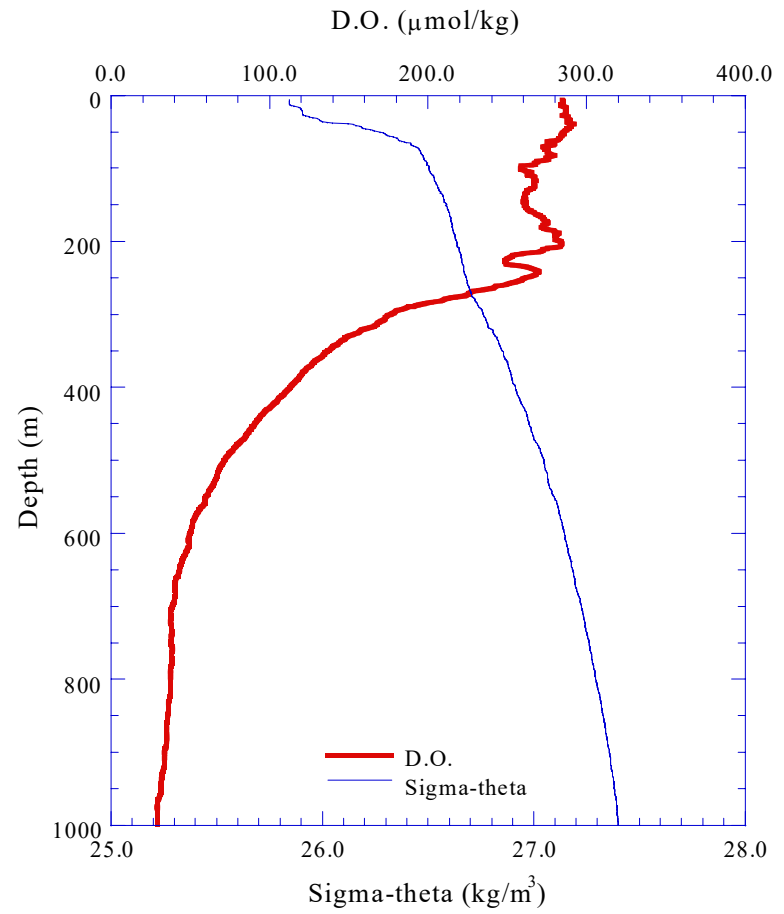
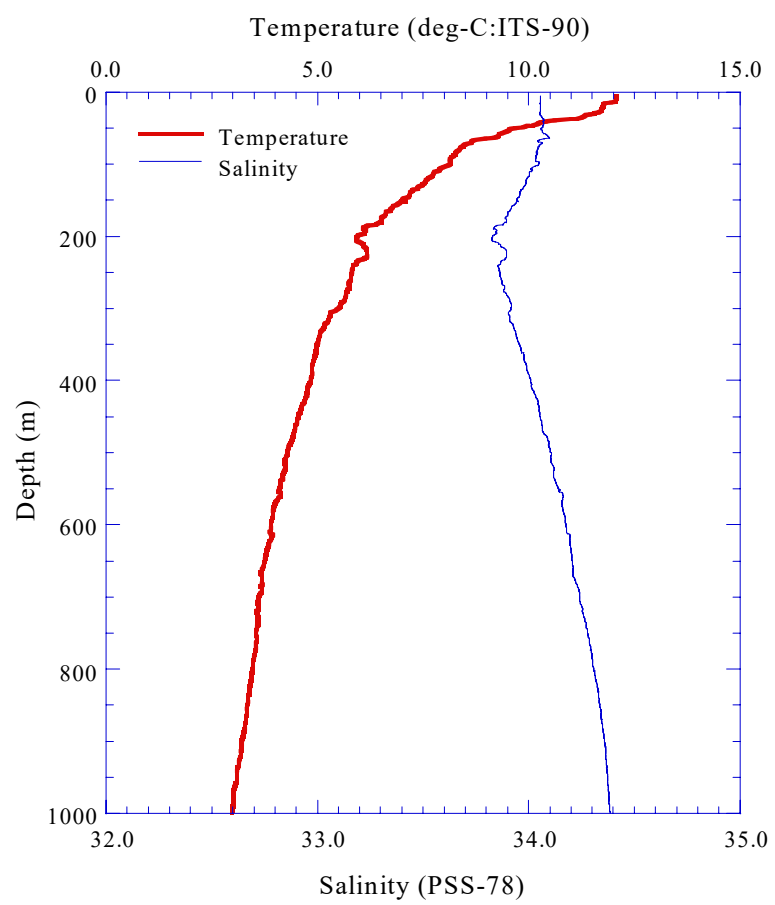


Fig.3.2.10.(b) CTD profile to 1,000m (Stn.12;012L01)

3.2-25

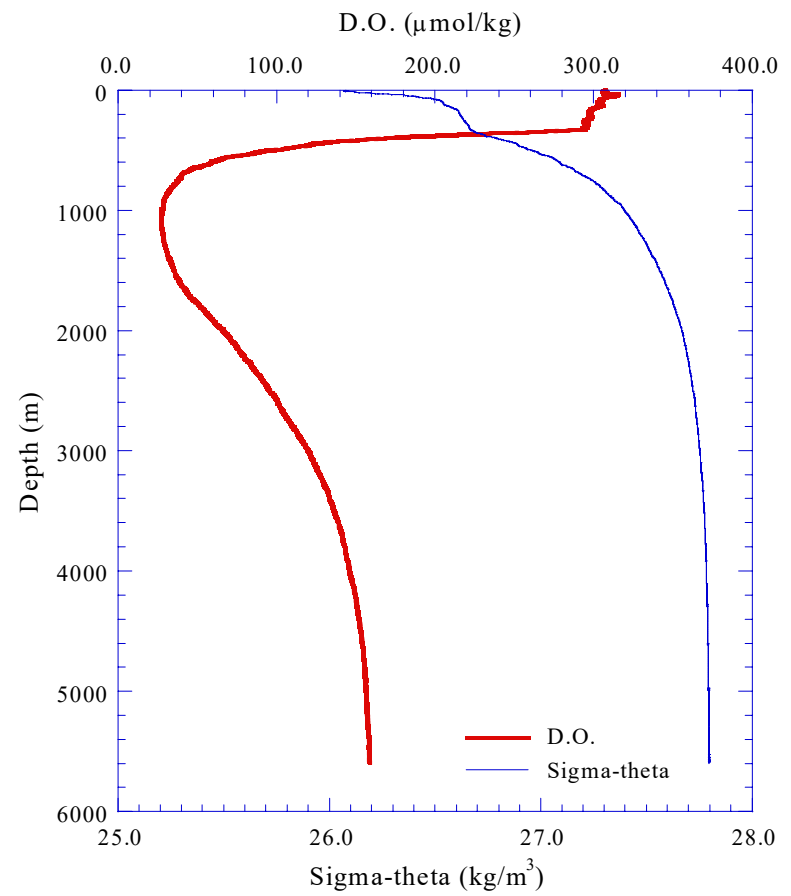
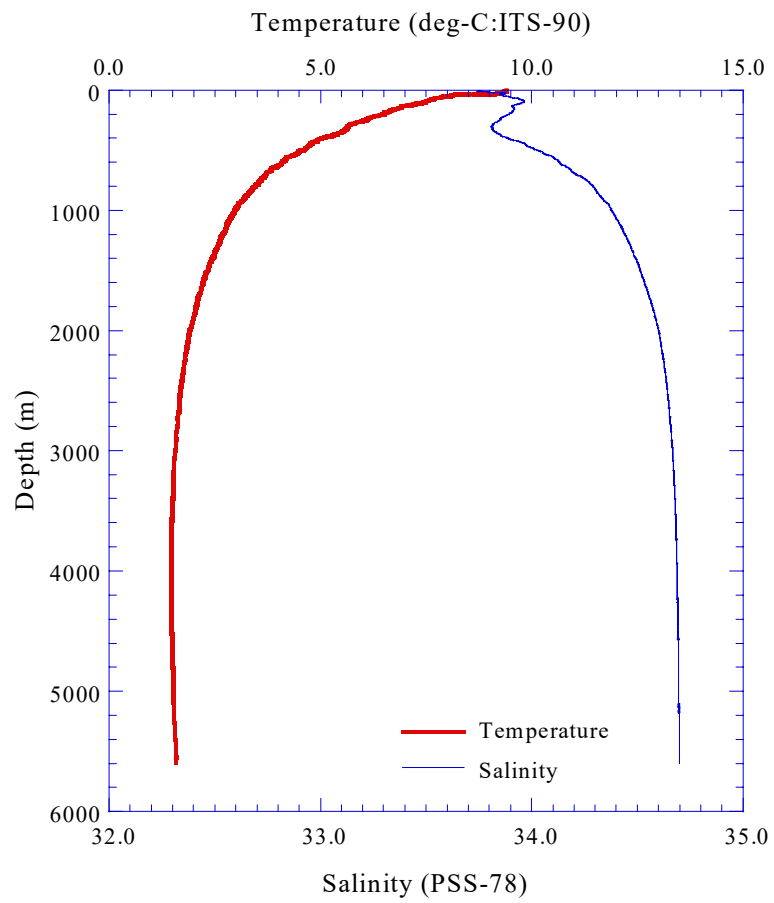


Fig.3.2.11.(a) CTD profile (Stn.13;013L01)

3.2-26

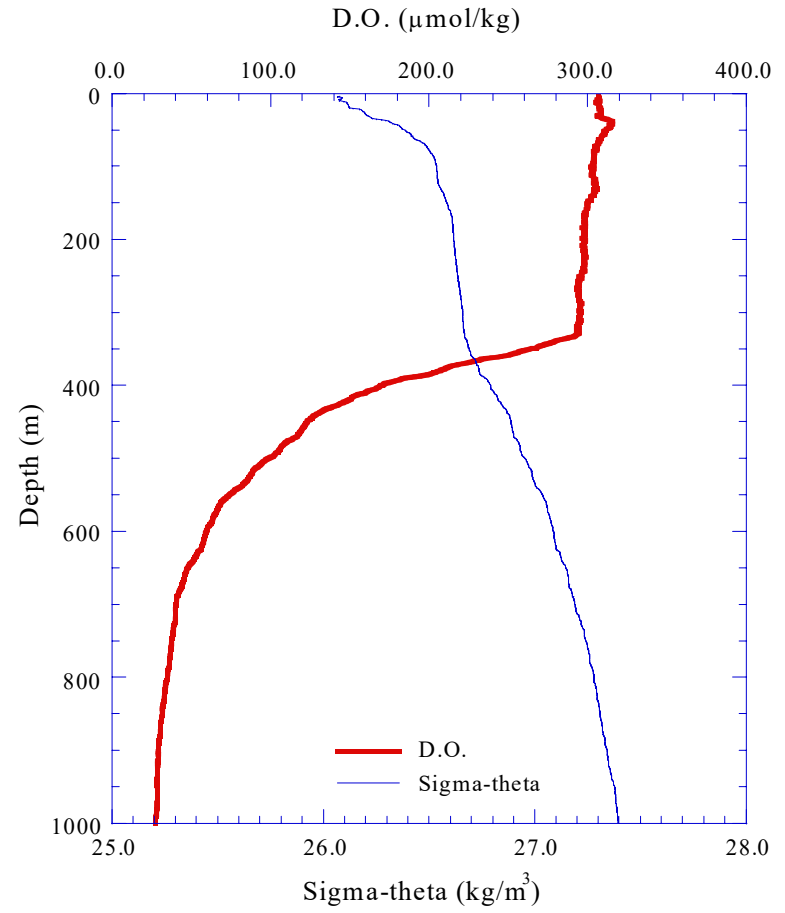
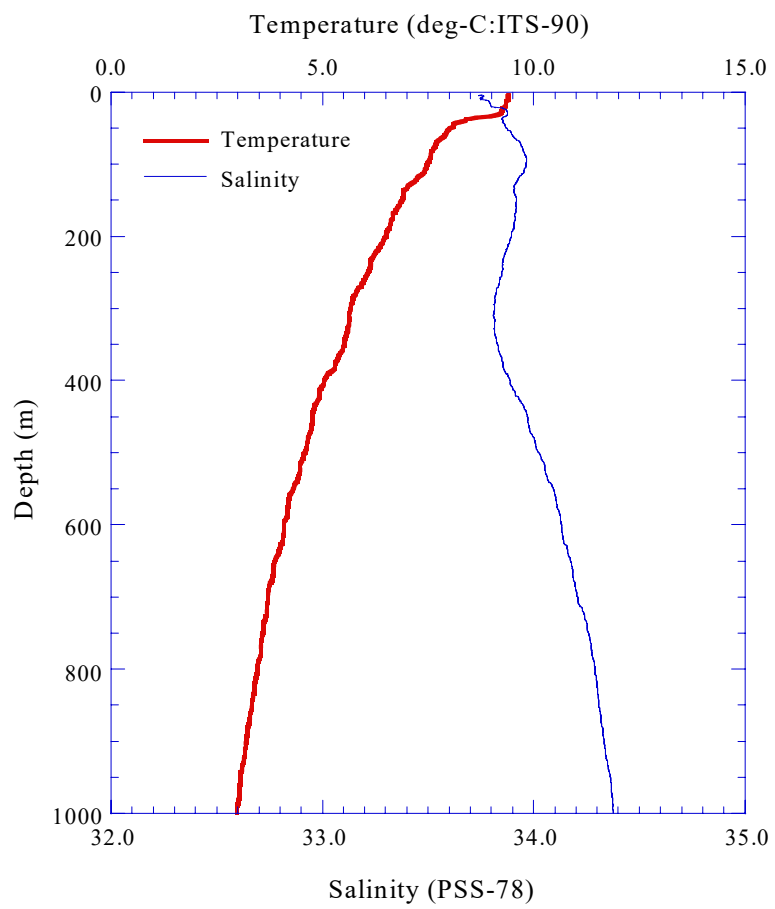


Fig.3.2.11.(b) CTD profile to 1,000m (Stn.13;013L01)

3.2-27

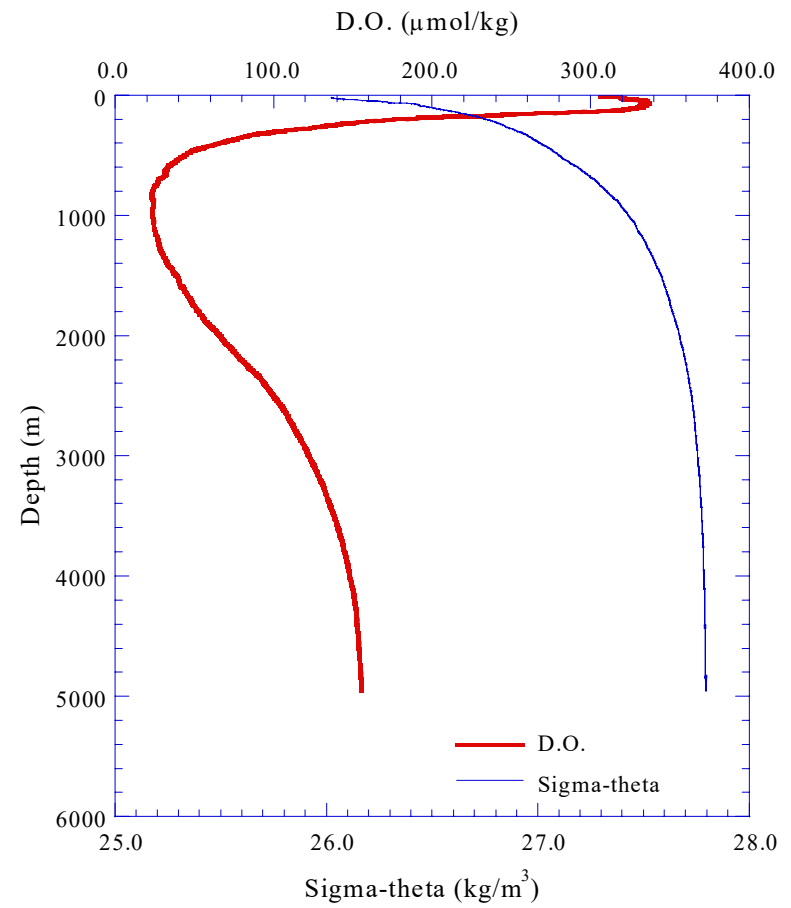
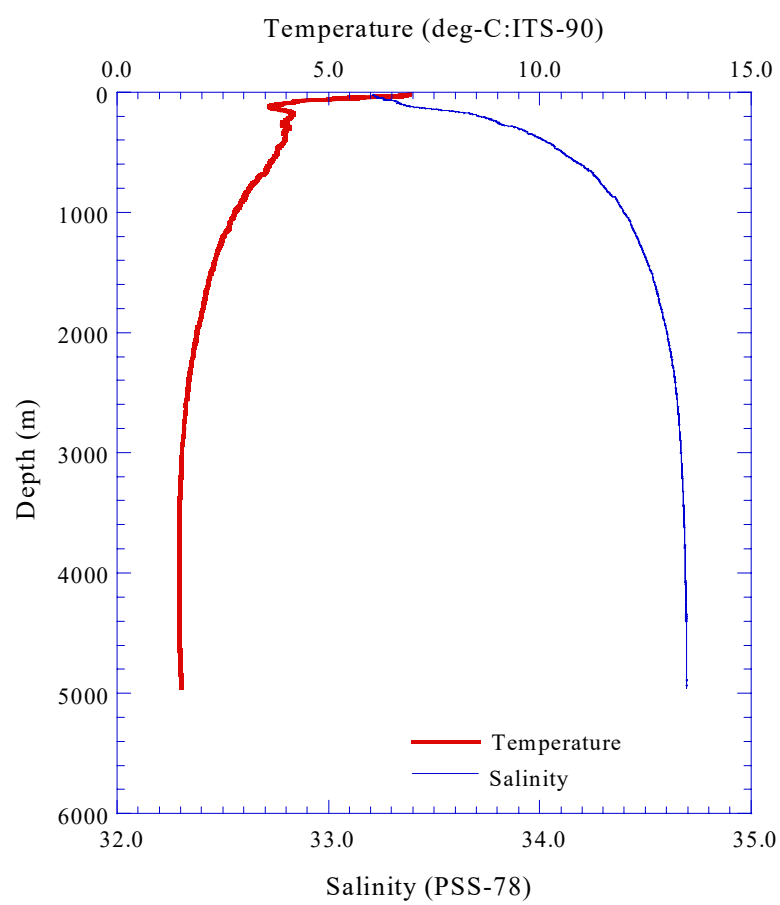


Fig.3.2.12.(a) CTD profile (Stn.10;010L01)

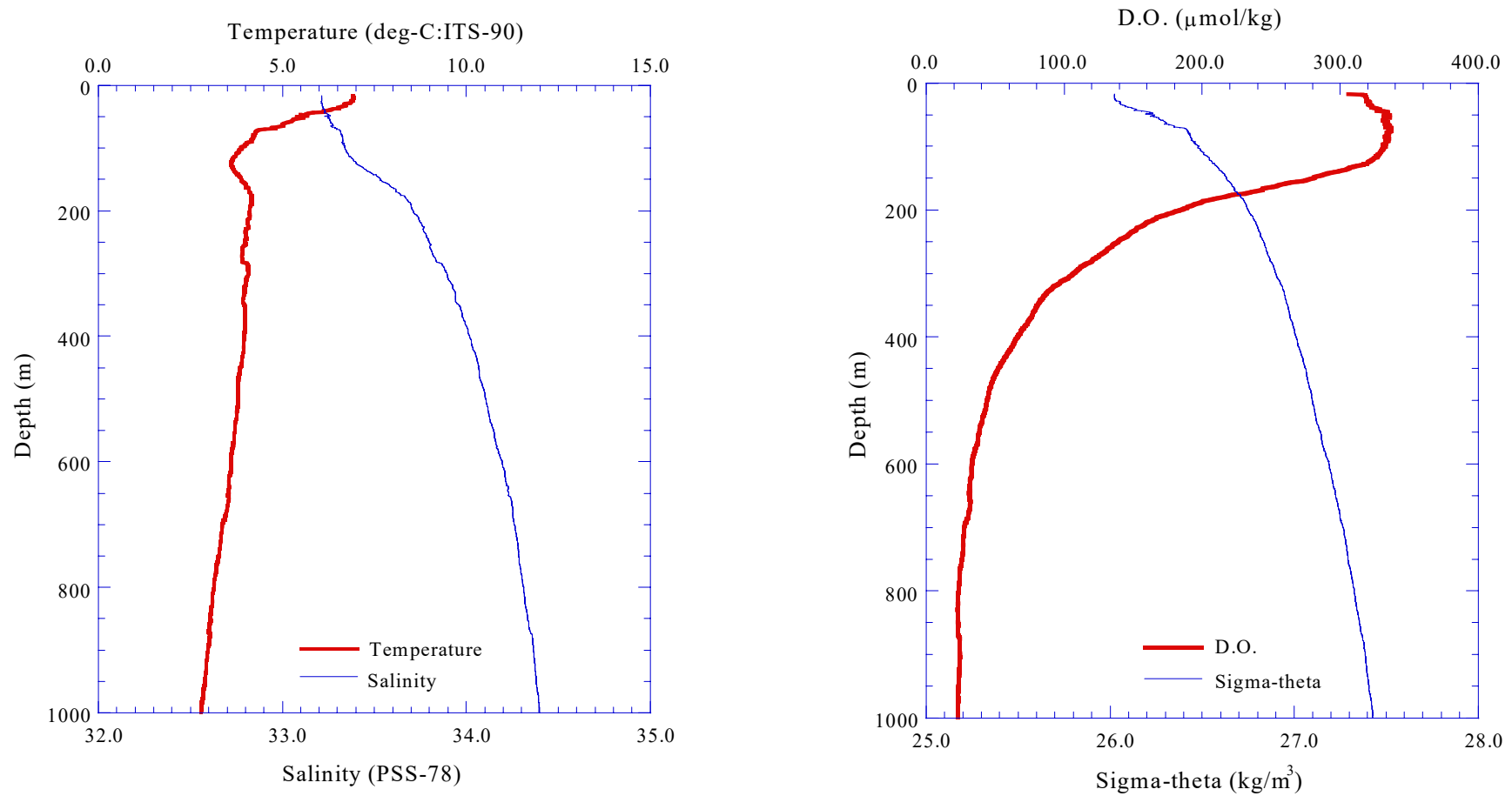


Fig.3.2.12.(b) CTD profile to 1,000m (Stn.10;010L01)

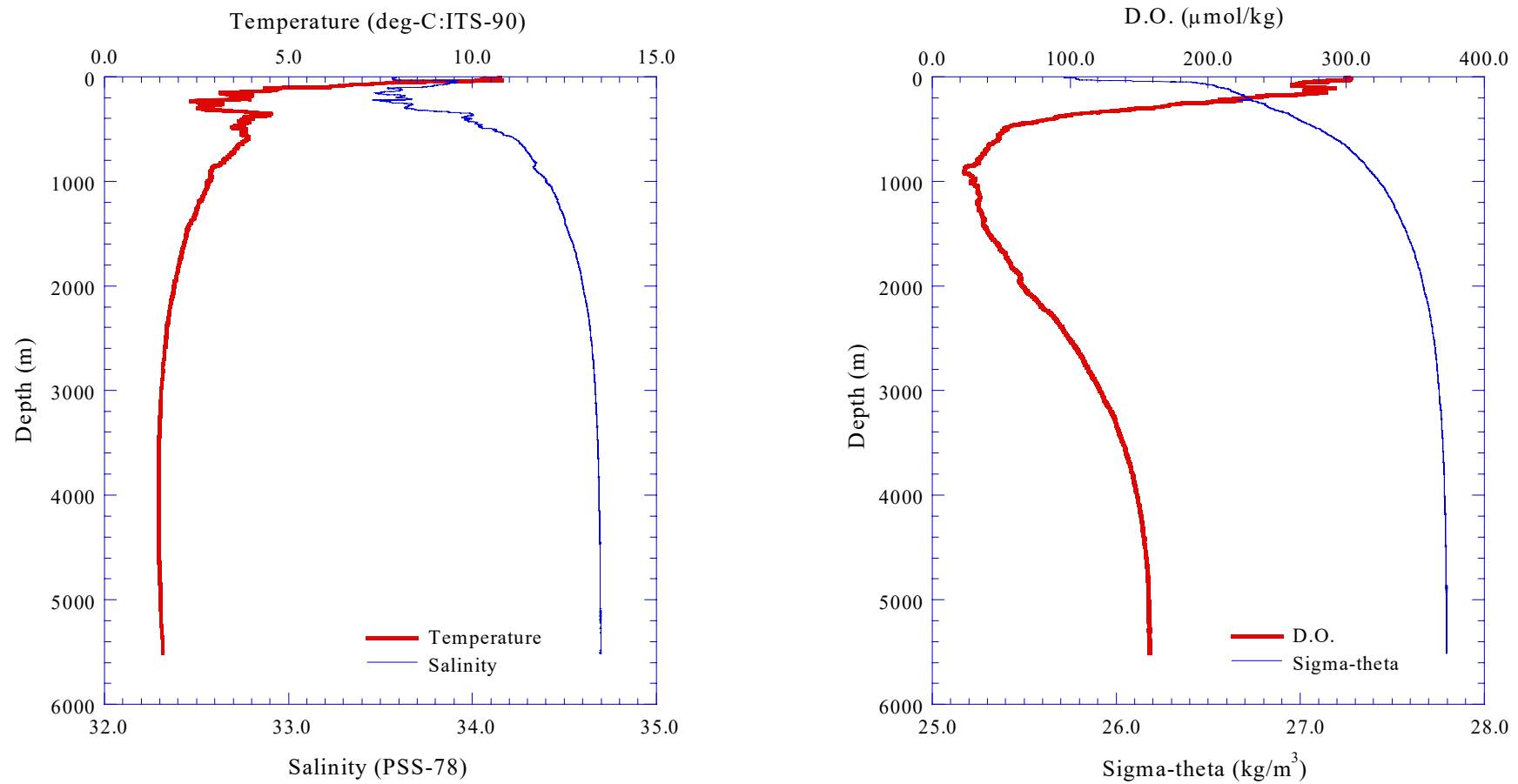


Fig.3.2.13.(a) CTD profile (Stn.14;014L01)

3.2-30

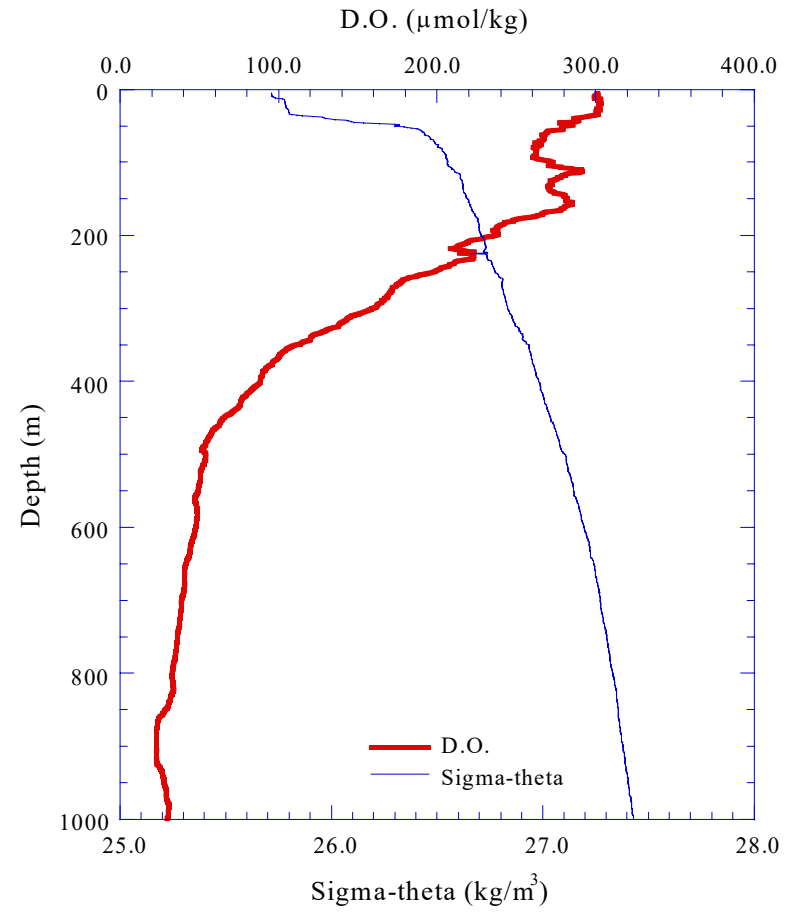
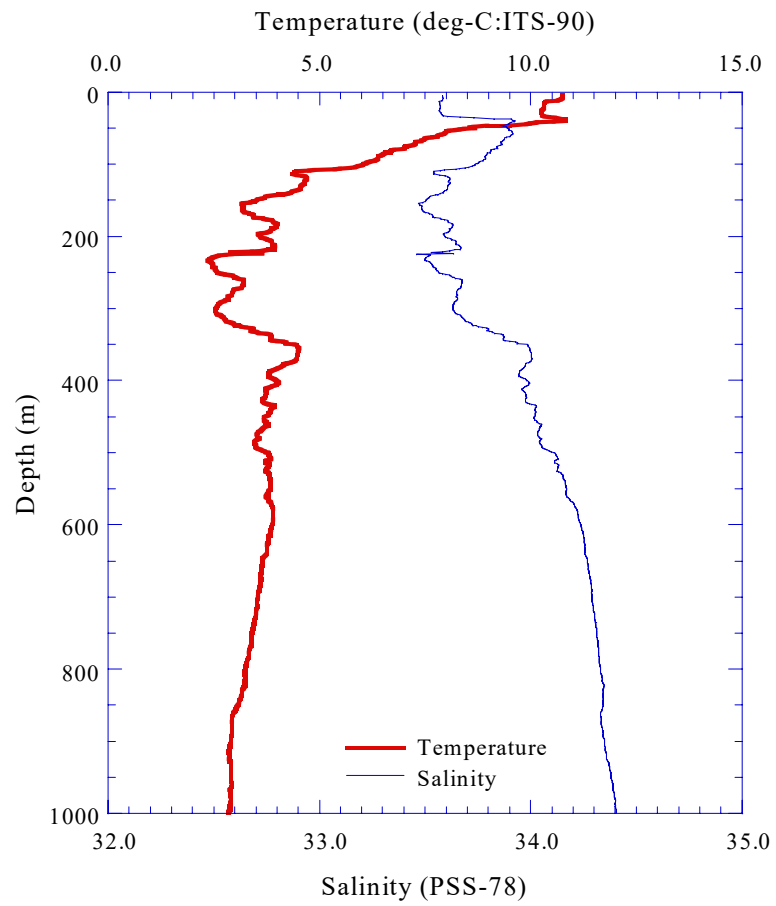


Fig.3.2.13.(b) CTD profile to 1,000m (Stn.14;014L01)

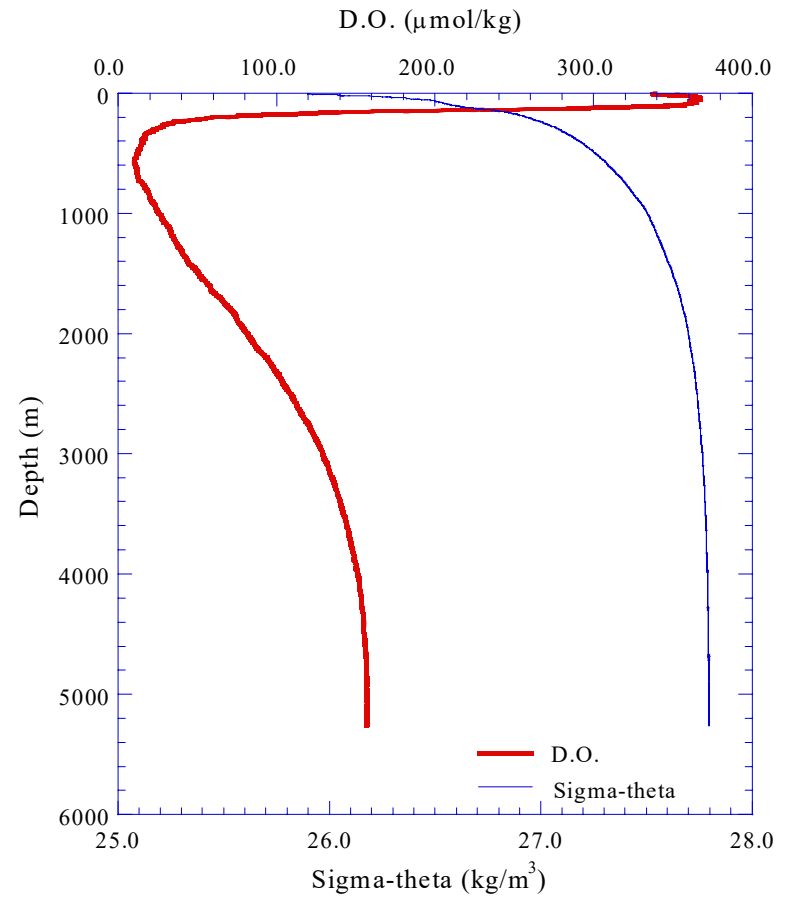
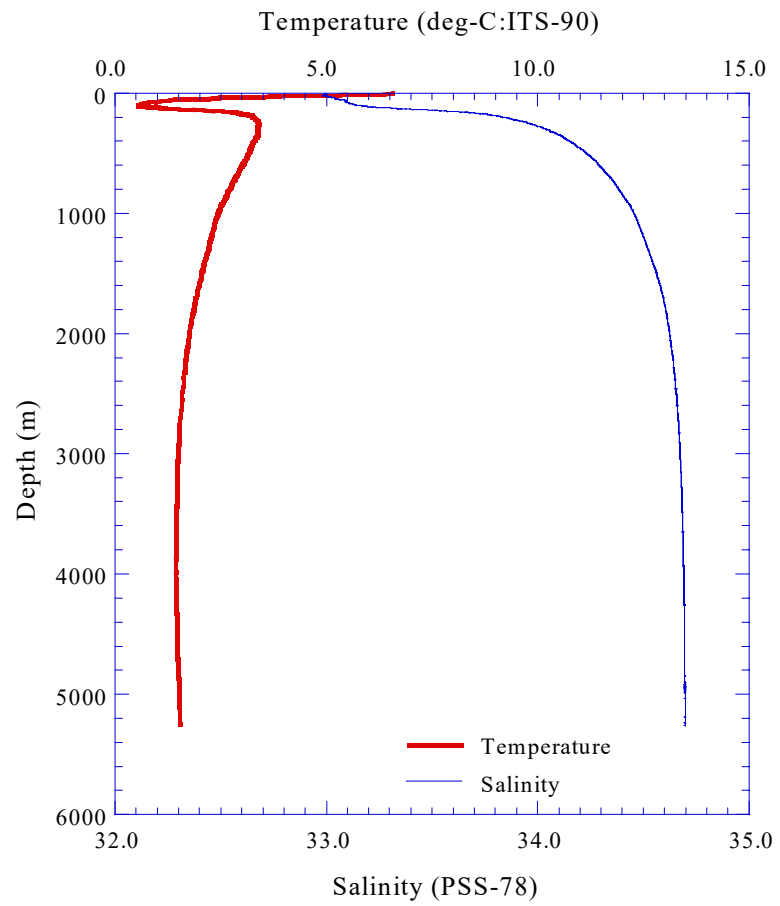


Fig.3.2.14.(a) CTD profile (Stn.1R;01RL01)

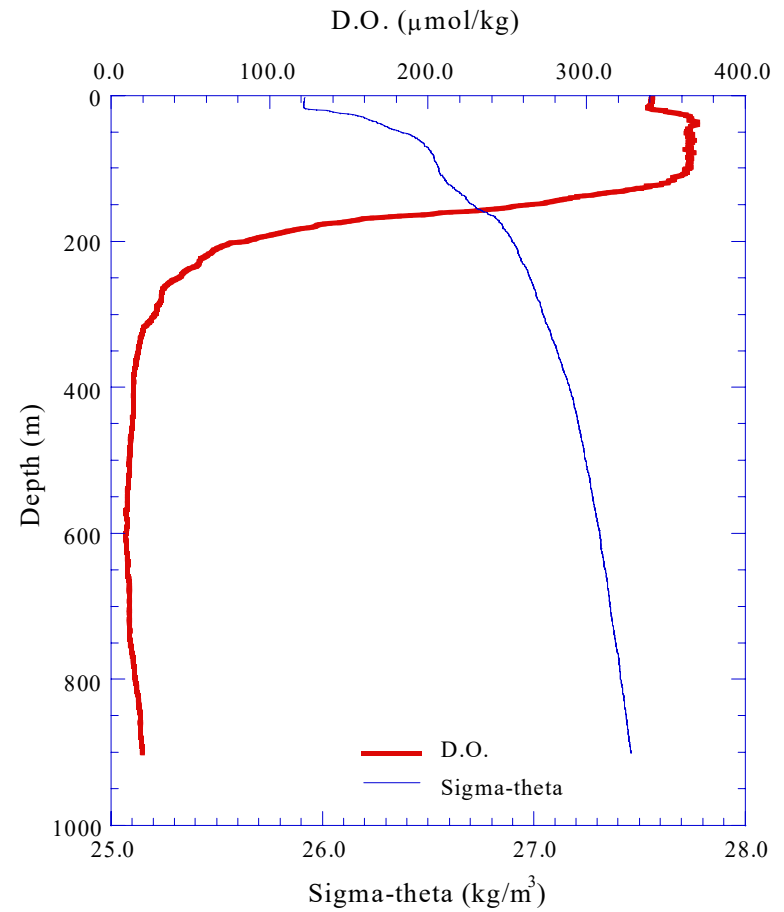
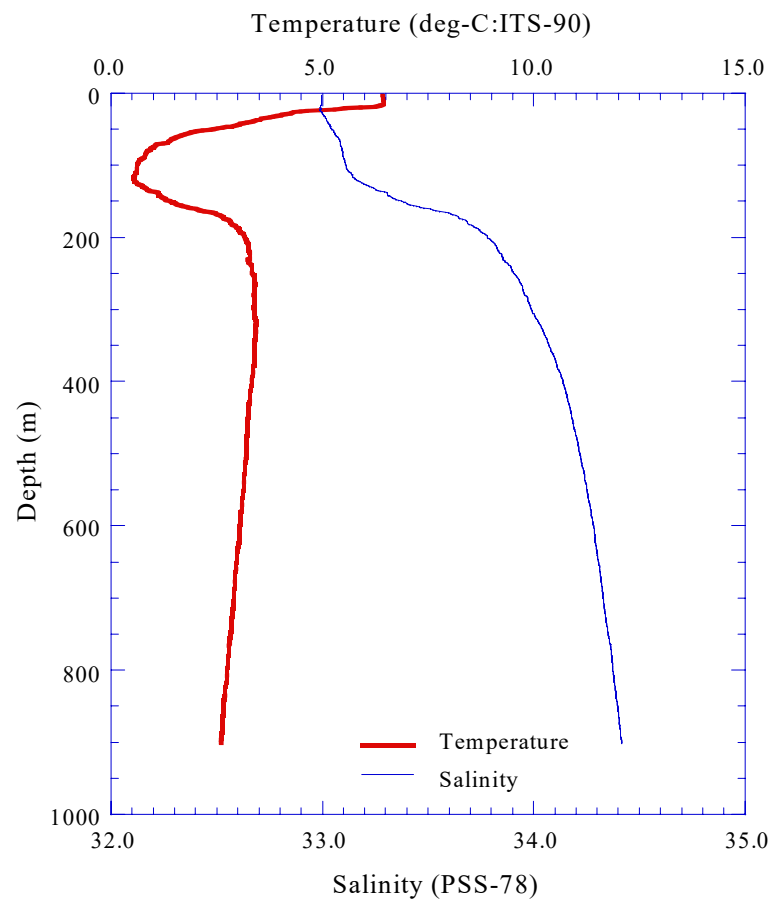


Fig.3.2.14.(b) CTD profile to 1,000m (Stn.1R;01RL02)

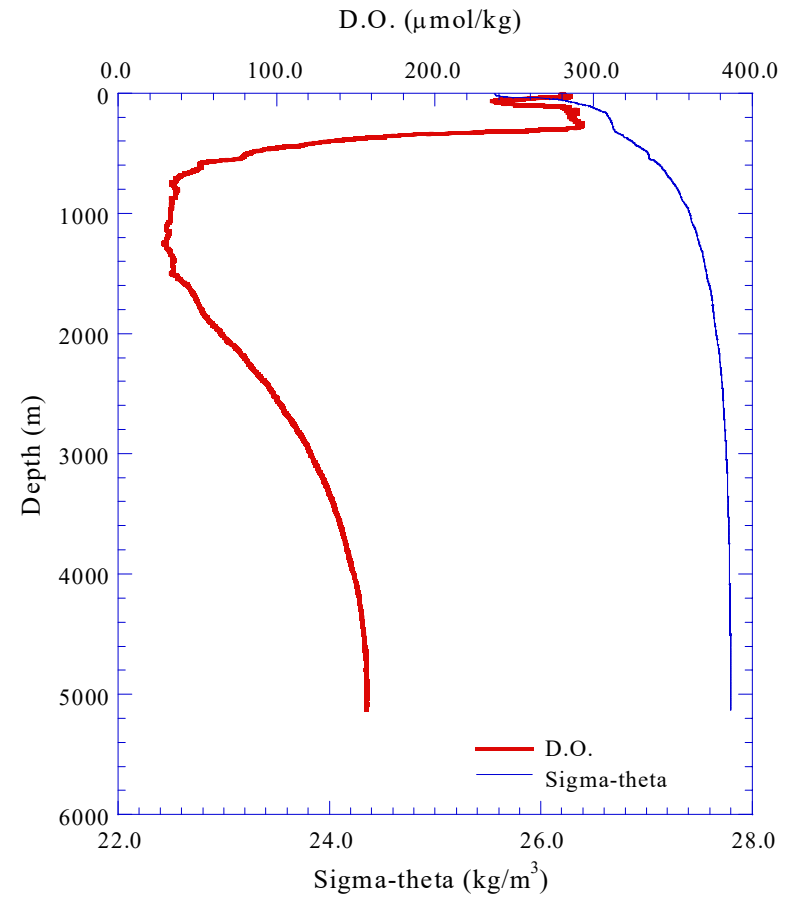
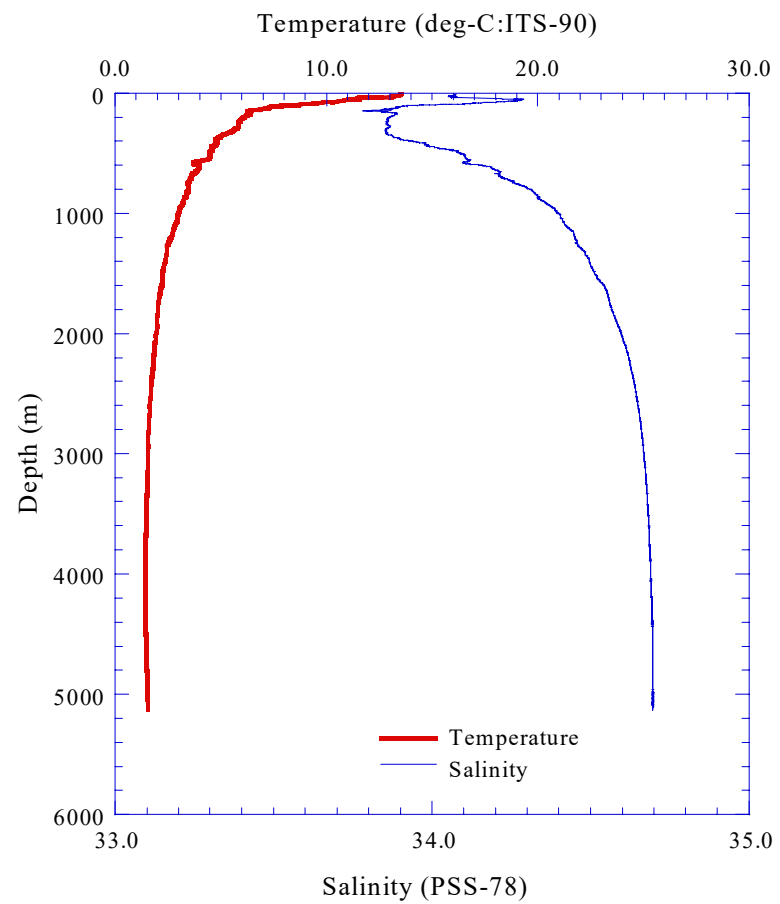


Fig.3.2.15.(a) CTD profile (Stn.15;015L01)

3.2-34

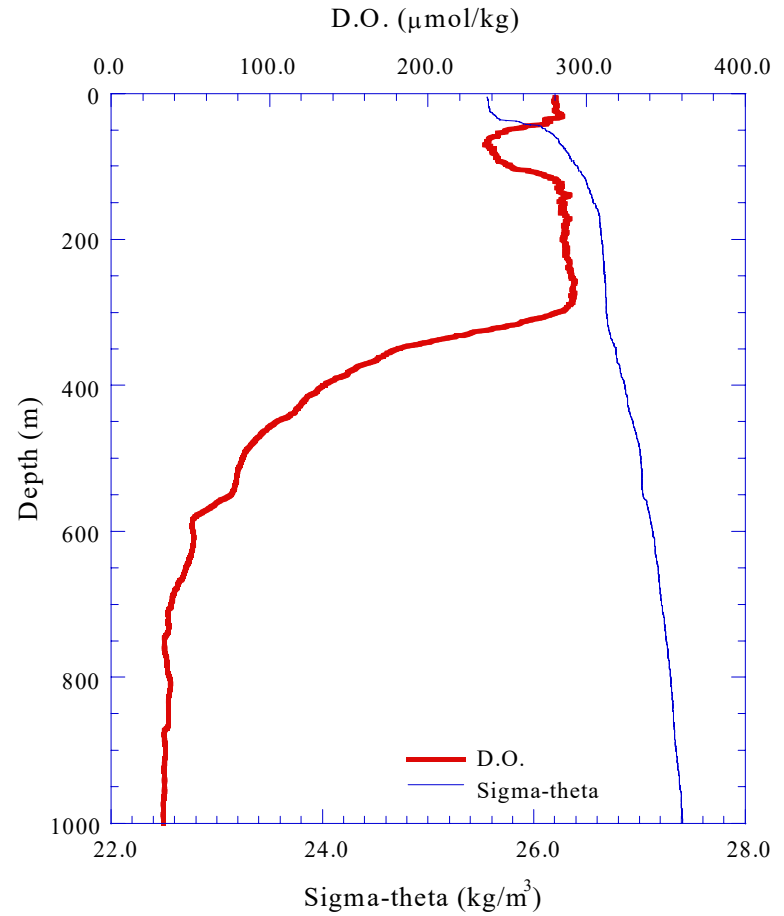
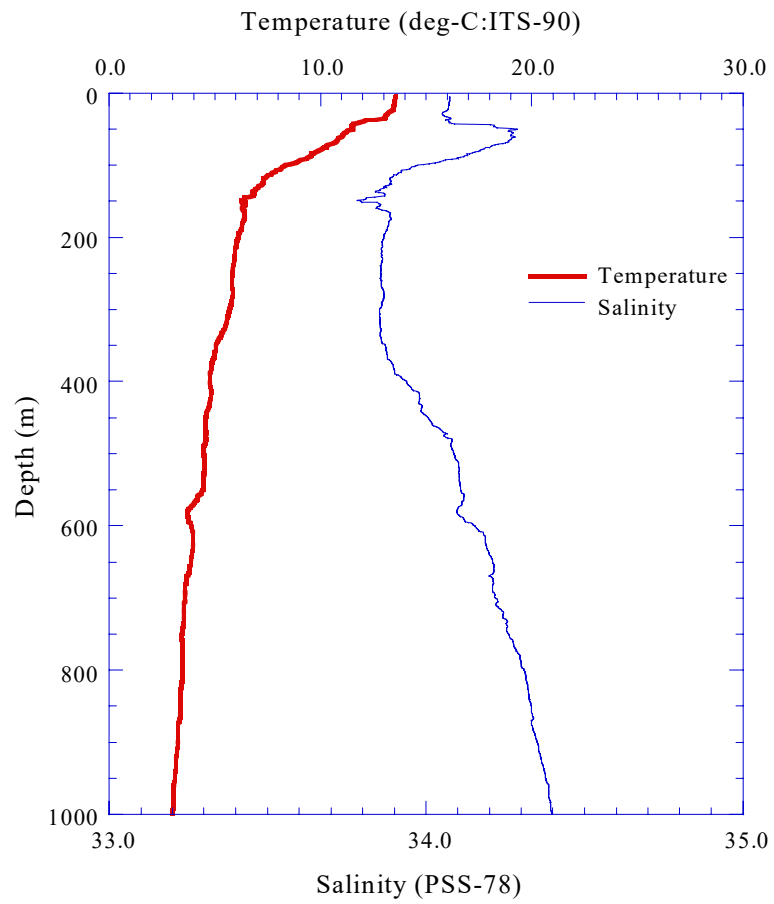


Fig.3.2.15.(b) CTD profile to 1,000m (Stn.15;015L01)

3.2-35

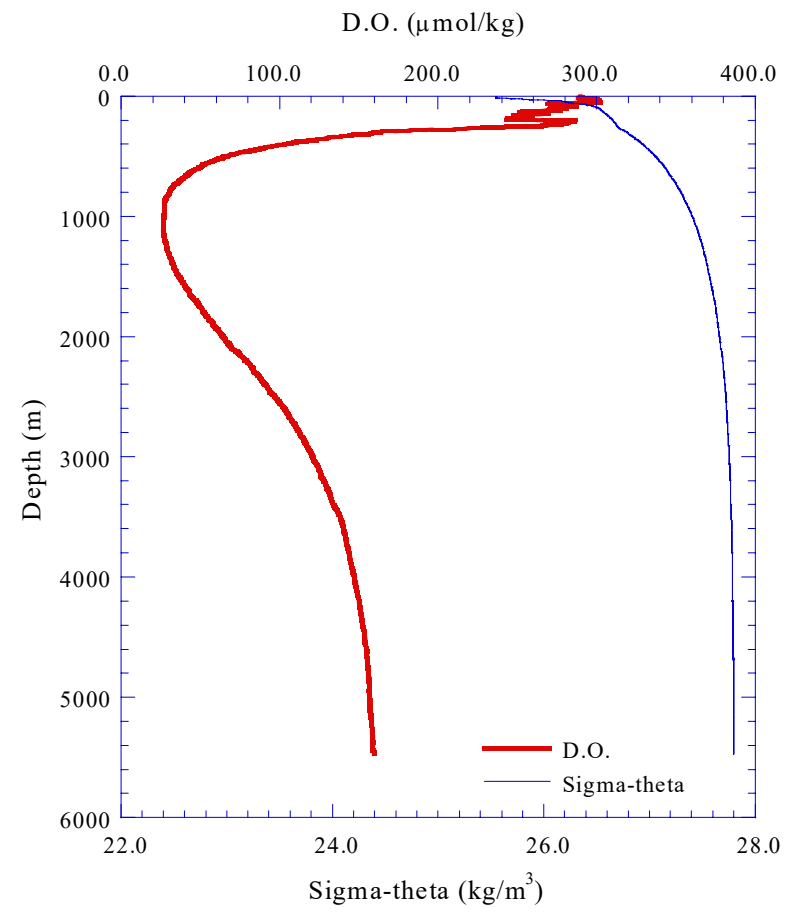
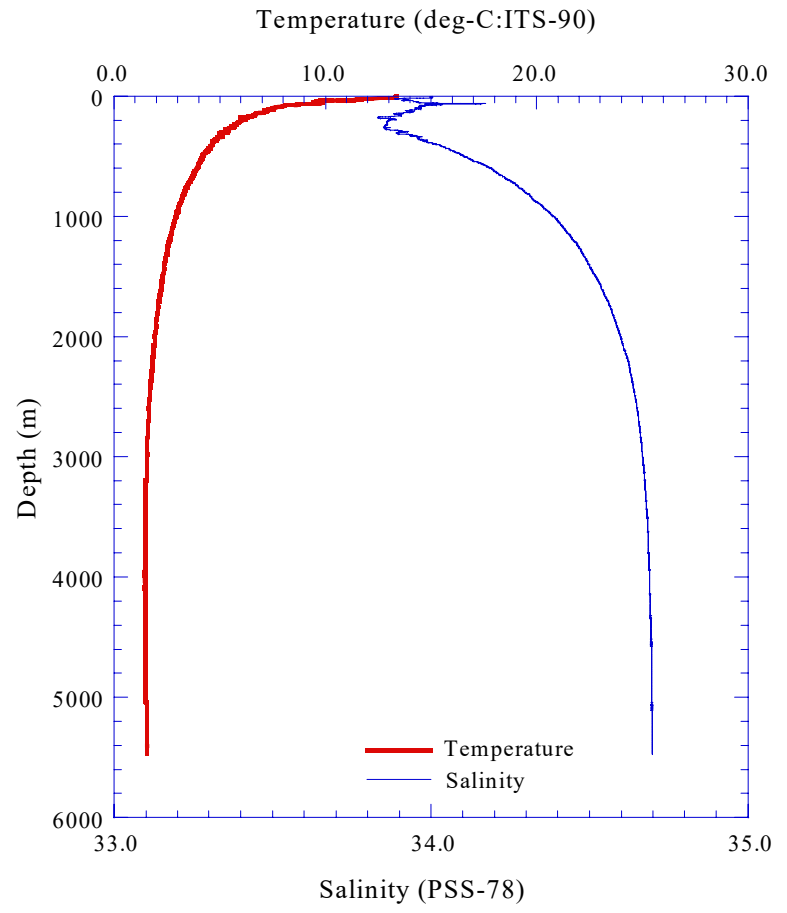


Fig.3.2.16.(a) CTD profile (Stn.16;016L01)

3.2-36

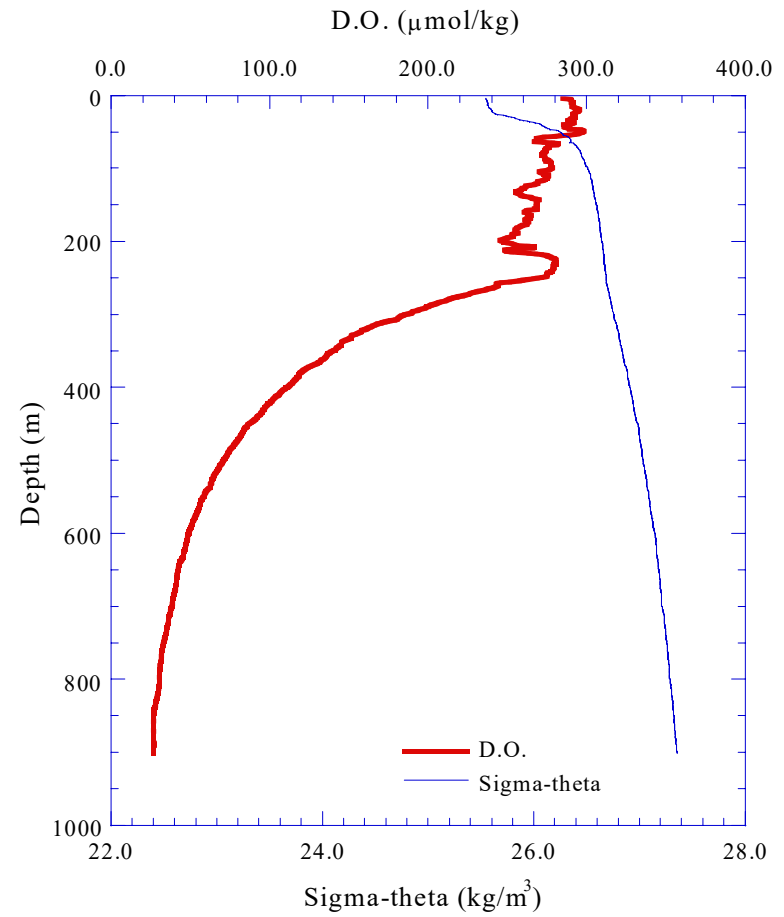
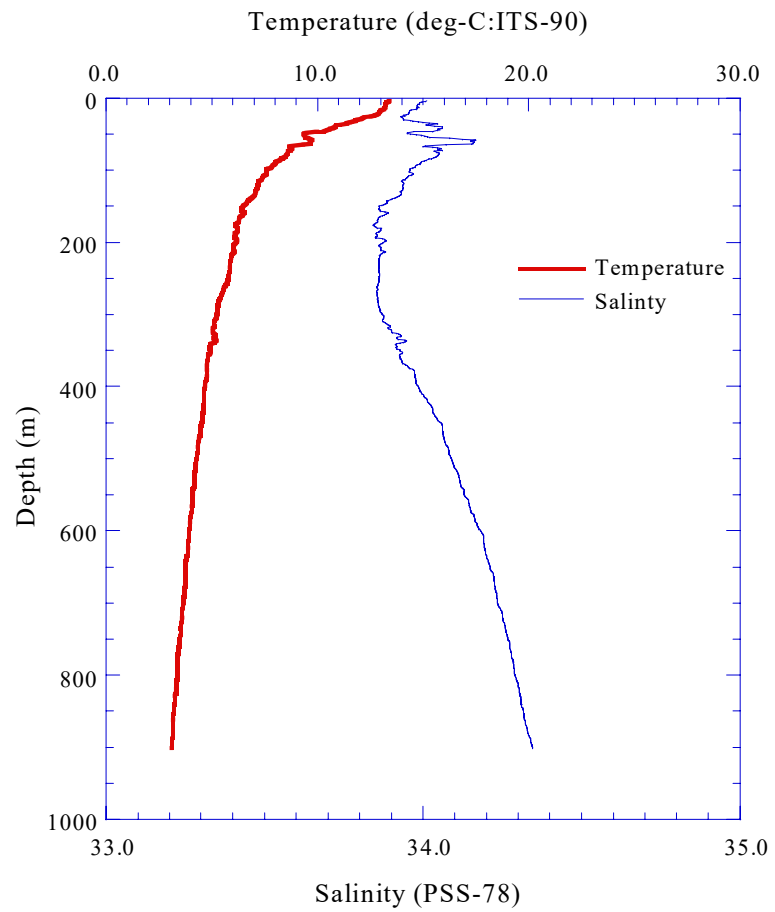


Fig.3.2.16.(b) CTD profile to 1,000m (Stn.16;016L02)

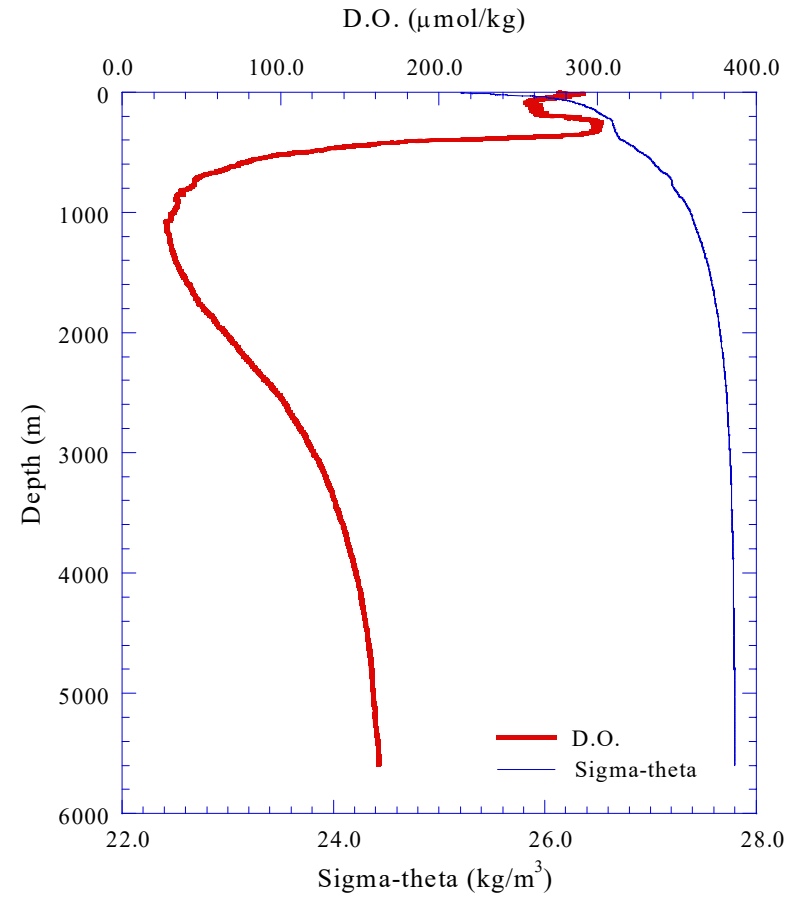
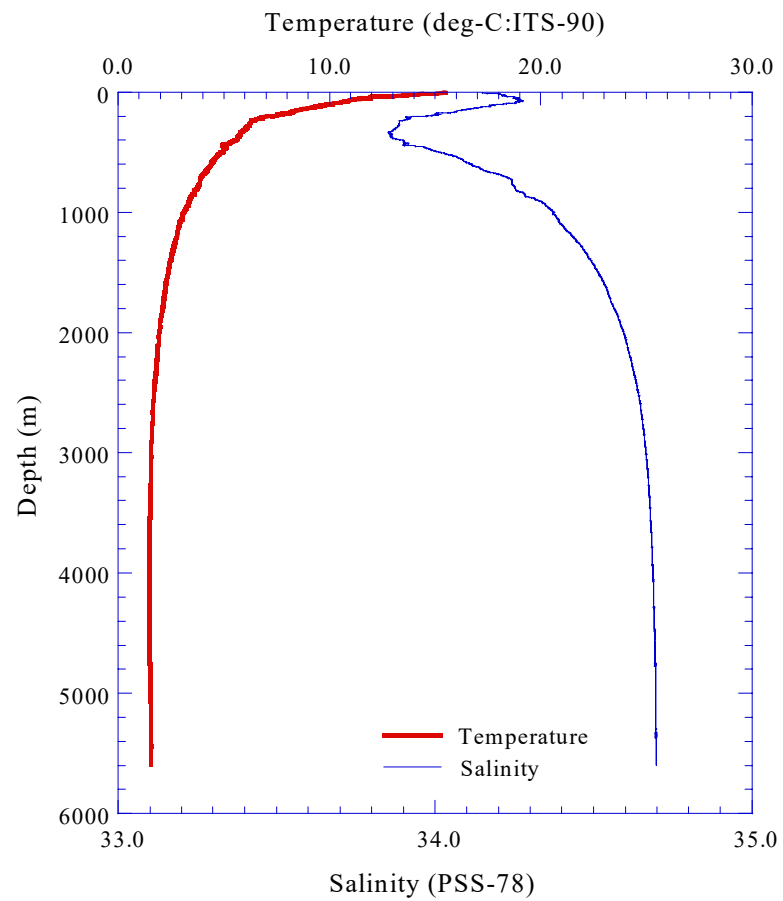


Fig.3.2.17.(a) CTD profile (Stn.17;017L01)

3.2-38

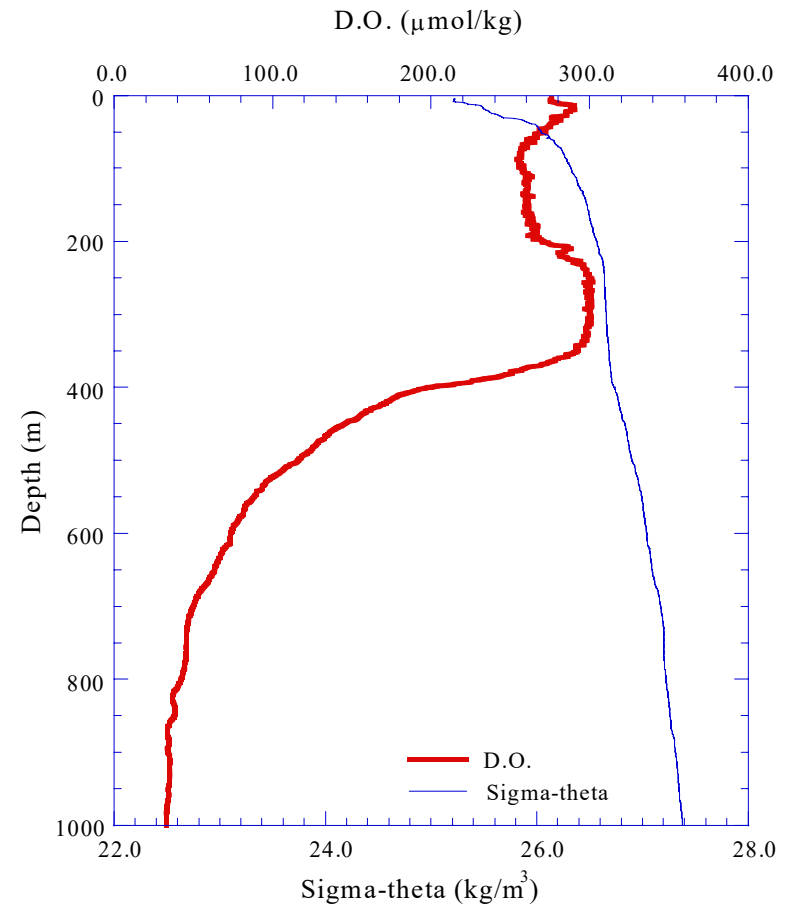
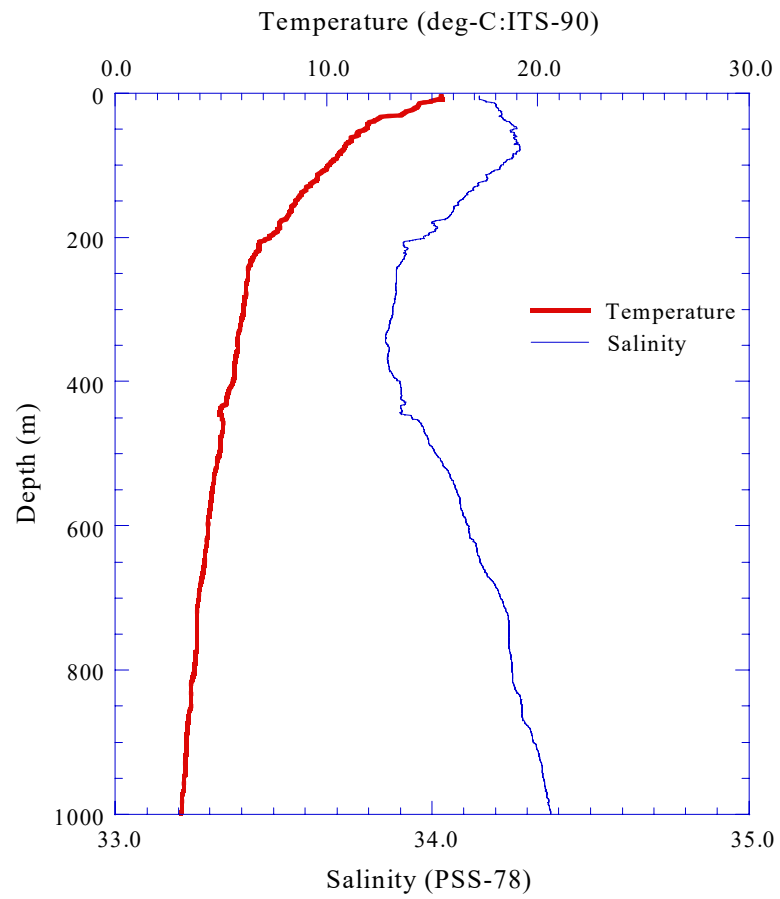


Fig.3.2.17.(b) CTD profile to 1,000m (Stn.17;017L01)

3.2-39

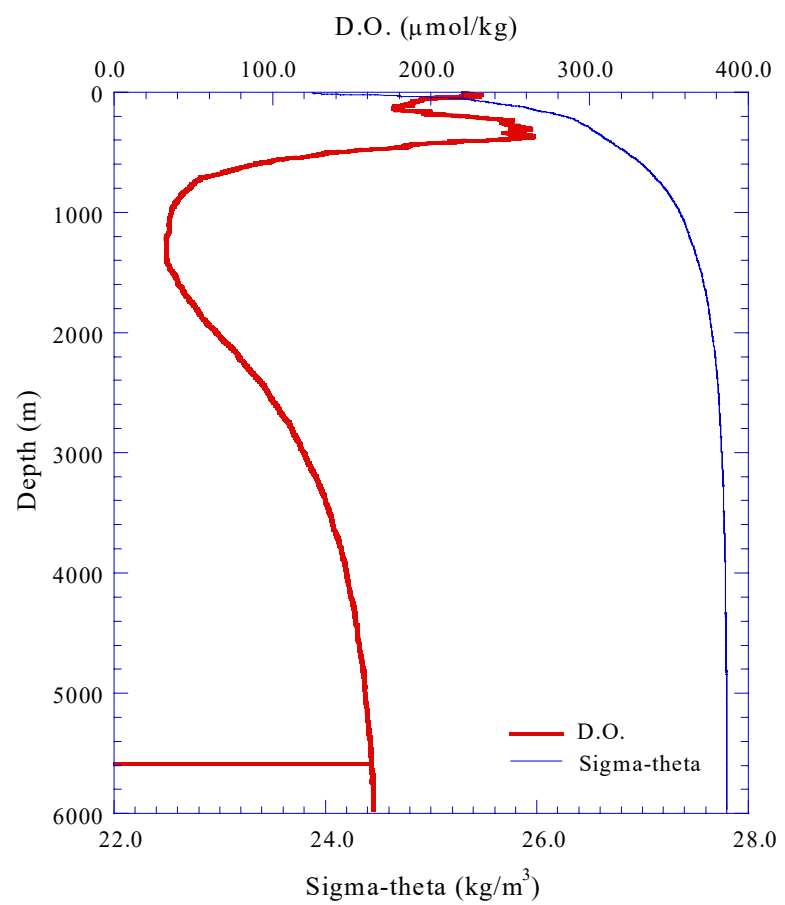
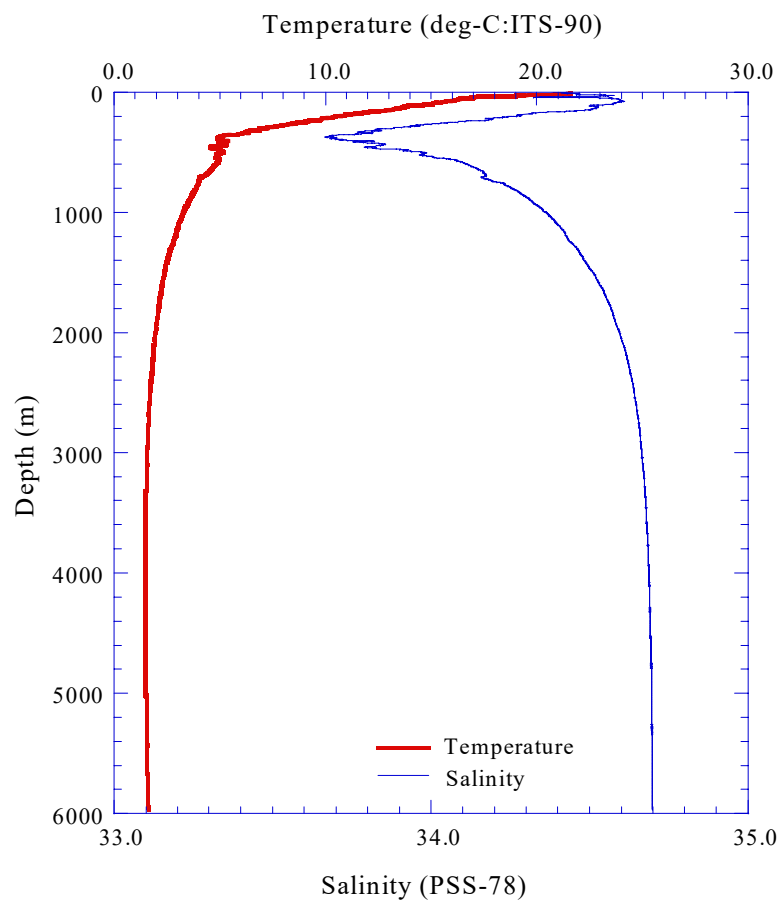


Fig.3.2.18.(a) CTD profile (Stn.18;018L01)

3.2.40

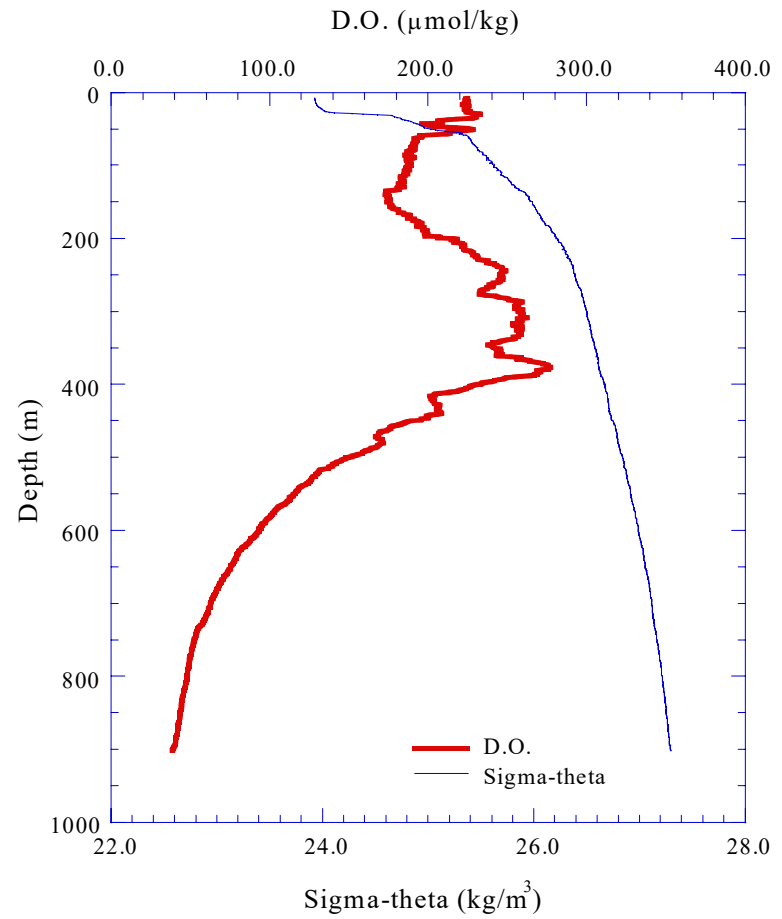
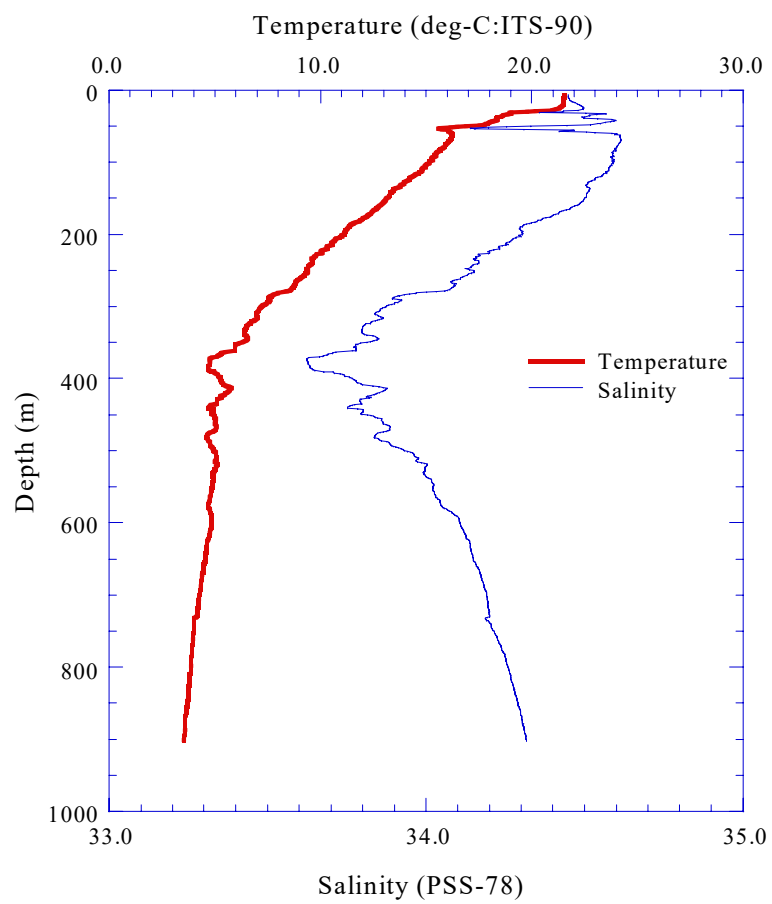


Fig.3.2.18.(b) CTD profile to 1,000m (Stn.18;018L02)

3.2-41

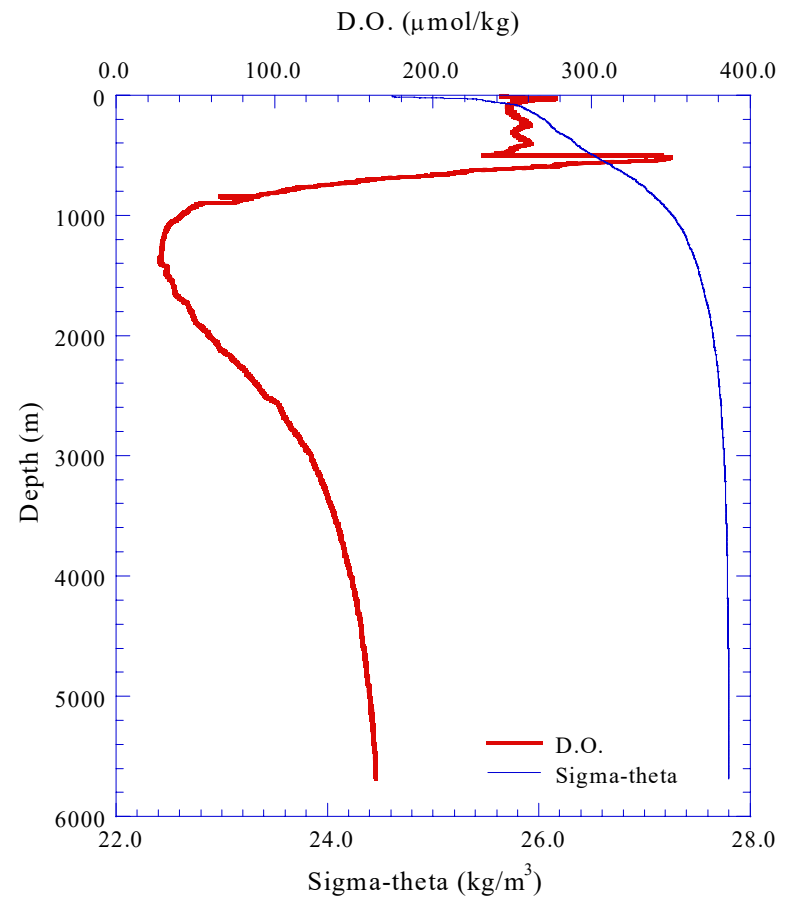
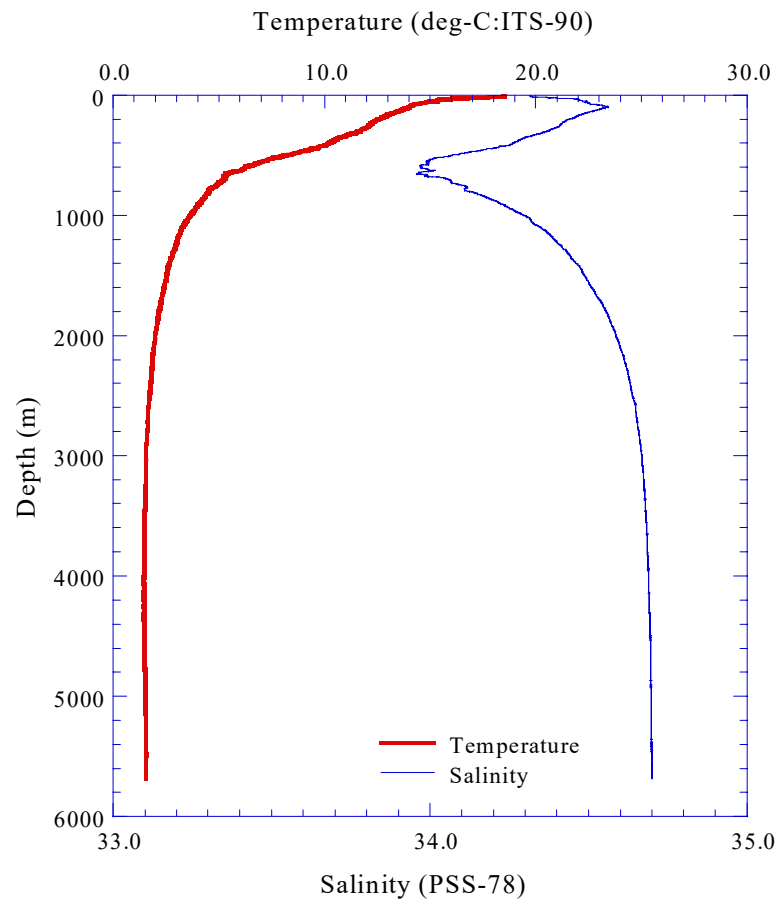


Fig.3.2.19.(a) CTD profile (Stn.19;019L01)

3.2.42

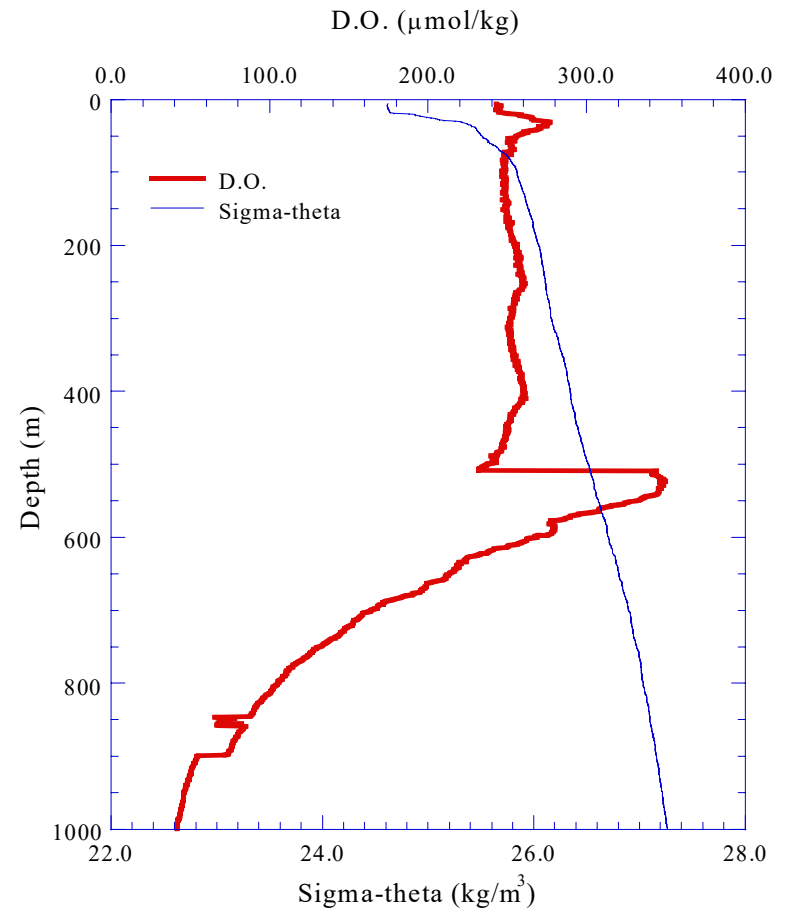
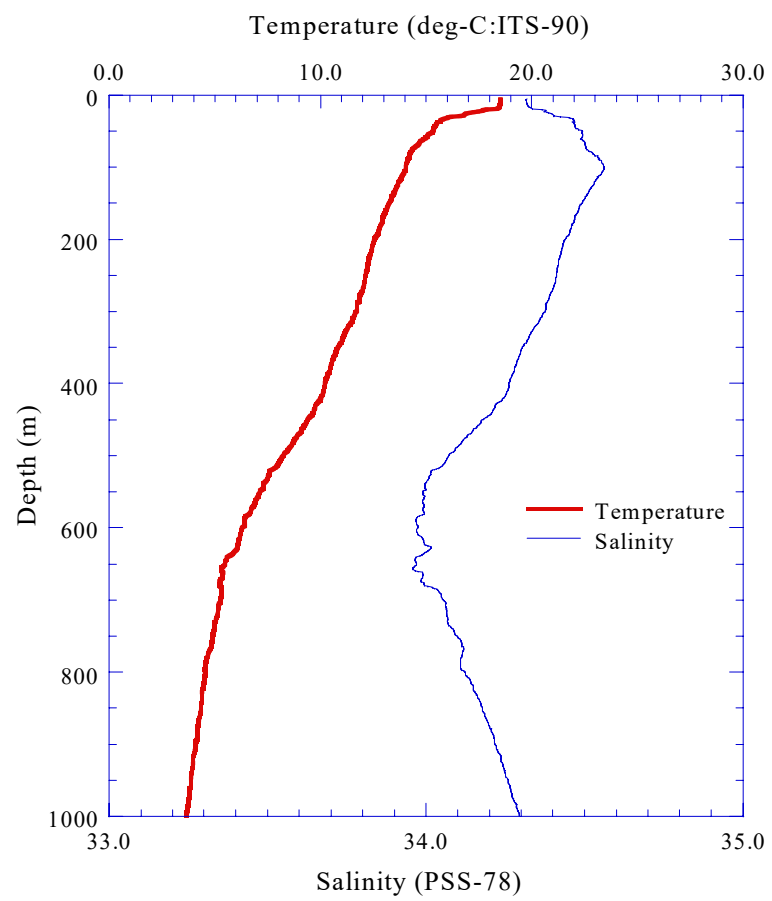


Fig.3.2.19.(b) CTD profile to 1,000m (Stn.19;019L01)

3.2-43

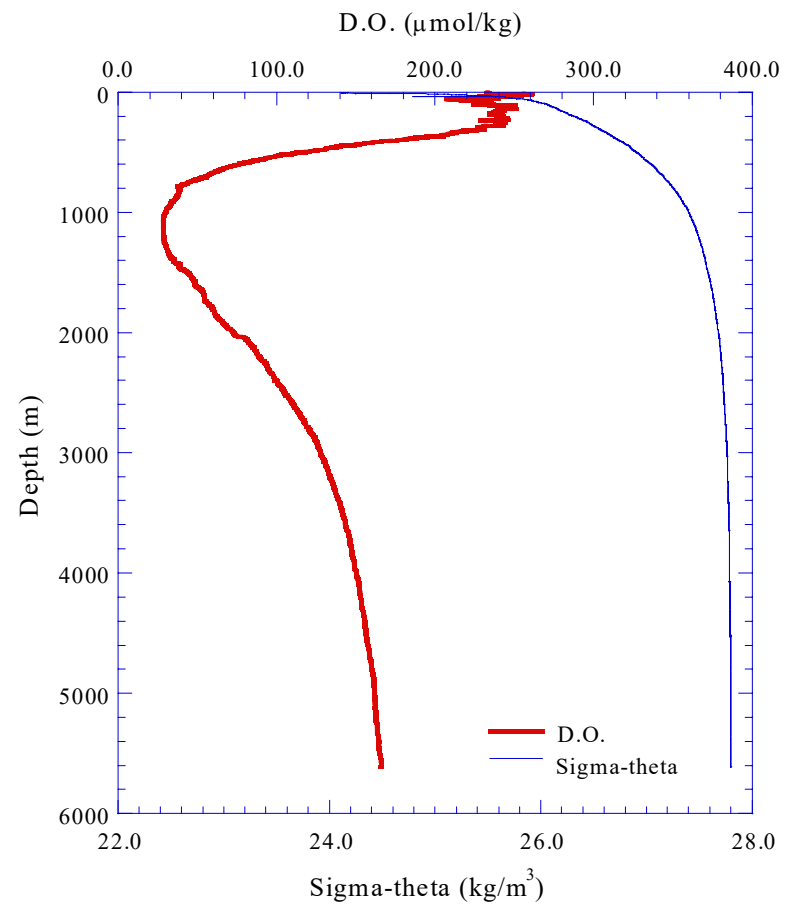
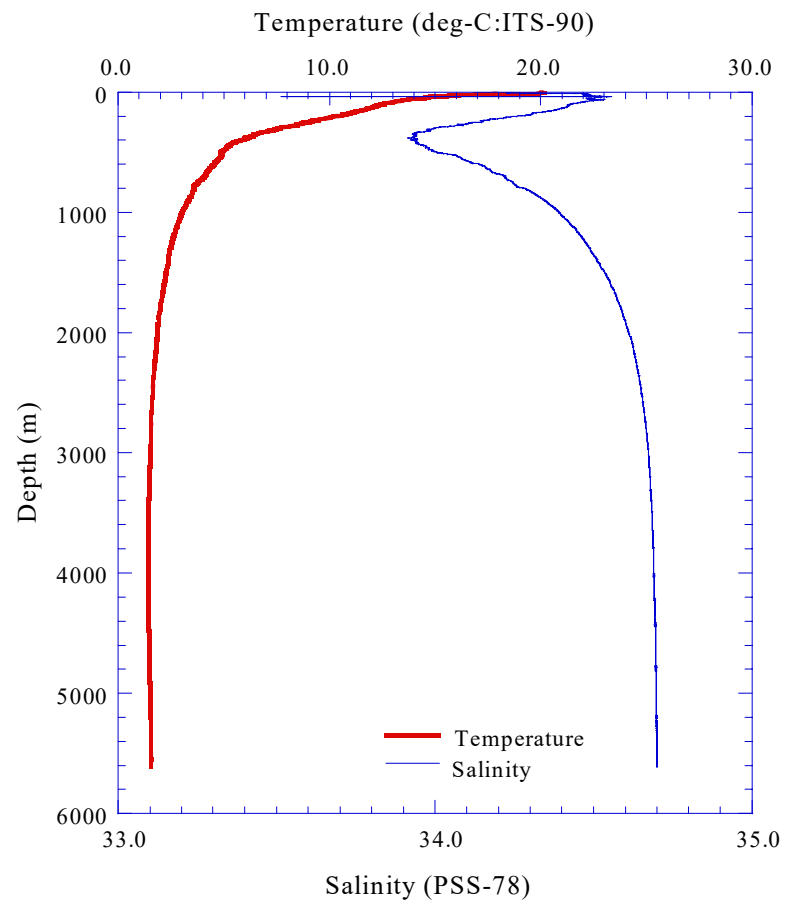


Fig.3.2.20.(a) CTD profile (Stn.20;020L01)

3.2-44

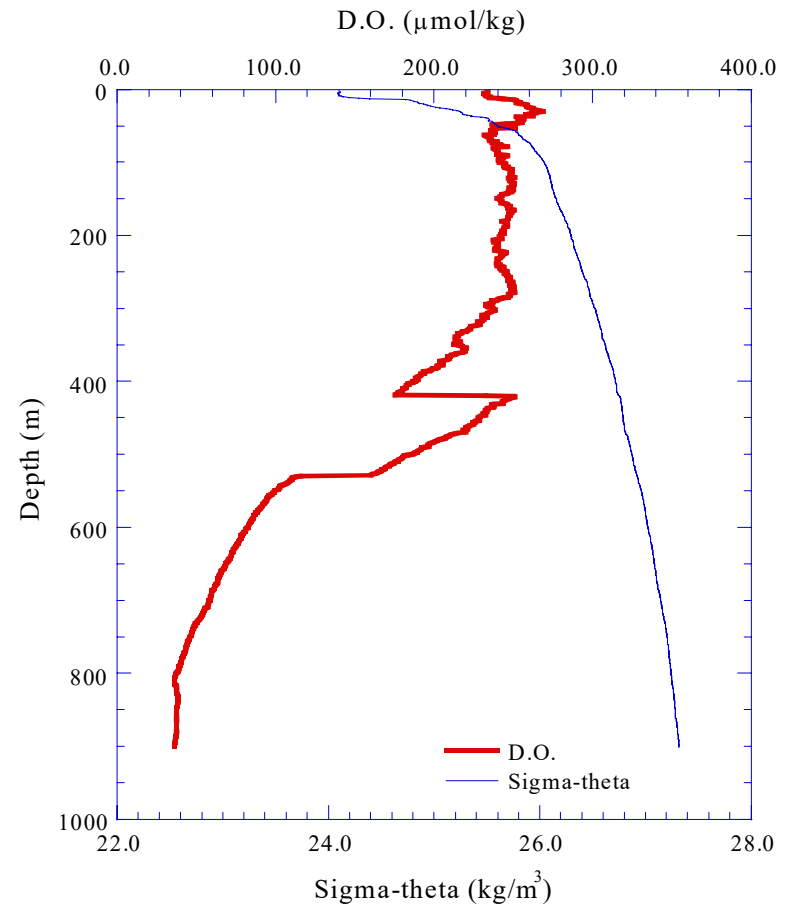
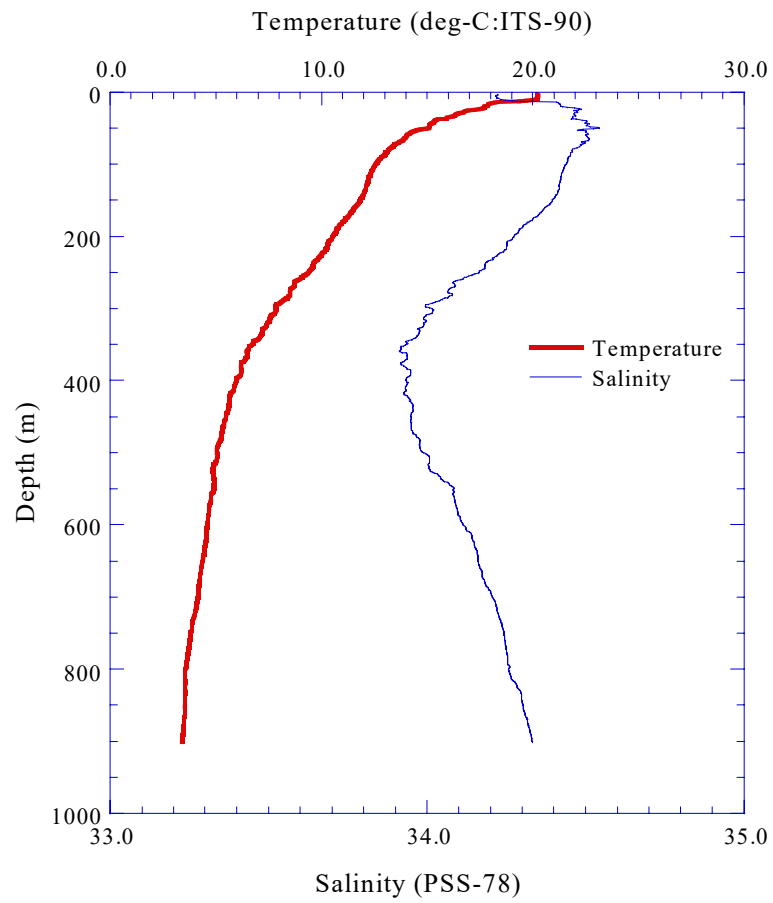


Fig.3.2.20.(b) CTD profile to 1,000m (Stn.20;020L02)

3.2-45

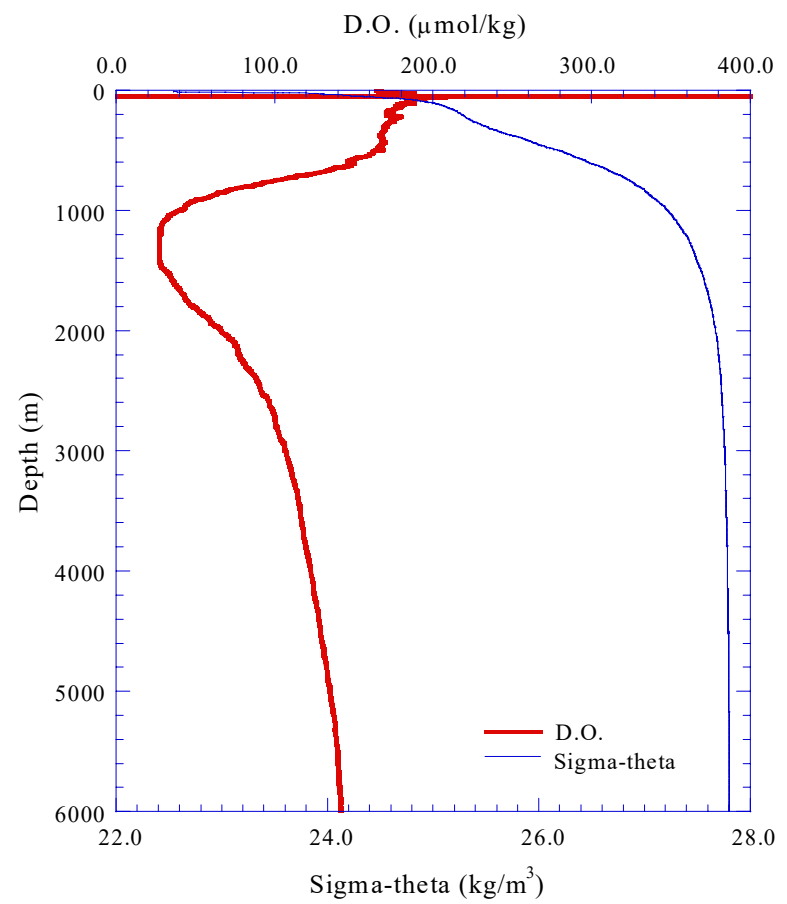
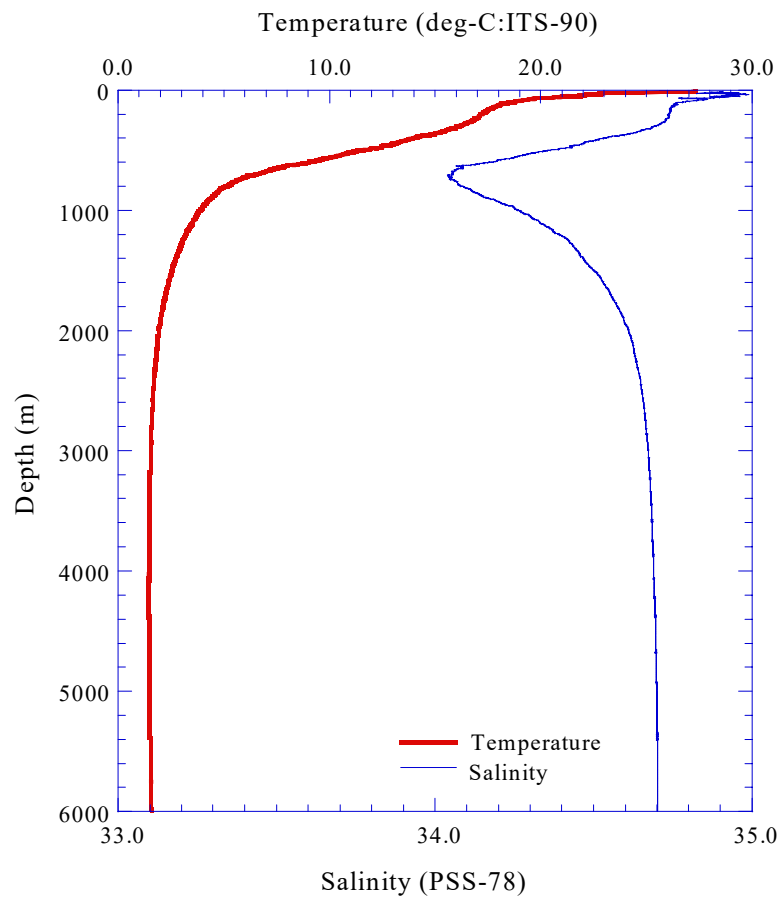


Fig.3.2.21.(a) CTD profile (Stn.25;025L02)

3.2-46

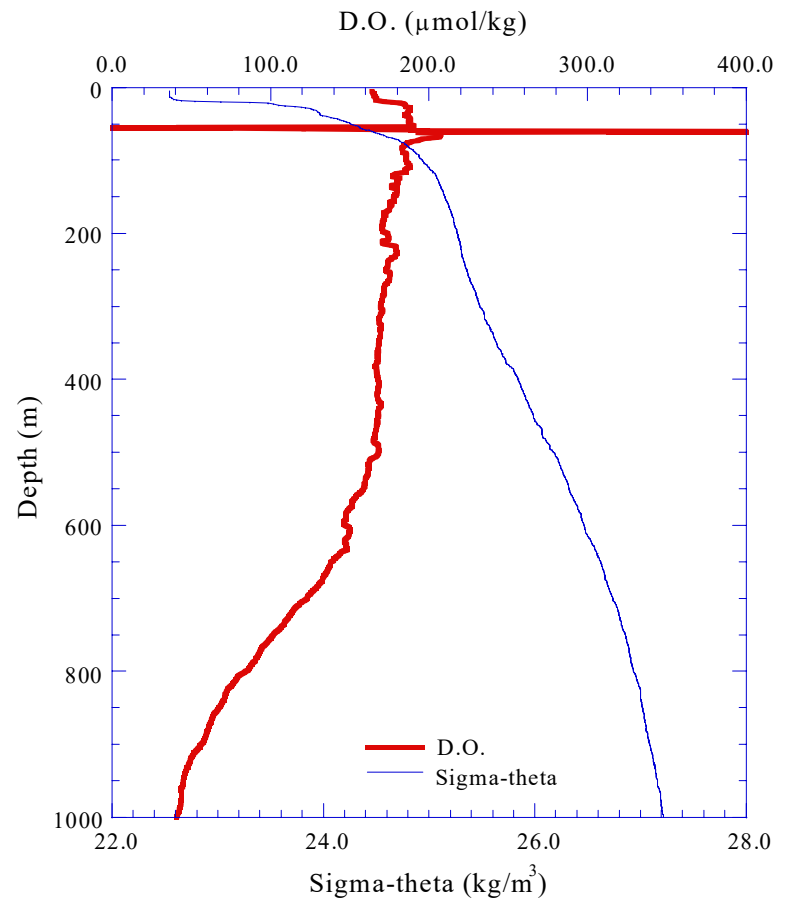
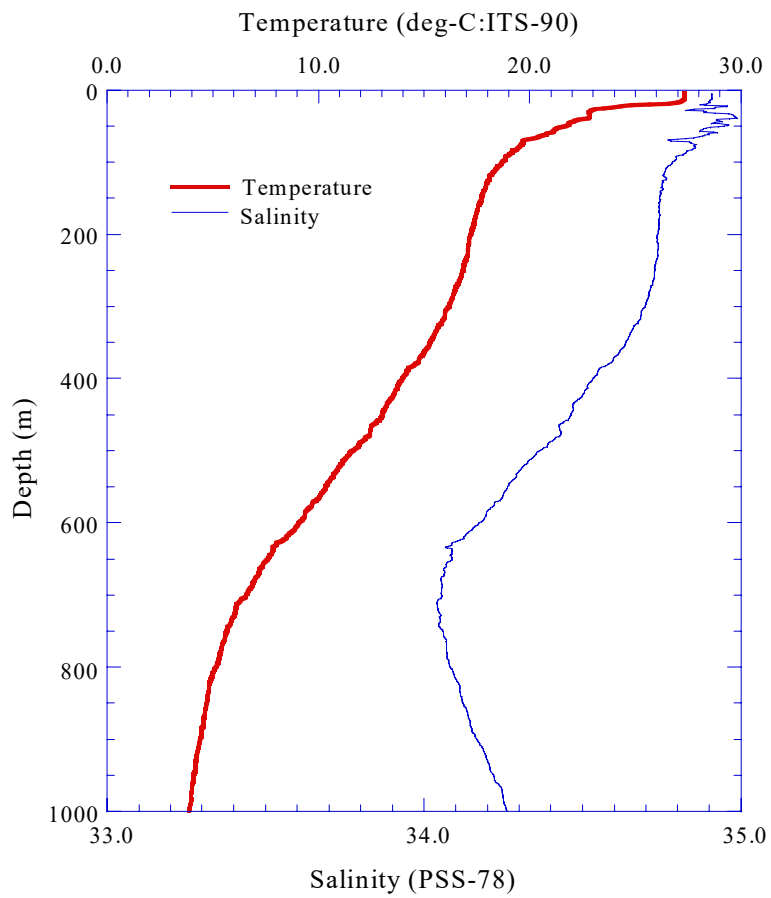


Fig.3.2.21.(b) CTD profile to 1,000m (Stn.25;025L02)

3.2-47

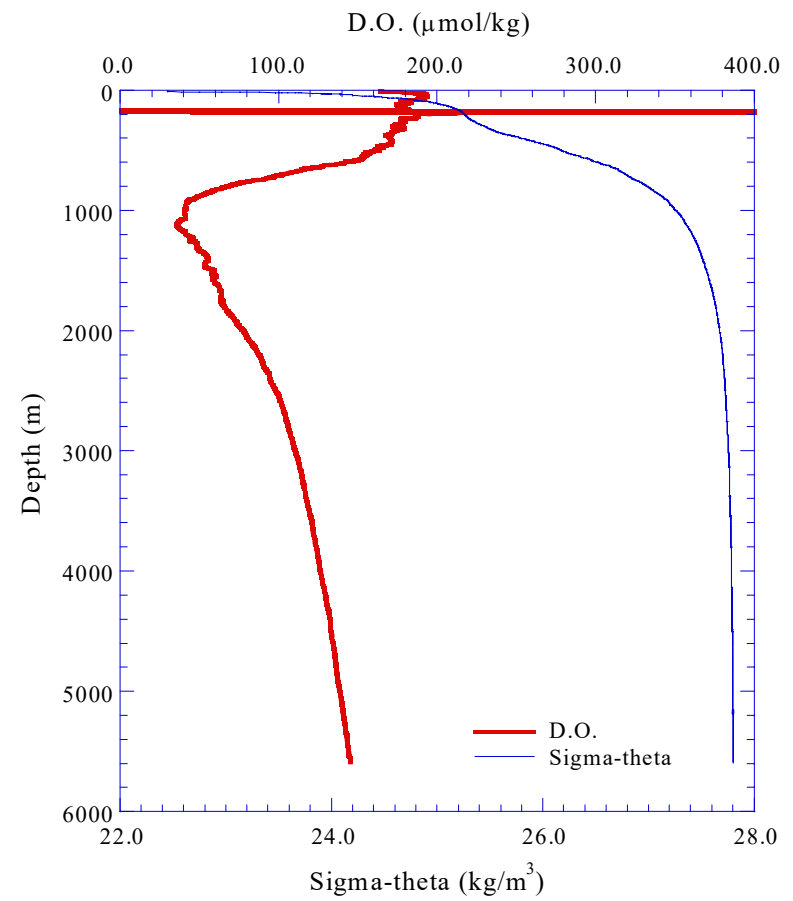
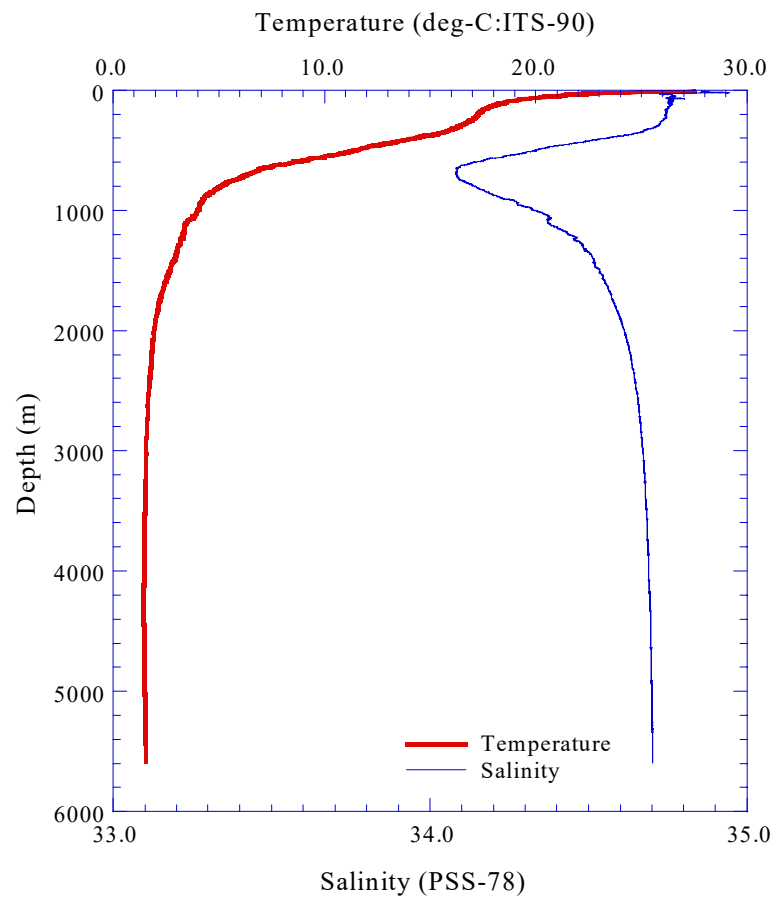


Fig.3.2.22.(a) CTD profile (Stn.26;026L01)

3.2.48

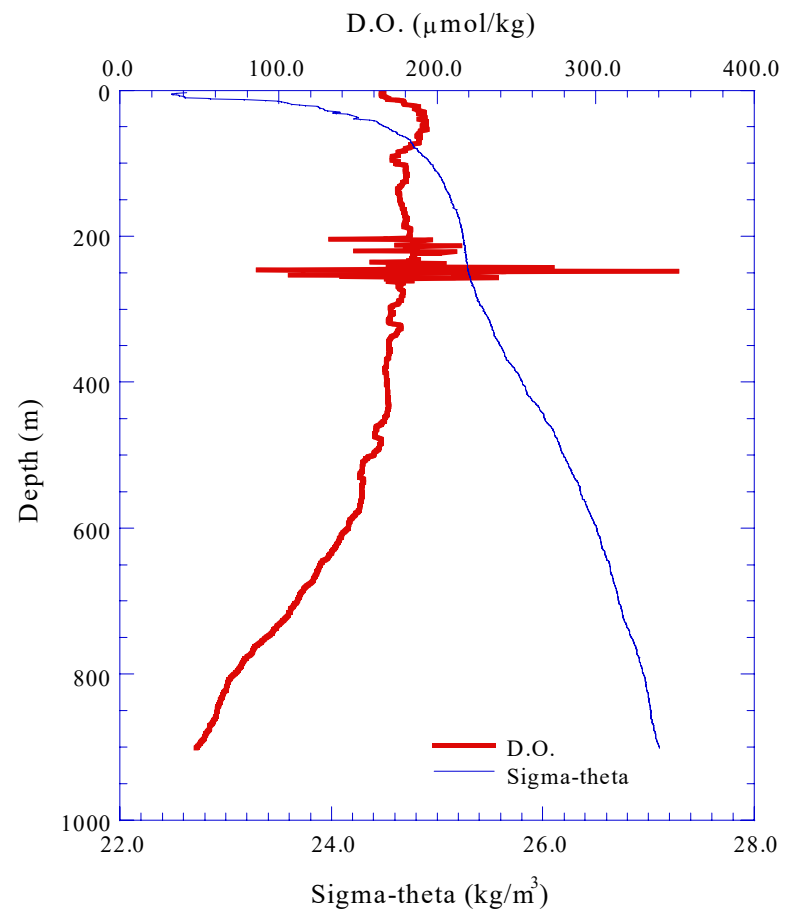
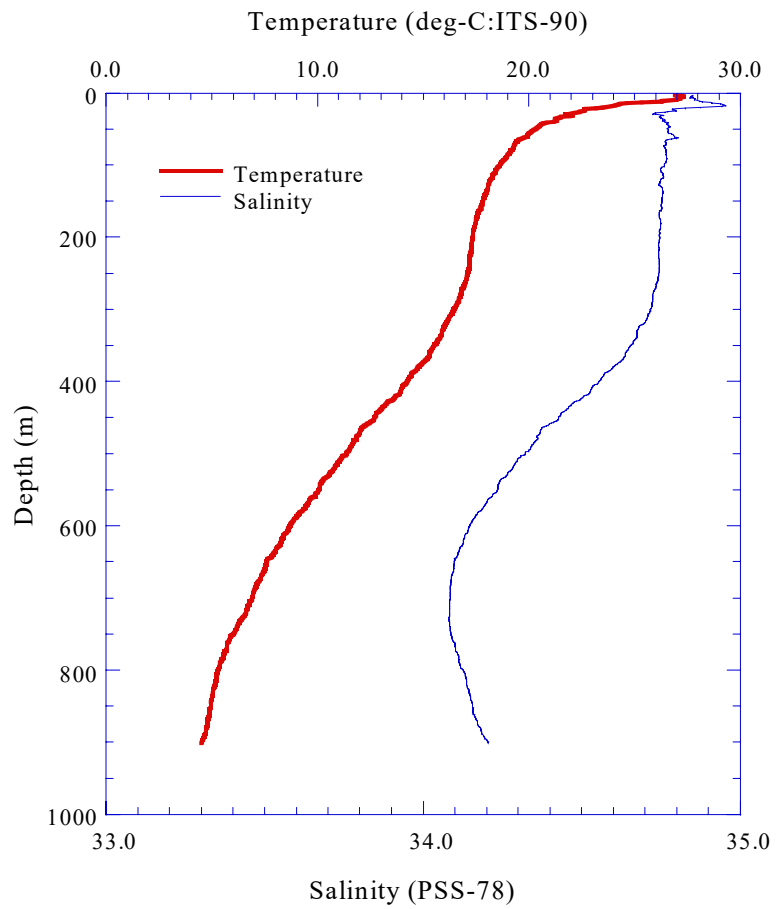


Fig.3.2.22.(b) CTD profile to 1,000m (Stn.26;026L02)

3.2-49

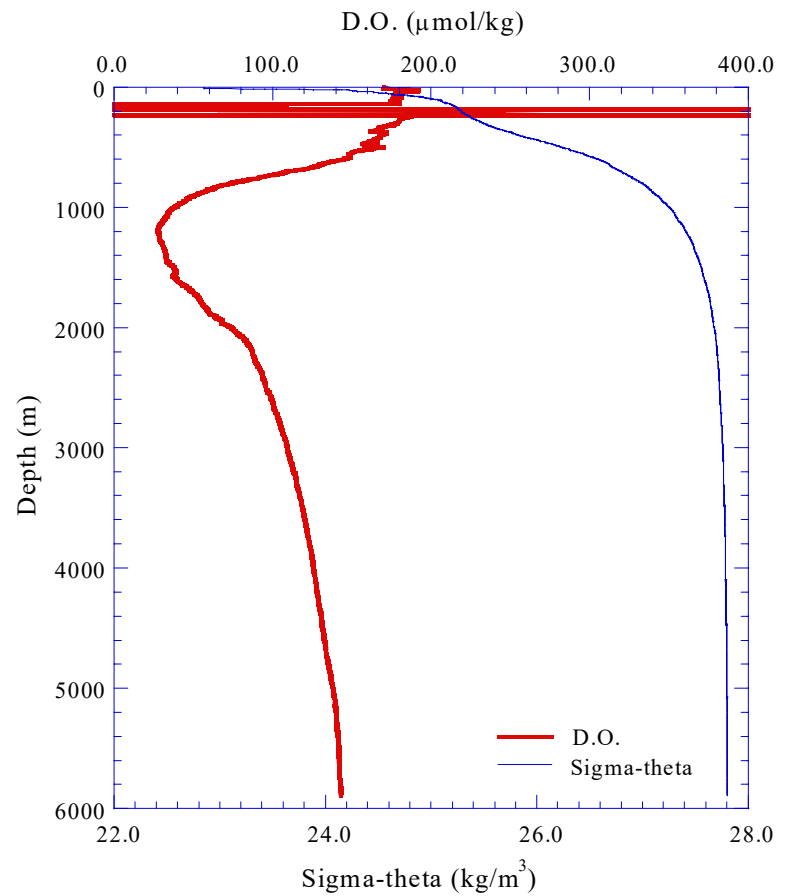
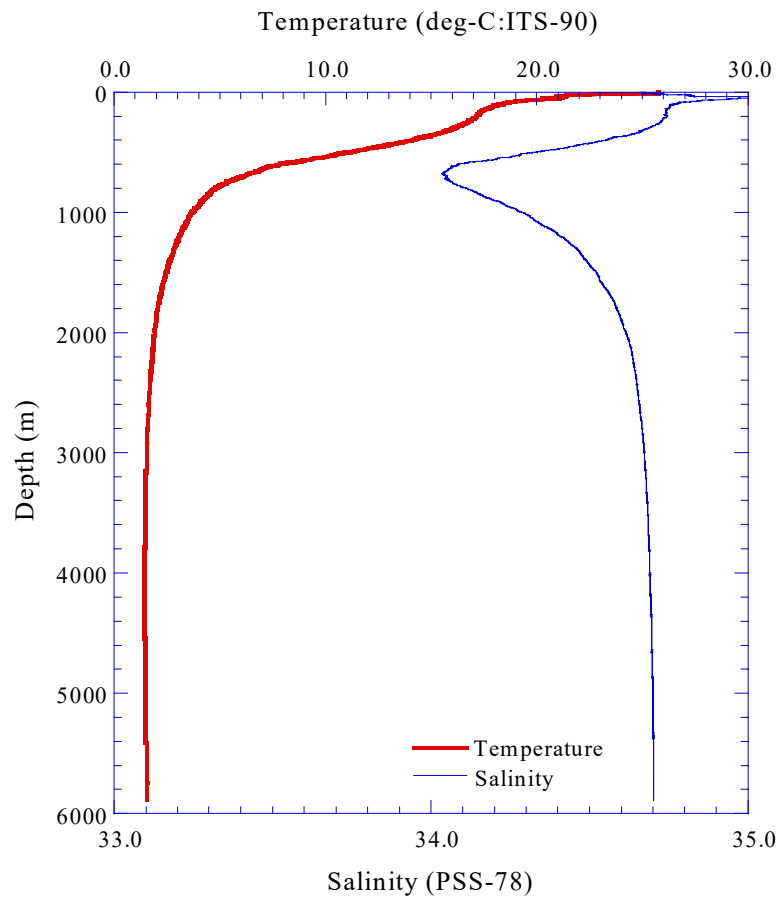


Fig.3.2.23.(a) CTD profile (Stn.24;024L01)

3.2-50

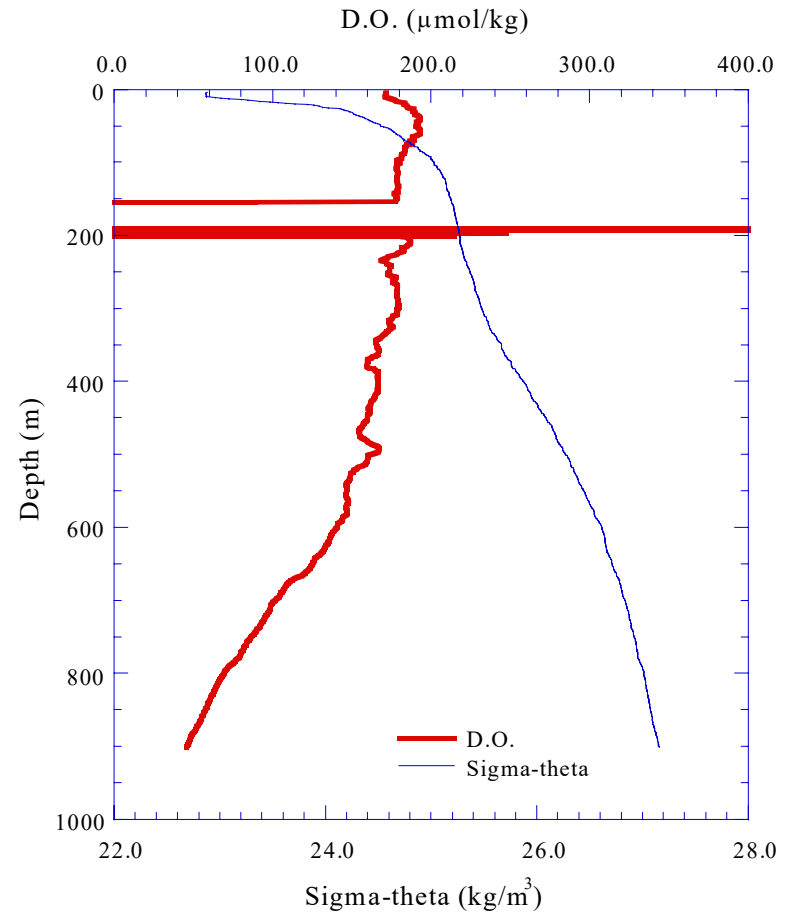
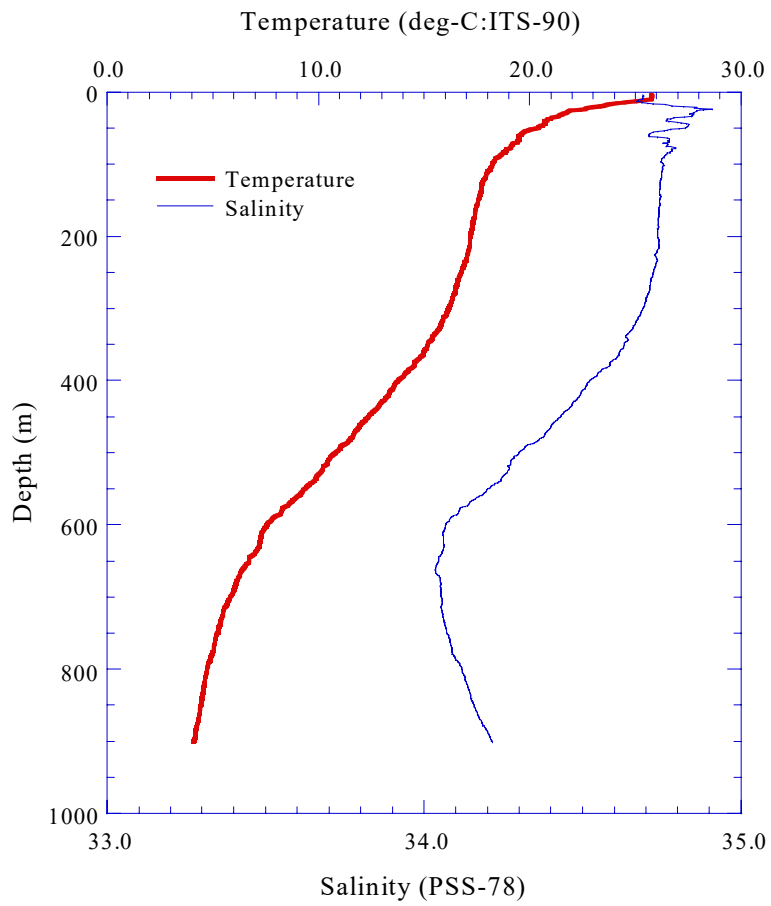


Fig.3.2.23.(b) CTD profile to 1,000m (Stn.24;024L02)

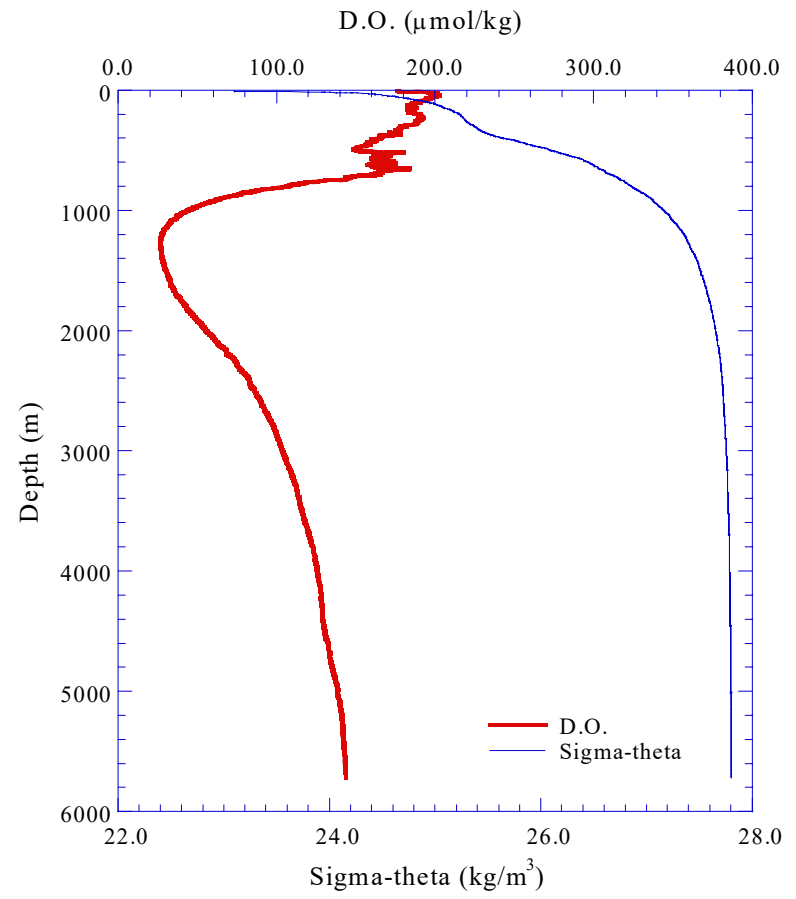
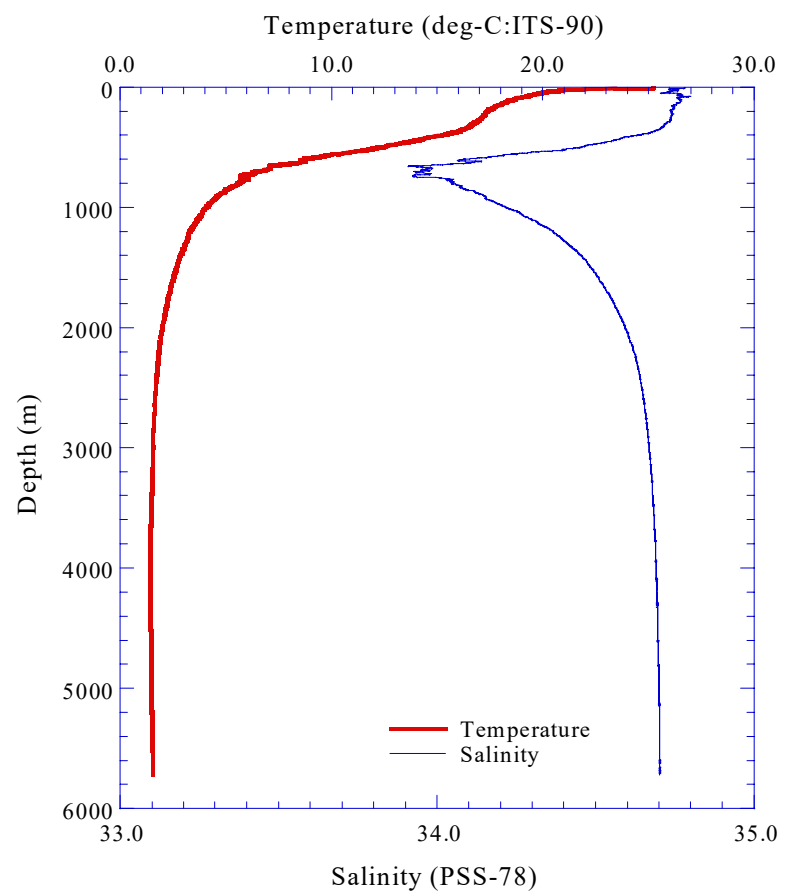


Fig.3.2.24.(a) CTD profile (Stn.23;023L01)

3.2-52

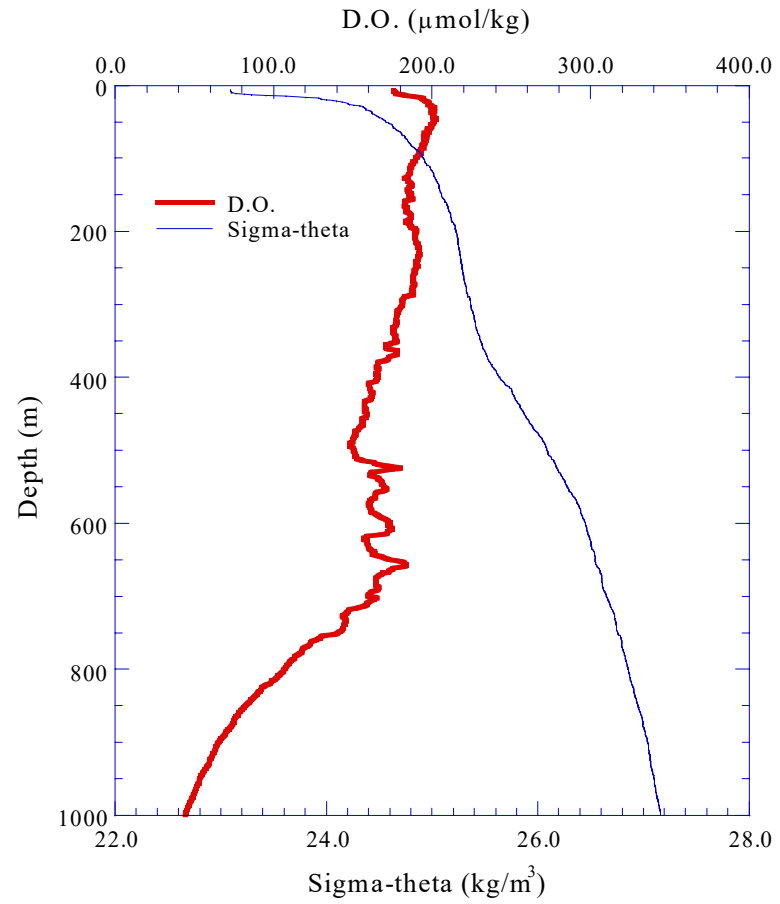
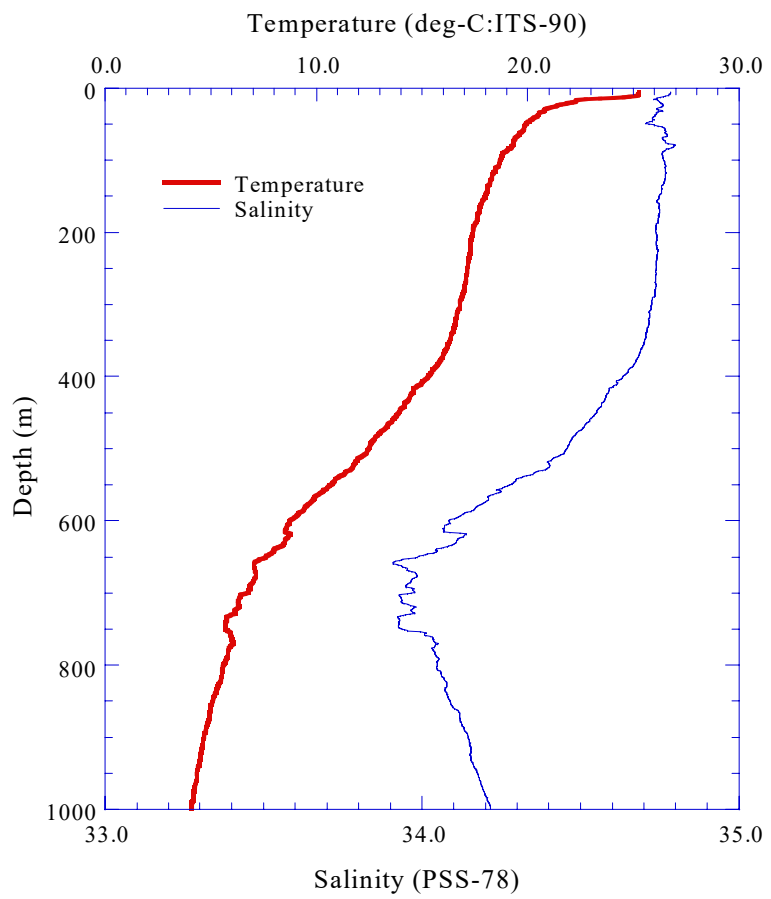


Fig.3.2.24.(b) CTD profile to 1,000m (Stn.23;023L01)

3.2-53

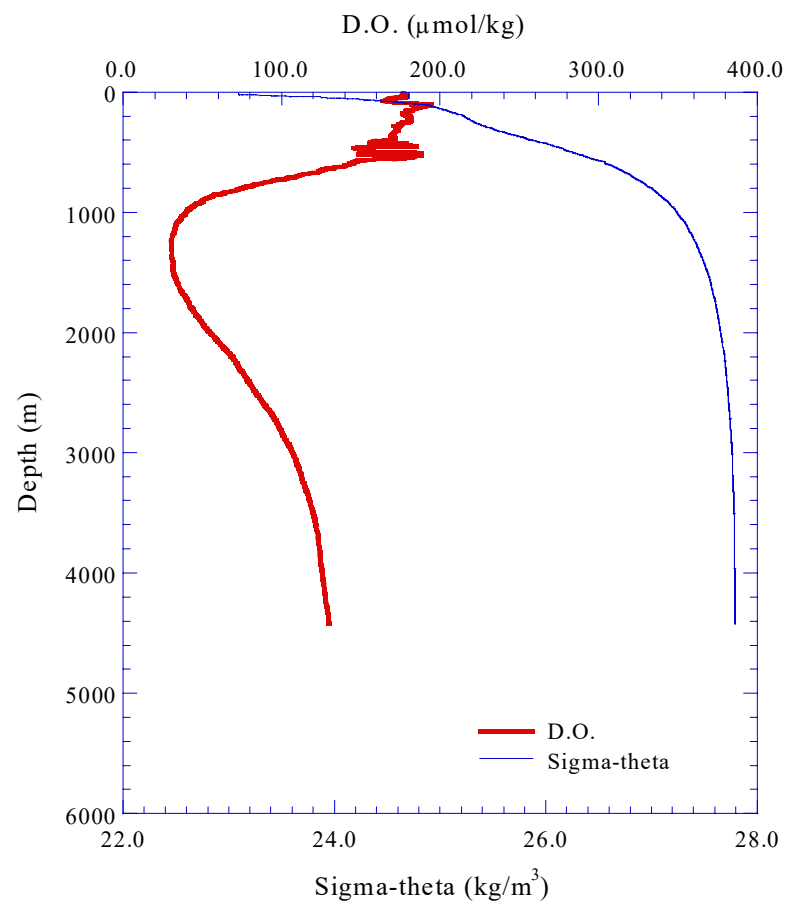
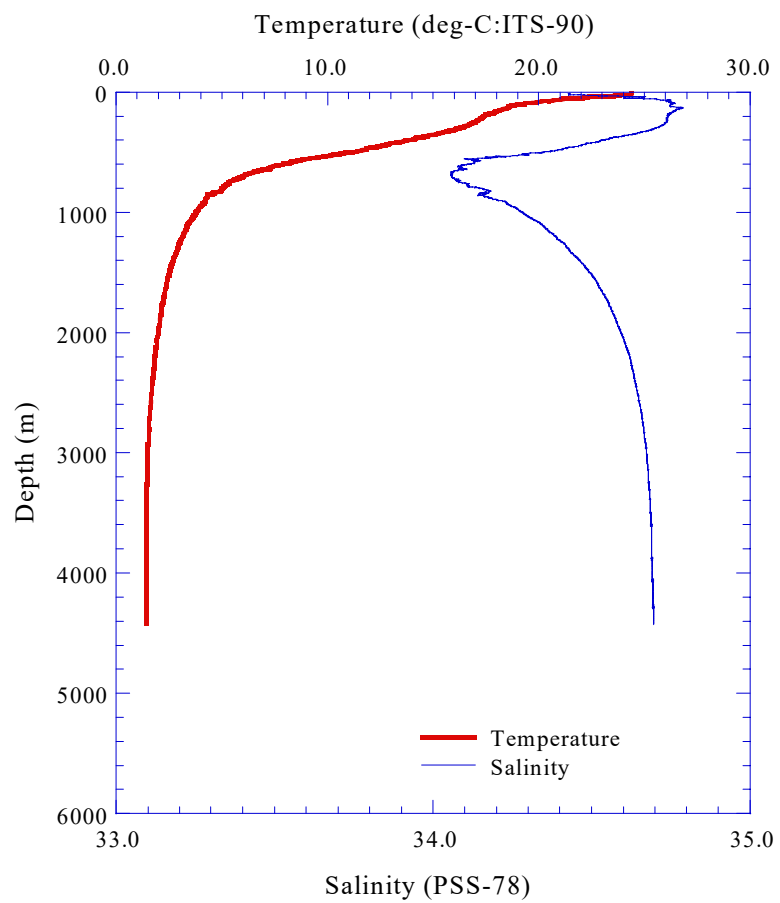


Fig.3.2.25.(a) CTD profile (Stn.22;022L01)

3.2-54

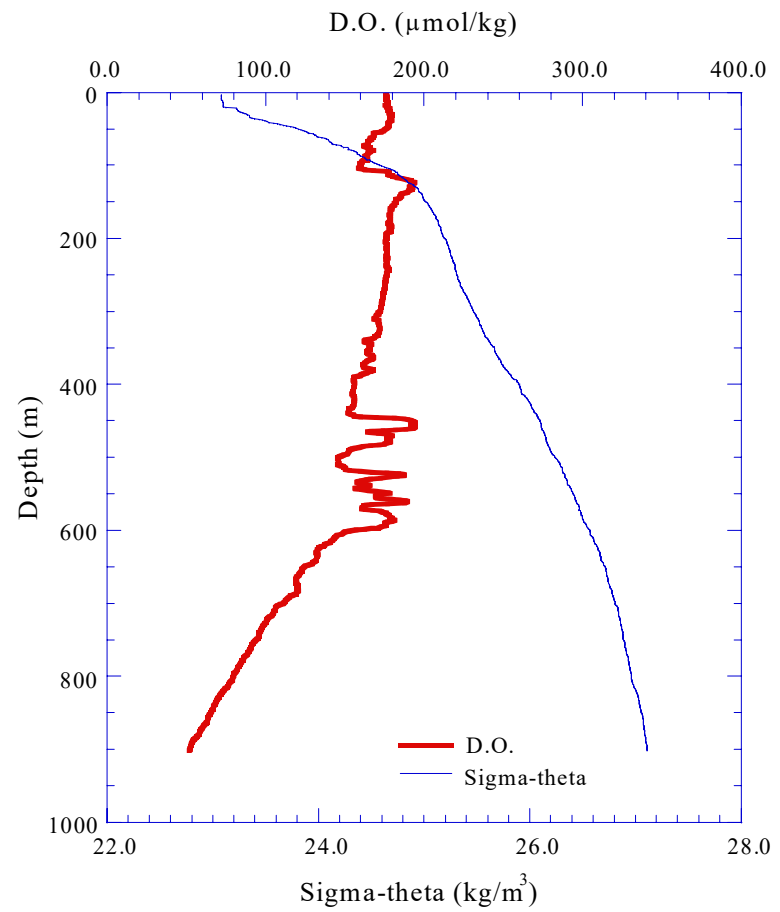
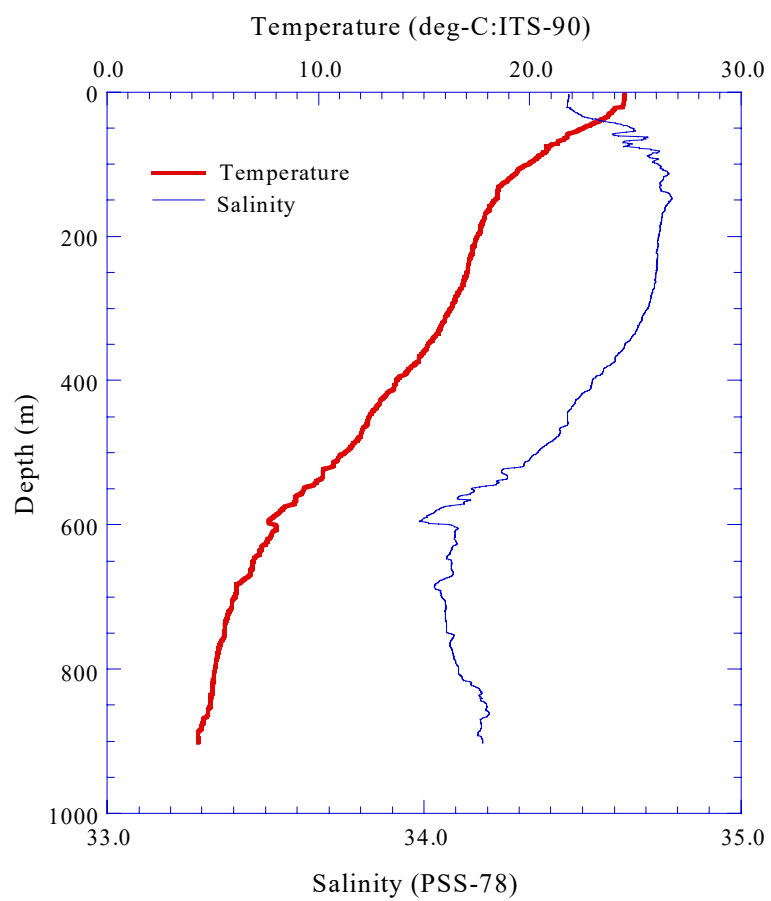


Fig.3.2.25.(b) CTD profile to 1,000m (Stn.22;022L02)

3.2-55

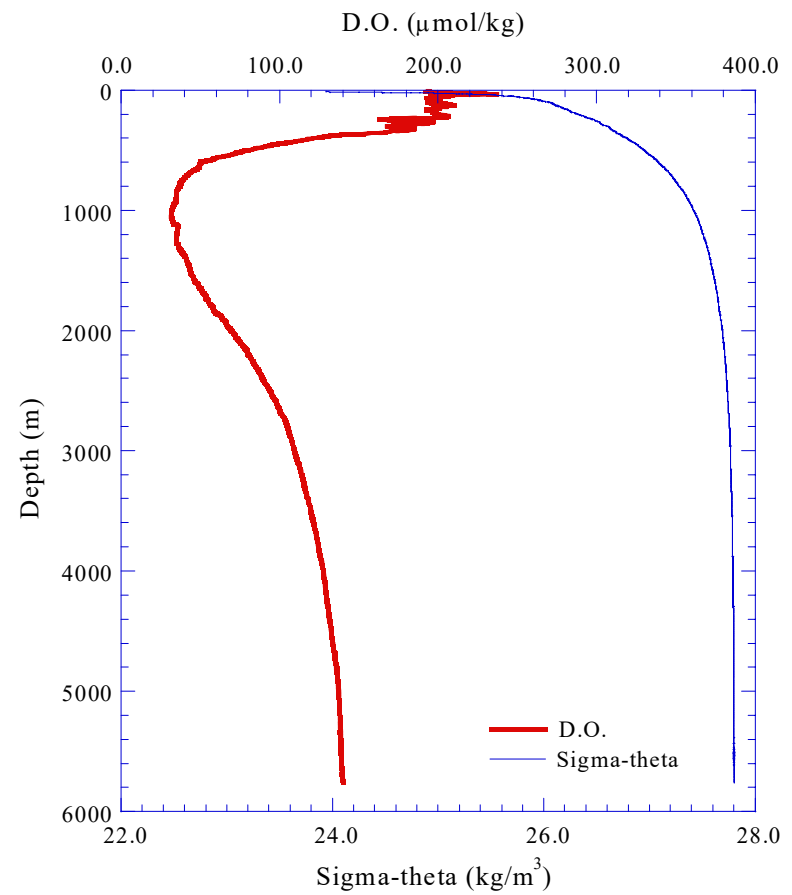
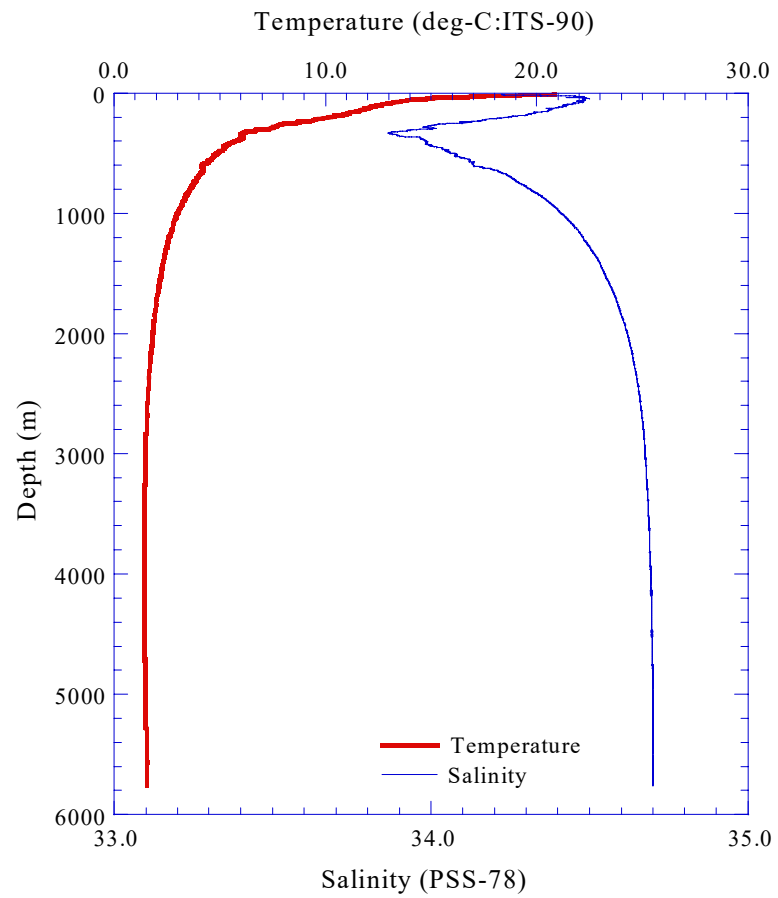


Fig.3.2.26.(a) CTD profile (Stn.21;021L01)

3.2-56

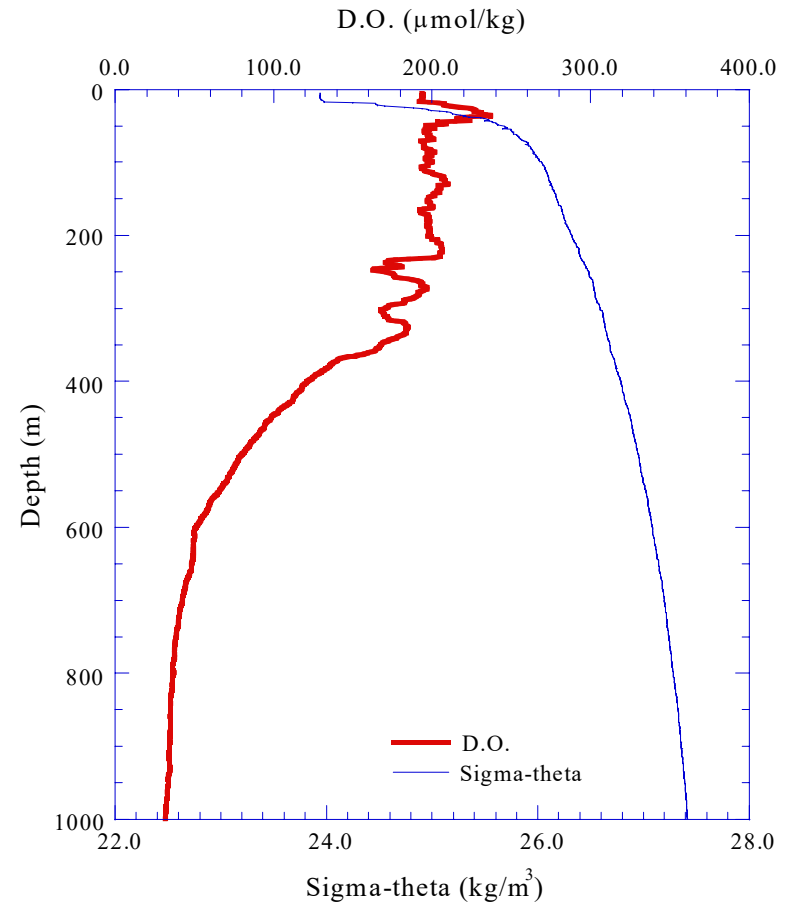
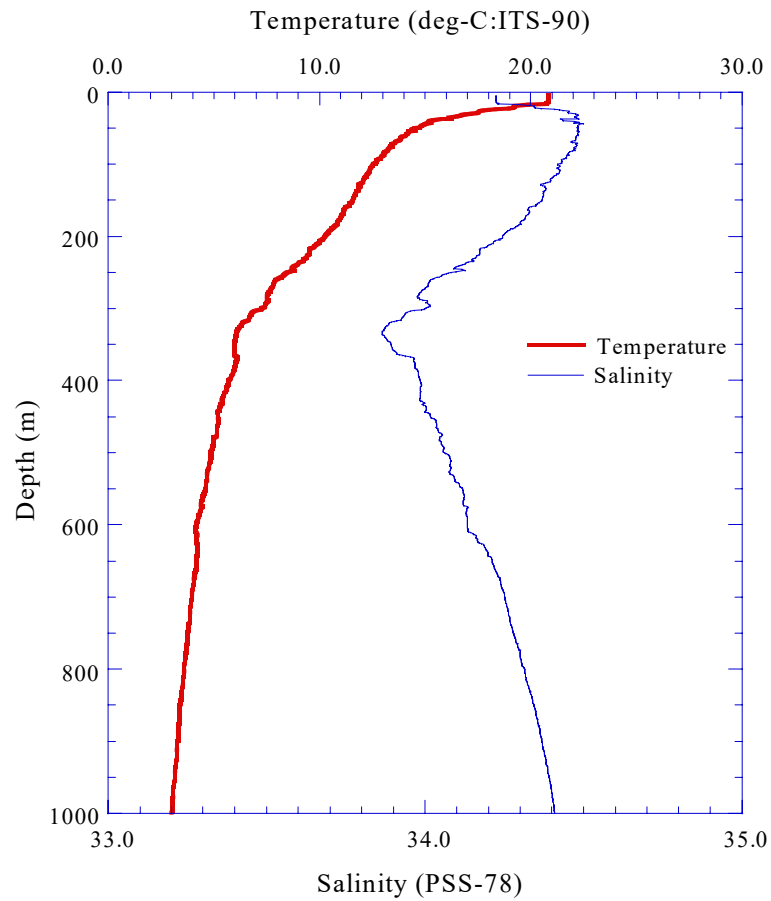


Fig.3.2.26.(b) CTD profile to 1,000m (Stn.21;021L01)

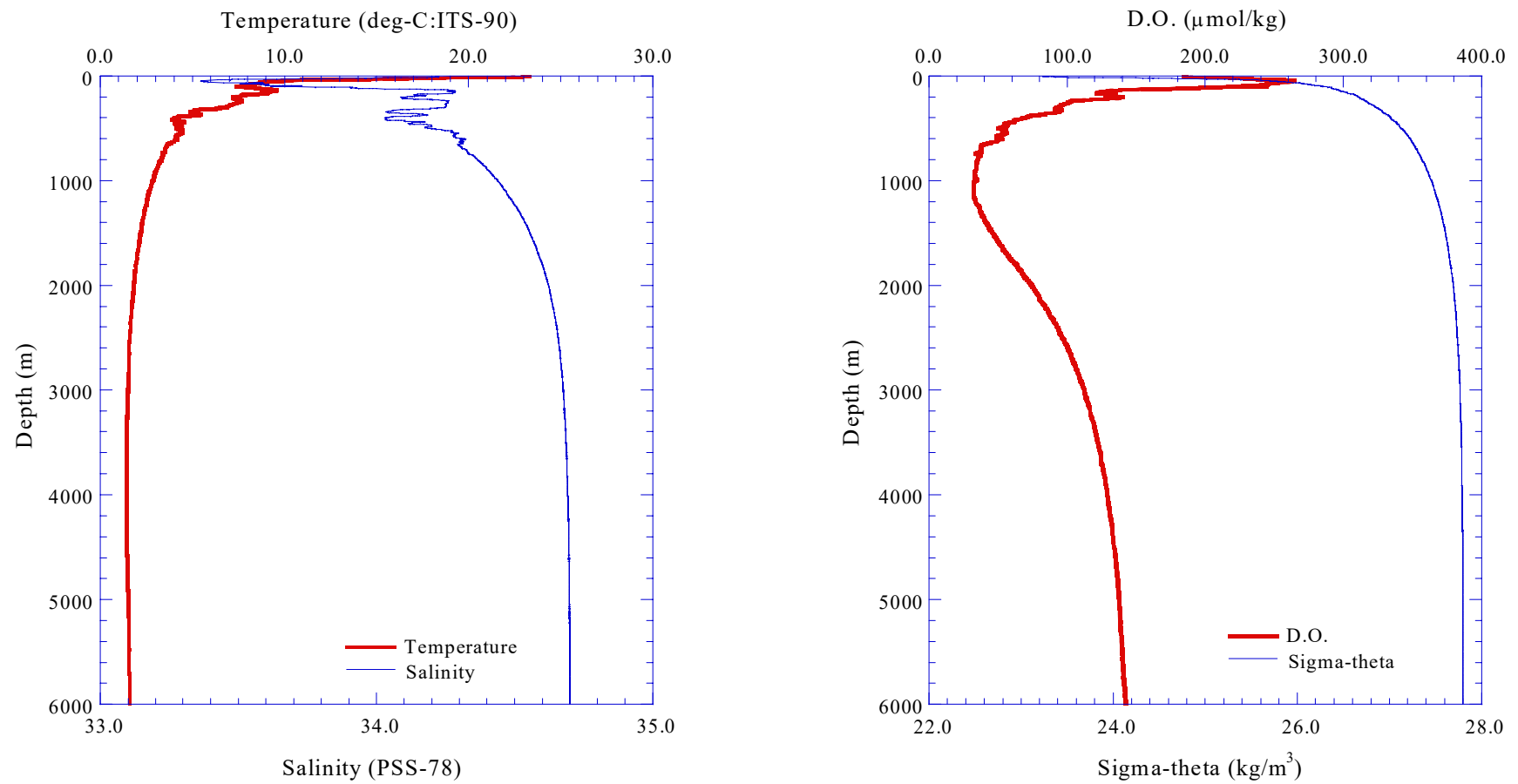


Fig.3.2.27.(a) CTD profile (Stn.27;027L01)

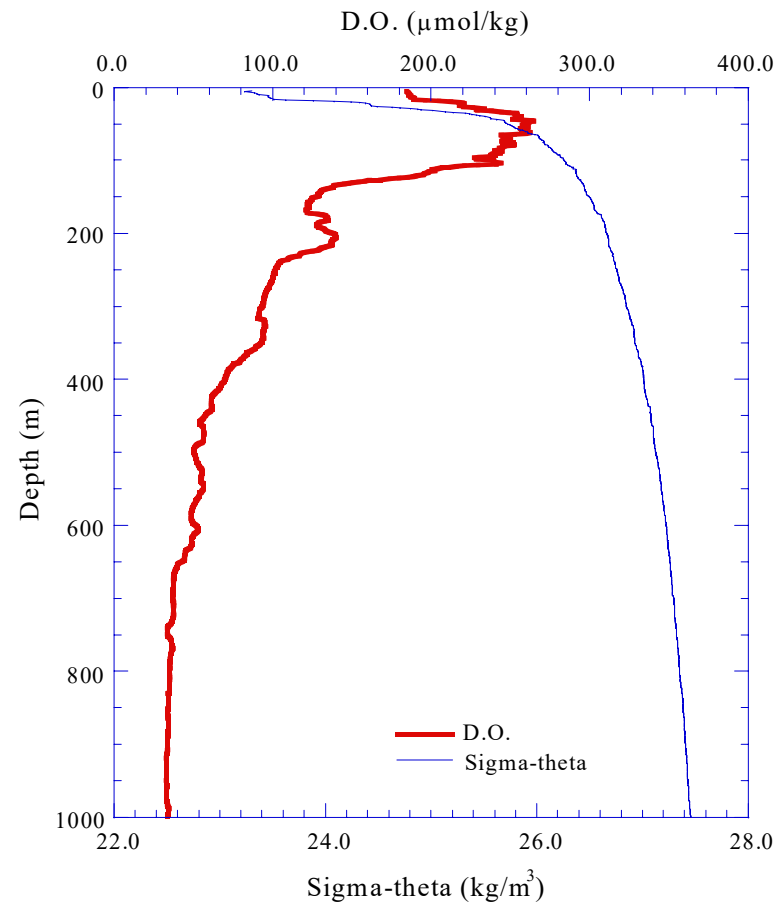
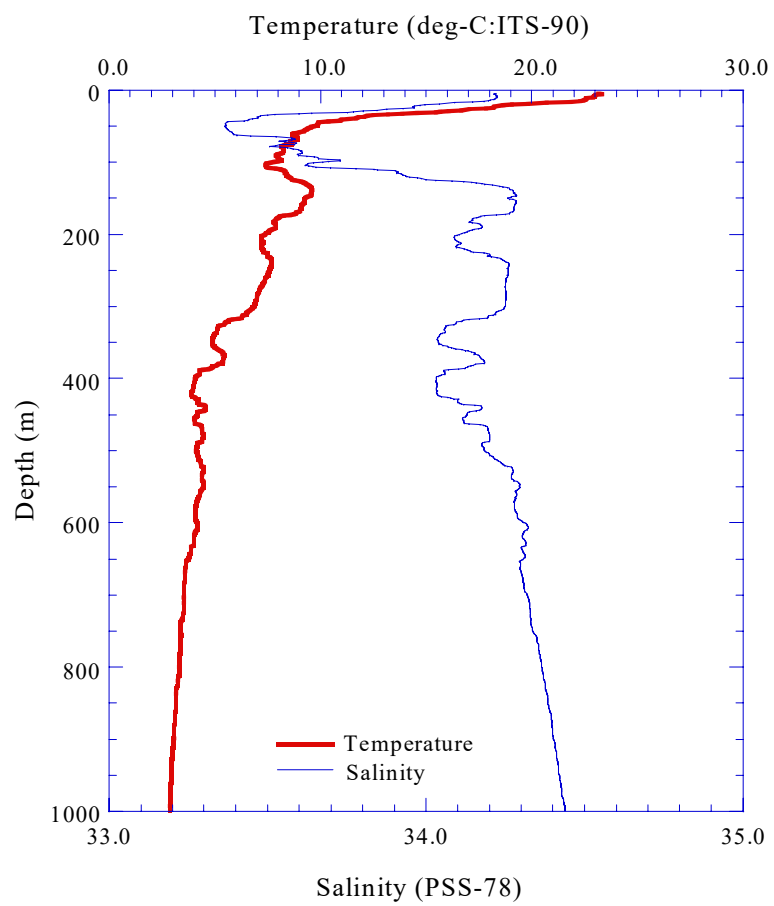


Fig.3.2.27.(b) CTD profile to 1,000m (Stn.27;027L01)

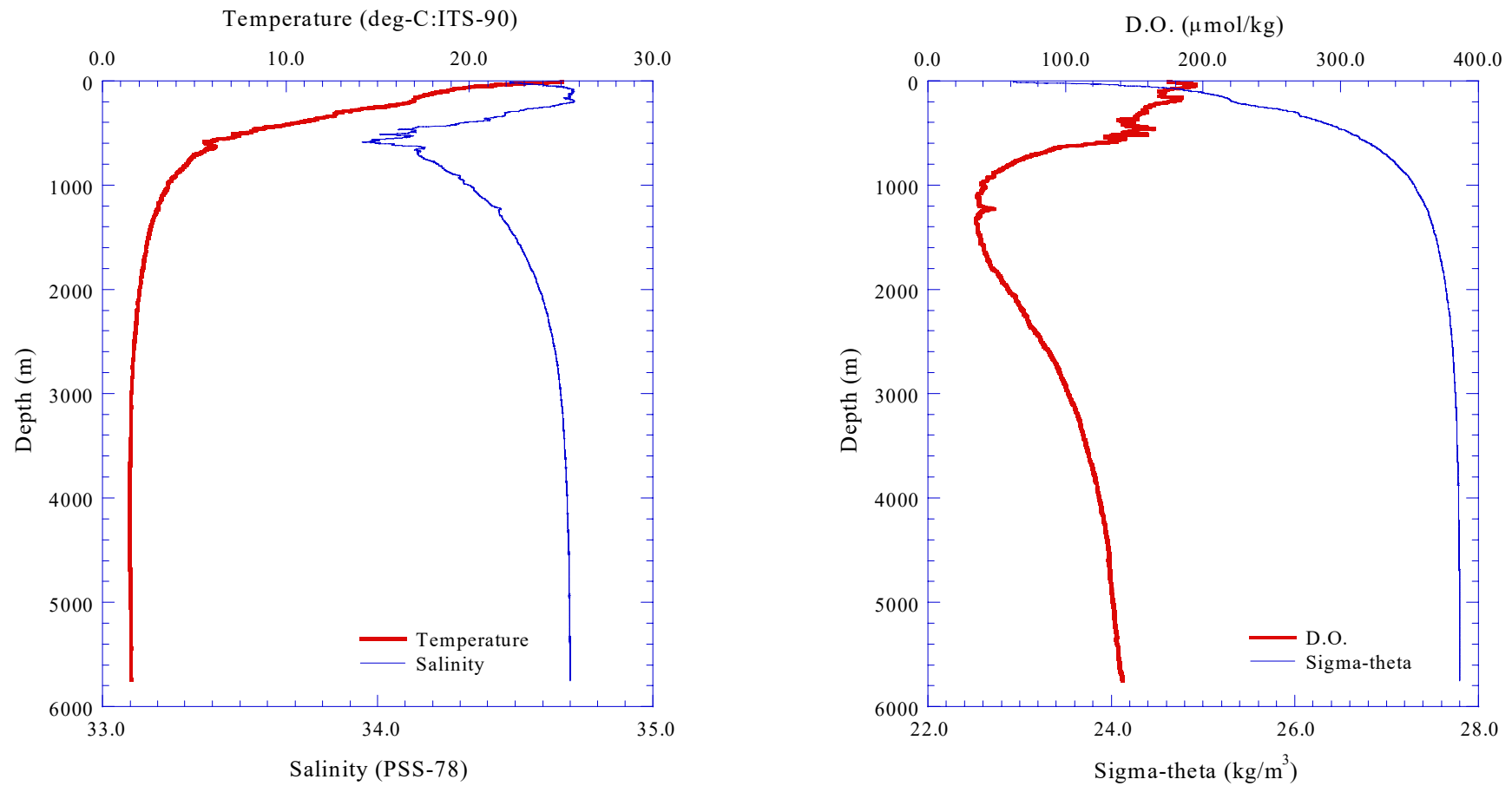


Fig.3.2.28.(a) CTD profile (Stn.28;028L01)

3.2-60

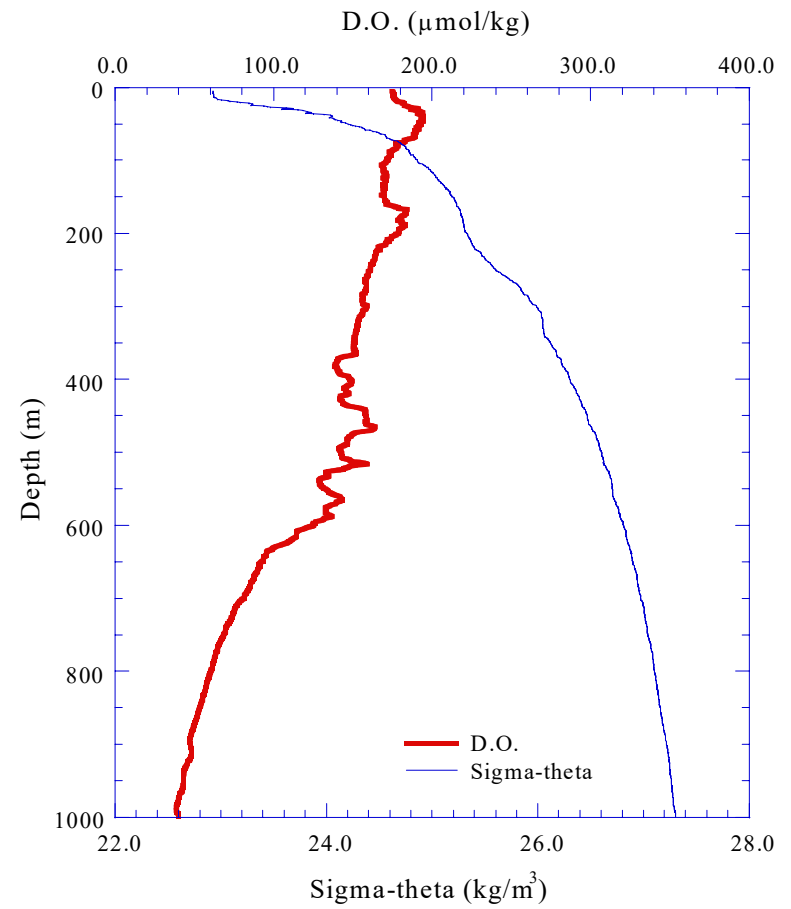
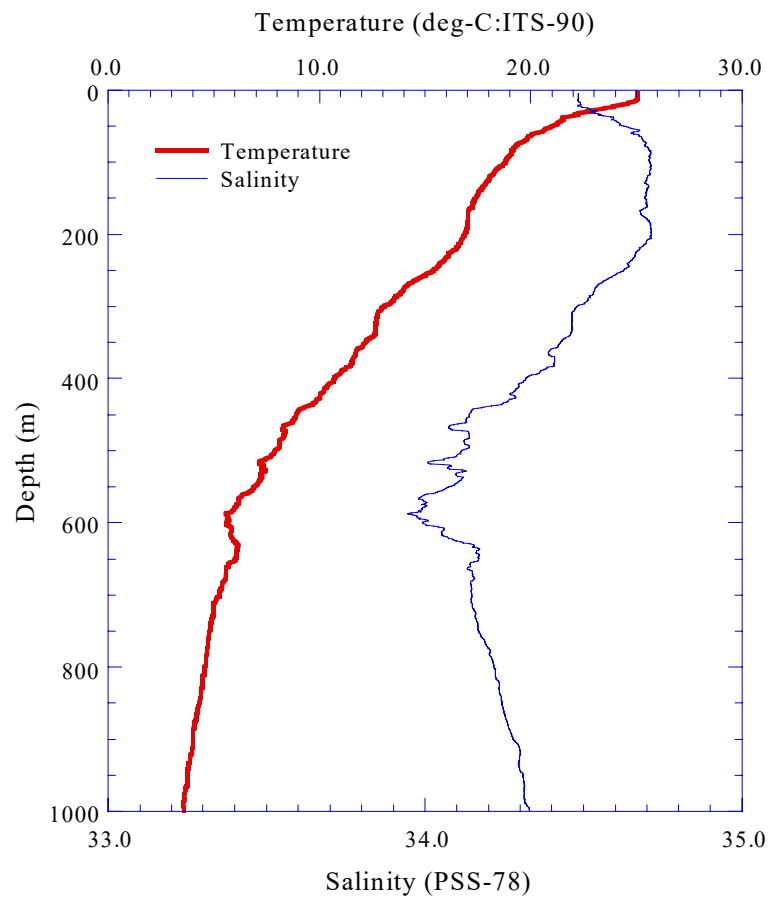


Fig.3.2.28.(b) CTD profile to 1,000m (Stn.28;028L01)

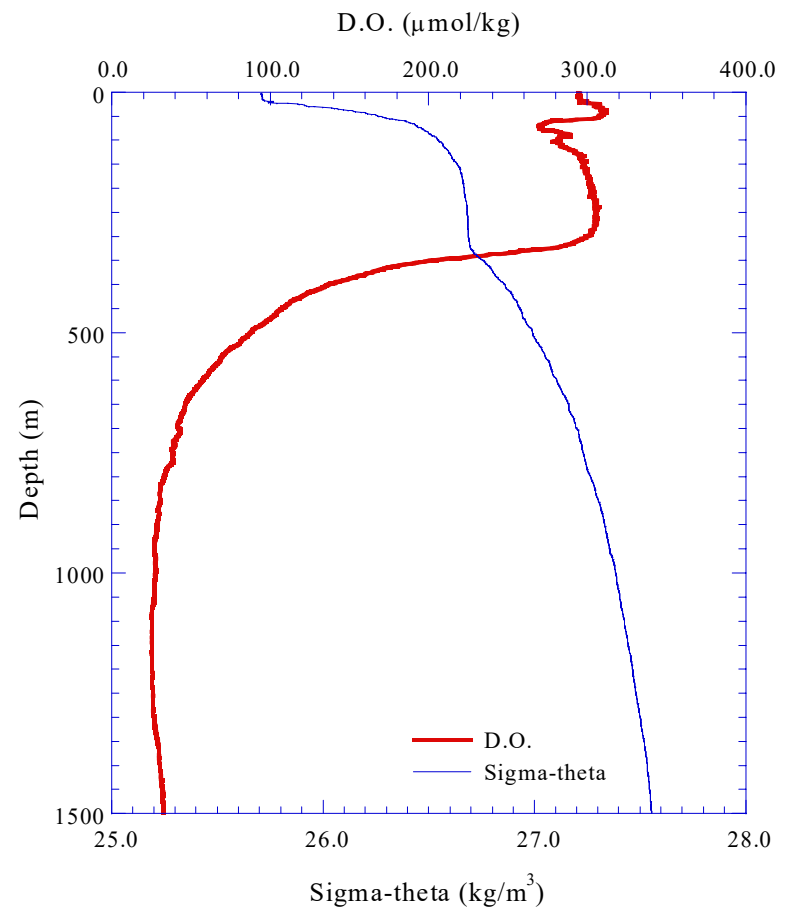
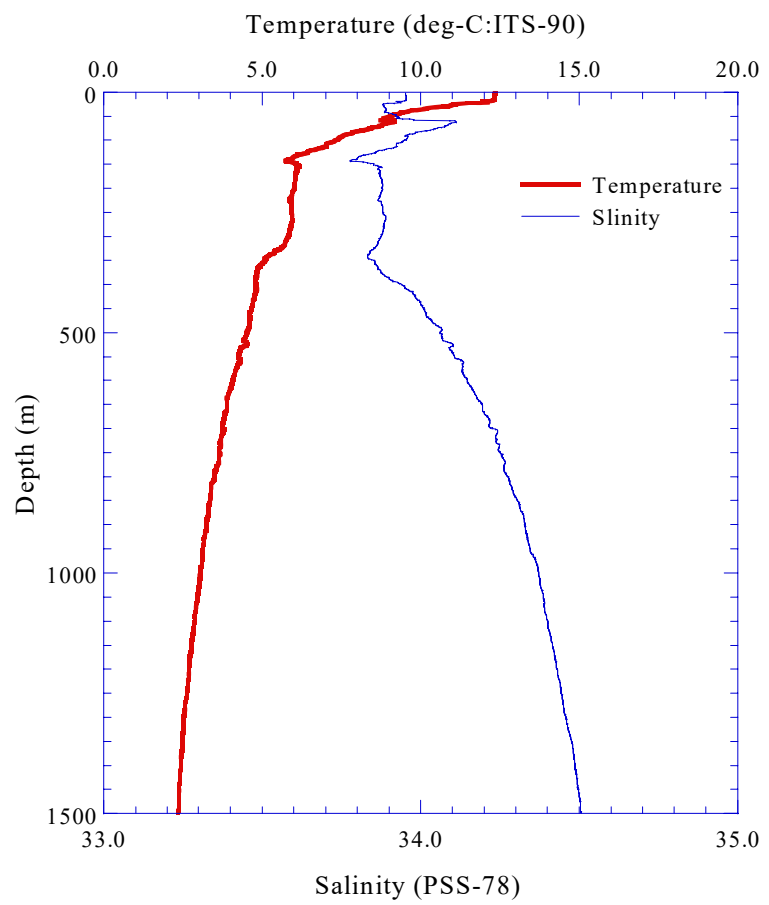


Fig.3.2.29 CTD profile (Stn.E01;E01S01)

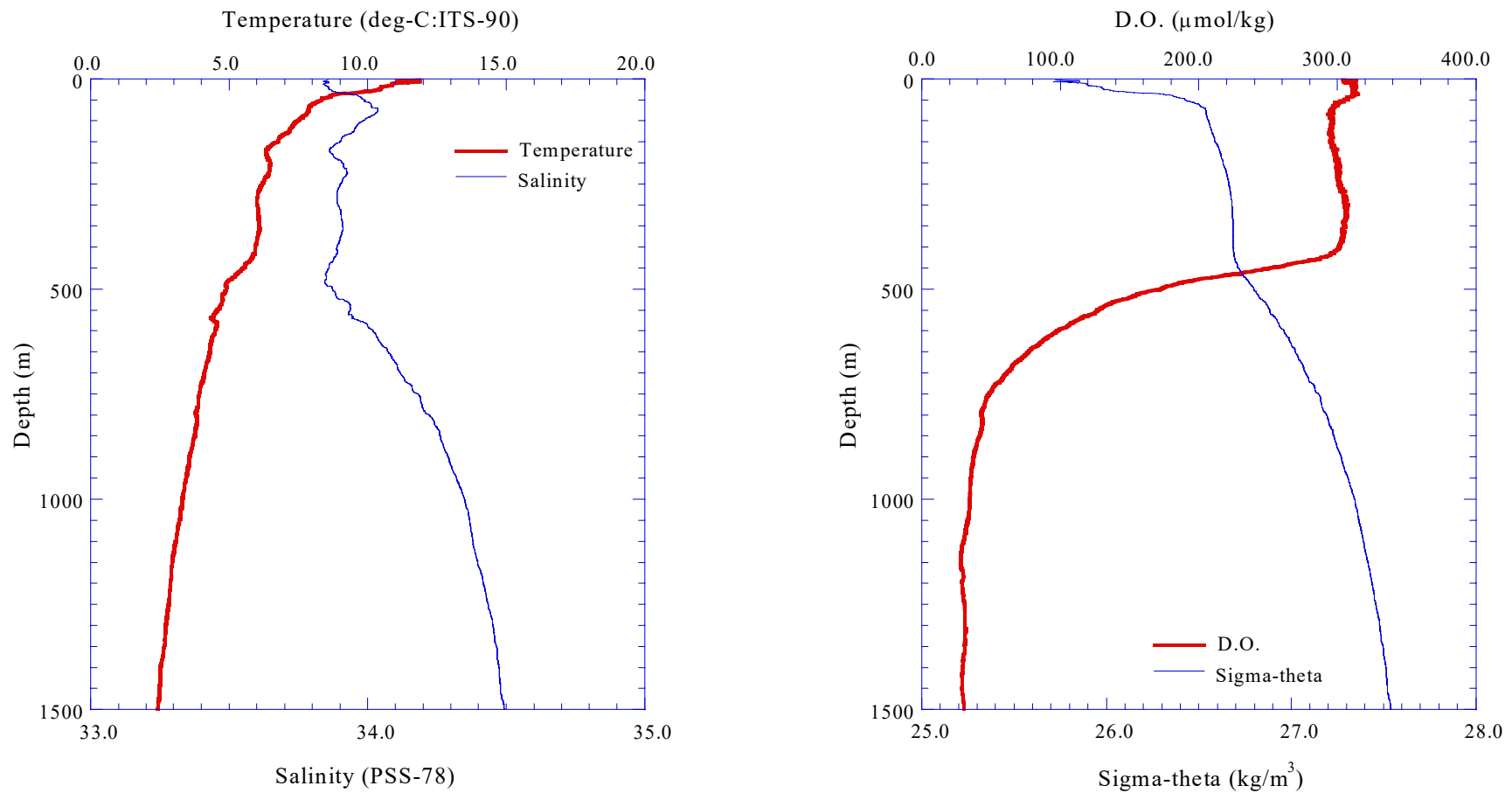


Fig.3.2.30 CTD profile (Stn.E02;E02S01)

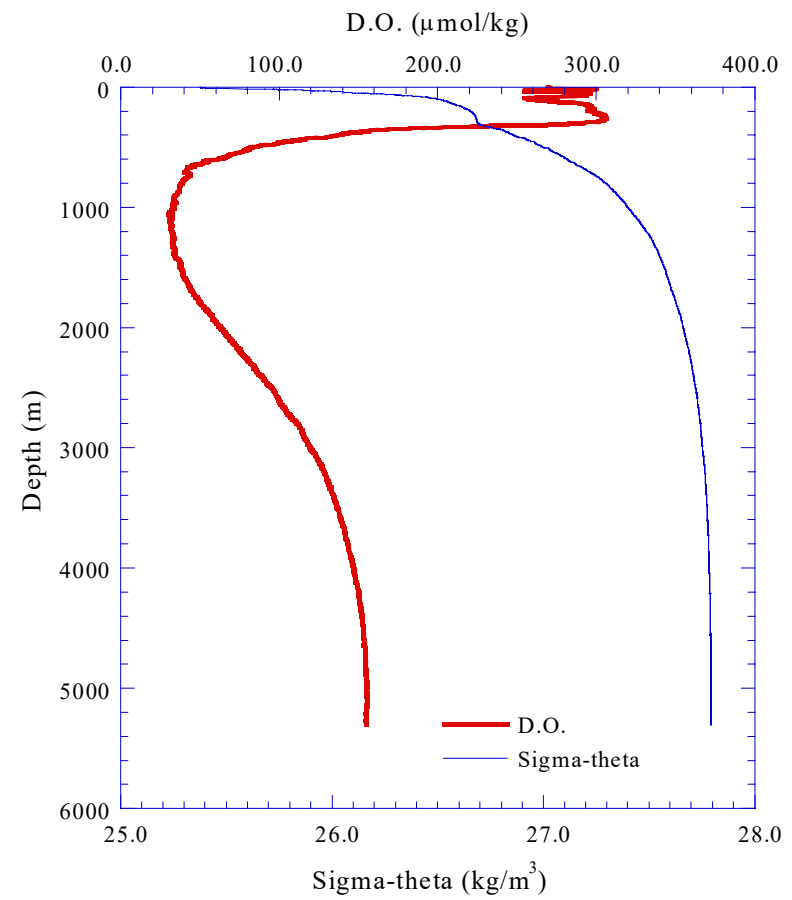
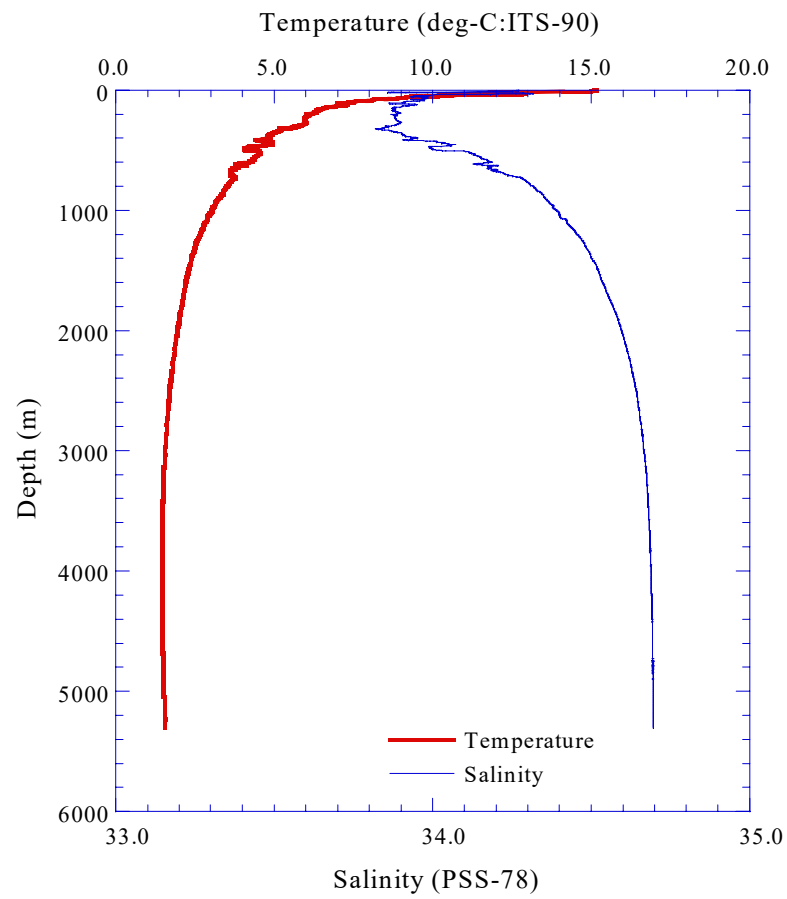


Fig.3.2.31.(a) CTD profile (Stn.E03;E03S01)

3.2-64

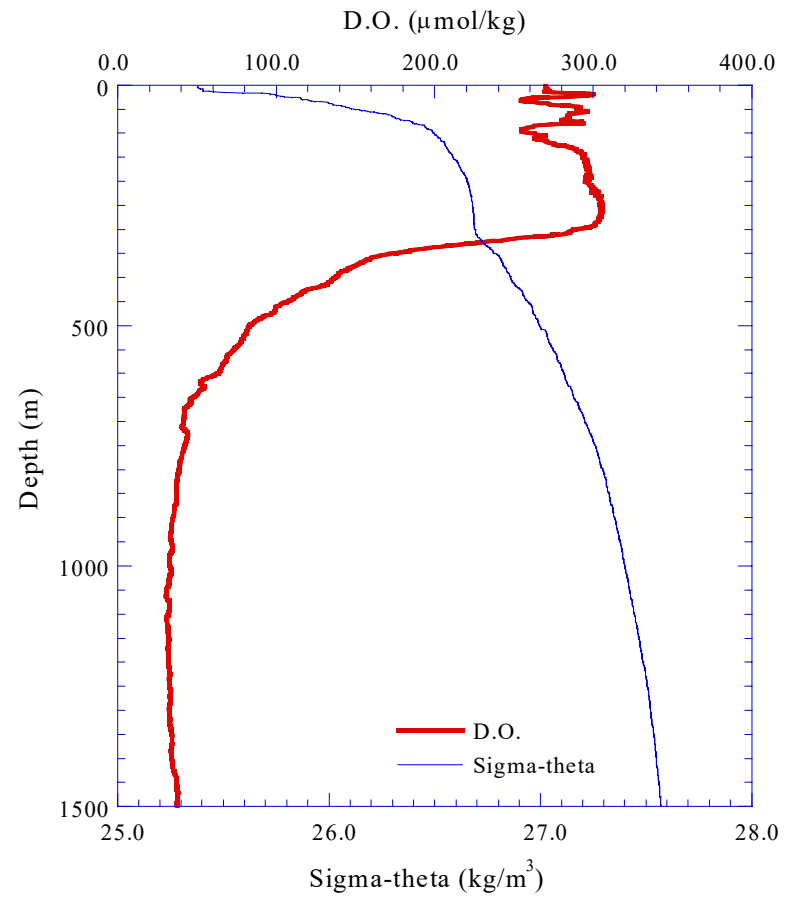
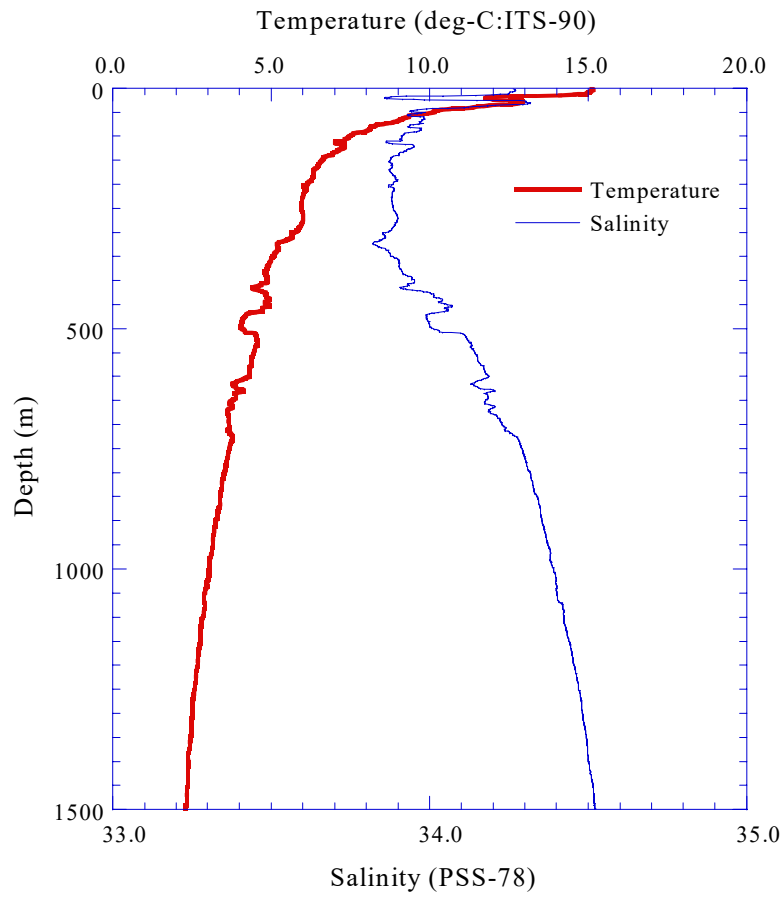


Fig.3.2.31.(b) CTD profile to 1,500m (Stn.E03;E03S01)

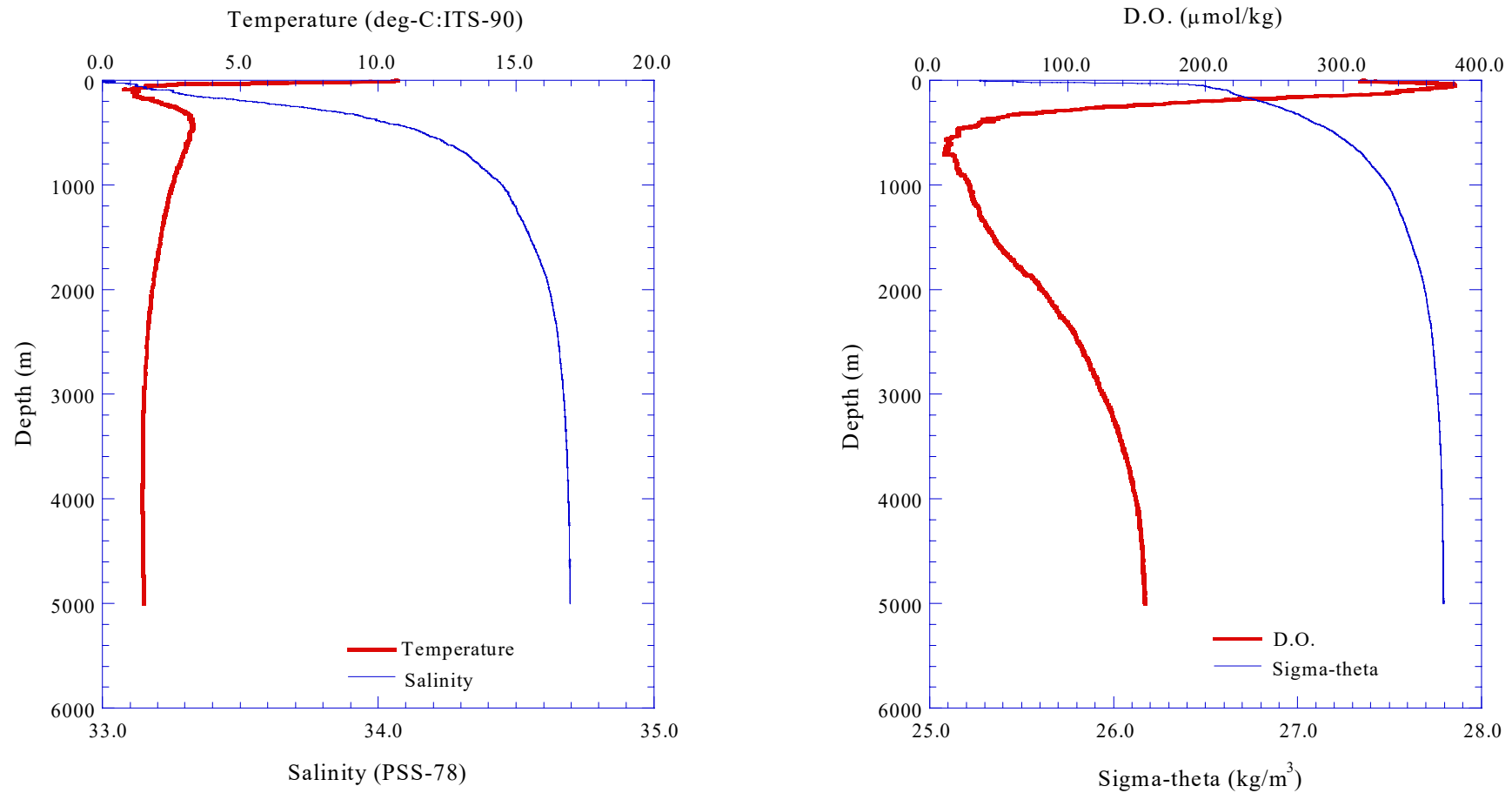


Fig.3.2.32.(a) CTD profile (Stn.E04;E04S01)

3.2-66

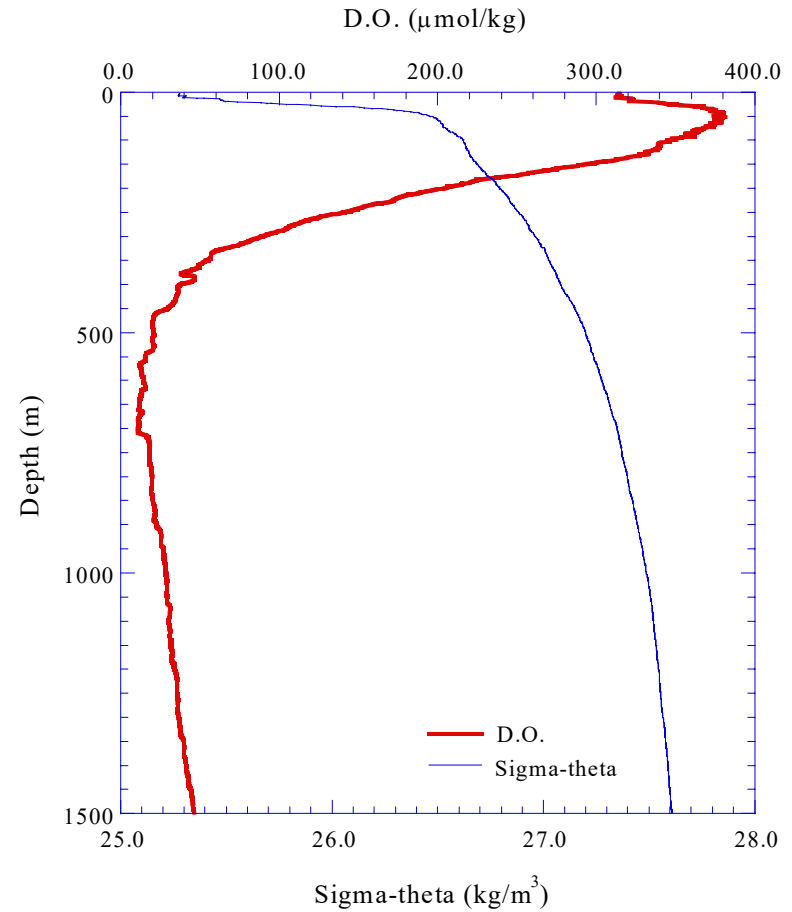
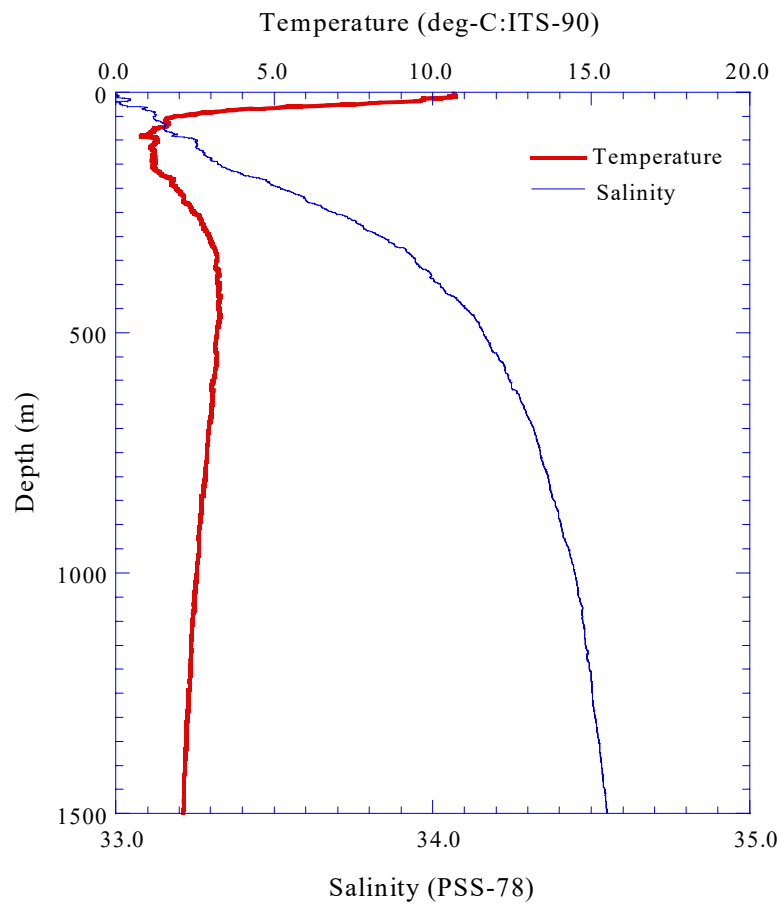


Fig.3.2.32.(b) CTD profile to 1,500m (Stn.E04;E04S01)

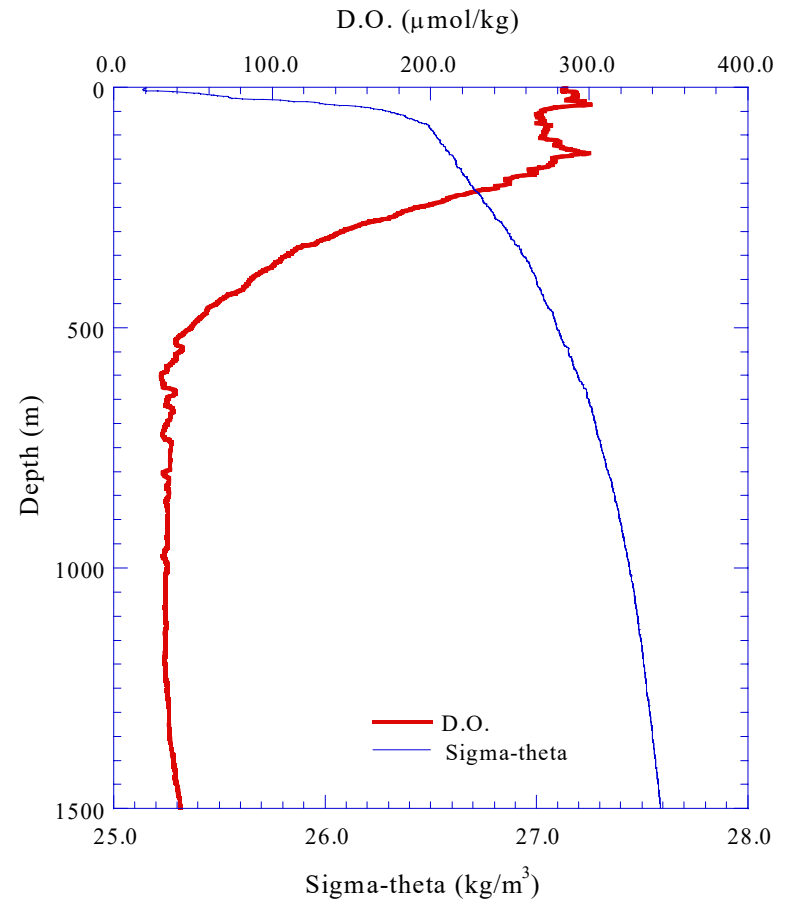
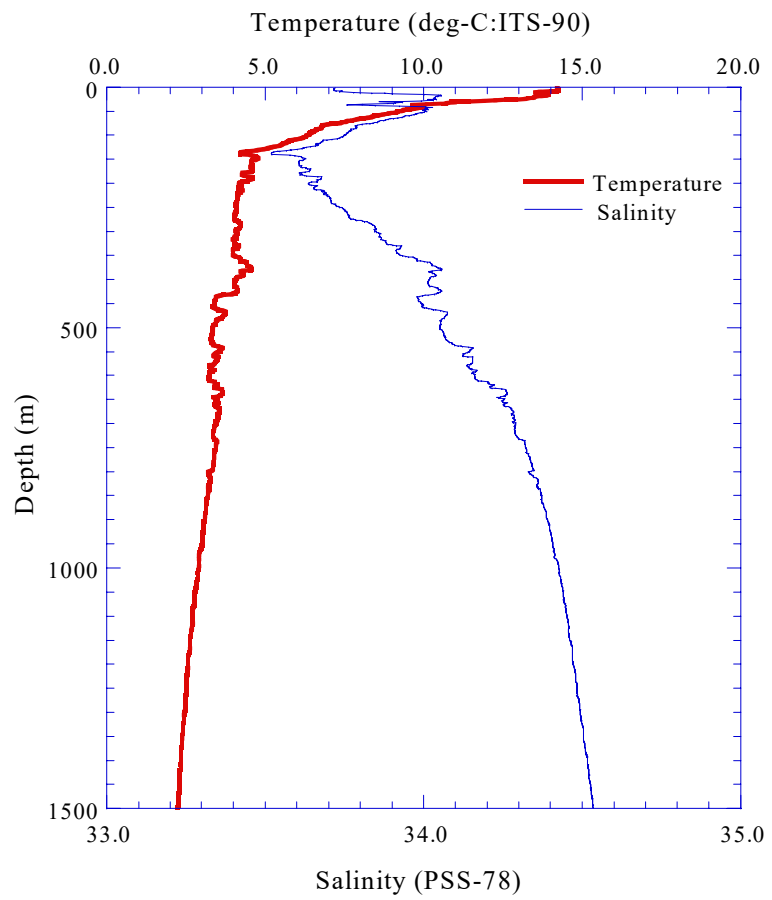


Fig.3.2.33 CTD profile (Stn.E05;E05S01)

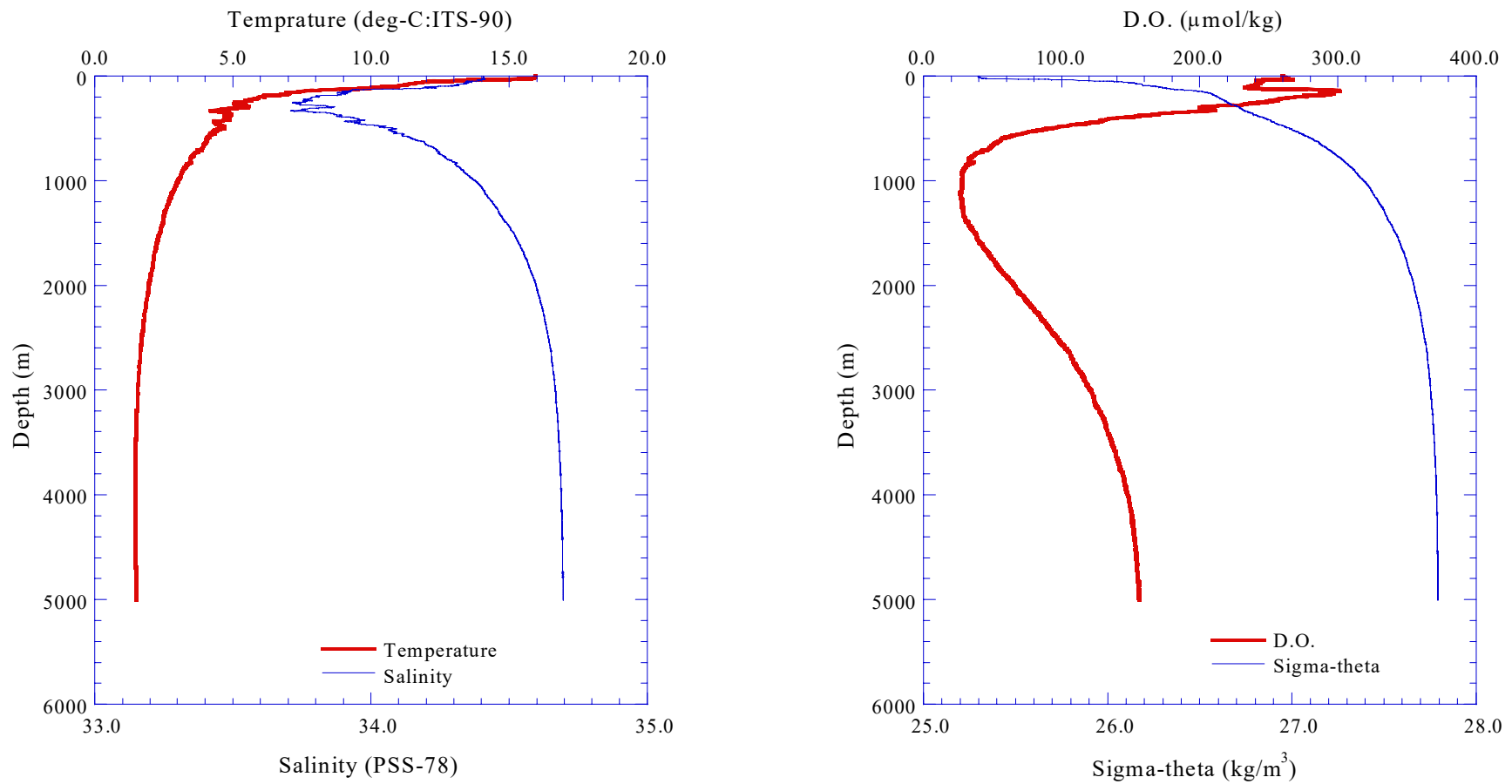


Fig.3.2.34.(a) CTD profile (Stn.E06;E06S01)

3.2-69

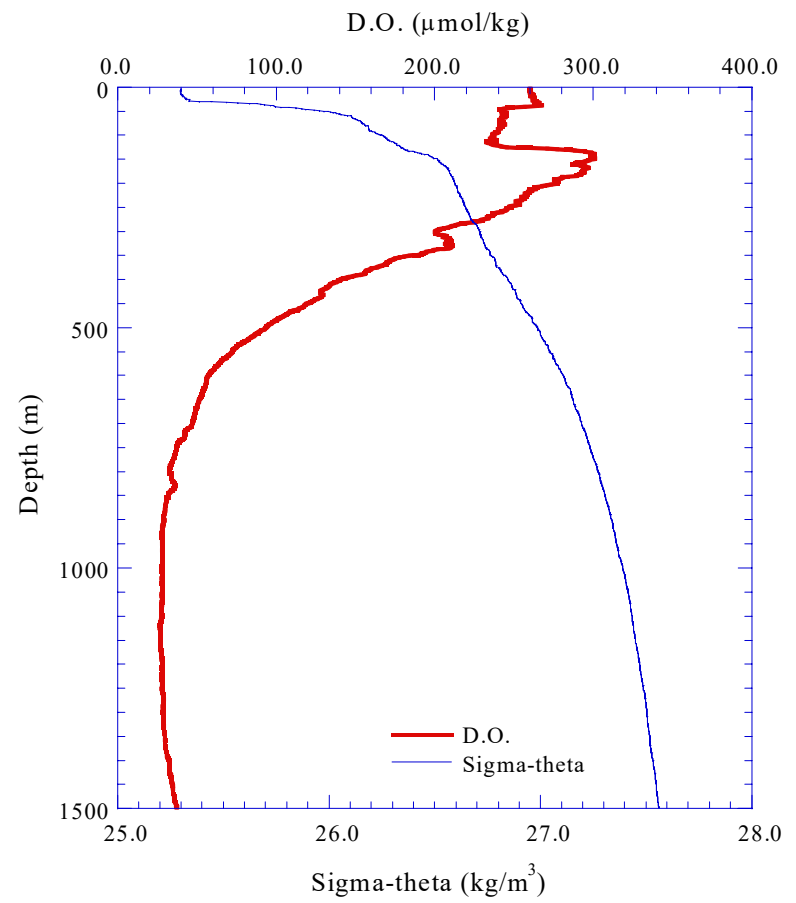
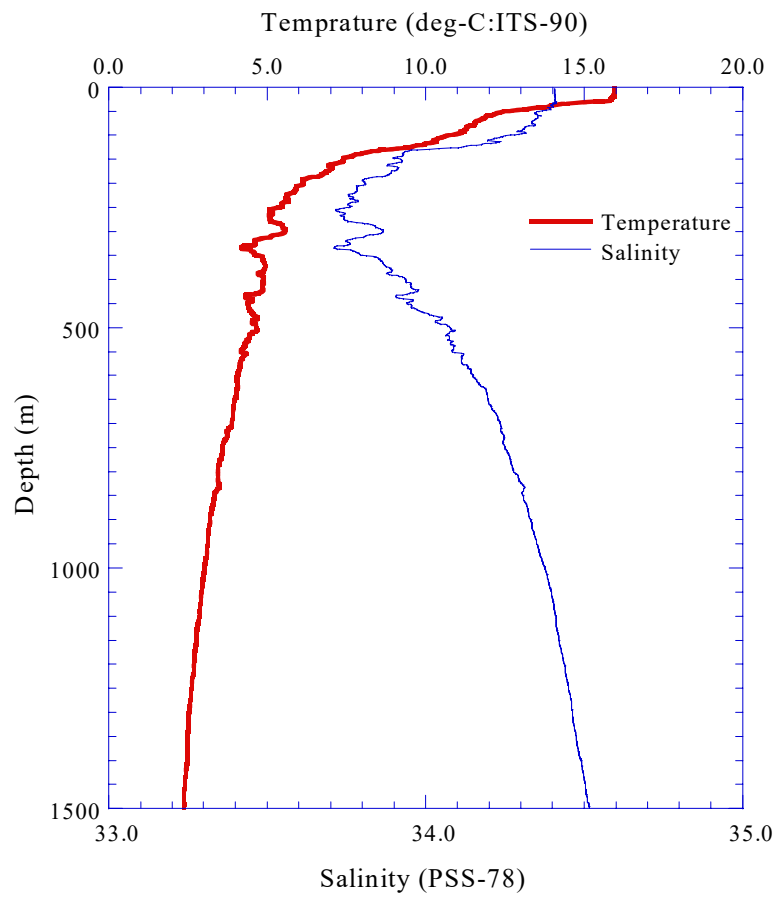


Fig.3.2.34.(b) CTD profile to 1,500m (Stn.E06;E06S01)

3.2-70

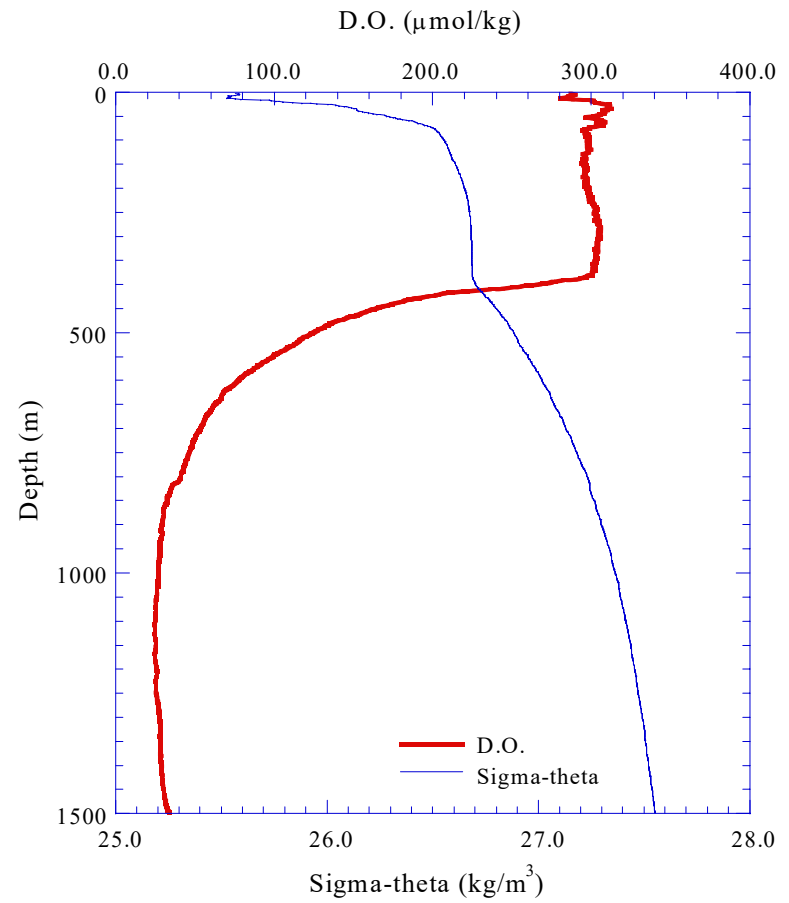
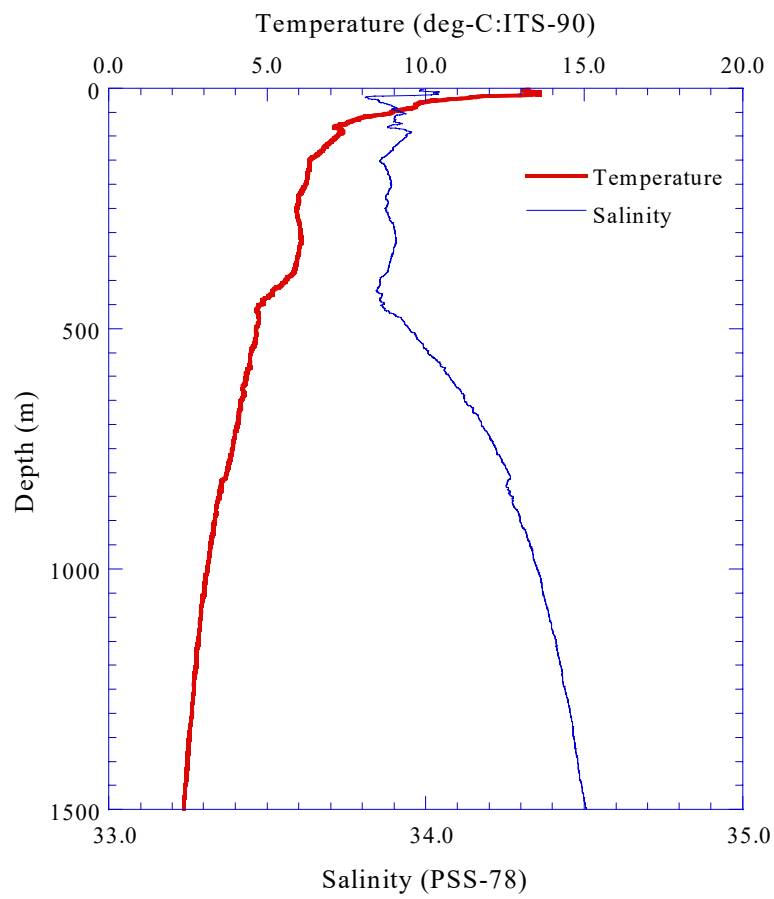


Fig.3.2.35 CTD profile (Stn.E07;E07S01)

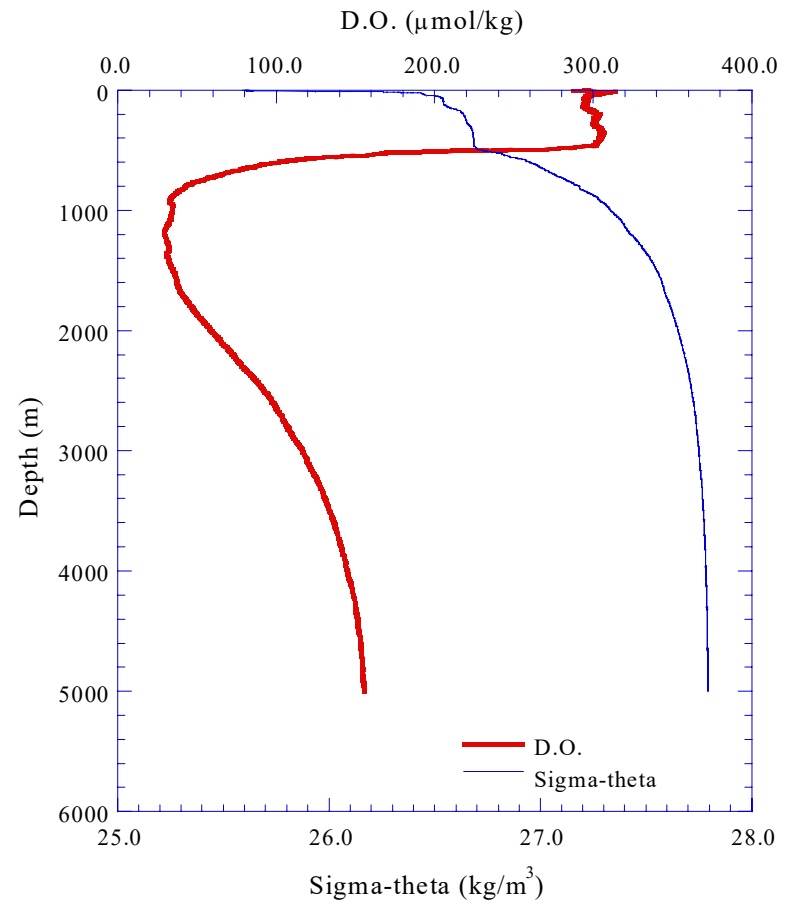
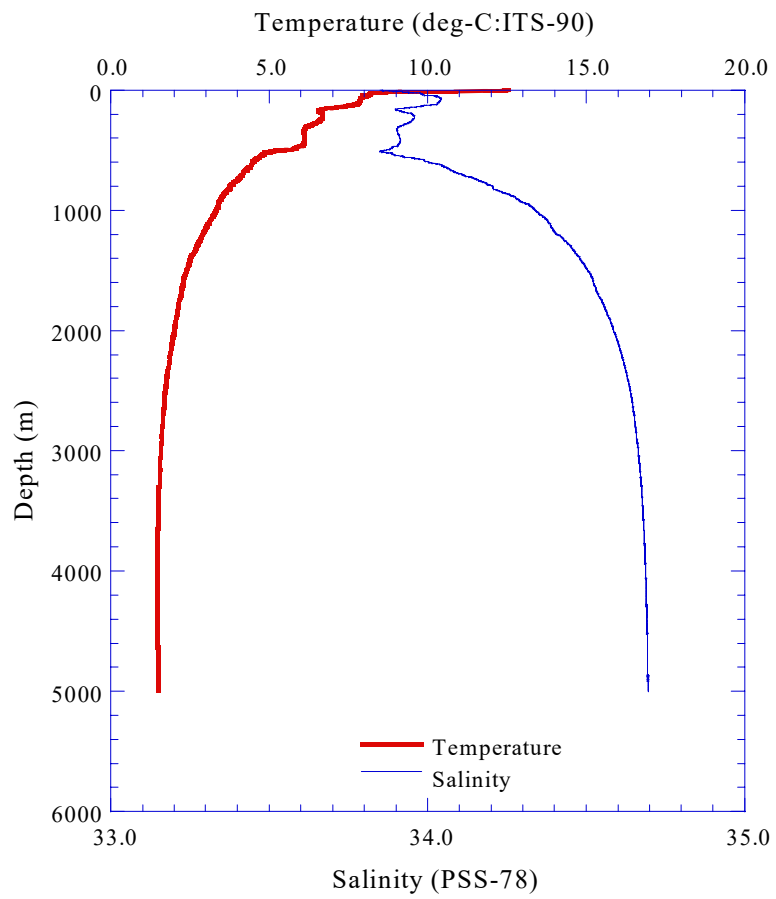


Fig.3.2.36.(a) CTD profile (Stn.E08;E08S01)

3.2-72

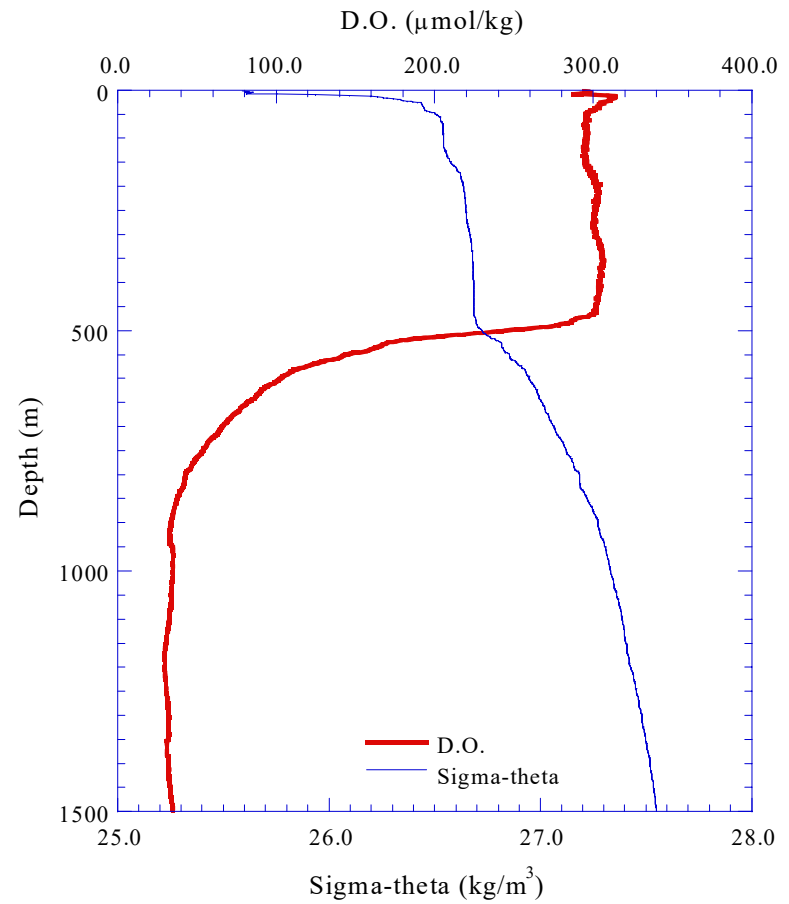
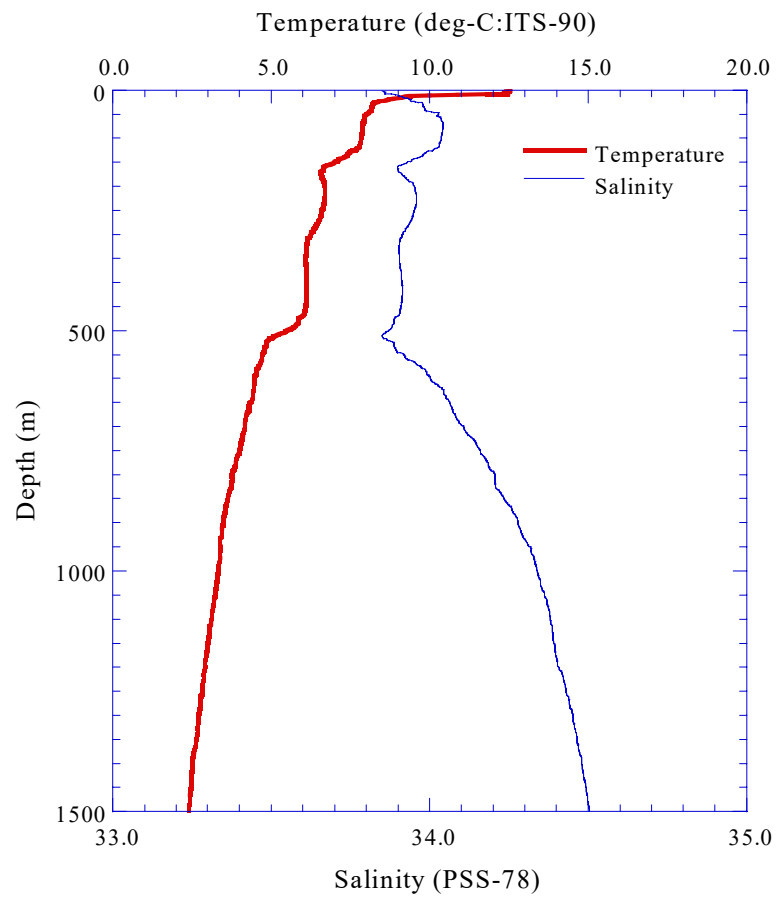


Fig.3.2.36.(b) CTD profile to 1,500m (Stn.E08;E08S01)

3.2-73

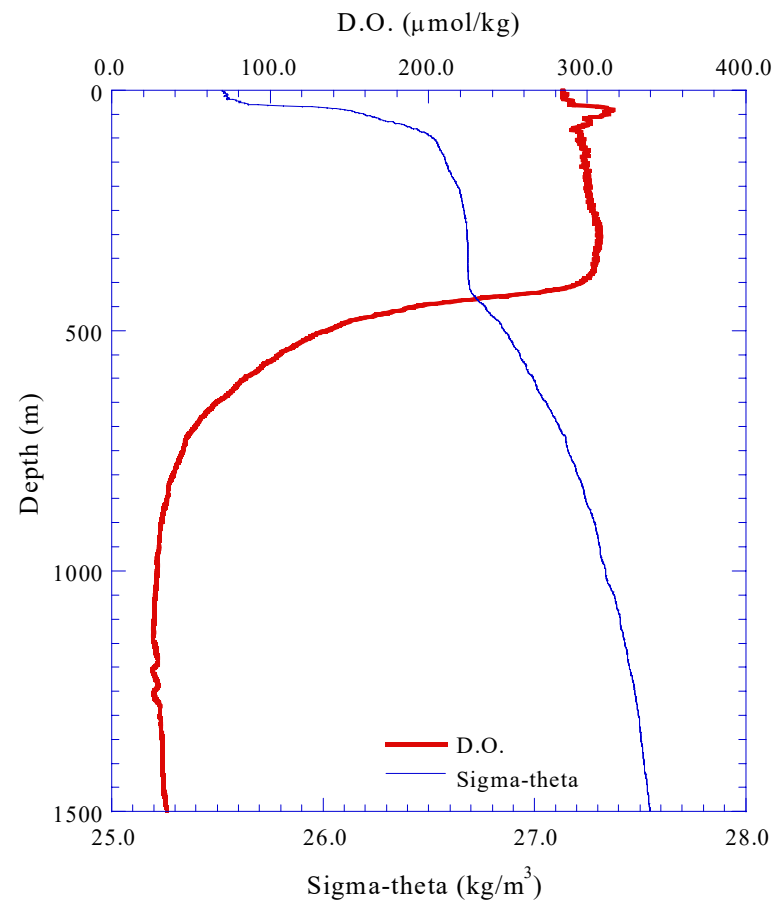
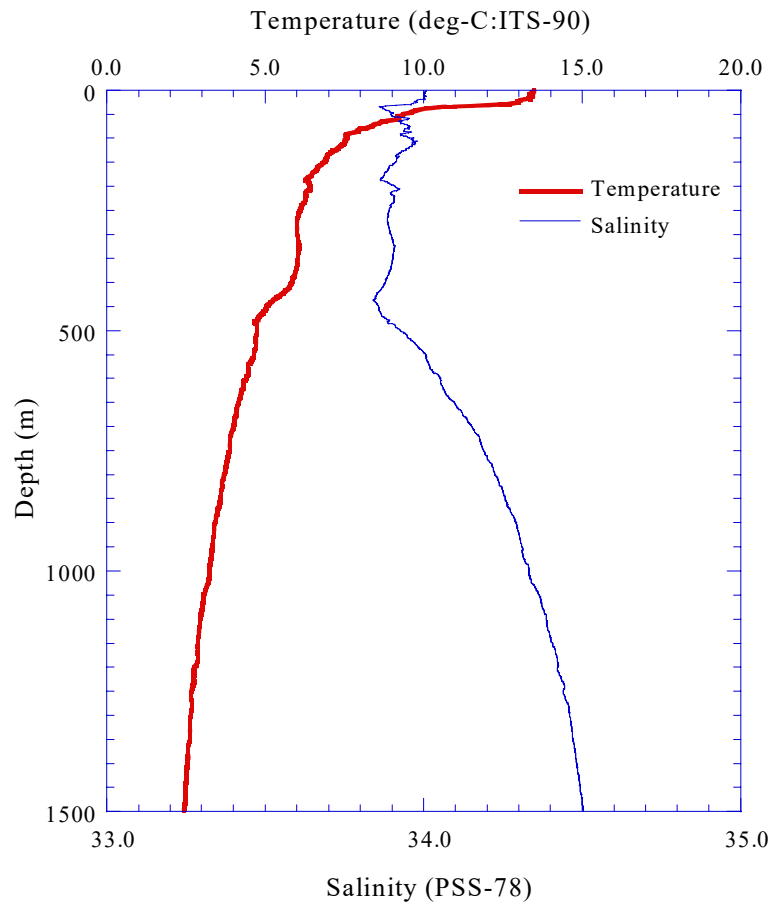


Fig.3.2.37 CTD profile (Stn.E09;E09S01)

3.2-74

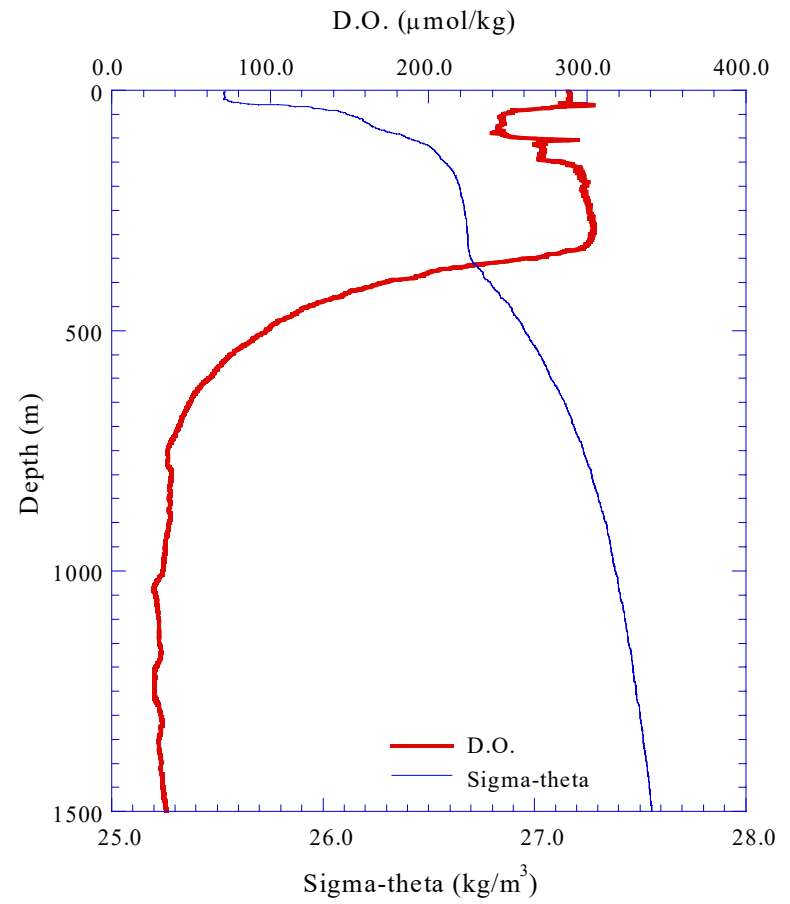
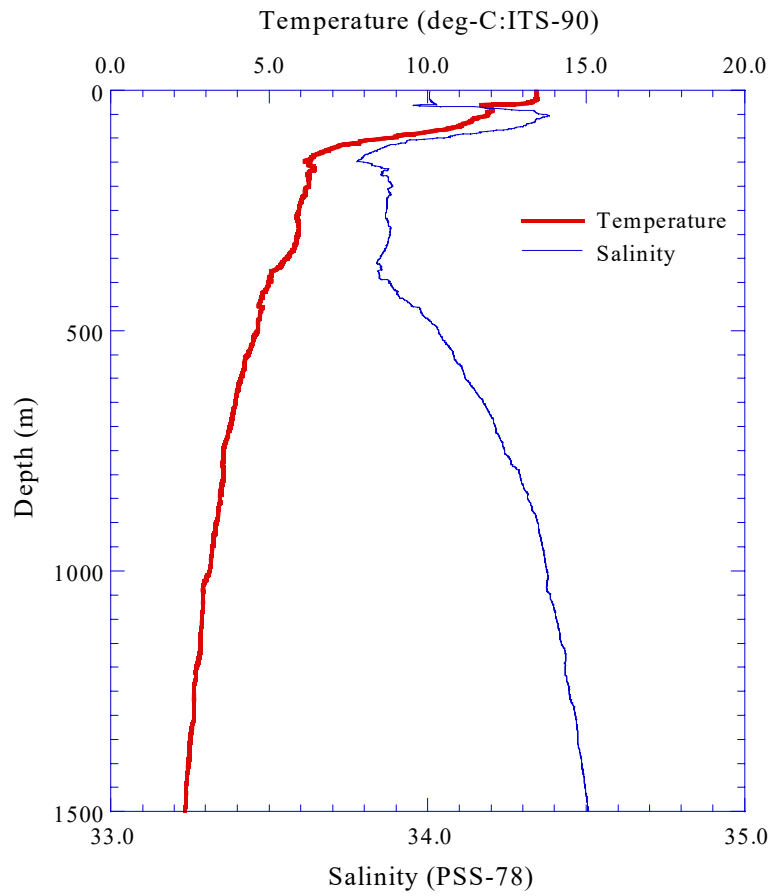


Fig.3.2.38 CTD profile (Stn.E10;E10S01)

3.2-75

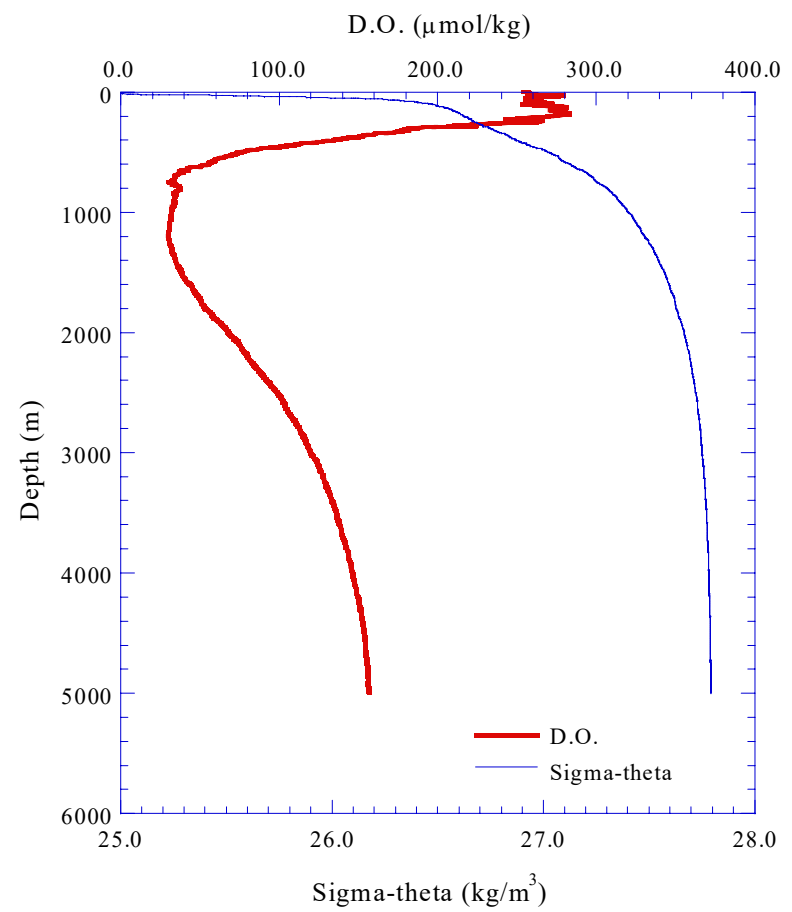
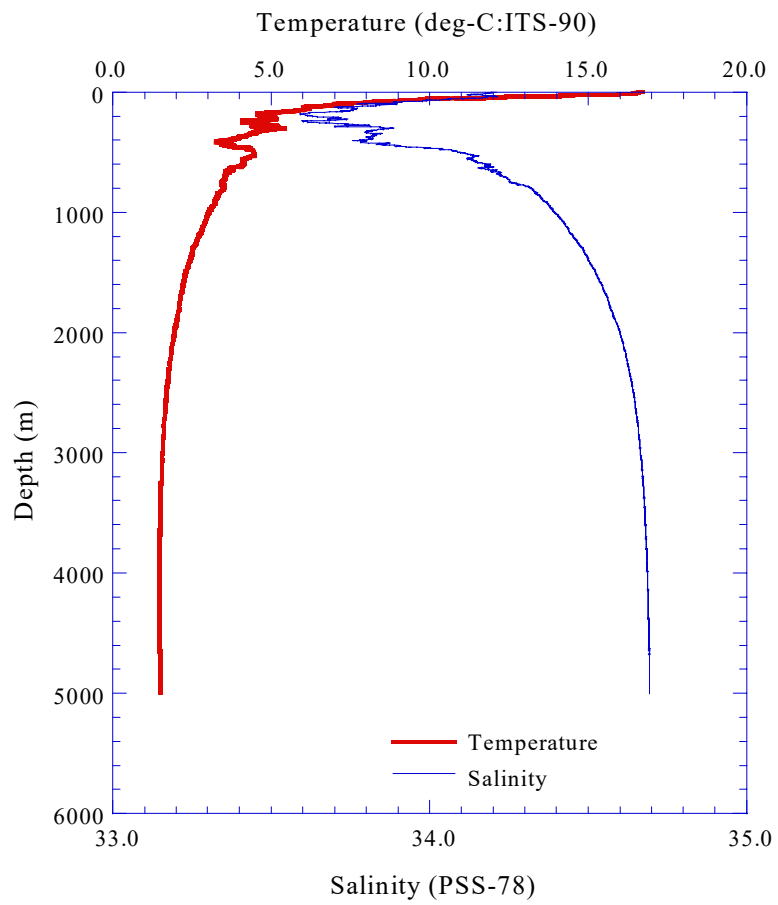


Fig.3.2.39.(a) CTD profile (Stn.E11;E11S01)

3.2-76

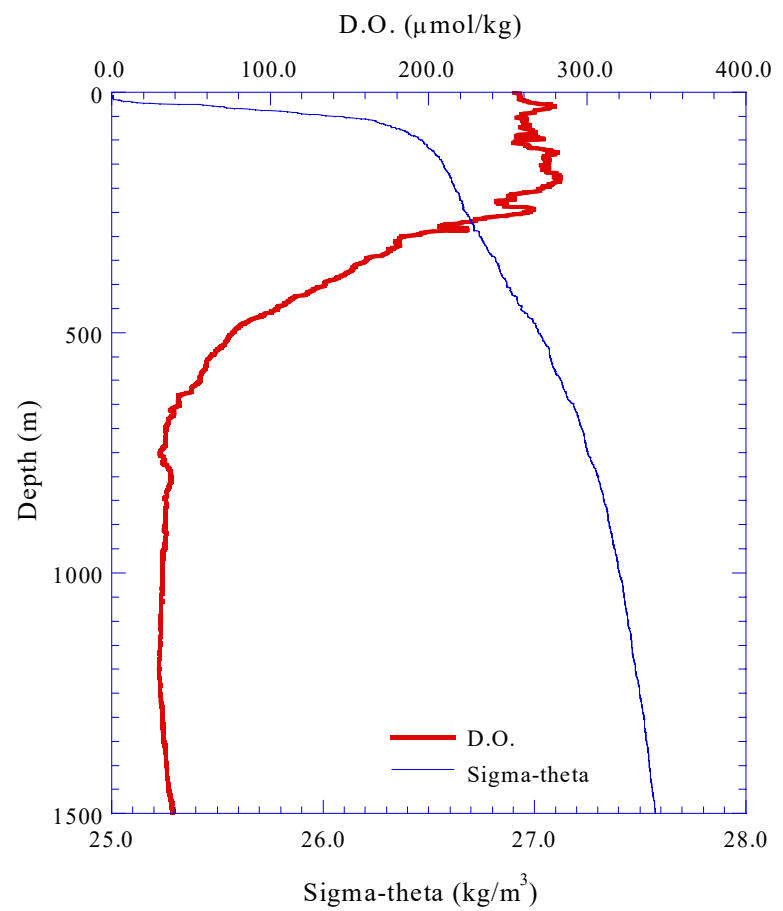
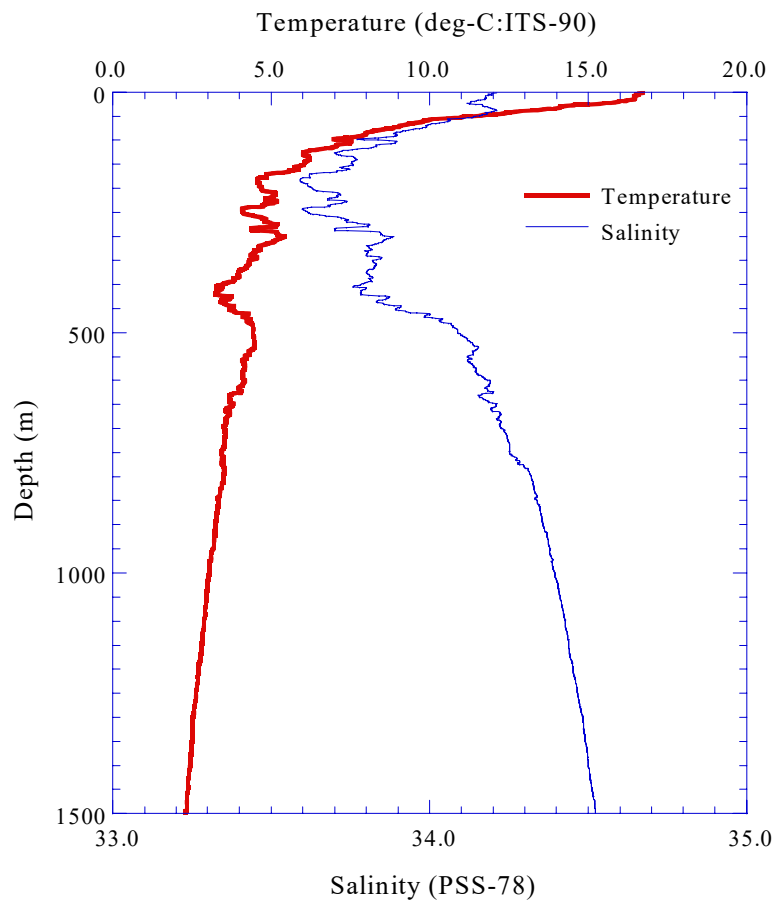


Fig.3.2.39.(b) CTD profile to 1,500m (Stn.E11;E11S01)

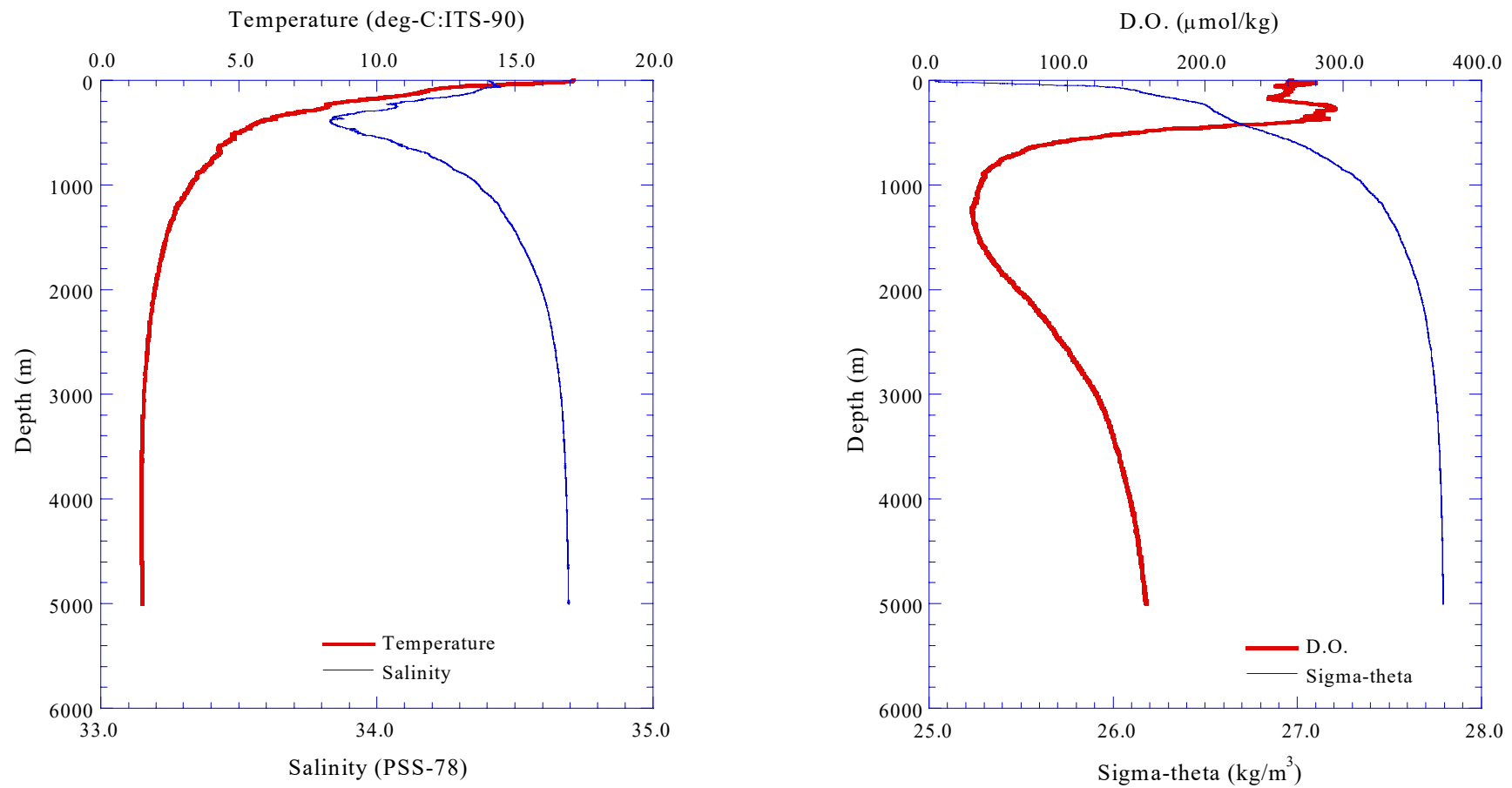


Fig.3.2.40.(a) CTD profile (Stn.E12;E12S01)

3.2-78

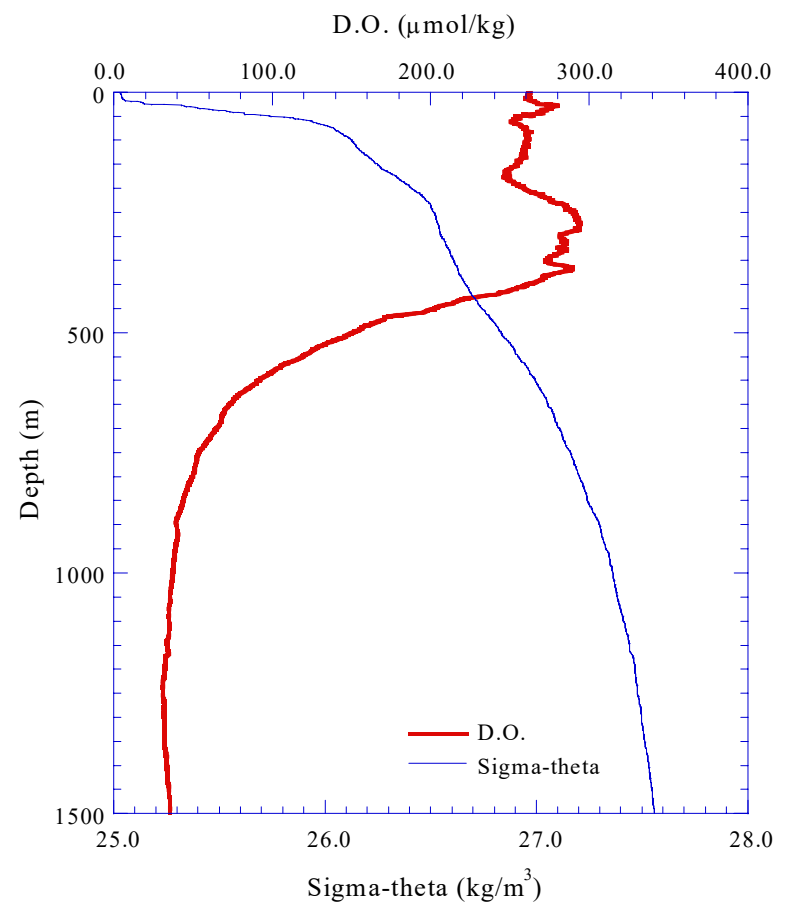
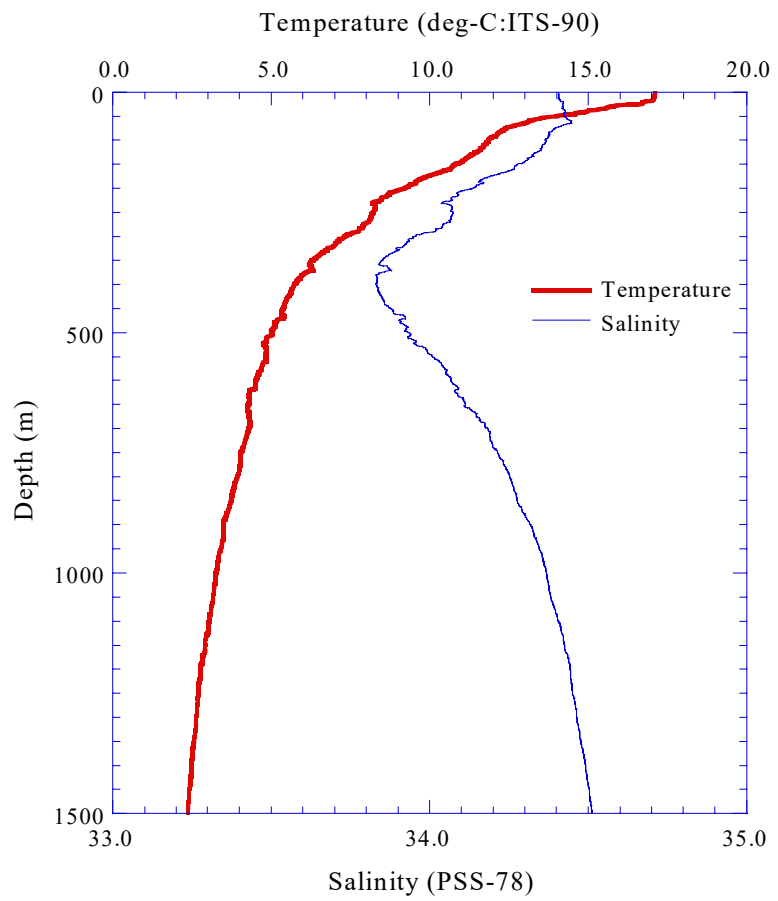


Fig.3.2.40.(b) CTD profile to 1,500m (Stn.E12;E12S01)

3.2-79

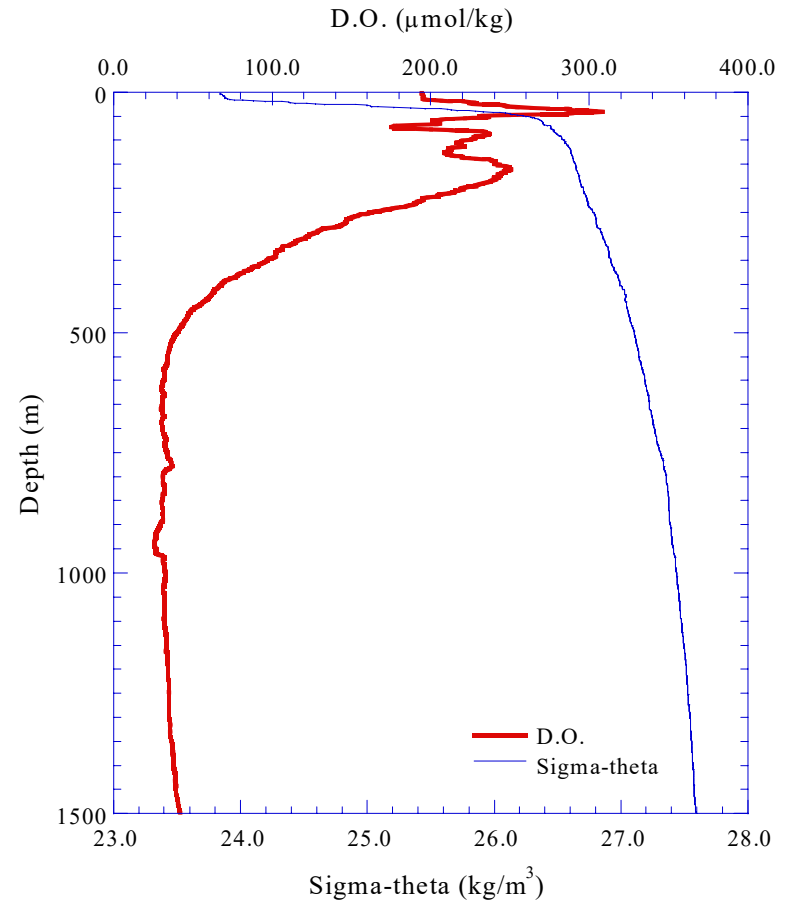
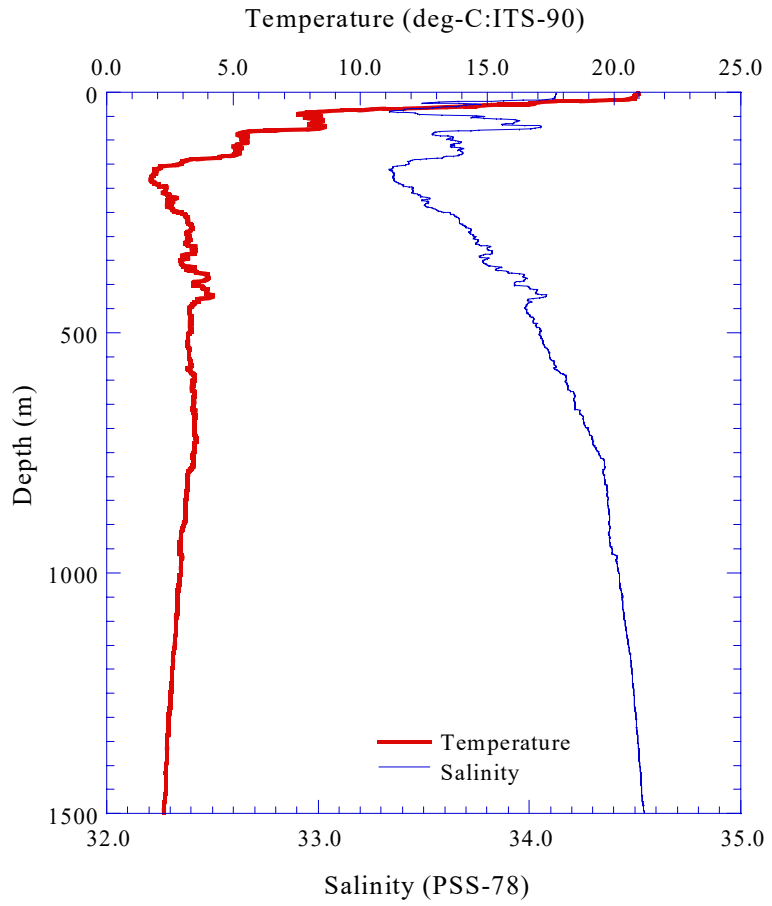


Fig.3.2.41 CTD profile (Stn.R01;R01S02)

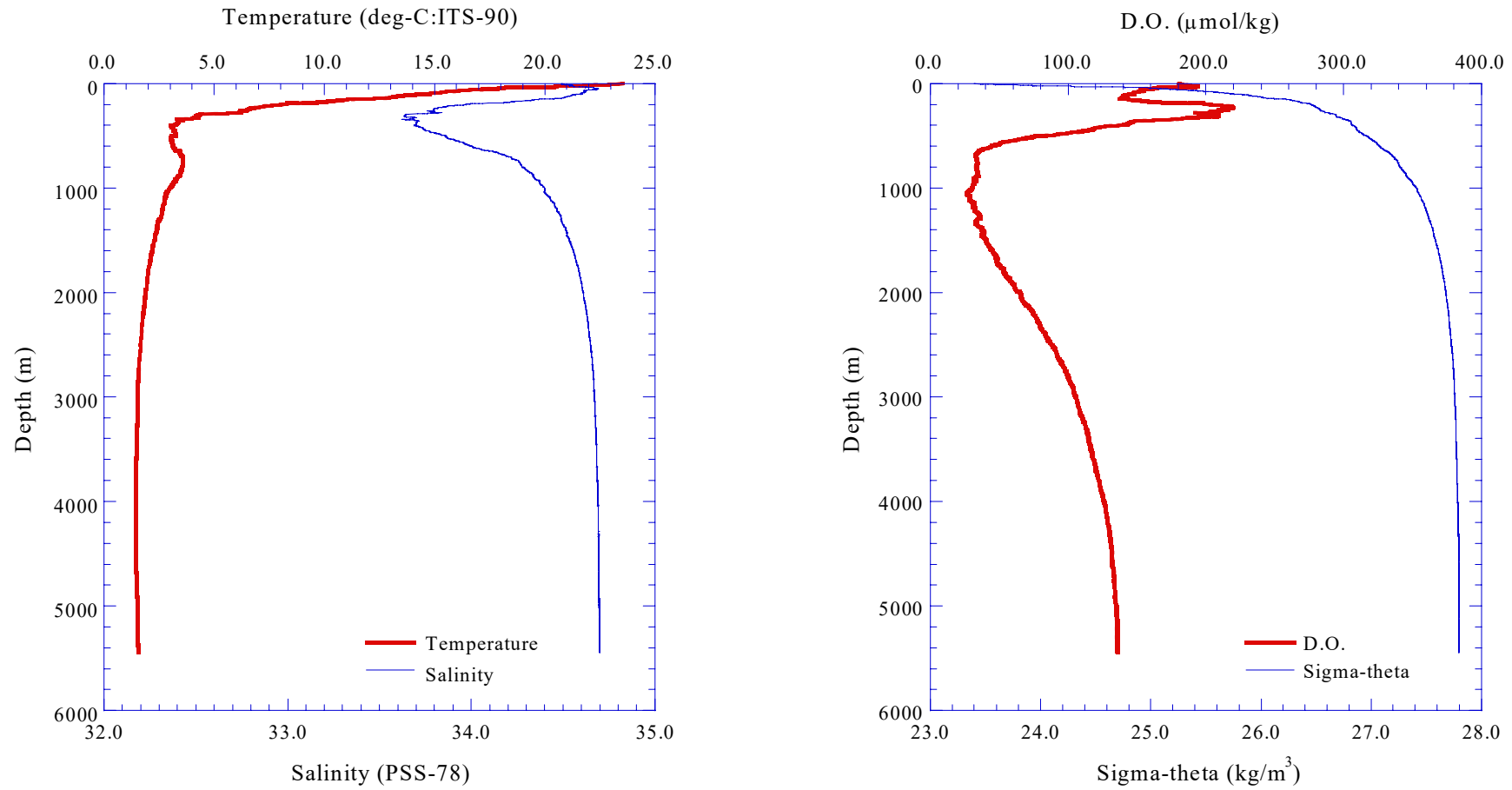


Fig.3.2.42.(a) CTD profile (Stn.R02;R02S02)

3.2-81

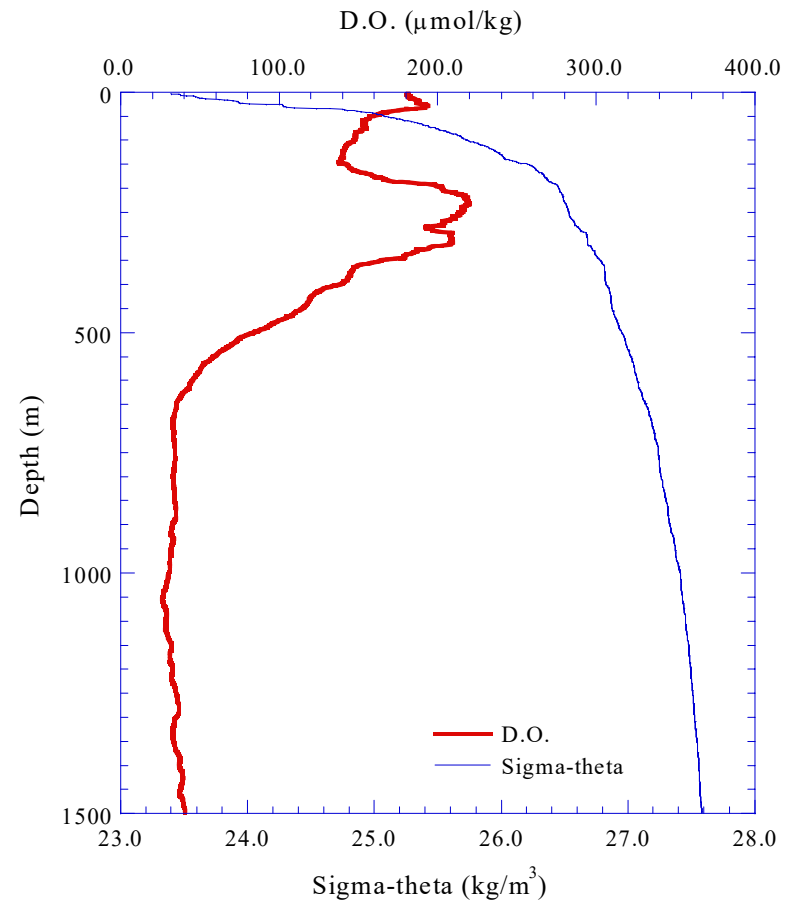
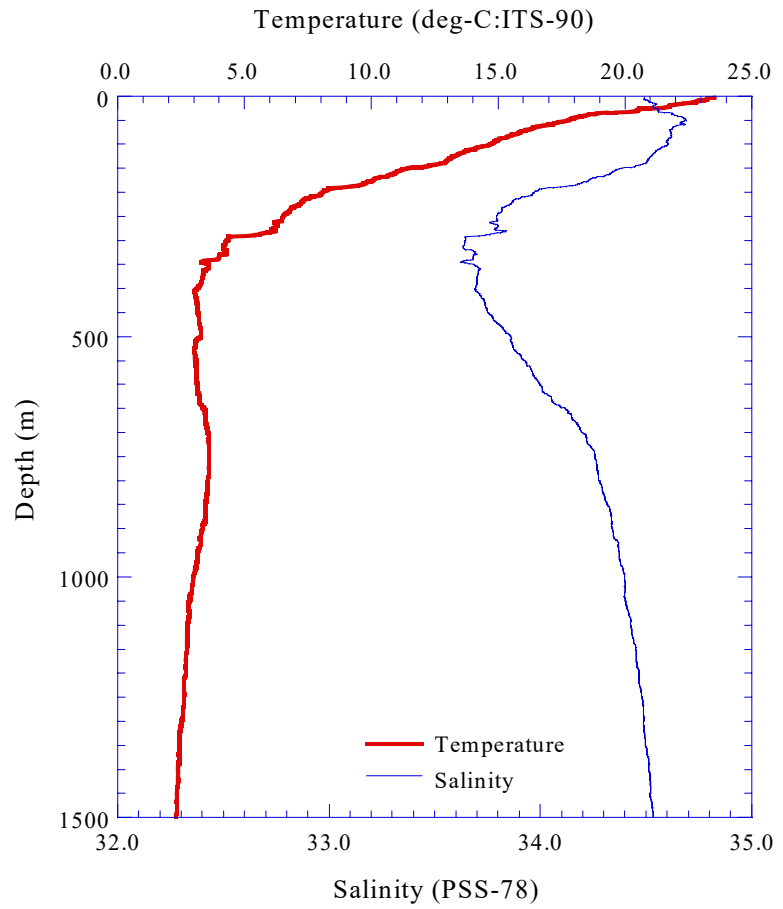


Fig.3.2.42.(b) CTD profile to 1,500m (Stn.R02;R02S02)

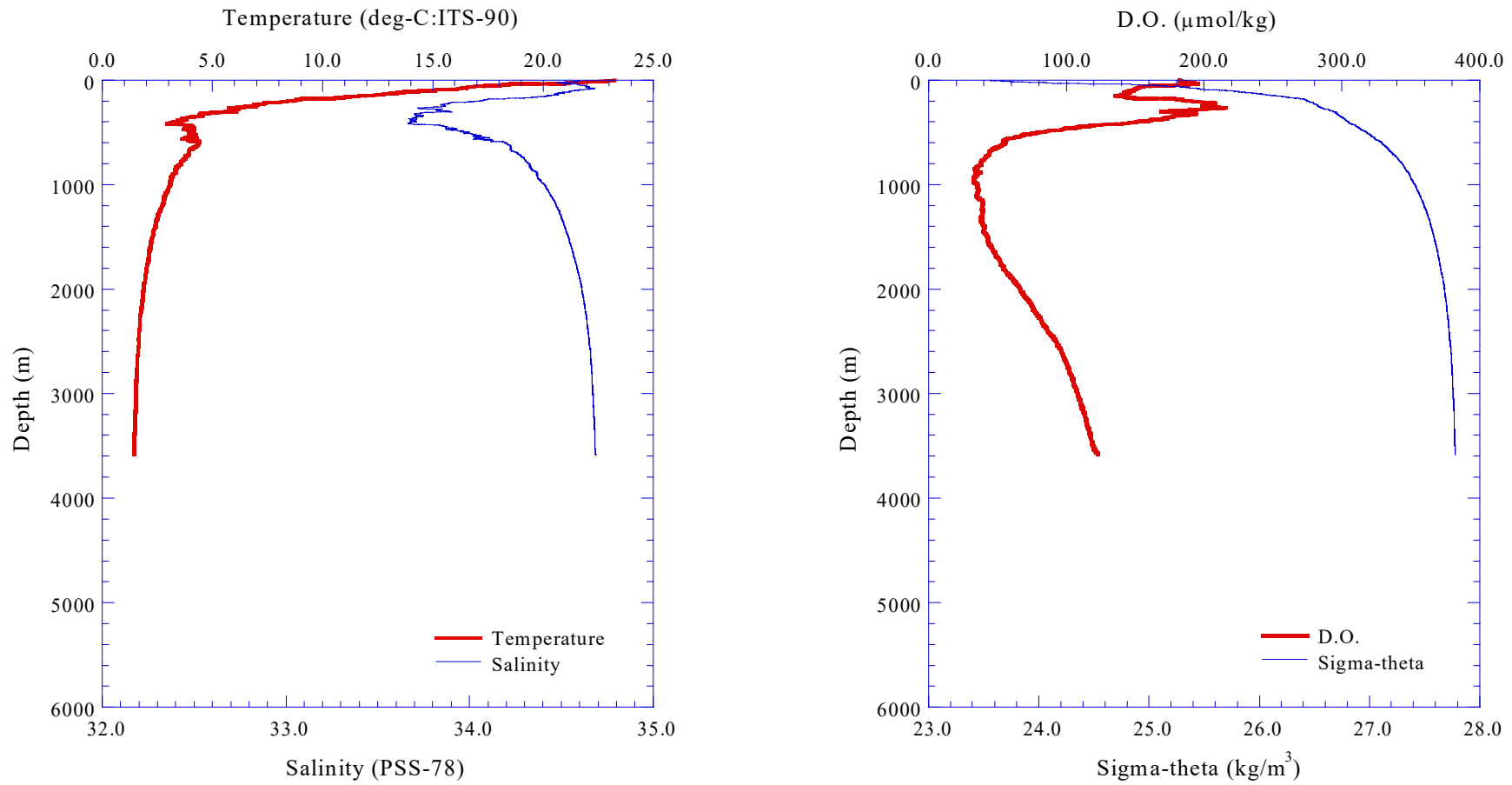


Fig.3.2.43.(a) CTD profile (Stn.R03;R03S01)

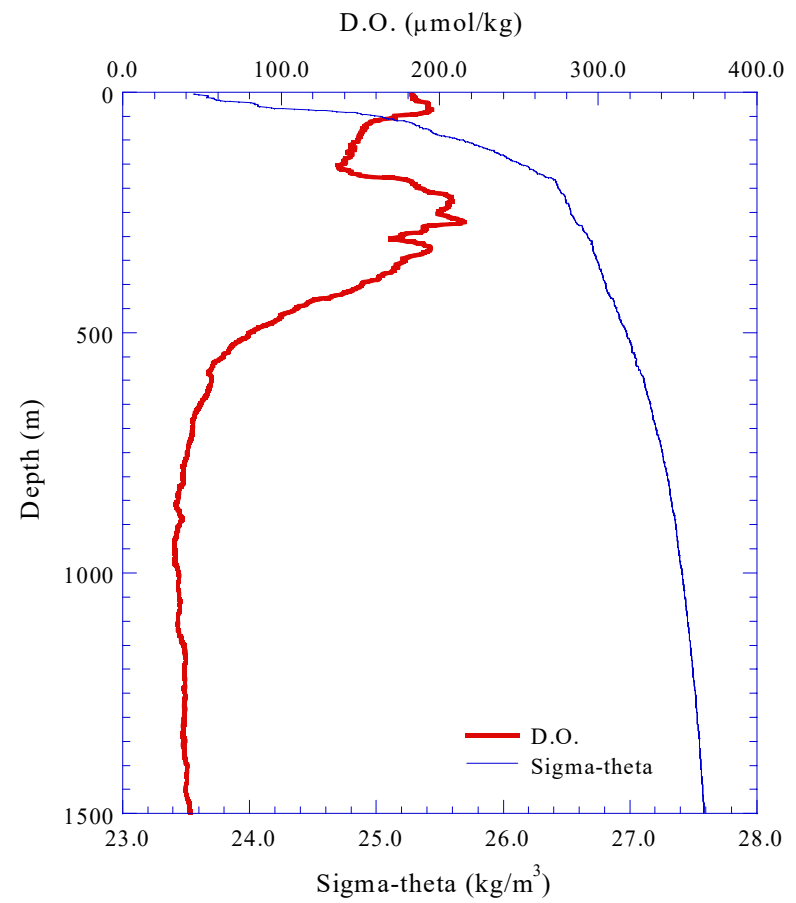
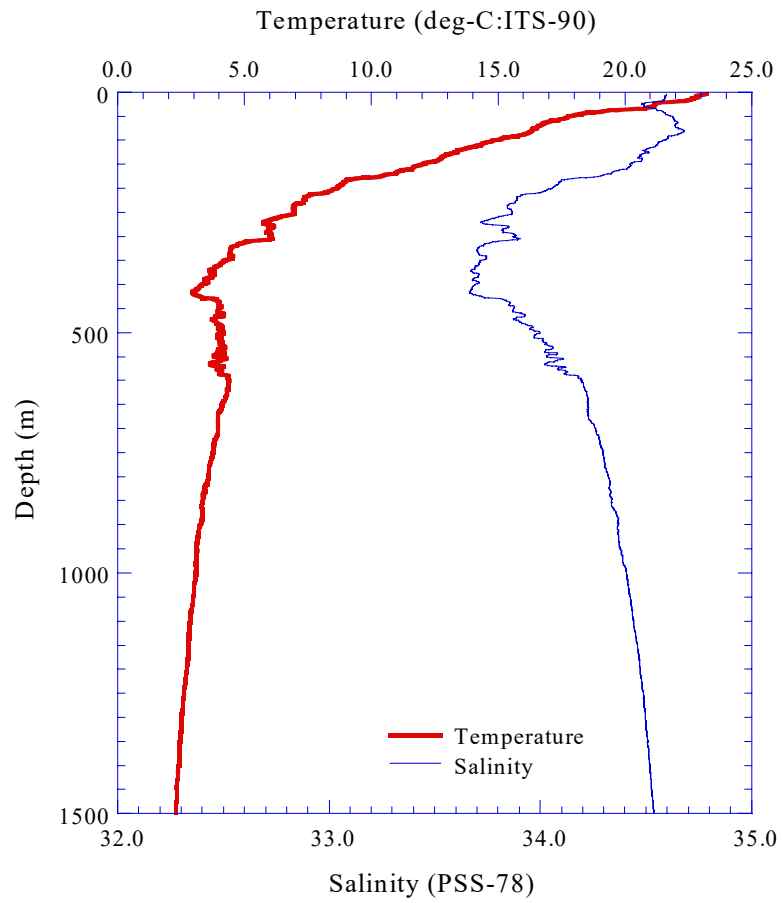


Fig.3.2.43.(b) CTD profile to 1,500m (Stn.R03;R03S01)

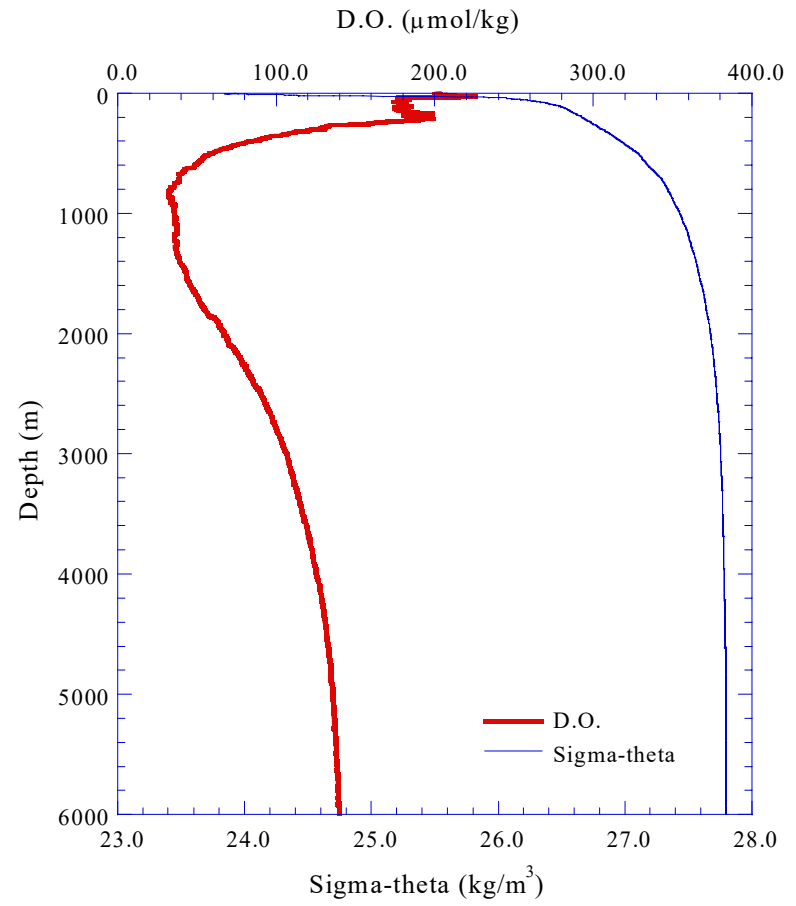
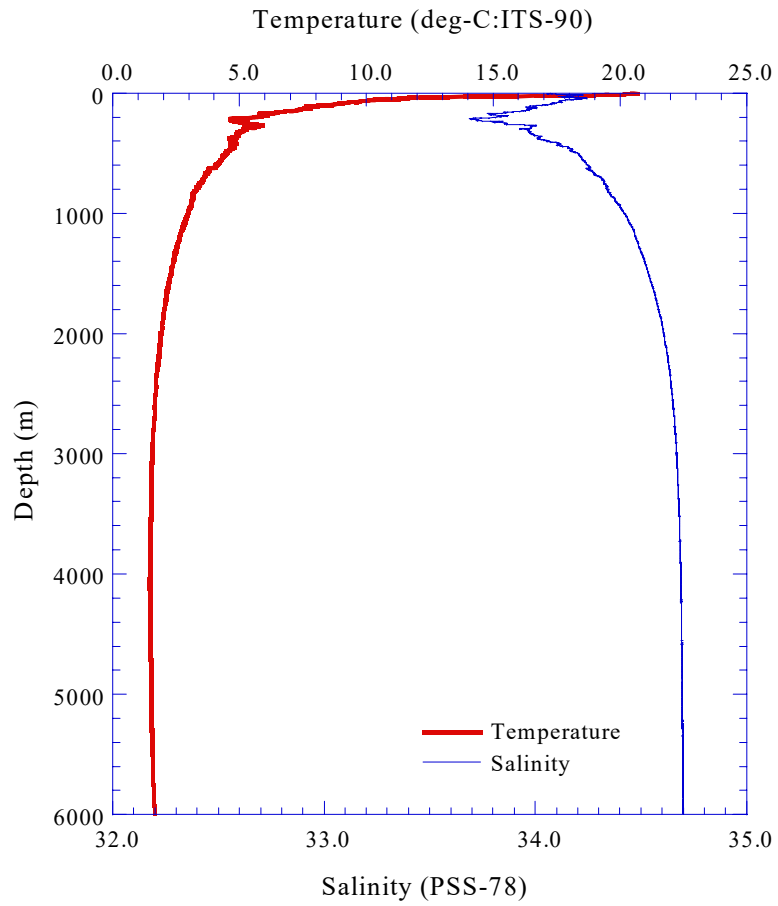


Fig.3.2.44.(a) CTD profile (Stn.R04;R04S01)

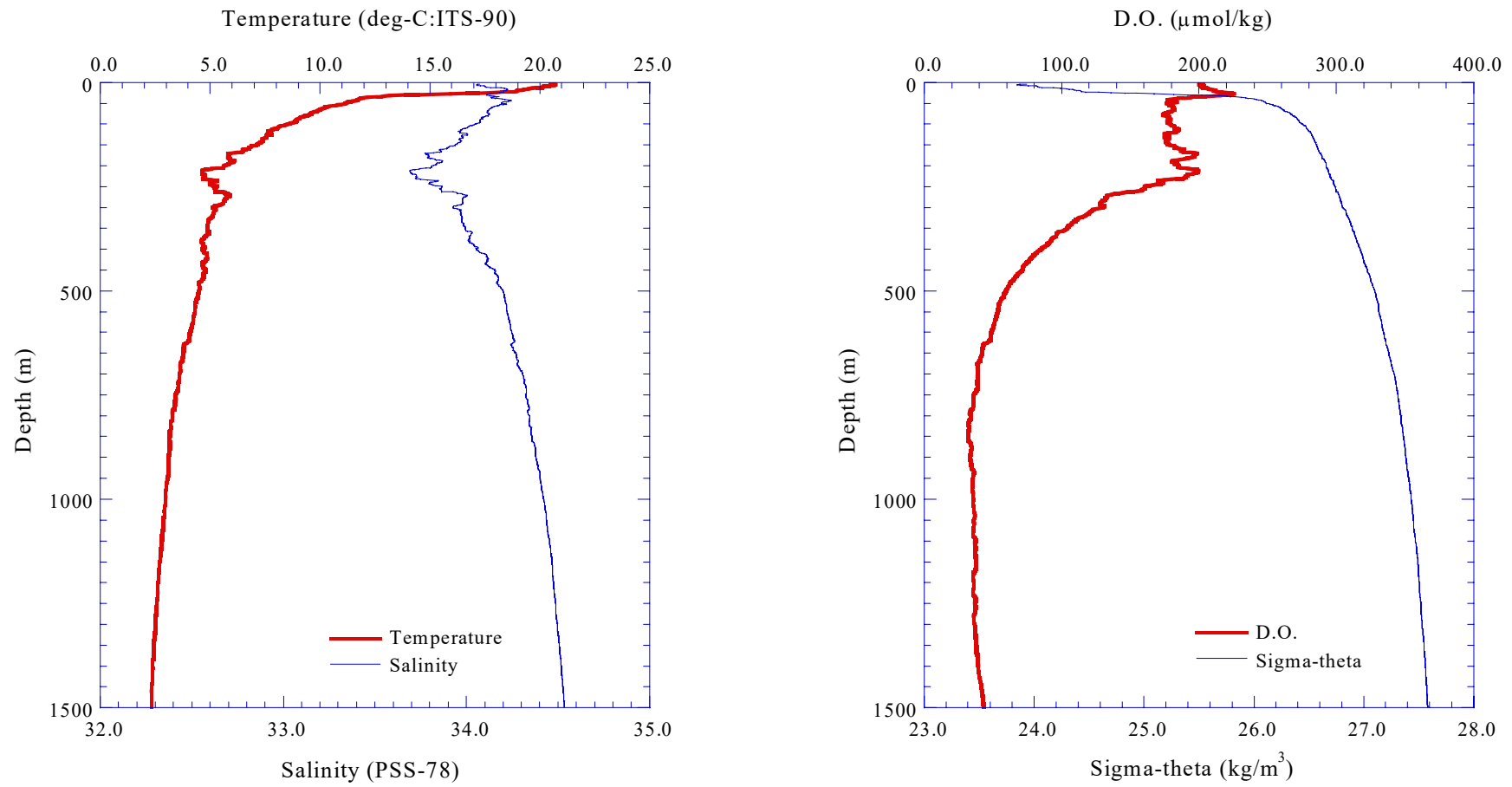


Fig.3.2.44.(b) CTD profile to 1,500m (Stn.R04;R04S01)

3.2-86

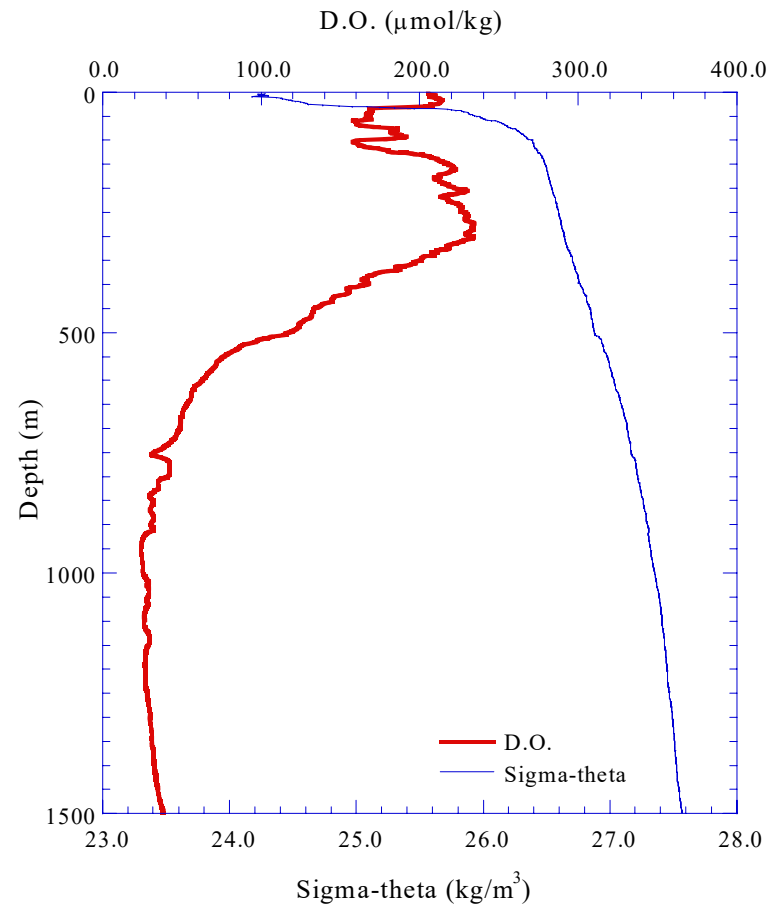
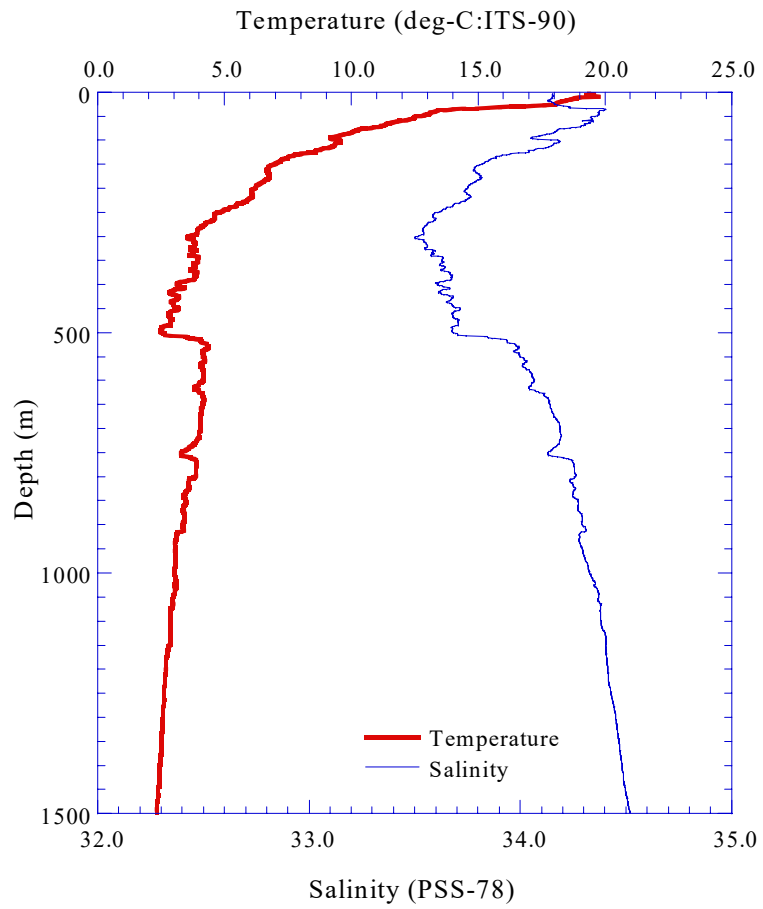


Fig.3.2.45 CTD profile (Stn.R05;R05S01)

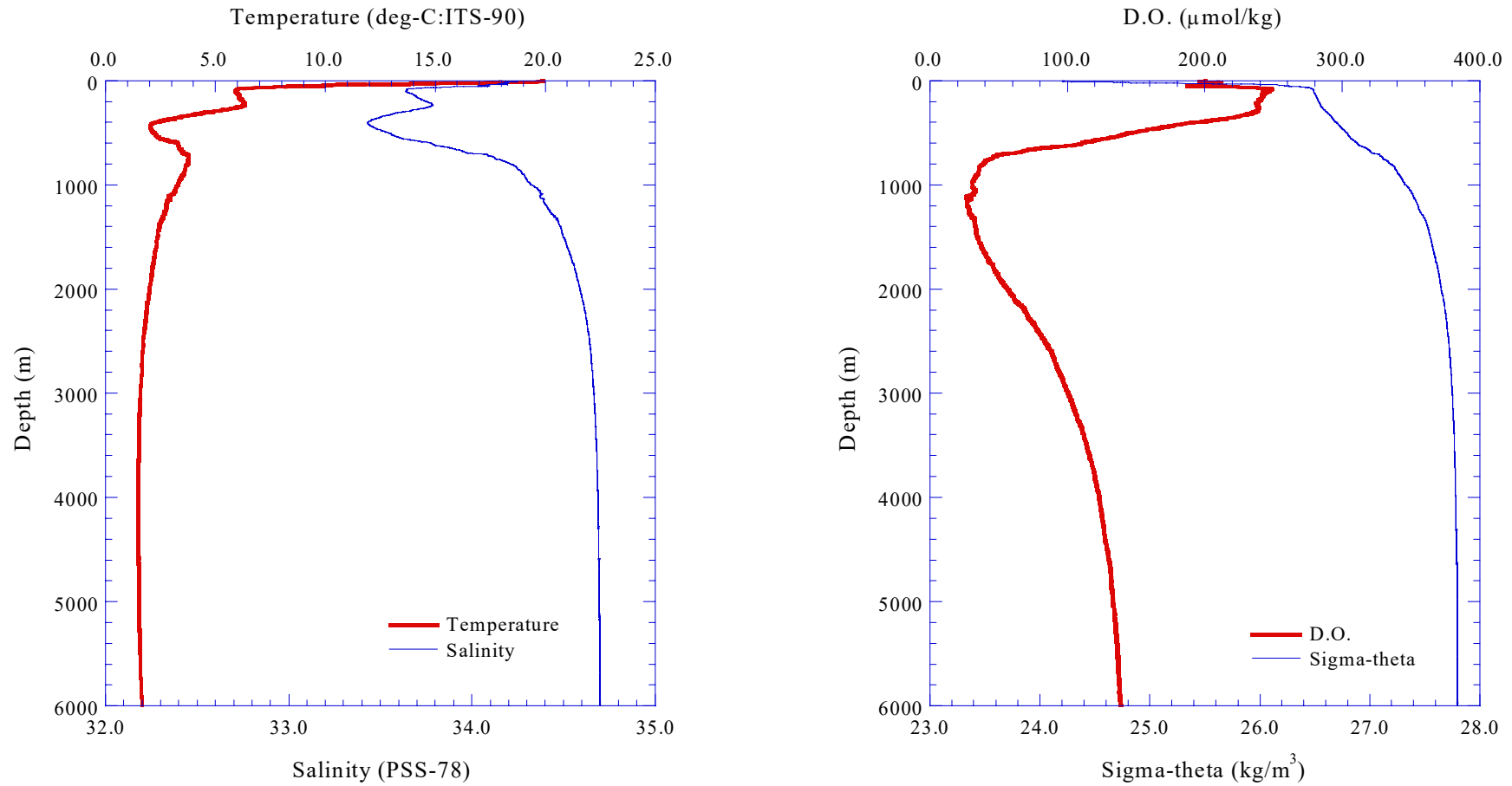


Fig.3.2.46.(a) CTD profile (Stn.R06;R06S01)

3.2-88

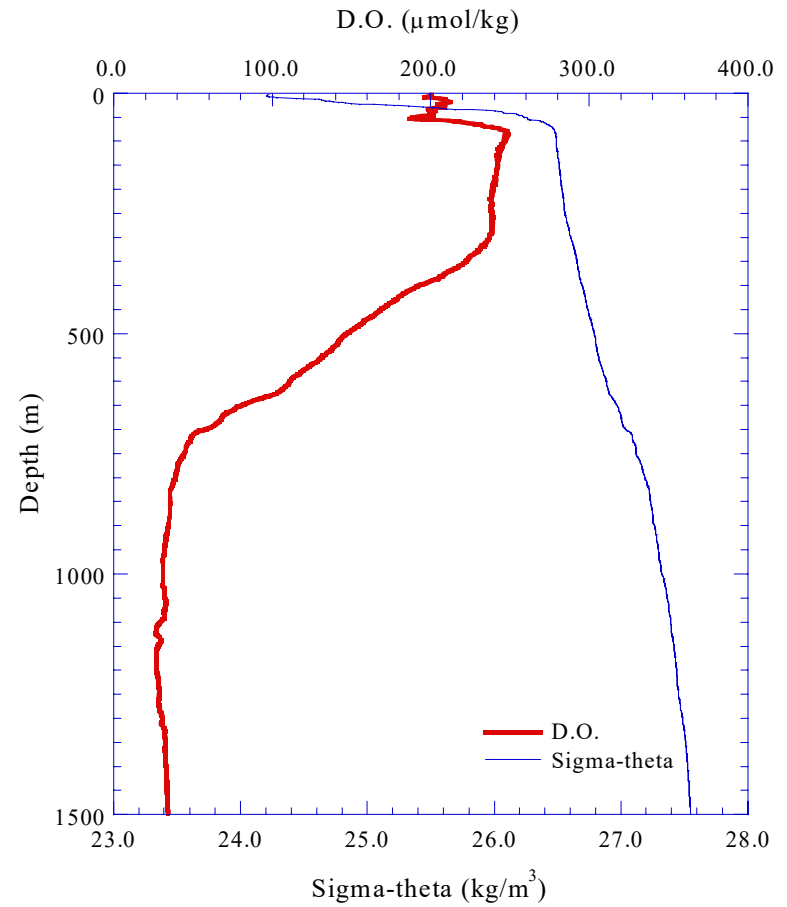
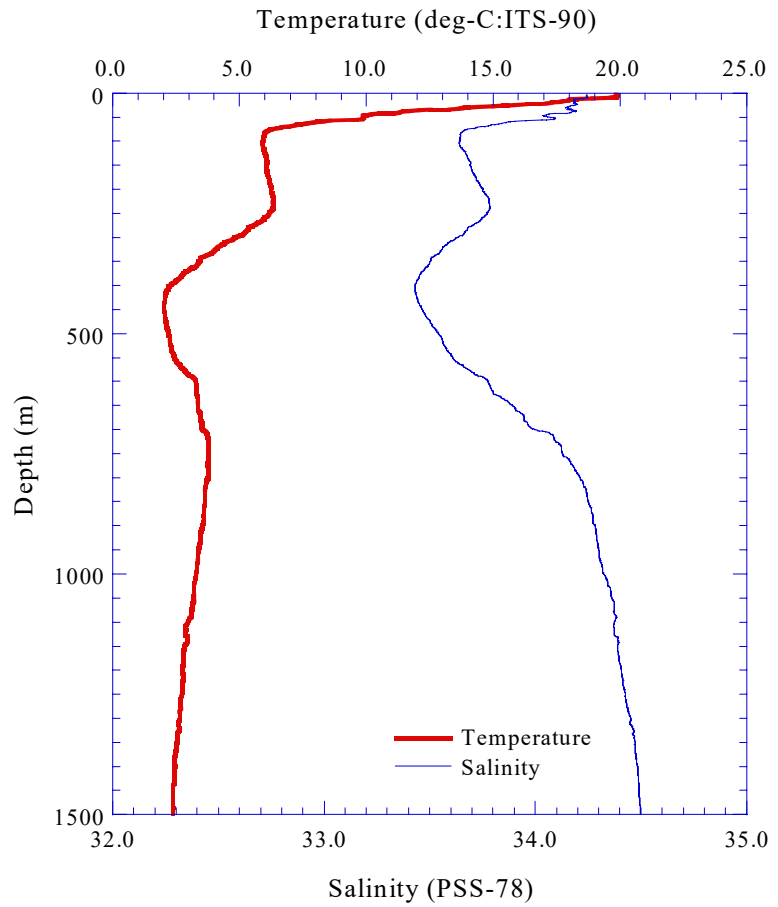


Fig.3.2.46.(b) CTD profile to 1,500m (Stn.R06;R06S01)

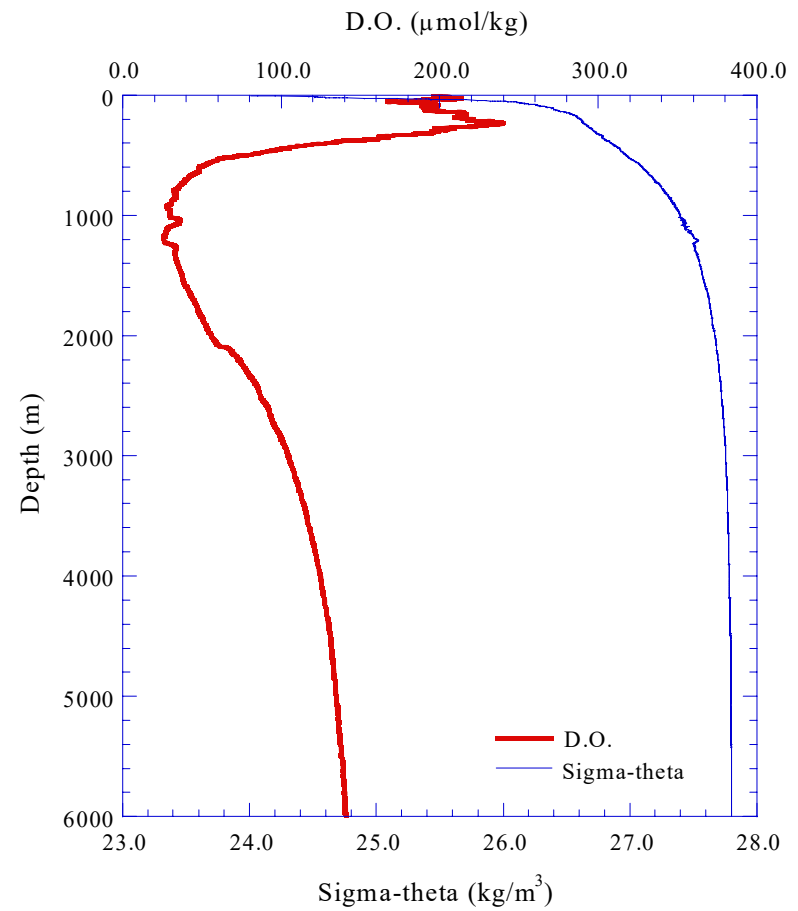
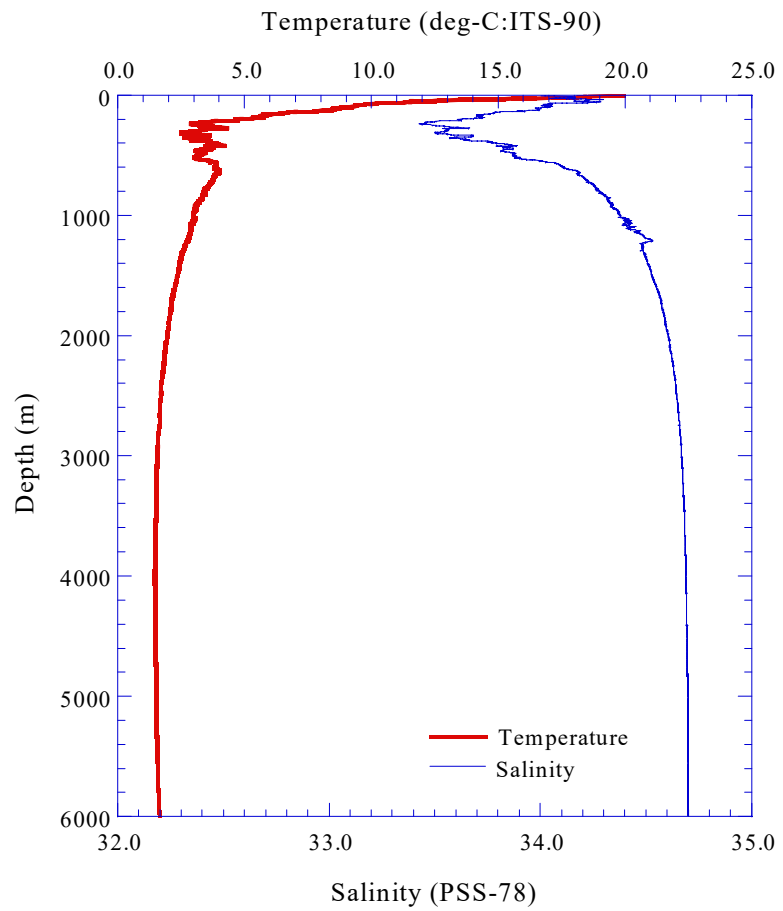


Fig.3.2.47.(a) CTD profile (Stn.R07;R07S01)

3.2-90

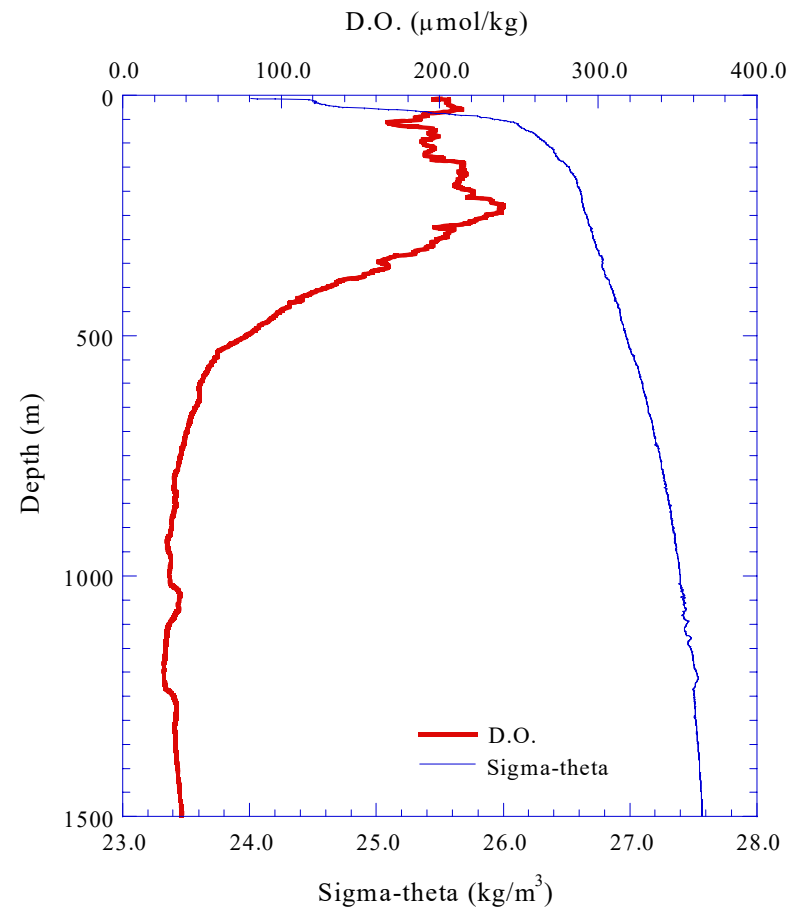
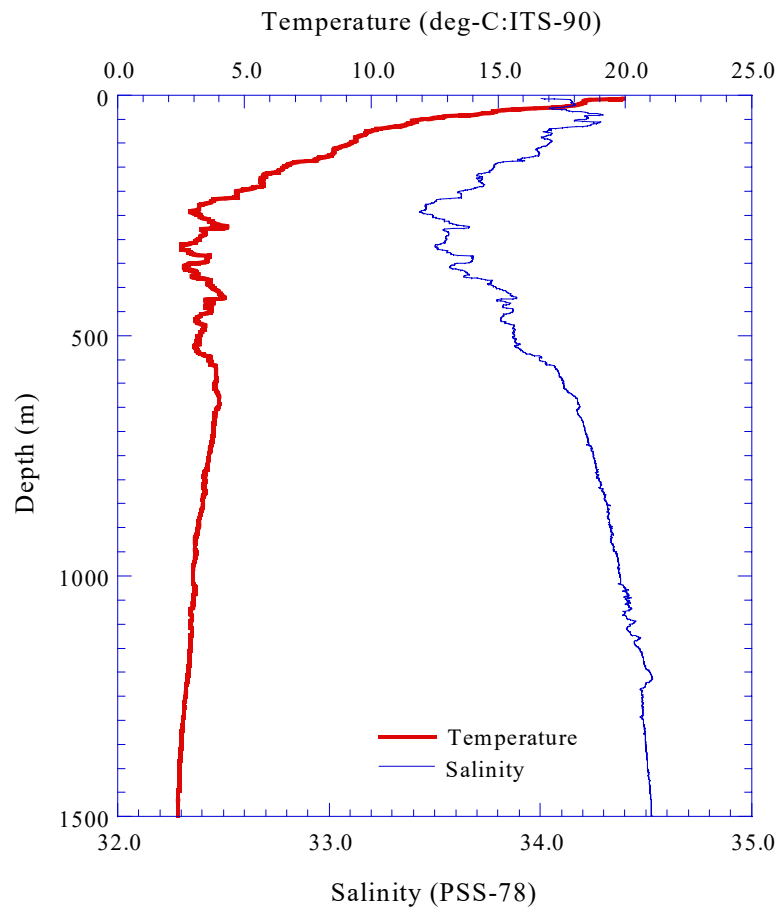


Fig.3.2.47.(b) CTD profile to 1,500m (Stn.R07;R07S01)

3.2-91

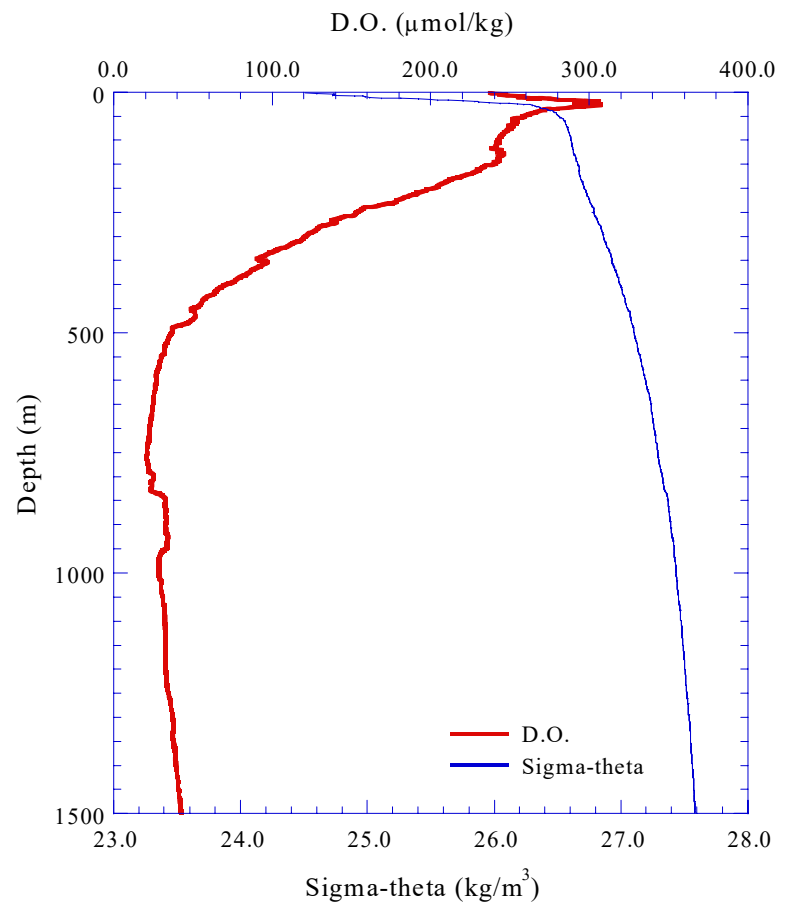
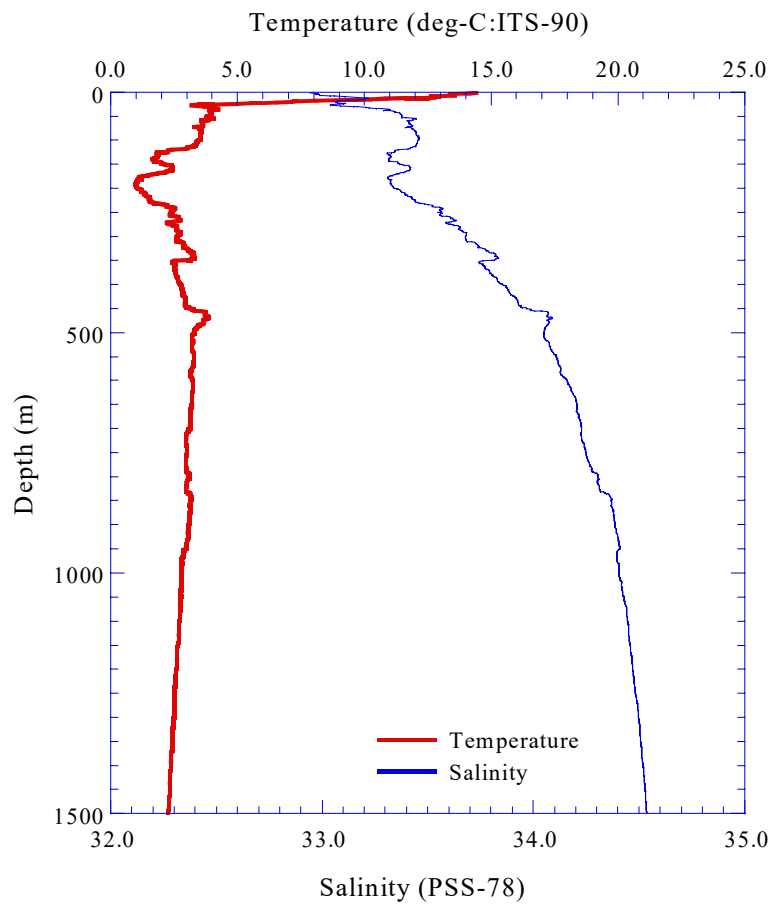


Fig.3.2.48 CTD profile (Stn.R08;R08S01)

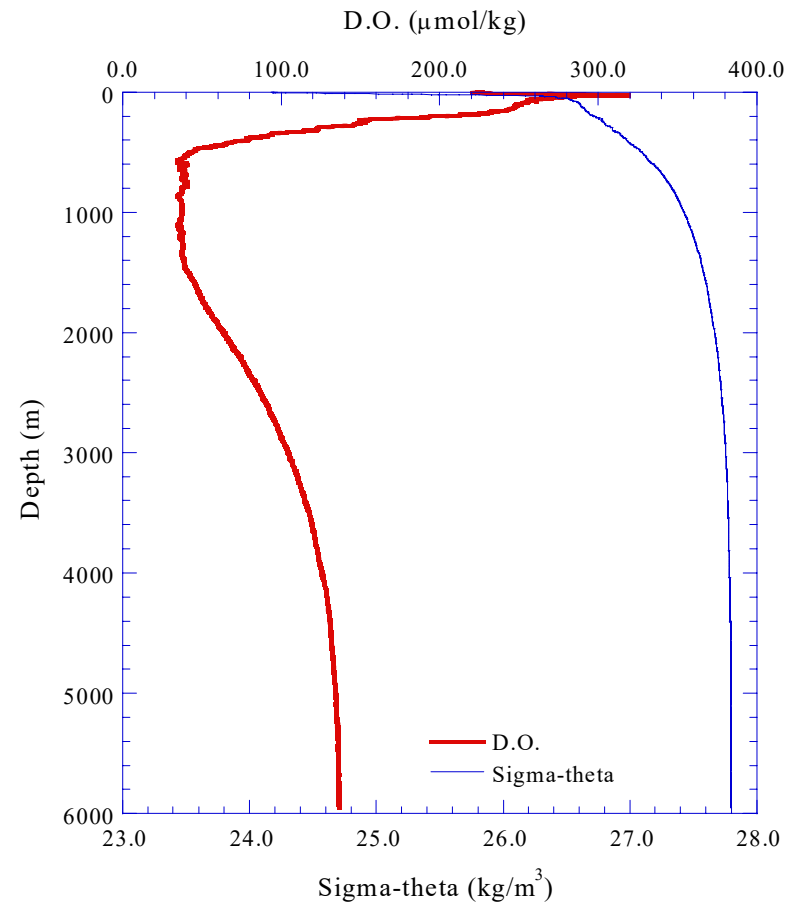
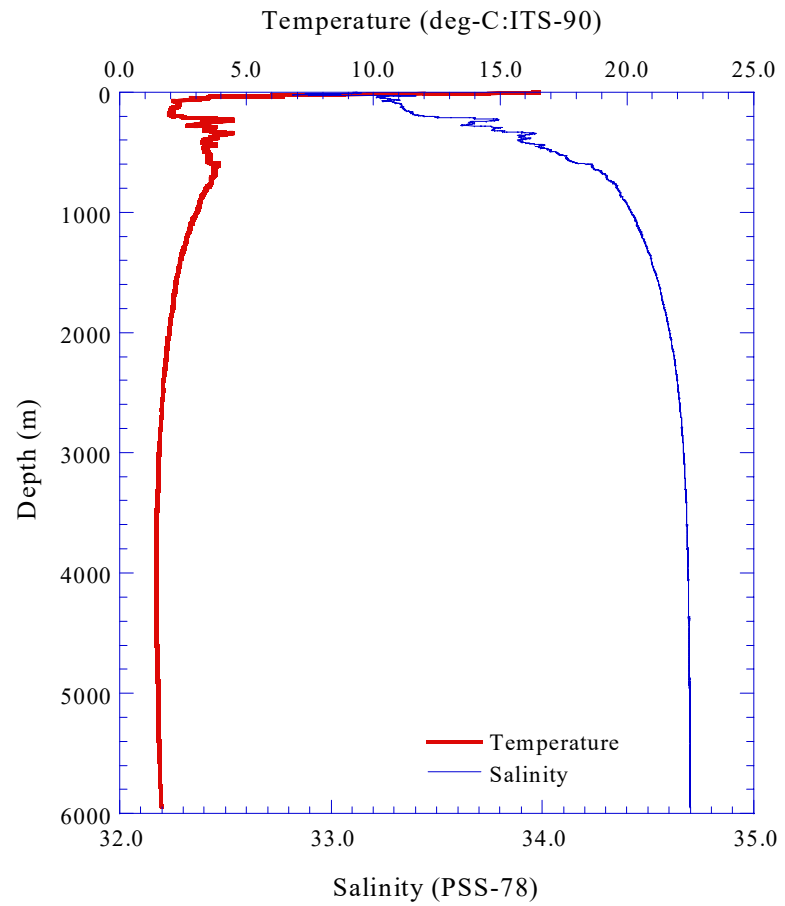


Fig.3.2.49.(a) CTD profile (Stn.R09;R09S01)

3.2-93

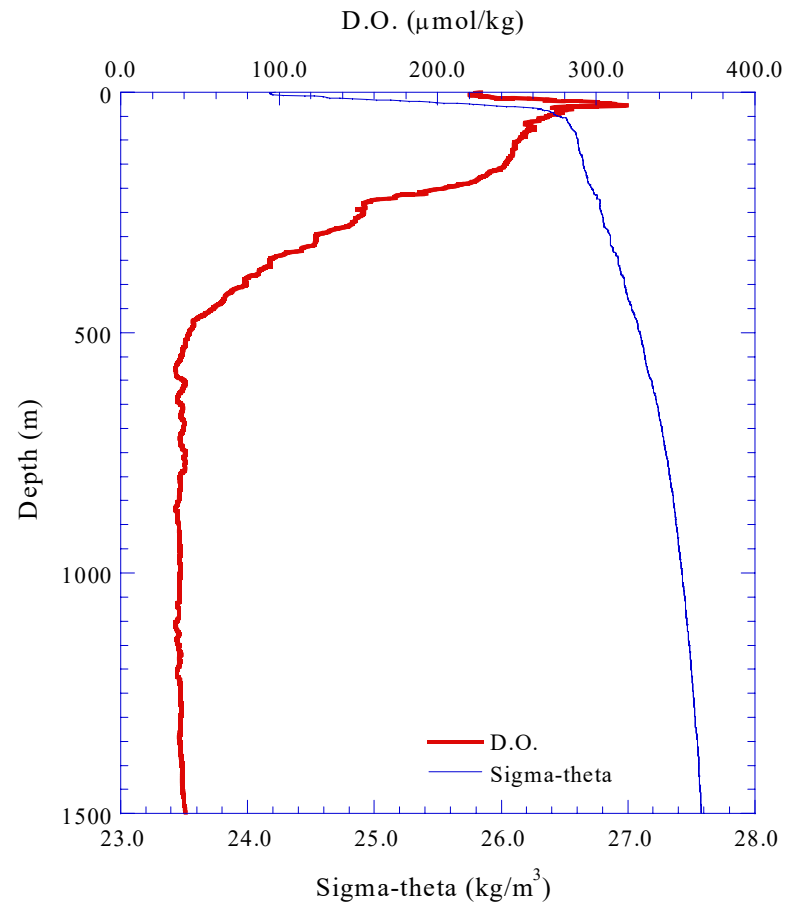
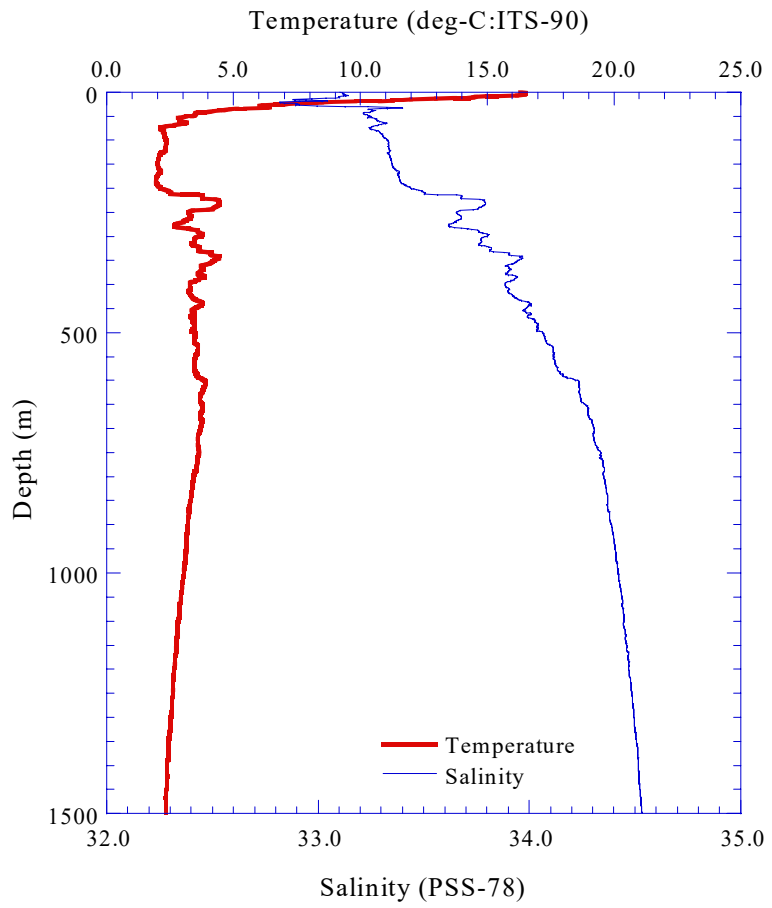


Fig.3.2.49.(b) CTD profile to 1,500m (Stn.R09;R09S01)

3.2-94

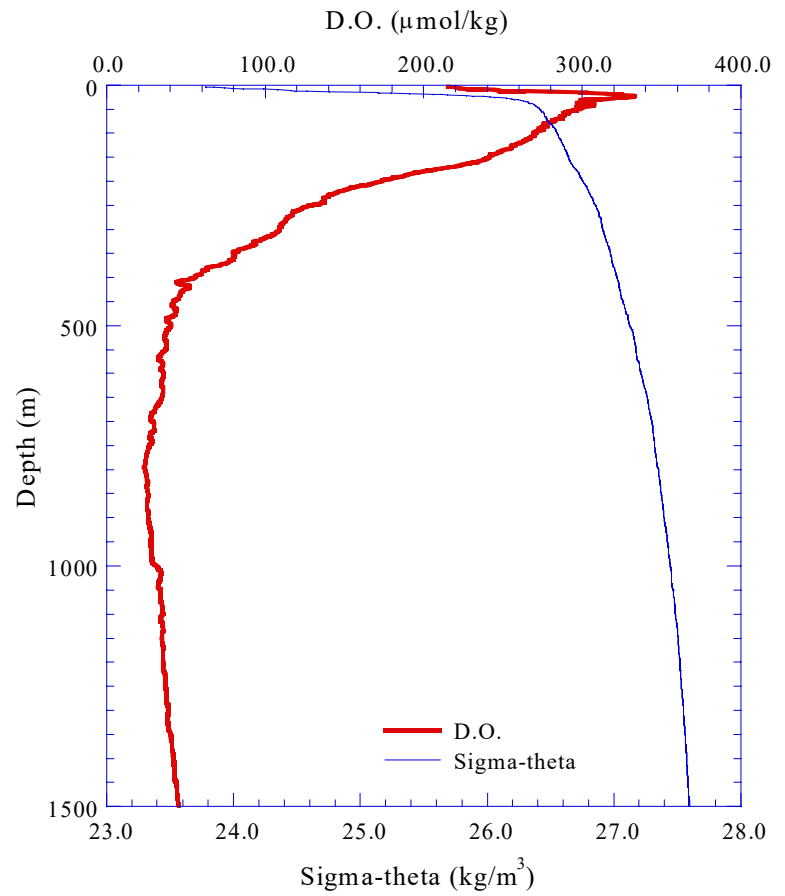
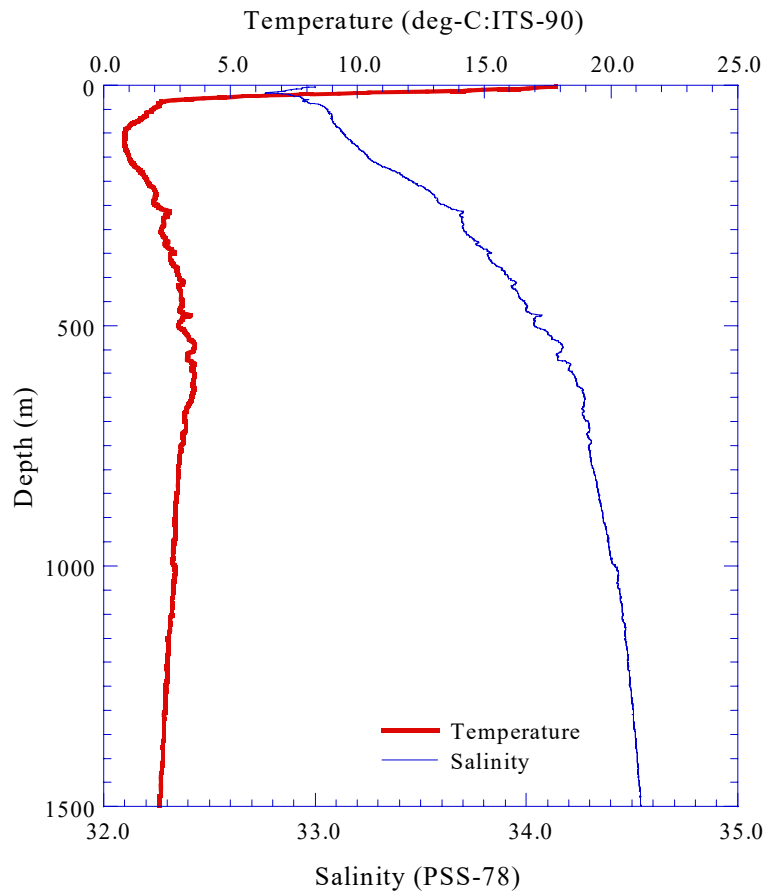


Fig.3.2.50 CTD profile (Stn.R10;R10S01)

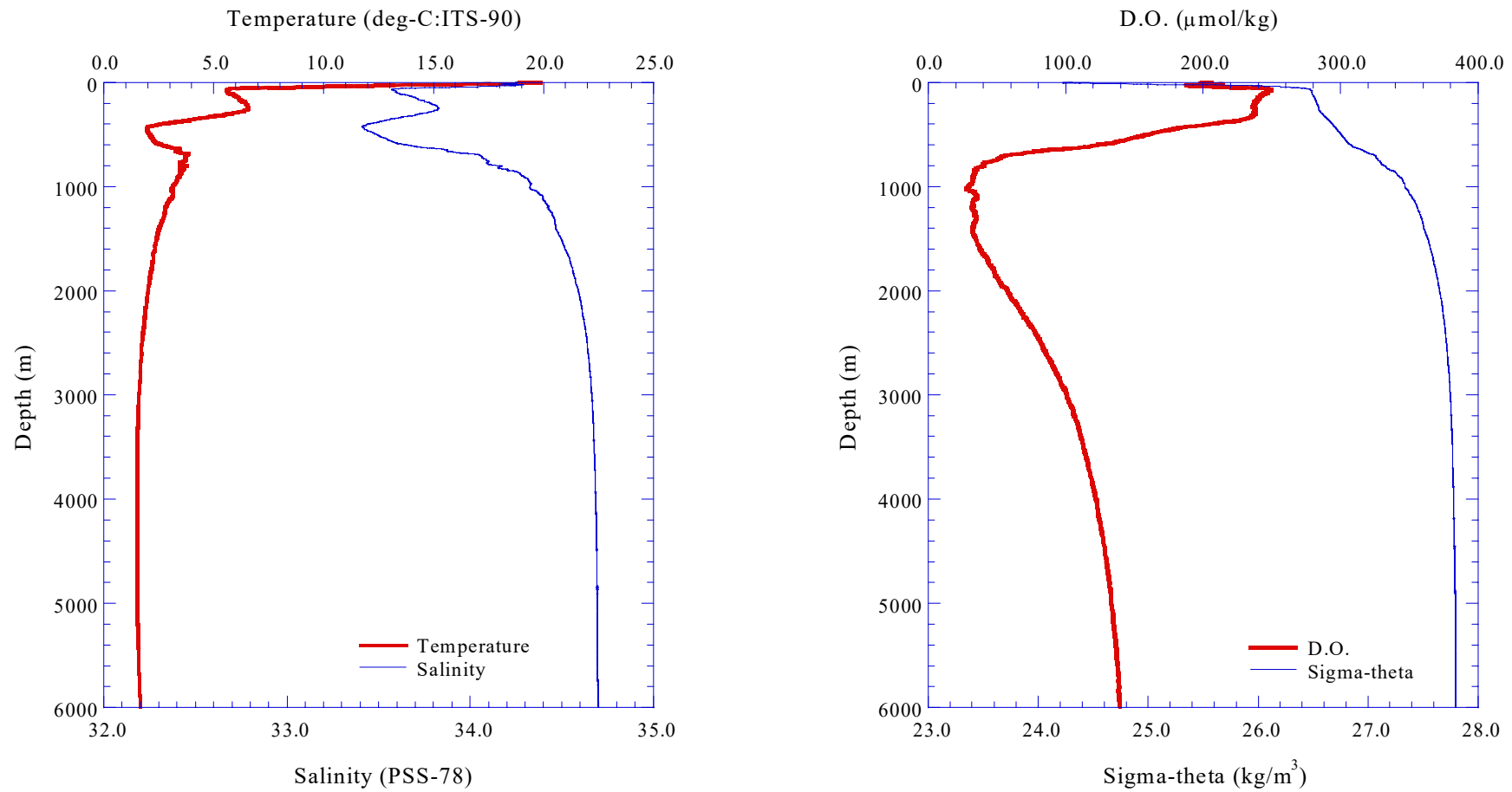


Fig.3.2.51.(a) CTD profile (Stn.R11;R11S01)

3.2-96

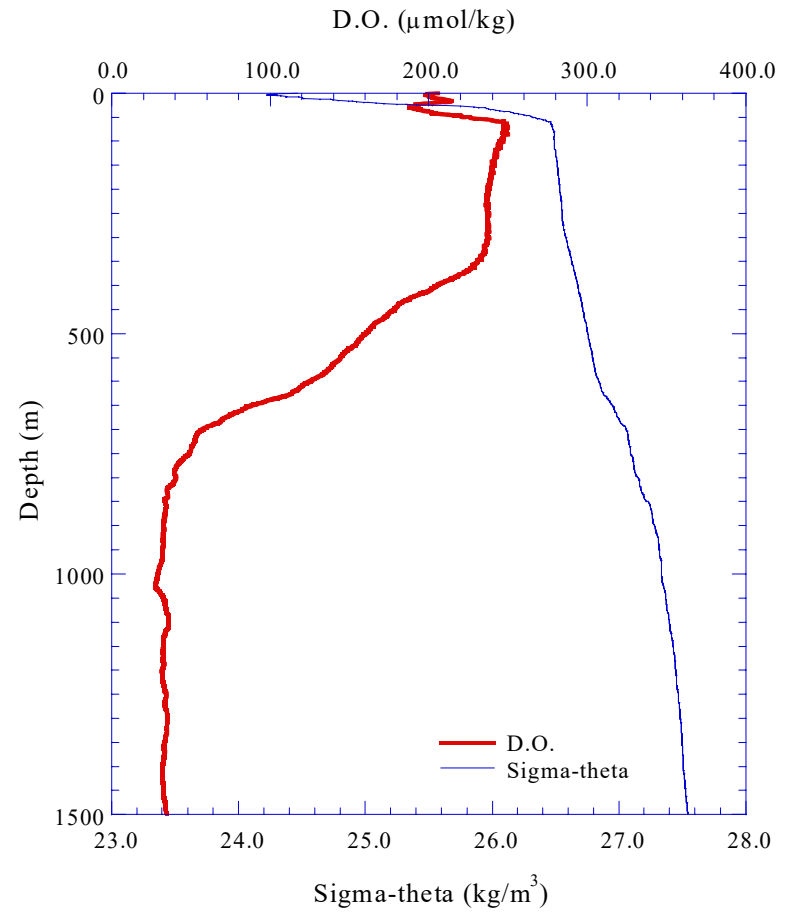
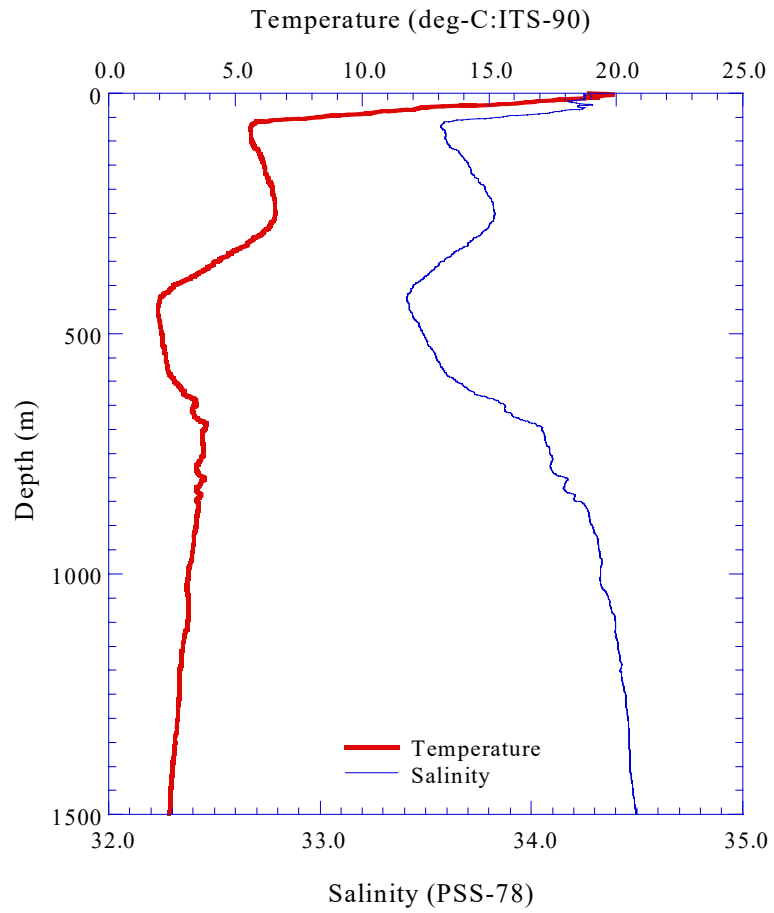


Fig.3.2.51.(b) CTD profile to 1,500m (Stn.R11;R11S01)

3.3 Hydrocast

3.3.1 Salinity

Hirokatsu UNO (MWJ): Operation Leader

Fujio KOBAYASHI (MWJ)

Miki YOSHIIKE (MWJ)

Kenichi KATAYAMA (MWJ)

Kei SUMINAGA (MWJ)

(1) Instrument and Method

The salinity measurements were carried out using the laboratory salinometer (Model 8400B AUTOSAL S/N 62823 and 62525; Guildline Instruments Ltd.), which was modified with Ocean Scientific International peristaltic-type sample intake pump. The instrument was operated in the “AUTOSAL Room” of R/V Mirai with a bath temperature 24 deg-C. A double conductivity ratio was defined as a median of 31 readings of the salinometer. Data collection was started after 15 data readings and it took about 10 seconds by a PC. We obtained two conductivity readings for each sample, and averaged values were used to calculate salinity.

1. Salinity Sample Bottle

The bottles in which the salinity was sampled were 250ml Phoenix brown glass bottles with screw caps.

2. Salinity Sample collection and Temperature Equilibration

Each bottle was rinsed three times and filled with sample water. Salinity samples were stored more than 24 hours in the same laboratory as the salinity measurement was made.

3. Standardization

The salinometer was standardized with IAPSO Standard Seawater batch P139 whose conductivity ratio is 0.99993 (salinity 34.997).

4. Sub-Standard Seawater

We also use sub-standard seawater which was deep-sea water filtered by pore size of 0.45 micrometer and stored in a 20 liter container made of polyethylene for at least 24 hours before measuring. It was used to check the drift of the AUTOSAL and measured in every 8 sampled.

(2) Results

Analysis data for each layer were shown in Appendix. The standard deviation of the difference of Salinity with CTD and AUTOSAL was 0.0022.

The 54 pairs of duplication samples taken by the same Niskin Bottle were analyzed to estimate the precision of this method. The standard deviation of the difference induplicate samples was 0.0013.

(3) Data archive

The salinity data at each station are listed in the Appendix. The data of sample will be submitted to the Data Management Office (DMO) in JAMSTEC together with the MO disk of CTD data in this cruise.

3.3.2 Dissolved oxygen

Takayoshi Seike (Marine Works Japan Ltd.) : Operation leader

Tomoko Miyashita (Marine Works Japan Ltd.)

Soichi Moriya (Marine Works Japan Ltd.)

(1) Objectives

Measurement of dissolved oxygen using the Winkler titration processed the WHP Operations and Methods manual (Culberson, 1991).

(2) Measured Parameter

Dissolved oxygen content in sea water

(3) Instruments and Methods

(a) Instruments and Apparatus

Glass bottle: Glass bottle for dissolved oxygen measurements consist of the ordinary BOD flask (ca. 200 ml) and glass stopper with long nipple, modified from the nipple presented in Green and Carritt (1966). These bottles were calibrated before this cruise.

Dispenser: Eppendorf Comforpette 4800/1000 μ l

OPTIFIX/2 ml (for $MnCl_2$ & NaOH/NaI aq.)

Metrohm Model 725 Multi Dosimat/20 ml (for KIO_3)

Titration: Metrohm 716 DMS Titrino/10 ml of titration vessel

Pt Electrode/6.0403.100(NC)

Software: Data acquisition and endpoint evaluation/Metrohm, METRODATA/606013.000

(b) Methods

Samples for dissolved oxygen measurement were collected from 12-liters Niskin bottles to dry glass bottles. During each sampling, at least 2 bottle volumes of sample water were overflowed in order to minimize contamination with atmospheric oxygen. We also measured the water temperature at the time of sampling for correction of sample bottle. After each sample is drawn, 1 ml of both $MnCl_2$ and NaOH/NaI reagents were added into the sample bottle.

The samples were stored about 2 hours in dark place after sampling to finish precipitation. After precipitation, the samples for the Winkler method were

analyzed by Metrohm piston burette of 10 ml with Pt Electrode using whole bottle titration in the laboratory under controlled temperature (ca. 21 ~ 24 °C). Before titration, H₂SO₄ were added to the sample after removing a glass stopper, and then a glass stopper was rinsed by deionized water well. Before sample analysis, the standardization and blank determination have performed at each station. Concentration of dissolved oxygen was calculated by equation (8) of WHP Operations and Methods (Culberson, 1991). Dissolved concentrations we calculated were not corrected by seawater blank.

(4) Data archive

The dissolved oxygen data at each station are listed in the Appendix. The data of titration of samples and worksheets of calculation of D.O. concentration were stored on floppy disks. All data will be to JAMSTEC Data Management Office (DMO) and under its control.

(5) References:

- Culberson, C. H. (1991) Dissolved Oxygen, in WHP Operations Methods, Woods Hole, pp.1-15.
- Green, E. J. and D. E. Carritt (1966) An improved iodine determination flask for Whole-bottle titrations, *Analyst*, 91, 207-208.

3.3.3 Nutrients

Kenichiro SATO (MWJ): Operation Leader

Jyunko HAMANAKA (MWJ)

Kaori AKIZAWA (MWJ)

(1) Objectives

The distributions of the nutrients are one of the most important factors on the primary production. During this cruise nutrient measurements will give us the important information on the mechanism of the primary production and seawater circulation.

(2) Instruments and Methods

There are 2 TRAACS 800 systems, which is BRAN+LUEBBE continuous flow analytical 4-channel system model, in the R/V MIRAI to analyze the nutrients in seawater. We usually used one system for nitrate + nitrite (1ch.), nitrite (2ch.), silicate (3ch.) and phosphate (4ch.). And the other one was for ammonia (3ch.) measurement, which was almost constructed for a closed line system. The laboratory temperature was maintained between 20-25 deg C.

a. Measured Parameters

Nitrite: Nitrite was determined by diazotizing with sulfanilamide and coupling with N-1-naphthyl-ethylenediamine (NED) to form a colored azo dye that was measured absorbance of 550 nm using 5 cm length cell.

Nitrate: Nitrate in seawater is reduced to nitrite by reduction tube (Cd - Cu tube), and the nitrite determined by the method described above, but the flow cell used in nitrate analysis was 3 cm length cell. Nitrite initially present in the sample is corrected.

Silicate: The standard AAI molybdate-ascorbic acid method was used. Temperature of the sample was maintained at 45-50 deg C using a water bath to reduce the reproducibility problems encountered when the samples were analyzing at different temperatures. The silicomolybdate produced is measured absorbance of 630 nm using a 3 cm length cell.

Phosphate: The method by Murphy and Riley (1962) was used with separate additions of ascorbic acid and mixed molybdate-sulfuric acid-tartrate. Temperature of the samples was adjusted to be 45-50 deg C using a water bath. The phospho-molybdate produced is measured absorbance of 880 nm using a 5 cm length cell.

Ammonia: Ammonia in seawater was determined by coupling with phenol and sodium hypochlorite to form a colored indophenol blue and by being measured the absorbance of 630 nm using 3 cm length flow cell.

b. Sampling Procedures

Samples were drawn into polypropylene 100 ml small mouth bottles. These were rinsed three times before filling. The samples were analyzed as soon as possible. Five ml sample cups were used for analysis.

c. Low Nutrients Sea Water (LNSW)

Ten containers (20L) of low nutrients seawater were collected in February 2001 at equatorial Pacific and filtered with 0.45mm pore size membrane filter (Millipore HA). They are used as preparing the working standard solution.

(3) Results

Precision of the analysis

We have made the repeat analysis of about 3000 m layer samples at each station. At this repeat analysis range of CV (concentration average to standard deviation) was 0.02 to 0.95 % except for nitrite and ammonia.

(4) Data Archive

All the nutrients data measured in this cruise are listed in the Appendix. These data are also stored in MO disk in Ocean Research Department in JAMSTEC.

3.3.4. pH

Andrey Andreev (JAMSTEC)

(1) Method and Instruments

pH ($-\log [H^+]$) of the seawater was measured potentiometrically in a closed cell at 25⁰ C. To measure pH a pH/Ion meter (model PHM95), pH electrode and Ag/AgCl reference electrode of the 'Radiometer' company were used. The temperature of the test solution was monitored by a temperature sensor (Radiometer) within 0.1⁰ C. To calibrate the electrodes a TRIS buffer (0.04 m TRIS+ 0.04 m TRISHCL) in the synthetic seawater (S=35 psu) (Total hydrogen scale) (Dickson and Goyet, 1994) was applied.

The pH was calculated by following equation

$$pH = pH(\text{TRIS buffer}) + F(E_s - E_t)/RT \cdot \ln(10)$$

where pH (TRIS buffer) is 8.0936 pH unit [DelValls and Dickson, 1998], ($E_s - E_t$) is the difference in EMF of standard and test solutions, $RT \cdot \ln(10)/F$ is Nernst constant (59.16 mv/pH unit at the temperature 25⁰ C).

The precision of the pH measurements was ± 0.0017 pH unit (± 0.1 mv in EMF). The accuracy of pH determinations (computed as total uncertainty related with an error of pH measurement in water samples, calibration, and drift in electrodes) was accepted to be ± 0.006 pH unit. The repeatability [Dickson and Goyet, 1994] of the pH measurements (based on 60 duplicate measurements) was ± 0.003 pH unit (2σ).

(2) Results

The pH data at each station are listed in the Appendix. To verify our pH values we consider the internal consistency between the pH and other chemical parameters (total alkalinity and dissolved oxygen) changes in the deep water layer (~ 4500 m (4000 – 5000 m)) of the study region. In the deep and bottom water layers of the North Pacific the pH changes are due to organic matter degradation ($\Delta pH_{org.}$) and carbonate dissolution ($\Delta pH_{carb.dis.}$) [Millero, 1996]. $\Delta pH_{org.}$ and $\Delta pH_{carb.dis.}$ can be computed by the respective changes in total alkalinity (TA) and dissolved inorganic carbon (DIC) concentrations using the coefficient of 360 $\mu\text{mol/pH unit}$ [Andreev et al., 2001]. Organic matter oxidation should lead to the decrease in pH and dissolved

oxygen. Fig. 3.4.1-1 shows that there is such tendency in the deep water layer of the study area. However due to high total uncertainty of our calculations (± 0.006 pH unit in pH, $\pm 2 \mu\text{mol}$ in TA and $\pm 1-2 \mu\text{mol/kg}$ in DO) it is difficult to accept where the ratio between the variation of pH due to organic matter oxidation and DO is equal to Redfield one ($\Delta\text{pH}_{\text{org.ox.}} = -\Delta\text{DIC}_{\text{org.ox.}} / 360 = 0.76 \cdot \Delta\text{DO}_{\text{org.ox.}} / 360$) (solid line on Fig.3.3.4-1).

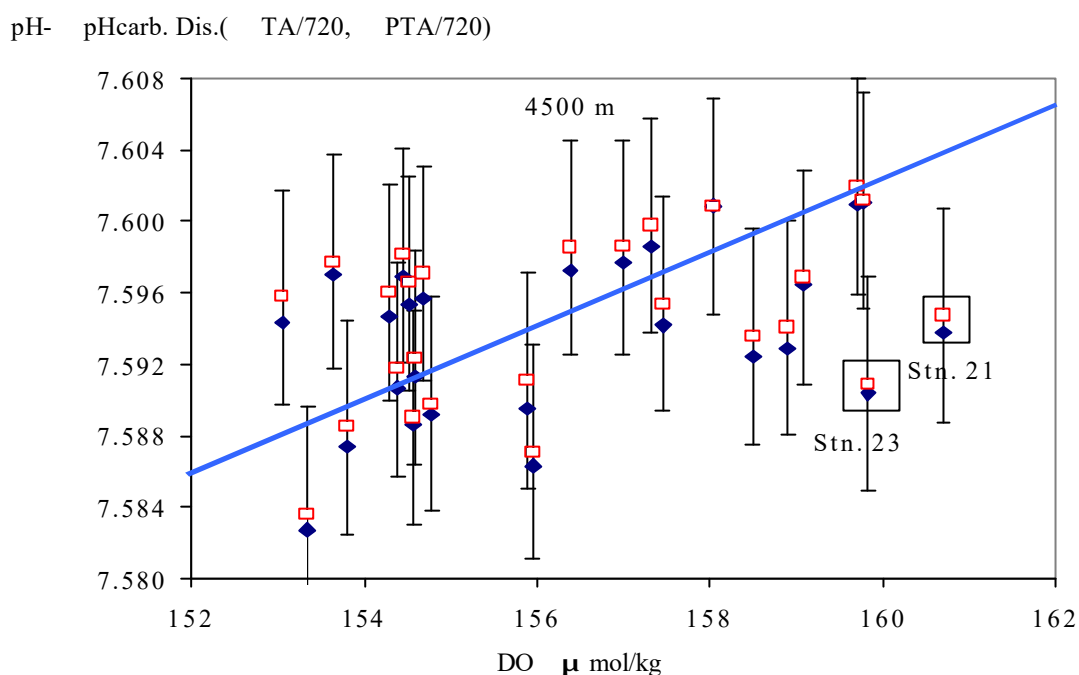


Fig. 3.3.4-1. pH corrected for the carbonate dissolution (by total alkalinity ($\Delta\text{TA}/720$) and potential alkalinity ($\Delta\text{PTA} ([\text{TA}] + [\text{NO}_3])/720$) [Millero, 1996]) versus dissolved oxygen in the deep water (~ 4500 m) of the Northwestern Pacific. Solid line shows where $(\text{pH} - \Delta\text{pH}_{\text{carb. dis.}})$ is $0.76 \cdot \Delta\text{DO}/360$.

Figs. 3.3.4-2 (A- D) show the vertical section of pH_{25} along 165° E, 155° E, 153° E and 144° E in the North Pacific. In the surface water layer there is a tendency to pH increase with an increase of temperature due to the decrease in the carbon dioxide solubility. In the intermediate water layer the lowest pH (and DO) is observed in the subarctic area (Fig. 3.3.4-2.). From the high to lower latitudes the pH increase with an increase of DO. The strong lateral gradients in pH are observed in the zones of fronts (Subarctic front ($41-42^\circ$ N) and Kuroshio Extension front ($32-34^\circ$ N)) and anticyclone eddies ($36-37^\circ$ N (Fig. 3.3.4-2 B), $41-42^\circ$ N (Fig. 3.3.4-2 C), $38-39^\circ$ N and $40-41^\circ$ N (Fig. 3.3.4-2 D).

From 26° N to 40° N the distribution of the pH at the isopycnal surfaces (Fig. 3.3.4-3) in the intermediate water layer ($\sigma_\theta = 26.7- 27.5$) was quite uniform. The significant isopycnal gradients in pH are observed in the zone of the Subarctic front (42- 44° N) (trans. along 155° (Fig. 3.3.4-3.B) and 153° E (Fig. 3.3.4-3.C)) and in the zone of the confluence of the Oyashio and Kuroshio Extension Current (Fig. 3.3.4-3. D).

The part of the cruise activity was focused on the study of structure and characteristics of the anticyclone eddies of the Subarctic frontal zone (Fig. 3.3.4-3 C) and Kuroshio – Oyashio Mixed Water region (Fig. 3.3.4-3 D) (see section 3.11). Due to its non-conservative behavior the pH itself is not a good tracer to clarify the role of the anticyclone eddies on the fluxes of the chemical elements in the study area. For this purpose the excess pH [Andreev et al., 2001] can be used. pH excess is a decrease of pH in the seawater due to an increase of the carbon dioxide in the atmosphere. This decrease in pH takes place in the surface water layer. The penetration of the pH excess into deep water is determined by advection and turbulent diffusion. Figs.3.3.4-4 show the vertical section of the computed excess pH and salinity along 144° E. At the $\sigma_\theta = 26.6- 27.0$ there is a strong correlation between the distribution of salinity and pH excess. High (absolute value) pH excess coincides with a lower salinity (Fig. 3.3.4-4). Low salinity water is Oyashio Current water formed by a mixing of the East Kamchatka and Okhotsk Sea waters in the Kuril Islands area. Intermediate water formation and transformation processes that take place in the Okhotsk Sea and Kuril islands area [Talley and Nagata, 1995] result in the increase of pH excess (by absolute value) in the intermediate water layer [Andreev et al., 2001]. By Oyashio Current a low salinity and high pH excess water supplies to the Kuroshio- Oyashio Mixed Zone where it can be trapped by anticyclone eddies (Fig. 3.3.4-4.).

(3) References

Andreev A., M. Honda, Yu. Kumamoto, M. Kusakabe and A. Murata (2001) Excess CO₂ and pH excess in the Intermediate water layer of the Northwestern Pacific. *J. Of Oceanography*. V. 57, 177-188.

Dickson, A. G. and C. Goyet (Eds.) (1994) Handbook of Methods for the Analysis of the Various Parameters of the Carbon Dioxide System in Seawater, ORNL/CDIAC-74. 107 p.

DelValls T.A. and A. G. Dickson (1998) The pH of buffers based on 2-amino-2-hydroxymethyl-1,3- propanediol ('tris') in the synthetic sea water. *Marine Chemistry*. V.45, 1541- 1554.

Millero F. J. (1996) *Chemical Oceanography*. 469 p.

Talley L. D. And Y. Nagata (eds.) (1995) *The Okhotsk Sea and Oyashio region*. PICES Sci. Rep. 6,150-157.

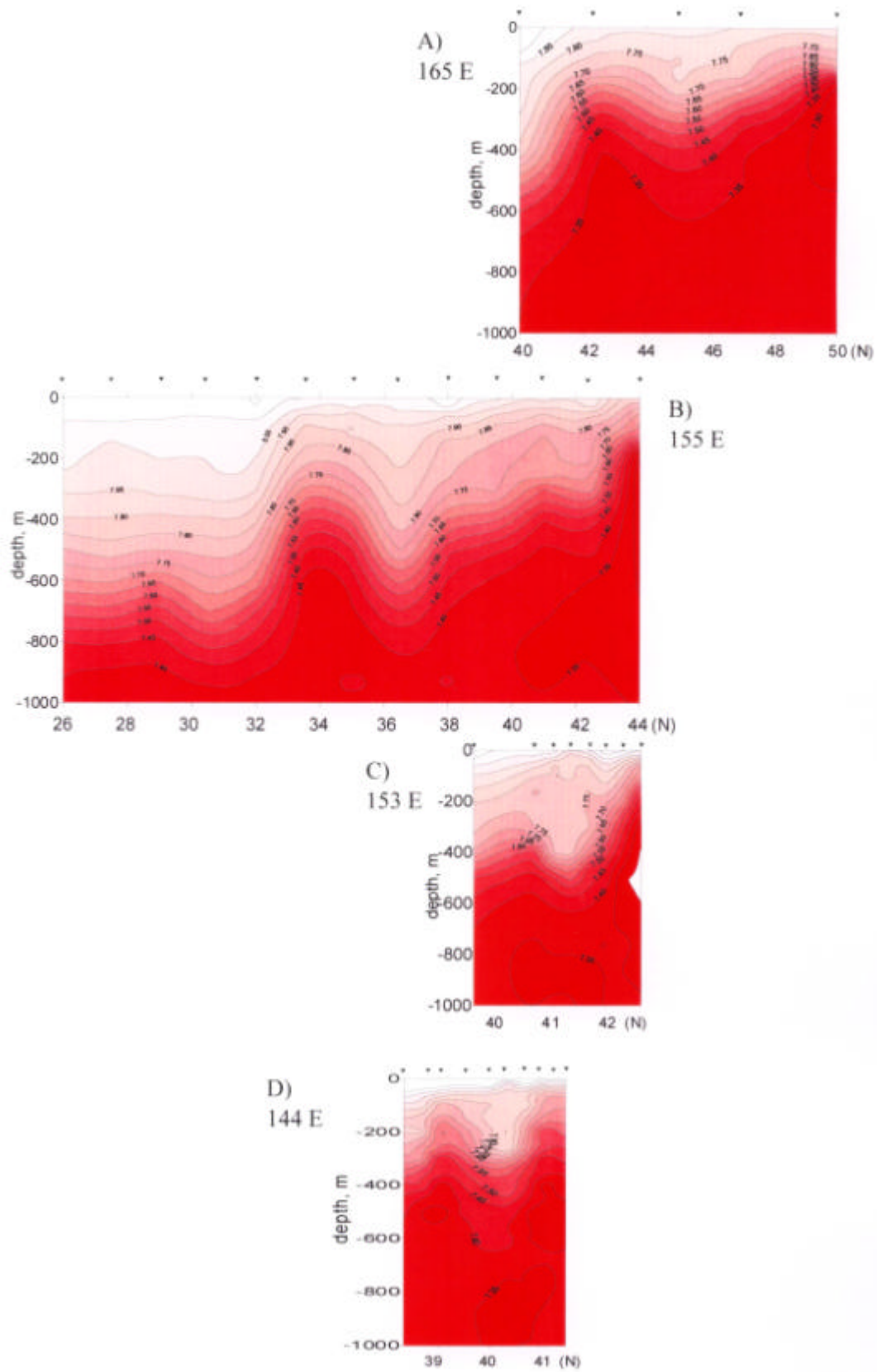


Fig.3.3.4-2 Vertical section of the pH along 165 ° E(A), 155 ° E(B), 153 ° E(C) and 144 ° E(D).

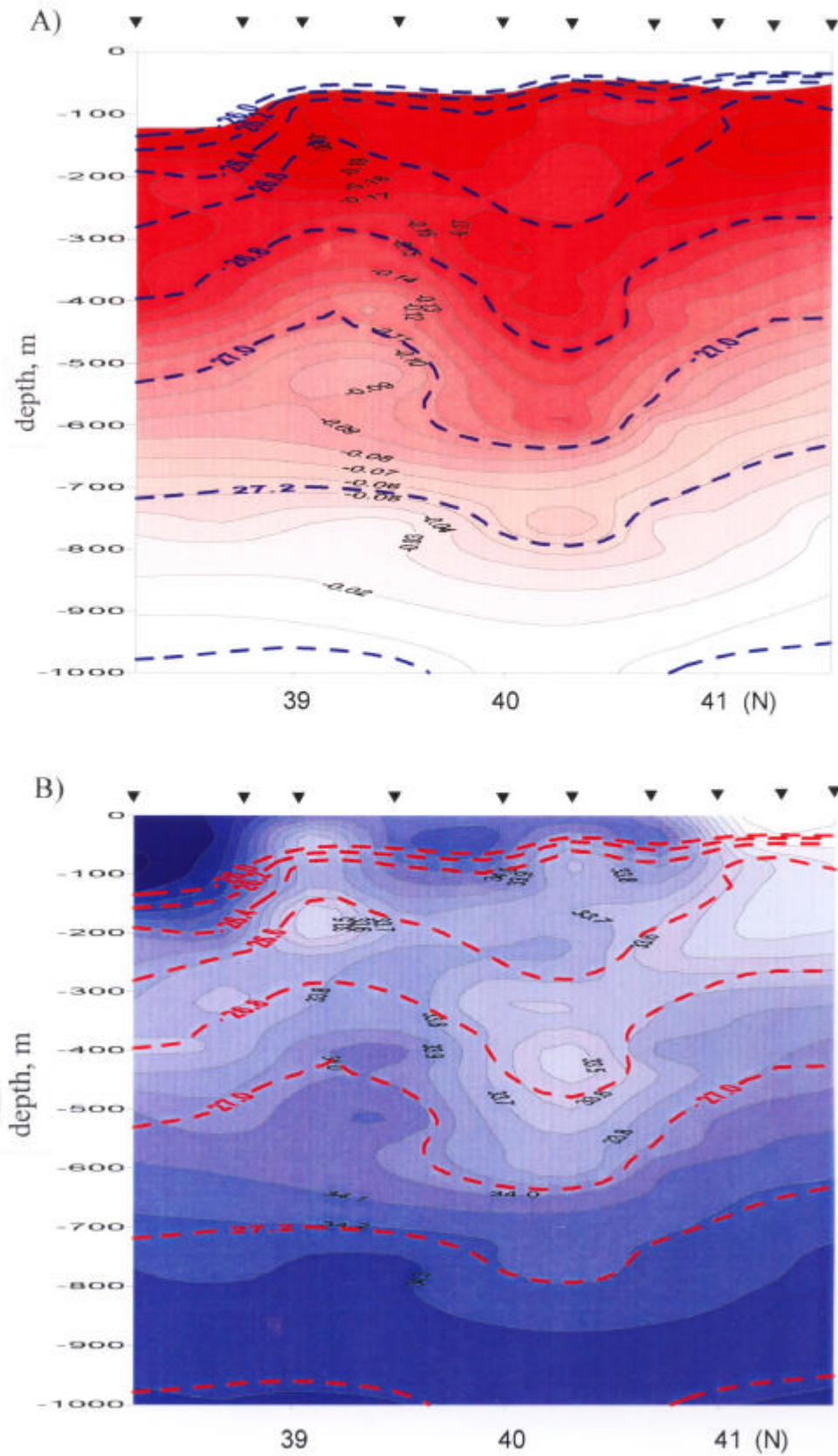


Fig.3.3.4-4 Vertical section of the pH excess (A) and salinity (B) along 144° E.

The solid dotted line is the potential density

3.3.5 Total dissolved inorganic carbon

Mikio Kitada (MWJ)

Minoru Kamata (MWJ)

(1) Objective

Global warming caused by green house gas such as CO₂ has become much attention all over the world. In order to verify carbon cycle in the northwestern North pacific, total dissolved inorganic carbon (TDIC) was measured with analytical instruments installed on R/V MIRAI.

(2) Instruments and Methods

Concentration of TDIC in seawater collected at the station Test, 1, 2, 3, 4, 5, 7, 8, 10, 11, 12, 13, 14, 1R, 15, 16, 17, 18, 19, 20, 21, 22, 23, 24, 25, 26, 27, and 28 was measured by a coulometer (Carbon Dioxide Coulometer Model 5012, UIC Inc.). A volume of seawater (nominal 32 cm³) was taken into a receptacle and 2 cm³ of 10 percents (v/v) phosphoric acid was added. The CO₂ gas evolved was purged by CO₂ free nitrogen gas for 13 minutes at the rate of 130 cm³ min.⁻¹ and adsorbed into an electrolyte solution, containing ethanolamine, dimethylsulfoxide, and thymolphthalein indicator. Acids formed by reacting with adsorbed CO₂ in the solution were titrated with hydroxide ions using coulometer. Calibration of the coulometer was carried out using sodium carbonate solutions (0-2.5mM). The coefficient of variation of 3 replicate determinations was approximately less than 0.1 percents for 1 sigma. All the data were referenced to the Dickson's CRM (Batch #53).

(3) Data archive

All data are listed in the Appendix and will be submitted to JAMSTEC Data Management Office (DMO).

3.3.6 Total alkalinity

Fuyuki Shibata (operation leader)
(Marine Works Japan Ltd.)

Keisuke Wataki
(Marine Works Japan Ltd.)

(1) Introduction

Global warming that caused by green house gas such as carbon dioxide has become much attention all over the world. In the flux study of northwestern pacific, understanding formation of the North Pacific Intermediate Water and its volume of transportation is very important. In order to verify carbon dioxide parameters including total Alkalinity were measured on in this R/V MIRAI cruise.

(2) Methods

Seawater samples were drawn from 30L Niskin bottles into 250ml Nalgene polyethylene bottles with sampling tubes. The bottles were rinsed twice and filled with seawater by overflowing taking care not to entrain bubbles. The bottles were then sealed with screw and inner caps and stored at a refrigerator. Before measurement, bottles were in the water bath about 25 degree C.

The titration system consisted of a titration manager (Radiometer, TIM900), an auto-burette (Radiometer, ABU901), a pH glass electrode (pHG201-7), a reference electrode (Radiometer, REF201), a thermometer (Radiometer, T201) and two computers, the one was installed burette operation software (Lab Soft, Tim Talk 9) and the another one was for calculated total alkalinity. The method of total alkalinity measurement was as follows: approx. 100ml of seawater was placed in a 200ml tall beaker with a Knudsen pipette, and titrated with a solution of 0.1M hydrochloric acid. The acid was made up in a solvent of sodium chloride (0.7M) as same as the ionic strength of seawater. The titration by the acid was carried to the carbonic acid point using a set of electrodes that were used to measure electromotive force at 25 degree C. The value of total alkalinity was calculated by titrated acid volume, electromotive force, and seawater temperature pipetted.

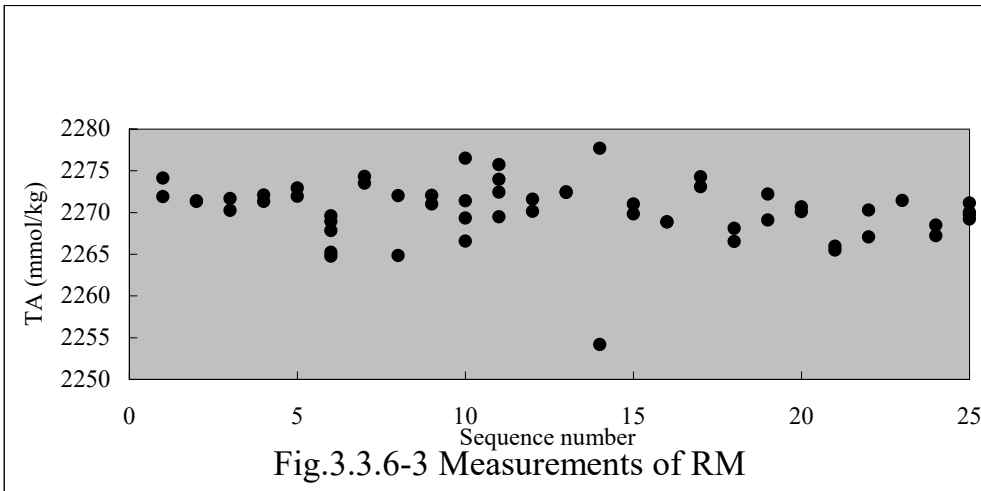
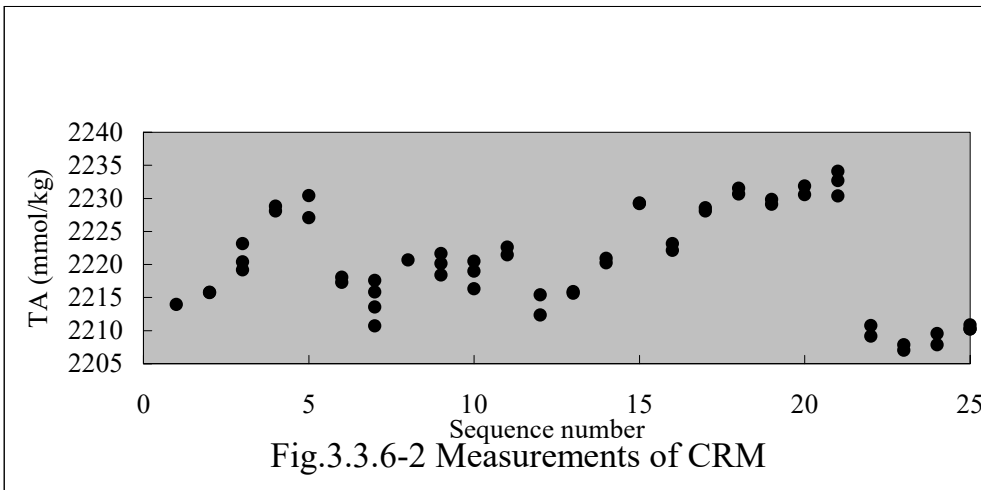
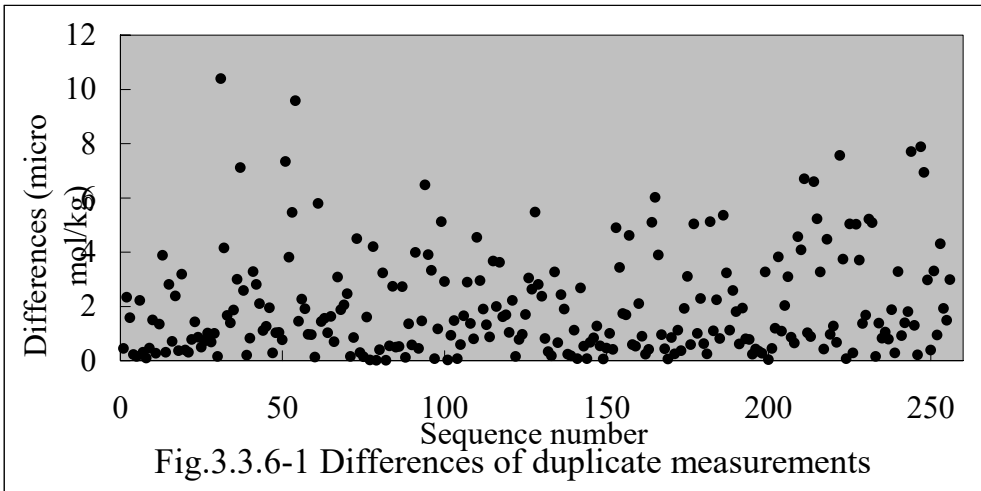
(3) Preliminary results

Preliminary data of total alkalinity are shown in the Appendix. In Fig.3.3.6.1, difference of duplicate measurement was shown sequentially to evaluate the precision of the measurement. The average and standard deviation of the repeatability measurements were 2.0 and 1.9 $\mu\text{mol/kg}$, respectively.

We measured two kinds of control sample, SIO CRM batch 53 and JAMSTEC RM to evaluate the stability of the measurement. Values of the CRM were plotted sequentially in Fig.3.3.6.2. The batch of the acid solution changed between the sequence number 21 and 22. Measurements values of RM (Fig.3.3.6.3) and seawater samples were corrected by the CRM values.

(4) References

DOE (1994) Handbook of methods for the analysis of the various parameters of the carbon dioxide system in sea water; version 2, A.G. Dickson & C. Goyet, eds. ORNS/CDIAC-74.



3.3.7 Carbon-13

Takayuki Tanaka, Shizuo Tsunogai (Hokkaido University) and Syuichi Watanabe (JAMSTEC)

In order to understand carbon cycles in the ocean related with biogeochemical and hydrographic systems, seawater samples for analysis of stable carbon isotope of total dissolved inorganic carbon ($\delta^{13}\text{C}$) was collected in the western North Pacific during the MR01-K03 cruise. The station collected water samples for $\delta^{13}\text{C}$ is listed the following;

Stn. 1, 2, 3, 4, 5, 1R, 15, 16, 17, 18, 19, 20, 21, 22, 23, 24, 25 and 26.

Seawater samples were collected in a 100 ml glass bottle and 50 μl of saturated mercuric chloride (HgCl_2) was added as preservative. Then the samples were stored in the cold storage (4°C) on board and until analysis after transporting to the laboratory. In the laboratory, total dissolved inorganic carbon will be extracted as CO_2 and $\delta^{13}\text{C}$ will be measured using mass spectrometer.

3.3.8 Carbon-14

Yuichiro Kumamoto (JAMSTEC), Mikio Kitada (MWJ), and Minoru Kamata (MWJ)

In order to study the role of intermediate water in carbon cycle in the western North Pacific, seawater for radiocarbon and stable carbon isotopes of TDIC was collected by the hydrocast at the stations 18, 20, 22, 24, and 26. Seawater was collected in a 250 ml glass bottle. Then a head-space of 2 % of the bottle volume was left by removing seawater sample with a plastic pipette. Saturated mercuric chloride (HgCl_2) of 0.05 cm^3 was added as preservative. Finally, the bottle was sealed using a greased ground glass and a clip was secured. We collected about 120 seawater samples during this cruise. All the samples were stored in a laboratory of JAMSTEC Mutsu Branch in Mutsu City. In the laboratory, TDIC will be extracted as CO_2 and converted to graphite for measurements of stable and radiocarbon isotopes, respectively.

3.3.9 Iodine-129

Takashi Suzuki and Takafumi Aramaki
Marine Research Laboratory
Mutsu Establishment
Japan Atomic Energy Research Institute

(1) Objective

^{129}I is a radioactive element with half-life 1.57×10^7 y. The natural ^{129}I is produced by spontaneous fission of ^{238}U and the interaction of cosmic ray with Xe atom in the atmosphere. Recently, the anthropogenic ^{129}I was increased by nuclear weapon tests and nuclear activity. This ^{129}I was used for an oceanographic tracer in the North Atlantic Ocean and the Arctic Ocean (Raisbeck et al., 1995; Smith et al., 1999), because the anthropogenic ^{129}I was discharged from nuclear reprocessing plants in Europe (LaHuge in France, Sellafield in England). In Japan, nuclear reprocessing plant was operated in the Tokai, Ibaraki and large nuclear reprocessing plant will be operated near future in the Rokkasho, Aomori. High concentration ^{129}I was observed from seawater and seaweed around the Tokai, Ibaraki (Muramatsu and Ohmomo 1986). We investigate the background level and the potential of oceanographic tracer of ^{129}I in the western North Pacific Ocean.

(2) Methods

1. Sampling

Sample bottles used the polyethylene made after washing in hydrochloric acid solution (pH=2). One-Liter seawater was sampled from Niskin bottles at Stn. 1, 17 and 27 (24 layers) and Stn. 20 (38 layers). These samples were brought back to the laboratory.

2. Sample preparation

After bringing back to the laboratory, seawater samples were added iodine carrier. All iodine is reduced to iodide (I^-). This solution is transferred into a separation funnel. The iodide (I^-) oxidized to iodine (I_2) by addition of sodium nitrate and extracted into carbon tetrachloride. The iodine is back-extracted into the water phase by addition of sodium sulfite. The iodine is precipitated by addition of silver nitrate. The precipitated AgI is washed with ammonium solution and distilled water. The AgI is finally mixed with niobium and pressed in a target holder. Iodine isotopic ratio is measured by Accelerator Mass Spectrometry installed Japan Atomic Energy Research Institute, Mutsu establishment.

(3) References

- Raisbeck et al., (1995) *Journal of Marine Systems*, 6, 561-570
Smith et al., (1999) *Journal of Geophysical Research*, 104, 29663-29677
Muramatsu and Ohmomo (1986) *The Science of Total Environment*, 48, 33-43

3.3.10 Freon

Shinichi Tanaka

Marine & Atmospheric Geochemistry Lab.
Division of Ocean & Atmospheric Science,
Graduate School of Environmental Earth Science
Hokkaido University

(1) Introduction

CFCs are useful chemical tracers to study on the water circulation in ocean and air-sea gas exchange. In this study, we purposed to obtain the distribution of CFCs in the northern North Pacific and study formation of North Pacific Intermediate Water (NPIW) and air-sea gas exchange.

(2) Method

(a) Sampling and sealing

Water samples were collected at 28 station; Station test, 1 ~ 5, 7, 8, 10 ~ 28. Seawater samples were collected with Niskin bottles. Each sample was collected in a 100 ml-glass ampoule bottle with a tygon rubber tube. At the sampling, seawater was allowed to overflow more than four times the bottle volume. Then, the ampoule was seal off by burner when the ampoule's headspace was filled by pure N₂.

(b) Analysis

Concentration of CFCs will be determine in laboratory. CFCs dissolved in seawater are stripped and pre-concentrated using a purge-and-trapping system with ECD-GC. This procedure is based on that described by Bullister and Weiss(1988)

(3) Result

Concentration of CFCs will be determined in laboratory. The obtain data during this cruise will be discussed with the past data by way of time series change of CFCs concentration, and surface data will be estimated for the air-sea gas exchange.

3.3.11 Ar/N₂/O₂

Shinichi Tanaka

Marine & Atmospheric Geochemistry Lab.
Division of Ocean & Atmospheric Science,
Graduate School of Environmental Earth Science
Hokkaido University

(1) Introduction

It is essential to estimate the role of bubble effect for the air-sea gas exchange. However, the mechanism is not sufficiently made clear. Bubbles are enormously produced air-sea gas exchange under heavy storms. In this study, we purposed to obtain the distribution of O₂/N₂/Ar ratio in the surface water and the role of bubble effect by change of N₂/Ar ratio.

(2) Method

(a) Sampling

Water samples were collected at 15 stations. Station 1,3,5,8,10,11,13,1R,16,18, 20,22,24, and 26. Seawater samples were collected with Niskin bottle. Each sample was collected in a 100ml-glass bottle with a tygon rubber tube. At the sampling, seawater was allowed to overflow more than four times the bottle volume. A 100 μl aliquot of saturated HgCl₂ solution was added to each sample to avoid biological change after sampling and it was stored in cold water before analysis.

(b) Analysis

O₂/N₂/Ar ratio was determined on board immediately. O₂/N₂/Ar dissolved in the seawater sample were stripped and divided into two. One of them is carried to a capillary column cooled by dry ice – ethanol bath (-72 °C) in TCD GC, and determine Ar/O₂ ratio. Another gas is carried to capillary column cooled by ice-water (0 °C) in TCD-GC, and determine (Ar + O₂)/N₂ ratio.

(3) Results

Data is not completed. These data need more adjustment.

3.3.12 DMS/DMSP

Nobue Kasamatsu and Shizuo Tsunogai (Hokkaido University)

(1) Objective

Dimethylsulfide (DMS) is the most abundant biogenic sulfur-bearing compounds emitted from the ocean to the atmosphere. DMS is formed from its precursor dimethylsulfonio-propionate (DMSP) which is produced by marine phytoplanktons. This observation is conducted to improve our basic knowledge on production DMS biochemistry in the western North Pacific. We also adapted the dilution technique to study microzooplankton grazing of algal DMSP vs Chl.*a*, and to estimate the impact of microzooplankton grazing on DMS production in the western North Pacific.

(2) Method

Water samples were collected with CTD systems attached with Niskin samplers of 30 or 12 L capacity and a plastic bucket from surface to 200 m water depth at more than 20 stations. Dilution experiments for DMS/DMSP were carried out at Stn.1, 1R, 8, 17, 26 and R-4. The sample water was transferred to a 100 ml glass syringe and kept at about 4°C in the dark until analysis. All the samples for DMS were analyzed within 12 hours after the sampling. For DMS measurement, an aliquot of 20ml of seawater sample was filtered using Whatman GF/F filter (47 mm) and introduced into glass purge chamber with stoppers at each mouth. The concentration of DMS in the seawater samples was determined using a purge-and-trap system followed by a gas chromatograph equipped with a flame photometric detector (Shimadzu GC-14B). For DMSPt (total DMSP) measurement, an aliquot of 14 ml of seawater sample was injected into 30 ml vial containing 4 ml of 6N NaOH to cleave DMSPt (dissolved DMSP and particulate DMSP) into gaseous DMS. For dissolved DMSP (DMSPd), an aliquot of 14 ml seawater sample was injected through a Watman GF/F filter into the vial. The vials were stored at 4°C for at least 6 hours. DMSP samples were sparged in the vials. The particulate DMSP (DMSPp) concentrations can be determined by subtracting the DMS and DMSPd values from DMSPt values. The analytical error for each measurement was 14 %.

3.3.13 Chlorophyll-*aa* and pigment

Nobue Kasamatsu, Shizuo Tsunogai (Hokkaido University), Keiri Imai (CREST) and Syuichi Watanabe (JAMSTEC)

(1) Objective

In order to clarify the spatial variability and vertical structure of Chlorophyll *a* (Chl-*a*) distribution, and understand the relationship between production and predation of phytoplankton in the western North Pacific, we measured Chl-*a* concentrations and phytoplankton pigment signatures and cultivated phytoplankton using dilution technique

(2) Methods

Water samples were collected from surface to 200 m water depth at more than 20 stations, using CTD systems attached with Niskin sampler of 30 and 12 L capacity. Surface water samples were collected with a plastic bucket. For Chl-*a* samples, the seawater were collected in 3 L dark bottles and filtered through the three different pore sizes filters; 10 μ m Nuclepore (Millipore), 2 μ m Nuclepore (Millipore), and Whatman GF/F filter under low vacuum pressure (<100 mmHg). Filtered samples were extracted in 6 ml of N, N-dimethylformamide (DMF) and stored at -17°C until analysis on land. Chl-*a* concentration will be determined by the fluorometric method with a Turner Designs Fluorometer.

Surface water for dilution experiment was taken with a plastic bucket at Stn.1, 1R, 5, 8, 11, 17, 26 and R-4. Water for the dilution was filtered using gravity through 15 cm GF/F (Whatman). A dilution series was prepared, in 350 or 600ml polycarbonate bottles, consisting of 100, 75, 50, and 25% unfiltered water (on several occasions different dilutions were used). These were incubated for 24-76 h in a water-bath deck incubator.

Phytoplankton pigments samples were collected to identify the major classes of phytoplankton present. Seawater was filtered through a Whatman GF/F filter and filter samples were stored in a deep freezer (-80°C) until analysis on land. Pigments will be measured with high-performance liquid chromatography (HPLC).

3.3.14 CREST samples

Takeshi Egashira (Japan Science and Technology Corporation)

Fujio Shimano (Japan Science and Technology Corporation)

Keiri Imai (Japan Science and Technology Corporation)

Nobuo Tsurushima (National Institute for Resources and Environment)

Yukihiro Nojiri (National Institute for Environment Studies)

(1) Study of carbon system at the station KNOT

Introduction

A new ocean time series station has been established in the western subarctic Pacific. This is one of the activities of JGOFS-Japan and JGOFS-NPTT (North Pacific Task Team). This station was named “KNOT” (Kyodo Northwest Pacific Ocean Time series; Kyodo is Japanese word meaning collaborative) and located at 44 ° N, 155 ° E. The station KNOT is in the southwestern part of western subarctic gyre and the area is characterized by high biological production in spring/summer and deepening of surface mixed layer in winter season by surface cooling. The purpose of this study is to understand the seasonal variation of carbon system in the area around the KNOT.

Sampling

We collected samples for measurement of total carbon dioxide (TC) and total alkalinity (TA), and nutrients. Water samples were collected with CTD rosette systems attached with Niskin bottles of 30L capacity. Sample waters were drawn from Niskin samplers into individually numbered, clean bottles.

Sample storage

TC and TA samples (250ml) were poisoned with 0.05ml of saturated HgCl₂ solution and stored in glass bottles at room temperature. Nutrients samples (100ml) were stored in polypropylene bottles at a freezer (-20 °C).

(2) Phytoplankton pigment

Chlorophyll-a and pigments separated by HPLC are measured for comparison with phytoplankton species and number. The seawater sub samples for phytoplankton pigments were collected from 13 layers (0, 5, 10, 20, 30, 40, 50, 60, 80, 100, 125, 150, 200m) by Niskin sampler attached to CTR-RMS at station KNOT. At other same station as primary production experiments, their samples were collected by Niskin bottle from 0 to 100m of depth. And chlorophyll-a samples were collected at all CTD/Hydrocast station by Niskin bottle from 0 to 100 or 200m of depth. At same

station as primary production experiments, chlorophyll-a samples were carried out size fraction with nuclepore filter (pore size 10 and 2um) and grass fiber filter (Whatman GF/F). These chlorophyll-a samples will be measured with Turner.

3.4 Hydrocast for trace metals

Naoyuki Sato (Kanazawa Univ.)

(1) Objective

The distribution and speciation of trace elements in seawater are controlled by various physical, chemical and biological processes. Deficiency of trace elements may limit phytoplankton growth. Our object is to reveal the behavior of trace elements and to elucidate the processes occurring in the ocean.

(2) Measured parameters

On the present cruise, we are studying the distribution of trace elements (Al, Sc, Ti, V, Mn, Fe, Co, Ni, Cu, Zn, Ga, Y, Zr, Nb, Mo, Cd, Hf, Ta, W, Th, U, Au, Pd, etc.) in seawater.

(3) Instruments and Methods

Seawater samples were collected with X-Niskin bottles mounted on a CTD carousel water sampling system. Seawater (500 ml, 5 l) was transferred from the sampler using a silicon tube and bell to avoid contamination by airborne particles.

Immediately after sampling, 250 ml of seawater were filtered through a 0.2 μm Nuclepore filter using a closed filtration system in the clean room. The filtered seawater, which is used for determination of trace bioelements, such as Mn, Fe, Co, Ni, Cu, Zn and Cd, was added with 0.01 M of hydrochloric acid for preservation. In our laboratory, the samples will be adjusted to pH 5 with ammonium acetate buffer and passed through a column of 8-quinolinol immobilized fluoride containing metal alkoxide glass (MAF-8HQ). Collected trace elements on MAF-8HQ will be eluted with 25 ml of 0.5 M nitric acid. The trace bioelements in the eluates will be determined with a high resolution ICP-mass spectrometer (HR-ICP-MS; JEOL JMS-PLASMAX1).

Unfiltered seawater (250 ml), which is used for determination of elements of groups 4, 5 and 6 (Ti, Zr, Hf, V, Nb, Ta, Mo and W), was added with 0.01 M of hydrochloric acid and 0.002 M of hydrofluoric acid for preservation. The method is basically the same as that for trace bioelements except that the eluent is 0.5 M nitric acid containing 0.001 M oxalic acid. The samples will be brought back to our laboratory and subjected to preconcentration with MAF-8HQ and determination by HR-ICP-MS.

Seawater (5 l), which is used for determination of platinum-group elements, was added with 0.01 M of hydrochloric acid for preservation. In our laboratory, the samples will be adjusted to pH 3 with ammonium acetate buffer and passed through a column of poly(N-aminoethyl)acrylamide chelating fiber. Collected trace elements on poly(N-aminoethyl)acrylamide chelating fiber will be eluted with 25 ml of 0.1 M ammonia and 0.001 M potassium cyanide. Pd and Au in the eluates will be determined by ICP-MS.

(4) Results

312 samples were collected during this cruise. We are now analyzing these samples, and it will be ended by October 2002.

(5) Data archive

Raw data of trace elements will be submitted to DMO (Data Management Office), JAMSTEC.

3.5 Optical observation and primary production

Takeshi Egashira (Japan Science and Technology Corporation)

Imai Keiri (Japan Science and Technology Corporation)

(1) Optical observation

The underwater downward irradiance and upward radiance were measured using the underwater unit, PRR-600(Biospherical Instrument Inc.). The measurements were carried out from the sea surface down to depth about 85m. The incident solar spectral irradiance was measured using the deck unit, PRR-610 (Biospherical Instrument Inc.). The measurements were carried out before primary production sampling. The data by measurements of PRR were decided on primary production sampling depth layer.

(2) Primary production

In western region of North Pacific Ocean time series survey was started since June 1998. In this region it is important to estimate primary production by phytoplankton in spring. Therefore the mission of this study is to measure primary production of spring season by phytoplankton in this region.

In this cruise, using ^{13}C as a tracer for inorganic ^{13}C uptake by phytoplankton photosynthesis, incubation experiments carried out in similar in-site. Water samples were collected with Niskin-X sampling bottles attached to CTD-RMS from 6 layers corresponding to 100, 34, 17, 8.5, 4, 0.9% of surface irradiance and drained into 250ml polycarbonate bottles. After addition of $^{13}\text{C}\text{-NaHCO}_3$ those bottles were incubated for 24 hours. And particle matter was filtered onto pre-combusted (450°C, 4h) grass fiber filter (Whatman GF/F) after incubation. Primary production will be calculated with concentration and ^{13}C -atom % of particle organic carbon (POC) determined by tracer. Incubation date and station are as follows.

Table 3.5-1 Incubation date, station and sampling depth

Date	Station	Sampling depth
9-Jun	Stn.1	0, 3, 7, 13, 19, 29m
9-Jun	Stn.2	0, 7, 15, 24, 32, 48m
10-Jun	Stn.3	0, 4, 10, 16, 21, 32m
12-Jun	Stn.5	0, 5, 12, 21, 31, 50m
13-Jun	Stn.7	0, 5, 12, 20, 29, 46m
14-Jun	Stn.8	0, 3, 5, 16, 28, 54m
19-Jun	Stn.11	0, 9, 21, 33, 45, 72m
20-Jun	Stn.13	0, 5, 17, 27, 38, 60m
21-Jun	Stn.10	0, 4, 13, 25, 41, 66m
23-Jun	Stn.14	0, 4, 9, 21, 42m
25-Jun	Stn.1R	0, 14, 21, 32, 46m
3-Jul	Stn.26	0, 11, 34, 52, 70, 90m

3.6 Plankton net

Takeshi Egashira (Japan Science and Technology Corporation)

Naonobu Shiga (Faculty of Fisheries, Hokkaido University)

(1) Net zooplankton

These samplings aim to reveal the biomass, horizontal and vertical distribution, and species composition of net zooplankton in northwestern subarctic Pacific. Net zooplankton was collected using single type NORPAC nets. Single type NORPAC nets were towed vertically, and sampling depth strata were 0 to 150m and 0 to 500m. Sampling stations were station 1 to 14 except for station 6 and 9. Volumes of water filtered through the net were estimated from readings of a Rigosha flowmeter mounted in the mouth of each net. All net samples were immediately preserved in 5% buffered formalin to seawater solution.

(2) Phytoplankton

The subject of this study is to reveal the species succession of phytoplankton in northwestern subarctic Pacific. Water samples for taxonomic analysis and counting for phytoplankton were collected using Niskin bottles at 0 to 200m of depth. Sampling stations were station 1 to 14 except for station 6 and 9. All water samples were preserved with 1% buffered formalin to seawater solution. Collected samples will be used for identifying the species of phytoplankton.

3.7 Time-series sediment trap experiment

3.7.1 JAMSTEC Sediment trap

Hiroaki Muraki, Aya Kato, Kazuhiro Sugiyama, Masumi Ishimori
(Marine Works Japan Ltd.)

Makio Honda *

(Japan Marine Science and Technology Center)

(1) Introduction

One of characteristics in the northwestern North Pacific is strong seasonal variability in the biological activity and its related marine chemistry. In order to study seasonal variability in biological pump and its role in materials cycle with the emphasis on the carbon cycle, time-series sediment trap experiment has been conducted since December 1997 at three stations (stn. KNOT : Japanese biogeochemical time-series station, stn. 50N: western Subarctic gyre, and stn. 40N: Subarctic front). During MR01-K03 cruise, the sediment trap mooring systems were recovered.

(2) Methods

1) Mooring system

The mooring system at three stations consists of three sediment traps with 21 collecting cups (McLane Mark 7G-21 or Mark 78-21), glass floatation, wire / nylon ropes, and acoustic release (Benthos 865A). Sediment traps were positioned at approximately 1000 m, 3000 m, and 5000 m depths. Before deployment, collecting cups were filled with sea water based 5 % buffered formalin to preserve collected settling particles. Sampling started in August 2000 and February 2000 at station 50N and 40N, respectively. Each cup was scheduled to rotate every 17.38 days for station 50N and 23.14 days for station 40N.

2) Recovery

Thanks to the enthusiastic assistance by captain Hashimoto, chief officer Dowaki and crew members, the sediment trap mooring systems at stations 50N and 40N were recovered successfully on 11, June and 19, June, respectively. Every collecting cups rotated on schedule. Although some collecting cups at station 40N missed sampling (clogging ?), a lot of valuable samples were collected.

On the other hand, mooring system at station KNOT could not be recovered because of malfunction of acoustic release system. It is planned that this mooring

system is recovered by “drag” method during the next cruise (MR01-K04) held in coming summer.

3) Sample collection

On board, condition of sample collection was checked. Fig. 3.7.1.1 and 3.7.1.2 show heights of sample collected in cups, which measured by a scale.

From station 50N, 18 samples (last sample was recovered before completion) for respective depths were obtained. During autumn 2000, relatively high fluxes were observed. From station 40N, 21 samples at 1000 m and 5000 m were obtained. During June and August, high flux was observed and the maximum was higher than that at station 50N. At 3000 m, no sample was collected after high flux was observed in June 2000. Judging from previous experiments, high flux might clog the bottom of conical funnel of the sediment trap.

(3) Chemical analysis

These samples will be transported to laboratory being kept in refrigerator. At laboratory, chemical components such as carbon, nitrogen, carbonate, opal and trace elements will be measured.

(4) New mooring system

By sediment trap experiment for three years, seasonal variability in biogenic and lithogenic materials' flux in deep sea in the northwestern North Pacific has been verified. However information of seasonal variability in the biological activity in the shallow water have not been necessary obtained enough to compare fluxes in deep sea. We have prepared new mooring systems, which consists of not only time-series sediment traps in deep sea, but also multilayer profiler of CTD / current meter and water sampler, plankton collector and time-series incubation device in the euphotic zone. These new mooring systems will be deployed near stations 50N and KNOT during MR01-K04.

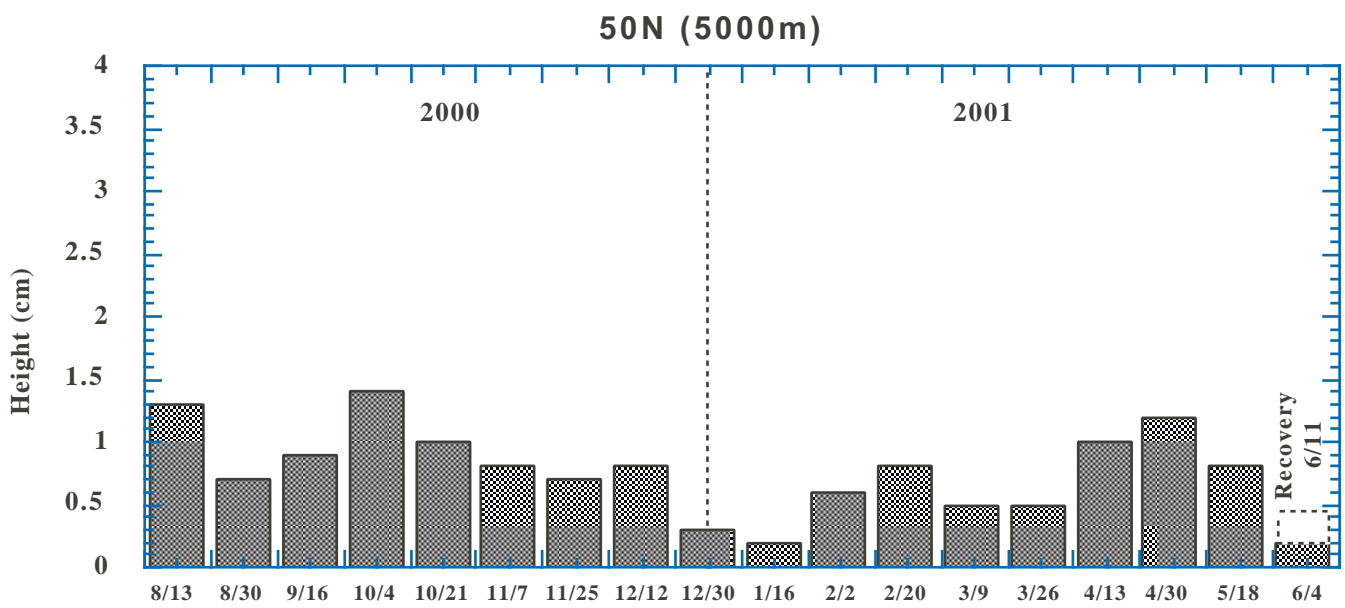
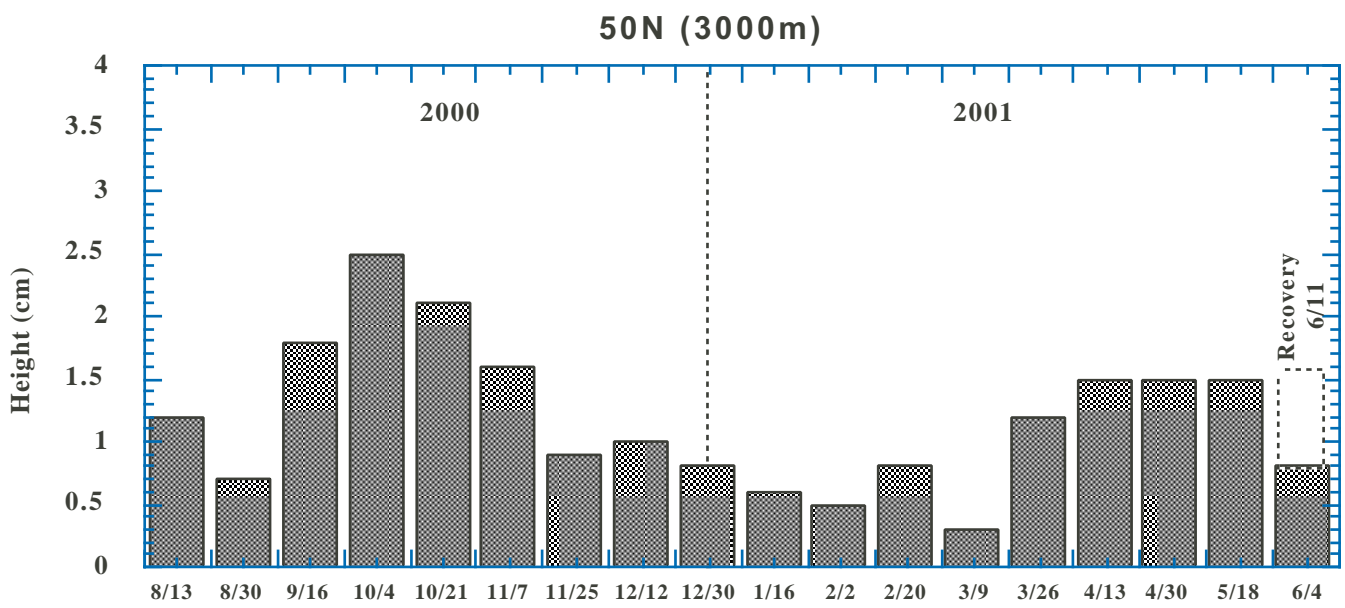
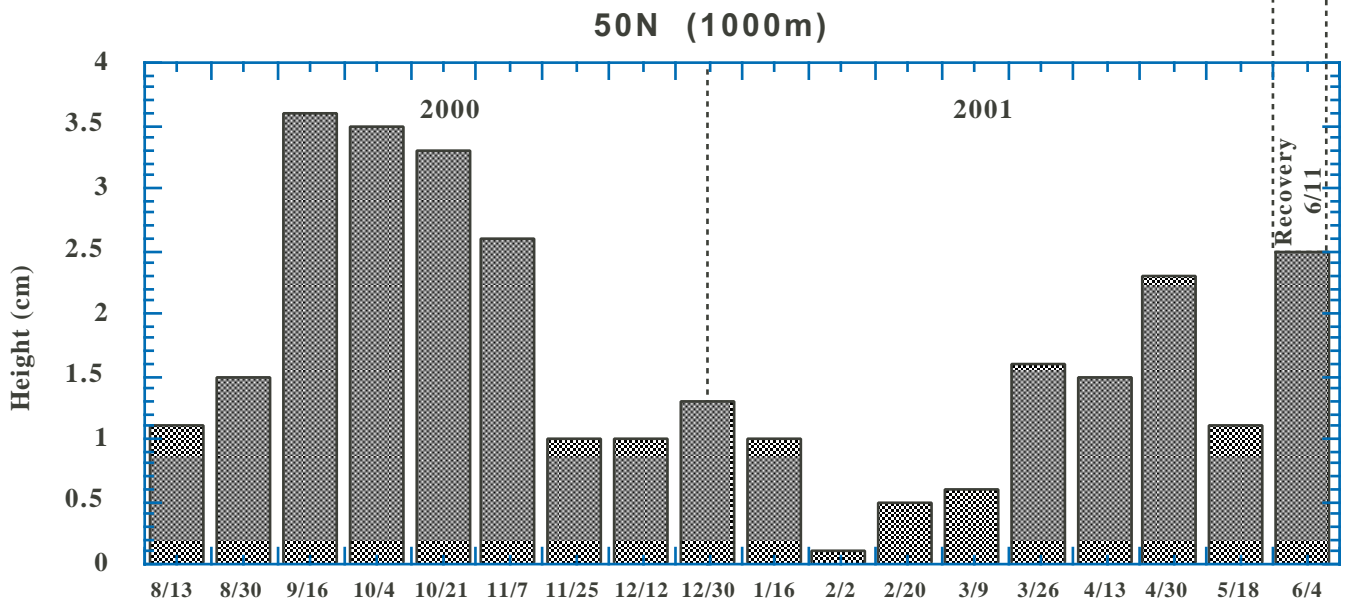


Fig. 3.7.1-1 Seasonal variability in collected samples at station 50N
 Unit is height of samples measured by a scale on board.
 Date for each period is an starting day of sample collection.

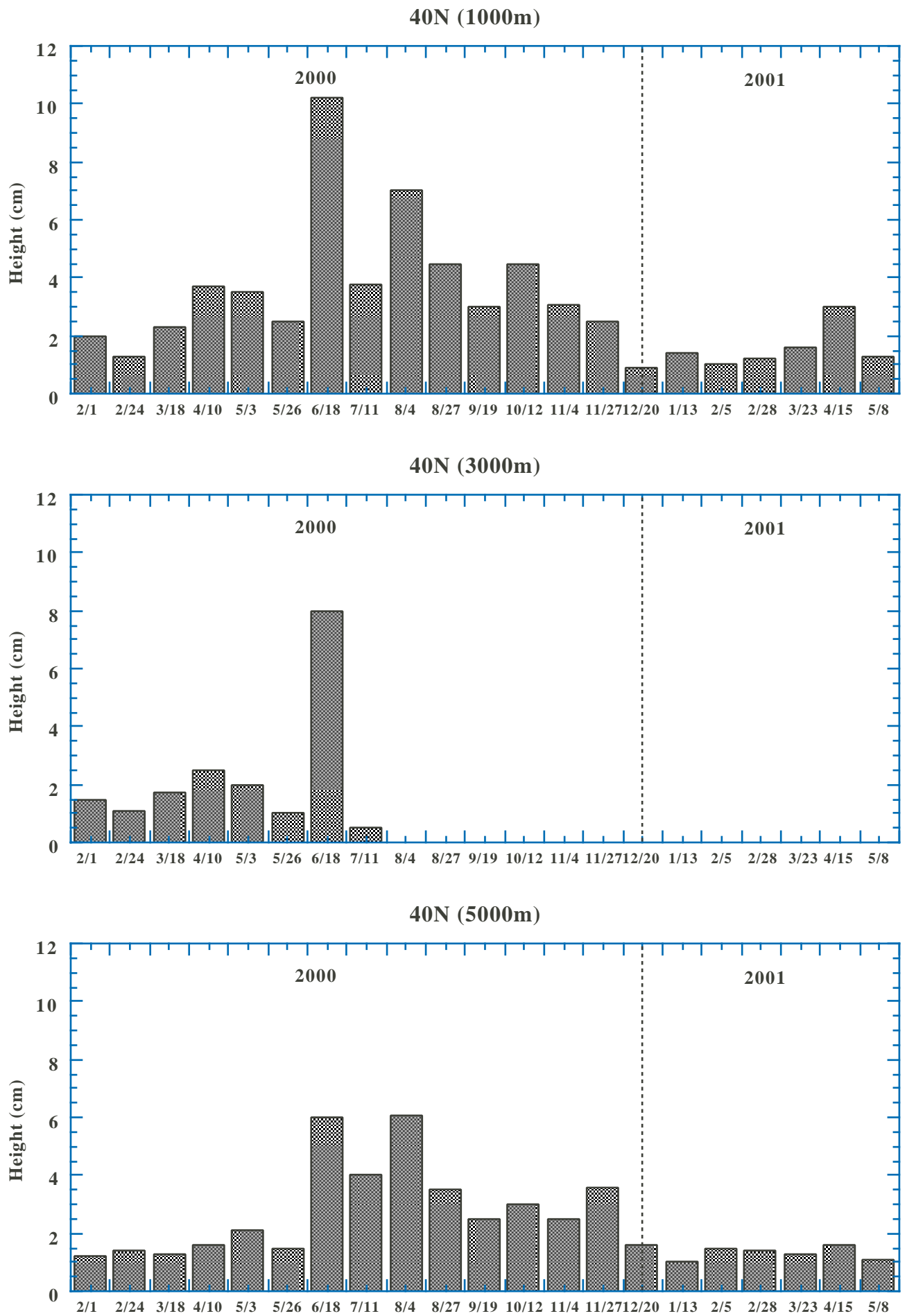


Fig. 3.7.1-2 Seasonal variability in collected samples at station 40N
 Unit is height of samples measured by a scale on board.
 Date for each period is an starting day of sample collection.

3.7.2 Hokkaido Univ. sediment trap

Shinitiro Noriki and Hisashi Narita (Hokkaido University)

(1) Introduction

The most important feature in the northwestern North Pacific is the strong seasonal variation of biogenic productivity. The sediment trap experiment was conducted for understanding the seasonal variations of the biological productivity, its related oceanic environments and its influence on biogeochemical cycles of various chemical species. At St. KNOT, which is a Japanese biogeochemical time-series station, the sediment trap experiment had been carried out during three years from 1989 by our group and has been going on by JAMSTEC since December 1997.

The sediment trap had been deployed by using T/V Bosei Maru on October 1999, where located in the northwestern North Pacific basin about 50 miles northwest of St. KNOT (44° 42.478 N, 155° 37.811 E) and has been re-deployed the same position (44° 42.550 N, 155° 37.410 E) by using R/V Mirai on 26 May 2000. Our objectives are investigation into biochemical cycles in the northwestern North Pacific, and the comparison with results of the St. KNOT. The sediment trap mooring system was recovered.

(2) Methods

Sediment trap was deployed on 26 May 2000. The settling particles samples were collected at about 1,000 m with sediment trap consisting twin cones type (NICHYU GIKEN KOGYO CO., Ltd., STM-13-6000) each with 13 cups working in time series. Sampling cups were rotated 10 days spring to summer and 40 days from fall to the recovered time.

(3) Future work

Samples were transported to the laboratory on land, and will be separated into several portions by rotary splitting systems. Chemical analysis, such as organic and inorganic carbon, biogenic opal and trace elements will be measured, and will be discussed their variations and its reflected of the oceanic environments.

3.8 Sediment

Personnel:

Naokazu AHAGON (MIO, JAMSTEC)

Hisashi NARITA (GEES, Hokkaido Univ.)

Ken'ichi OHKUSHI (LBA, Tsukuba Univ)

Toshiaki MISHIMA (DRD, JAMSTEC)

Masao UCHIDA (ORD, JAMSTEC)

Aya KATO (Marine Works Japan, Ltd.)

Hiroaki MURAKI (Marine Works Japan, Ltd.)

Masumi ISHIMORI (Marine Works Japan, Ltd.)

Kazuhiro SUGIYAMA (Marine Works Japan, Ltd.)

3.8.1 Objectives

Main objective of sediment coring in this cruise is to investigate paleoceanographic changes in the Northwest Pacific during late Quaternary as follows:

(1) changes in deep-water circulation, (2) changes in sea surface temperature, (3) variations in paleo-flux of biogenic components, (4) millennial-scale changes of North Pacific Intermediate Water ventilation from the last glacial to Holocene, (5) developing new paleoceanographic proxies such as compound-specific radiocarbon analysis, (6) searching geomagnetic events and utilizing rock-magnetic analysis for paleoenvironmental reconstruction.

3.8.2 Coring equipments

(1) Multiple Core Sampler

Multiple Core Sampler was used for taking the surface sediment. This sampler consists of a main body of 620kg-weight and acrylic eight sub-core samplers (I.D. 73mm and length of 60cm).

(2) Piston Core Sampler

Piston Core Sampler consists of a 1500kg-weight, a total 20m-long duralumin tube (5m x 4), and a pilot core sampler. The inner diameter of core tube is 80mm. We used a multiple-type pilot core sampler "Ashura", which is equipped with an 80kg-weight and three acrylic sub-cores as same as Multiple Core sampler.

(3) Site survey

The site survey was carried out using 12-kHz SEA BEAM 2100 Multi-Narrow Beam Bathymetric Survey System with Sub-bottom Profiler (SeaBeam Instruments, Inc.).

(4) Positioning System

Global positioning system (GPS) of WGS84 was adopted to determine a geographic position.

3.8.3 Sampling Locations

In total, seven piston and four multiple cores were obtained during this cruise at five stations (Table 3.8.1). Paired coring of piston and multiple cores on proposed sites were performed except for Station 31. Bathymetric survey map of each cored sites are shown in *Appendix*.

Table 3.8.1. Sediment samples collected during MR01-K03 cruise.

Core ID	Date	Station No.	Equipment	Latitude*	Longitude*	Depth (m)	Cored Length† (cm)
MR01-K03 MC-01	15.June.01	9A	MC	45° 02.32'N	170° 14.72'E	2647	28
MR01-K03 MC-02	16.June.01	9B	MC	44° 57.41'N	170° 21.45'E	3140	29
MR01-K03 MC-03	17.June.01	8	MC	45° 00.50'N	164° 56.93'E	6027	31
MR01-K03 MC-04	9.July.01	30	MC	41° 07.11'N	142° 24.15'E	1362	35
MR01-K03 MC-05	12.July.01	29	MC	39° 57.38'N	145° 29.90'E	5266	34
MR01-K03 PC-01	15.June.01	9A	20m-PC	45° 02.33'N	170° 14.85'E	2642	1071
MR01-K03 PC-02	16.June.01	9B	20m-PC	44° 57.50'N	170° 21.44'E	3144	1659
MR01-K03 PC-03	22.June.01	8	20m-PC	45° 00.50'N	164° 56.94'E	6027	1801
MR01-K03 PC-04	9.July.01	30	20m-PC	41° 07.10'N	142° 24.17'E	1363	1334
MR01-K03 PC-05	10.July.01	30	20m-PC	41° 07.09'N	142° 24.15'E	1366	1337
MR01-K03 PC-06	11.July.01	31	15m-PC	42° 21.42'N	144° 13.36'E	1066	712
MR01-K03 PC-07	12.July.01	29	20m-PC	39° 57.37'N	145° 29.91'E	5266	1432

*WGS84

†excluded flow-in materials

3.8.4 Method and preliminary results

Core Handling

After retrieving the corer on deck, piston core tube was sectioned into every 1m in length using a rotary band saw. The sediment were pushed out from the tube using a

hydraulic core pusher, and then transferred into PVC liners. After carrying the sections into wet-laboratory, routine analysis was performed as following order:

- (1) Whole-round sections were equilibrated at room temperature, and then run through Multi-Sensor Core Logger (MSCL).
- (2) Whole-round section was split lengthwise into working and archive halves with a stainless steel wire. After splitting, two halves of cores were first scraped across to expose a fresh surface for visual core description and color reflectance measurement, and then sediments were photographed with a color film.
- (3) Slab samples of 1cm thick were taken for Soft X-ray Photograph using a plastic case of 20 cm-long and 3cm-wide from archive halves.
- (4) After this process, archive halves of the samples were placed into plastic bags, and then sealed with Ar gas. The archive halves were transferred to a cold storage aboard the R/V MIRAI. After the cruise, the archive halves are going to be stored at a storage of MIO-JAMSTEC under 4°C. The working halves were processed for routine sampling as requested by researcher.

In the case of multiple and pilot core materials, at least one sub-core in each sites was processed for on-board routine analysis. The remaining sub-cores were sliced in every 1 or 2 cm, which depended on researcher.

Multi-Sensor Core Logging

H. MURAKI, T. MISHIMA and H. NARITA

Gamma-ray attenuation (GRA) and magnetic susceptibility (MS) were measured on whole-core section before splitting using the onboard GEOTEK multisensor core logger (MSCL). The MSCL have three sensors, which is gamma-ray attenuation, P-wave velocity (PWV), and magnetic susceptibility. However, PWV sensor was not used in this cruise, because there was always gap between the core liner and the sediment, which causes inaccurate P-wave transfer through the sediment.

The principle of GRA is based on the facts that medium-energy gamma rays (0.1-1MeV) interact with the formation material mainly by Compton scattering, that the elements of most rock-forming minerals have similar Compton mass attenuation coefficients, and that the electron density measured can easily be related to the material bulk density. The ^{137}Ce source used transmits gamma rays at 660 KeV. A standard NaI scintillation detector is used in conjunction with a universal counter. GRA calibration assumes a two-phase system model for sediments and rocks, where the two phases are the minerals and the interstitial water. Aluminum has an attenuation coefficient similar to common minerals and is used as the mineral phase standard. Pure water is used as the

interstitial-water phase standard. The actual standard consists of a telescoping aluminum rod (five elements of varying thickness) mounted in a piece of core liner and filled with distilled water. GRA measurement was carried on every 1 or 2-cm whole-core with 20-seconds counting. GRA data provide wet bulk density and fractional porosity for core thickness is constant (multiple core:74mm, piston core:80mm)

MS was measured using Bartington MS2C system installed in MSCL. The main unit is the widely used, versatile MS2 susceptometer. The unit has a measuring range of 1×10^{-5} to 9999×10^{-5} (SI, volume specific). The loop sensor has an internal diameter of 100mm. It operates at a frequency of 0.565 kHz and an alternating field (AF) intensity of 80 A/m (=0.1mT). MS data measurement was also carried on every 1 or 2-cm whole-core with 1 second. All results are processed to eliminate data gaps between sections and then plotted in Fig. 3.8.1-3.8.9.

Visual Core Description

N. AHAGON, K. OHKUSHI and K. SUGIYAMA

Archive half sections were visually described for lithology, coring disturbance, sedimentary structure and sediment color etc. Smear slide analysis under a polarized microscope was also carried out for determining grain size, mineral and microfossil compositions of the sediment. Optical identification of mineral under smear slide sample was based on Rothwell (1989) and some were determined by X-ray diffraction (XRD) method. The sediment color was described using standard Munsell notation for convenience, but more objective color measurement was also performed using spectrophotometer (*see* color reflectance measurement). Description was done for every section basis using description form, and then summarized to a column in each sites (Fig.8.3.10-16).

Color reflectance measurement

M. ISHIMORI and A. KATO

Color reflectance was measured by using the Minolta Photospectrometer CM-2002. This is a compact and hand-held instrument, and can measure the spectral reflectance of sediment surface with a scope of 8 mm in diameter. High-speed and accuracy measurements of spectral reflectance in the range from 400 to 700 nm can be obtained by ultracompact spectral sensors, hybrid IC analog circuitry, and a 32-bit, 16-MHz microcomputer. To ensure accuracy, the CM-2002 uses a double-beam feedback system, monitoring the illumination on the specimen at the time of measurement and automatically compensating for any changes in the intensity or spectral distribution of

the light. Calibration was carried out with the zero and white calibration pieces (Minolta CM-2002 standard accessories) before the measurement of core samples. The color of working half core was measured on every 2-cm through crystal clear polyethylene wrap.

The color reflectance data are indicated as color parameters of L*, a*, and b* (L*: black to white, a*: red to green, b*: yellow to blue). All results are processed to eliminate data gaps between sections and then plotted in Fig. 3.8.2-3.8.9 with MSCL results.

Core Photographs

K. SUGIYAMA and H. MURAKI

After splitting each sections of piston, pilot and multiple cores into working and archive halves, sectional photographs of archive halves were taken using a Nikon single-lens reflex camera and a Cannon digital camera. Both working and archive halves were photographed on PC-01 since sediments were so soupy that recovery of archive halves was very low. When using the Nikon reflex camera, shutter speed was selected on 1/250 and 1/320. Sensitivity ISO 100 was used on negatives. The photos will be stored at DMO of JAMSTEC.

Soft X-ray Photographs

K. SUGIYAMA

Soft X-ray photograph analysis system (Soft-X), PRO-TEST 150 (SOFTEX), was used to observe sedimentary structures of samples. The total 553 sediment slabs were collected from cores using original plastic cases (200x30x7mm). X-ray photographs of samples through the plastic cases were taken under a standard condition that is practically known (50kVp, 3mA, in 200 seconds). During this cruise, the samples were photographed in 110 negatives that were developed on board. The results will be stored at DMO of JAMSTEC.

X-Ray Diffraction (XRD)

A. KATO and N. AHAGON

RIGAKU RINT 2002 X-ray diffractometer was used for the XRD analysis of mineral phases. Ni filtered CuK radiation generated at 40kV and 50mA was used. Peaks were scanned from 2 ° to 90 ° 2 θ , with a step size of 0.02 ° and a counting time of 0.04s per step. Bulk samples were dried, ground, and mounted in random orientation in glass planchettes. The

powder was then pressed into the glass sample holders for analysis. The raw data will be stored at DMO of JAMSTEC.

3.8.5 Future work (shore-based study)

The working halves of the core were continuously sub-sampled for shore-based analysis. The following measurements will be performed on shore-based laboratories:

JAMSTEC group

- *Stable isotopes ($\delta^{18}\text{O}$ & $\delta^{13}\text{C}$) of foraminifera for PC01, PC02, MC01 and MC02.
- *Trace elements in foraminifera for PC01, PC02, MC01 and MC02.
- *Alkenones and specific organic compounds for PC02 and MC02.
- *AMS14C age and compound-specific radiocarbon analysis for PC05 and MCs.
- *Carbonate C & organic C analysis for PC01, PC02, PC03 and PC07.
- *Paleomagnetic & rock-magnetic analysis for all sites.
- *Index physical properties for all sites.

Hokkaido University group

- *Biogenic opal analysis for PC01, PC02, PC03 and PC07.
- *Trace elements in opal & bulk sediments for PC01, PC02, PC03 and PC07.

Tsukuba University group

- *Stable isotopes ($\delta^{18}\text{O}$ & $\delta^{13}\text{C}$) of foraminifera for PC04, PC06 and MC04.
- *Microfossil analysis (radiolaria, diatom, foraminifera) for PC04, PC06 and MC04.
- *AMS 14C age for PC04, PC06 and MC04.

3.8.5 Reference

Rothwell, R.G., 1989. *Minerals and mineraloids in marine sediments: An optical identification guide*, Elsevier Applied Science, LN & NY., 279pp.

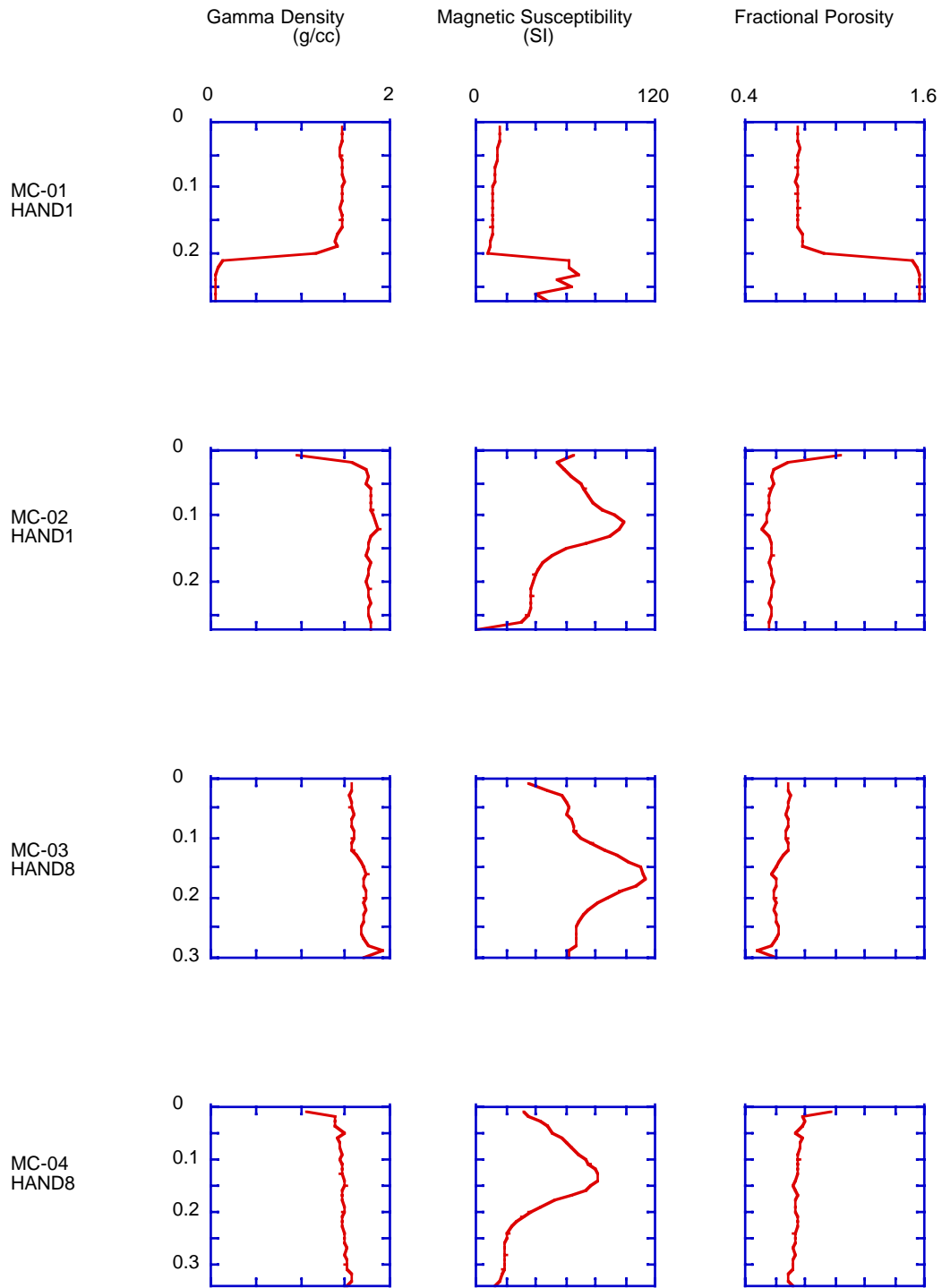


Fig. 3.8-1 MSCL results of MR01-K03 Multiple Core samples.
Vertical axis indicates depth in core (M).

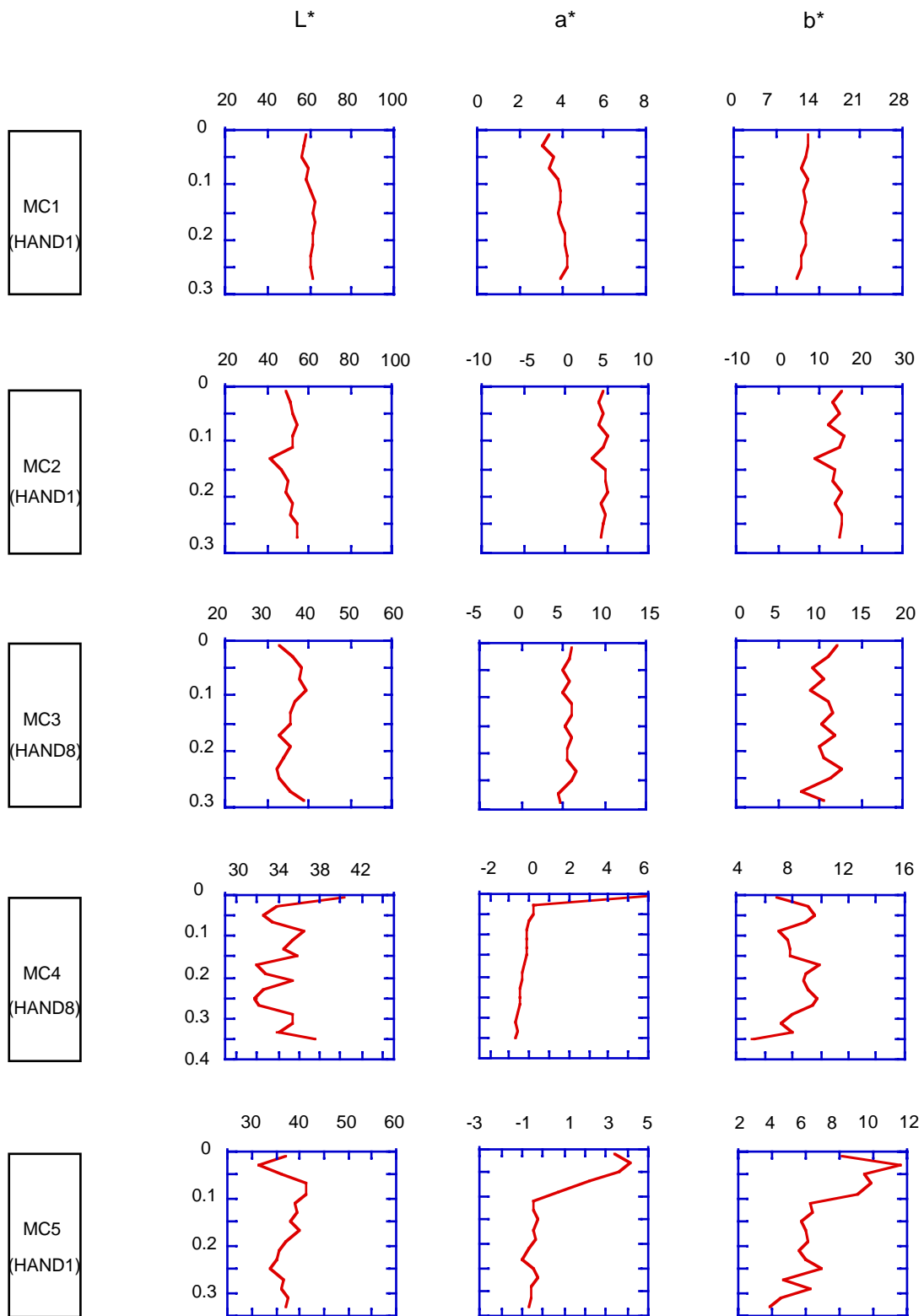


Fig. 3.8-2 Color reflectance plots of MR01-K03 Multiple Core Samples. Vertical axis indicates depth in core (M).

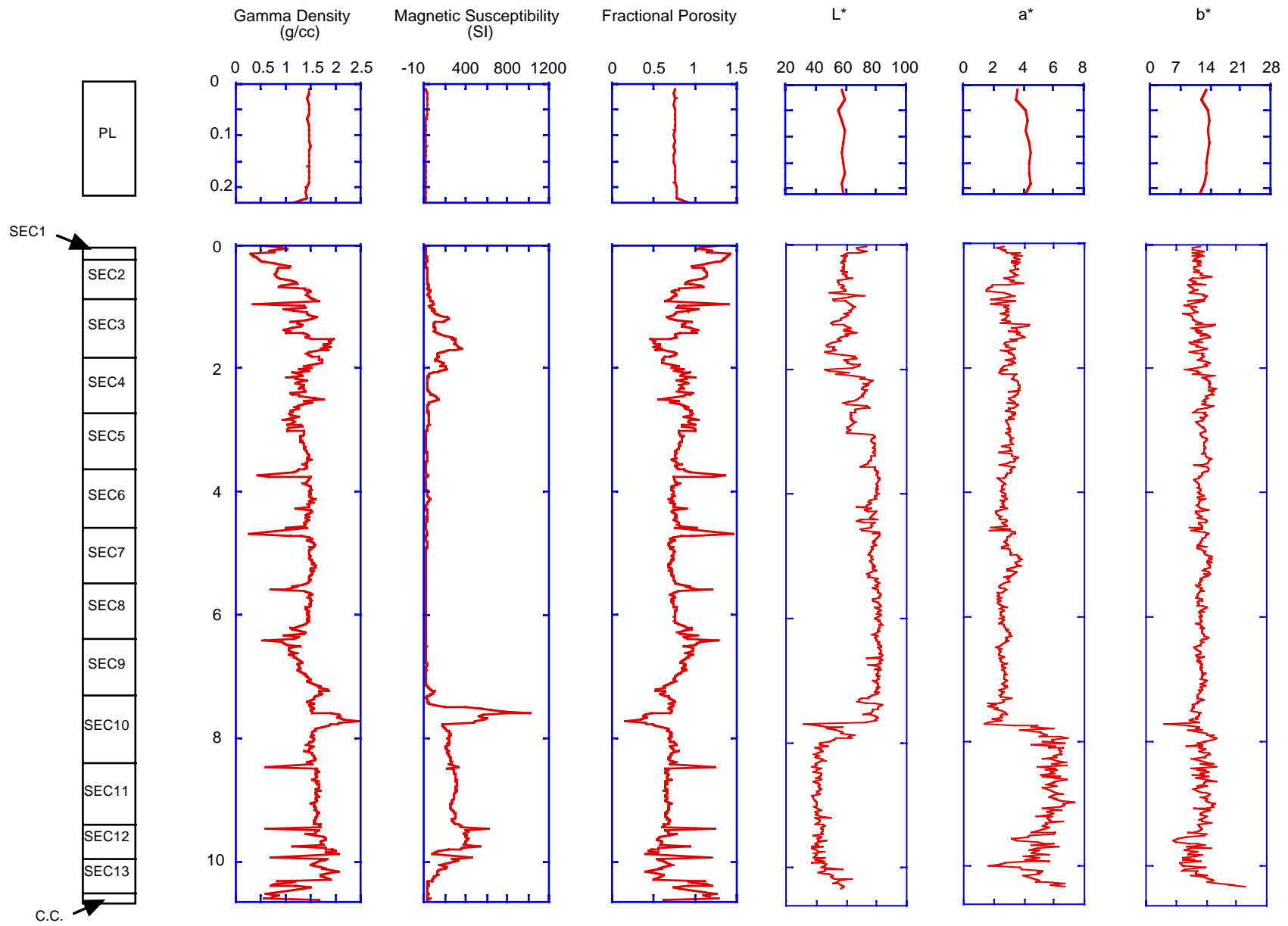


Fig. 3.8-3. MSCL and Color reflectance results of MR01-K03 PC01&PL01(HAND2).

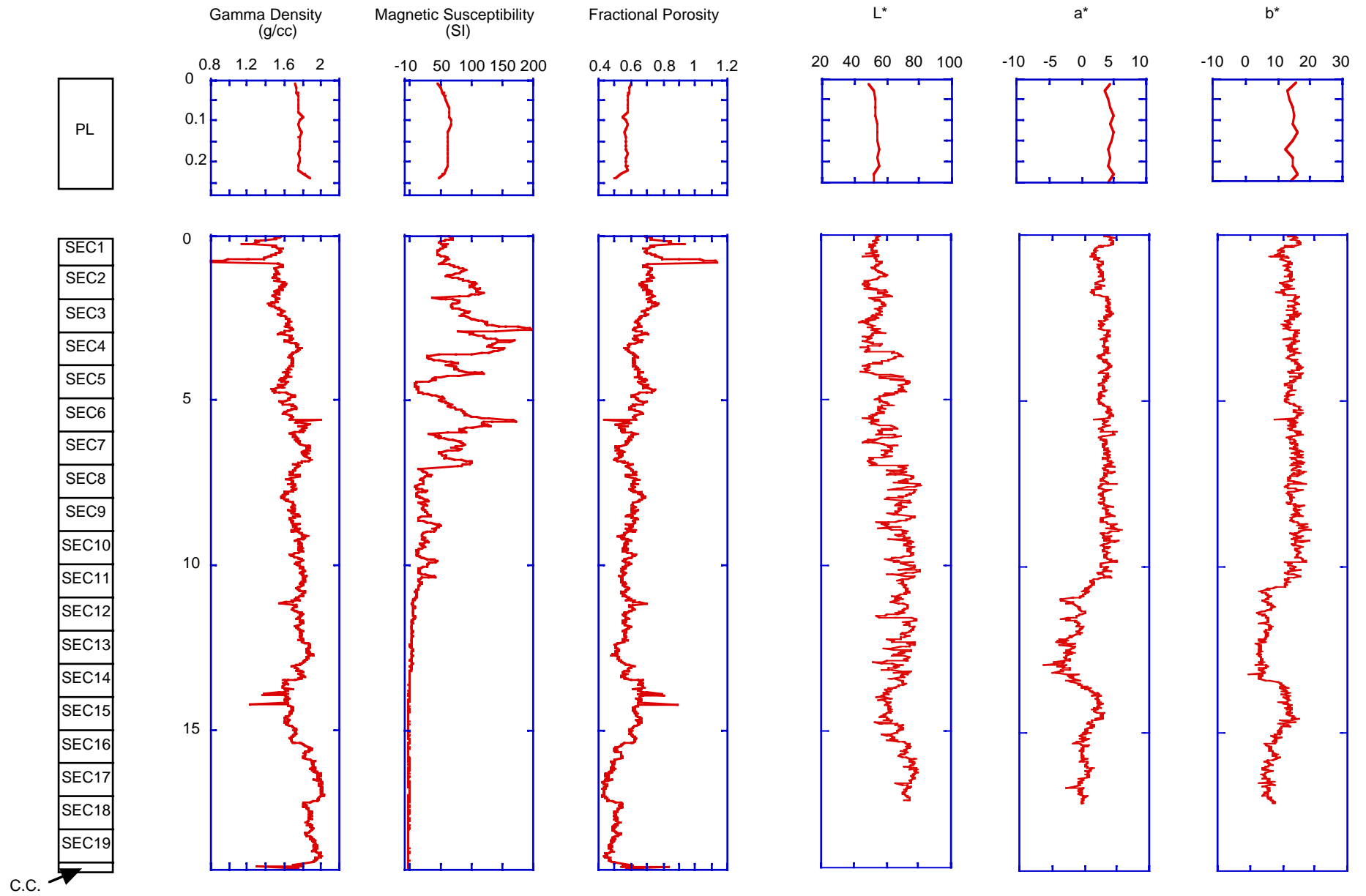


Fig.3.8-4. MSCL and Color reflectance results of MR01-K03 PC02&PL02(HAND3).

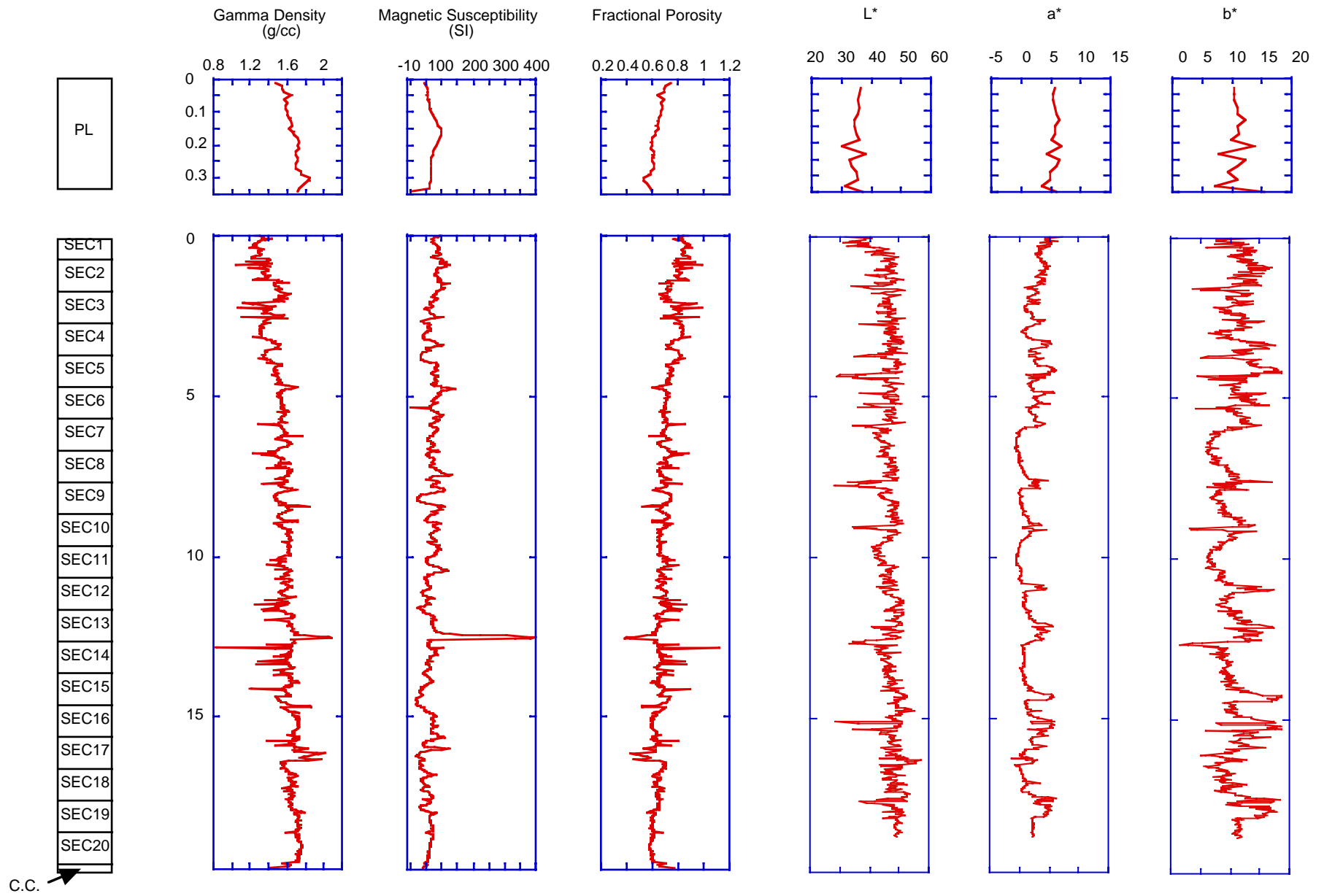


Fig. 3.8-5. MSC/L and Color reflectance results of MR01-K03 PC03&PL03(HAND2).

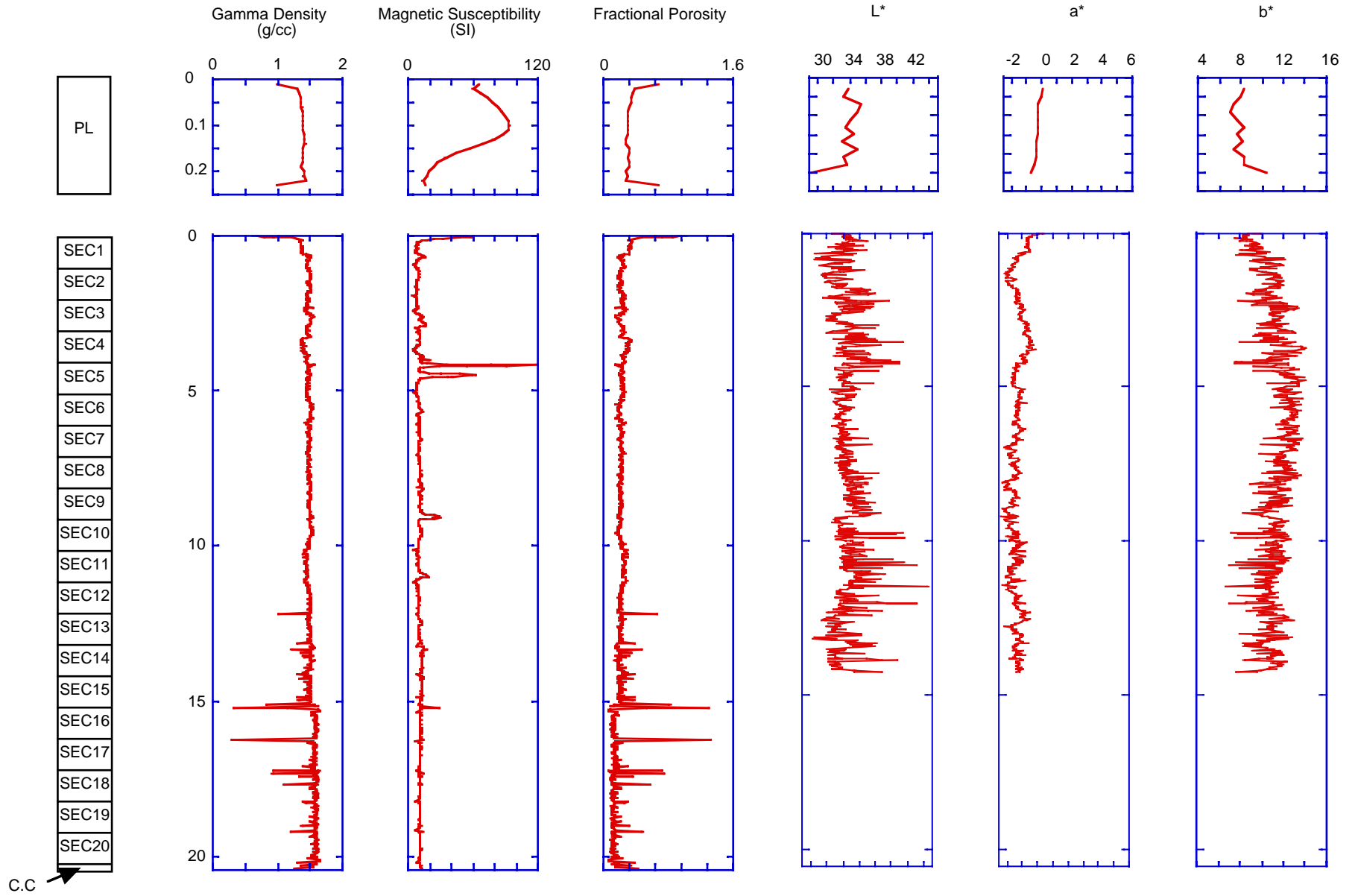


Fig. 3.8-6. MSCL and Color reflectance results of MR01-K03 PC04&PL04(HAND1).

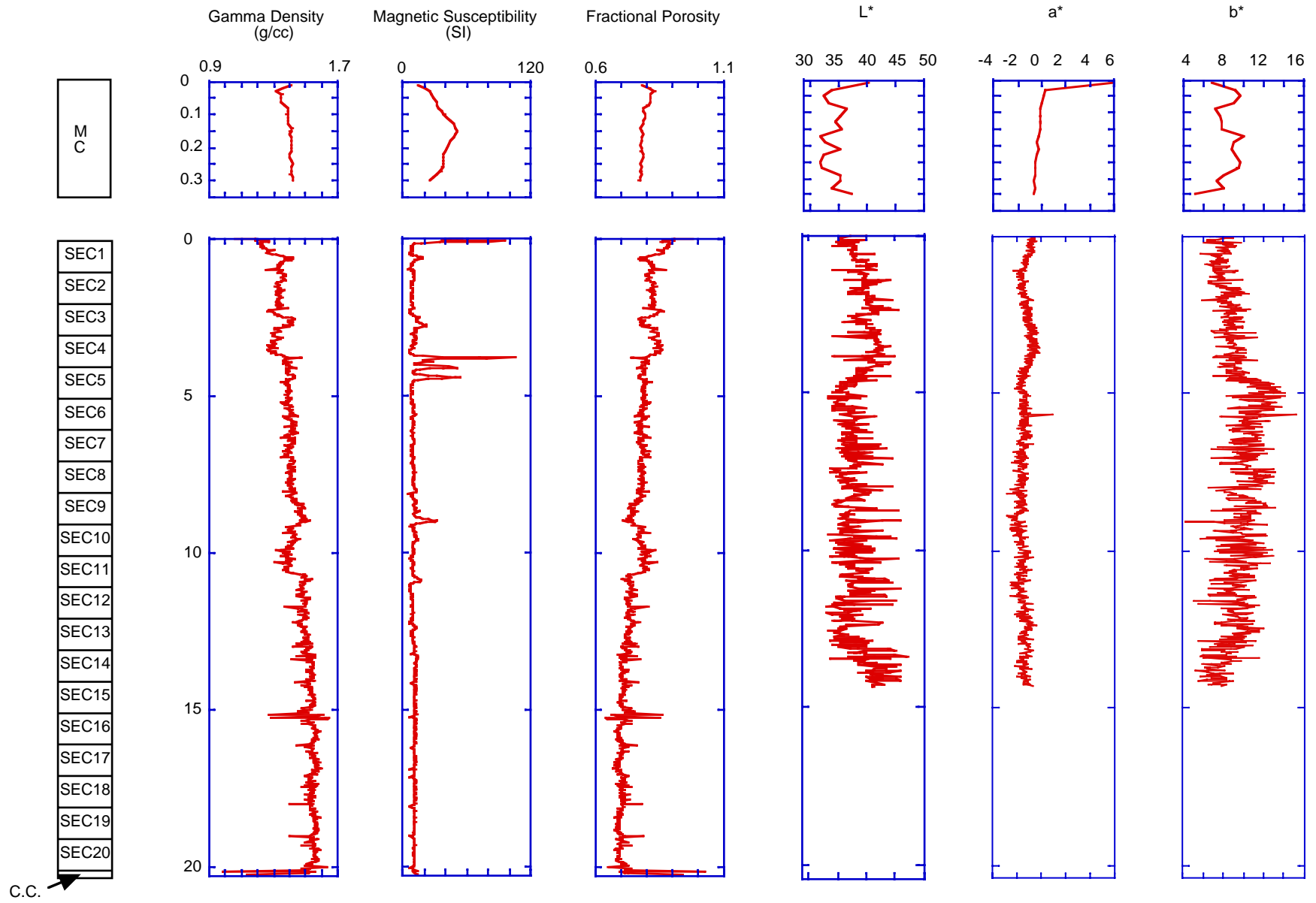


Fig. 3.8-7. MSCL and Color reflectance results of MR01-K03 PC05&MC04(HAND2).

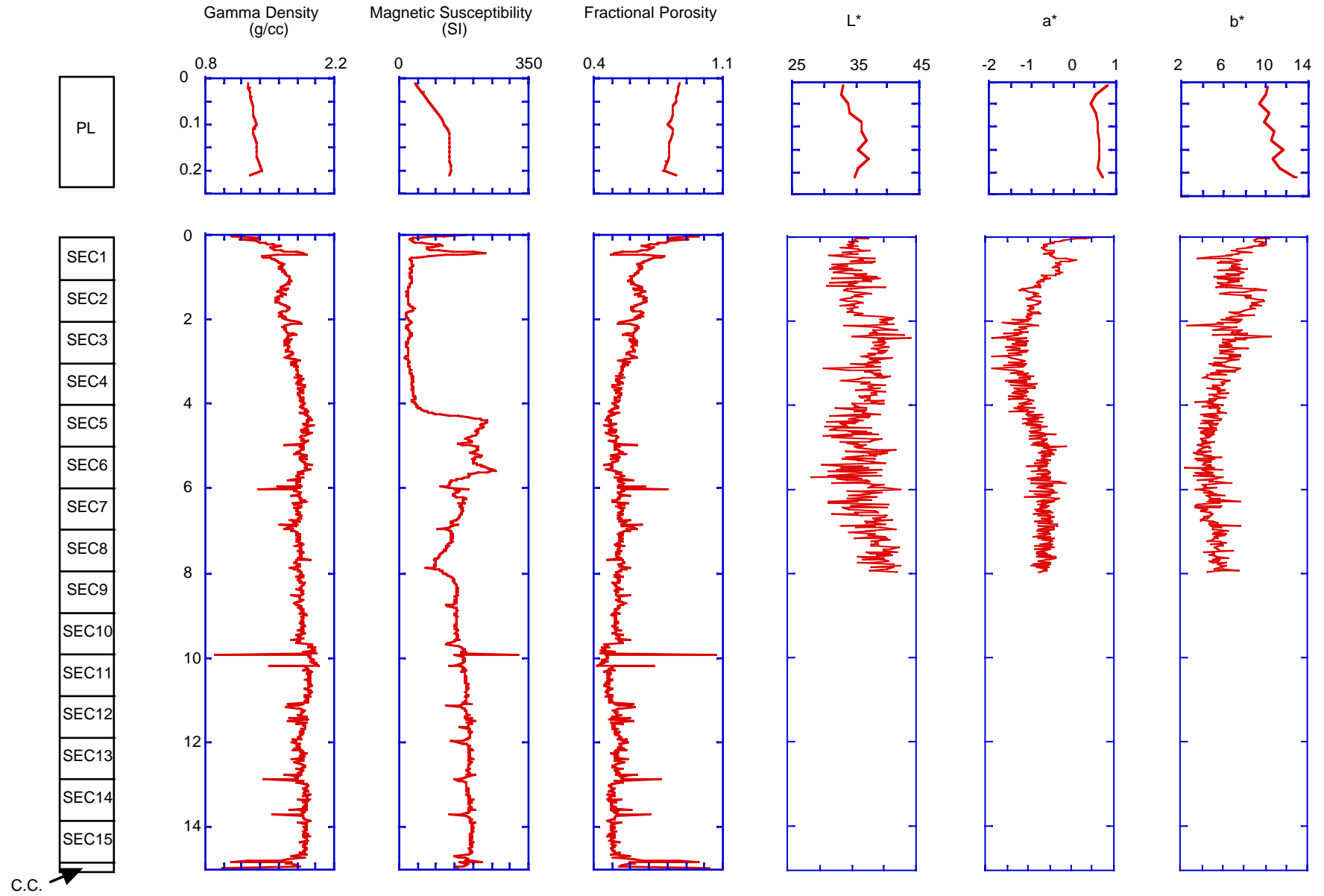


Fig. 3.8-8. MSCL and Color reflectance results of MR01-K03 PC06&PL06(HAND2).

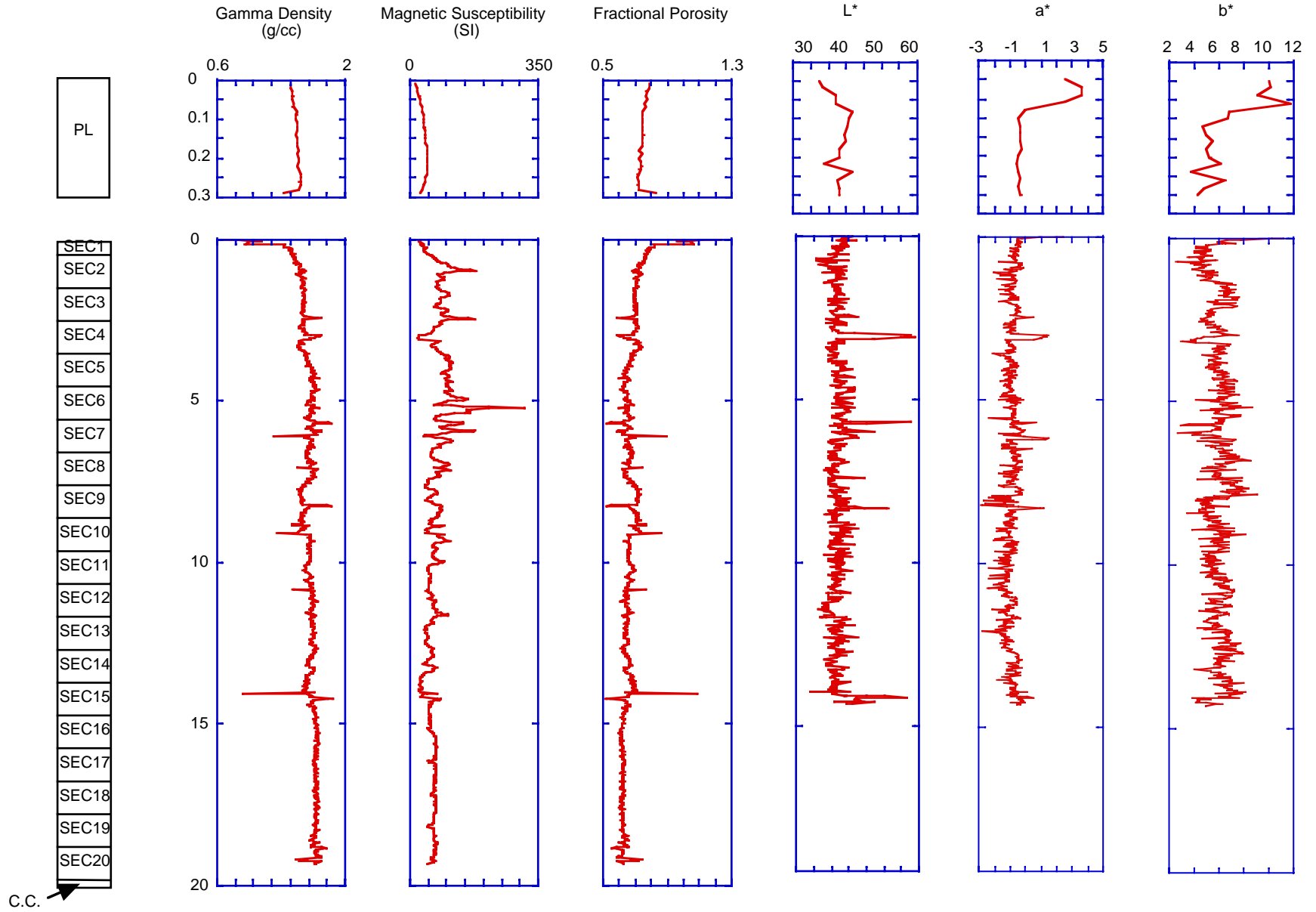


Fig. 3.8-9. MSCL and Color reflectance results of MR01-K03 PC07&PL07(HAND3).

Visual Core Description Summary: MR01-K03 PC-01

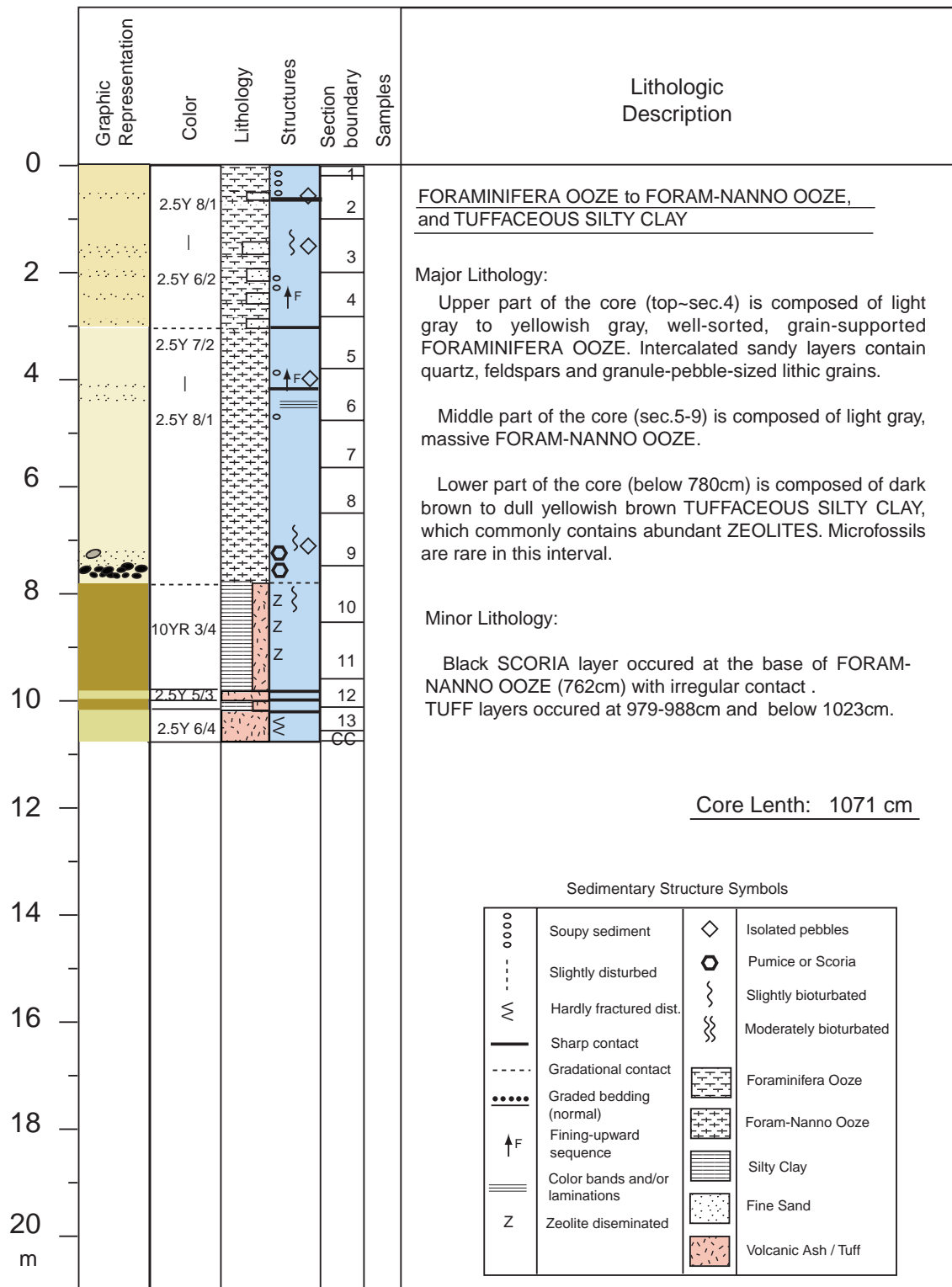


Fig. 3.8.10. Core Description Summary of PC01.

Visual Core Description Summary: MR01-K03 PC-02

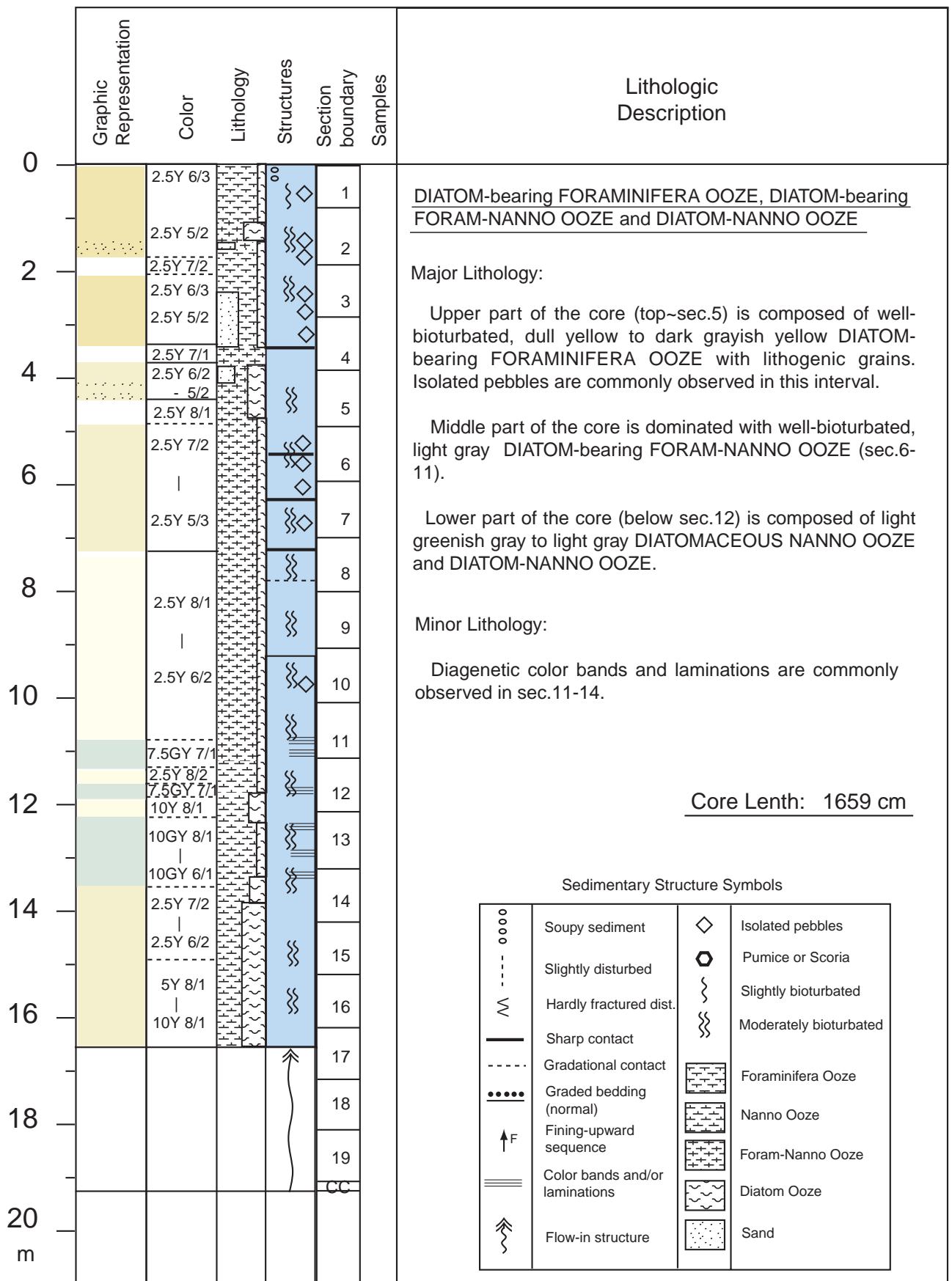


Fig. 3.8-11. Core Description Summary of PC02.

Visual Core Description Summary: MR01-K03 PC-03

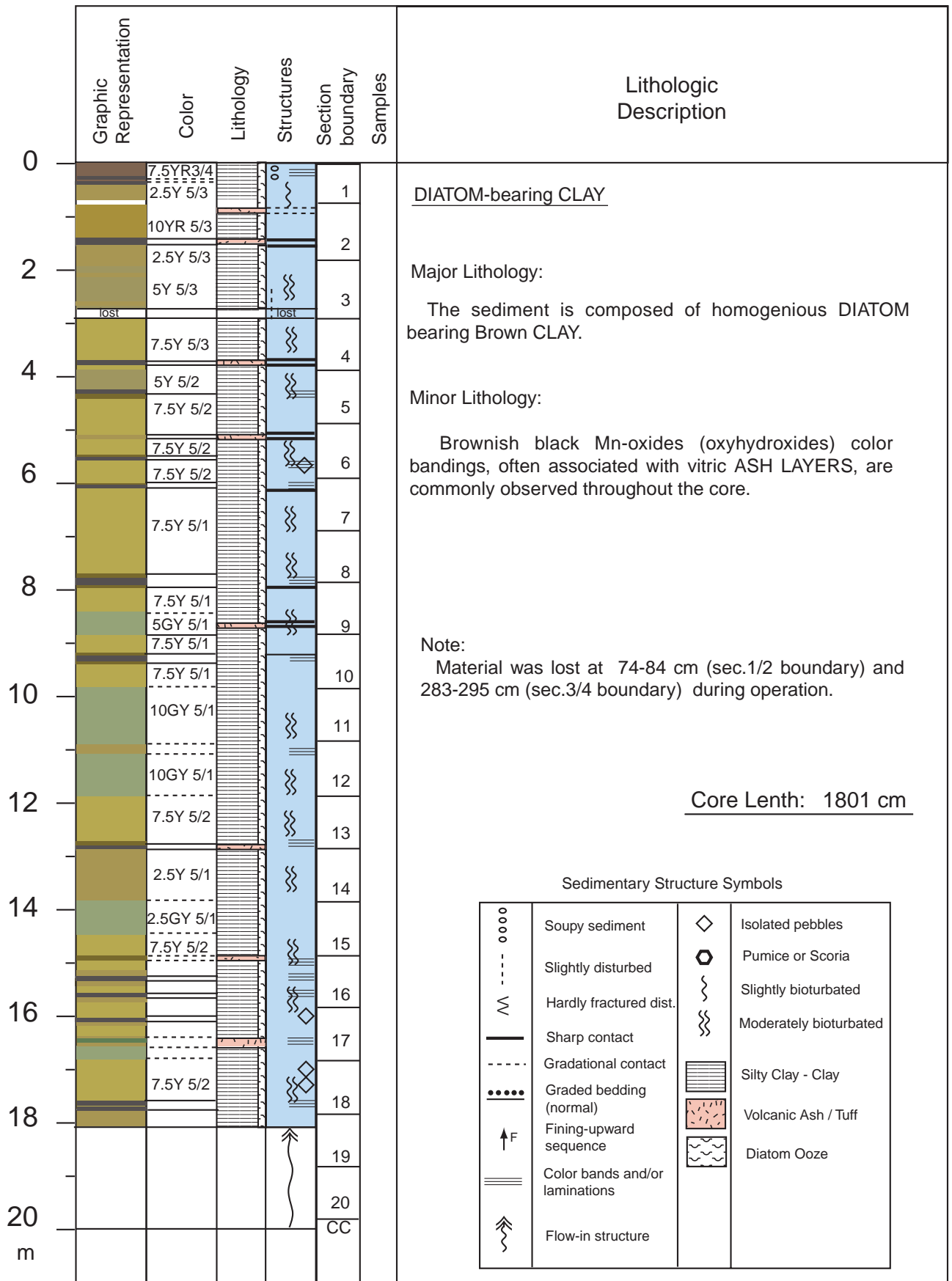


Fig. 3.8-12. Core Description Summary of PC03.

Visual Core Description Summary: MR01-K03 PC-04

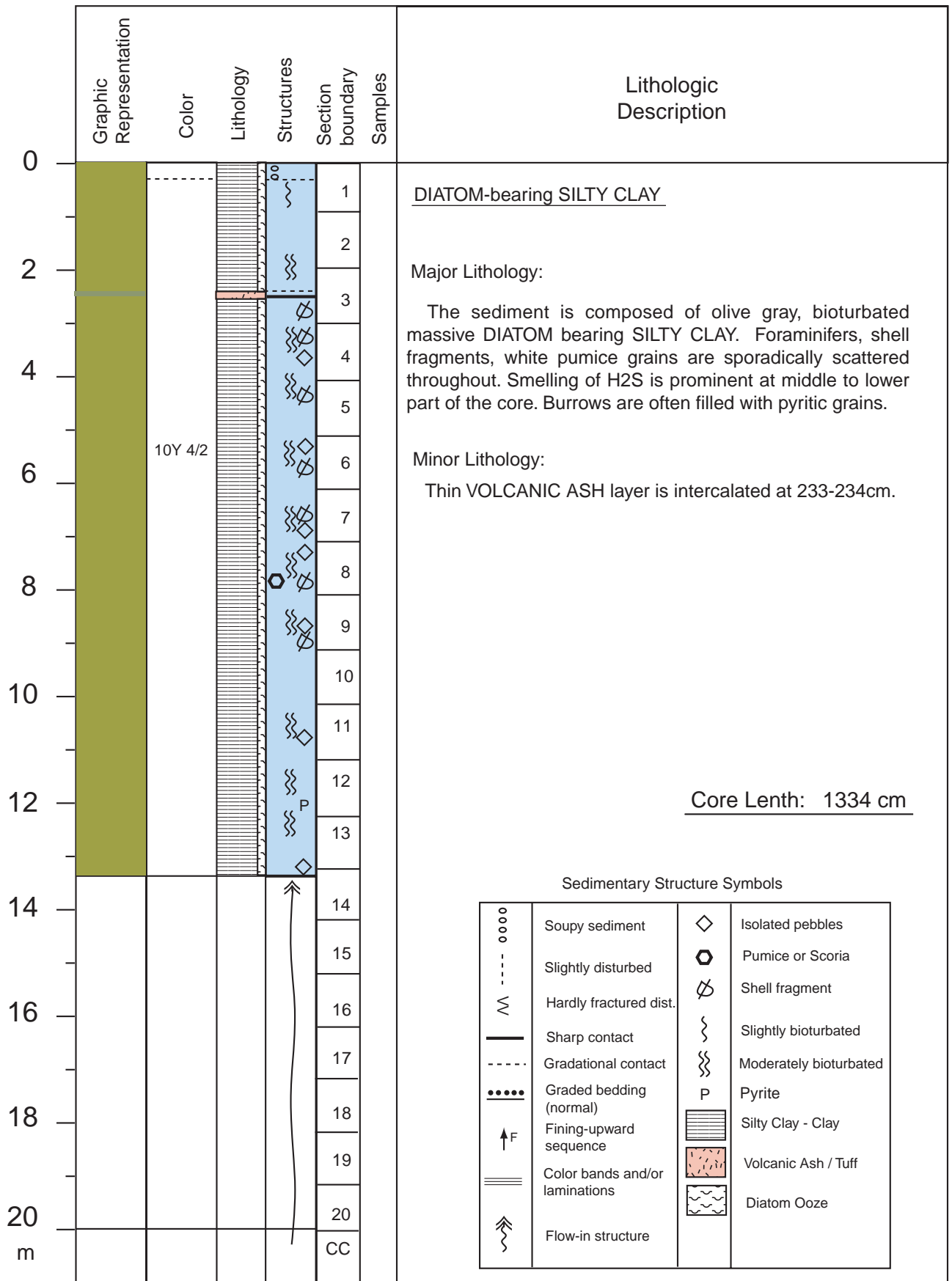


Fig. 3.8-13. Core Description Summary of PC04.

Visual Core Description Summary: MR01-K03 PC-05

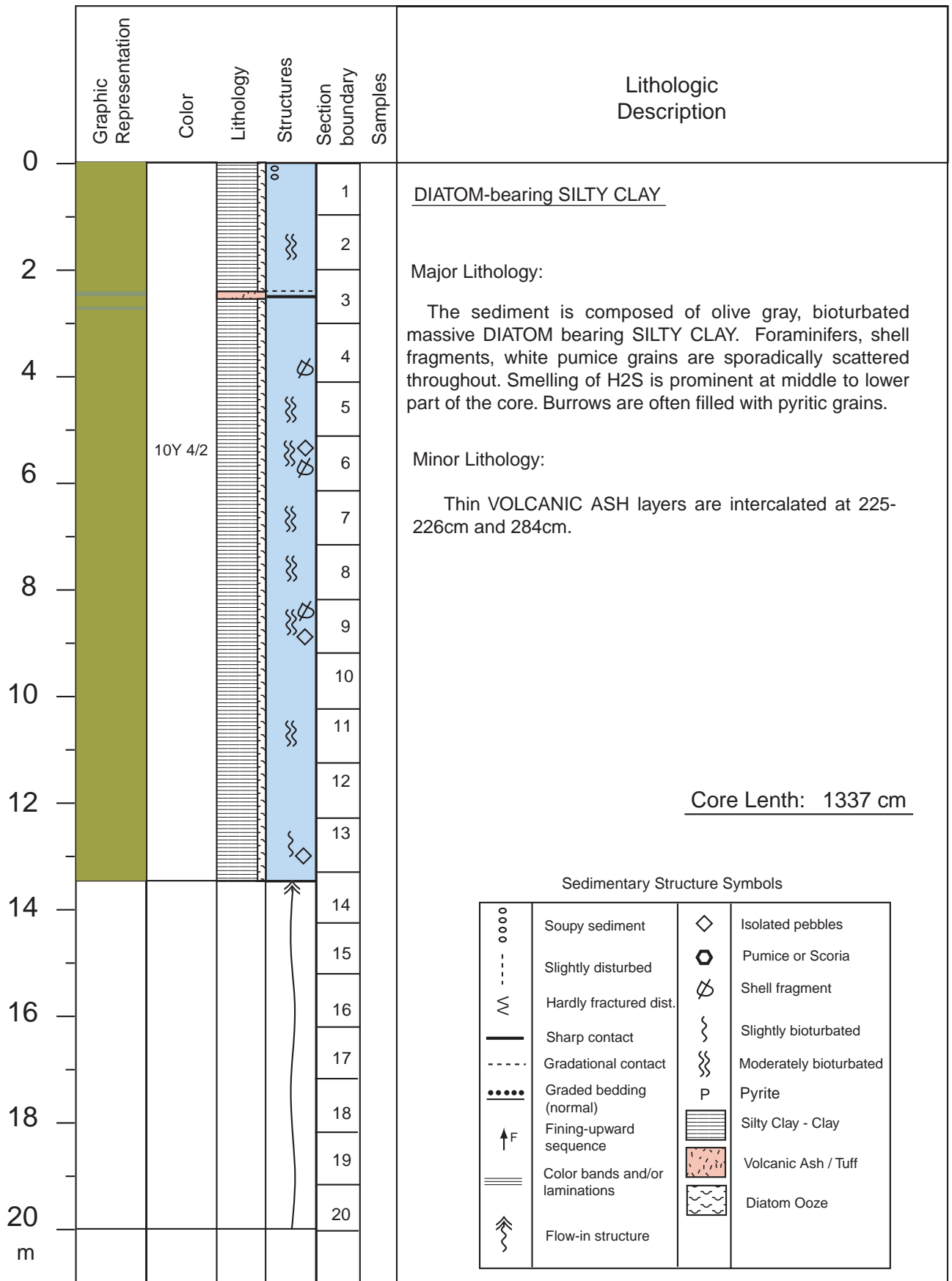


Fig. 3.8-14. Core Description Summary of PC05.

Visual Core Description Summary: MR01-K03 PC-06

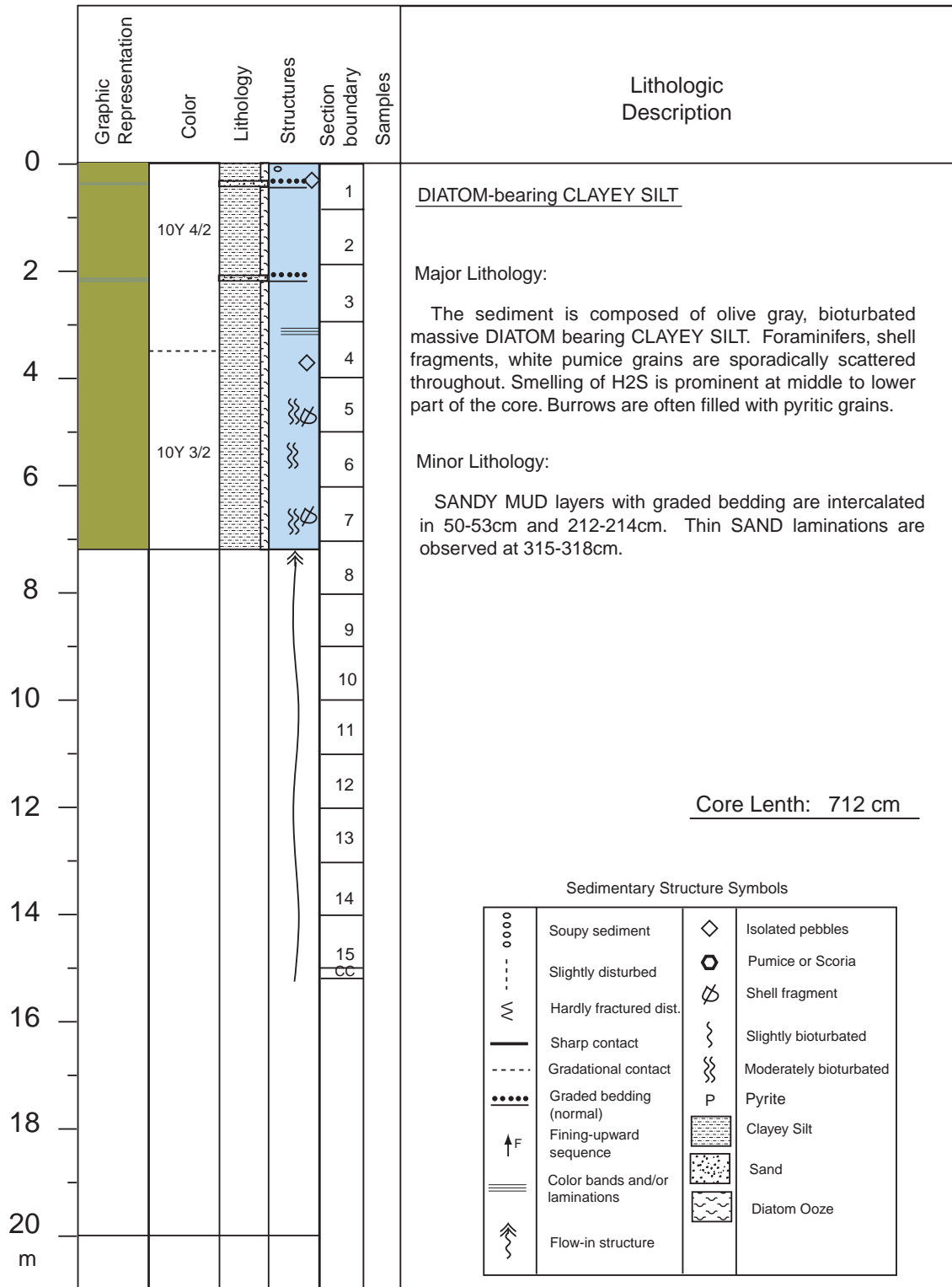


Fig. 3.8.15. Core Description Summary of PC06.

Visual Core Description Summary: MR01-K03 PC-07

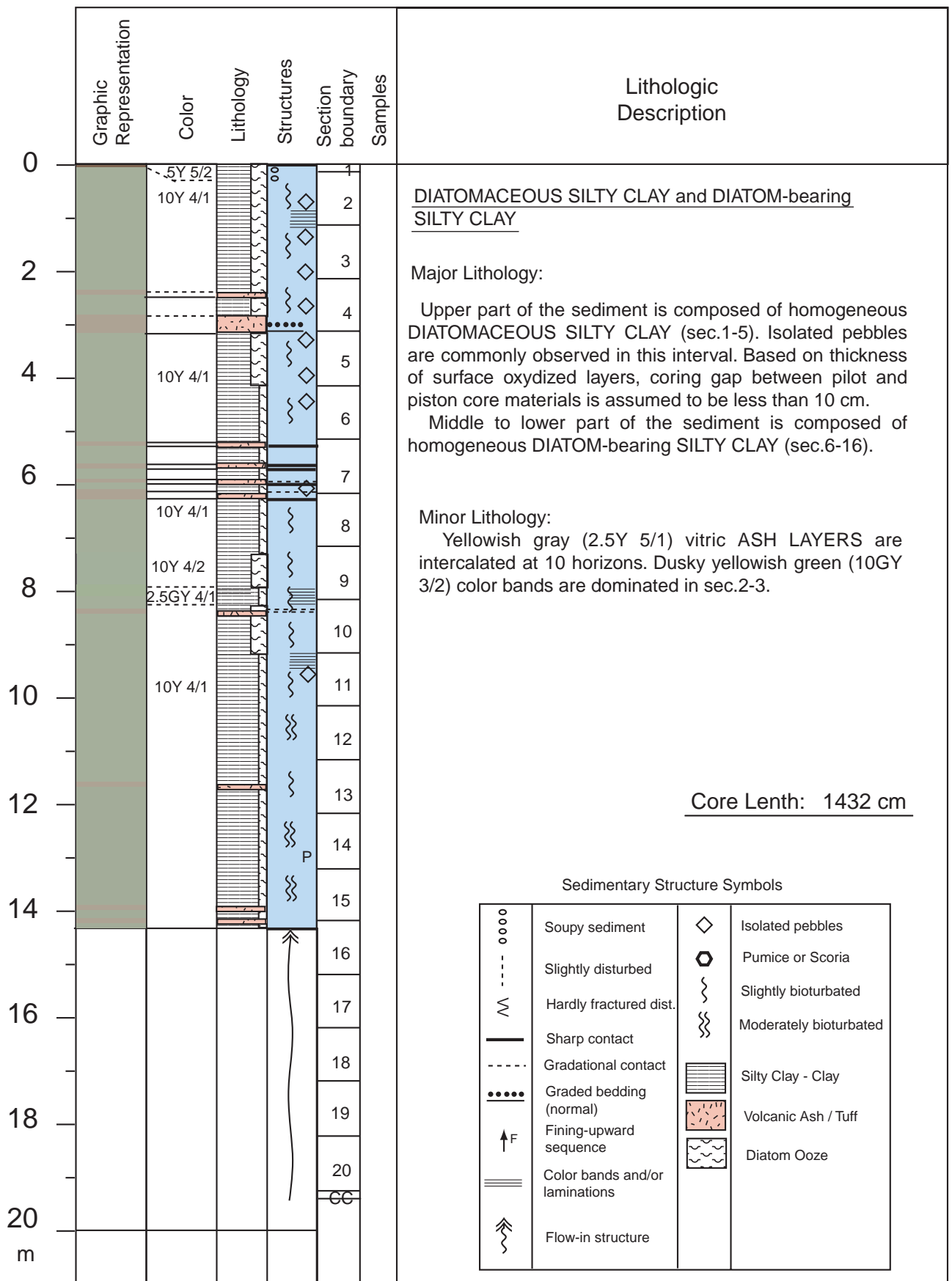


Fig. 3.8-16. Core Description Summary of PC07.

3.9 Atmospheric Observation

3.9.1 Aerosol

Jiahong WU (Toyama University)

Co-workers not on board:

Jing ZHANG (Toyama University)

Mariko HATTA (Toyama University)

(1) Objective

It is well known that the exchange of material and energy between the atmosphere and ocean has especially significance. Global geographical and seasonal distributions of troposphere aerosol have attracted considerable attention during the past several decades. The natural aerosol has been substantially perturbed by anthropogenic activities, e.g. increases of sulfates, nitrates, organic condensates, soot, and soil dust. Since the long-range transport of anthropogenic aerosols from East Asia have important influence to the bio-geochemical environments of high latitude northern Pacific Ocean, it is of great moment to elucidate the chemical properties of aerosols and their transportation over the Ocean. In order to prove the origin and elucidate the transport mechanism of the aerosol from Asian continent, the aerosol sampling and measurements were carried out in this study. In addition, surface seawater and particulate matter were also collected for analysis.

(2) Instruments and Analytical Methods:

-Aerosol Collection:

The instruments used in this work are shown in Table 3.9.1-1. The aerosol samples were collected on the compass deck, during this cruise (MR01-K03, from 6/4/2001 to 7/19/2001). Aerosols were collected on quartz fiber filters while the vessel is sailing, the pumping time for each collector is about 30 hours and the flow rate is about 1097 ± 13 L/min (19 L/min).

-Aerosol Analysis:

On board: samples were dealt with as Figure 3.9.1-1 and nutrients (nitrite, nitrate, phosphate, silicate) were analyzed.

Not on board: heavy metals and so on

-Surface seawater and its particles:

The seawater samples (2L) were collected at stations, KNOT1, 3, 5, 8, 11, 13, KNOT2, 17, 20, 23, 26, 27, 28, according to the sampling plan. Suspended particles were collected by filtering 20L seawater with smaller pore size (0.1 μ m) membrane filters.

(3) Preliminary results

As an example, temporal variation of the nutrients is shown in Figure 3.9.1-2.

According to latitude and the size of aerosol, the variation of each nutrient can be seen. It is one of the dates that can be used for further discussions.

(4) Future plan

Heavy melts and so on

(5) Tables and Figures

Type		AH-600	
Characteristics	Diameter range	1.1 - 7.0 μ m	
	particle size classification.	5 stages.	
composition	Pump	Flow Rate	556l/min(450-750l/min)
		Flow range	max.1600l/min
		Motor	AC100V、 1KW
Dimension		600 (W) *460(D)*1,258(H)mm	
Weight		~ 3 9 k g	

Talbe3.9.1-1 Instrument of Air-sample

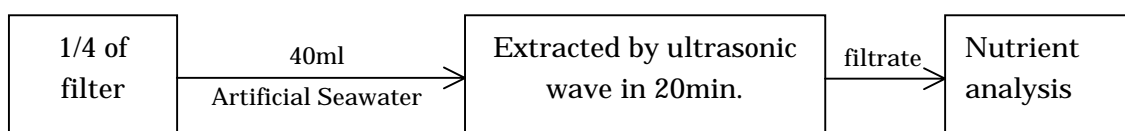
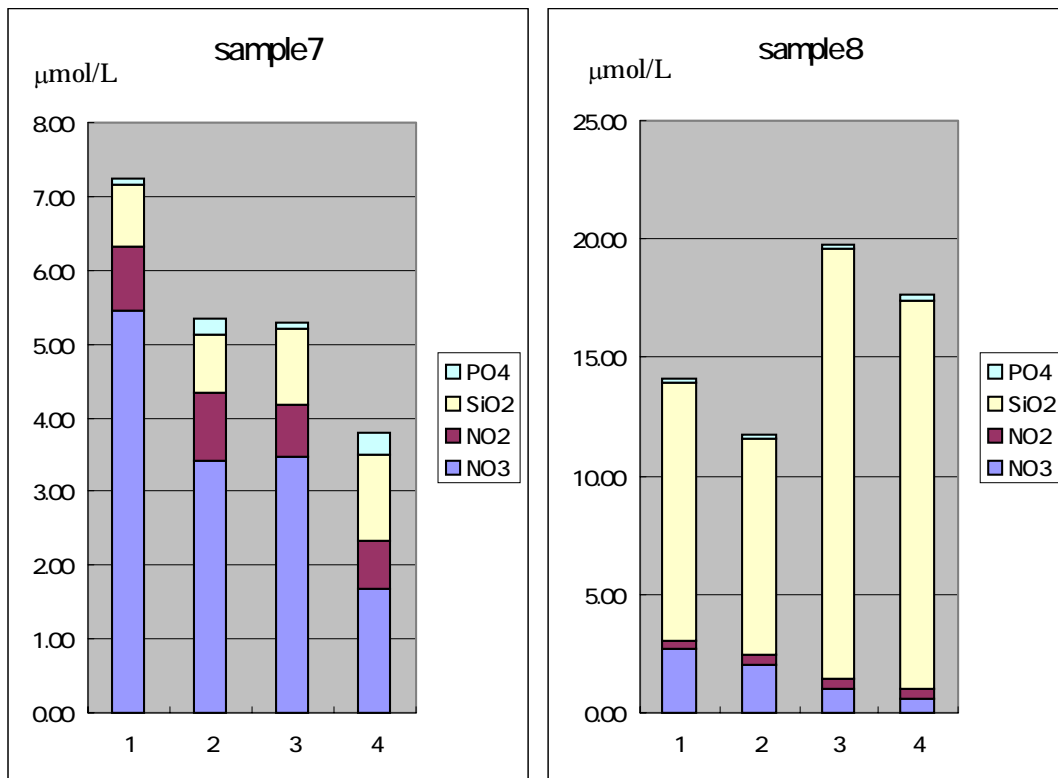


Figure 3.9.1-1 The experiment processes of nutrients

sample7 6/24/2001-6/27/2001
45E 155N 40E 155N

sample8 6/29/2001-7/2/2001
40E 155N 27E155N



it is just relative relations.
the concentration of silicate is divided 10.
the concentration of nitrate is also divided 10.

Figure 3.9.1-2 Temporal results of nutrients of aerosol

(6) Data Archive

All of the raw and processed data will be submitted to the JAMSTEC Data Management Office (DMO) as soon as our analysis is completed and will remain under its control.

3.9.2 Radiometer / particle counter

Tatsuo Endoh (Institute of Low Temperature Science, Hokkaido University) Associate Professor

Naoshi Narita (Graduate school of earth environmental science, Hokkaido University) Research Associate

Syuichi Watanabe (JAMSTEC) Chief Research Scientist

Tamio Takamura (Center of environmental remote sensing science, Chiba University) Professor

Sachio Ohta (Engineering environmental resource laboratory, Graduate school of engineering, Hokkaido University) Professor

Teruyuki Nakajima (Center of climate system research, University of Tokyo) Professor

(1) Objects/Introduction

One of the most important objects is the collection of calibration and validation data from the surface (Nakajima et al.1996, 1997 and 1999). It may be considered for the observation over the widely opening of the huge ocean to be desired ideally because of horizontal homogeneity. Furthermore, the back ground values of aerosol concentration are easily obtained over there (Ohta et al.1996, Miura et al. 1997 and Takahashi et al. 1996) and vertical profile of aerosol concentration are obtained by means of extrapolation up to the scale height. It is desired to compare the integrated value of these profiles of aerosol concentration with optical thickness observed by the optical and radiative measurement (Hayasaka et al. 1998, Takamura et al.1994). Facing this object, the optical and radiative observations were carried out by mean of the Sky Radiometer providing more precise radiation data as the radiative forcing for global warming.

(2) Measuring parameters

Atmospheric optical thickness, Ångström coefficient of wave length efficiencies, Direct irradiating intensity of solar, and forward up to back scattering intensity with scattering angles of 2-140degree and seven different wave lengths
GPS provides the position with longitude and latitude and heading direction of the vessel, and azimuth and elevation angle of sun. Horizon sensor provides rolling and pitching angles.

Concentration and size distribution of atmospheric aerosol.

(3) Methods

The instruments used in this work are shown as following in Table3.9.2-1.

Sky Radiometer was measuring irradiating intensities of solar radiation through seven different filters with the scanning angle of 2-140 degree. These data will provide finally optical thickness, Ångström exponent, single scattering albado and size distribution of atmospheric aerosols with a kind of retrieval method.

Optical Particle Counter was measuring the size of large aerosol particle and counting the number concentration with laser light scattering method and providing the size distribution in 0.3,0.5,1.0,2.0 and 5.0 micron of diameter with real time series display graphically.

(4) Results

Information of data and sample obtained are summarized in Table 3.9.2-2. The sky radiometer has been going well owing to more calm and silent condition and circumstances about shivering problems provided by the R/V Mirai whose engines are supported by well defined cushions. Therefore, measured values will be expected to be considerably stable and provide good calculated parameters in higher quality. However, some noise waves were found to interfere the 16, 13 and 12 channel marine bands of VHF from sky radiometer. Fortunately the origin and source were identified by using a VHF wide band receiver and the interference waves were kept by fairly separating from two VHF antennae and decreased to recovery of 100%.

Aerosols size distribution of number concentration have been measured by the Particle Counter and data obtained are displayed in real time by a kind of time series *in situ* with 5 stages of size range of 0.3, 0.5, 1.0, 2.0, and 5.0 micron in diameter.

(5) Data archive

This aerosol data by the Particle Counter will be able to be archived soon and anytime. However, the data of other kind of aerosol measurements are not archived so soon and developed, examined, arranged and finally provided as available data after a certain duration. All data will archived at ILTS (Endoh), Hokkaido University, CCSR (Nakajima), University of Tokyo and CEReS (Takamura), Chiba University after the quality check and submitted to JAMSTEC within 3-year.

References

- Takamura, T., et al., 1994: Tropospheric aerosol optical properties derived from lidar, sun photometer and optical particle counter measurements. *Applied Optics*, Vol. 33, No. 30, 7132-7140.
- Hayasaka, T., T. Takamura, et al., 1998: Stratification and size distribution of aerosols retrieved from simultaneous measurements with lidar, a sunphotometer, and an aureolemeter. *Applied Optics*, 37(1998), No 6, 961-970.
- Nakajima, T., T. Endoh and others (7 persons) 1999: Early phase analysis of OCTS radiance data for aerosol remote sensing., *IEEE Transactions on Geoscience and Remote Sensing*, Vol. 37, No. 2, 1575-1585.
- Nakajima, T., et al., 1997: The current status of the ADEOS-1/GLI mission. *Advanced and Next-generation Satellites*, eds. H. Fujisada, G. Calamai, M. N. Sweeting, SPIE 2957, 183-190.
- Nakajima, T., and A. Higurashi, 1996: AVHRR remote sensing of aerosol optical properties in the Persian Gulf region, the summer 1991. *J. Geophys. Res.*, 102, 16935-16946.
- Ohta, S., et al., 1997: Variation of atmospheric turbidity in the area around Japan. *Journal of Global Environment Engineering*, Vol.3, 9-21.
- Ohta, S., et al., 1996: Chemical and optical properties of lower tropospheric aerosols measured at Mt. Lemmon in Arizona, *Journal of Global Environment Engineering*, Vol.2, 67-78.
- Takahashi, T., T. Endoh, et al., 1996: Influence of the growth mechanism of snow

particles on their chemical composition. Atmospheric Environment, Vol.30, No. 10/11, 1683-1692.

Miura, K., S. Nakae, et al.,: Optical properties of aerosol particles over the Western Pacific Ocean, Proc. Int. Sym. Remote Sensing, 275-280, 1997.

Table3.9.2-1. Information of obtained data inventory (Method)

Item,	No.data	Name	Instrument	Site position
Optical thickness Ångström exponent.		Endoh	Sky Radiometer(Prede,POM-01MK2)	roof of stabilizer
Aerosol Size dis- tribution		Endoh	Particle Counter(Rion,KC-01C)	compass deck(inlet) & environmental research laboratory

Table3.9.2-2. Data and Sample inventory

Data/Sample	rate	site	object	name	state	remarks
Sun & Sky Light	1/5min (fine& daytime)	roof of stabilizer	optical thickness Ångström expt.	Endoh	land analysis	6/5'01- 7/19'01
Size distri- bution of aerosols	1/2.5min	compass deck	concentration of aerosols	Endoh	on board	6/5'01- 7/19'01

3.10 Surface water underway observations

3.10.1 pCO₂ (JAMSTEC)

Mikio Kitada (MWJ)

Minoru Kamata (MWJ)

(1) Objectives

The objective of this observation is continuous measurement of partial pressure of CO₂ in the atmosphere and surface seawater .

(2) Instrument and Methods

Concentrations of CO₂ in the atmosphere and the sea surface were measured continuously during the entire cruise by a automated system with a non-dispersive infrared (IR) analyzer (BINOS). During 1.5 hour cycle, the system analyzed four standards, an ambient air sample, and a headspace sample in an equilibrator sequentially.

The ambient air sample that was taken from the bow is introduced into the IR through a mass flow controller which controls the air flow rate at about 0.5 L/min, a cooling unit, a parma pure dryer, and a desiccant holder (Mg(ClO₄)₂).

The equilibrator has shower head through which surface water is forced at a rate of 5-8 L/min. Air in the head space is circulated with an air pump at 0.5-0.8 L/min. in a closed loop through two cooling units, a perma pure dryer, and the desiccant holder. For calibration, compressed gas standards with nominal mixing ratios of 270, 329, 360 and 410 ppmv (parts per millions by volume) were used.

(3) Data archive

All data will be submitted to JAMSTEC Data Management Office (DMO).

3.10.2 pCO₂ (CREST)

Principal Investigator

Fujio Shimano (Japan Science and Technology)

(1) Objective

Continuous measurement of the partial pressure of CO₂ (pCO₂) in surface seawater.

(2) Method

Surface seawater is pumped up to a Tandem-style equilibrator (Kimoto Electric Co., Ltd.) and the gases were equilibrated with a headspace of the equilibrator. After equilibration the headspace gas was dried and analyzed using a standardized non-dispersive infrared (NDIR) gas analyzer (LI-6252 LI-COR, inc.) .

(3) Precision

The pCO₂ in surface seawater was measured using the NDIR gas analyzer with an estimated precision of approximately 0.05 ppm.

(4) Sampling stations

Measuring data included all stations of MR01-K03.

(5) Comments

The CO₂ system in seawater is described by four carbon system parameters: TA, TCO₂, pH, and either fCO₂ or pCO₂. pCO₂ has the largest dynamic range of the four parameters and is an excellent parameter to use in calculations.

This report contained tables of the following data:

Time(GMT)

Latitude, Longitude, Ship speed, Ship heading

Pressure

SST and seawater temperature of equilibrator headspace

Salinity

DO

pCO₂ and fCO₂

3.10.3 Salinity, temperature, dissolved oxygen, and fluorescence

Takayoshi SEIKE (Marine Works Japan LTD.)

Tomoko MIYASHITA (Marine Works Japan LTD.)

(1) Objective

Measurements of salinity, temperature, dissolved oxygen, fluorescence, and particle size of plankton in near-sea surface water.

(2) Methods

The *Continuous Sea Surface Water Monitoring System* (Nippon Kaiyo co.,Ltd.) has sensors for automatic and continuous measurements of salinity, temperature, dissolved oxygen, fluorescence and particle size of plankton in near-sea surface water every 1-minute. This system is located in the “*sea surface monitoring laboratory*” on R/V Mirai. This system is connected to shipboard LAN-system. Measured data is stored in a PC hard disk every 1-minute together with date and position of the ship, and displayed on a monitor of the PC.

Near-surface water was continuously pumped up to the laboratory and flowed into the *Continuous Sea Surface Water Monitoring System* through a vinyl-chloride pipe. The seawater flow rate is controlled by several valves to be 12 L/min except with the fluorometer (about 0.3 L/min). The flow rate is measured by two flow meters and each values were checked everyday.

Specification of the each sensor of this system is listed below.

a) Temperature and Salinity sensor

SEACAT THERMOSALINOGRAPH

Model: SBE-21, SEA-BIRD ELECTRONICS, INC.

Serial number: 2118859-2641

Measurement range: Temperature -5 to +35 °C, Salinity 0 to 6.5 S m⁻¹

Accuracy: Temperature 0.01 °C, Salinity 0.001 S m⁻¹

Resolution: Temperatures 0.001 °C, Salinity 0.0001 S m⁻¹

b) Bottom of ship thermometer

Model: SBE 3S, SEA-BIRD ELECTRONICS, INC.

Serial number: 032607

Measurement range: -5 to +35 °C

Resolution: ± 0.001

Stability: 0.002 year^{-1}

c) Dissolved oxygen sensor

Model: 2127, Oubisufair Laboratories Japan INC.

Serial number: 44733

Measurement range: 0 to 14 ppm

Accuracy: $\pm 1\%$ at 5 of correction range

Stability: $1\% \text{ month}^{-1}$

d) Fluorometer

Model: 10-AU-005, TURNER DESIGNS

Serial number: 5562 FRXX

Detection limit: 5 ppt or less for chlorophyll a

Stability: $0.5\% \text{ month}^{-1}$ of full scale

e) Particle Size sensor

Model: P-05, Nippon Kaiyo LTD.

Serial number: P5024

Measurement range: 0.02681 mmt to 6.666 mm

Accuracy: $\pm 10\%$ of range

Reproducibility: $\pm 5\%$

Stability: $5\% \text{ week}^{-1}$

f) Flow meter

Model: EMARG2W, Aichi Watch Electronics LTD.

Serial number: 8672

Measurement range: 0 to 30 l min⁻¹

Accuracy: $\pm 1\%$

Stability: $\pm 1\% \text{ day}^{-1}$

The monitoring Periods (UTC) during this cruise are listed below.

5-Jun.-'01 8:28 to 16-Jul.-'01 23:48

(3) Date archive

The data were stored on a magnetic optical disk, which will be kept in Ocean Research Department, JAMSTEC.

3.10.4 Nutrients

Junko Hamanaka (MWJ)

Kenichiro Sato (MWJ)

Kaori Akizawa (MWJ)

(1) Objectives

Phytoplankton requires nutrient elements for growth, chiefly nitrogen, phosphorus, and silicon. The data of nutrients in surface seawater is important for investigation of phytoplankton productivity.

(2) Parameters

- Nitrate+ Nitrite
- Nitrite
- Silicate
- Phosphate

(3) Methods

The nutrients monitoring system was performed on BRAN+LUEBBE continuous monitoring system Model TRAACS 800 (4 channels) from June 5 to July 17, 2001. This system was located at the surface seawater laboratory in R/V Mirai. Seawater at the depth of about 4 m was continuously pumped up to the laboratory and introduced direct to monitoring system with a narrow tube. The methods are as follows.

Nitrate + Nitrite: Nitrate in the seawater was reduced to nitrite by a reduction tube (Cd-Cu tube), and the reduced nitrate was measured as nitrite by the nitrite method as shown below. The flow cell was 3 cm length type.

Nitrite: Nitrite was determined by diazotizing with sulfanilamide by coupling with N-1-naphthyl-ethylendiamine (NED) to form a colored azo compound, and by being measured the absorbance of 550 nm using 3 cm length flow cell in the system.

Phosphate: Phosphate was determined by complexing with molybdate, by reducing with ascorbic acid to form a colored complex, and by being measured the absorbance of 800 nm using 5 cm length flow cell in the system.

Silicate: Silicate was determined by complexing with molybdate, by reducing with ascorbic acid to form a colored complex, and by being measured the absorbance of 800 nm using 3 cm length flow cell in the system.

3.10.5 Total dissolved inorganic carbon

Mikio Kitada (MWJ)

Minoru Kamata (MWJ)

(1) Objective

Continuous measurement of total dissolved inorganic carbon (TDIC) in the surface seawater.

(2) Instruments and Methods

Concentration of TDIC in surface seawater collected by a pump from a depth of 4.5m was continuously measured every 55 minutes by a coulometer (Carbon Dioxide Coulometer Model 5012, UIC Inc.). Seawater was introduced into a receptacle (nominal 30cm³) and 2 cm³ of 10 percents (v/v) phosphoric acid was added to evolve CO₂ gas. The evolved CO₂ gas was purged by CO₂ free nitrogen gas (purity 99.9999%) for 13 minutes at a flow rate of 130 cm³/min. and was absorbed into an electrolyte solution. Acids formed by reacted with the absorbed CO₂ in the solution were titrated with hydrogen ions. The titration was monitored by the coulometer. Calibration of the coulometer was carried out using sodium carbonate solutions (0-2.5mM). The coefficient of variation of 3 replicate determinations was approximately less than 0.1 percents for 1 sigma. TDIC were determined from titration values. All the values reported are set to the Dickson's CRM (Batch #53).

(3) Data archive

All data will be submitted to JAMSTEC Data Management Office (DMO).

3.11 Eddy observations

Vyacheslav LOBANOV, Igor ZHABIN
 (V.I.Il'ichev Pacific Oceanological Institute, Far Eastern Branch,
 Russian Academy of Sciences)
 Satoshi OKUMURA, Wataru TOKUNAGA
 (GODI)

(1) Introduction

The XBT and XCTD observations were implemented to find out location and to obtain detailed thermohaline structure of mesoscale eddies, and to support AGRO drifters deployment program.

(2) Equipment and calibration

To implement the observations we used the T.S.K.(Tsurumi-Seiki)/Sippican T-7 and T-5 Expandable Bathythermographs (XBT) and T.S.K. Expendable Conductivity, Temperature & Depth Profiler XCTD-1 with data registration by T.S.K. MK-30N and MK-100 digital converters. Characteristics of expandable probes are listed in Table 3.11-1.

Table 3.11-1 Characteristics of expandable probes

Probe type	Depth, m	Ship speed, knots	Temperature accuracy (C)	Conductivity accuracy (mS/cm)	Coefficients for depth calculation	
					a	b
XCTD	1100	12	0.02	0.03	3.425432	-4.7026039
T-07	760	15	0.2	-	6.691	-2.25
T-05	1830	6	0.2	-	6.828	-1.82

The following formula was used for depth calculation:

$$z = a*t + (10^{-3})*b*t^2$$

where z – depth (m)
 t – elapsed time (seconds)
 a, b – coefficients

For the XCTD observations the coefficients of depth, temperature and conductivity calculation were installed in the probe.

(3) The data

In total 72 XCTD and 40 XBT probes were used at 111 stations. Observations at station XC-9 were repeated. At 4 stations XB-35, 36, 37 and 38 T-5 probes were launched, the rest of the XBT were of T-7 type. The list of the stations is shown in Table 3.11-2 and 3.11-3. Location of the stations is demonstrated at figures of the eddy study preliminary results (next paragraph). Vertical profiles of temperature and salinity for every station are attached below.

Table 3.11-2 XBT stations locations

Station	Date	Time	Lat.	N	Lon.	E
xb-01	626	1:53	41	20.1	153	24.9
xb-02	626	2:37	41	20	153	9.72
xb-03	626	3:06	41	20	152	59.89
xb-04	626	5:59	41	20.2	152	29.76
xb-05	626	6:44	41	20	152	14.71
xb-06	627	13:35	41	30	153	0.04
xb-07	627	14:34	41	15	152	59.96
xb-08	627	15:15	41	4.92	152	59.92
xb-09	627	16:08	41	4.97	152	45.03
xb-10	628	8:05	40	29.7	153	0.1
xb-11	712	7:48	39	57.1	145	23.79
xb-12	712	8:30	40	4.09	145	12.92
xb-13	712	9:11	40	11.1	145	2.15
xb-14	712	9:53	40	18.1	144	51.22
xb-15	712	10:36	40	25.1	144	40.18
xb-16	712	11:18	40	32.1	144	29.18
xb-17	712	12:01	40	39	144	18.13
xb-18	712	12:45	40	46	144	7.21
xb-19	712	15:58	40	20.3	143	56.97
xb-20	712	18:00	39	50.3	143	58.26
xb-21	713	13:30	38	10	143	53.19
xb-22	713	14:44	38	16	144	15.16
xb-23	713	16:14	38	23.1	144	37.5
xb-24	713	16:58	38	25.9	144	25.38
xb-25	713	18:25	38	34.1	144	1.07
xb-26	713	19:51	38	42.1	143	36.99
xb-27	713	20:32	38	46	143	25
xb-28	713	21:14	38	49.9	143	12.83
xb-29	713	23:23	39	0.06	143	22.44
xb-30	714	0:28	39	6.08	143	43.43
xb-31	714	10:07	40	5.53	144	35.07
xb-32	714	10:59	40	16.6	144	40.93
xb-33	714	15:20	40	27.5	144	46.79
xb-34	714	16:07	40	38.3	144	52.16
xb-35	715	14:39	40	22.4	146	3.73
xb-36	715	15:27	40	22.1	145	51.85
xb-37	716	7:12	40	22	144	14.14
xb-38	716	8:57	40	22.2	143	41.8
xb-39	716	12:50	41	3.3	143	46.18
xb-40	716	13:44	41	13.9	143	36.09

Table 3.11-3 XCTD stations locations

Station	Date	Time	Lat.	N	Lon.	E
xc-01	611	20:46	48	60	165	0.04
xc-02	611	22:46	48	30	165	0.06
xc-03	612	0:46	48	0.04	165	0.06
xc-04	612	2:49	47	30	165	0.02
xc-05	613	4:57	46	59.8	165	1.84
xc-06	613	7:09	46	30	165	0
xc-07	613	9:17	46	0.02	165	0.13
xc-08	613	11:24	45	30	164	59.92
xc-09-1	614	4:58	44	59.6	165	0.63
xc-09-2	614	5:12	44	59.6	165	4.43
xc-10	614	7:43	44	60	166	0.34
xc-11	614	10:24	45	0.06	167	0.02
xc-12	614	13:06	44	59.9	167	59.99
xc-13	614	15:48	45	0.03	168	59.98
xc-14	614	18:18	44	60	169	55.26
xc-15	617	4:16	44	30	164	58.78
xc-16	617	6:17	44	0.09	164	59.69
xc-17	617	8:14	43	30.1	164	58.85
xc-18	617	10:12	43	0.03	164	59.46
xc-19	617	12:15	42	29.8	165	0.02
xc-20	617	14:17	42	0.02	164	59.97
xc-21	617	16:19	41	30	165	0.47
xc-22	617	18:22	41	0.01	165	0.76
xc-23	617	20:23	40	30	165	0.95
xc-24	617	22:33	40	0	165	0.82
xc-25	619	3:27	39	48.2	164	47.66
xc-26	619	4:36	39	57.7	164	29.64
xc-27	619	5:42	40	6.73	164	12.5
xc-28	619	6:48	40	15.8	163	55.41
xc-29	619	7:54	40	24.7	163	37.98
xc-30	619	9:02	40	33.6	163	20.39
xc-31	619	10:35	40	45.7	162	56.95
xc-32	625	4:57	41	45.1	154	59.89
xc-33	625	15:34	41	9.98	154	39.89
xc-34	625	16:49	41	20.1	154	19.91
xc-35	626	1:09	41	20	153	39.79
xc-36	626	13:18	41	20.1	151	29.81
xc-37	626	16:55	42	0.21	152	20.2
xc-38	628	5:28	40	48.4	152	59.87
xc-39	628	13:08	39	59.8	153	0.02
xc-40	628	14:08	39	45	152	59.96
xc-41	629	3:26	39	29.9	153	30.03
xc-42	629	4:54	39	30.1	153	56.91
xc-43	629	6:41	39	30.1	154	30.05
xc-44	629	16:14	38	30	155	0.02

xc-45	630	4:12	37	42.9	154	49.96
xc-46	630	5:34	37	24.9	154	39.51
xc-47	630	6:48	37	9.03	154	29.96
xc-48	630	8:20	36	49.1	154	45.08
xc-49	630	14:38	36	9.93	154	59.99
xc-50	630	16:38	35	39.8	155	0
xc-51	707	14:28	37	30.1	145	13.29
xc-52	707	16:12	37	54.6	145	15.02
xc-53	707	17:14	38	8.63	145	16.16
xc-54	710	3:44	41	24	143	25.49
xc-55	711	8:47	41	25	144	37.4
xc-56	712	6:50	39	50	145	35
xc-57	712	13:34	40	54.5	143	55.24
xc-58	713	1:46	38	49	143	55.06
xc-59	713	7:46	38	27.1	143	42.96
xc-60	713	11:59	38	3	143	29.93
xc-61	713	17:40	38	30.1	144	13.15
xc-62	713	21:58	38	54.3	143	0.32
xc-63	714	1:46	39	13.3	144	8.21
xc-64	714	7:28	39	46	144	25.09
xc-65	714	10:32	40	11	144	38.04
xc-66	714	15:44	40	33.3	144	49.63
xc-67	715	2:01	40	54.6	145	1.15
xc-68	715	5:02	41	18	145	14.25
xc-69	715	23:56	40	22	145	25.07
xc-70	716	0:43	40	22	145	10.02
xc-71	716	9:52	40	22	143	24.92

(4) Preliminary results: Eddy Study

Introduction

Mesoscale eddies are an important mechanism of water mass modification, heat and matter transport across the oceanic frontal zones. Recent observations have proved that mesoscale eddies are dominant features of water dynamics in the confluence zone of Kuroshio and Oyashio currents. They play a key role in physical and biological fluxes in this transition area between subarctic and subtropical waters. From them the most known are warm core rings of Kuroshio that pitch off in the area of first anticyclonic meander of the Kuroshio Extension between 142 and 146 E and then move to the north influencing on water dynamics off Honshu and Hokkaido and transporting subtropical properties into subarctic area (e.g. Kawai, 1972; Tomosada, 1986; Lobanov et al., 1991; Yasuda et al 1992). Similar anticyclonic eddies are observed along the whole chain of Kuril Islands up to Kamchatka (Bulatov and Lobanov, 1983; Rogachev 2000; Yasuda et al., 2000). They contribute to water exchange at the western boundary of subarctic gyre and were studied at the MR00-K03 cruise in May-June 2000.

Anticyclonic mesoscale eddies were also reported in the area of Subarctic front to the east of 150 E (e.g. Maximenko et al., 2001). However there are not many data on their structure and dynamics. Meanwhile, some cloud-free infrared satellite images and satellite altimetric data show existence of many well developed mesoscale eddies along Kuroshio Extension at least down to 170-180 E and location of the eddies to the north up to 45-50 N. Characteristics of these eddies were studied in the present cruise. Main objectives of the eddy study are:

- water mass structure of the eddies (including physical and chemical parameters);
- eddy dynamical characteristics;
- comparative characteristics of eddies of different location and origin;
- role of the eddies in cross-frontal transport and water mass modification;
- horizontal and vertical fluxes in the eddies.

Methods

To identify the eddies we used satellite sea surface temperature (SST) and sea surface height (SSH) data obtained correspondingly by infrared measurements from NOAA AVHRR and altimeter observations from TOPEX/POSEIDON and ERS-2 satellites. These data were collected prior to the cruise on January-May 2001. Real-time NOAA AVHRR data were received during the cruise by the Terrascan ship-borne satellite receiving station. Using standard multi-channel algorithm (MCSST) daily composite images of SST were prepared.

To find the location of eddies and their structure we also used operational data of ship-borne continuous water monitoring system and data on current velocities of ship navigation system and ADCP.

To study vertical structure of water masses we used CTD observations with Rosette multisampling system. In the area of anticyclonic eddies of subarctic front B and C in total 12 additional CTD stations were implemented (6 deep stations down to 5000-6000 m and 6 shallow stations down to 1500 m) marked as E01-E12. In the area of Kuroshio warm-core rings E and F 7 deep and 4 shallow stations were made marked as R01-R11. In addition to this 47 XCTD and 40 XBT observations were made for eddy studies.

To study current velocity in the area of the eddies we used ship borne ADCP observations and data from the LADCP attached to the CTD/RMS system.

Mesoscale structure of the Kuroshio-Oyashio confluence zone

According to classical view, the large-scale circulation in the mid-latitude Northwestern Pacific is dominated by the warm and saline Kuroshio and its seaward extension (Kuroshio Extension) in the south, and the cold and less saline Oyashio and its seaward extension (Subarctic Current) in the north. Instabilities of the large scale flows give rise to prominent mesoscale features such as fronts and eddies.

A synoptic view of this area based on NOAA AVHRR satellite infrared images is shown in Fig. 3.11-1 where red colors correspond to warmest Kuroshio water of subtropical origin while blue colors represent cold Oyashio and Subarctic Current water. Meandering stream of the Kuroshio Extension can be seen in lower part of the images. Sharp thermal front at its northern edge can be seen around 38 N at 145 E and around 33 N at 155 E.

Propagation of warm water to the north is associated with mesoscale meanders, filaments and anticyclonic eddies. A large number of the eddies marked by characters A-P can be seen in the area just east of Japan and down to 170 E. Most of them were seen at satellite SST and SSH data a few months prior the cruise with exception of eddy E that was just formed in the beginning of June. Another exception is warm water areas marked as H and I that represent a result of merging of three anticyclonic eddies and intrusion of Kuroshio water happened in early June and followed by a process of new eddies formation.

Propagation of cold subarctic water to the south is associated with intrusions of the Oyashio located just east of Hokkaido and east of eddies G and F. Other intrusions of cold water can be seen along 154 E just east of eddies B and C and in the eastern area. Thus it is seen that advection of both warm and cold water in the Kuroshio-Oyashio confluence zone is associated with mesoscale eddies. Structure and characteristics of 6 individual anticyclonic eddies samples during the cruise is discussed in the next paragraphs.

General features of thermohaline structure across the transition area

Satellite images of Fig. 3.11-1 does not show northern part of the transition area between subarctic water and Kuroshio Extension because of cloud cover. Here we will discuss large-scale features of the frontal zone structure using hydrographic observations along two meridional sections of 155 E and 165 E implemented in the cruise.

We will use most common nomenclature of transition area that assume 3 major fronts. The Polar Front extends northeastward from 41°N, 150°E as continuation of Oyashio Front and southern boundary of subarctic water mass structure (Uda, 1963). The Subarctic Front locates some distance southward as a boundary between modified subarctic water and modified subtropical water. This front is not well defined due to meanders and eddies and occurs around 40°N between 150°E and 170°E. The Kuroshio Extension Front is the northern boundary of subtropical mode water. It corresponds to northern edge of Kuroshio Extension.

The vertical temperature and salinity structure in the upper 1000 m across the Polar Front, transition domain and Subarctic Front is shown at XCTD section taken along 165°E (Fig. 3.11-18). The Polar Front usually defined as the 4°C isotherm at 100 m depth (Favorite et al., 1976) is seen near 48°N (XCTD stations 4-5). Along front Subarctic Current is characterized by the dynamic height anomaly relatively 1000 db $\Delta h=10$ cm. This front separates western subarctic water with subsurface temperature minimum <2°C (dichothermal water according to Uda, 1963) and intermediate temperature maximum about 3.5°C (mesothermal water) from more warm waters of the transition domain, where salinity increase with depth without salinity minimum. The transition domain is observed between 42°N and 48°N. This domain is limited from the south by the Subarctic Front (XCTD stations 20-21) defined as the salinity 34 psu at the surface (Favorite et al., 1976) that represents boundary between the subarctic and subtropical water mass structure around northern edge of the anticyclonic eddy A (Fig. 3.11-1).

Vertical sections of potential temperature, salinity and potential density in the upper 1000 m along 155°E are shown in Fig. 3.11-19. Typical western subarctic structure with cold subsurface (dichothermal) layer was observed at the station KNOT. An examination of the thermohaline structure reveals that the front at 42°N (stations KNOT-15) is Subarctic

Front. Transition domain is not well defined along this sections. The Subarctic Front is the boundary between the subtropical and subarctic water masses. According ADCP data the strong frontal current (Oyashio Extension or Subarctic Current) with velocity up to 65 cm/s was observed near 43°N (Fig. 3.11-7). The dominant front at 34°N (stations 20-21) is the Kuroshio Extension front. The Kuroshio Extension front is strongest between 100 and 300 m where cross-frontal differences reach 8°C and 0.7 psu. South of this front typical subtropical structure with mode water in thermocline and “old” intermediate salinity minimum (NPIW) was observed. The zone between 34°N and 42°N is transition area with a vertical thermohaline structure characterized by “new” salinity minimum centered around isopycnal 26.65 σ_θ . In addition to the dominant Kuroshio Extension front a secondary front associated with northern boundary of the warm core anticyclonic Kuroshio eddy D was found at 39°N (stations 17-18). North of the eddy D more fresh and cold salinity minimum was seen (station 18).

Basic vertical profiles of temperature, salinity, and density in the Kuroshio-Oyashio confluence zone are shown in Fig. 3.11-20. This area is considered as a formation site for North Pacific Intermediate Water (NPIW). In this area the low salinity Oyashio water contacted with Tsugaru Current water, warm core ring and Kuroshio Extension waters. Low salinity water intrusions along the Kuroshio front is possible mechanism of formation of NPIW (Talley et al., 1995, Yasuda et al., 1996). The vertical thermohaline structure of Kuroshio and coastal Oyashio is represented by stations xc-51 and xc-54 (source waters for subtropical and subarctic structures, respectively). The salinity of the Oyashio water increases with depth while the salinity of the Kuroshio has maximum in subsurface layer and minimum around the depth of 550 m. Warm and saline water of subtropical origin is found in area of Kuroshio front (xc-52) in the upper 400 m. cold and low salinity Oyashio water is located beneath it. Thus at the Kuroshio front subarctic intermediate water is overrun by subtropical water. Numerous intrusions occurs along Kuroshio front (xc-52 and xc-53).

The processes leading to the formation of salinity minimum in the Kuroshio-Oyashio interfrontal zone and in the eddies need to be investigated more fully because they have important influence on the NPIW formation and spreading.

Eddy A

The eddy A is the most eastern eddy sampled in the cruise. It was located around 39°50'N, 164°50'E just to the east of Shatskiy Rise and had an elliptical shape of 110x140 miles at the surface. Dynamic height relatively 1000 dbar in the eddy A center was high (142 cm) in comparison with the area of transition domain (112 cm). Large dynamic height anomaly corresponds relatively strong near surface ADCP current velocity up to 75 cm/s (Fig. 3.11-4). At the vertical section (Fig. 3.11-3) strong currents associated with the eddy are seen to penetrate down to 400-450 m with the area of maximum velocities shifting toward the eddy center with a depth.

Eddy A had a warm, saline upper layer, with subsurface salinity maximum and warm (T=7.5-9°C) and relatively saline (S=33.9-34.1 psu) core at intermediate depth of 200-400 m indicating the Kuroshio origin water (Fig. 3.11-5). Vertical section of potential density

(Fig. 3.11-5 d) shows thick isopycnal layer in the density range $26.4-26.6 \sigma_{\theta}$. Thus, the eddy core is characterized by low potential vorticity suggesting that enhanced mixing processes occurred in the internal part of eddy.

Eddy B

This eddy was located at the subarctic front and was seen at altimetry data at least since January as an elliptical area of anticyclonic rotation with the size of 160 x 110 miles and large axis directed eastward and northeastward. During this period the eddy was staying at approximately the same position. Satellite infrared images indicated a permanent flow of warm water (warm streamer) along the western and northern part of the eddy and cold water flow (cold streamer) around its eastern periphery. The eddy B area was mostly covered with the clouds, however, a few clear images collected during the cruise (Fig. 3.11-6) shows a tendency of decreasing of the eddy size and its weakening from May to July. ADCP velocities of 30-45 cm/s were observed in the eddy down to 425-475 m (Fig. 3.11-7) showing anticyclonic rotation with maximum currents at the western and northern segments. The eddy might seem like a stationary meander of subarctic front. However some satellite images (Fig. 3.11-6,a) clearly shows an anticyclonic flow of water streamers with convergence area in the eddy center.

Distribution of hydrographic data also clearly shows the eddy as isolated anticyclonic feature down to 2500-3000 m (Fig. 3.11-8-9). Probably because of a lack of deep CTD stations at the southern part of the eddy it seems to be merged with another eddy C at Fig. 3.11-8, c and 3.11-9, c showing density distribution at the near bottom layer. Vertical density profile for the eddy center at station E08 (Fig. 3.11-9) demonstrated an existence of three very uniform (isopycnal) layers around 60-120, 200-270 and 320-470 m. The last isopycnal layer of $26.685 \sigma_{\theta}$ is also seen at other stations located close to the eddy center and represents its core water with $T=6.08-6.12$ C and $S=33.90-33.91$ psu (Fig. 3.11-10). This water of very low potential vorticity has been forming in the eddy center and then transporting southward along the periphery of other eddies C and D at (Fig. 3.11-11). The eddy core has a shape of intra-thermocline lens with a shallow seasonal thermocline in the eddy center and deep upper mixed layer at its periphery.

Eddy C

This eddy of smaller size was located just to the south of eddy B and had a diameter of 60-80 miles. XCTD stations 39-41 and CTD station E12 taken in the eddy area show a much less developed pycnocline layer in its center in compare with eddy B. It may be a result of our observation not exactly at the eddy center or some specific feature of its structure. However the eddy C had a clear signature at the satellite imagery prior the CTD survey and can be identified at the dynamic topography and ADCP data as an anticyclonic structure with currents of 40 cm/c (Fig. 3.11-6-8).

In the layer of minimum potential vorticity (235-290 m) it had a water of $T=7.8-8.3$ C and $S=34.01-34.07$ psu. At subsurface layer (70-180 m) the eddy contained a water with maximum salinity $S=34.2-34.4$ and $T=9.6-12.4$. Surface layer was occupied by recent

intrusion of warm water from the south ($T=16.8-17.2$ C $S=34.4$). These water masses represent modified Kuroshio water.

Eddy D

According to satellite altimetry and infrared data this eddy was formed from the meander of the Kuroshio Extension around 37 N, 158 E in middle March and was moving westward at typical speed of 3-5 cm/s. It is the largest and most energetic eddy in the area. It has a circular shape with diameter of 150-170 miles. Strong currents associated with the eddy were observed by the ADCP along the 155 E to occupy an area of 170 miles with maximum velocities of 95-100 cm/s observed at 35-50 miles off the eddy center (Fig. 3.11-13). The eddy had a thermohaline structure typical for Kuroshio warm-core rings with a core of warm and high salinity (34.2-34.5 psu) water at the upper layer down to 550 m (Fig. 3.11-14). The salinity minimum densities in the eddy center (station XC47) were higher than in the surrounding water. A streamer wrapping clockwise along the eddy and carrying warm saline water in the upper layer and cold fresh water at the intermediate depth (350-450 m) were observed at station 18.

Eddy E

This comparatively small and the youngest eddy was formed in the beginning of June just a few days before the survey as a result of instability of an anticyclonic meander of Kuroshio Extension around 143-144 E. It had a near circular shape with a diameter of 55-60 miles and thermohaline structure similar to eddy D and typical to Kuroshio warm core rings (Fig. 3.11-15-17). This eddy however does not have an isopycnal core. Transformed Kuroshio water with $T > 8$ C and $S > 34.0$ psu was observed only at upper 0-220 m layer. This may be explained as the beginning stage of eddy evolution or a fact that our observation were not exactly at the eddy center. During the period of survey the eddy made a chaotic motion around the site at pretty high speed of 8-12 cm/s (up to 6 miles a day). So at the moment of survey its center was located to the east of station R03 and south of stations R02 and XB25. Maximum ADCP velocities up to 80-90 cm/s were observed at the northern and eastern edge of the eddy.

Eddy F

This eddy is a typical warm-core ring of the Kuroshio at a middle stage of its evolution. It had an elliptical shape of 70 x 90 miles and at the period of survey its center was located just over the deepest part of Japan Bottom trench (Fig. 3.11-15). The eddy had a relatively isopycnal layer of 26.5-26.8 at its center at depth 70-600 m and two lens-like cores. The upper core (120-300 m) contained a relatively warm and saline water of $T=5.9-6.6$ C and $S=33.66-33.82$ psu. While the lower core (400-600 m) contained extremely cold and fresh water of $T=1.96-2.60$ C and $S=33.41-33.60$ psu.

ADCP measured velocities were up to 75-80 cm/s with maximum at 100-200 m layer. Many inversions at T and S vertical profiles around the eddy periphery at depth of

200-600 m suggest an intensive mixing process at intermediate depth (between 26.6-27.0 isopycnals) which lead to formation of uniform core of the eddy. Like eddy B the eddy

F had a much more shallow pycnocline at the central part center than at its periphery which should have an important biological implication.

Comparative characteristics of the eddies

A summary characteristics of 6 anticyclonic eddies are presented at the Tables 3.11-4 and 3.11-5. We estimated eddy diameter using satellite, hydrographic and ADCP data, which are in a good agreement. Dynamic height anomaly was calculated relatively to 1000 db surface. Dynamic height and depth of isopical layer values for eddies C, D, and E might be underestimated because of the measurements not exactly at their centers.

Table 3.11-4 General characteristics of anticyclonic eddies

Eddy	Center * location	Diameter (miles)	Dyn. height anomaly (din.cm)	ADCP max velocity (cm/s)	Estimated age (months)	Description
A	39°48' 164°48'	110-140	30	75	4	East KWCR
B	41°12' 152°52'	110-160	12	50	> 6	Eddy of subarctic front
C	39°30' 153°00'	60-80	18	40	-	Eddy of subarctic front
D	37°09' 154°30'	150-170	44	100	3	East KWCR
E	38°34' 144°01'	55-60	24	80	0.3	West KWCR, newly formed
F	40°22' 144°28'	70-90	20	75	> 6	West KWCR

*- location of the station nearest to the eddy center

Table 3.11-5 Characteristics of the eddy core water

Eddy	Depth (m)	T (C)	S (psu)	Density
A	180-350	8.0-9.1	34.01-34.14	26.43-26.54
B	200-370	6.0-6.1	33.90-33.91	26.68-26.69
C	235-290	7.8-8.3	34.01-34.07	26.50-26.55
D	70-200	14.1-14.5	34.56-34.58	25.62-25.88
E	-	-	-	-
F	120-300	5.9-6.6	33.66-33.82	26.50-26.58
	400-600	2.0-2.6	33.41-33.60	26.68-26.83

Conclusion

(1) Six different anticyclonic eddies were observed in the transition area off Japan and down to 165 E having a comparatively similar thermohaline and dynamical characteristics. All of the eddies penetrated down to bottom layer. The eddies in the eastern area were the same (or even more) energetic feature as Kuroshio warm core rings located just east of Japan. Numerous number of eddies presented at satellite data suggests importance of eddy induced transport and mixing in the transition area.

(2) All of the observed eddies contained a relatively warm and saline water at their core (typical depth 100-400 m) originated from the Kuroshio. A secondary core of cold and fresh water originated from the Oyashio was observed at the eddy F located below its main warm core.

(3) Horizontal advection of low salinity subarctic water along the eddy periphery to the south and enhanced mixing with subtropical mode water at intermediate depth in the eddy area are important mechanism of water exchange in the transition area.

(4) A doming of main pycnocline over the eddy core results in more shallow seasonal pycnocline at the eddy center. This fact along with intrusions of warm and cold streamers around the eddy periphery should have significant biological implication.

References

- Favorite F., A. Dodimead, and K. Nasu (1976) Oceanography of the subarctic Pacific region, 1960-1971, Bull. Int. N. Pac. Comm., 33, 187 p.
- Kawai H. (1972) Hydrography of the Kuroshio Extension. In: The Kuroshio: Its Physical Aspects (Ed. H.Stommel and K.Yoshida), U.Wash. Press, 235-352.
- Lobanov V.B., K.A. Rogachev, N.V. Bulatov, A.F. Lomakin and K.P. Tolmachev (1991) Long term evolution of the Kuroshio warm eddy. Doklady (Trans.) USSR Acad. Sci., 317, 984-988 (in Russian).
- Maximenko N. A., M. N. Koshlyakov, Y.A. Ivanov, M.I. Yaremchuk and G.G. Panteleev (2001) Hydrophysical experiment "Megapoligon-87" in the northwestern Pacific subarctic frontal zone. J. Geophys. Res., 106 (C7), 14143-14163.
- Talley L.D., Y. Nagata, M. Fujimura, T. Kono, D. Inagake, M. Hirai and K. Okuda (1995) North Pacific Intermediate Water in the Kuroshio/Oyashio mixed water region. J. Phys. Oceanogr., v. 25, 475-501.
- Tomosada A. (1986) Generation and decay of Kuroshio warm-core rings. Deep-Sea Res., 33, 1475-1486.
- Uda M. (1963) Oceanography of the subarctic Pacific Ocean, J. Fish. Res. Board Can., 20, N1, 119-179.
- Yasuda I., K. Okuda and Y. Shimizu (1996) Distribution and modification of North Pacific Intermediate Water in the Kuroshio-Oyashio interfrontal zone. J. Phys. Oceanogr., v. 26, 448-465.

Aknowledgements

We like to thank Dr. S.Watanabe, Dr. Y.Kumamoto, Captain Hashimoto, all members of research group and crew of r/v Mirai for their kind attention and cooperation during the eddy studies.

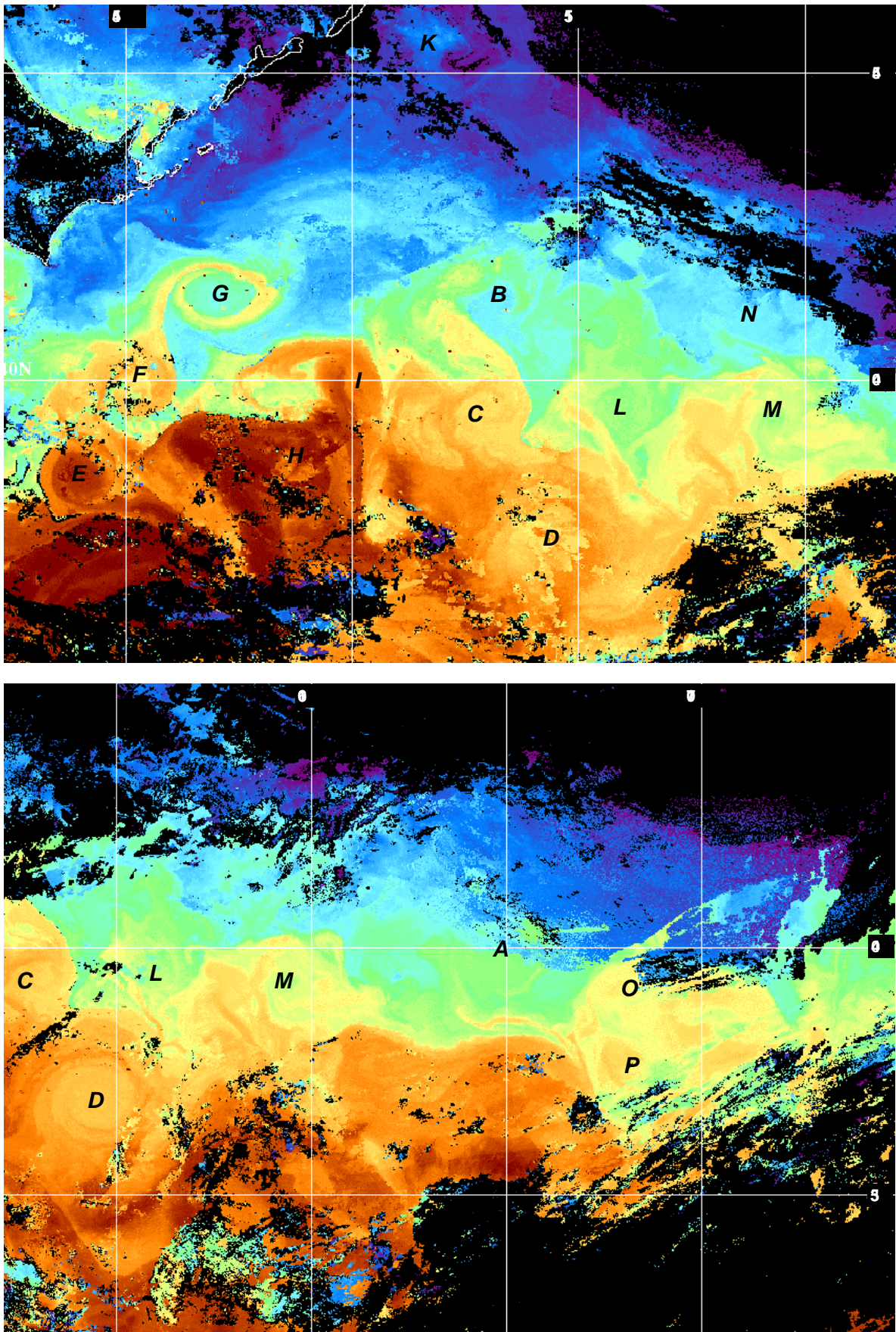


Fig. 3.11-1 NOAA AVHRR MCSST daily composite satellite images of the subarctic front area for June 17 (upper) and 18 (lower), 2001 showing numerous anticyclonic eddies marked by characters (A-P). Red colors correspond to warmer waters, dark blue and black are cold water and clouds.

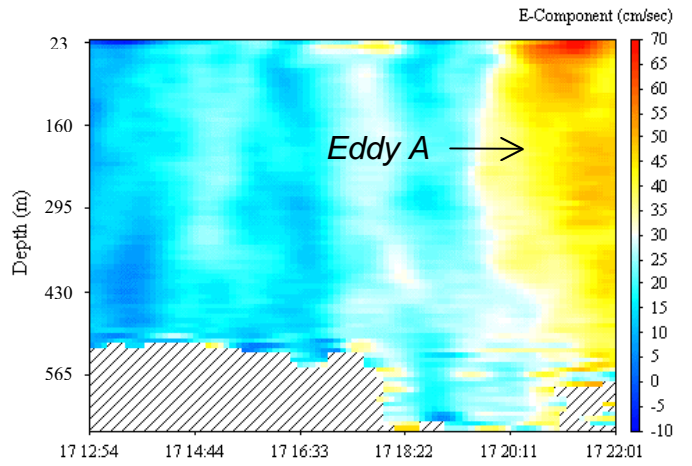
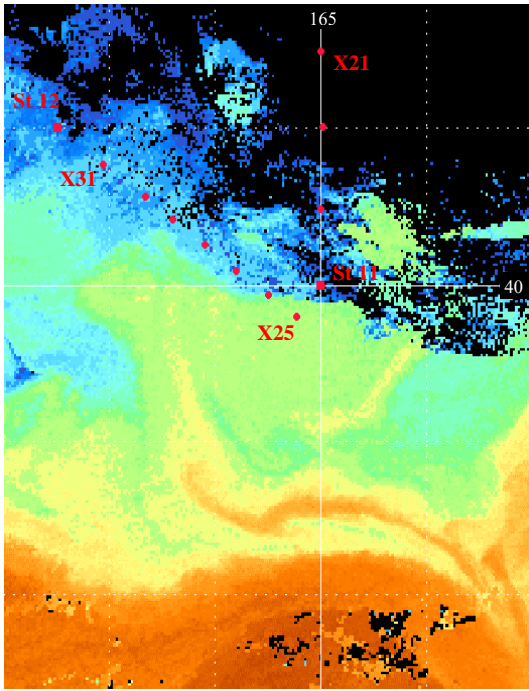


Fig. 3.11-3 Vertical section of current velocity along 165 E from 44 to 40 N (right) by ADCP measurements.

Fig. 3.11-2 Anticyclonic eddy A on NOAA MCSST infrared satellite image for June 18 and location of CTD and XCTD stations of June 17-19, 2001.

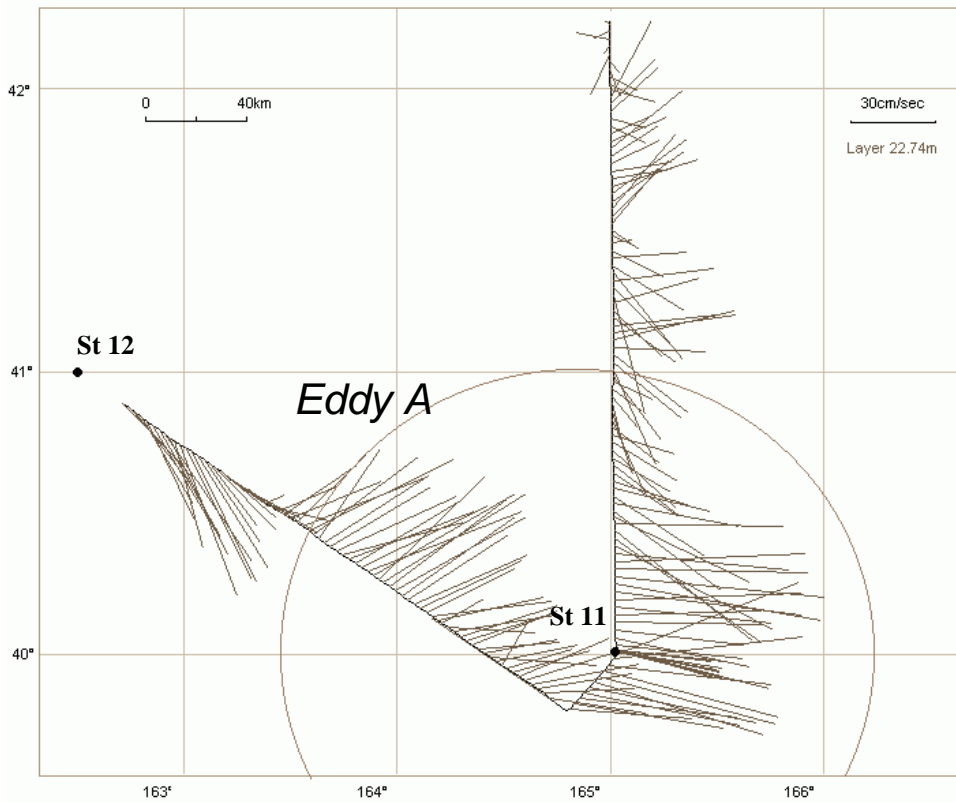


Fig. 3.11-4 Currents in upper layer of Eddy A measured by ADCP system on June 17-19, 2001

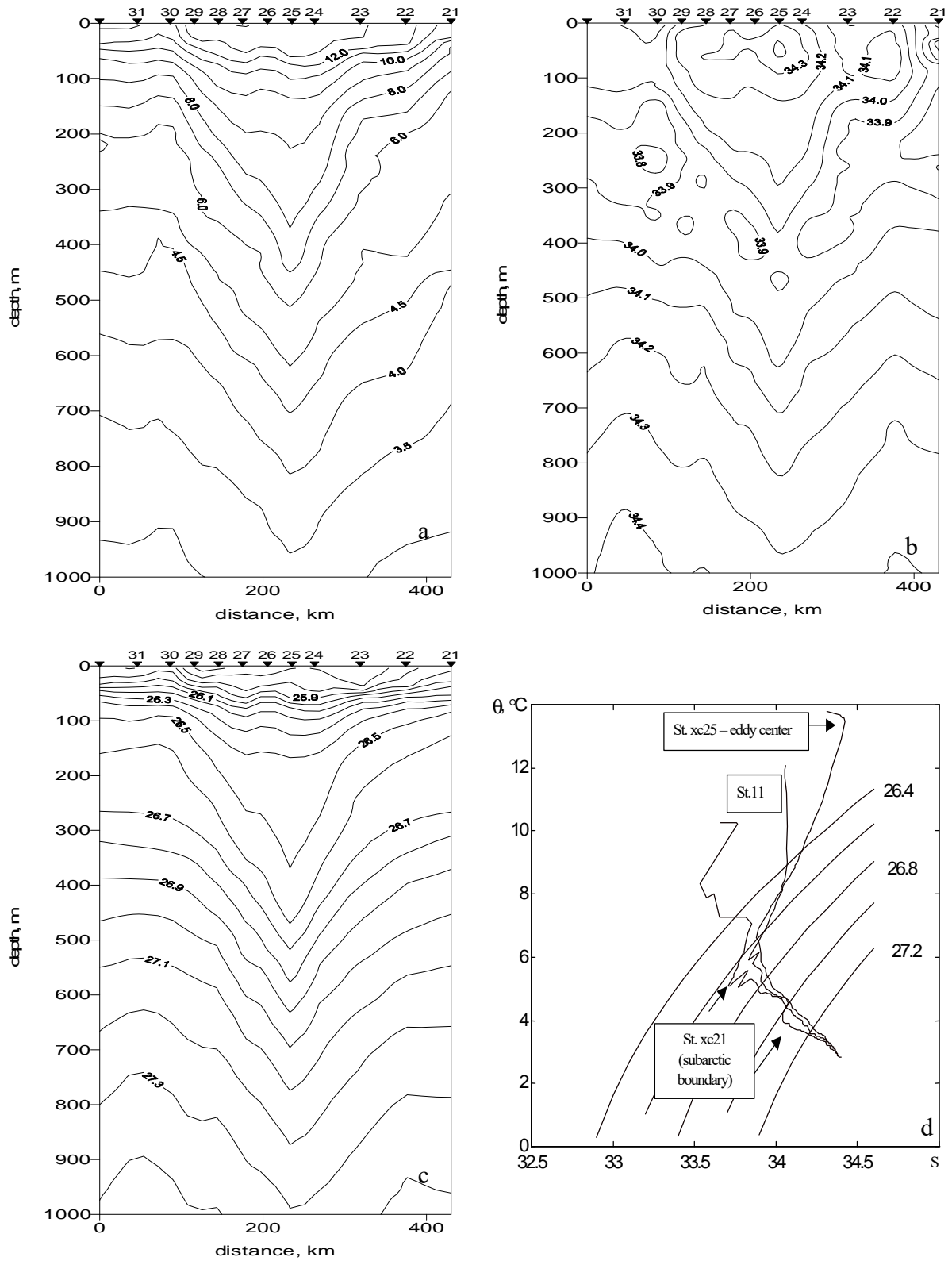


Fig. 3.11-5 Vertical sections of potential temperature (a), salinity (b), potential density (c) across eddy A and TS-diagram (d) for the station located in the eddy area.

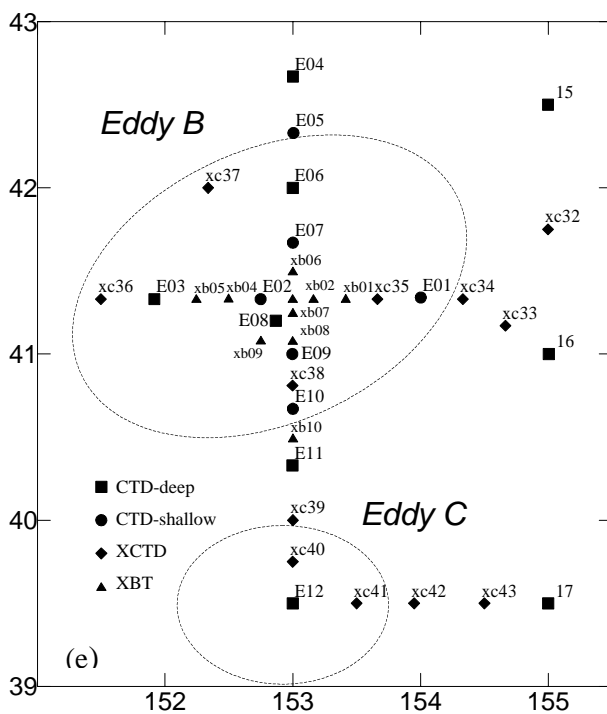
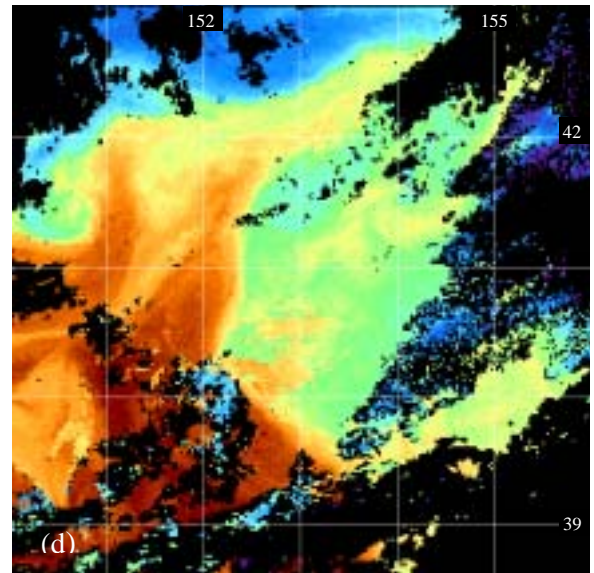
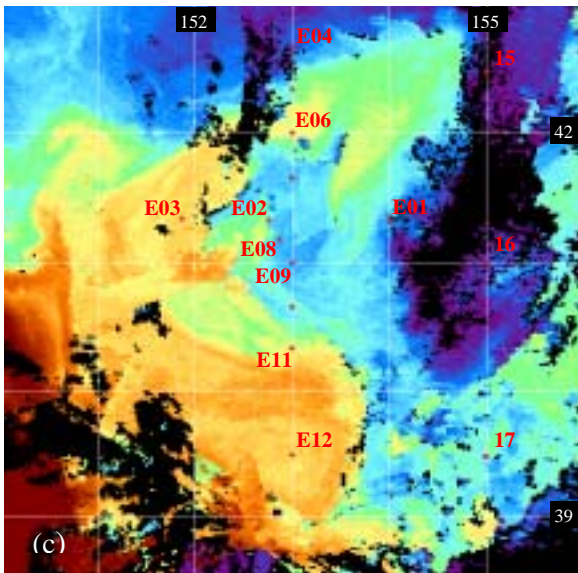
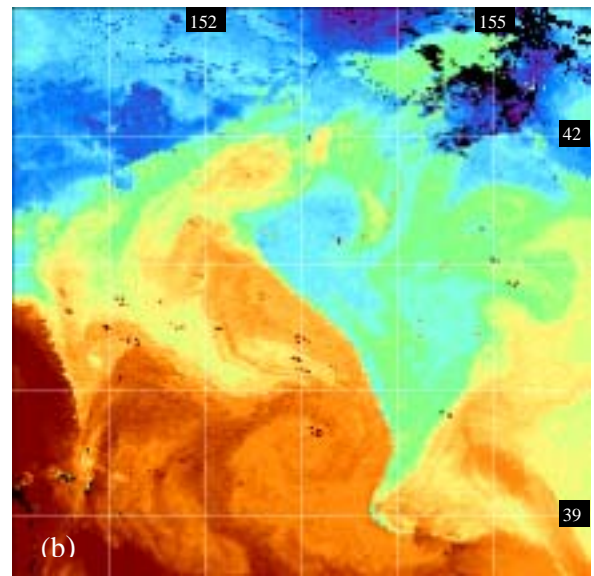
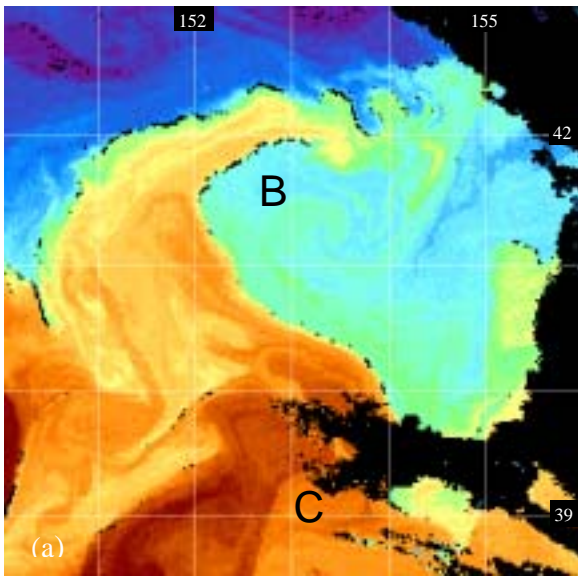
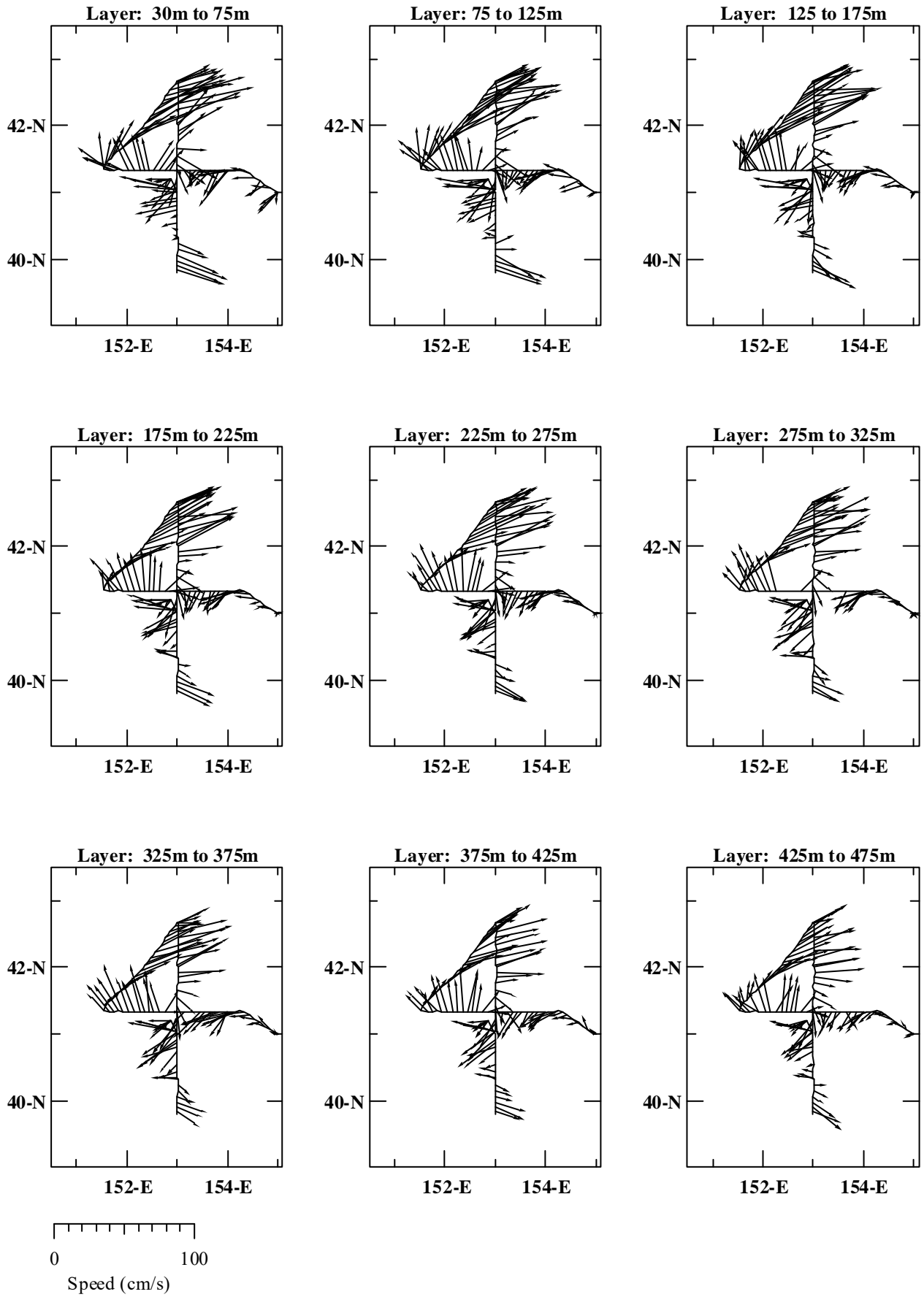


Fig. 3.11-6 Anticyclonic eddies B and C on satellite images for May 30 (a), June 17 (b), June 23 (d) and July 8 (d) and scheme of hydrographic survey (e) of June 25-29, 2001. Location of CTD stations down to bottom (CTD-deep), CTD stations down to 1500 m (CTD-shallow), XCTD and XBT is shown.



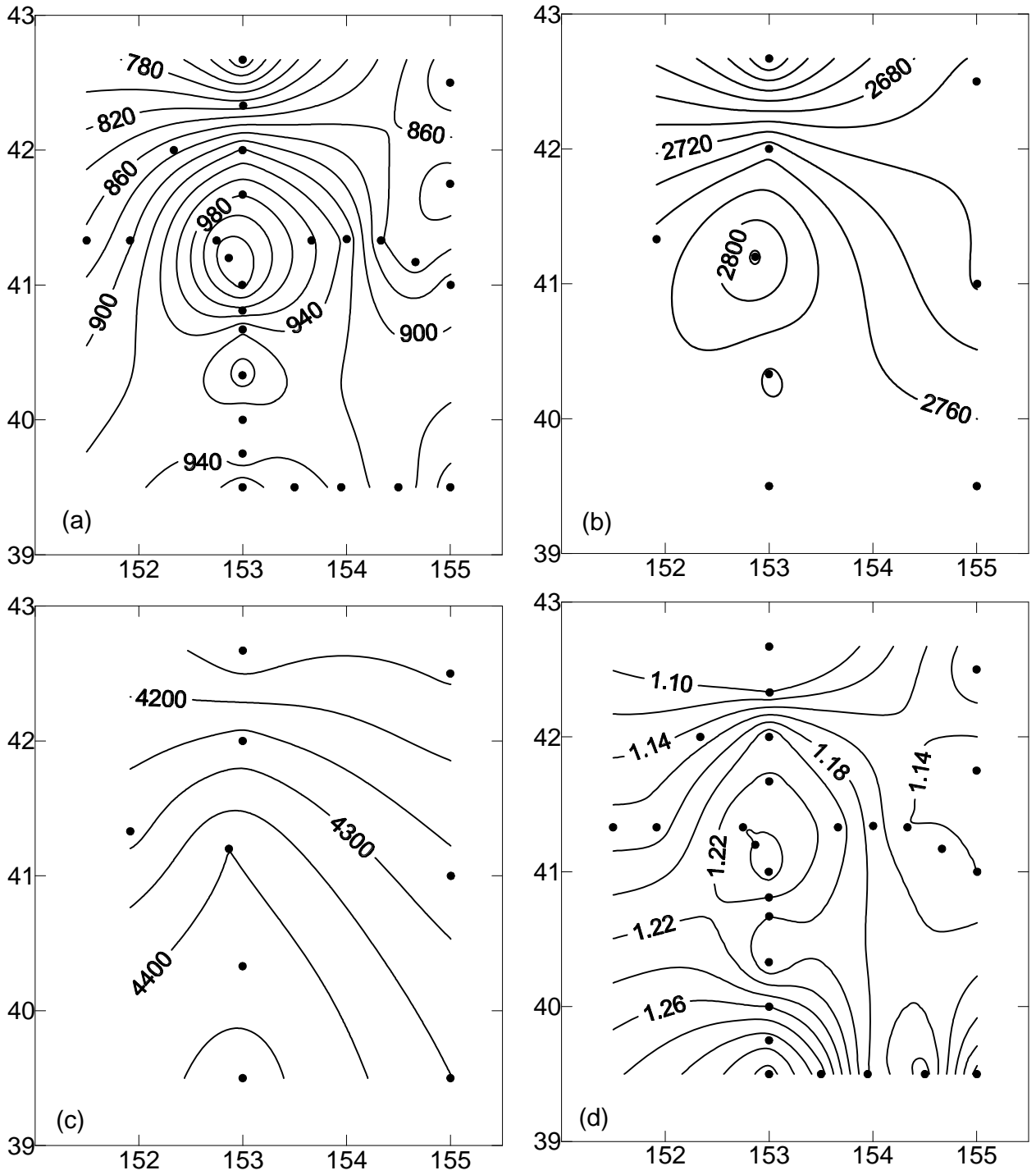


Fig. 3.11.8 Depth of potential isopical surfaces 27.35 (a), 27.74 (b), 27.79 (c) and dynamic height at the surface relative to 1000 db (in dyn. m) (d) in the area of eddy B

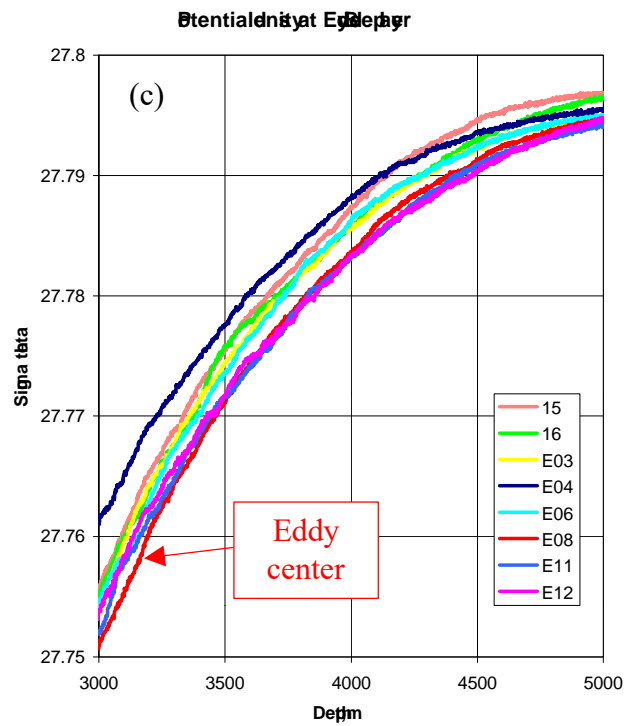
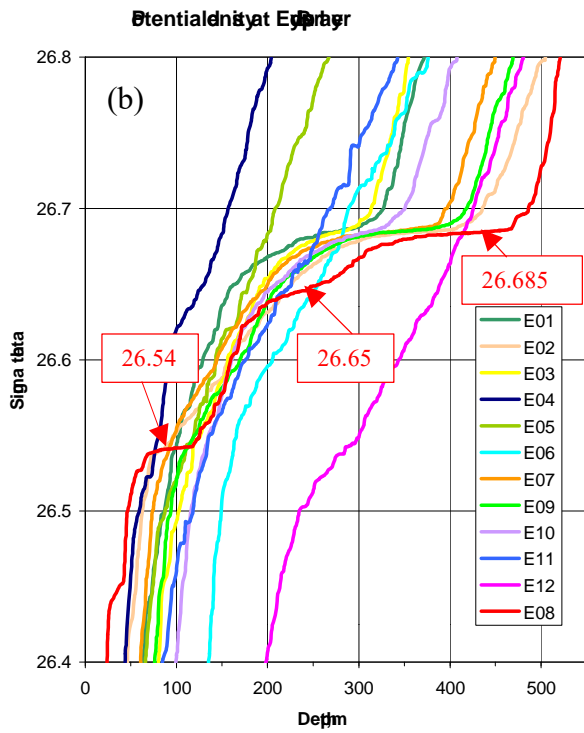
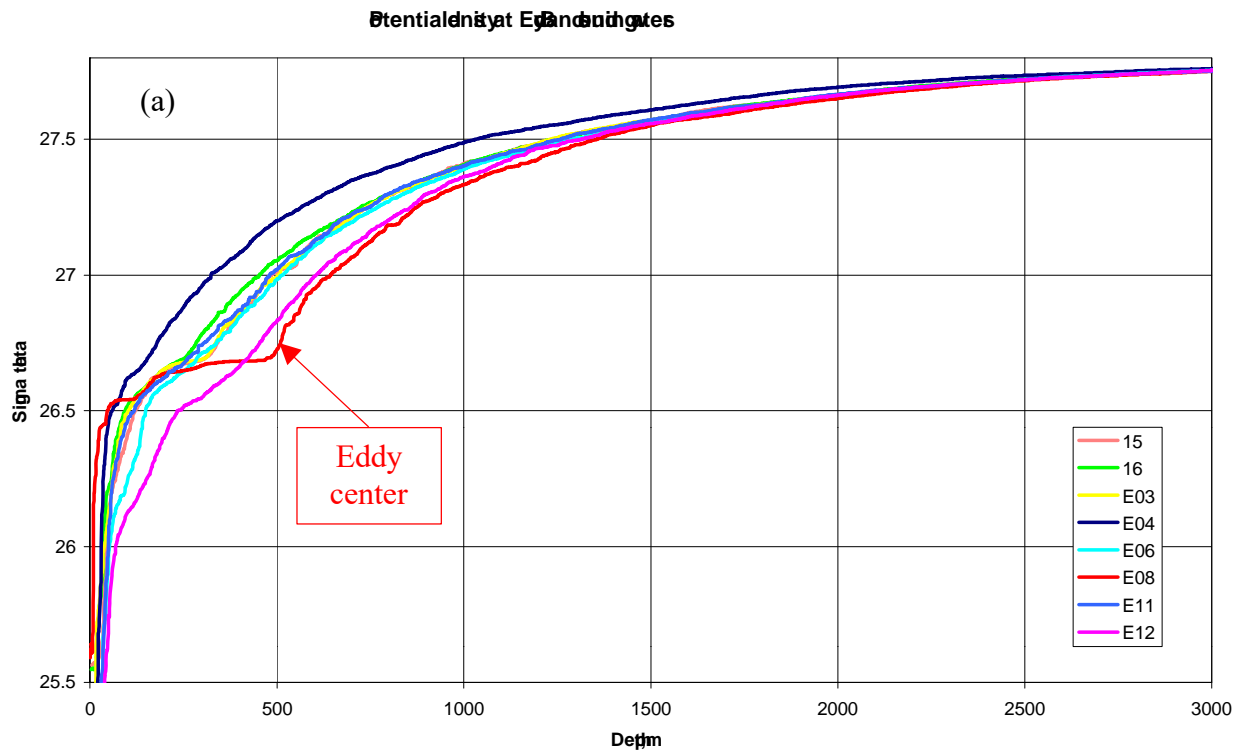


Fig. 3.11-9 Vertical profiles of potential density at the eddy B central part and surrounding waters.

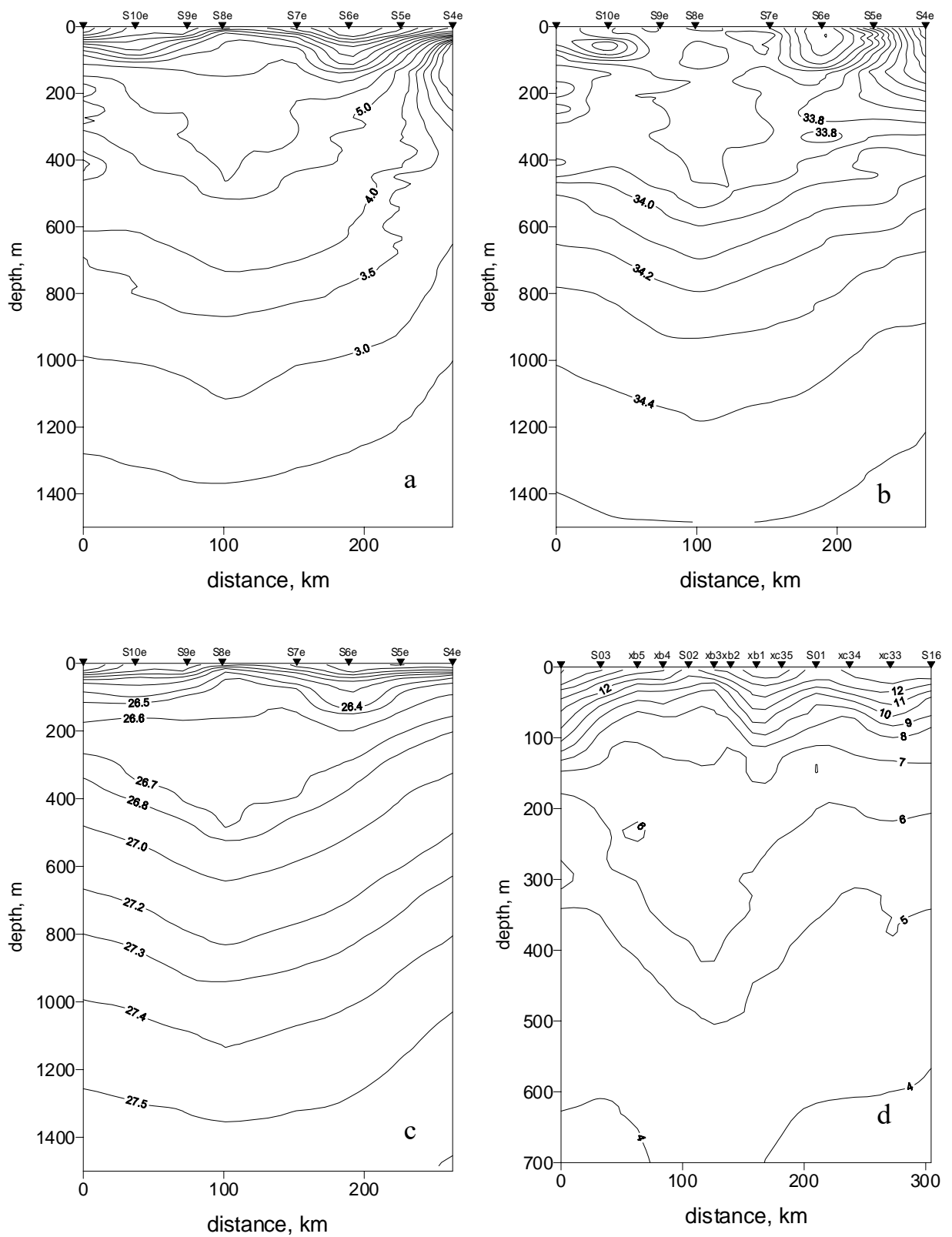


Fig. 3.11-10 Meridional vertical sections of potential temperature (a), salinity (b), potential density (c) and zonal section of temperature across eddy B.

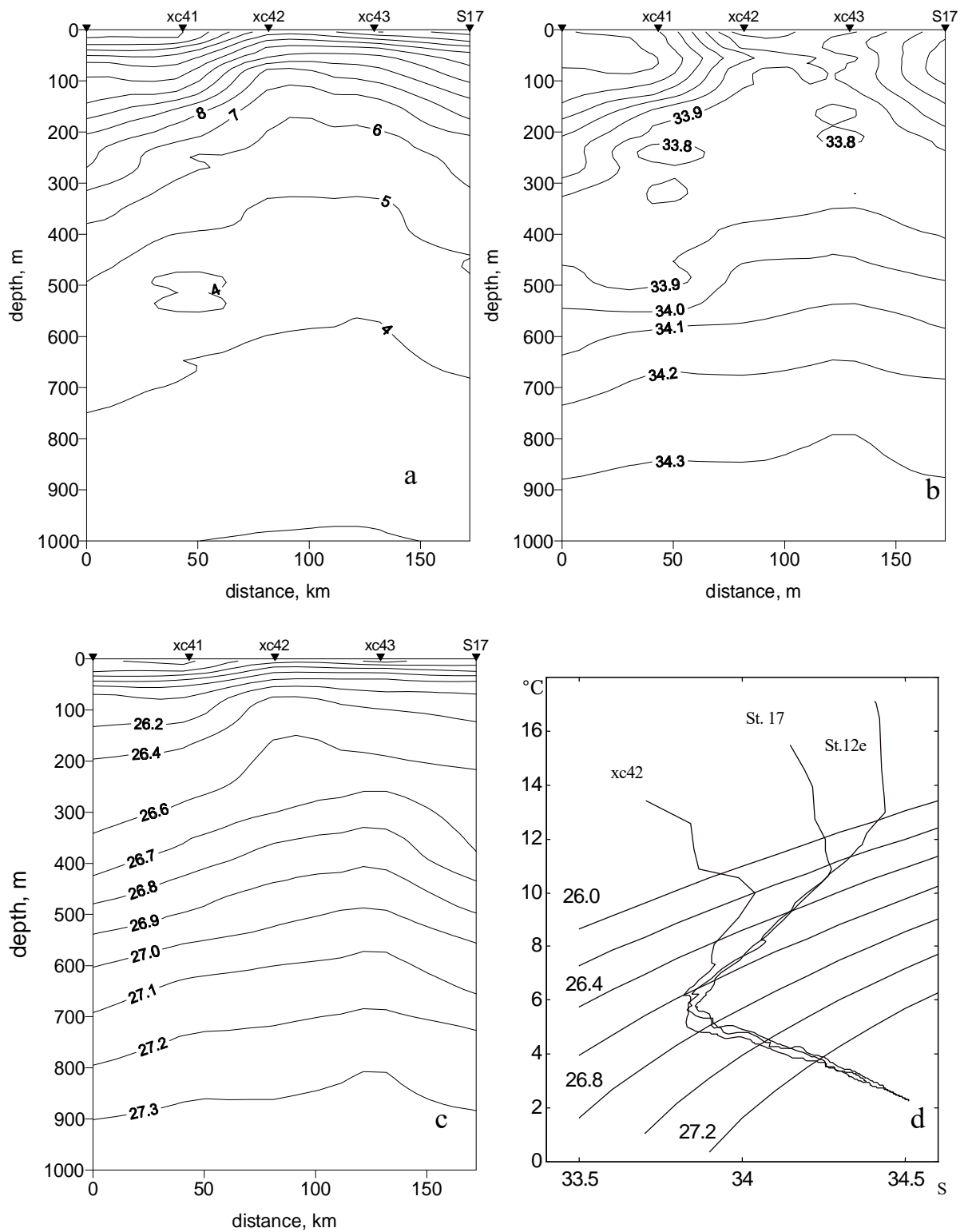


Fig. 3.11-11. Vertical sections of potential temperature (a), salinity (b), potential density (c) across the could streamers near eddy B and TS-diagram (d) for stations inside (xc42) and outside streamer.

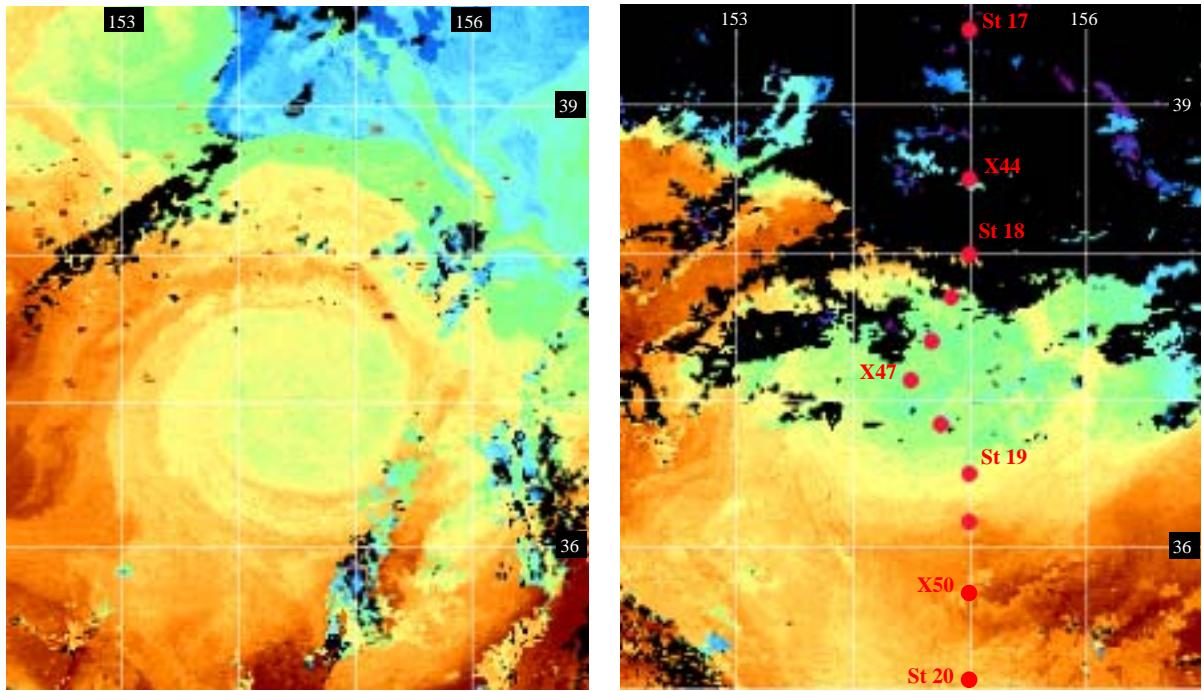


Fig. 3.11-12 Anticyclonic eddy D on satellite images for June 18 (left) and 26 (right) and location of CTD and XCTD stations on June 29-30, 2001.

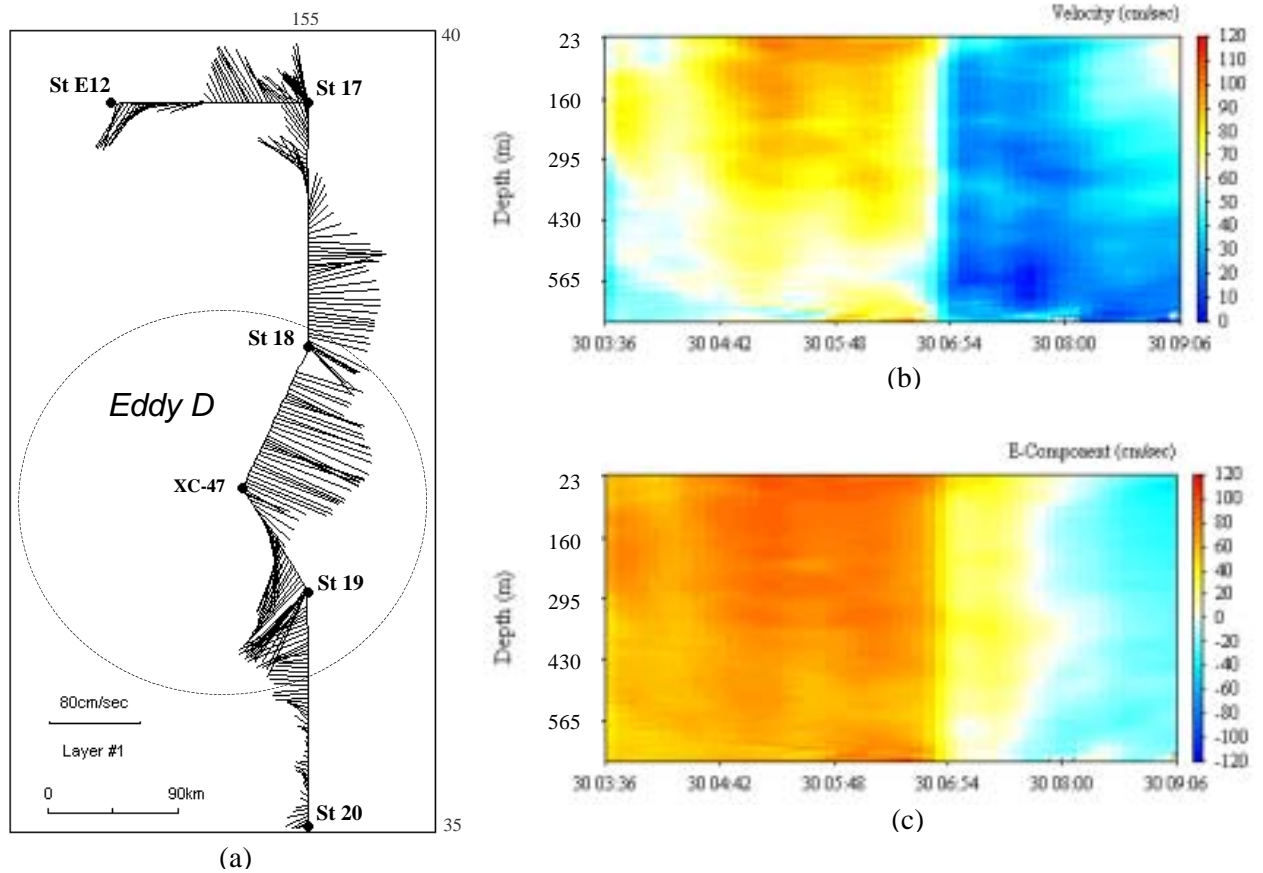


Fig. 3.11-13 Currents by the ADCP at the area of eddy D at surface layer (a) and vertical plots of absolute velocity (b) and east-west component of current vectors between st. 18 and 19 (c).

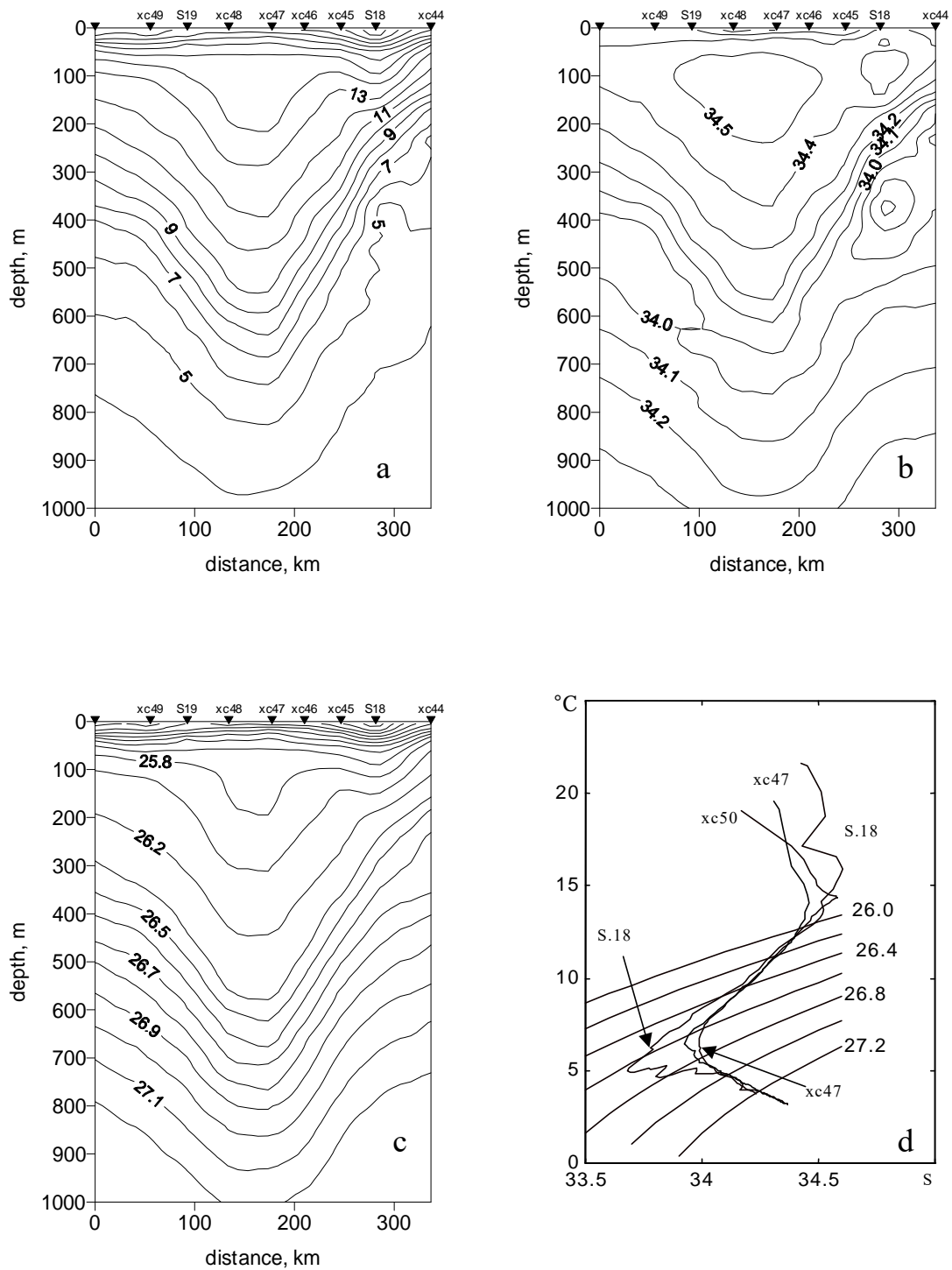


Fig. 3.11-14. Vertical sections of (a) potential temperature, (b) salinity, (c) potential density across eddy D and TS-diagram (d) for stations inside (xs47) and at the edge (S18, xc50) of the eddy.

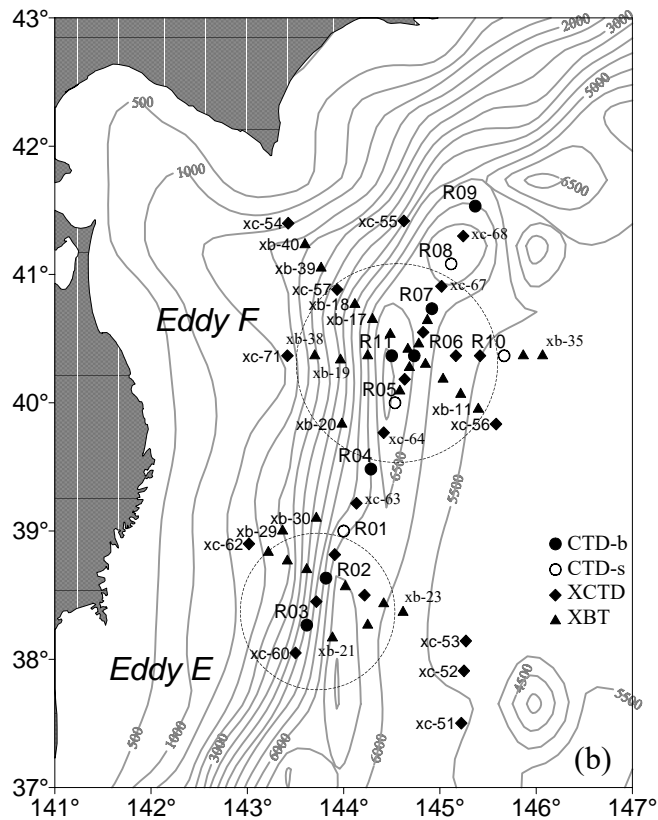
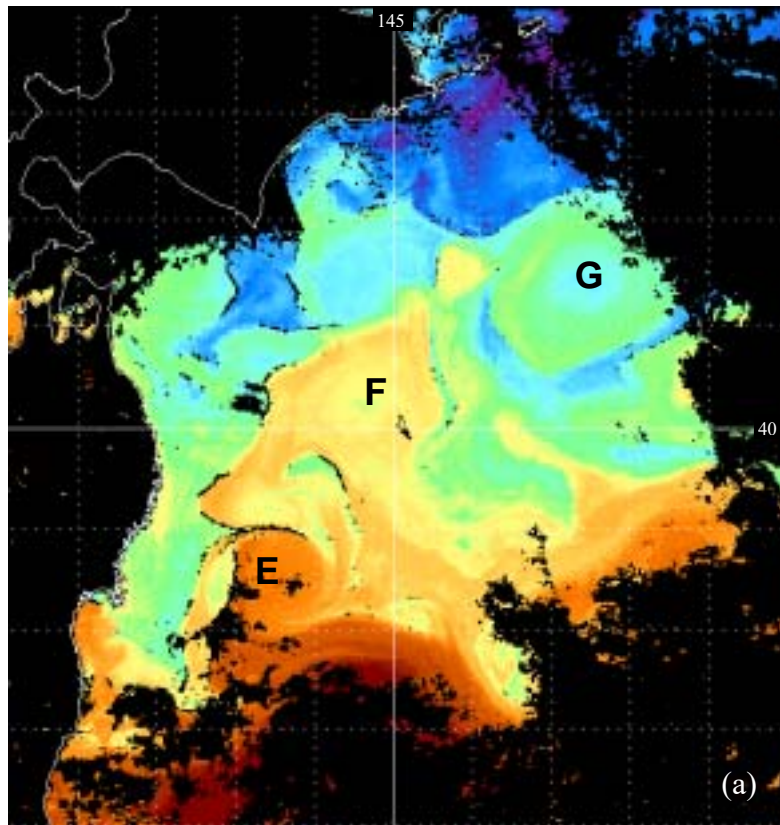


Fig. 3.11-15 Satellite image for July 7, 2001 showing the eddies E, F and G (a) and scheme of hydrographic survey of July 12-16, 2001 (b)

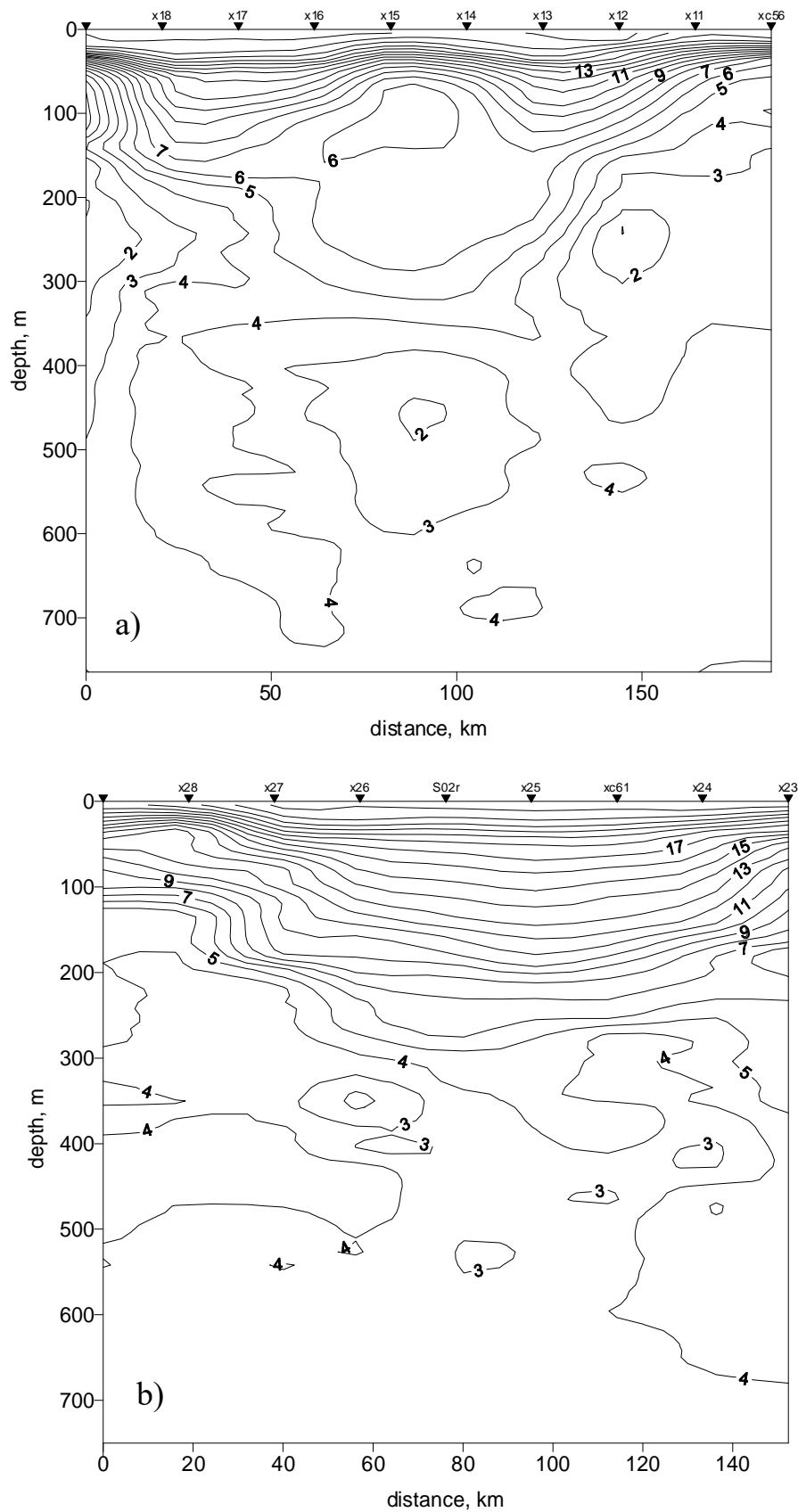


Fig. 3.11-16 Thermal structure across the Kuroshio anticyclonic rings F (a) and E (b).

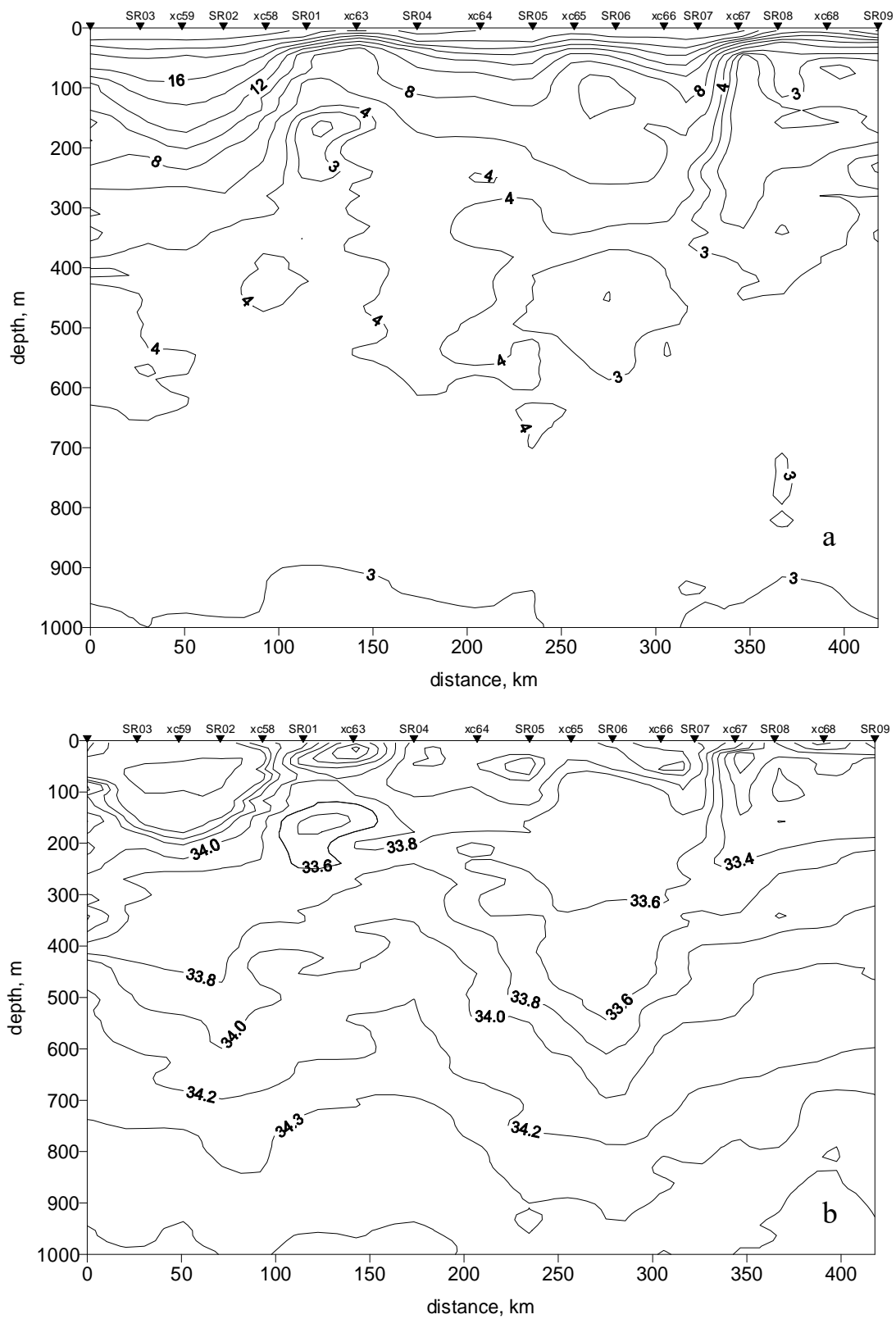


Fig. 3.11-17 Vertical sections of potential temperature (a), salinity (b) and potential density across Kuroshio anticyclonic rings E (left) and F (right).

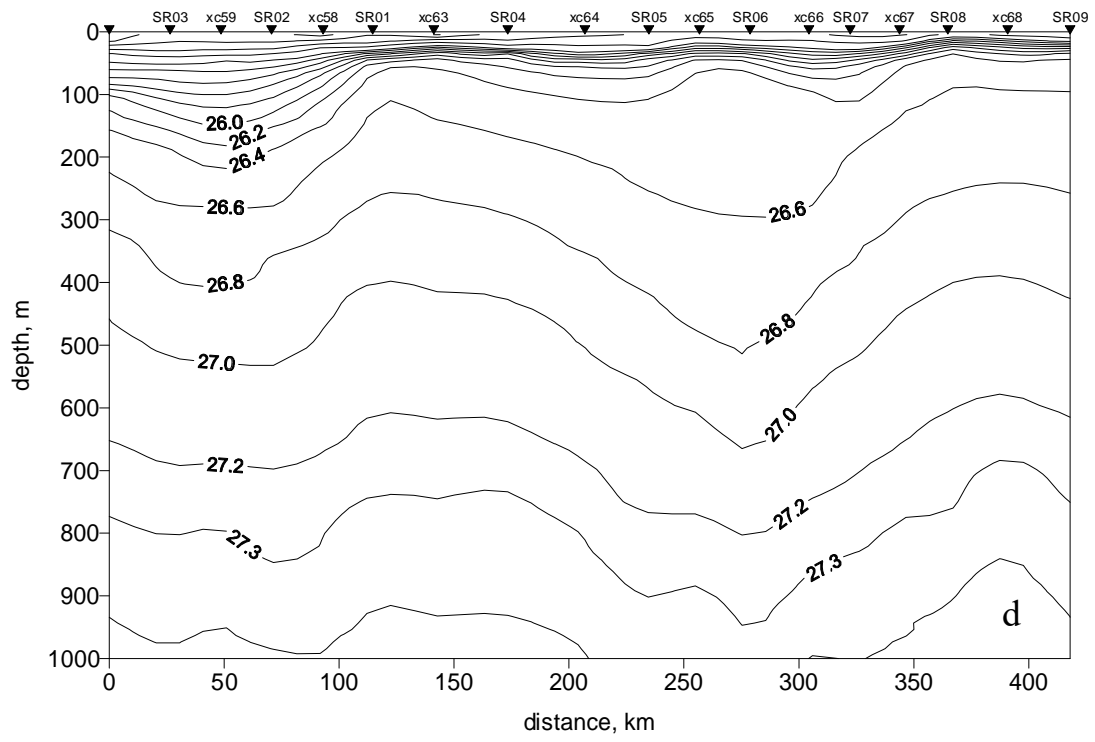


Fig. 3.11-17 Continued.

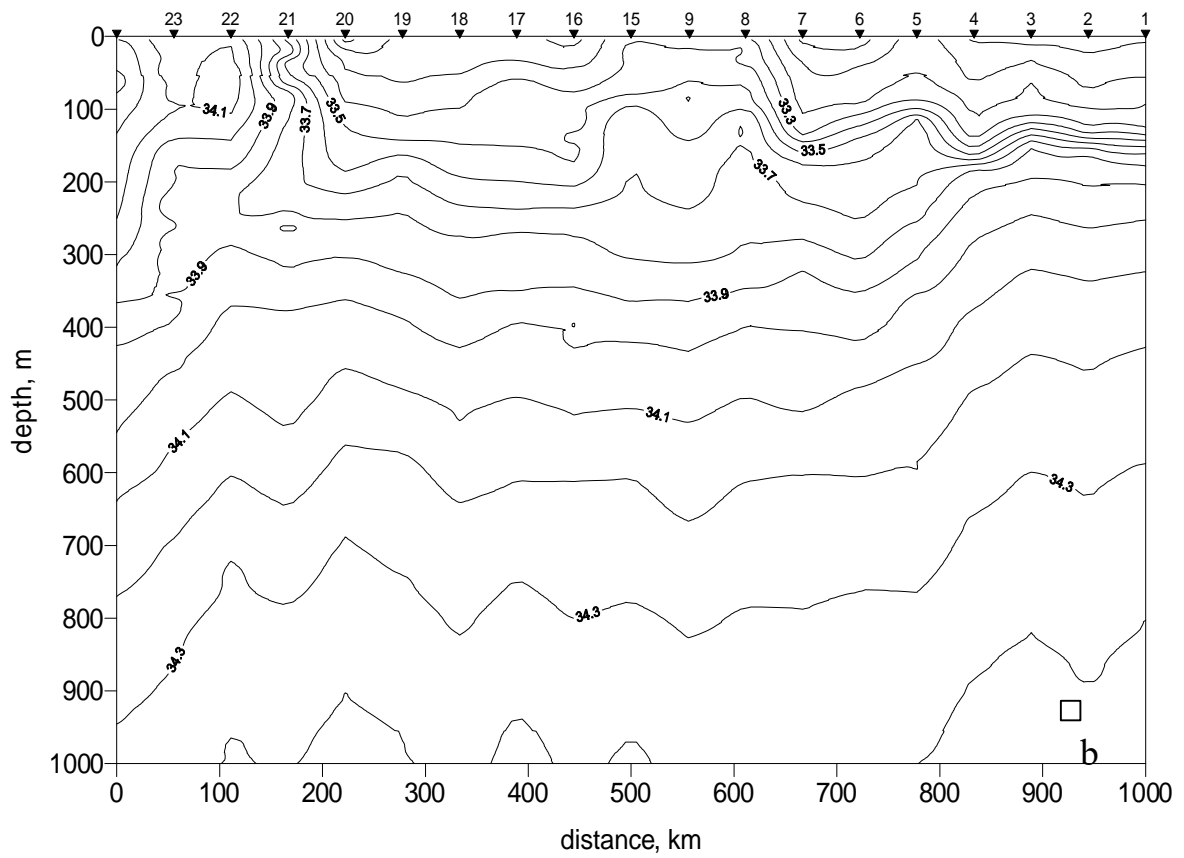
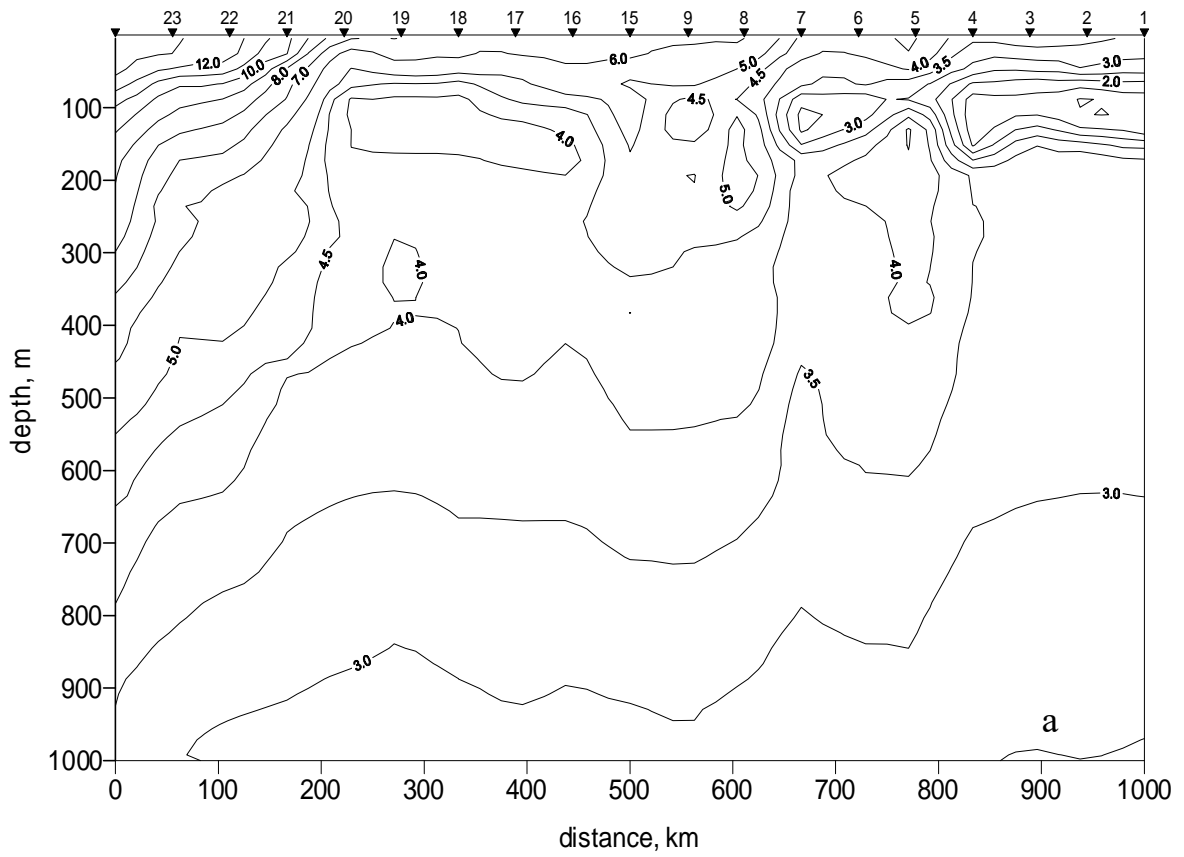


Fig. 3.11-18 Vertical sections of potential temperature (a), salinity (b), potential density (c) along 165° E (between 40° - 50° N) and TS-diagram (d) for different types of thermohaline structure

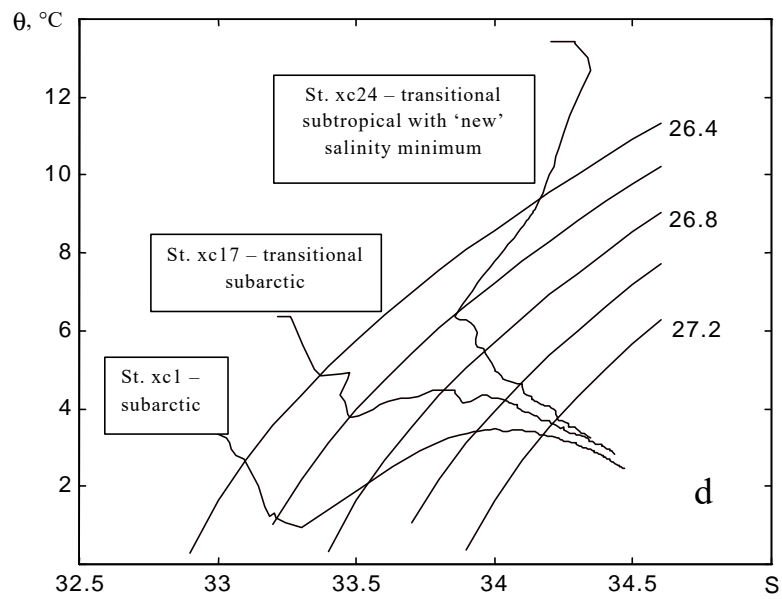
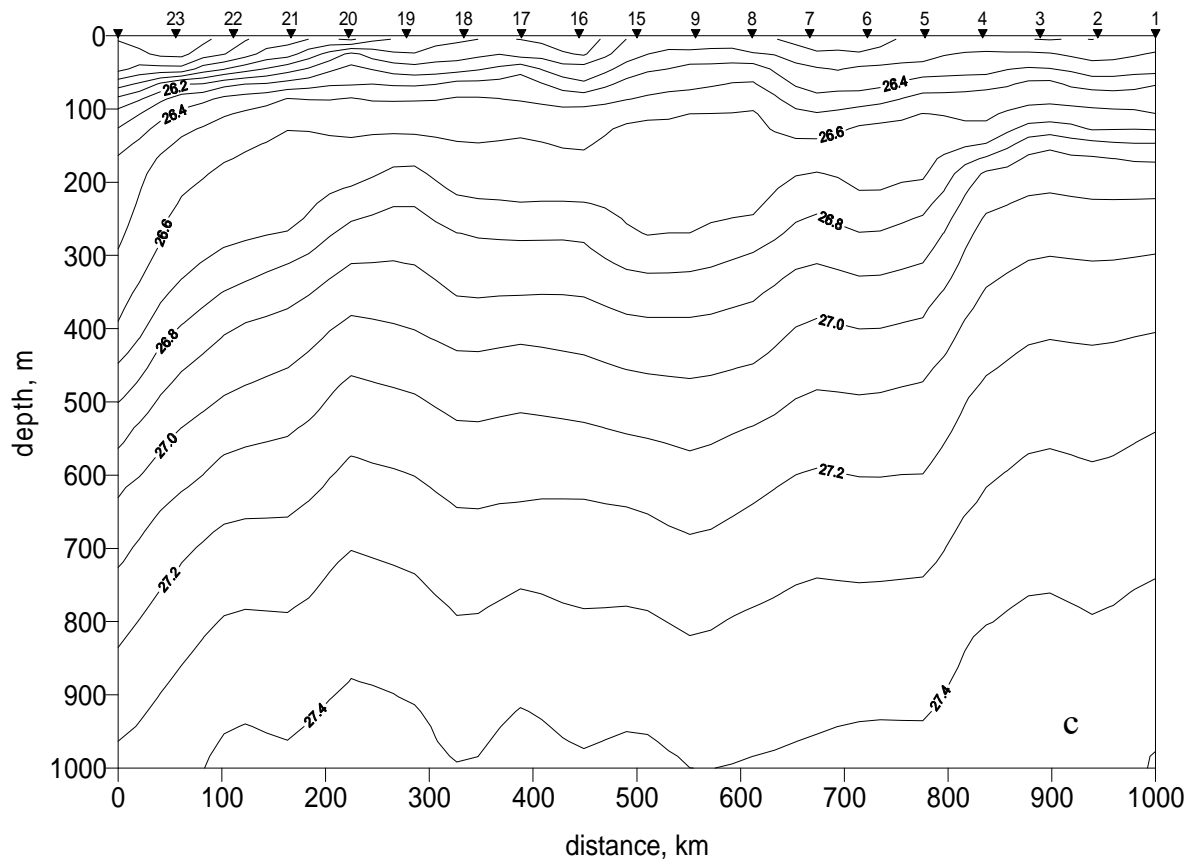


Fig. 3.11-18 Continued.

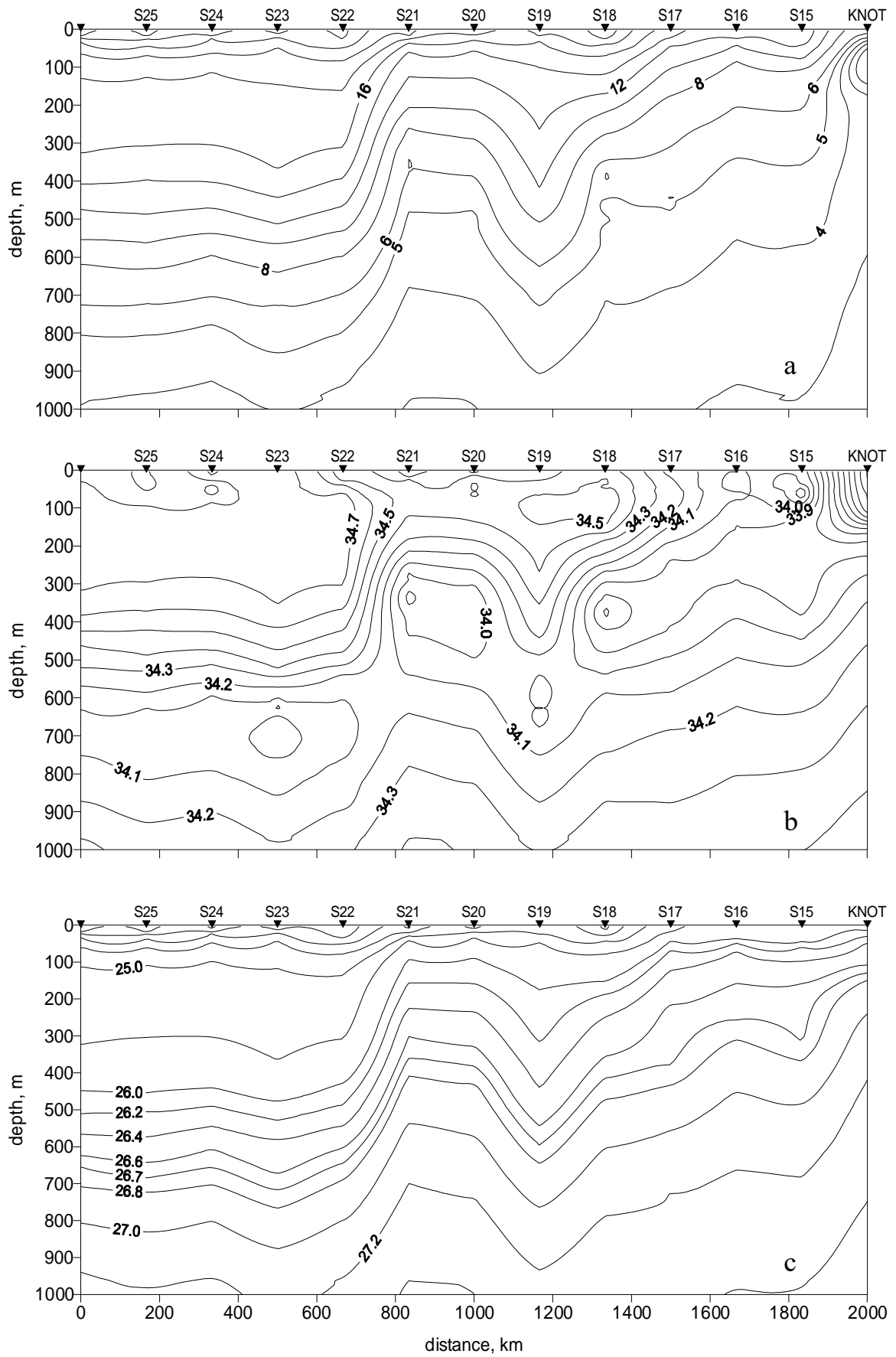


Fig. 3.11-19 Vertical sections of potential temperature (a), salinity (b) and potential density (c) along 155°E.

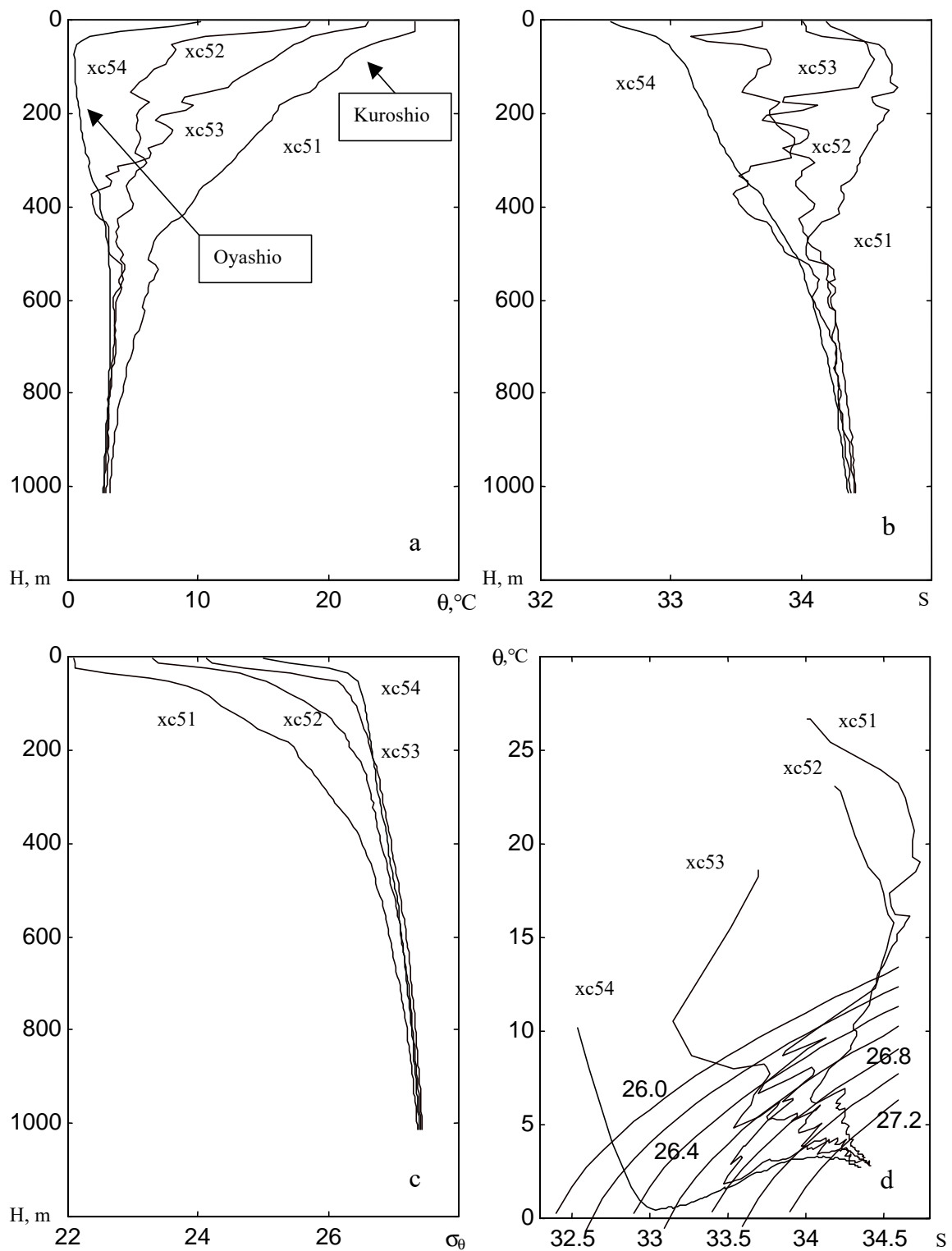


Fig. 3.11-20 Vertical profiles of potential temperature (a), salinity (b), potential density (c) and TS diagram shows main features of thermohaline structure in the Kuroshio-Oyashio interfrontal zone

Temperature

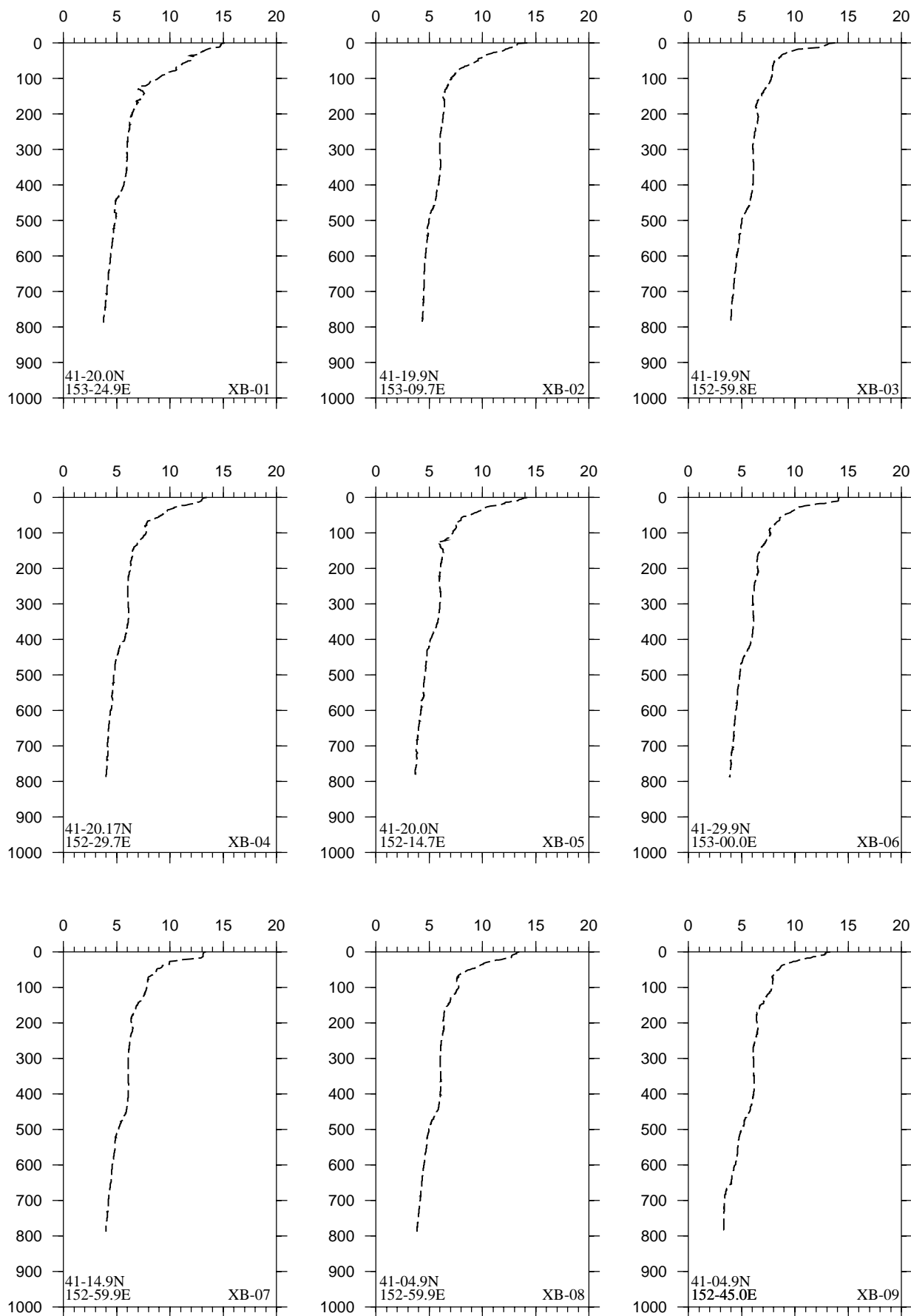


Fig.3.11-21 Vertical profiles of XBT temperature

Temperature

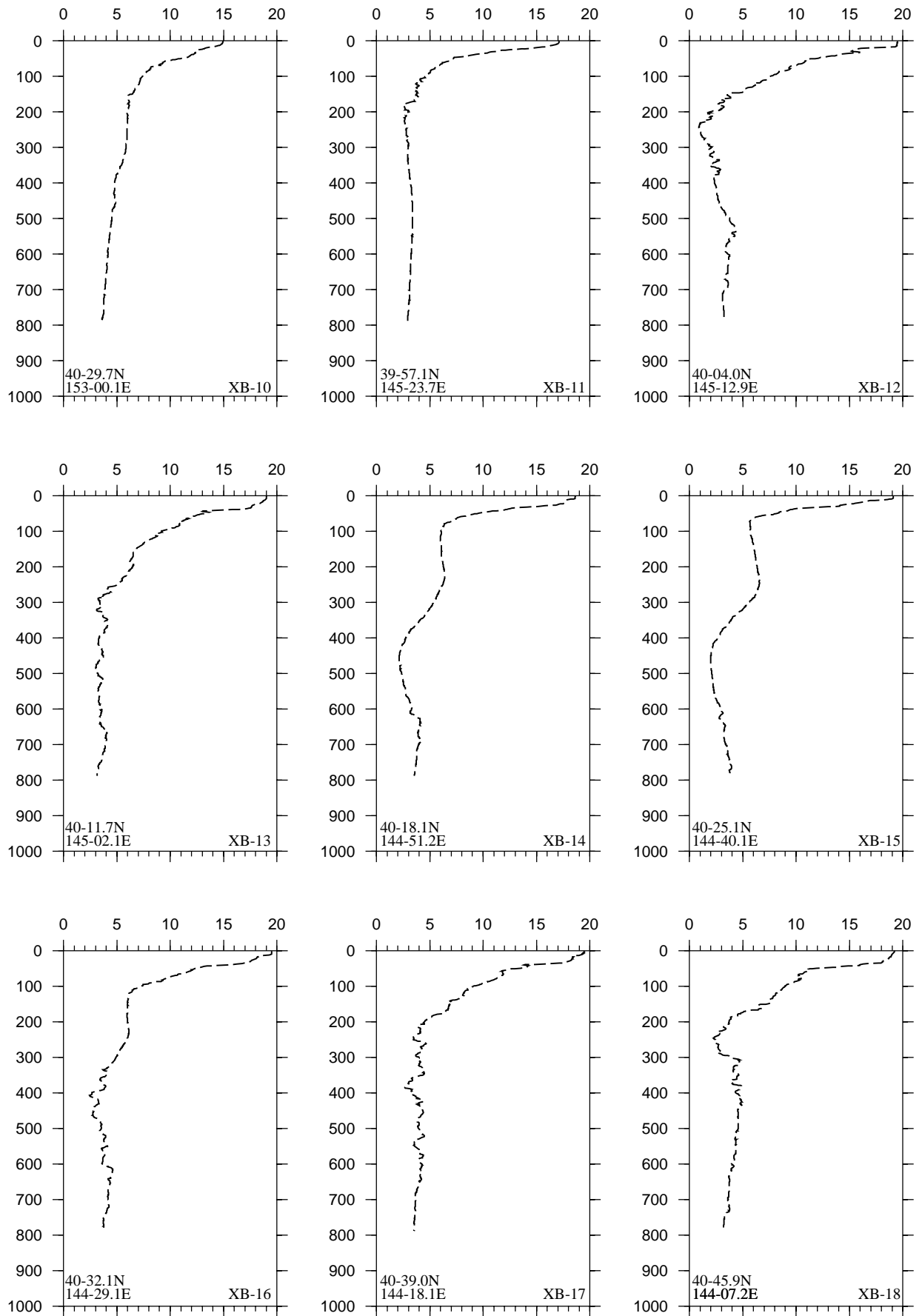


Fig.3.11-21 (continued)

Temperature

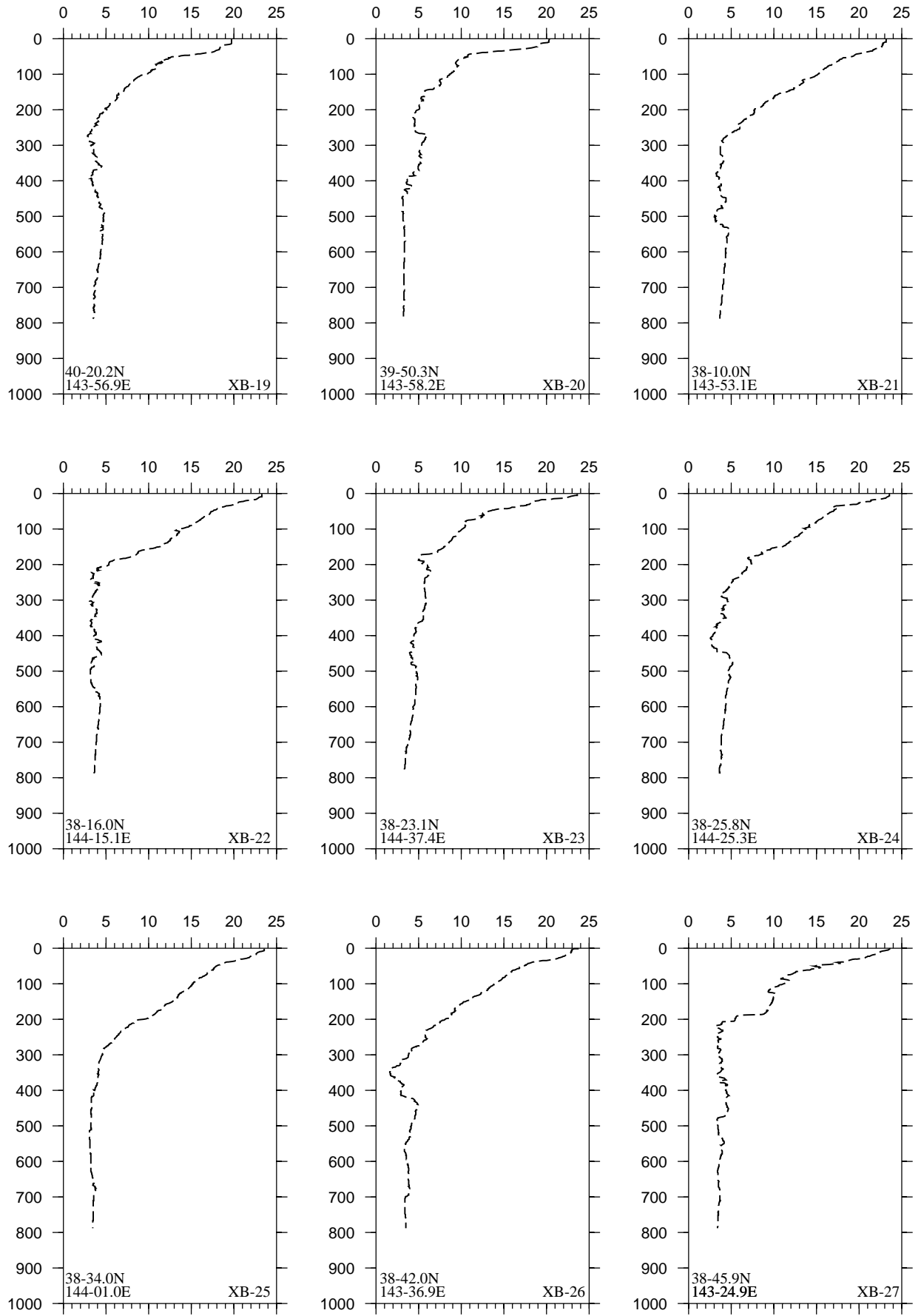


Fig.3.11-21 (continued)

Temperature

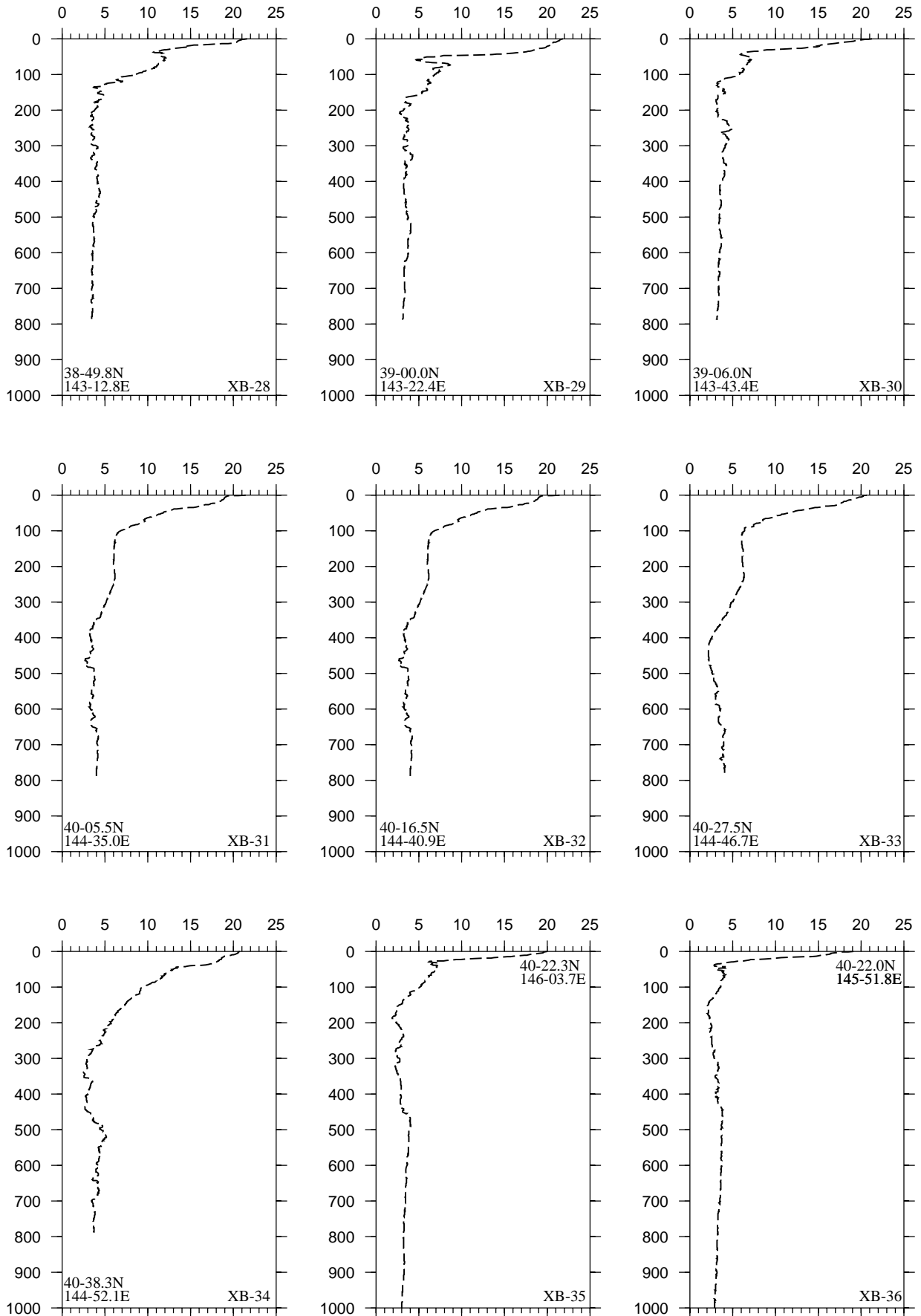


Fig.3.11-21 (continued)

Temperature

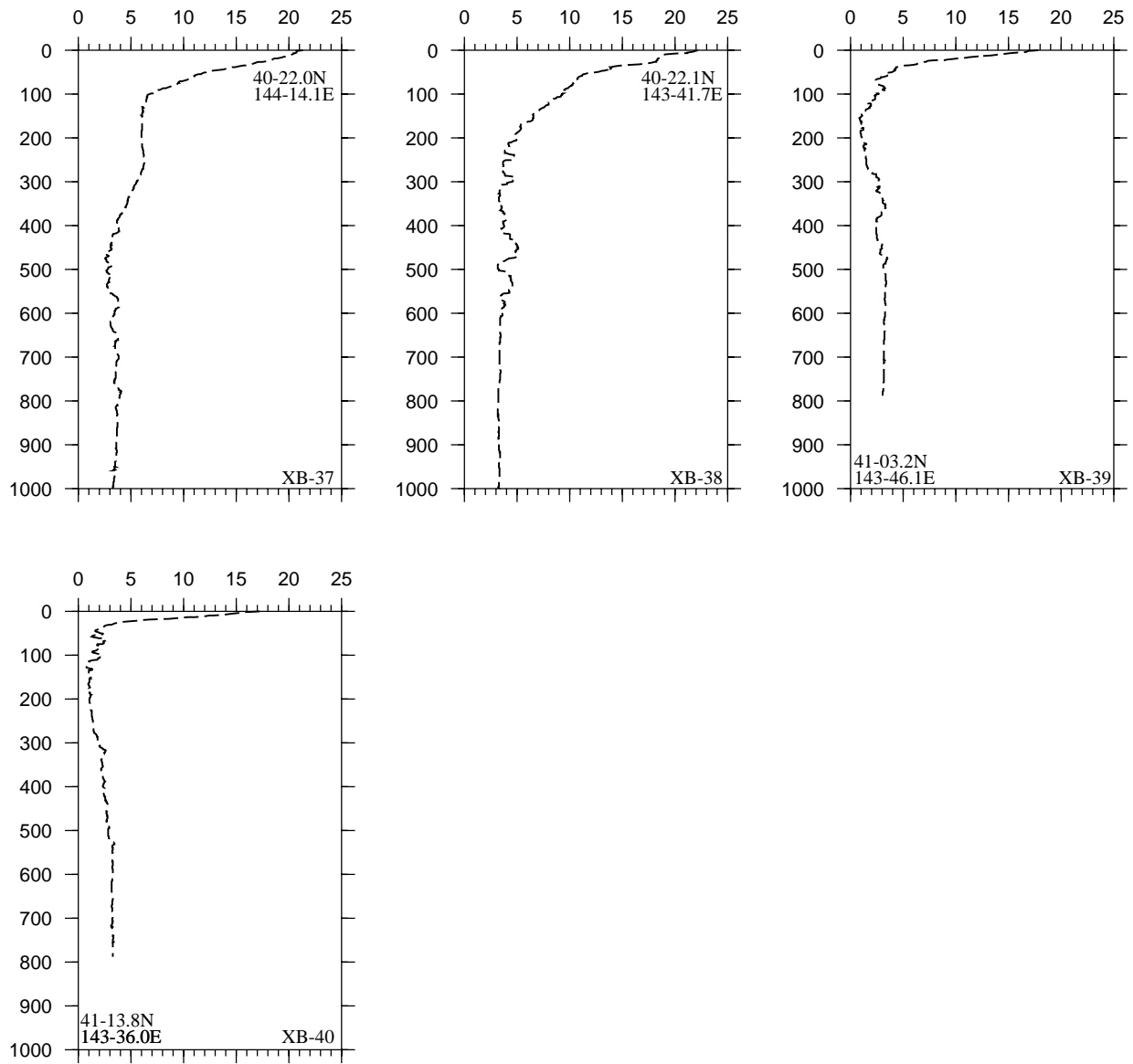
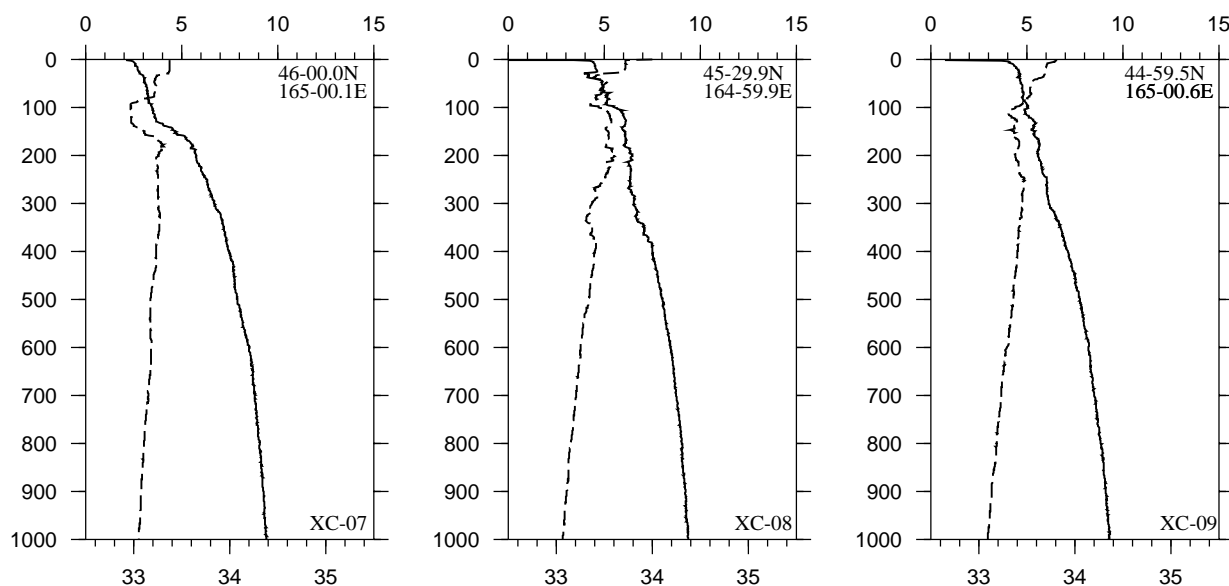
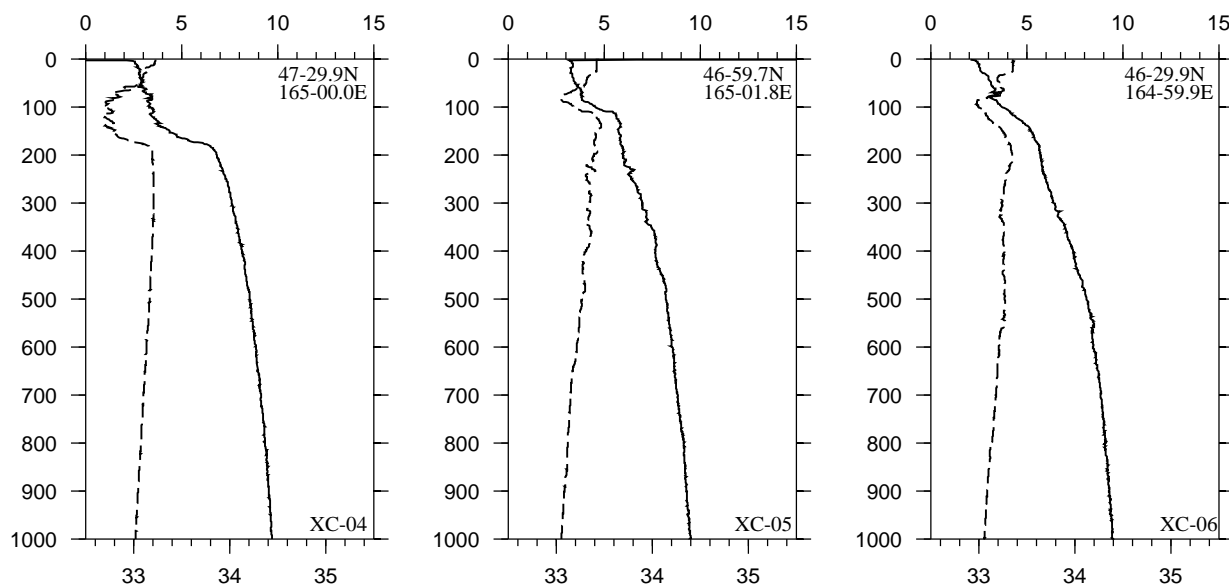
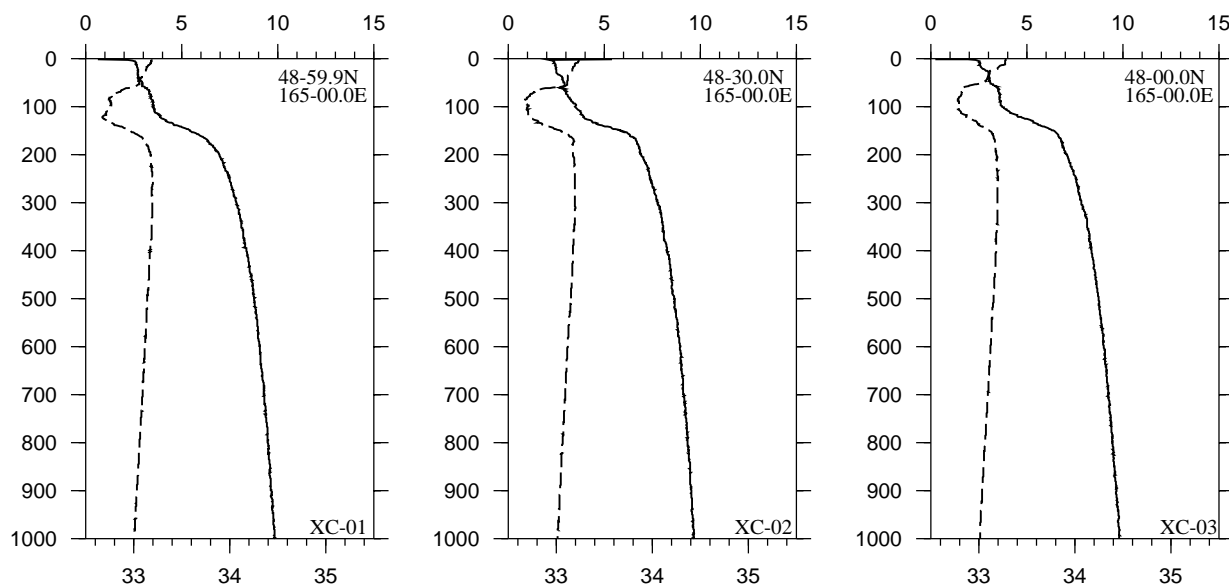


Fig.3.11-21 (continued)

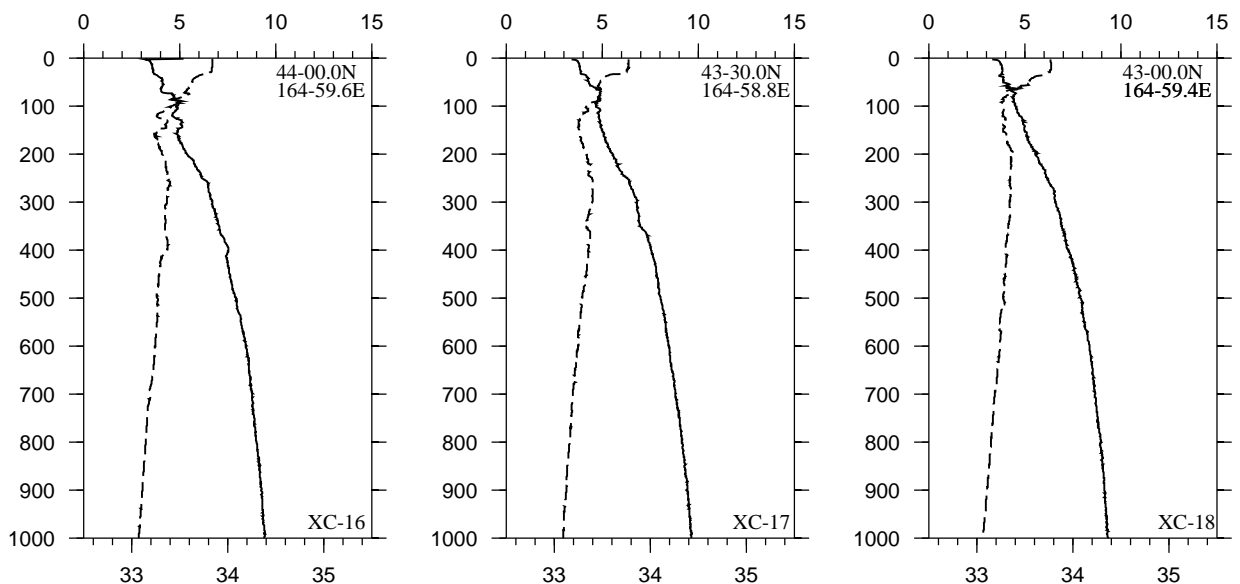
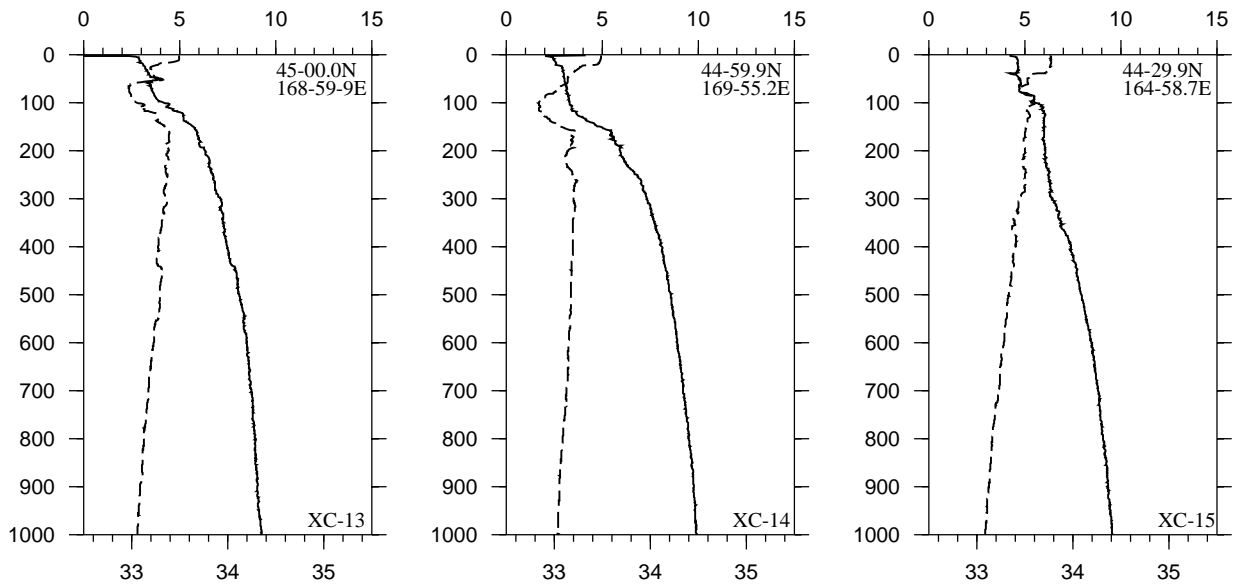
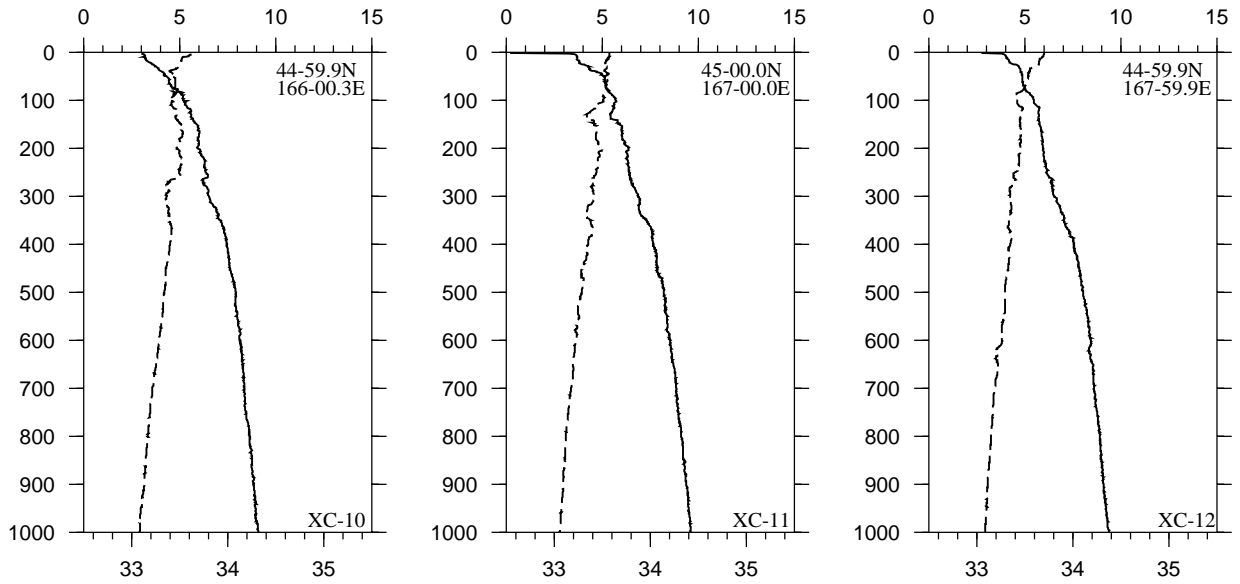
Temperature



Salinity

Fig.3.11-22 Vertical profiles of XCTD temperature and salinity

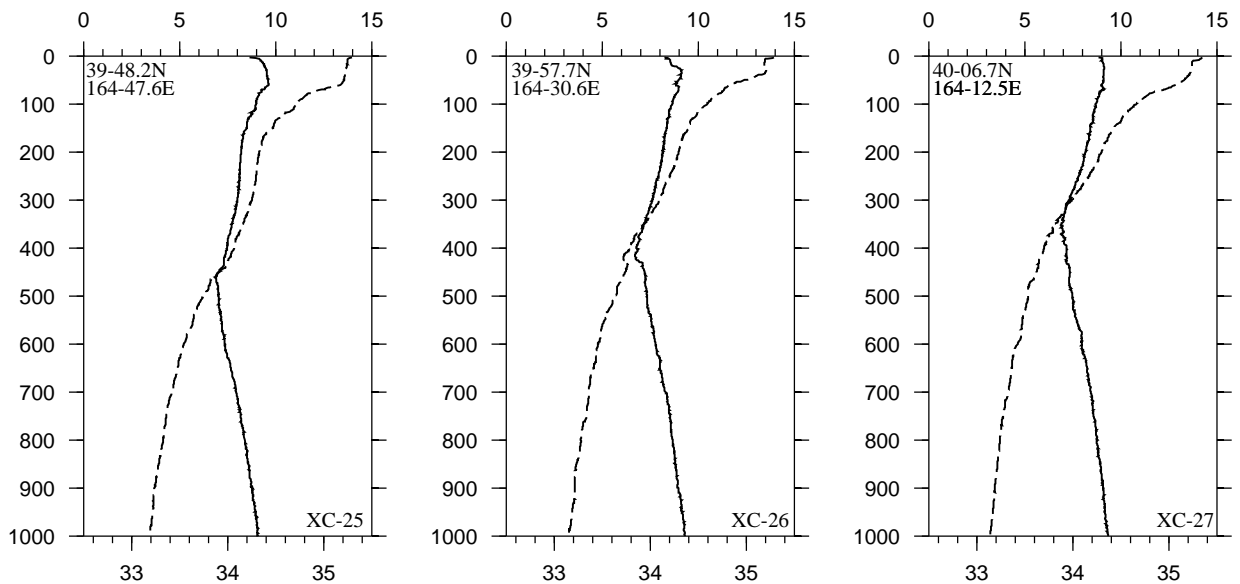
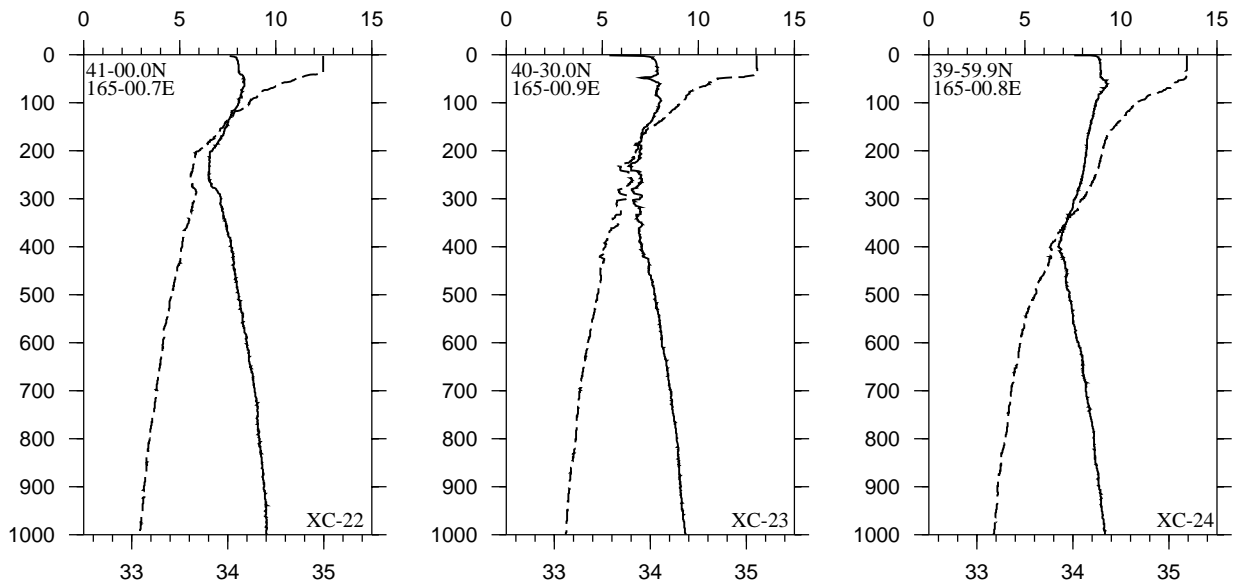
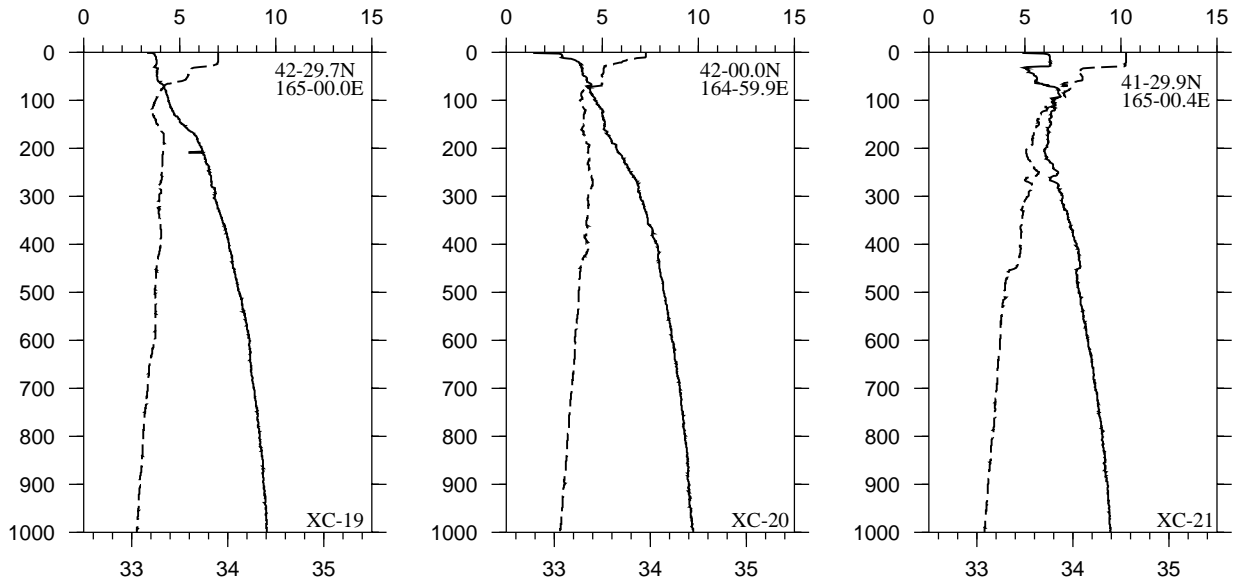
Temperature



Salinity

Fig.3.11-22(continued)

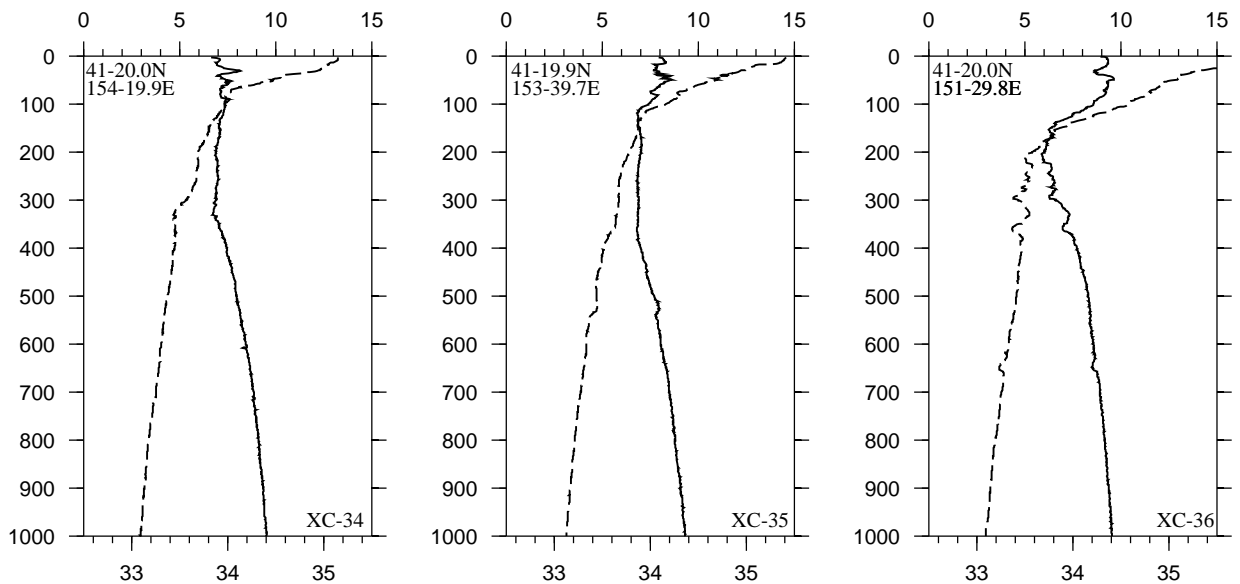
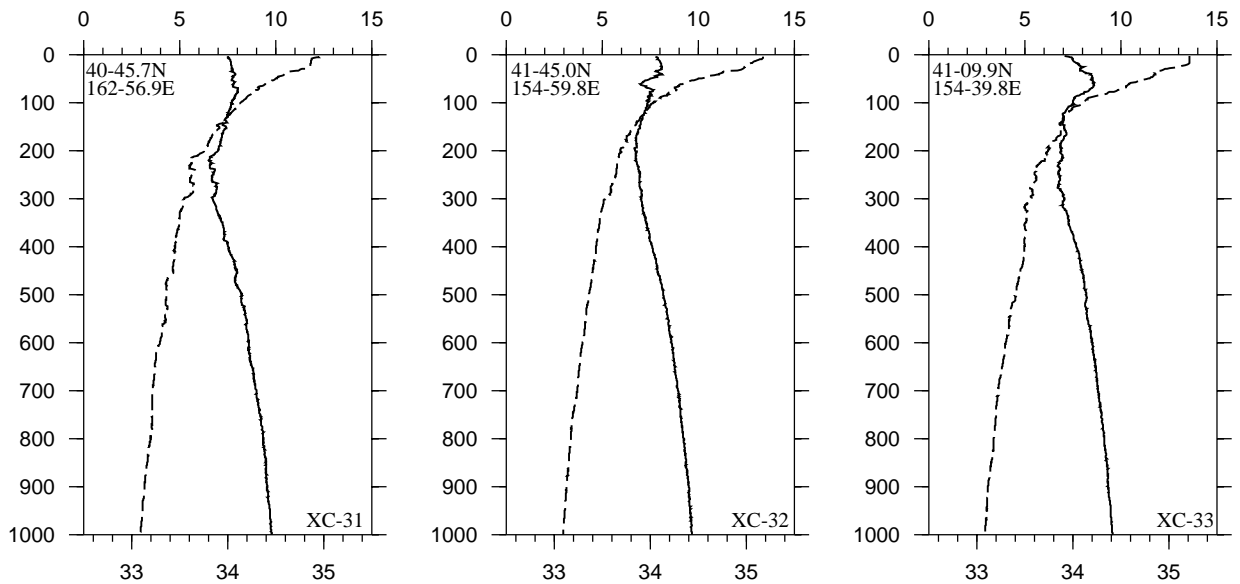
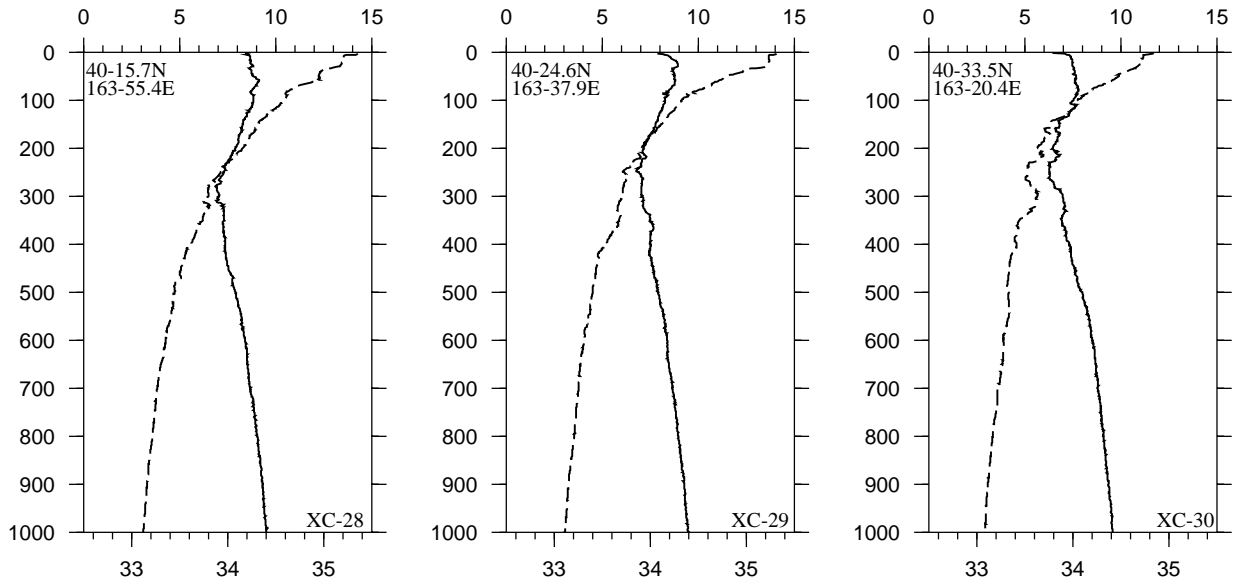
Temperature



Salinity

Fig.3.11-22(continued)

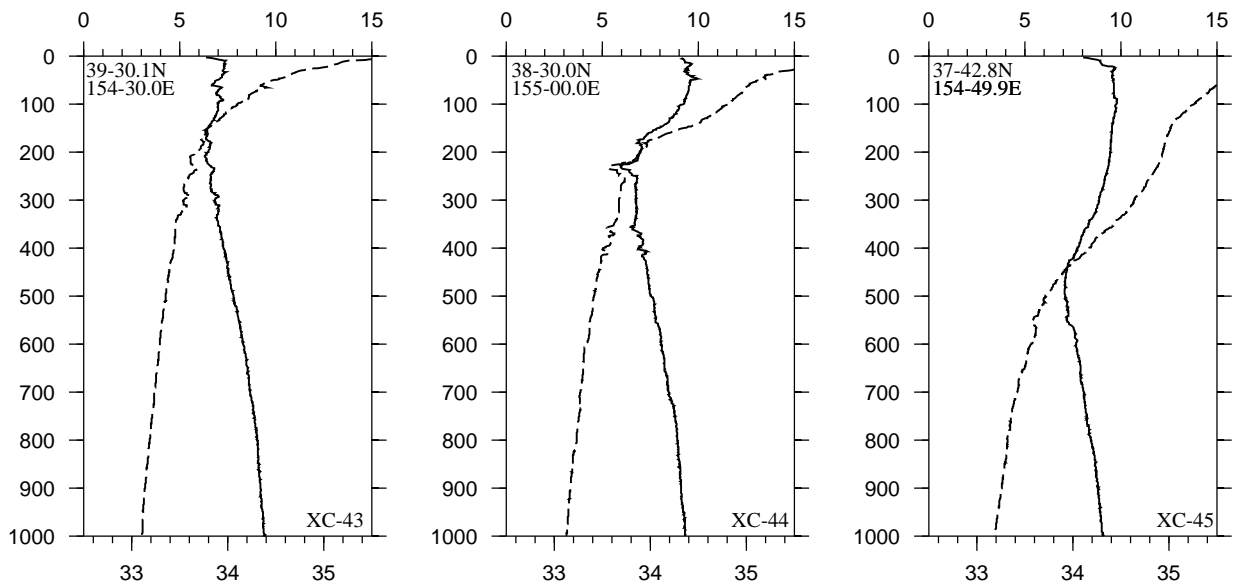
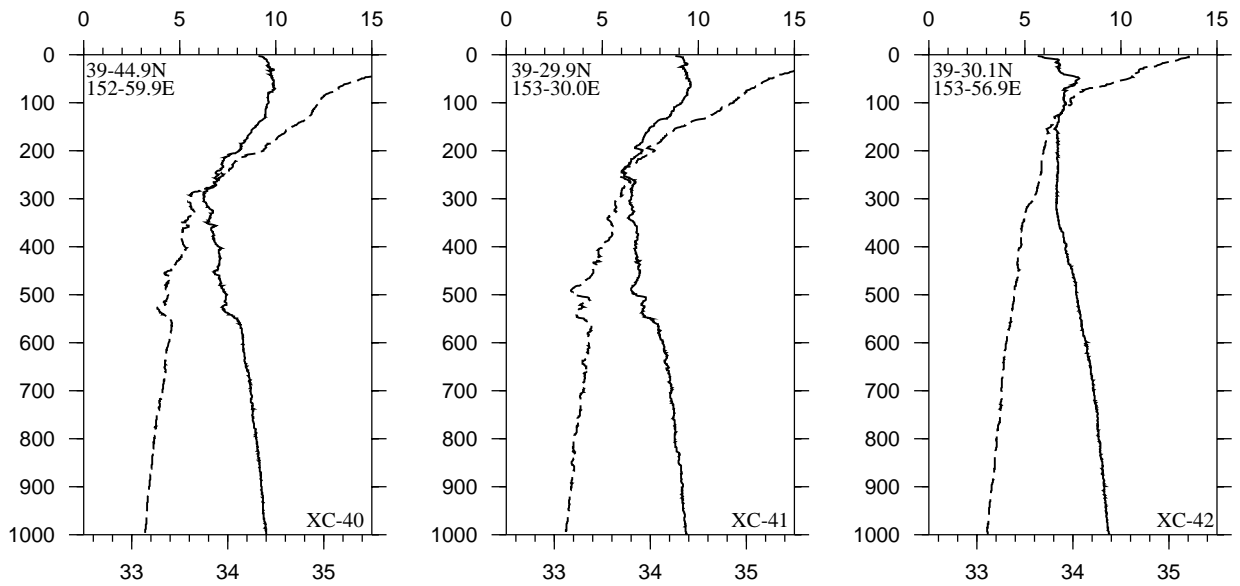
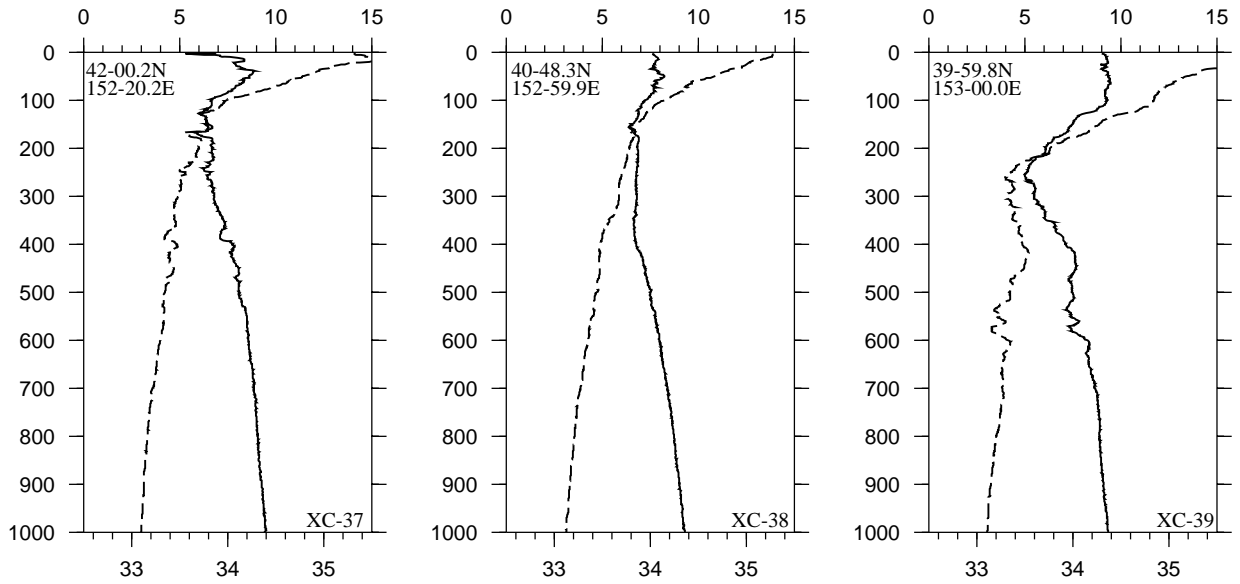
Temperature



Salinity

Fig.3.11-22(continued)

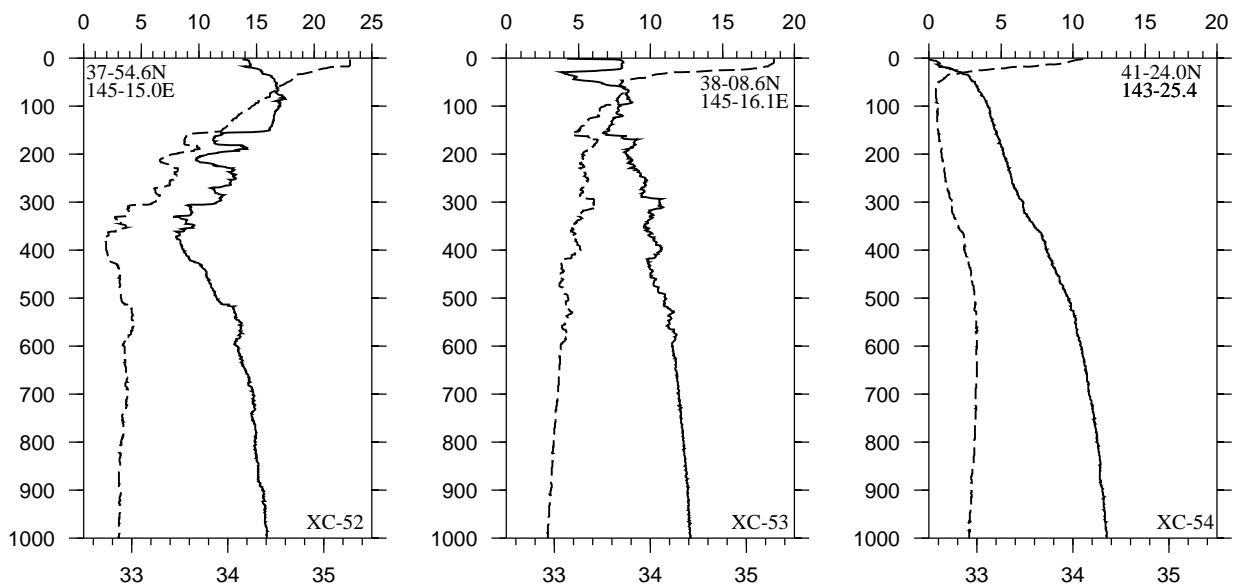
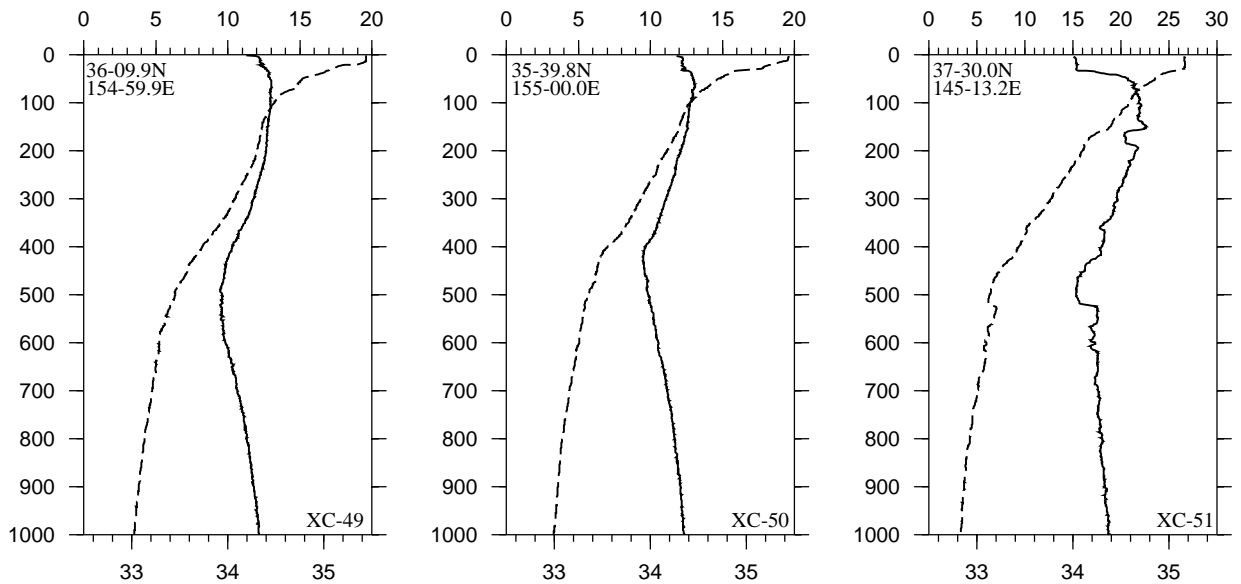
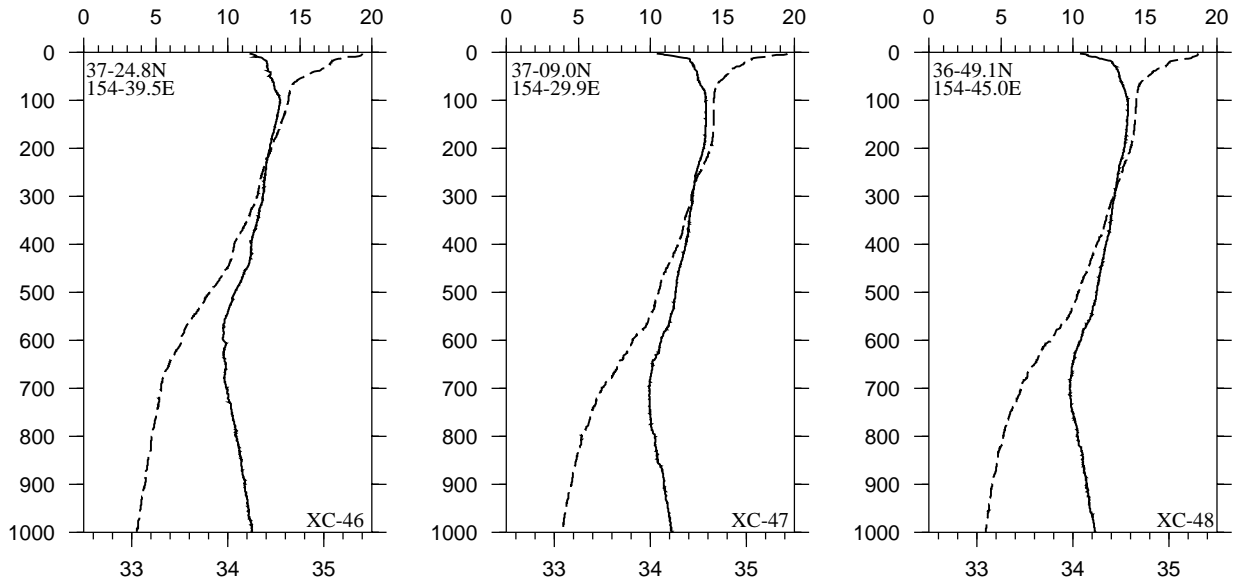
Temperature



Salinity

Fig.3.11-22(continued)

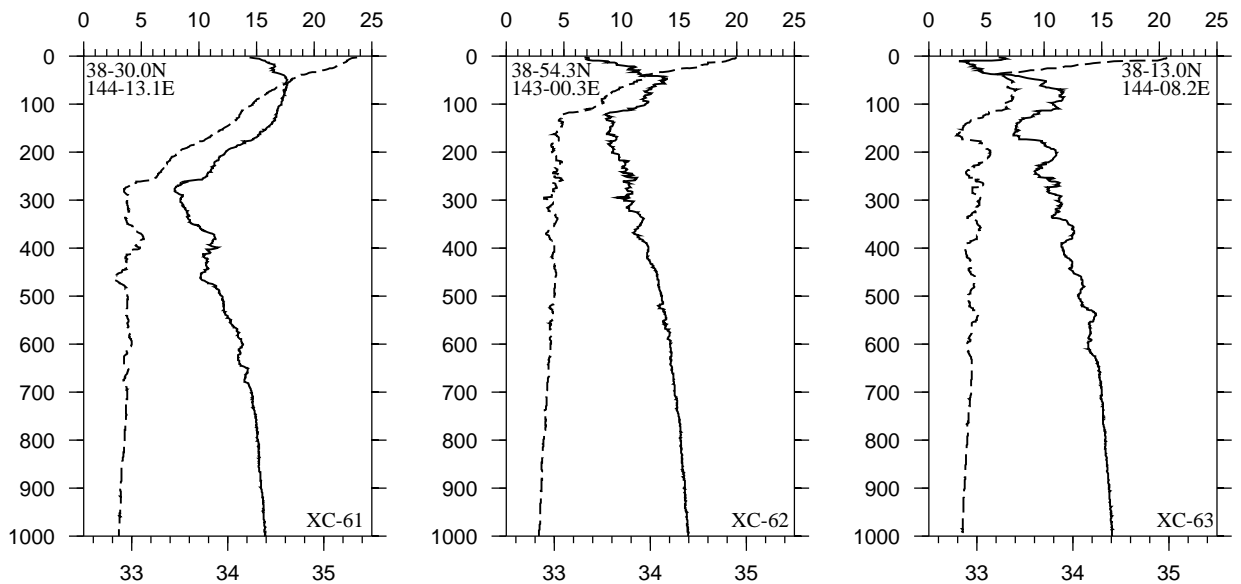
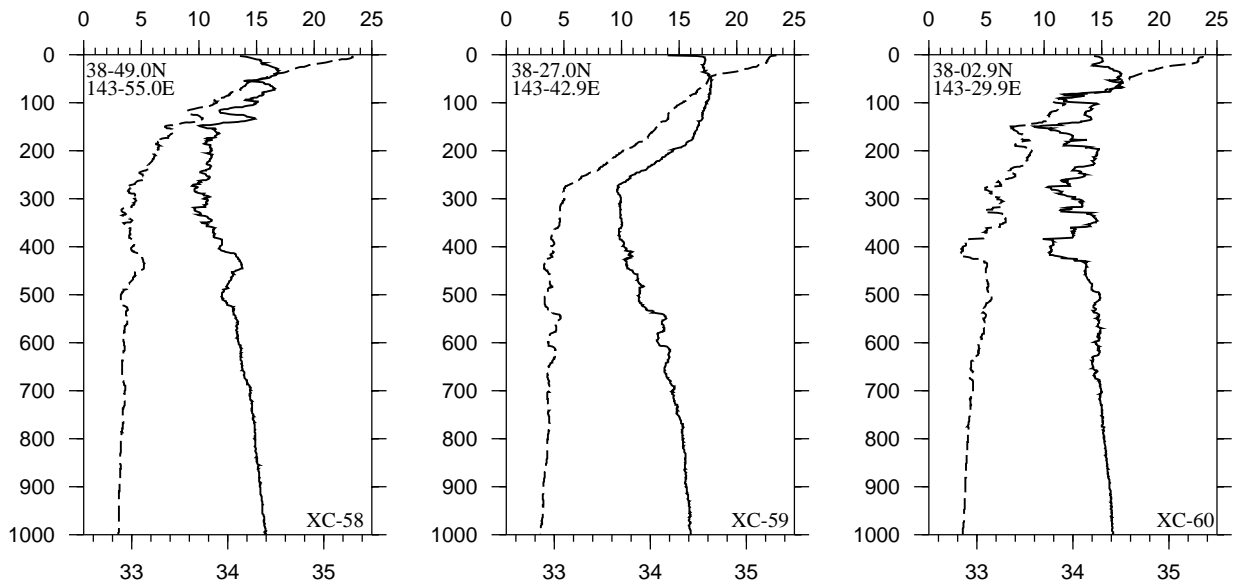
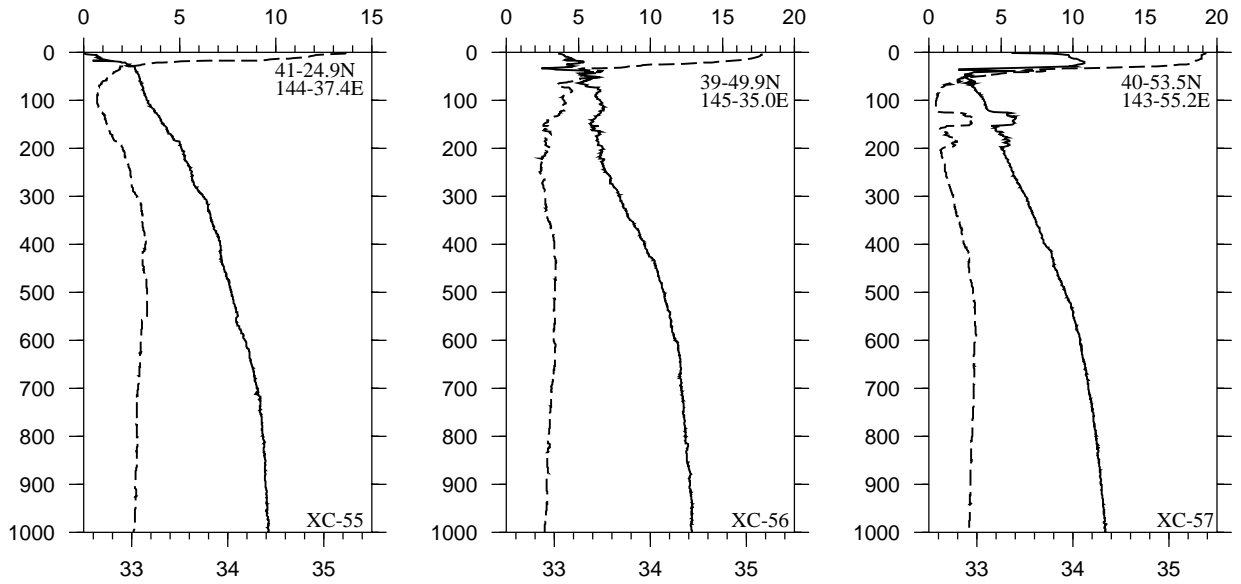
Temperature



Salinity

Fig.3.11-22(continued)

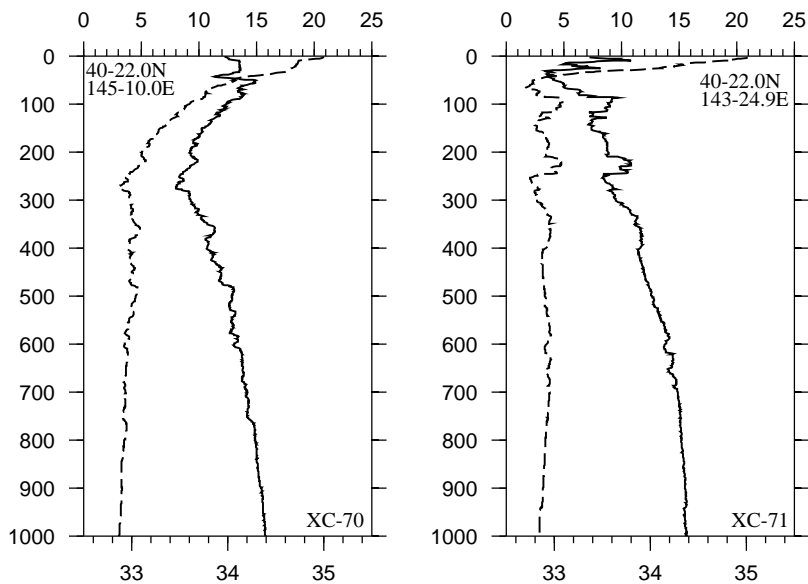
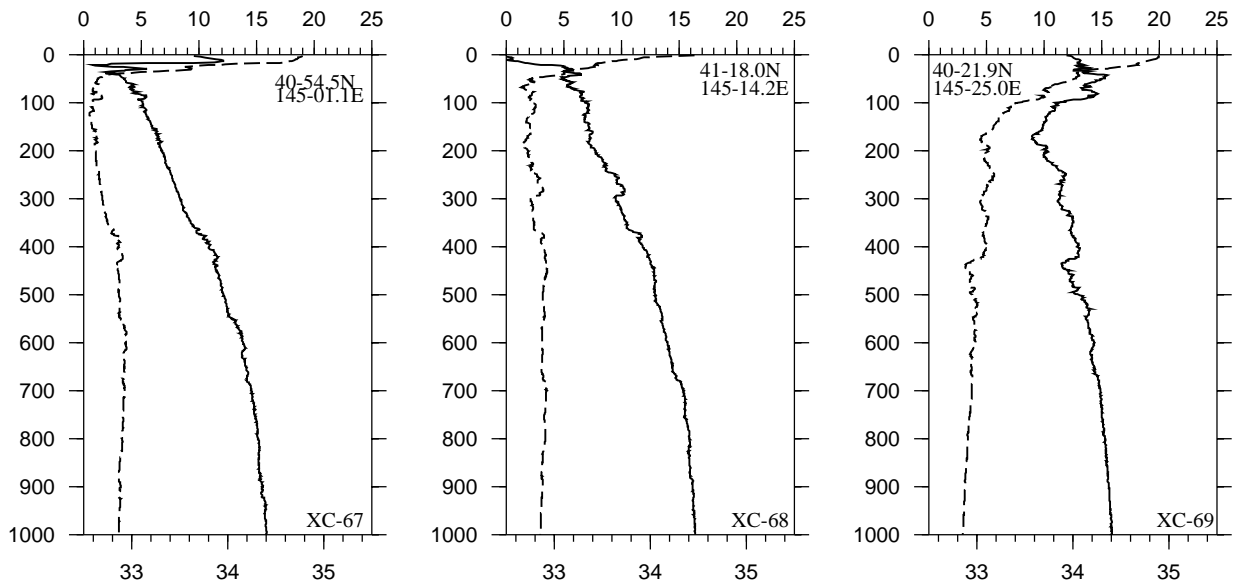
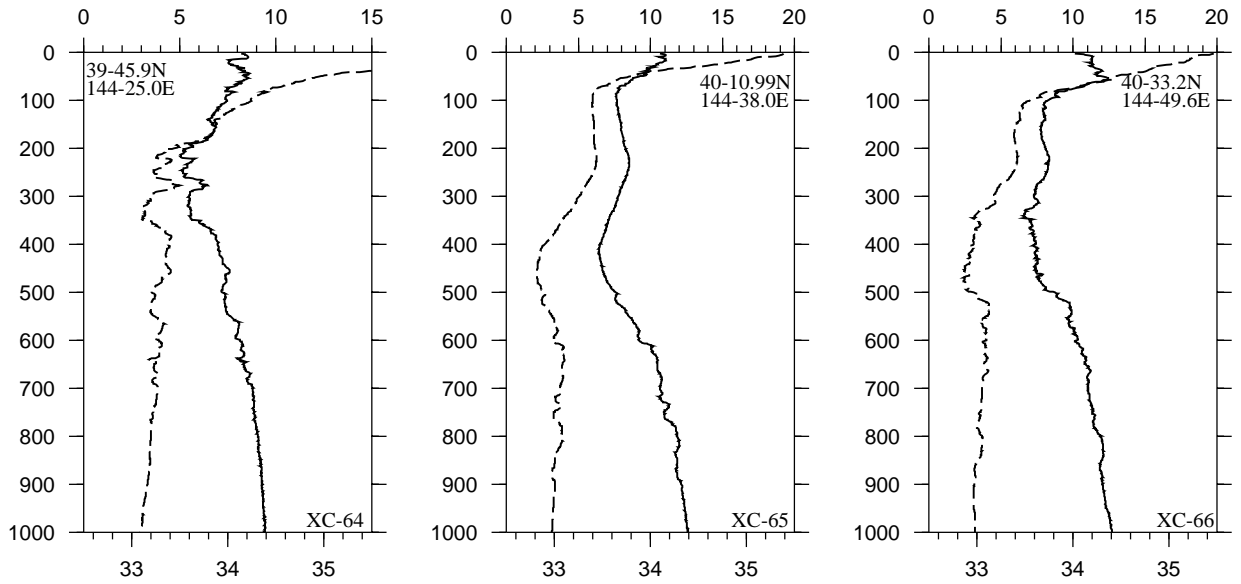
Temperature



Salinity

Fig.3.11-22(continued)

Temperature



Salinity

Fig.3.11-22(continued)

3.12 ARGO buoy

Naoto Iwasaka (FORSGC): Principal Investigator (not on board)
Taiyo Kobayashi (FORSGC) not on board
Yasuko Ichikawa (FORSGC) not on board
Hirokatsu Uno (MWJ)
Fujio Kobayashi (MWJ)
Kennichi Katayama (MWJ)
Miki Yoshiike (MWJ)
Kei Suminaga (MWJ)
Satoshi Okumura (GODI)
Wataru Tokunaga (GODI)

(1) Objectives

The objective of deployment is to clarify the structure and temporal /spatial variability of the dichothermal and the mesothermal waters in the western subarctic region of the North Pacific.

The dichothermal water, characterized by a temperature minimum, is formed by wintertime cooling in the western subarctic region, and spreads away from its formation region by lateral advection. The mesothermal water, characterized by a temperature maximum, is formed by the northward advection of the warm and saline subtropical water beyond the subarctic front in the subsurface layer. Formation and advection processes of the dichothermal and mesothermal waters have been studied in the climatological feature.

The profiling floats deployed in this cruise measure vertical profiles of temperature and salinity automatically every ten days.

The data from the floats will enable us to understand the formation and advection processes of the dichothermal and the mesothermal waters with time scales much smaller than the past studies.

(2) Parameters

- water temperature, salinity, and pressure
- time-averaged current velocity at the sea surface and a depth of 2000 dbar, calculated from the float positions at the sea surface

(3) Methods

1) Profiling float deployment

We deployed three APEX floats manufactured by Webb Research Ltd. The floats equip a CTD sensor of an electrode type SBE-41 made by Sea-Bird Electronics Inc.

The floats are designed to drift at a specified depth (called a parking depth) for a specified period, and then change their buoyancy by increasing volume and rise up to the sea surface. During their ascent, they measure temperature, salinity, and pressure. The floats remain at the sea surface for about one day (WMO2900055) or a half-day (WMO2900056 and 2900057), transmit their positions and the CTD data to ARGOS satellites, and then return to the parking depth by decreasing

volume. Each of the ascent and descent takes about six hours. The parameters of the deployed floats are as follows:

ARGOS PTT ID: 28937
WMO No.: 2900055
APEX Serial No.: 128
CTD sensor: SBE-41 made by Sea-Bird Electronics Inc.
Cycle: 10 days (Parking Depth: 213 hours, Sea Surface: 27 hours)
Target Parking Pressure: 2000 dbar
Reset Date and Time: 02:20 June 13, 2001 (GMT)
Deployed Date and Time: 04:56 June 13, 2001 (GMT)
Deployed Position: 46°59.79'N, 165°01.85'E

ARGOS PTT ID: 06501
WMO No.: 2900056
APEX Serial No.: 227
CTD sensor: SBE-41 made by Sea-Bird Electronics Inc.
Cycle: 10 days (Parking Depth: 225 hours, Sea Surface: 15 hours)
Target Parking Pressure: 2000 dbar
Reset Date and Time: 02:41 June 14, 2001 (GMT)
Deployed Date and Time: 04:56 June 14, 2001 (GMT)
Deployed Position: 44°59.57'N, 165°00.54'E

ARGOS PTT ID: 06508
WMO No.: 2900057
APEX Serial No.: 234
CTD sensor: SBE-41 made by Sea-Bird Electronics Inc.
Cycle: 10 days (Parking Depth: 225 hours, Sea Surface: 15 hours)
Target Parking Pressure: 2000 dbar
Reset Date and Time: 10:03 June 17, 2001 (GMT)
Deployed Date and Time: 12:13 June 17, 2001 (GMT)
Deployed Position: 42°29.96'N, 165°00.01'E

It should be noted that the periods for which the floats are actually at the parking depth or the sea surface are less than those specified by the periods for descent and ascent, respectively.

2) CTD observation

A CTD cast was made just before the deployment of floats for calibration of the float sensor at St. 7 and 8. A CTD cast at St. 10 was done four days after the deployment of float due to bad weather condition (Sec. 3.2).

3) XCTD observation

XCTD observations to a depth of about 1000 dbar were made at 19 stations between 49°N and 40°N along 165°E with an interval of 30 latitude minutes and at six stations between 165°E and 170°E along 45°N with an interval of one latitude degree in order to understand the distributions of salinity and temperature around the float-deployment point (Sec. 3.2).

(4) Preliminary result

1) Sea conditions around the deployment point of floats

Distributions of temperature, salinity and potential density measured with the XCTD are shown in Figs. 3.12-1, 3.12-2 and 3.12-3, respectively. In the surface layer above about 20 dbar, the salinity from the XCTD has lower values than that from the CTD probably due to bubbles attached to the conductivity sensor, so we do not use the data above 20dbar in this analysis.

Temperature minimum layer lies at about 100 dbar to the north of 42°N, and it also corresponds to the upper part of the halocline at about 150 dbar. Temperature maximum layer lies at about 200-400 dbar, below the halocline. This temperature minimum layer is called the dichothermal water and the temperature maximum layer is called the mesothermal water, respectively. They are the typical waters of the western subarctic region of the North Pacific. The temperature of the dichothermal water is generally lower in the north; it is less than 1°C at the northern end of this section. Around 44-46°N relatively warm and saline water spreads in the upper of 600 dbar, thus the characteristics of the dichothermal and the mesothermal waters are less distinct.

Around 47°N the isopycnal surfaces denser than 26.6 sigma_theta have relatively steep slopes. This shows a stronger eastward flow in this region. A break of the dichothermal water core (colder than 2°C) will be caused to this strong flow.

Around 41-42°N the temperature and the salinity change largely, more than 6°C and 0.8 psu. There is the Subarctic (Oyashio) Front. The change of potential density in the Subarctic Front is relatively small, about 0.3 sigma_theta, due to the offset of the changes of temperature and salinity for density.

An intrusion of low salinity water from the Subarctic Front makes clear salinity minimum at the depth of about 400 dbar in the south of 41°N. The density of this salinity minimum is about 26.2 sigma_theta, which is much less dense than the North Pacific Intermediate Water, 26.8 sigma_theta.

2) Observation with profiling float

2.1. Vertical profiles of temperature and salinity

The three floats made the first ascent on the time expected from the establishment in mechanical, and transmitted the temperature and salinity data. Their earliest positions recorded at the sea surface are 47.107°N, 165.582°E for WMO2900055, 44.905°N, 165.159°E for 2900056, and 42.342°N, 164.801°E for 2900057, respectively (Fig 3.12-4).

The vertical profiles of temperature and salinity from the three floats during their first ascent and from the CTD at the station of float deployment are shown in Figs. 3.12-5, 3.12-6 and 3.12-7, respectively. Both observations are about 10-20 nautical miles apart in space and about 6-9 days in time.

The temperature and salinity from floats of WMO2900055 and 2900057 have very similar vertical profiles to those of the CTD data except at depths less than 100 dbar. The salinity profile observed by WMO2900056 has a little difference around 200-900 dbar, but the difference in the T-S diagram is relatively small.

Subsequently to the first ascent, all floats work successfully up to now.

2.2. Velocity at a 2000-m depth

The floats of WMO2900055 and 2900057 drifted westward and 2900056 drifted eastward. Averaged speeds at the parking depth are 5.4, 1.7, and 2.8 cm s⁻¹, respectively, if their drifts during the ascent and descent are ignored.

(5) Data archive

All data acquired through the ARGOS system is stored at JAMSTEC/FORSGC. The real-time data are provided to meteorological organizations via Global Telecommunication System (GTS) and utilized for analysis and forecasts of sea conditions.

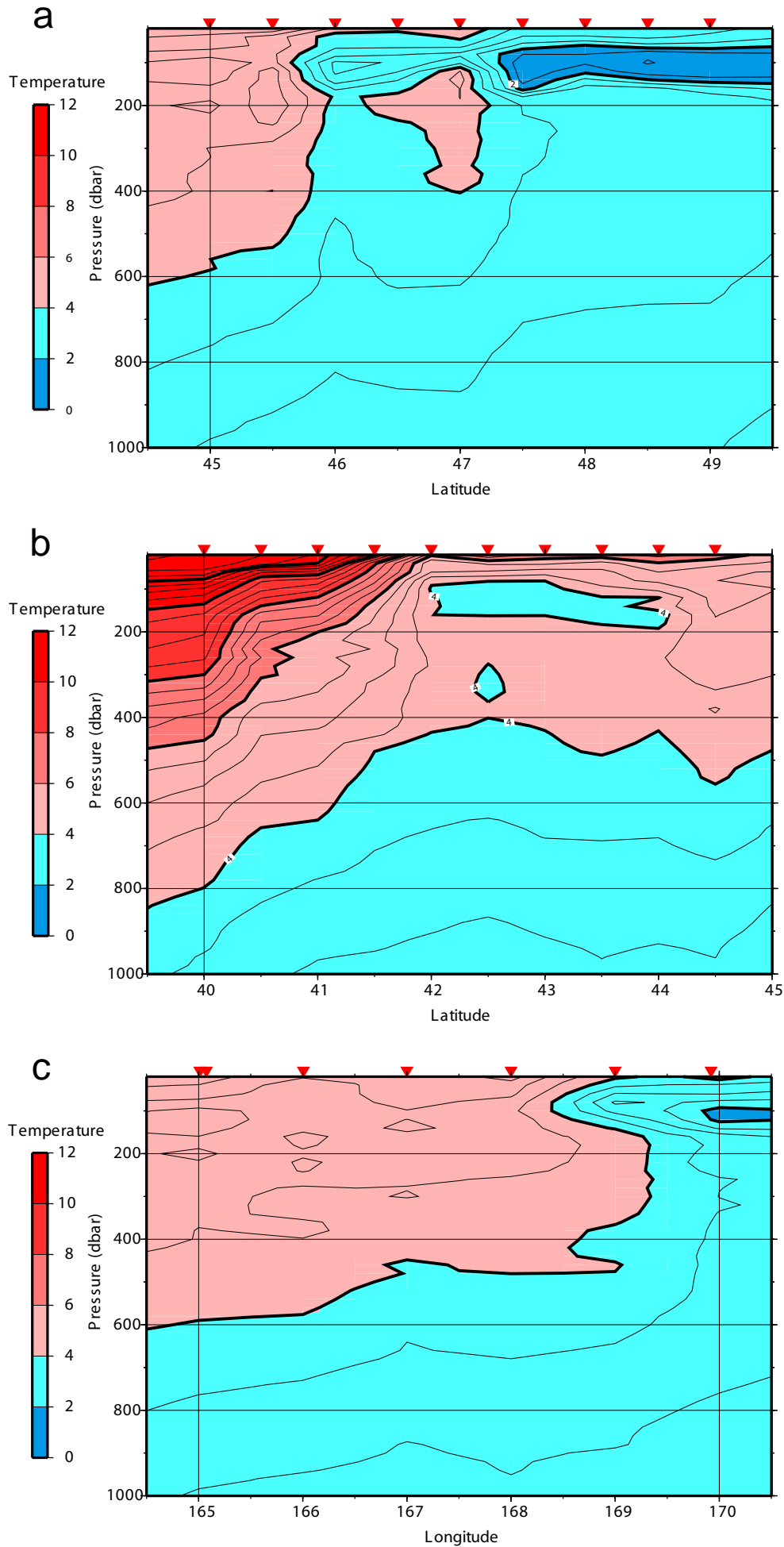


Fig. 3.12-1: Distribution of temperature (oC) measured with the XCTD.
 (a) 45-49oN and (b) 40-45oN along 165oE, and (c) 165-170oE along 45oN

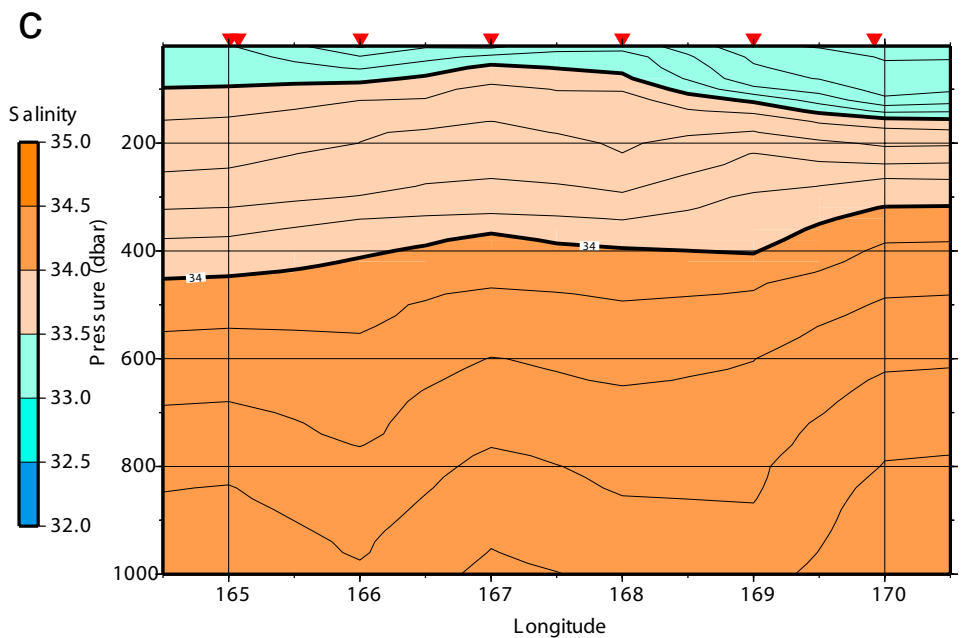
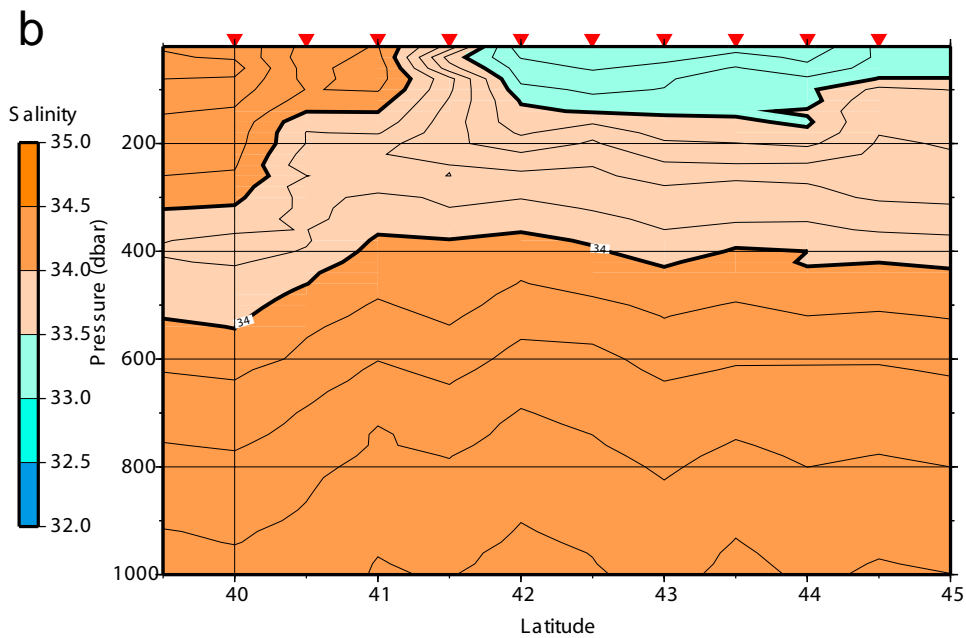
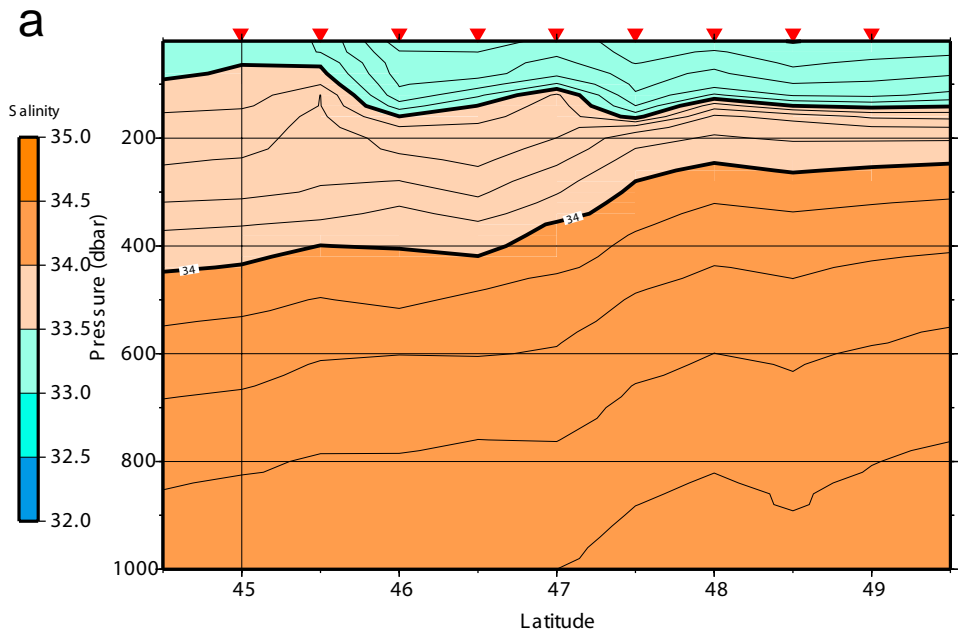


Fig. 3.12-2: Same as Fig. 3.12-1 but for salinity.

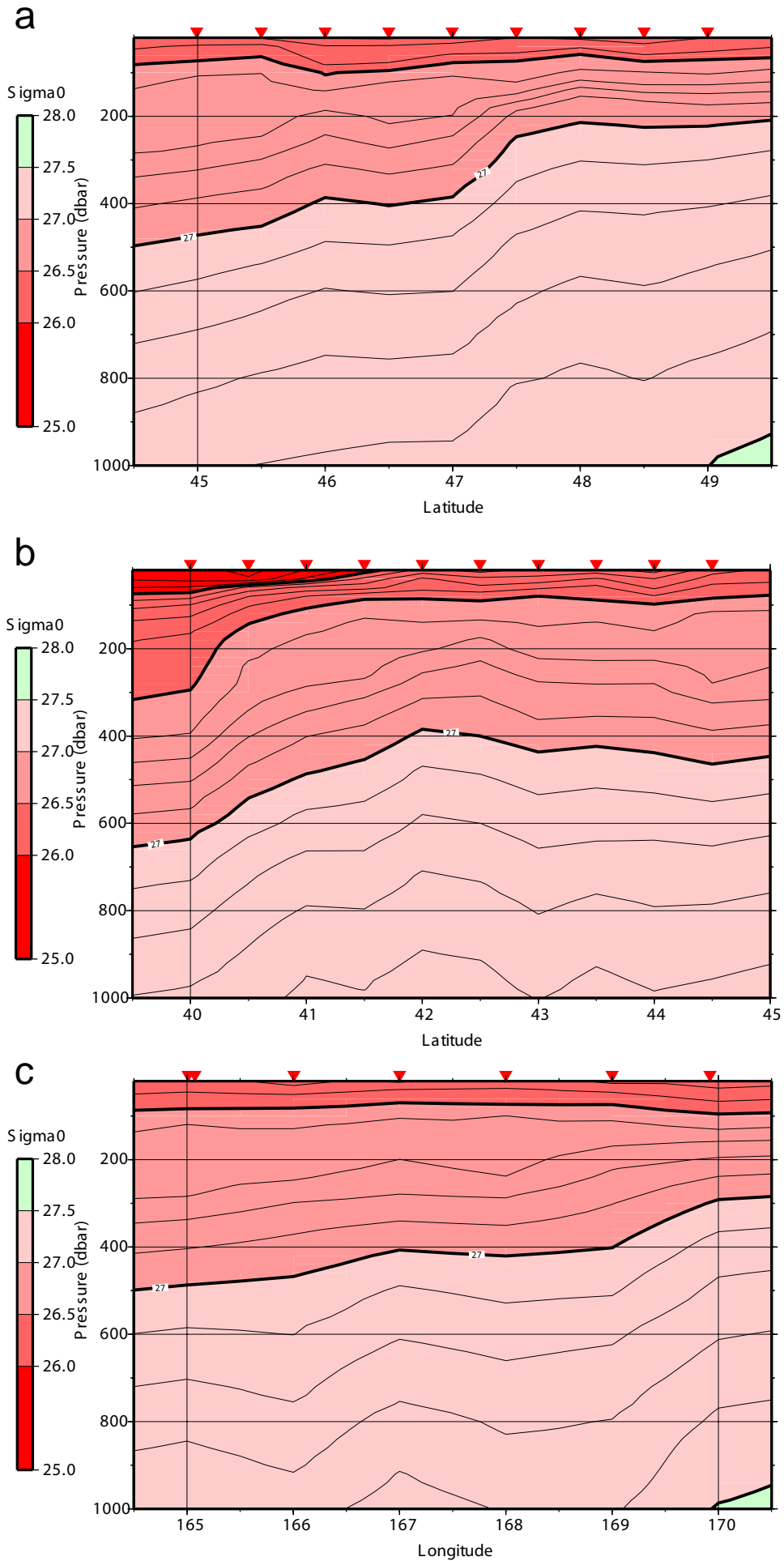


Fig. 3.12-3: Same as Fig. 3.12-1 but for potential density.

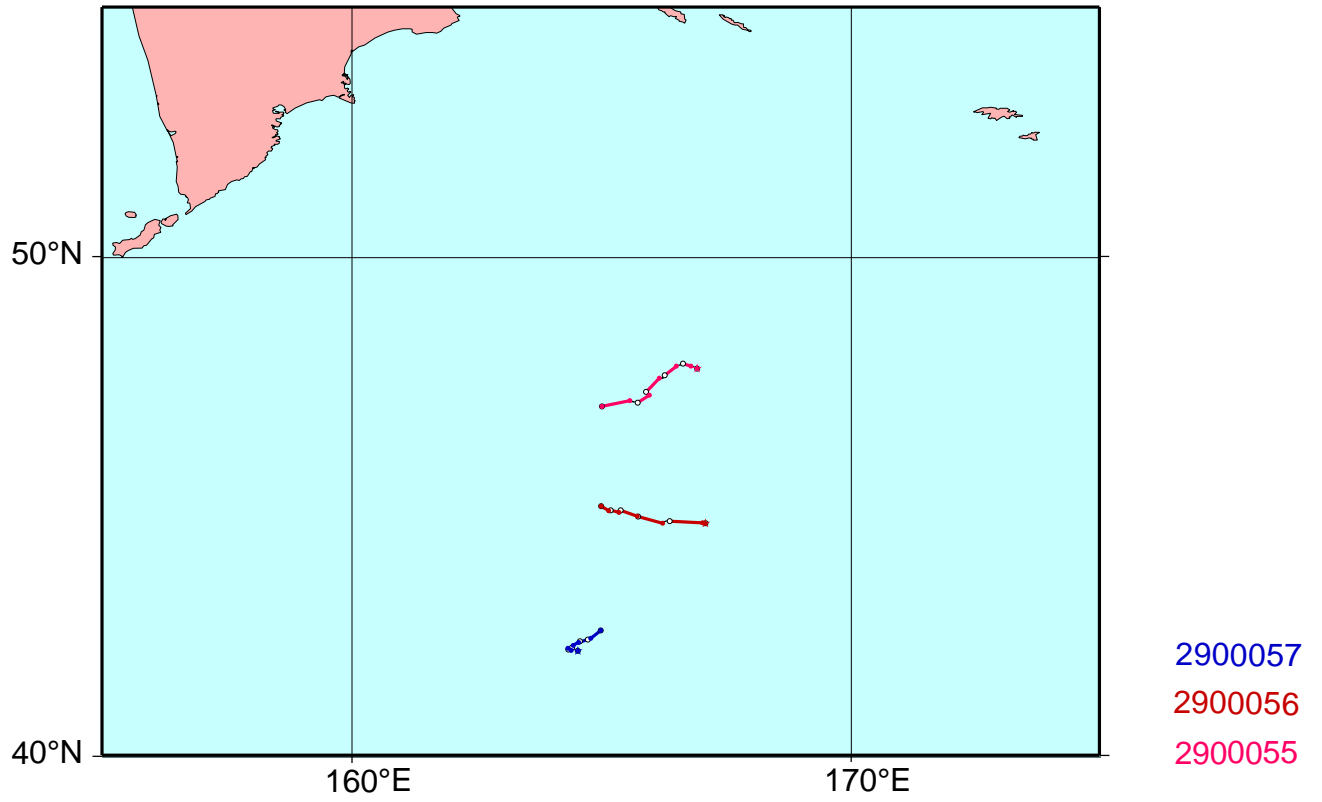


Fig. 3.12-4: Trajectories of the profiling floats during the deployments to August 6, 2001.

CTD: 2001-Jun-13 Lat: 47.0005
Lon: 165.015

Float: 2900055 2001-06-22 Lat: 47.087
Ascent No. 1 19:19:35 Lon: 165.642

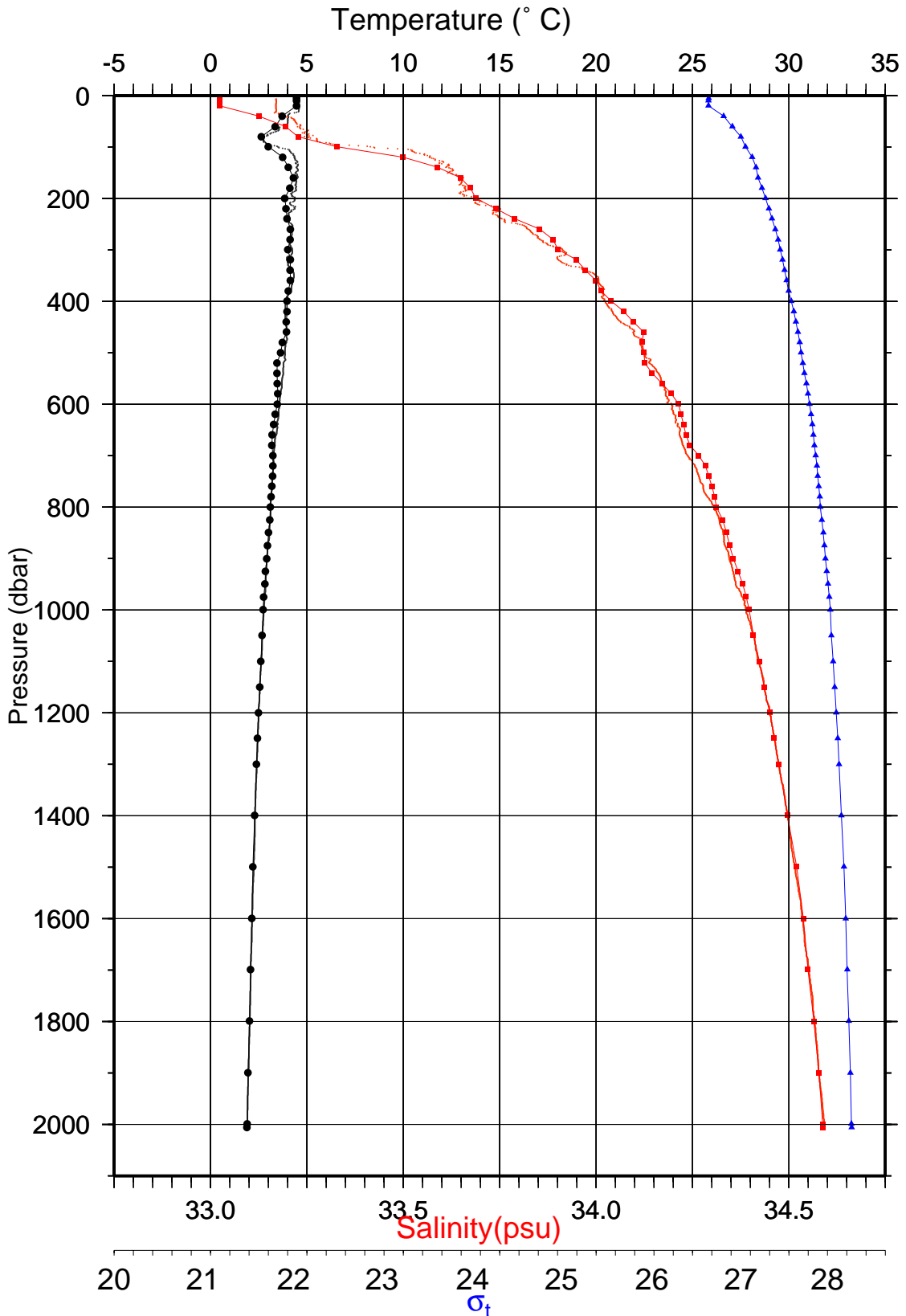


Fig. 3.12-5: Vertical profiles of temperature (oC), salinity, and potential density observed by the profiling float WMO2900055 during first ascent on Jun. 22 and with the CTD at the St. 7 of the float deployment on Jun. 13.

CTD: 2001-Jun-13 Lat: 45.0012
Lon: 165.001

Float: 2900056 2001-06-24 Lat: 44.908
Ascent No. 1 02:35:28 Lon: 165.161

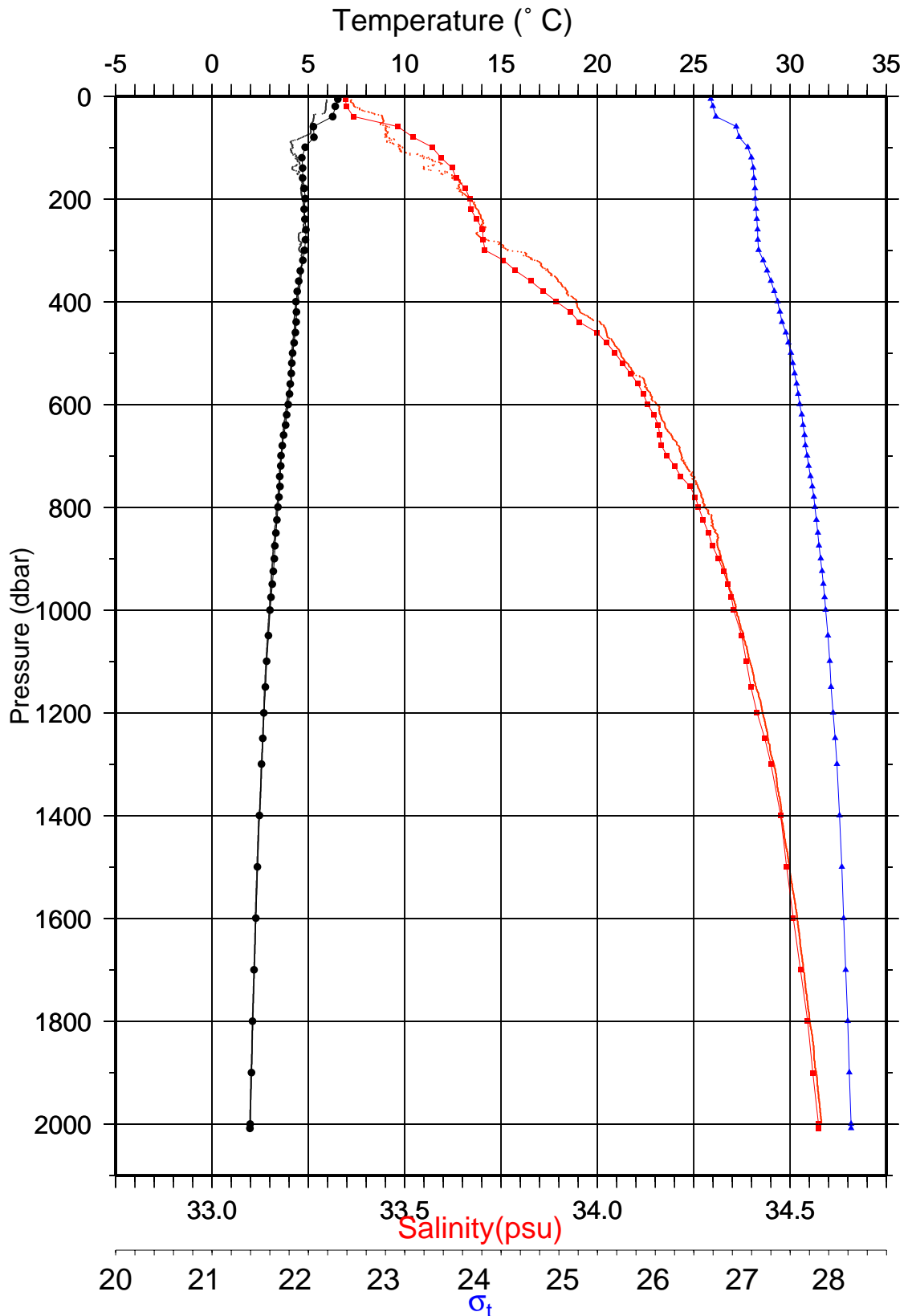


Fig. 3.12-6: Same as Fig. 3.12-5 but for the float WMO2900056 on Jun. 24 and St. 8 on Jun. 13.

CTD: 2001-Jun-21 Lat: 42.5088
Lon: 164.993

Float: 2900057 2001-06-27 Lat: 42.331
Ascent No. 1 09:12:22 Lon: 164.795

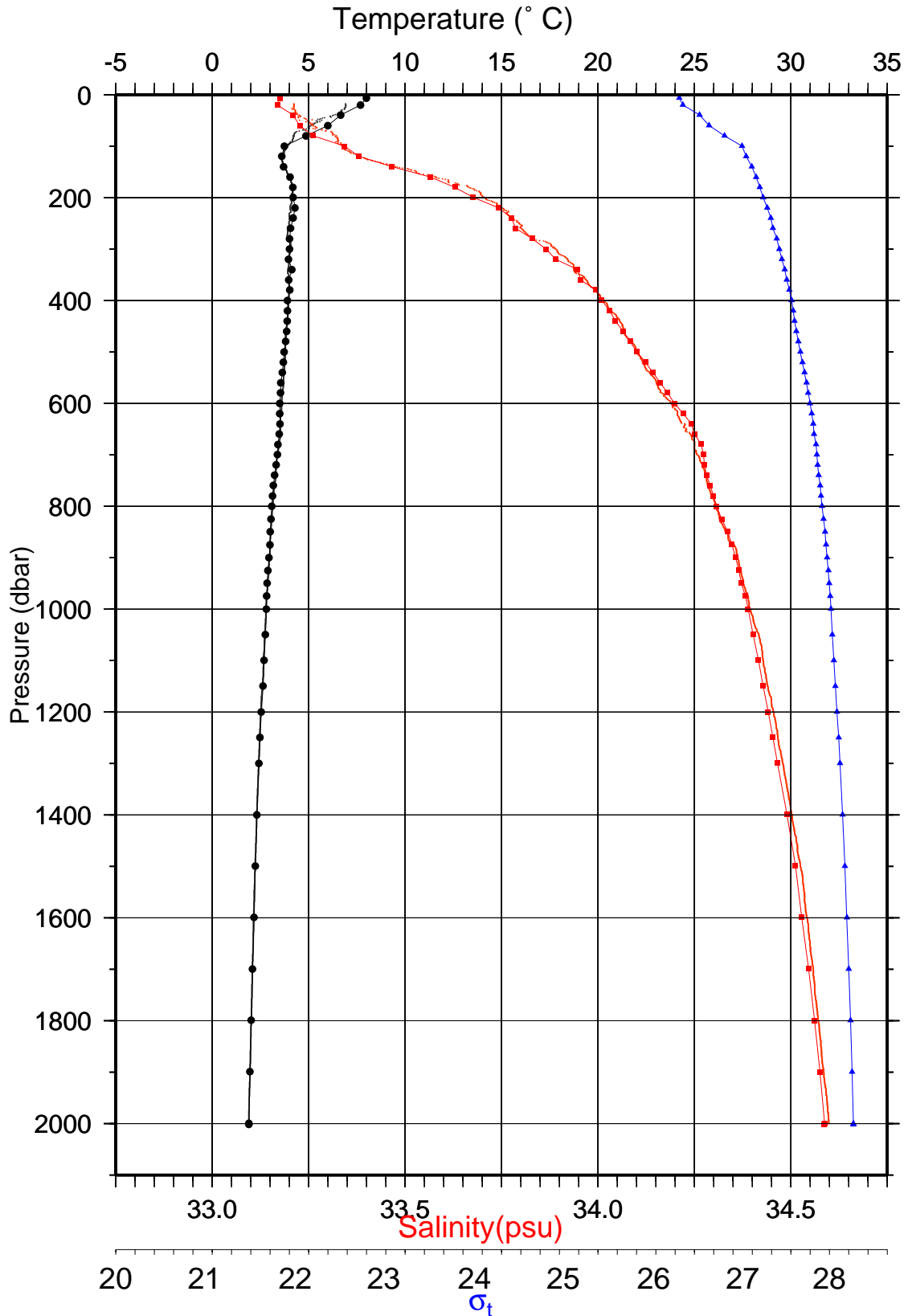


Fig. 3.12-7: Same as Fig. 3.12-5 but for the float WMO2900057 on Jun. 27 and St. 10 on Jun. 21.

3.13 Shipboard ADCP

Satoshi Okumura (Global Ocean Development Inc.)

Wataru Tokunaga

(1) Parameters

(1.1) N-S(North-South) and E-W(East-West) velocity components of each depth cell [cm/s]

(1.2) Echo intensity of each depth cell [dB]

(2) Methods

We had measured current profiles by shipboard ADCP (Acoustic Doppler Current Profiler ;VM-75, RD Instruments, Inc. U.S.A.) from the departure of Sekinehama on 4 June 2001 to the arrival of Sekinehama 19 July 2001.

Major parameters for the measurement configuration are as follows;

Frequency:	75 kHz
Average(process data):	every 300 sec.
Depth cell length:	800 cm
No. of depth cells:	80
Ping per ensemble:	60 (No bottom track pings)
Time between pings:	2.0 sec
Coordinate system:	Earth

(3) Preliminary results

The results will be public after the analysis.

(4) Data archives

ADCP data obtained in this cruise will be submitted to JAMSTEC Data Management Division and will be under their control.

3.14 Geological and geophysical observation

3.14.1 Sea beam

Satoshi Okumura (Global Ocean Development Inc.)

Wataru Tokunaga

(1) Objective

R/V Mirai has installed a multi narrow beam echo sounding system (MNBES), SeaBeam 2112.004 (SeaBeam Inc., USA). The main objective of MNBES observation is collecting continuous bathymetry data along ship's track to make a contribution to geological and geophysical investigations.

(2) System configuration and performance

Frequency:	12 kHz
Transmit beam width:	2 degree
Transmit power:	20 KW
Transmit pulse width:	3 msec to 20 msec
Depth range:	100 to 11,000 m
Beam spacing:	1 ° athwart ship
Swath width:	max 150 °
	120 ° to 4,500 m
	100 ° to 6,000 m
	90 ° to 11,000m
Depth accuracy:	Within < 0.5% of depth or ± 1 m, (whichever is greater, over the entire swath)

(3) Method

We carried out bathymetric survey from the departure of Sekinahama on 4 June 2001 to the arrival of Sekinahama on 19 July 2001. Additional survey performed around several sites (St. 8, 9, 29, 30, 31) for determination of sediment core sampling positions.

The data we've got there were post-processed immediately and visualized image as color contour map.

To get accurate sound velocity of water column, we used temperature and salinity profiles from CTD (deep casts) data and calculated sound velocity by equation in Mackenzie (1981).

(4) Preliminary result

The results will be public after the analysis.

(5) Data archives

The raw data obtained during this cruise will be submitted to JAMSTEC Data Management Division and will be under their control.

3.14.2 Sea surface gravity

Satoshi Okumura (Global Ocean Development Inc.)

Wataru Tokunaga

(1) Method

We had measured relative gravity value by LaCoste-Ronberg onboard gravity meter S-116 throughout MR01-K03 cruise. To determine the drift ratio of the onboard gravity meter and the absolute gravity value, we also measured relative gravity value at comparative points of the Sekinehama port, already known absolute gravity value, using by portable gravity meter CG-3M Autogav (SCINTREX, Canada)

(2) Preliminary results

The Measured gravity values should be corrected based on the bathymetry (free-air) and ship's movement (etoves). The results will be public after the analysis.

(3) Data archives

Sea surface gravity data obtained during this cruise will be submitted to JAMSTEC Data Management Division and will be under their control.

Reference Table of Port Call Gravity Calibration

Cruise No: MR01-K03

No.	Date (yyyy/mm/dd)	UTC (hh:mm)	Port	Absolute G (if known)	Sea Level (cm)	Draft (cm)	G at sensor* (mgal)	L&R Reading Value(mgal)	Remarks
Ex.	2000/1/1	3:30	Sekinehama	980371.85	230.0	620	980372.60	12345.6	example
1	2001/6/2	3:00	Sekinehama	980371.85	245.0	628	980372.65	12656.2	
2	2001/7/19	5:06	Sekinehama	980371.85	233.5	600	980372.60	12658.4	

note: Gravity values at the sensor position of onboard gravimeter are calculated the follows;

$$\text{absolute G} + \text{sealevel} * 0.3086 / 100 + (\text{draft} - 530) / 100 * 0.0431$$

3.14.3 Surface three component magnetometer

Satoshi Okumura (Global Ocean Development Inc.)

Wataru Tokunaga

(1) Objective

In order to continuously obtain the geomagnetic field vectors on the sea surface, a three component magnetometer is a very useful equipment. The magnetic force on the sea is affected by induction of magnetized body beneath the seafloor in addition to the earth dipole magnetic field. The magnetic measurement on the sea is, therefore, one of utilities for geophysical reconstruction of crustal structure and so on. The geomagnetic field can be divided into three components, i.e., two horizontal(x&y) and one vertical(z) moments. Three-component observation instead of total force includes much information of magnetic structure of magnetized bodies.

(2) Method

The sensor is a three axes fluxgate magnetometer on the top of foremast and sampling period is 8 Hz. The timing of sampling is controlled by the 1pps standard clock of GPS signal. Every one second data set which consists of 310 bytes; navigation information, 8 Hz three component of magnetic forces, ship's roll and pitch data were recorded.

(3) Preliminary result

The results will be public after the analysis. The procedure of quality control is mainly to eliminate the effect of ship's magnetized vector condition.

(4) Data archives

Magnetic force data obtained during this cruise will be submitted to JAMSTEC Data Management Division and will be under their control.